The Evolving Role of Extreme Weather Events in the U.S. Power System with High Levels of Variable Renewable Energy

Josh Novacheck,[1] Justin Sharp,[2] Marty Schwarz,[1]
Paul Donohoo-Vallett,[3] Zach Tzavelis,[1] Grant Buster,[1]
and Michael Rossol[1]

1 National Renewable Energy Laboratory
2 Sharply Focused, LLC
3 U.S. Department of Energy

NREL is a national laboratory of the U.S. Department of Energy
Office of Energy Efficiency & Renewable Energy
Operated by the Alliance for Sustainable Energy, LLC

This report is available at no cost from the National Renewable Energy Laboratory (NREL) at www.nrel.gov/publications.

Contract No. DE-AC36-08GO28308

Technical Report
NREL/TP-6A20-78394
December 2021

The Evolving Role of Extreme Weather Events in the U.S. Power System with High Levels of Variable Renewable Energy

Josh Novacheck,[1] Justin Sharp,[2] Marty Schwarz,[1] Paul Donohoo-Vallett,[3] Zach Tzavelis,[1] Grant Buster,[1] and Michael Rossol[1]

1 National Renewable Energy Laboratory
2 Sharply Focused, LLC
3 U.S. Department of Energy

Suggested Citation
Novacheck, Josh, Justin Sharp, Marty Schwarz, Paul Donohoo-Vallett, Zach Tzavelis, Grant Buster, and Michael Rossol. 2021. *The Evolving Role of Extreme Weather Events in the U.S. Power System with High Levels of Variable Renewable Energy*. Golden, CO: National Renewable Energy Laboratory. NREL/TP-6A20-78394. https://www.nrel.gov/docs/fy22osti/78394.pdf.

NREL is a national laboratory of the U.S. Department of Energy
Office of Energy Efficiency & Renewable Energy
Operated by the Alliance for Sustainable Energy, LLC

This report is available at no cost from the National Renewable Energy Laboratory (NREL) at www.nrel.gov/publications.

Contract No. DE-AC36-08GO28308

Technical Report
NREL/TP-6A20-78394
December 2021

National Renewable Energy Laboratory
15013 Denver West Parkway
Golden, CO 80401
303-275-3000 • www.nrel.gov

NOTICE

This work was authored in part by the National Renewable Energy Laboratory, operated by Alliance for Sustainable Energy, LLC, for the U.S. Department of Energy (DOE) under Contract No. DE-AC36-08GO28308. Funding provided by the U.S. Department of Energy Office of Energy Efficiency and Renewable Energy Strategic Analysis Team and Water Power Technologies Office. The views expressed herein do not necessarily represent the views of the DOE or the U.S. Government.

This report is available at no cost from the National Renewable Energy Laboratory (NREL) at www.nrel.gov/publications.

U.S. Department of Energy (DOE) reports produced after 1991 and a growing number of pre-1991 documents are available free via www.OSTI.gov.

Cover Photos by Dennis Schroeder: (clockwise, left to right) NREL 51934, NREL 45897, NREL 42160, NREL 45891, NREL 48097, NREL 46526.

NREL prints on paper that contains recycled content.

Foreword

The central research questions we investigate in this report are whether increasing levels of wind and solar generation make it more challenging to reliably operate the power system during extreme weather events and whether that increase changes which events would be considered extreme, due to large impacts to power system operations. To address these questions, we used high-resolution data sets of historical load, weather, wind, and solar resources for 2007–2013, identified periods of extreme weather events, and then modeled grid operations during those same events under high wind and solar future systems. Twelve events were selected for detailed modeling, and while this is not a large enough sample size or period to robustly determine the future likelihood of recurrence and risk, it allows an initial assessment at how potential weather impacts will change as penetration increases.

Four levels of technical detail are provided in the report:

Report Component	Description
Executive Summary	• Brief summary of the study approach and type of weather events considered • Brief summary of the eight common findings from the data sets and modeling as they relate to power sector planning and operations
Technical Summary	• More extensive summary of the study approach and type of weather events considered • More extensive summary discussion of the eight common findings from the data sets and modeling as they relate to power sector planning and operations
Report Main Text	• Detailed review of categories of weather events and their impact on power sector operations and planning • Detailed description of the development of future power sector infrastructures, methods used to identify events of interest, and the power sector operational modeling approaches used to evaluate each event • Detailed exploration of eight common findings from the data sets and modeling as they relate to power sector planning and operations
Appendix	• Detailed description of each event analyzed, including salient meteorological features, specific impacts on load and net load, and wind and solar generation • Analysis of production cost modeling results for a subset of the events

The events and associated data considered in this report may be useful to system planners, policy makers, and researchers to test the weather resilience and resource adequacy of future power system infrastructure. The events could be used to assess the performance of integrated resource plans, assess the operation of future power systems analyzed in grid integration studies, or to explore tradeoffs between different policy options.

Acknowledgments

We gratefully acknowledge the many people whose efforts contributed to this report. Many NREL colleagues reviewed and improved this report, including and Doug Arent, Jaquelin Cochran, David Palchak, Wesley Cole, Melinda Marquis, Caitlin Murphy, Gian Porro, and Greg Stark. We also thank our external reviewers for providing technical peer review, including Hannah Bloomfield, Michael Milligan, Steve Rose, Priya Sreedharan, and Aidan Tuohy. We also thank our DOE colleagues for providing critical review of interim and final work products, including Hill Balliet, Cindy Bothwell, Zachary Eldredge, Aaron Ng, Joe Paladino, Allan Ward, Guohui Yuan, and Johanna Zetterberg. This work was funded by the U.S. Department of Energy's Office of Energy Efficiency and Renewable Energy Strategic Analysis Team and Water Power Technologies Office and under contract number DE-AC36-08GO28308. All errors and omissions are the sole responsibility of the authors.

Acronyms and Abbreviations

AEO	Annual Energy Outlook
ATB	Annual Technology Baseline
CAISO	California Independent System Operator
CONUS	conterminous United States
EI	Eastern Interconnection
EIA	U.S. Energy Information Administration
ERCOT	Electric Reliability Council of Texas
EST	Eastern Standard Time
FRCC	Florida Reliability Coordinating Council
gas-CC	gas-combined cycle
gas-CT	gas-combustion turbine
GW	gigawatt
ISO	independent system operator
ISO-NE	ISO New England
km	kilometer
LCD	Local Climatological Data (NOAA)
LST	local standard time
mb	millibars
MISO	Midcontinent Independent System Operator
MW	megawatt
NCEP	National Centers for Environmental Prediction
NOAA	National Oceanographic and Atmospheric Administration
NREL	National Renewable Energy Laboratory
NSRDB	National Solar Resource Database
NYISO	New York Independent System Operator
PCM	production cost model/modeling
PJM	PJM Interconnection
RE	renewable energy
SERC	SERC Reliability Corporation
SPP	Southwest Power Pool
TI	Texas Interconnection
TVA	Tennessee Valley Authority
TWh	terawatt-hours
UTC	Coordinated Universal Time
VRE	variable renewable energy
WI	Western Interconnection
WIND	Wind Integration National Dataset

Executive Summary

The central research questions we investigate in this report are whether increasing levels of wind and solar generation make it more challenging to reliably operate the power system during extreme weather events and whether such increases change our consideration of the type of events that could be considered "extreme" based on their significant impact to power system operations. In this report, we (1) review categories of weather events and their impact on power sector operations and planning; (2) describe the development of future power sector scenarios, methods used to identify weather events of interest, and the power sector operational modeling approaches used to evaluate each event; and (3) explore eight common findings from the data sets and modeling as they relate to power sector planning and resource adequacy. The findings do not explicitly explore the resilience of the system to the weather events. The appendix contains a detailed description of each event analyzed from which the common findings were synthesized, including salient meteorological features; specific impacts on load, wind and solar resource and generation, and net load (i.e., load minus available renewable generation); and analysis of production cost modeling results for a subset of the events.

Study Approach and Weather Events

Our study leverages high-resolution wind and solar data, renewable technology modeling, and geospatial analysis developed by the National Renewable Energy Laboratory (NREL) to identify and model the generation profiles of wind and solar for future high variable renewable energy (VRE) penetration systems. The data sets allow for investigation of weather events that occurred between 2007 and 2013. While 2007–2013 does not provide a complete sample of all high-impact weather events that could impact the future system, this historical range does allow us to identify case study events that may not occur annually, but do come about with some regularity, such as a 1 in 10-year event.

Weather events were categorized into two broad categories, "High Impact Events" and "Events Posing Planning Challenges". Table ES-1 defines the general type of event that falls into each category. Data sources to identify specific events within these categories included the historical weather record and wind and solar modeled resource availability from the Wind Integration National Dataset (WIND) Toolkit and National Solar Radiation Database (NSRDB).

Table ES-1. Categorization of Weather Events

Weather Event Category	Weather Event Type
High Impact Events	Cold Waves Midlatitude Storms Heat Waves Tropical Systems
Events Posing Planning Challenges[a]	Low Variable Renewable Energy Resource with High Demand High Variable Renewable Energy Resource with Low Demand

[a]The events we identified and studied in this category are often milder versions of the events in the "High Impact Events."

We selected three future years from a scenario produced by the NREL Regional Energy Deployment System (ReEDS) capacity expansion model, designed with assumptions that are generally consistent with Low RE cost scenario from the 2019 Standard Scenarios (Cole et al. 2019), to determine the size and location of new generators (e.g., wind, solar, or thermal), generators to retire, new energy storage of various durations[1], and additions of interregional transmission capacity. The three selected years—2024, 2036, and 2050—have corresponding projected system infrastructure plans that reach variable renewable generation (VRE) penetrations of 17%, 50%, and 65% of annual demand, respectively.[2] While 2036 and 2050 systems experience large growth in wind and solar, a significant portion of thermal capacity, mostly in the form of gas, remains on the system and contributes to meeting the reserve margin requirements of the ReEDS model. Brinkman et al. (2021) contains further explanation about the shift of thermal generators to providing more capacity than energy as is the case in scenarios explored in this paper. As an example of one future scenario, Figure ES-1 shows the distribution of utility-scale PV and wind generators for the 2050 infrastructure plan. Using a future buildout, a final set of events was selected, informed by the wind and solar generation profiles from the infrastructure plans, to represent a diversity of events the future system may encounter rather than to determine the most extreme events or to rank the events against each other.

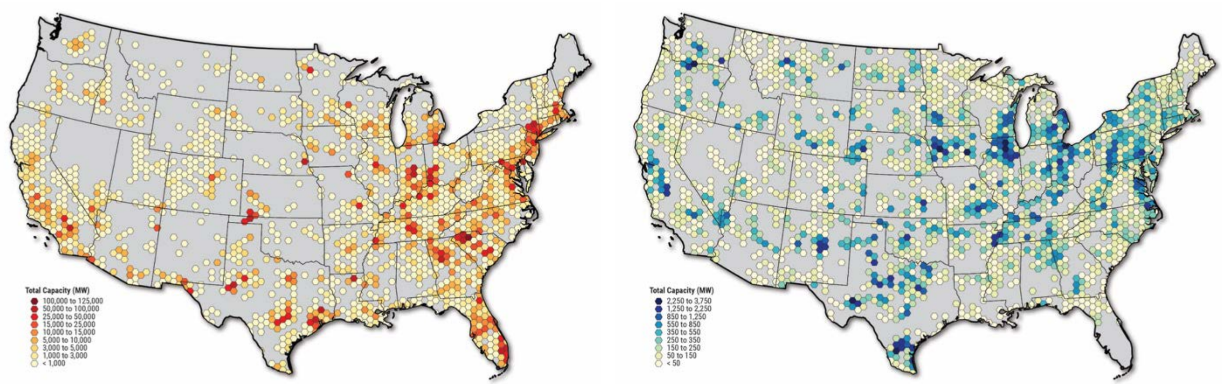

Figure ES-1. Locations and capacity of utility-scale PV (left) and wind (right) generators in the 2050 infrastructure plan

For a select number of these events, we performed production cost modeling (PCM) of the three infrastructure plans to understand how operations of systems with higher penetrations of variable renewable generation may change when subjected to the same weather as the historical weather event we identified. We focused the modeling and analysis on a subset of similar weather events with different intensities (e.g., different intensity heat and cold waves) to better understand how the operations evolve as the VRE penetration changes. The operational analysis focuses on understanding the implications for meeting load during the specific events in the three

[1] The infrastructure plans have low deployment of storage, especially relative to newer versions of the Standard Scenarios. This report used assumptions from the 2018 Standard Scenarios. The cost of storage was revised down in the 2019 Standard Scenarios resulting in greater deployment of storage.

[2] The resulting clean electricity penetrations of the infrastructure plans fall below those needed to achieve the carbon pollution-free power sector by 2035 goal set by President Biden. There may be different weather events that are more relevant to 100% clean electricity systems with higher levels of VG than we identified and studied. However, several of the events we analyzed lead to widespread low wind and solar generation potential. These events would likely be relevant to systems with even higher VG penetrations than those we studied.

interconnections (Eastern, Western, Texas). In addition, we conducted sensitivity analysis of the 2050 infrastructure plan on events where hydropower or the impact of turbine blade icing and cold temperature shutdown would have large impact. Implications for operational costs and electricity prices are not analyzed.

Findings

Our analysis of the case study weather events informs eight key findings. These findings are specific and limited to the events from the historical data set and to the grid infrastructure futures considered, but they point to an overarching conclusion: the most concerning events to the resource adequacy of the future system are different than the concerning events of today. Future research is needed to investigate applicability of these findings to: (1) other weather conditions, beyond the limited sample of weather events from 2007–2013 explored here and including those that capture further influence of climate change in the coming decades; and (2) other grid infrastructure futures.

Finding 1. Wind and solar generation tend to be available during the extreme weather events of today and do not introduce new resource adequacy concerns or system operation stress as their annual energy penetration increases. Exceptions exist, but they tend to be short periods of elevated net load.

In general, the variable renewables added in these scenarios generate at statistically common levels for the season during the extreme weather events we studied. Often the generation from these resources can reduce the burden of extreme high loads that are typical of these extreme weather events. There are days and hours during these events when net load is still among the highest in the data set, suggesting wind and solar do not mitigate all periods of resource adequacy stress caused by these events. However, the periods of high net load are not as protracted as the periods of high load, and net load peaks are always well below load peaks. In some cases, adding wind and solar can change which day of a weather event would require the most non-VRE generation to meet demand.

The largely normal wind and solar availability during extreme weather events are due to the common meteorology of the events. Heat inducing summertime high loads occur on sunny days and wintertime high loads tend to coincide with the arrival of cold air that is brought in by strong winds. This suggests the events that historically caused major disturbances on the power system are not made worse by the growth of wind and solar generation and do not introduce new planning challenges beyond what already exist during normal weather conditions (e.g., the need for wind/solar forecasting and ramping flexibility). Greater exploration of wind and solar availability can be found in the discussion of Finding 1 in the Technical Summary, the full report, and in each event case study description in the appendix.

Finding 2. Mild weather conditions can produce extended periods of low wind and solar resource. Historically, the weather during these events would not be a reason for concern among system planners and operators, but with the increasing contribution of wind and solar generation, these events need to become a focus of planners in order to ensure system adequacy.

As the penetration of variable renewable generation increases, a new type of “extreme” will become increasingly important to system planners: widespread low wind and solar resource during moderate to high loads leading to extremely high net loads. These very high net load days may not coincide with the summer or winter peak load, which tend to determine generation and transmission capacity needs under the existing prevalent approach to system planning.

We identified four events within the time frame characterized by periods of high net load driven by moderate to high load and low output from wind and solar generators. The type of weather that leads to these conditions can occur throughout the year, but the events that cause the most severe risk to power system resource adequacy over a broad area tend to occur in the winter or summer. Load during these events is closer to the middle of the distribution of seasonal loads and therefore more common for the system to encounter. But due to low wind and solar output relative to normal, the net load during the event ends up in the high tail of the seasonal net load distribution, a system state that occurs infrequently. The summer events tend to have higher hourly net load peaks, which occur around sunset. However, winter events tend to have more prolonged periods of poor wind and solar resource over larger areas, leading to extended periods (i.e., multiple days) of high net load.

Finding 3. Because cold waves occur in winter when solar generation is already low, system operations during cold waves is most heavily influenced by the performance of wind generation. Generally, wind generation is abundant as the cold front moves through, but there is uncertainty in the extent of the wind lull that follows the front, both temporally and spatially. The severity of the lull determines the magnitude of the required response from the rest of the system.

The limited sample size of weather events (2007–2013) we explored in this study suggest cold waves are among the weather events with the largest impact on system operations relative to today as the system utilizes more VRE. This is predominately because of wind generation dynamics driven by the cold waves. Initially, the front that brings cold temperatures also brings high winds. In the two cold waves we studied with production cost modeling (PCM), this means wind generation ramps up at the same time as load increases. However, as the front moves through, but temperatures remain cold, the wind generation tends to decrease. In some cases, such as an extreme cold wave that occurred in February 2011, there is enough geographic diversity in the wind and solar resource and utilizable transmission capacity to trade the available VRE over long distances. During this event, after the initial cold front moved through, wind generation potential dropped in much of the southern portions of the Eastern Interconnection (EI) and in Texas but remained well above normal throughout the Upper Midwest. However, a milder cold wave from February 2008 had a widespread negative impact on the wind resource throughout the EI. In our system operations modeling, the prolonged wind generation deficit after the front moved on necessitated a large ramp-up of available thermal capacity to meet load for an extended period. Both cold wave events we examined suggest the days following the onset of a cold wave may be among the most important for planners to consider when determining capacity needs for future systems that rely on high levels of VRE. Our results also suggest the days following milder cold waves may be the most concerning due to the widespread reduction in wind generation potential. This information could be useful to planners as they prepare for the winter season and need to identify key periods to study as they assess the forecasted adequacy of their system. However, we suggest additional research on a larger sample size of cold waves to more fully explore the differences between cold wave intensities.

Finding 4. Increased PV capacity drives system operational changes during summer months and this does not change during heat waves. However, the contribution from wind after sunset differentiates the level of system operation stress caused from one heat wave to another.

The heat waves we studied had little to no impact on PV generation, but they do impact total wind generation. Increasing PV capacity, and thus generation, on a system can have a large impact on system operations, pushing more thermal and hydropower generation toward a narrower net load peak, but this is typical of most summer days. On average, wind generation is at its lowest in the summer, but, on an interconnection-wide scale and accounting for transmission constraints, wind plays a critical role providing resource adequacy to the 2036 and 2050 infrastructure plans as it reliably increases its generation in the evening as solar generation decreases. For the specific heat waves examined, events associated with extreme heat and high electricity demand did not lead to lower than normal wind generation potential. However, more moderate heat waves could severely depress wind generation, especially during the key net load peak in the evening. Based on the weather years of 2007–2013, the most pressing events for planners and operators to ensure sufficient capacity at the net load peak appear to be moderate heat waves accompanied by persistent high pressure and very low wind generation. One critical aspect of heat waves that we did not study are coincident widespread wildfires. More research is required to understand system risk associated with the reduction of PV generation caused by wildfire smoke and other infrastructure outages due to wildfires.

Finding 5. Understanding the characteristics and diversity of wind and solar resources—at small and large geographic scales—is key to assessing their contribution to resource adequacy. Operating existing and expanded transmission more flexibly than today enables that contribution.

Several of the weather events we explored include periods of low wind and solar output. Even in these circumstances, these variable resources can still contribute to resource adequacy through the application of interregional coordination and system flexibility. These events feature extremely high net loads and demonstrate how careful planning and an understanding of the regional diversity of wind and solar resource can enable reliable operations by utilizing the bidirectional trading of power through the transmission system, while avoiding overbuilding local generation. But for wind and solar to contribute to resource adequacy during these events, the direction and magnitude of transmission flows must change more rapidly relative to today and as the overall penetration of wind and solar increases.

In these types of events, trading power with neighboring regions in both directions and taking advantage of geospatially separate VRE subject to diverse weather conditions is critical to maintaining resource adequacy. Enabling this trading behavior requires an understanding of the wind and solar for multiple weather years, ensuring that transmission infrastructure exists to take advantage of the geographic diversity of the resource, and use of planning and operations models that capture the full geographic scale of the power system.

Finding 6. In areas where hydropower is abundant, its availability and flexibility are key to mitigating system stress during extreme weather events.

Water availability and flexibility to shift when water is used impact whether hydropower can achieve the change in the desired operations to support higher variable renewable energy penetration systems. In our sensitivity analysis, dry conditions, leading to less water available for hydropower generation, led to less generation at peak, but hydropower output was still shaped, subject to operational and regulatory constraints, to provide as much power as possible at the peak net load hours. While our modeling partially captured the coincident weather affecting hydropower availability and wind and solar generation, more research using a weather data set that considers weather variability over a longer multiyear period is needed to fully understand the correlation between hydropower, wind, and solar.

Even more important than availability of water to hydropower's ability to provide value and resilience during key weather events is how much flexibility a hydropower unit has to shift energy day-to-day and hour-to-hour. One sensitivity we modeled made hydropower operations less flexible. The modeled inflexibility is costly to the Western Interconnection (WI), where hydropower's contribution is the largest of all three interconnections, as the modeled system is unable to focus hydropower's water use to the events or hours of the event where it is most valued. Further research is needed to understand which is of higher value—shifting energy day-to-day or hour-to-hour—and how the type of event affects the value. We also suggest more investigation into how the same value could be extracted from other forms of energy storage for areas without abundant hydropower resources.

Finding 7. Broad, interconnection-wide impacts from wind turbine blade icing and cold temperature shutdowns are rare. However, regional icing and cold temperature events can be significant and rely on local gas generation dispatch and interregional transmission flows to maintain adequate supply to meet demand.

Ability to forecast icing and cold temperature events and coordinate operations across regions will be key to determining the extent to which these events are a resource adequacy concern. In our modeling of high variable renewable energy systems, the reduction of total wind generation caused by the cold or icing events was limited to 10% of the available wind generation. Though this is a significant reduction, the remaining available wind generation is still well above events with widespread low wind speed. However, our modeling shows local icing and cold temperature cutoffs do reach more concerning levels during these events. Our results suggest, with proper coordination with neighboring system and usage of available gas dispatch, which also is derated due to cold weather in our modeling, such events can be managed. Note we were unable to explore potential impacts of snow cover on solar panels due to data and modeling limitations.

Finding 8. Tropical storm impact on renewable resource availability is localized and of less impact than direct damage to generation, transmission, and distribution infrastructure.

Tropical storms and hurricanes can significantly impact the power sector. However, these storms primarily impact local transmission and distribution infrastructure due to local high winds and flooding, which was not the focus of this study. The extent of the impact is small compared to both the size of the electrical system and the larger pressure systems that drive the extreme temperature events. For the tropical storms and hurricanes we investigated, outside the band of damaging wind speeds, their impact on wind and solar generation is primarily through the broad extent of cloud cover and net increase in wind resource, even when accounting for the cut-out windspeed for the typical wind turbine.

Conclusions

This report contains a first of its kind analysis investigating how various weather events could impact U.S. power system operations when wind and solar are large contributors to the energy mix. Using case study weather events from 2007 to 2013, we found that the transition to a system with more VRE changes which weather events lead to largest threats to the resource adequacy of the future system. We found that wind and solar do not lead to new operational or resource adequacy concerns during the high-impact weather events during the period studied (e.g., extreme cold waves, extreme heat waves, and midlatitude storms). Wind and solar generators are generally available during these events. However, weather events that were not particularly concerning historically, and tend to be milder versions of the high-impact events, can lead to large and extended periods of wind and solar deficits. Often the low wind and solar generation can be well-forecasted on weekly and daily timescales and therefore well-represented in operational forecasts used by system operators to commit and dispatch generation resources. However, these types of events are often not considered in resource adequacy studies used by planners to ensure enough generation and transmission resources exist to serve load.

The events identified by this study and the associated data may be useful to system planners, policy makers, and researchers to test the weather resilience and resource adequacy of future power system infrastructure. The events could be used to test the performance of integrated resource plans or to explore tradeoffs between different policy options. This report also describes a methodology for identifying additional events relevant to different regions or from additional weather years.

There are several areas where further research is required. Most importantly, we need to better understand how frequently the concerning events we identified occur, while capturing events we may have missed by only using an historical weather data set covering 2007–2013. This would require the creation of wind, solar, hydropower, and load data sets for a longer historical period, as well as those that capture the potential prospective effects of climate change. Climate change may vary the frequency and magnitude of the weather events we studied or introduce new types of weather events not explored in this work. Using the expanded data sets, future work can also explore new methods to statistically quantify risks to system operations presented by these weather events by pairing PCM with other resource adequacy models and tools, while exploring a greater number of infrastructure plans that investigate higher penetrations of VRE and 100% clean electricity systems.

Technical Summary

As weather-dependent renewable generation grows, it is important for power system planning to understand the broad trends and correlations between weather, renewable resources, and load. The traditional planning, performed by utilities and system operators, includes the study of system resource adequacy during peak load periods in the summer and winter to ensure the generation and transmission system is appropriate to meet load. But in a power grid with a high penetration of variable renewable energy (i.e., wind and solar), periods of high risk to system resource adequacy may no longer correspond only to hours of peak load. In particular, high shares of variable renewable energy, even when well-forecasted to inform system operations, can further complicate the stress extreme weather events already place on the grid. They also may lead to changes to the types of weather conditions that are most problematic to system operations and resource adequacy due to widespread and extended deficits of wind and solar generation. Accordingly, the focus of reliability assessments in long-term planning studies may need to evolve in the coming years to more fully incorporate weather events that lead to these deficits. This report seeks to identify these new weather events and understand the characteristics of the events that lead to system risk of future systems with higher penetrations variable renewable energy.

Two examples of such events that may require changes to long-term planning assessments are periods of extreme cold or heat. During the February 2021 cold wave that led to large-scale load shedding in Texas, peak load, gas outages, and low wind output all exceeded even the most extreme values used in ERCOT's winter planning[3,4]. The 2020 historic West-wide heat wave in August and September, created a spike in demand and resulted in rolling blackouts. Also, the increase in variable renewable energy penetration has exposed the U.S. power system to new and unforeseen stressors. For example, unforecasted wind turbine low temperature shutdowns occurred throughout the MISO footprint during an intense cold wave in January 2019 (Rose 2019). Also, erroneous tripping of a large amount of solar PV capacity due to manufacturer inverter settings during the August 2016 Blue Cut Fire in Southern California[5] exacerbated an already major contingency event. The MISO and California examples are now well understood. MISO now represents low temperature shutdowns in their wind forecasts (Rose 2019), while NERC and inverter manufacturers have implemented recommendations on changes to inverter settings to avoid erroneous tripping in the future[6]. But the events demonstrate the importance of incorporating weather-related risks in resource adequacy modeling and system planning[7].

The central research questions we investigate in this report are whether increasing levels of wind and solar generation make it more challenging to reliably operate the power system during extreme weather events and whether such increases change our consideration of the type events that could be considered "extreme" based on their significant impact to power system operations

[3] http://www.ercot.com/content/wcm/key_documents_lists/225373/2.2_REVISED_ERCOT_Presentation.pdf

[4] http://www.ercot.com/content/wcm/lists/197378/SARA-FinalWinter2020-2021.pdf

[5] https://www.nerc.com/pa/rrm/ea/1200_MW_Fault_Induced_Solar_Photovoltaic_Resource_/1200_MW_Fault_Induced_Solar_Photovoltaic_Resource_Interruption_Final.pdf

[6] https://www.nerc.com/pa/rrm/ea/1200_MW_Fault_Induced_Solar_Photovoltaic_Resource_/1200_MW_Fault_Induced_Solar_Photovoltaic_Resource_Interruption_Final.pdf

[7] This study focuses on weather events that occurred between 2007 and 2013 due to available data. The examples given in this paragraph are outside of this range and were not studied in this report.

and resource adequacy. In this report, we (1) review categories of weather events and their impact on power sector operations and planning; (2) describe the development of future power sector scenarios, methods used to identify weather events of interest, and the power sector operational modeling approaches used to evaluate each event; and (3) explore eight common findings from the data sets and modeling as they relate to power sector planning. The findings do not explicitly explore the resilience of the system to the weather events. The appendix contains a detailed description of each event analyzed from which the common findings were synthesized, including salient meteorological features; specific impacts on load, wind and solar resource and generation, and net load; and analysis of production cost modeling results for a subset of the events.

Study Approach and Events

Our study leverages high-resolution wind and solar data, technology modeling, and geospatial analysis developed by the National Renewable Energy Laboratory (NREL) to identify and model the generation profiles of wind and solar generating for future high VRE penetration systems. The data sets allow for investigation of weather events that occurred between 2007 and 2013. While 2007–2013 does not provide a complete sample of all high-impact weather events that could impact the future system, this historical range does allow us to identify case study events.

Weather events were categorized into two broad categories, "High Impact Events" and "Events Posing Planning Challenges". Table TS-1 defines the general type of event that falls into each category. Further details on the categorization and the weather events can be found in the Taxonomy of Extreme Weather Events section in the main body of the report. Methods to identify the events are more fully described in the main body of the report, but data sources included the historical weather record, wind and solar modeled resource availability from the Wind Integration National Dataset (WIND) Toolkit and National Solar Radiation Database (NSRDB), and historical load profiles. reported by utilities, Independent System Operators (ISO), or Regional Transmission Operators (RTO).

Table TS-1. Categorization of Weather Events

Weather Event Category	Weather Event Type
High Impact Events	Cold Waves Midlatitude Storms Heat Waves Tropical Systems
Events Posing Planning Challenges[a]	Low Variable Renewable Energy Resource with High Demand High Variable Renewable Energy Resource with Low Demand

[a]The events we identified and studied in this category are often milder versions of the events in the "High Impact Events."

We selected three future years from a scenario produced by the NREL Regional Energy Deployment Systems (ReEDS) capacity expansion tool determine sizes and locations of new generators (e.g., wind, solar, or thermal), generators to retire, and additions of interregional transmission capacity. The ReEDS scenarios were designed with assumptions that generally consistent with Low Renewable Energy (RE) cost scenario from the 2019 Standard Scenarios (Cole et al. 2019); specific assumptions are shown in Table TS-2. The three selected years—2024, 2036, and 2050—have corresponding projected system infrastructure plans that reach variable renewable generation (VRE) penetrations of 17%, 50%, and 65% of annual demand, respectively.[8] Figure TS-1 shows the total generation capacity by type for the three infrastructure plans in each of the three interconnections: Eastern (EI), Western (WI), and Texas (TI). Figure TS-2 shows the national distribution of utility-scale PV and wind generators for the 2050 infrastructure plan. While 2036 and 2050 systems experience large growth in wind and solar, a significant portion of thermal capacity, mostly in the form of gas, remains on the system and contributes to meeting the reserve margin requirements of the ReEDS model. Brinkman et al. (2021) contains further explanation about the shift of thermal generators to providing more capacity than energy as is the case in scenarios explored in this paper.

Table TS-2. Summary of Assumptions for Creation of Each Infrastructure Plan

<table>
<tr><th>Infrastructure Plan Name and ReEDS year</th><th>Generator Cost and Performance Assumptions</th><th>RE Resource Supply Curves[a]</th><th>Distributed Generation Assumptions[b]</th><th>All Other Assumptions</th><th>Wind and PV Annual Energy Penetration</th></tr>
<tr><td>2024</td><td>2019 ATB Mid-Case (NREL 2019)</td><td rowspan="3">2019 Standard Scenarios Mid-Case (Cole et al. 2019)</td><td>dGen Mid-Cost RE adoption</td><td rowspan="3">Standard Scenarios 2019 Mid-Case (Cole et al. 2019); ReEDS version 2018 (Cohen et al. 2019)</td><td>17%</td></tr>
<tr><td>2036</td><td rowspan="2">2019 ATB Low for PV and Wind (NREL 2019)</td><td rowspan="2">dGen Low-Cost RE adoption</td><td>50%</td></tr>
<tr><td>2050</td><td>65%</td></tr>
</table>

[a] See ReEDS documentation (Cohen et al. 2019) for an in-depth explanation of the renewable energy resource supply curves.

[b] See ReEDS documentation (Cohen et al. 2019) for discussion of dGen usage with ReEDS.

[8] The resulting clean electricity penetrations of the infrastructure plans fall below those needed to achieve the carbon pollution-free power sector by 2035 goal set by President Biden. There may be different weather events that are more relevant to 100% clean electricity systems with higher levels of VG than we identified and studied. However, several of the events we analyzed lead to widespread low wind and solar generation potential. These events would likely be relevant to systems with even higher VG penetrations than those we studied.

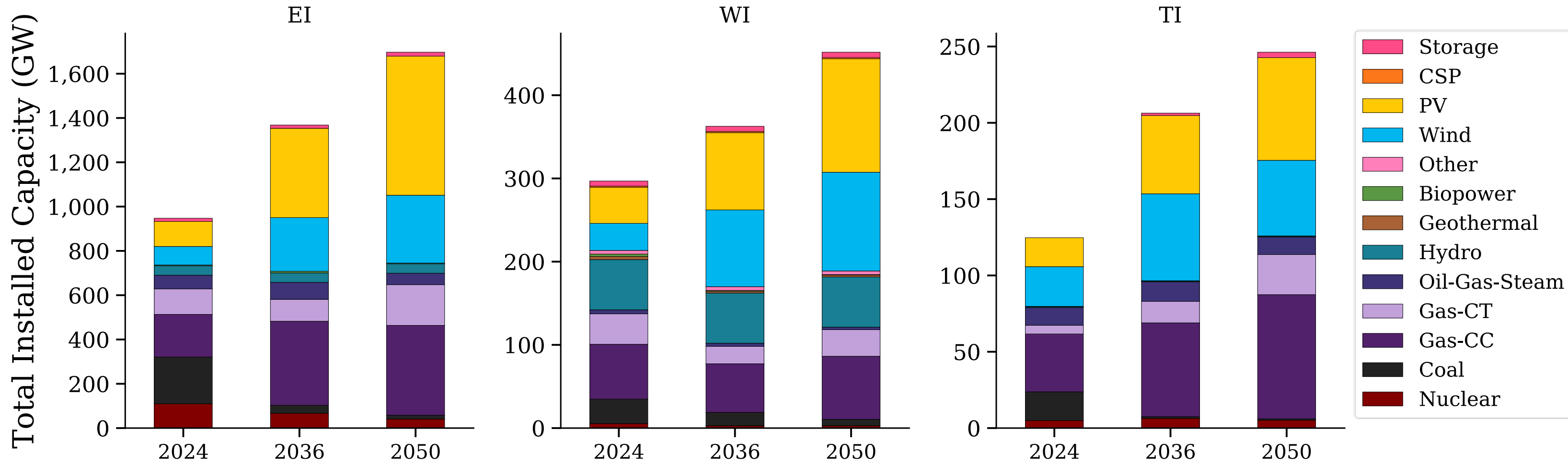

Figure TS-1. Total installed capacity for the Eastern Interconnection (EI, left), Western Interconnection (WI, middle), and Texas Interconnection (TI, right) for the three infrastructure plans

The 2024, 2036, and 2050 infrastructure plans reach 17%, 50%, and 65% annual wind and solar energy penetrations, respectively.

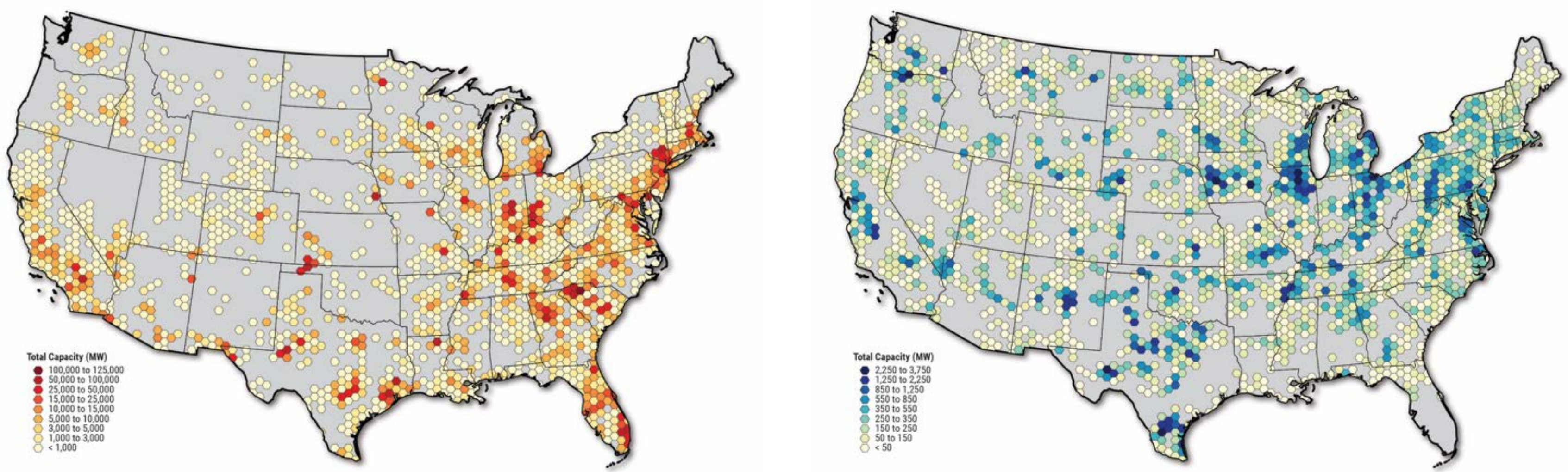

Figure TS-2. Locations and capacity of utility-scale PV (left) and wind (right) generators in the 2050 infrastructure plan

ReEDS also builds new transmission between zones in its least cost optimization. Table TS-3 shows the interzonal transmission expansion in the 2036 and 2050 infrastructure plans and the percent increase in transmission capacity relative to the 2024 plan, which is incorporated into the production cost model. Intrazonal transmission is also expanded, but it is not shown in the table.

Table TS-3. Expanded Transmission Capacity Between Zones for 2036 and 2050 Infrastructures

Percentage value in parenthesis is the increase from 2024.

Zone From	Zone To	2036	2050
CAISO	West Connect	422 MW (9%)	4,424 MW (96%)
Columbia Grid	Canada	523 MW (349%)	523 MW (349%)
Columbia Grid	Northern Tier	1,027 MW (14%)	2,758 MW (36%)
Columbia Grid	West Connect	12 MW (24%)	532 MW (1064%)
ISO-NE	Canada	0 MW (0%)	3,051 MW (72%)
MISO	Canada	1,813 MW (76%)	3,786 MW (158%)
MISO	SPP	625 MW (11%)	1,313 MW (22%)
MISO	TVA	2,515 MW (73%)	4,450 MW (129%)
Mountain West	Northern Tier	3 MW (3%)	12 MW (13%)
Mountain West	SPP	1,604 MW (458%)	1,604 MW (458%)
Northern Tier	SPP	131 MW (31%)	131 MW (31%)
NYISO	Canada	792 MW (198%)	4,012 MW (1003%)
NYISO	ISO-NE	5,353 MW (611%)	5,573 MW (636%)
PJM	MISO	3,165 MW (27%)	5,013 MW (44%)
PJM	NYISO	6,702 MW (791%)	6,702 MW (791%)
SERC	FRCC	2,298 MW (64%)	3,566 MW (99%)
SPP	ERCOT	508 MW (69%)	508 MW (69%)
SPP	TVA	1,182 MW (23%)	1,677 MW (33%)
TVA	PJM	853 MW (106%)	853 MW (106%)
TVA	SERC	491 MW (68%)	522 MW (72%)
West Connect	Mountain West	0 MW (0%)	0 MW (0%)
West Connect	Northern Tier	929 MW (91%)	929 MW (91%)
West Connect	SPP	340 MW (110%)	340 MW (110%)

ERCOT: Electric Reliability Council of Texas; FRCC: Florida Reliability Coordinating Council; ISO-NE: ISO New England; MISO: Midcontinent Independent System Operator; NYISO: New York Independent System Operator; PJM: PJM Interconnection: SERC: SERC Reliability Corporation; SPP: Southwest Power Pool; TVA: Tennessee Valley Authority

A final set of events was selected for analysis, informed by the wind and solar generation profiles from the infrastructure plans, to represent a diversity of events the future system may encounter rather than to determine the most extreme events or to rank the events against each other. Table TS-4 lists the events we analyzed, which method or methods identified the event as being of interest, and any unique characteristics of the event. The "High-Impact Events" all caused disruptions to power systems operations when they occurred. All the events shown drove load higher and, in many cases, also impacted transmission and generation infrastructure. For a select number of these events, we performed production cost modeling (PCM) of the three infrastructure plans to understand how operations of systems with higher penetrations of variable renewable generation may change when subjected to the same weather as the historical weather event we identified. We focused the modeling and analysis on a subset of similar weather events with different intensities (e.g., different intensity heat and cold waves) to better understand how the operations evolve as the VRE penetration changes in each of the three interconnections. In addition, we conducted sensitivity analysis of the 2050 infrastructure plan on events where hydropower or the impact of turbine blade icing and cold temperature shutdown would have large impact.

Table TS-4. Summary of 2007–2013 Events Selected for Analysis

Event Name	Event Dates	Identification Methods[9]	Unique Characteristics of the Event	Production Cost Modeling[10]
High-Impact Events				
Cold Wave	Feb 1–4, 2011	1.1, 1.2, 3	Intensity, record-breaking low temperatures, geographic extent, and southerly reach	2024, 2036, 2050 Plans
Heat Wave 1	July 19–24, 2011	1.1, 1.2, 3	Long-lasting heat wave, hottest summer countrywide in 75 years	2024, 2036, 2050 Plans
Heat Wave 2	June 29–Jul 7, 2012	1.1, 1.2, 3	Heat over much of the East, historic derecho storm event	—
Hurricane Irene	Aug 25–30, 2011	2.2, 3	Potential impact on wind and eastern solar	—
Hurricane Gustav	Sep 1–6, 2008	2.2, 3	Wide geographic extent and longevity over land	—
Winter Storms	Dec 4–12, 2013	1.1, 1.2, 2.2, 3	Three back-to-back storms with wide geographic impacts and long-lasting cold air reaching southern states	2050 Plan + Hydro Sensitivities + Icing Sensitivity
Events Posing Planning Challenges				
Winter Net Load 1	Feb 20–23, 2008	1.1, 1.2, 2.1, 2.2	Otherwise calm weather yielding extremely low-wind resource across CONUS and low-solar across south	2024, 2036, 2050 Plans

[9] Refers to methods described in the "Identification Methodology" section of the main body of the report.
[10] The "Power Sector Infrastructure" section of the report describes the characteristics of the scenarios, while the "Power Sector Event Modeling: Production Cost Modeling" describes the sensitivities.

Event Name	Event Dates	Identification Methods[9]	Unique Characteristics of the Event	Production Cost Modeling[10]
Winter Net Load 2	Dec 6–11, 2009	1.1, 1.2, 2.2	Concurrent high net load across all three interconnections, poor wind in the West and Texas	—
Winter Net Load 3	Feb 2–5, 2010	2.1, 2.2	Nationwide poor wind and solar	2050 + Icing Sensitivity
Summer Net Load 4	Aug 8–11, 2010	1.2, 2.2	High net load in the EI despite no extremes in either renewable resource or load	2024, 2036, 2050 Plans
Lowest Net Load	April 17, 2011	1.2, 2.1, 2.2	Widespread high wind and solar resource with low load results in lowest net load observed in data set	2050 Plan + Hydro Sensitivities + Icing Sensitivity
Wind Drought	Oct 1–24, 2010	2.2	Three weeks of well-below-normal wind CONUS-wide	—

Findings

Our analysis of the case study weather events informs eight key findings. These findings are specific and limited to the events from the historical data set and to the grid infrastructure futures considered, but they point to an overarching conclusion: the most concerning events to the resource adequacy of the future system are different than the concerning events of today. Future research is needed to investigate applicability of these findings to: (1) other weather conditions, beyond the limited sample of weather events from 2007–2013 explored here and including those that capture further influence of climate change in the coming decades; and (2) other grid infrastructure futures.

Finding 1. Wind and solar generation tend to be available during the extreme weather events of today and do not introduce new resource adequacy concerns or system operation stress as their annual energy penetration increases. Exceptions exist, but they tend to be short periods of elevated net load.

The “High-Impact Events” from Table TS-4 are all weather events that caused disruptions to power systems operations when they occurred. All the events drove load higher and, in many cases, also impacted transmission and generation infrastructure. Using the four multiday extreme cold and heat waves events listed in Table TS-4, we compare load to net load, and examine how the distribution of daily average load compares to the distribution of daily average net load, to isolate the impact of increased VRE. In each case, the distributions used for this comparison include the 29 days surrounding the middle of the event (fourteen days on either side and inclusive of the event) for all 7 years of available data. In other words, they are the seasonal distributions and help determine how atypical an individual event is for that time of year. Table TS-5 shows the percentile within the seasonal distribution of load and net load across the full data set for each day of each event for the 2050 plan. In the table, values of 100 or close to that are examples of days with highest load or net load in the data set for that time of year. The full meteorological summary and impact of each event is examined in detail in the appendix.

Table TS-5. Comparison of Daily Average Load and Net Load Percentiles within the Month around the event over the Full 7-Year Data Set for the 2050 Infrastructure Plan

Load percentiles are color coded on a green (low percentile) to yellow (high percentile) gradation.

Interconnect		TI		EI		WI	
Event	Day	Load Percentile	Net load Percentile	Load Percentile	Net load Percentile	Load Percentile	Net load Percentile
Cold Wave	1-Feb	91.8	31.1	69.4	32.7	92.9	58.2
	2-Feb	99.5	81.1	71.9	21.9	98.0	70.4
	3-Feb	100.0	100.0	90.3	57.1	95.4	52.0
	4-Feb	99.0	87.2	82.7	62.2	74.0	4.6
Winter Storms	4-Dec	39.6	51.9	29.2	18.2	79.9	89.9
	5-Dec	81.2	83.8	40.3	46.8	84.2	100.0
	6-Dec	98.7	85.1	61.7	66.9	96.1	90.3
	7-Dec	100.0	100.0	67.5	90.9	91.6	77.3
	8-Dec	96.8	99.4	78.6	94.2	90.9	64.3
	9-Dec	98.1	98.1	91.6	72.7	98.7	49.4
	10-Dec	99.4	94.2	92.2	57.8	96.8	85.7
	11-Dec	97.4	95.5	96.5	70.8	92.9	72.7
	12-Dec	92.9	88.3	96.8	77.9	89.6	76.6
Heat Wave 1	19-Jul	59.5	91.1	97.6	99.4	75.0	13.1
	20-Jul	72.0	32.7	98.8	80.4	65.5	22.6
	21-Jul	85.7	13.1	100.0	95.2	49.4	26.2
	22-Jul	78.6	8.3	99.4	98.8	38.7	25.6
	23-Jul	71.1	5.4	87.5	83.3	13.1	50.0
	24-Jul	60.1	20.8	65.5	94.0	8.9	50.6
	25-Jul	92.3	54.8	81.0	97.0	51.2	28.6
Heat Wave 2	29-Jun	79.9	64.9	98.7	80.5	73.4	55.8
	30-Jun	29.2	55.8	79.2	80.5	34.4	48.7
	1-Jul	6.5	18.8	76.6	76.0	20.1	2.0
	2-Jul	45.5	15.6	96.1	89.0	58.4	57.8
	3-Jul	58.4	19.5	98.7	87.7	59.7	26.0
	4-Jul	38.3	13.6	90.9	66.2	10.4	36.4
	5-Jul	72.7	44.2	99.4	98.1	24.0	65.6
	6-Jul	75.3	68.8	100.0	99.4	42.2	82.5
	7-Jul	39.6	75.3	98.1	92.2	26.0	79.2
	8-Jul	20.8	75.3	76.0	83.8	26.6	76.0

As Finding 1 states, there are exceptions during these events that do lead to elevated net load for a short period. As seen in Table TS-5, the Winter Storms at different points hits the 100th percentile of the seasonal average net load in the TI and WI, and reaches the 94th percentile in the EI. The Cold Wave event in the TI also reaches the 100th percentile of the seasonal average net load. With the exception of December 5 during the Winter Storms event in the WI, the elevated net loads are the same days as the highest load day during the event. This supports the finding that during the extreme weather events of today, VRE is not adding additional resource adequacy concerns. VRE does shift the concerning day during the Winter Storms event in the WI. Load hits the 98th percentile of the seasonal distribution, the highest of the event, 5 days after the peak net load day. But after the peak net load day, the average daily net load drops out of the high end of the seasonal distribution. Operators and planners should be aware that days like these exceptions can occur, but they do not present the extended resource adequacy concerns of other weather events, which will be discussed in Finding 2.

In general, the variable renewables added in these scenarios generate at statistically common levels for the season during the extreme weather events we studied. The largely normal wind and solar availability during extreme weather events are due to the common meteorology of the events. Heat inducing summertime high loads occur on sunny days and wintertime high loads tend to coincide with the arrival of cold air that is brought in by strong winds. This suggests the events that historically caused major disturbances on the power system are not made worse by the growth of wind and solar generation and do not introduce new planning challenges beyond what already exist during normal weather conditions (e.g., the need for wind/solar forecasting, ramping flexibility, etc.). Greater exploration of wind and solar availability can be found in the discussion of Finding 1 the full report, and in each event case study description in the appendix.

Finding 2. Mild weather conditions can produce extended periods of low wind and solar resource. Historically, the weather during these events would not be a reason for concern among system planners and operators, but with the increasing contribution of wind and solar generation, these events need to become a focus of planners in order to ensure system adequacy.

As the penetration of variable renewable generation increases, a new type of "extreme" will become increasingly important to system planners: widespread low wind and solar resource during moderate to high loads leading to extremely high net loads. These very high net load days may not coincide with the summer or winter peak load, which tend to determine generation and transmission capacity needs under the existing prevalent approach to system planning.

We identified four events characterized by periods of high net load driven by moderate to high load and low output from wind and solar generators. These are listed in Table TS-4 as the Winter Net Load 1–3 events and the Summer Net Load event. Table TS-6 shows the percentiles of the load and net load for each day of each event relative to the seasonal distribution (as defined in Finding 1) for the 2050 plan. Load during these events is closer to the middle of the distribution of seasonal loads and therefore more common for the system to encounter. But due to low wind and solar output relative to normal, the net load during the event ends up in the high tail of the seasonal net load distribution, a system state that occurs infrequently.

Table TS-6. Comparison of Daily Average Load Percentile within Month around Date to Daily Average Net Load Percentile within Month around Date over the Full 7-Year Data Set for the 2050 Infrastructure Plan

Load percentiles are color coded on a green (low percentile) to yellow (high percentile) gradation.

Interconnection		TI		EI		WI	
Event	Day	Load Percentile	Net load Percentile	Load Percentile	Net load Percentile	Load Percentile	Net load Percentile
Winter Net Load 1	20-Feb	50.0	73.6	79.7	78	52.2	92.3
	21-Feb	71.4	93.4	89.6	98.9	61.5	90.7
	22-Feb	78.0	91.2	78.0	100.0	51.1	81.9
	23-Feb	50.5	30.8	34.1	96.2	16.5	62.6
	24-Feb	18.7	60.4	21.4	68.1	7.7	16.5
Winter Net Load 2	6-Dec	73.2	78.0	66.1	79.8	60.1	37.5
	7-Dec	75.0	95.2	85.1	100.0	95.8	95.2
	8-Dec	69.0	57.1	81.5	73.8	98.2	97.0
	9-Dec	87.5	75.6	82.1	10.1	100.0	92.9
	10-Dec	95.8	92.9	93.5	32.1	99.4	95.8
	11-Dec	89.3	88.1	98.2	54.2	97.6	94.0
	12-Dec	61.9	84.5	84.5	38.7	78.6	61.3
Winter Net Load 3	2-Feb	73.1	91.2	57.7	98.9	56.6	96.2
	3-Feb	78.0	58.2	51.6	85.2	58.2	97.8
	4-Feb	76.9	96.2	54.9	90.7	51.6	68.7
	5-Feb	56.0	79.1	42.3	55.5	42.3	64.8
	6-Feb	50.5	67.0	28.6	36.3	11.5	85.7
Summer Net Load 4	8-Aug	40.7	15.9	28.0	20.9	3.8	18.1
	9-Aug	81.3	57.7	90.7	96.2	23.6	54.9
	10-Aug	89.6	89.6	96.2	99.5	36.8	45.6
	11-Aug	97.3	98.4	97.3	100.0	40.7	31.3
	12-Aug	91.2	96.2	94.0	95.6	44.5	28.0

For the Winter Net Load 1 and 3 events, neither is noteworthy either meteorologically or from a load perspective: temperatures are not extreme, nor are there storm systems that would otherwise affect electric infrastructure. Winter Net Load 2 does see elevated loads, especially in the WI where the load is above the 95th percentile of the seasonal average daily load distribution for 5 consecutive days. The West Coast experienced very cold temperatures, which drove up load in the WI and is a weather event that would stress the contemporary system. However, the weather and load impacts in the EI and TI were not particularly noteworthy or concerning for today's system. Compared to the Cold Wave and Winter Storms events highlighted with Finding 1, these three events tend to have lower loads but significantly higher net loads.

The Summer Net Load event has 3 consecutive days with this combination of low wind and high load. Unlike cold waves, which are connected to changeable weather by atmospheric dynamics and thus have some synergy with wind generation and diverse solar resource, heat waves are associated with stable, quiescent conditions. Unless triggered by local scale circulations, winds tend to be light, and there is reduced vertical mixing, such that trapped aerosols and haze are prevalent. It is possible that in a larger meteorological data set there may be days where load is as high as the Heat Wave 1 event and which are accompanied by wind resource that is as low, or slightly lower, than in the Summer Net Load event. Because wind is low and net load is occurring after sunset, additional wind and solar capacity would add little additional capability to serve load during the Summer Net Load event without supporting infrastructure, such as storage or responsive demand. As the diversity value of generally high-quality wind is saturated, events like these need increased attention in planning activities and are a motivation for further research.

Finding 3. Because cold waves occur in winter when solar generation is already low, system operations during cold waves is most heavily influenced by the performance of wind generation. Generally, wind generation is abundant as the cold front moves through, but there is uncertainty in the extent of the wind lull that follows the front, both temporally and spatially. The severity of the lull determines the magnitude of the required response from the rest of the system.

Operations during all types of events change due to an increasing contribution from variable renewable generation, but no type of event that we studied changed operations as much as cold waves. Historically, both cold and heat waves impact load magnitude and shape, but the timing and magnitude of the wind and solar resource during a cold wave changes the operations paradigm in important ways, and the impact is specific to the geography and meteorology of each region. Importantly for planners, particularly in the EI and TI, we find that days that follow the initial cold wave may pose resource adequacy risk to the future system. On these days the cold remains, but the air is stagnant, leading to persistent high loads and the risk of low wind generation over a broad area. These dynamics and their impact to future system operations and adequacy are explored in this section and in more detail in the main body of the report.

The Rocky Mountains roughly separate the EI and TI from the WI, and from a meteorological regime perspective, they divide the country. A cold wave moving down the Rocky Mountains will bring wind, quickly followed by falling temperatures, possibly precipitation, and then clearing skies and diminishing wind. The cold air will then either deepen or gradually moderate depending on the balance of nighttime cooling and solar heating, until another disturbance brings in air to replace it.

We studied two different cold wave events with a PCM to understand how operations during those events changes as the penetration of VRE on the system increased:

- The Cold Wave event: A “high-impact” event in early February 2011.
- The Winter Net Load 1 event: a milder “planning-challenges” event in mid-to-late February 2008.

Both cold wave events impacted operations in the EI and TI. The Cold Wave event dropped temperatures across the county, while the Winter Net Load event mostly reduced temperatures in the central and eastern United States.

The difference between the two events in the way the wind resource recedes from its peak makes the 2008 Winter Net Load 1 event particularly challenging for future EI operations, while the resulting net load for the EI during the 2011 Cold Wave event is right at the average net load for that time of year. We simulated how the three different future power system infrastructures (2024, 2036, and 2050) would operate during both cold waves with different levels of wind and solar capacity. The resulting EI dispatch is shown in Figure TS-3. The cold wave hit the system on February 1, 2011, during the Cold Wave event and on February 18, 2008, during the Winter Net Load 1 event, and, in the 2036 and 2050 infrastructures, an increase in total wind generation comes with it. The system responds by reducing the gas-combined cycle (gas-CC) generation. In both events, wind generation decreases as load remains elevated in the days following the initial cold wave. Given the dynamics of cold waves described earlier, the decrease in wind generation is expected in both events. However, the amount of decrease differs between the two.

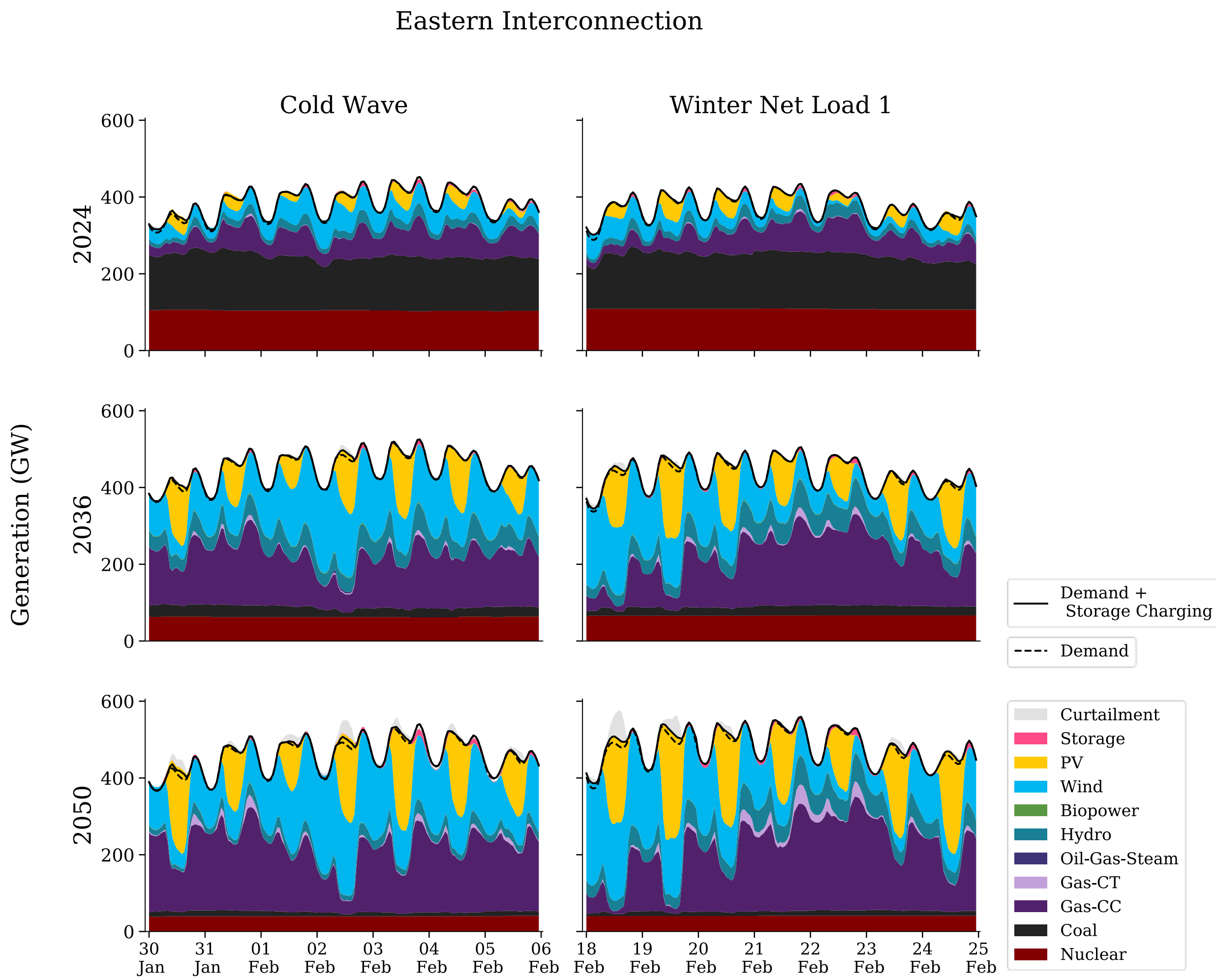

Figure TS-3. Generation dispatch for the EI during the February 2011 Cold Wave event (left column) and the February 2008 cold wave, or High Net Load 1 event (right column)

Both cold waves were simulated with three future infrastructure years: 2024 (top), 2036 (middle), and 2050 (bottom).

In the Cold Wave event in 2011, Upper Midwest wind generation remains above average, which limits the need for a large ramp back up of the gas fleet. Transmission to export the Upper Midwest wind generation also serves as an enabling technology to avoid the need for significant dispatchable capacity increases in the following days. Figure TS-4 shows the net interchange of power between MISO and its neighbors during the 2011 event. In 2024, the net interchange is not highly impacted by the changing wind generation. However, in both 2036 and 2050, when there is a higher wind penetration and an increase in transmission capacity, exports from MISO to PJM are more substantial. As wind generation in other parts of the EI decreases on the evening of February 2, MISO goes from importing 7 GW of power from PJM to exporting more than 15 GW to PJM in a matter of 24 hours. Exports to PJM quickly decrease from the peak, but MISO remains a net exporter to PJM for the next 2 days before the cold subsides.

In contrast, the milder cold wave during the Winter Net Load 1 event in 2008 does not have excess wind generation in any part of the EI. The 2008 cold wave requires more dispatchable generation to come online, including an extended period of gas-combustion turbine (gas-CT) generation from the evening of February 20 through the evening of February 22. Typically, gas-

CT capacity is used as a peaking unit, coming online for just a few hours before shutting back down. However, as the wind generation dies down but the cold persists in 2008, available thermal capacity is tight enough that these gas-CTs need to stay on longer, with some staying on for about 36 hours.

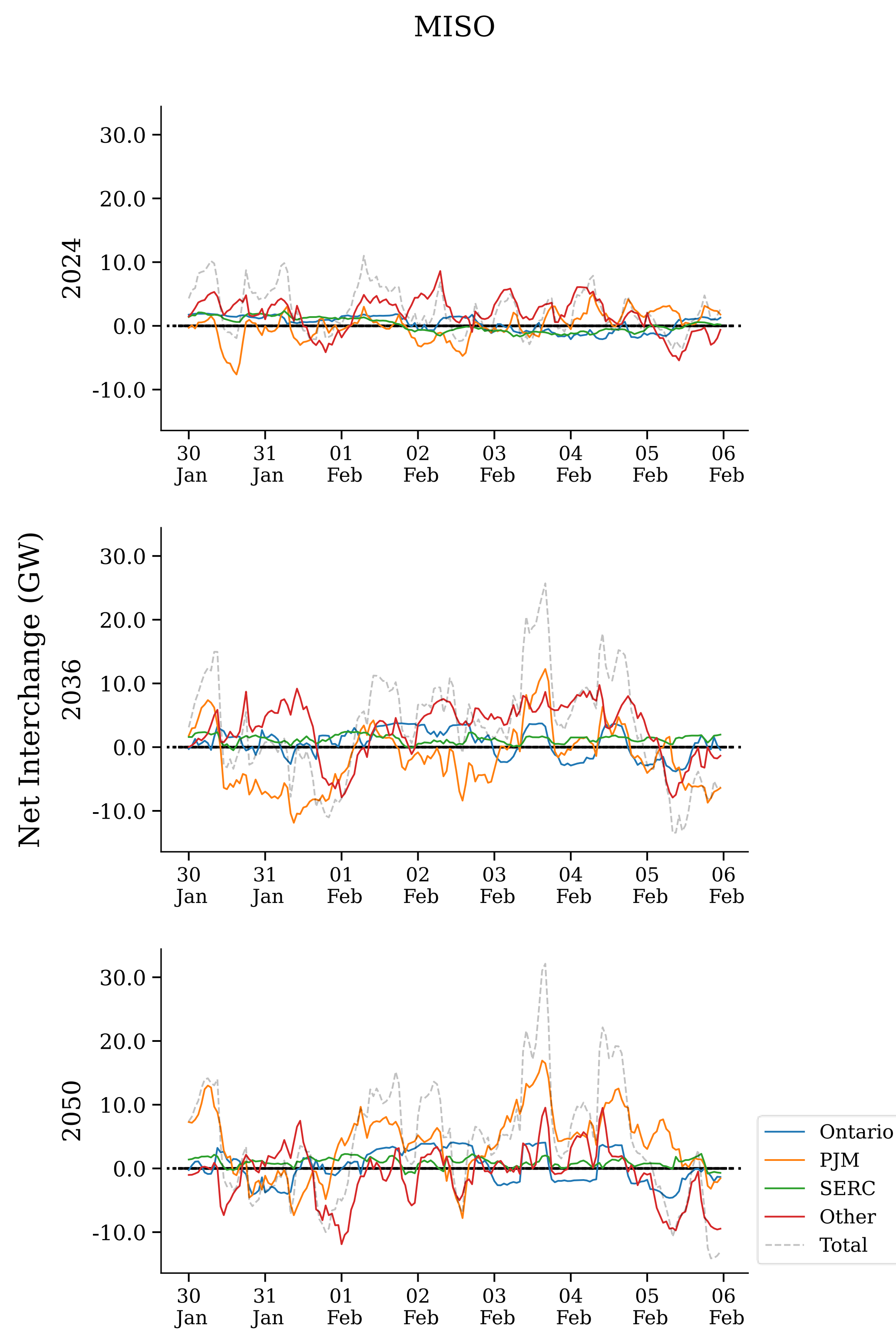

Figure TS-4. Net power flow between MISO and its neighbors during the February 2011 Cold Wave event

Positive flow means an export from MISO to its neighbor.

The limited sample size of weather events (2007–2013) we explored in this study suggests cold waves are among the weather events with the largest impact on system operations as the system utilizes more VRE. This is predominately because of wind generation dynamics driven by the cold waves. Initially, the front that brings cold temperatures also brings high wind resource. In the two cold waves we studied, this means wind generation ramps up at the same time as load increases. However, as the front moves through, but temperatures remain cold, the wind generation tends to decrease, requiring a response from the system. In some cases, such as the 2011 Cold Wave event in the EI, there is enough geographic diversity in the wind and solar resource and utilizable transmission capacity to trade the available VRE over long distances. In contrast, the 2008 Winter Net Load 1 event had a widespread negative impact on the wind resource throughout the EI and necessitated a large ramp-up of the thermal capacity. Two days during the Winter Net Load 1 event are among the highest net load days in the entire data set for the EI. This suggests the days following the onset of a cold wave may be among the most important for planners to consider when determining capacity needs for future systems that rely on high levels of VRE. Our results also suggest the days following milder cold waves may be the most concerning, but additional research on a larger sample size of cold waves is required to more fully explore these milder events.

Finding 4. Increased PV capacity drives system operational changes during summer months and this does not change during heat waves. The contribution from wind after sunset differentiates the level of system operation stress caused from one heat wave to another.

Heat waves drive the highest load days in most regions in the conterminous United States (CONUS); they send temperatures climbing and consequentially electric load also. Day-to-day operations in heat waves are largely the same, but the wind generation contribution to peak net load is the major driver of system operations and resource adequacy stress. The magnitude and shape of the solar generation profile is largely the same from one day to the next, and the rest of the system ramps and cycles on and off to utilize as much solar generation as possible in the middle of the day. This causes major differences in the system dispatch as the solar PV capacity increases from 2024 to 2036 to 2050, as can be seen in Figure TS-5. However, this is not unique to heat waves and constitutes typical operations, especially during summer months, in high VRE systems. What distinguishes system stress between heat waves is the contribution from wind generation after the sunset when solar PV does not contribute to resource adequacy.

We analyzed two distinct heat waves, a record-breaking heat wave in July 2011, Heat Wave 1, that had average wind generation, and a moderate heat wave in August 2010, Summer Net Load, that mostly impacted the EI and had below-average wind generation. For both heat wave events, we modeled system operations for the 2024, 2036, and 2050 infrastructures. Figure TS-5 shows the EI generation dispatch during the heat wave in July 2011 on the left and the moderate heat wave in August 2010 on the right. In both events, daily operations are largely the same and evolve similarly as the wind and solar penetration increases. As noted earlier, during these heat wave events the shape of wind and solar generation are largely consistent day-to-day. The two resources are largely anticorrelated; solar generation maxes out in the middle of the day when wind generation is very low, and wind picks up in the evening as the sun is setting and the solar generation ramps down. However, in the EI, the wind evening ramp only fills in a fraction of the solar generation peak, from earlier in the day. The major difference between the two heat waves is the amount of capacity needed at the net load peak, which depends on the coincidence of the heat wave with reduced wind generation.

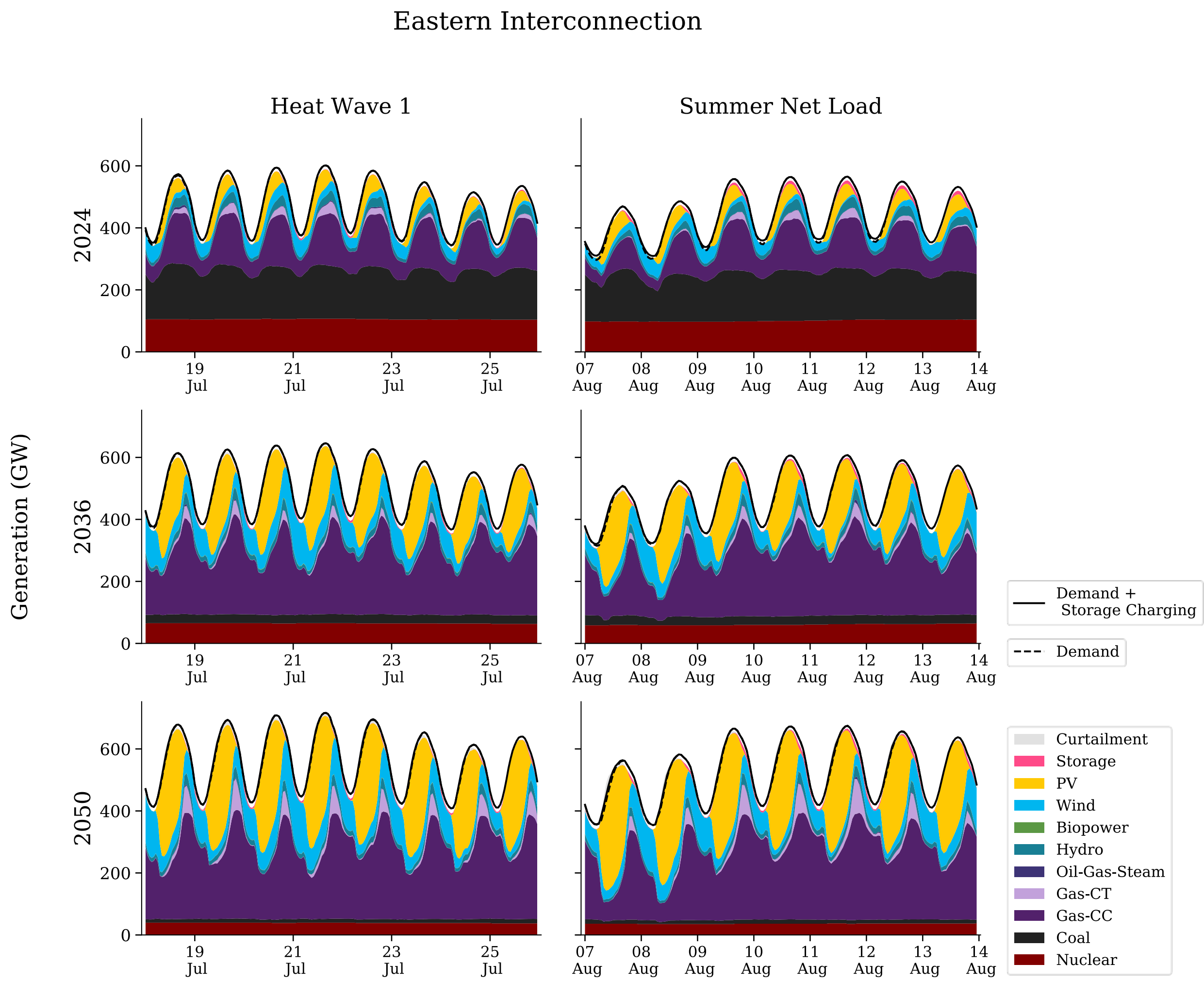

Figure TS-5. Generation dispatch for the EI during the Heat Wave 1 (left column) and the Summer Net Load (right column)

While the day-to-day operations during each heat wave look largely the same, the self-reliance of regions within the EI differ. As an example, Figure TS-6 shows the net exports between MISO and its neighbors. During both heat waves, net exports are more dynamic with increased wind and solar penetration. Net exports in 2024 are relatively stable, rarely changing much hour-to-hour. In both 2036 and 2050, net exports change rapidly, largely following when solar generation increases and decreases throughout the EI. The 2036 average hourly rate of change of MISO's net exports is 53% and 90% higher than the 2024 rate of change in Heat Wave 1 and Summer Net Load events, respectively. The analogous values for 2050 are 100% and 133% higher. In both heat waves and in all infrastructures, MISO is a net importer, though in 2050 there are hours every day where MISO is a net exporter. However, during the Summer Net Load heat wave, which had less impact on total load but unseasonably low wind generation, MISO relied more heavily on imports. On average, hourly MISO net imports were 2,100 MW and 1,600 MW higher in 2036 and 2050, respectively, during the Summer Net Load event than during Heat Wave 1.

In summary, the heat waves we studied had little to no impact on PV generation, but they do impact total wind generation.[11] Increasing PV capacity, and thus generation, on a system can have a large impact on system operations, pushing more thermal and hydropower generation toward a narrower net load peak. On average, wind generation is at its lowest in the summer, but, on an interconnection-wide scale and accounting for transmission constraints, wind plays a critical role providing resource adequacy to the 2036 and 2050 infrastructure plans as it reliably increases its generation in the evening as solar generation decreases. For the specific heat waves examined, events associated with extreme heat and high electricity demand did not lead to lower than normal wind generation potential. However, more moderate heat waves could severely depress wind generation, especially during the key net load peak in the evening. However, based on the weather years of 2007–2013, the most pressing events for planners and operators to ensure sufficient capacity at the net load peak appear to be moderate heat waves, such as the Summer Net Load event, that are accompanied by persistent high pressure and very low wind generation.

[11] A key limitation to our investigation of heat waves is we did not include the impact of coincident large-scale wildfires that could have severe impact on solar PV generation potential.

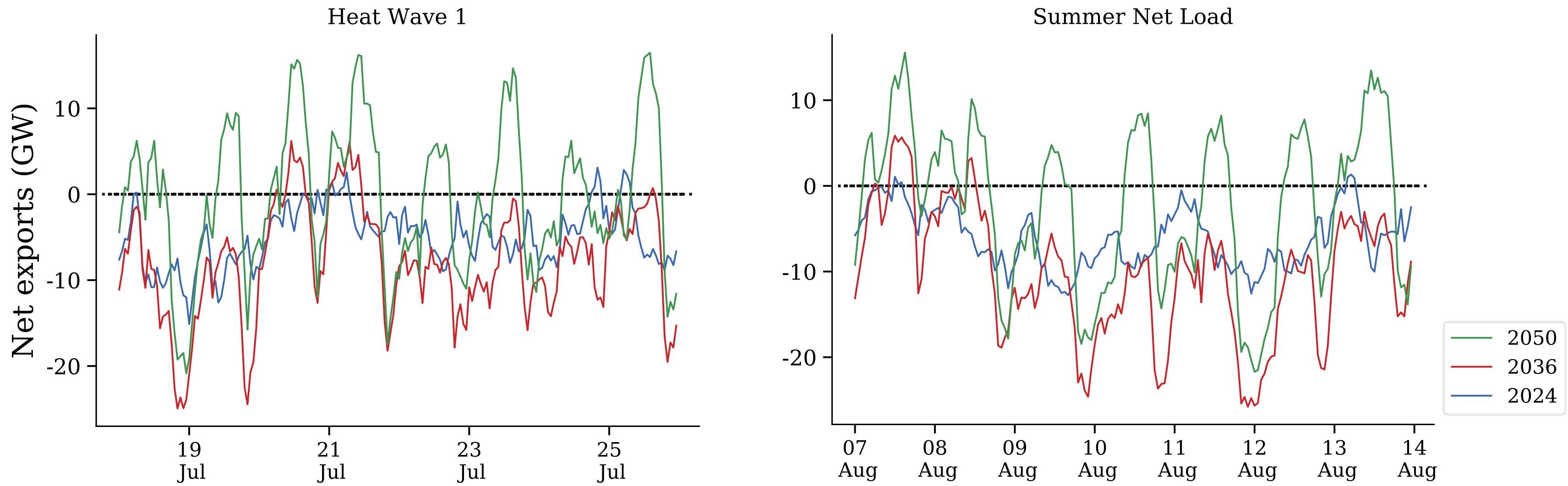

Figure TS-6. Net exports between MISO and its neighbors during the July 2011 Heat Wave 1 (left) and August 2010 Summer Net Load (right) heat waves for the three infrastructure plans 2024 (blue), 2036 (red), and 2050 (green)

Positive net export means MISO is exporting more power to its neighbors than importing.

Finding 5. Understanding the characteristics and diversity of wind and solar resources—at small and large geographic scales—is key to assessing their contribution to resource adequacy. Operating existing and expanded transmission more flexibly than today enables that contribution.

Several of the weather events we explored include periods of low wind and solar output. Even in these circumstances, these variable resources can still contribute to resource adequacy through the application of interregional coordination and system flexibility. Two events that feature extremely high net loads, one in the summer and one in the winter, demonstrate how careful planning and an understanding of the regional diversity of wind and solar resource can enable reliable operations without the need to overbuild generation, from the ability to trade power through the transmission system.

The first example involves the wind and solar resource in SPP during the Summer Net Load event in early to mid-August 2010. On August 10 and August 11, 2010, the EI experiences nearly the highest net load days within the data set because of the very low wind generation throughout the interconnection. During the daytime hours on August 10 and August 11, the fleetwide capacity factor of wind in the EI falls to 5% and 4%, respectively. For much of the Summer Net Load event, SPP relies on its transmission infrastructure to import power. SPP also taps into nearly all its thermal capacity in the evening hours after sunset. The left plot of Figure TS-7 shows the offline available thermal capacity (i.e., thermal capacity that is not committed and not on a planned or forced outage) in SPP throughout the event. In the 2036 and 2050 infrastructure plans, at 8 p.m. EST on August 11, there is nearly no offline thermal capacity available in SPP. At this time, imports from MISO have dropped to zero from a high of 9 GW a few hours earlier, as seen in the right plot. SPP is on its own, PV generation is quickly ramping down as the sun sets, and SPP lacks additional available thermal capacity. However, wind begins to ramp back up; at 8 p.m. EST, SPP's wind has a combined capacity factor of 22%, up from 5% only 6 hours earlier. During this event, SPP's wind follows a typical pattern for wind generation in the EI, picking up in the evening and overnight. This is not the case for MISO where wind reaches a maximum fleetwide capacity factor of only 9% overnight, while SPP reaches 58% in the early morning hours of August 12. SPP's wind recovers enough that it can turn thermal units off and export power to MISO.

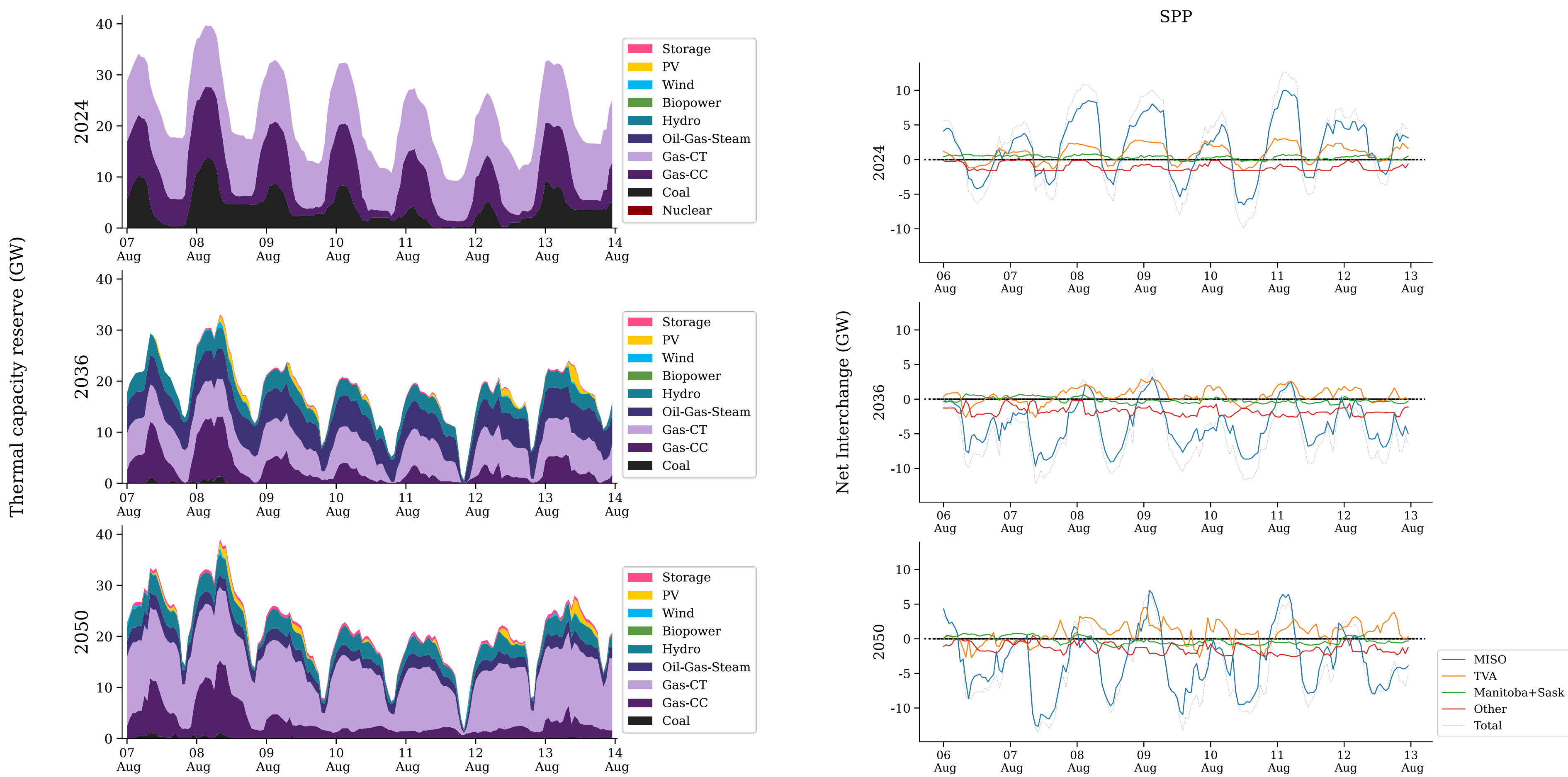

Figure TS-7. Offline thermal capacity reserve in SPP (left column) and net power flow between SPP and its neighbors (right column) during the Summer Net Load event

Positive flow means an export from SPP to its neighbor.

February 21–23, 2008 during the Winter Net Load 1 event is another example where the geographic diversity of VRE boosted its contribution to resource adequacy even though the overall and local wind and solar resource was low. During this period, the EI experienced cold temperatures that elevated load above normal. At the same time, stagnant air steadily reduced the wind generation output by more than 90%, hitting an extreme low output for the full data set on February 23. In addition, winter storm systems reduced PV output in the Southeast and in MISO on February 21, before extending into PJM the next day.

Figure TS-8 shows the trading between the three regions, which generally becomes more dynamic with higher wind and solar penetrations. The trading pattern on February 22, at the height of the net load in the interconnection, highlights the use of transmission to capture the potential of the diverse PV resource. Particularly in 2050, the interchange between PJM and the NYISO has a strong diurnal pattern throughout the week. PJM exports more power to NYISO when PV output is high in the interconnection. This happens even on August 22, when PJM PV output is low. These exports are actually coming from the FRCC and MISO with power wheeled through the SERC and PJM to get to NYISO. Without the transmission capacity, expanded in 2036 and 2050 as summarized in Table TS-2, and institutions in place to dynamically trade between regions, the interconnection would be unable to take advantage of the geographic diversity of the PV output.

In these types of events, trading power with neighboring regions in both directions and taking advantage of VRE subject to diverse weather conditions is critical to maintaining resource adequacy while keeping capacity reserve margins, and therefore system costs, lower. Understanding the behavior of the wind and solar resource based on generation profiles for multiple weather years, ensuring that transmission infrastructure exists to take advantage of the geographic diversity of the resource, and use of planning and operations models that capture the full geographic scale of the power system are all critical for enabling this trading capability.

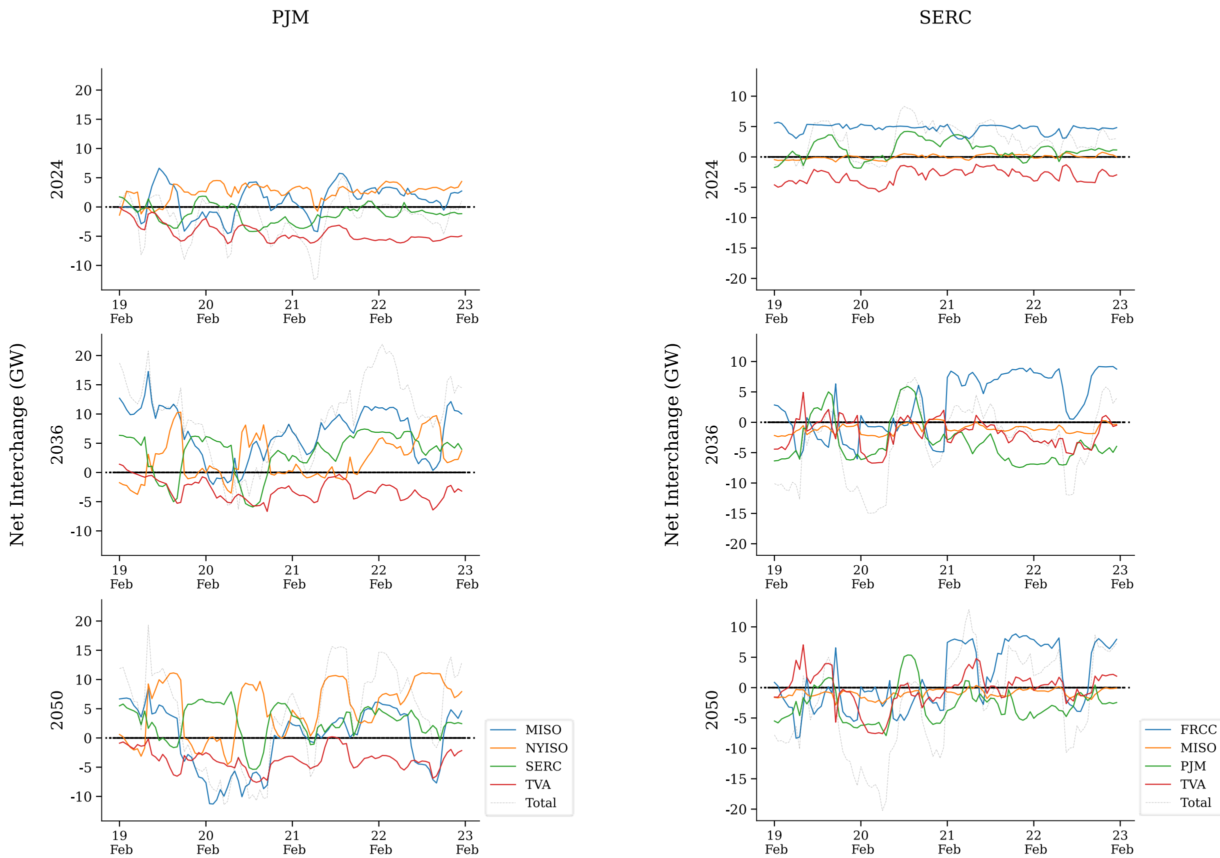

Figure TS-8. Net power flow between PJM (left) and the Southeast (right) and their respective neighbors for three future infrastructure plans, 2024 (top), 2036 (middle), and 2050 (bottom), during the High Net Load 1 event in February 2008

Positive flow means an export from PJM/Southeast to its neighbor

Finding 6. In areas where hydropower is abundant, its availability and flexibility are key to mitigating system stress during extreme weather events.

Hydropower provides valuable flexibility for the WI when water availability allows it. The way this flexibility is best used changes as the penetration of wind and solar increases. Rather than strictly following the load profile, hydropower is most valuable to the power system when used to follow net load (Brinkman et al. 2021; Bloom et al. 2016), which often means operating more as a peaking unit (i.e., ramping up quickly for a few hours after sunset before ramping back down). However, several factors impact whether hydropower can achieve this new behavior. These factors include whether it is a wet, dry, or normal hydropower year or season; and whether other water regulations and policies limit how much and when water stored in the reservoirs of dispatchable hydropower units (i.e., has a reservoir for water storage) can be used for generation.

To more fully understand hydropower's value to the WI, we simulated system operations under different hydropower availability and flexibility assumptions. These sensitives were only run on the 2050 system, and we focused the hydropower sensitivities on two weather events: a set of winter storms in December 2013 (the Winter Storms event) and the Lowest Net Load event April 2011. Availability assumptions focused on wetter and dryer conditions than what were actually experienced, but they were still plausible conditions for the time of year. The Inflexible Hydro sensitivity forced all dispatchable hydropower units to allocate their monthly or weekly hydropower water budgets equally for all hours and days. In other words, the dispatchable hydropower in the system was forced to operate at a constant output for the entire month, as determined by water availability. This assumption reflects that power is one of the last uses of a dam's water to be considered for many units, which limits the flexibility they might otherwise provide to the power system. Many hydropower units are at risk of losing this type of flexibility as they go through the relicensing process.

Figure TS-9 shows that inflexible hydropower leads to increased natural gas combined cycle (gas-CC) generation in the Lowest Net Load event. Curtailment of wind and solar generation also increases, by 6%. Similarly, dry hydropower conditions reduce total hydropower output, which is mostly met by gas-CC generation. However, dry hydropower conditions also lead to a 10% decrease in wind and solar curtailment. The reduced curtailment is due to dry hydropower conditions offering more flexibility to the dispatchable hydropower fleet in the WI.

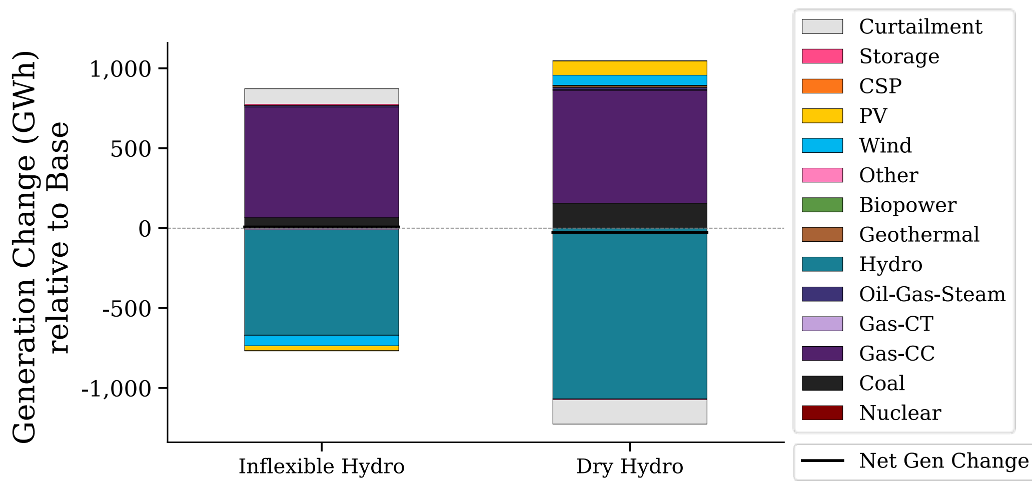

Figure TS-9. Change in total WI generation by type for different hydropower flexibility and availability assumptions during the April 2011 Lowest Net Load event, modeled with 2050 infrastructure

Figure TS-10 shows the change in generation by type for dry and wet hydropower conditions and inflexible hydropower operations during the December 2013 Winter Storms event, which affected much of the CONUS. Availability of hydropower had little impact during this event. Hydropower availability and variability is lower in December than in other months; a dry December does not look that different from a wet December. Inflexible hydropower, however, has a large impact on operations. Total hydropower generation during the Winter Storms event, specifically December 6–13, 2013, was 12% lower relative to base hydropower scenario conditions under the 2050 infrastructure plan. The event had higher net load than the rest of the month, and the base system's hydropower allocated more of December's hydropower generation to this event. Inability to shift more water for hydropower generation to the days of the Winter Storms event would impact the WI, leading to a large increase in peaker gas-CT usage (up 20%) and even imports from the EI. The 2050 plan modeled here does increase transfer capacity between the EI and WI.

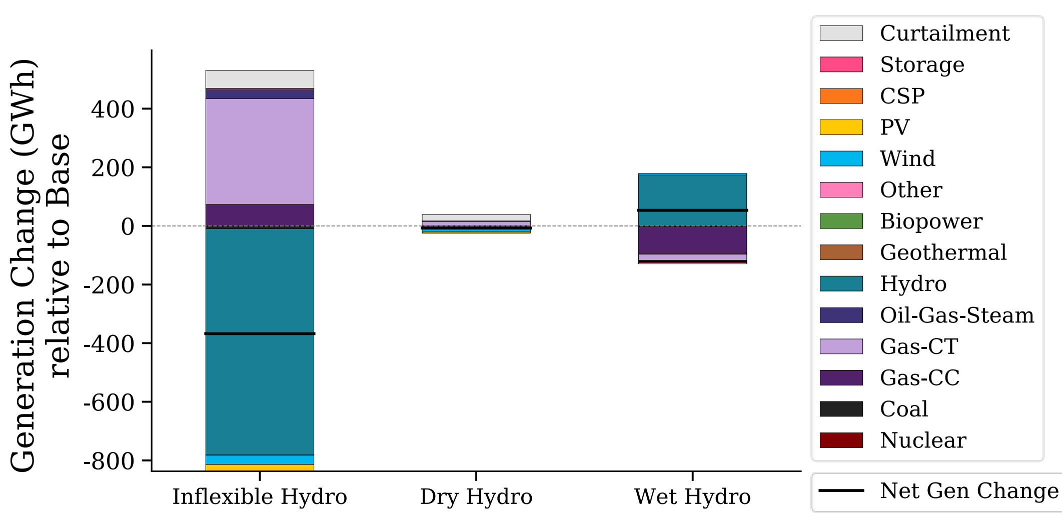

Figure TS-10. Change in total WI generation by type for different hydropower flexibility and availability assumptions during the 2013 Winter Storms event

As stated earlier, water availability and flexibility to shift when water is used impact whether hydropower can achieve the change in operations to support higher VRE penetration systems. In the Lowest Net Load event, dry hydropower led to less generation at peak, but hydropower was still shaped, subject to operational and regulatory constraints, to provide as much power as possible at the peak net load hours. While our modeling partially captured the coincident weather affecting hydropower availability and wind and solar generation, more research using a weather data set that considers weather variability over a longer multiyear period is needed to more fully understand the correlation between hydropower, wind, and solar. Even more important than availability of water to hydropower's ability to provide value and resilience during key weather events is how much flexibility a hydropower unit has to shift energy day-to-day and hour-to-hour. The modeled inflexibility is costly to the WI as the modeled system is unable to focus hydropower's water use to the events or hours of the event where it is most valued. Further research is needed to understand which is of higher value—shifting energy day-to-day or hour-to-hour—and how the type of event affects the value.

Finding 7. Broad, interconnection-wide impacts from wind turbine blade icing and cold temperature shutdowns are rare. However, regional icing and cold temperature events can be significant and rely on local gas generation dispatch and interregional transmission flows to maintain adequate supply to meet demand.

Two events—the December 2013 Winter Storms event and the February 2010 low VRE event (High Net Load 3 event in Table 44), were investigated for the impact of wind turbine blade icing and low temperature shutdowns on 2050 system operations. Blade icing and low temperature shutdowns led to a 7% (3.5 GWh) and 10% (2.7 GWh) decreases in total wind generation for the December 2013 Winter Storms and the February 2010 Winter Net Load 3 events, respectively. In both cases the differences are made up almost entirely by the gas fleet: both gas-CCs and gas-CTs. This finding highlights the importance of planning for potential icing and cold temperature cut-outs in forecasting along with anticipating the increased forced outage rates of thermal units, in order to ensure needed capacity is available. Options for reducing icing and cold-related derates through turbine cold weather packages can also be considered.

While system-wide icing does not lead to significant reductions in the wind generation, local impacts can be large for long periods of time. Figure TS-11 shows the wind generation reduction in Minnesota and Wisconsin due to icing and low temperature shutdowns during the Winter Net Load 3 event. Starting late on February 3 and lasting until midday on February 4, the two-state region experiences a large icing event that reduces wind output. At the height of the event, wind output is reduced by 7,500 MW, about a 75% decrease relative to base conditions for the 2050 infrastructure plan. The resulting gap is initially met by turning on quick start gas-CTs, but as the icing event continues and worsens, gas-CCs are also turned on. The region also reduces its exports to the Chicago area of PJM, meaning that region also must allocate other forms of generation to meet its load during this time.

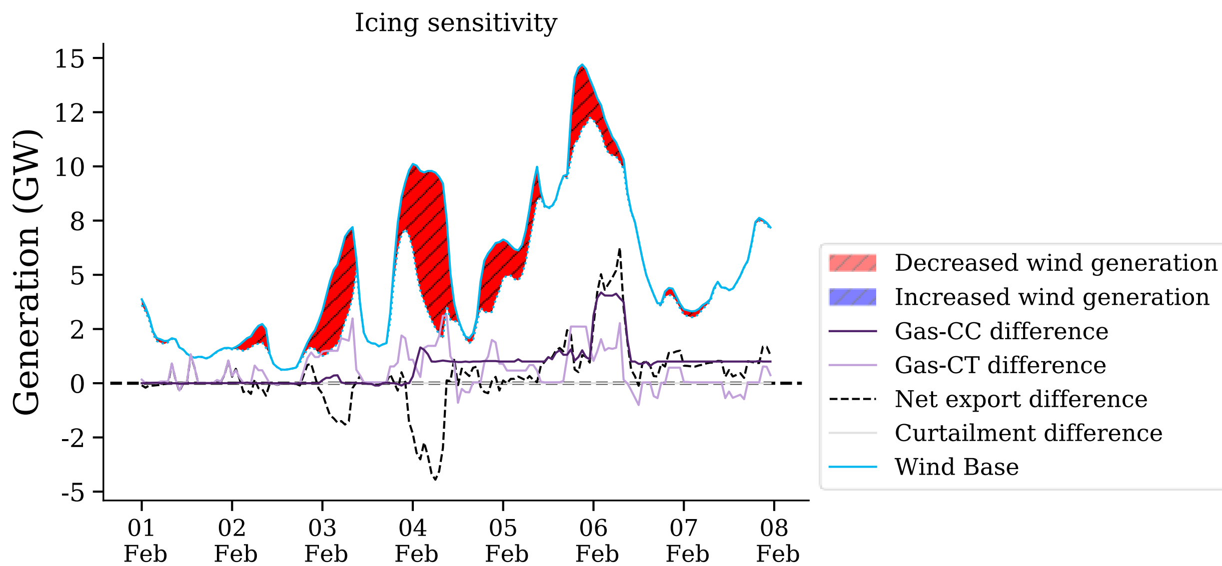

Figure TS-11. Icing and cold temperature cut-out impact on wind generation in Minnesota and Wisconsin for the Winter Net Load 3 event for the 2050 infrastructure plan

The differences in gas-CC and gas-CT generation, curtailment of VRE, and net interchange between Minnesota and Wisconsin and their neighbors are also shown. The differences are between a base conditions run and one that considered icing and cold temperature cut-outs.

System operators respond to system-wide and local icing and low temperature shutdown events by turning on gas units and utilizing transmission flexibility; however, gas units have historically tended to be forced out more frequently at cold temperatures than at moderate temperatures (Murphy, Sowell, and Apt 2019). Figure TS-12 shows the thermal forced outages during the December 2013 Winter Storms event. As the event progresses, a greater share of gas-CTs and gas-CCs begin to be forced offline, and at peak outage, about 10% of gas units are out in MISO. Enough reserve capacity is available during the event to withstand both the reduced wind output from icing and low temperature shutdowns, and the increased gas outages. However, having this extra capacity to ensure adequacy comes at a cost.

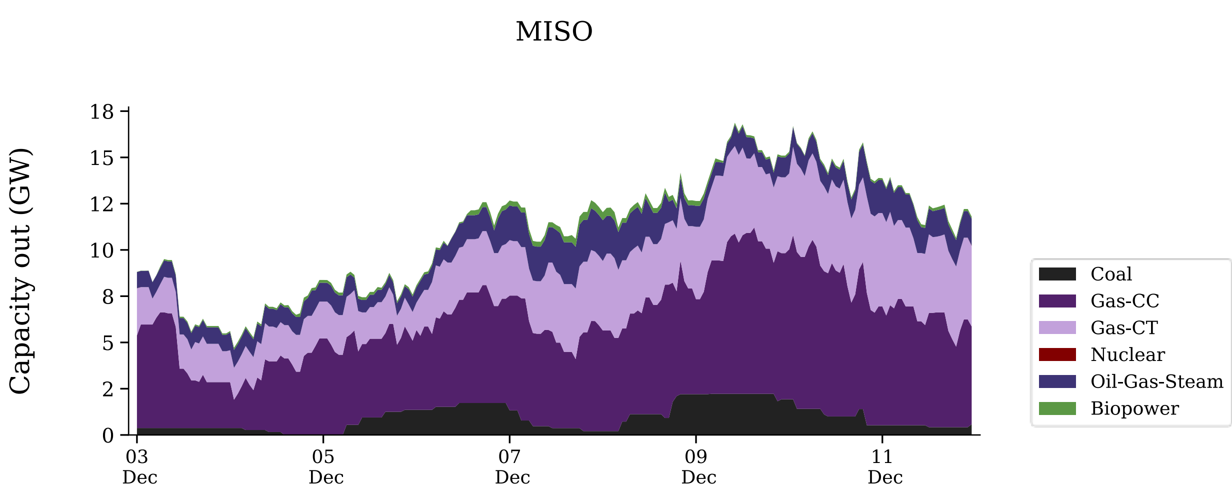

Figure TS-12. Total thermal capacity on an outage (forced or planned) in MISO during the December 2013 Winter Storms event for the 2050 infrastructure

Ability to forecast icing and cold temperature events and coordinate operations across regions will be key to determining the extent to which these events are a resource adequacy concern. In our modeling of the 2050 system, the cold or icing events were limited to reducing total wind generation in the EI by 10%. Though this is a significant reduction, it is not enough to force the event into the tail of the wind resource availability distribution. However, our modeling shows local icing and cold temperature cutoffs do reach more concerning levels during these events. Our results suggest, with proper coordination with neighboring system and usage of available gas dispatch, which also is derated due to cold weather in our modeling, such events can be managed We did not investigate the ability to forecasts these types of wind generation derates, which should be a focus of future research.

Finding 8. Tropical storm impact on renewable resource availability is localized and of less impact than direct damage to generation, transmission, and distribution infrastructure.

Tropical storms and hurricanes can significantly impact the power sector. However, these storms primarily impact local transmission and distribution infrastructure, and the extent of the impact is small compared to both the size of the electrical system and the larger pressure systems that drive the extreme temperature events. For the tropical storms and hurricanes we investigated, outside the band of damaging wind speeds, their impact on wind and solar generation is primarily through the broad extent of cloud cover and net increase in wind resource, even when accounting for the cut-out windspeed for the typical wind turbine.

While tropical storms and hurricanes may be much more concerning for island systems, the impact on renewable resource availability is minimal for CONUS. We examined Hurricane Maria because it tracked up the East Coast and was found to have slightly beneficial impact on wind generation. However, there is a chance that a powerful Category 4 or 5 hurricane tracking through a dense area of offshore wind along the East Coast or through the Gulf of Mexico could have a major impact if it caused major infrastructure loss. Such an evaluation was outside the scope of this study and should be considered in future work.

Conclusions

In this report, we present a first of its kind analysis investigating how various weather events could impact U.S. power system operations when wind and solar are large contributors to the energy mix. Using case study weather events from 2007 to 2013, we found that this power system transition does not lead to new operational or resource adequacy concerns during the high-impact weather events during the period studied (e.g., extreme cold waves, extreme heat waves, and midlatitude storms). Wind and solar generators are generally available during these events. However, weather events that were not particularly concerning historically, and tend to be milder versions of the high-impact events, can lead to large and extended periods of wind and solar deficits. Often the low wind and solar generation can be well-forecasted on weekly and daily timescales and therefore well-represented in operational forecasts used by system operators to commit and dispatch generation resources. However, these types of events are often not fully considered in resource adequacy studies used by planners to ensure enough generation and transmission resources exist to serve load during these periods.

Cold waves, both extreme and mild, present a new dynamic for system operators to be aware of. In the EI and TI, wind generation potential tends to be high as the initial front of the cold wave sweeps across these interconnections, but then decreases in the days that follow even as temperatures remain cold. The extent, both temporally and spatially, of this wind generation lull will differentiate between cold waves that cause resource adequacy concerns for operators and planners and those that do not. Based on the historical weather data set of 2007–2013, milder cold waves may have more severe lulls, presenting new weather conditions that can pose challenges to resource adequacy. Wind turbine blade icing and cold temperature shutdowns also introduce risk during cold waves, however, their impact tends to be local, while their interconnection-wide impact is less severe than the low wind generation caused by reduced wind speeds that can come after the initial cold front. Solar generation is lower in the wintertime, but winter precipitation and cloud cover can reduce solar generation even further. However, in the case study events we investigated, this impact tended to be spatially limited.

The resource adequacy risk of heat waves also evolves with greater penetrations of VRE. During heat waves, net load and resource adequacy risk tends to be highest after sunset when solar PV generation has gone to zero. During the record-breaking heat waves within in our data set, there was enough wind generation potential to reduce the system stress at the daily net load peak. However, more mild heat waves that are associated with broad-scale high pressure systems can lead to low wind generation potential in the evening and create higher net load periods than the record-breaking heat waves of the past. A key limitation to our investigation of heat waves is that we did not include the impact of coincident large-scale wildfires that could have severe impact on solar PV generation potential. Given the wildfires and associated blackouts in California in the late summer of 2020, we suggest further research on how wildfires may change future system operations during heat waves.

For both cold and heat waves, a geographically diverse wind and solar fleet enabled by expanded and flexible transmission reduces regional resource adequacy risks, even when the negative impact to the wind and solar resource is widespread. Also, in regions with large contributions from hydropower, the flexible operations of those units reduce the operations cost and resource adequacy concerns associated with the weather events we studied. Other enabling technologies, such as storage of different durations, responsive demand, as well as offshore wind generation, can also be considered for their weather resilience contribution in future work.

For this report, we used case study weather events to provide initial insights on the evolving role of weather events to U.S power system planning and operations. The events and associated data may be useful to system planners, policy makers, and researchers to test the weather resilience and resource adequacy of future power system infrastructure. The events could be used to test the performance of integrated resource plans or to explore tradeoffs between different policy options. This report also describes a methodology for identifying additional events relevant to different regions or from additional weather years.

We also identify several areas where further research is required. Most importantly, there is a need to better understand the frequency of the concerning events we identified in our limited 7-year data set. This would require the creation of wind, solar, hydropower, and load data sets for a longer historical period, as well as those that capture the potential prospective effects of climate change. Climate change may vary the frequency and magnitude of the weather events we studied or introduce new types of weather events not explored in this work. Using the expanded data sets, future work should also explore new methods to statistically quantify risks to system operations presented by these weather events by pairing PCM with other resource adequacy models and tools, while exploring a greater number of infrastructure plans that investigate higher penetrations of VRE and 100% clean electricity systems.

Table of Contents

List of Figures

List of Tables

Introduction

As weather-dependent renewable generation grows, it is important for power system planning to understand the broad trends and correlations between weather, renewable resources, and load. The traditional planning, performed by utilities and system operators, includes the study of system resource adequacy during peak load periods in the summer and winter to ensure the generation and transmission system is appropriate to meet load. But in a power grid with a high penetration of variable renewable energy (i.e., wind and solar), periods of high risk to system resource adequacy may no longer correspond only to hours of peak load. In particular, high shares of variable renewable energy, even when well-forecasted to inform system operations, can further complicate the stress extreme weather events already place on the grid. They also may lead to changes to the types of weather conditions that are most problematic to system operations and resource adequacy due to widespread and extended deficits of wind and solar generation. Accordingly, the focus of reliability assessments in long-term planning studies may need to evolve in the coming years to more fully incorporate weather events that lead to these deficits. This report seeks to identify these new weather events and understand the characteristics of the events that lead to system risk of future systems with higher penetrations variable renewable energy.

Historically, weather that stresses grid resilience typically does so by creating peak loads across a broad region while increasing the likelihood of transmission and generation outages (Murphy, Sowell, and Apt 2019; Allen-Dumas, KC, and Cunliff 2019). Two examples of such stresses are cold snap events like the cold waves that followed the disruption of the polar vortex in January 2014 (NERC 2014) or the 2021 winter storms in Texas and extreme heat events, such as what the Southwest experienced in June 2017 or the combination of wildfires and heat in California in August 2020. The January 2014 extreme cold weather event, which is colloquially known as a polar vortex event, saw record low temperatures extending from the northern tier states all the way to the Gulf Coast, which led to extreme heating loads and the forced outage of conventional generators in states where generating plants were ill-equipped to deal with temperatures well-below freezing. During the February 2021 cold wave that led to large-scale load shedding in Texas, peak load, gas outages, and low wind output all exceeded even the most extreme values used in ERCOT's winter planning[12]. Similarly, extreme heat events, such as the 2020 historic West-wide heat wave in August and September, created a spike in air conditioning load while reducing transmission and generation capacity. In addition, especially organized convection that covers a broad area that create extreme weather (e.g., hurricanes, tornados, thunderstorms, etc.), and winter storms can significantly impact transmission and distribution grids. Also, the increase in wind and solar penetration has exposed the system to new and unforeseen stressors, such as the wind turbine low temperature shutdowns that occurred throughout the MISO footprint during an intense cold wave in January 2019 (Rose 2019).

At high renewable energy penetrations, weather events that are important to the electric system will not just be those producing extreme loads and stressing traditional generators but will also include those that produce a large surplus or deficit in renewable energy resource availability. A number of recent studies in Europe (Bloomfield, Suitters, and Drew 2020; Li et al. 2020) and the U.S. (Handshcy, Rose, and Apt 2016; Cole, Greer, and Lamb 2020) have investigated the

[12] http://www.ercot.com/content/wcm/key_documents_lists/225373/2.2_REVISED_ERCOT_Presentation.pdf

weather events and frequency of these events that may pose supply deficits in a high renewable energy system. In addition to the evolving nature of weather risks to the electric system that will come from increased amounts of variable renewable energy (VRE), climate change is also changing the nature of weather risk, and its impact will be amplified and compounded by the energy transition. This topic is not the focus of this research. However, this is an important topic that we hope to address in future work, and the reader will find some references in the taxonomy section below to ways climate change may impact the weather events described.

The central research questions we investigate in this report are whether increasing levels of wind and solar generation make it more challenging to reliably operate the power system during extreme weather events and whether that increase changes which events would be considered extreme, due to large impacts to power system operations. To address these questions, we used a high-resolution data sets of historical load, weather, wind, and solar resources for 2007–2013, identified periods of extreme weather events, and then modeled grid operations during those same events under high wind and solar future systems. Twelve events were selected for detailed modeling, and while this is not a large enough sample size or period to robustly determine the future likelihood of recurrence and risk, it allows an original assessment at how potential weather impacts will change as penetration increases.

In this report, we (1) review categories of weather events and their impact on power sector operations and planning; (2) describe the development of future power sector infrastructures, methods used to identify events of interest, the power sector operational modeling approaches used to evaluate each event; and (3) explore eight common findings from the data sets and modeling as they relate to power sector planning and operations. The appendix contains a detailed description of each event, including salient meteorological features, specific impacts on load and net load, wind and solar generation, and analysis of production cost modeling results for a subset of the events.

Taxonomy of Extreme Weather Events

In this section, we categorize extreme weather events into common meteorological aspects and impacts to the power sector, focusing on impacts to load, wind and solar generation, and other electric infrastructure. The first category contains high-impact events, which we define as extreme weather events that had a profound societal impact at the time they occurred, including stress to the electric system. Examples of the type of events that fit this category are extreme cold along with winter precipitation, heat waves, bomb cyclones, and hurricanes. The second category is events that present challenges to planning for high VRE (i.e., wind and solar generation) systems. These are events with abnormal wind or solar resources, typically coincidental with high demand. In future high-penetration scenarios, these can result in high net load (i.e., load minus available renewable generation) or negative net load (i.e., large amounts of curtailment are needed). Though these categories do not encompass all possible extreme weather events that might pose challenges to power sector planning and operations, they do provide a useful framework that can be used to assess historical events in the context of higher renewable systems.

High-Impact Events

Cold Waves

Cold waves elevate loads as heating demand increases, and these loads tend to be largest in regions where electric heat predominates. However, even where gas and oil are the main heating fuels, load increases as electricity is often used to circulate air. Additionally, cold waves boost the demand for natural gas, which can then constrain gas-fired generation. Frigid air reaching locations where freezing is unusual can cause generation outages due to frozen lines or frozen fuel sources. Extreme cold can also lead to outages of renewable generators. Wind turbines may experience low temperature shutdowns. Should the cold wave also be accompanied by precipitation wind turbines blades may become ice-covered and solar panels can become snow- or ice-covered.

East of the Rocky Mountains in the United States, cold waves usually follow a general pattern of cold air channeled down the Canadian Rockies from the interior of Canada and the Arctic and into the northern United States. It can then spread south and east depending on the movement of the weather system associated with it. The cold air is typically very dry and arrives with moderate to strong northerly or northwesterly winds and clearing skies, leading to elevated wind and solar generation potential. However, as the system moves east, high pressure builds, and the wind resource typically weakens. In the Rocky Mountains and further west, cold waves also arrive from Canada, but they tend to be less intense because mountains block the coldest low-lying air. However, the cold can be long-lived with air getting trapped in mountain basins for days or even weeks and continuing to cool in place, causing stagnant and foggy conditions with poor wind and solar resource.

Recent research suggests that the frequency of cold waves entering the United States, and possibly the southerly extent of the cold waves, may increase due to climate change (Kretschmer et al 2018). However, this is an active area of research and contradictory results have also been found (Blackport and Screen 2020) and there is little current consensus (Cohen et al., 2020). What is clear is that the source air for cold waves in the Arctic is warming. So while it is possible such air masses may move south more frequently, that air may not be as cold as it once was.

Midlatitude Storms

Midlatitude storms are powerful, large-scale, non-tropical storms that occur most frequently during the shoulder and winter seasons. As their name suggests, they typically form and move in the region between the tropical and polar latitudes. That is between roughly 23° and 66° north or south. They are accompanied by strong winds, large temperature transitions, clouds, and precipitation, and they can dramatically impact renewable resource availability. In North America, these storms are fueled by large temperature gradients and their evolution transports warm air to the north ahead of the storm center, and cold air to the south behind it. When they are present, they are the primary determinant of renewable resource and temperature driven load. These storms can also impact utility infrastructure through high winds, embedded thunderstorms and, where temperatures are below freezing, snow and ice. The push of cold air to the south is what typically drives cold waves east of the Rocky Mountains, driving demand up and bringing frozen precipitation that impacts electric infrastructure. A bomb cyclone is a specific type of mid-latitude storm in this category that intensifies very rapidly with central pressure dropping by at least 24-mb in 24-hours. Because of the strong pressure gradients that result from this, bomb cyclones often yield especially strong winds that can damage infrastructure. The intensity of these storms may be modified by climate change, but attribution research is in its early stages.

Heat Waves

Heat waves cause a large increase in load over a broad area as a result of increases in air conditioner use and decreases in electric infrastructure efficiency. In most of the United States, they are responsible for annual peak loads.[13] They can also cause forced outages or derates of conventional generators, especially where cooling water is constrained, and they can reduce transmission capacity.

Heat waves are often associated with clear skies, which implies solar generation is synergistic with demand. However, photovoltaic efficiency is reduced as panel temperature increases. Extreme heat can be associated with haze, which reduce solar insolation, further lessening the solar generation on these days. As seen in the California blackouts in the late summer of 2020[14], wildfires can also be associated with heat waves. How widespread the reduction in solar insolation due to wildfires is and its impact on solar generation potential is an area of active research. These effects lead to neither high nor low solar generation, just average solar generation potential. In some locations, heat waves correlate with low wind conditions, reducing generation from wind generators. Excessive heat can also cause wind turbines to reach their high-temperature shutdown limits, around 98°F to 110°F at the nacelle depending on specific turbine designs and optional packages, forcing them offline.

Unlike cold waves, which typically only last a few days because the weather is more active in winter, heat waves can last many days or even weeks, waxing and waning in intensity. The subtleties of the weather pattern will determine whether the heat is accompanied by weaker or stronger wind and solar resources.

[13] Exceptions include the regions in the Pacific Northwest, which consistently is winter peaking, and the Southeast, which occasionally as peak or near peak loads in the winter. Electric heating loads drive winter peaks in both regions (Sun et al. 2020).

[14] http://www.caiso.com/Documents/Final-Root-Cause-Analysis-Mid-August-2020-Extreme-Heat-Wave.pdf

In the West, offshore air flow from land to ocean often leads to heat waves. In these cases, the air is dry and solar resource is usually good. Wind resource in the west is often driven by local terrain and there is a significant correlation between strong, hot, and dry offshore winds (i.e., from land to ocean) in the western lee of mountain ranges like the Cascades and the Sierra, and heat waves at major California, Oregon, and Washington load centers. However, the eastern end of mountain gaps is where the best average winds are found outside of heat waves and are thus where most of the existing wind generators in the West are located. Further, the hot, dry, and windy conditions typically present during heat waves are conducive to high wildfire risk and thus pose coincident risks for high demand, low wind generation, and well-above-normal fire and smoke risk that can affect infrastructure and solar generation.

In the East, subtle changes in pressure gradients that are due to weak weather systems impact the strength of the low-level jet that drives much of the warm season wind generation, so that there is no strong correlation between heat waves and changes in wind generation, but there is the possibility of patterns where heat and low wind resource are coincident. In the Eastern Interconnection and the Texas Interconnection, the low-level jet, warm temperatures, and overall weather patterns also profoundly impact fair weather cumulus formation, which is the primary cause of warm season scattered cloudiness as well as development of deep thunder clouds, both of which are drivers of solar variability.

There is strong observational evidence that the incidence of heat waves has increased dramatically due to climate change. The U.S. Global Change Research Program (USGCRP) reports that, "Heat waves are occurring more often than they used to in major cities across the United States, from an average of two heat waves per year during the 1960s to more than six per year during the 2010s. The average heat wave season across 50 major cities is 47 days longer than it was in the 1960s. Of the 50 metropolitan areas in this indicator, 46 experienced a statistically significant increase in heat wave frequency; and 45 experienced significant increases in season length, between the 1960s and 2010s."[15] In addition, there is growing evidence that wildfire risk is increasing due to climate change (Abatzoglou and Williams 2016).

Tropical Systems

Tropical systems consist of tropical depressions, tropical storms, and hurricanes. They have significant impacts on the electric system, most notably on transmission and distribution infrastructure. Large systems can also reduce load because of extensive cloud cover that reduces solar heating. Though there has been concern about damage directly to renewable energy infrastructure from hurricanes, to date, only a few wind plants have sustained significant damage from tropical storms. Hurricane Maria caused severe damage to the coastal Nuguabo Wind Farm in Puerto Rico, when it sustained an almost direct hit from the strongest part of the then Category 4 storm. However, the Santa Isabel Wind facility less than 90 km away sustained little damage. Typhoon Maemi, which struck the Japanese Miyakojima Island in September 2003, also caused severe damage to the island's six wind turbines (Ishihara et al. 2005). Since damaging winds from tropical systems extend less than 100 km at most from the storm center, and they diminish rapidly once the storm is over land, total wind and solar infrastructure at direct risk from any given storm is minimal. Storm surge risk is also minimal since most turbines are not located in

[15] "Heat Waves," https://www.globalchange.gov/browse/indicators/us-heat-waves.

the surge impacted area. Extensive build-out of offshore wind in the future might change these attributes and that risk should be evaluated in detail.

There is some evidence that the frequency and intensity of tropical storms might be increasing due to climate change, but results are not yet definitive. While this is concerning for coastal infrastructure, as mentioned the impact of tropical storms on land-based high penetration renewables is limited by their relatively small geographic scale, and lack of inland penetration, so the climate risk is minimal.

Aside from infrastructure risk, tropical storms also impact supply and demand balance and the impact of this with increasing wind and solar penetration will be examined in this report.

Events Posing Planning Challenges

Low Variable Renewable Energy Resource with High Demand

As renewable energy penetration increases, the risks to supply and demand balance will evolve considerably. In today's system, the primary weather risks that impact system wide supply and demand are typically temperature-driven extreme loads related to heating and cooling demand. In the future, weather variables that define the amount of available renewable generation will become increasingly important, and this will add considerable complexity to the multivariate weather dependence and increase the supply side impacts. Furthermore, given that weather phenomena tend to occur over broad regions, and that much of the country operates in interconnected grids with trading and taking advantage of resource diversity—it is important to understand how phenomena may affect an entire region and to evaluate the impact of additional transmission interconnection. Periods of poor renewable resource across a broad region that occur in conjunction with moderate, but not abnormal, demand may result in a net load—after accounting for wind and solar—that is difficult to meet with the remaining thermal and hydro fleet. The weather patterns that cause such a coincidence are unlikely to be newsworthy from today's perspective, and may include cold, foggy, and stagnant conditions in the winter and hot, hazy, low-wind periods in the summer.

The types of weather events that lead to low renewable energy resource are sometimes relatively benign from a societal impact perspective, and thus some of these conditions have not been studied in detail. However, at high renewables penetrations of renewables, these events could lead to supply shortages. There is speculation that the future the frequency of such stagnant weather may also become more common as the climate changes, due to the so-called wavier jet hypothesis leading to more atmospheric blocking[16] (Francis and Vavrus 2015). However, there are no definitive studies yet that indicate a direct connection to an increase in low resource periods across broad areas.

High Variable Renewable Energy Resource with Low Demand

The confluence of high-resource, low-load weather patterns can lead to oversupply problems. A real-life example is springtime in the Pacific Northwest, where sunny, moderately warm days can bring low demand, rapidly melting mountain snowpack, and good wind resource. These

[16] A lay description can be found at https://www.carbonbrief.org/jet-stream-is-climate-change-causing-more-blocking-weather-events

conditions lead to oversupply where, even with most thermal generators turned off, there is more renewable generation capability than load, when hydropower is factored in. This is more of an economic problem than a reliability concern, as curtailment, demand response, and storage (among other flexibility options) solves the issue. These periods also lead to lower levels of system inertia (Tsai et al. 2020) which could cause frequency stability problems, leading to reliability concerns. However, this may not be particularly concerning for large integrated interconnections such as the EI and WI, while smaller systems, such as the TI, may be able to rely on inverter technology to provide fast frequency response, replacing the need for inertia (Denholm et al. 2020).

Similar to low renewable resource and high demand events, a changing climate could lead periods of high resource and low demand in other regions during periods of atmospheric blocking, especially in the shoulder seasons, but again definitive studies of the potential impacts on the electric system at high penetrations of renewables are needed.

Methodology

In this section, we describe the development of future power sector infrastructures, methods used to identify events of interest, and the power sector operational modeling approaches used to evaluate each event.

Power Sector Infrastructure

Three future power sector infrastructures with varying penetrations of wind and solar generation were developed to assess their performance under extreme weather conditions. These infrastructures were developed using the National Renewable Energy Laboratory's (NREL's) capacity expansion tool, the Regional Energy Deployment System (ReEDS) model. ReEDS simulates electricity sector investment decisions based on system constraints and demands for energy and ancillary services (Cohen et al. 2019). The model determines the least-cost resource mix needed to satisfy regional demand requirements and maintain grid system adequacy, including the expansion and retirement of generators of all types and expanded transmission. Specifically, ReEDS identifies the type and location of thermal and renewable resource deployment, as well as a transmission infrastructure expansion to accommodate those installations. The ReEDS model is run sequentially for the entire conterminous United States (CONUS) in 2-year increments through 2050, using a wide range of possible futures for technology cost, thermal generator retirements, policy regulations, demand growth, and vehicle electrification. The results are documented in annual reports of the Standard Scenarios, an NREL-produced suite of forward-looking scenarios of the U.S. power sector (Cole et al. 2018, 2019, 2020). A customized set of these futures was run in ReEDS specifically for this study to create future infrastructure plans for 2024, 2036, and 2050. Table 1 defines the source for major assumptions to define our three infrastructure plans, and Figure 1 shows the resulting generation capacity mix in each interconnection. Further detail on these assumptions can be found in the appendix.

Table 1. Summary of Assumptions for Creation of each Infrastructure Plan

Infrastructure Plan and ReEDS Year	Generator Cost and Performance Assumptions	RE Resource Supply Curves[a]	Distributed Generation Assumptions[b]	All Other Assumptions	Wind and PV Annual Energy Penetration
2024	2019 ATB Mid-Case (NREL 2019)	2019 Standard Scenarios Mid-Case (Cole et al. 2019)	dGen Mid-Cost RE adoption	Standard Scenarios 2019 Mid-Case (Cole et al. 2019); ReEDS version 2018 (Cohen et al. 2019)	17%
2036	2019 ATB Low for PV and Wind (NREL 2019)		dGen Low-Cost RE adoption		50%
2050					65%

[a] See ReEDS documentation (Cohen et al. 2019) for an in-depth explanation of the renewable energy (RE) resource supply curves.

[b] See ReEDS documentation (Cohen et al. 2019) for discussion of dGen usage with ReEDS.

Though ReEDS determines the total generating capacity in each balancing area, the specific assumed location of each wind and solar generator is required to assess the generation from each wind and solar site during an extreme weather event. Using the Renewable Potential Model (reV), zonal capacity from ReEDS is translated into specific generator locations for use in determining generation. Further discussion of reV is included in the Weather, Demand, and Renewable Resource Data section and in the reV documentation (Rossol, Buster, and Bannister 2021; Maclaurin et al 2019). These modeled locations for wind and utility scale PV are shown in Figure 2 for the 2050 infrastructure plan.

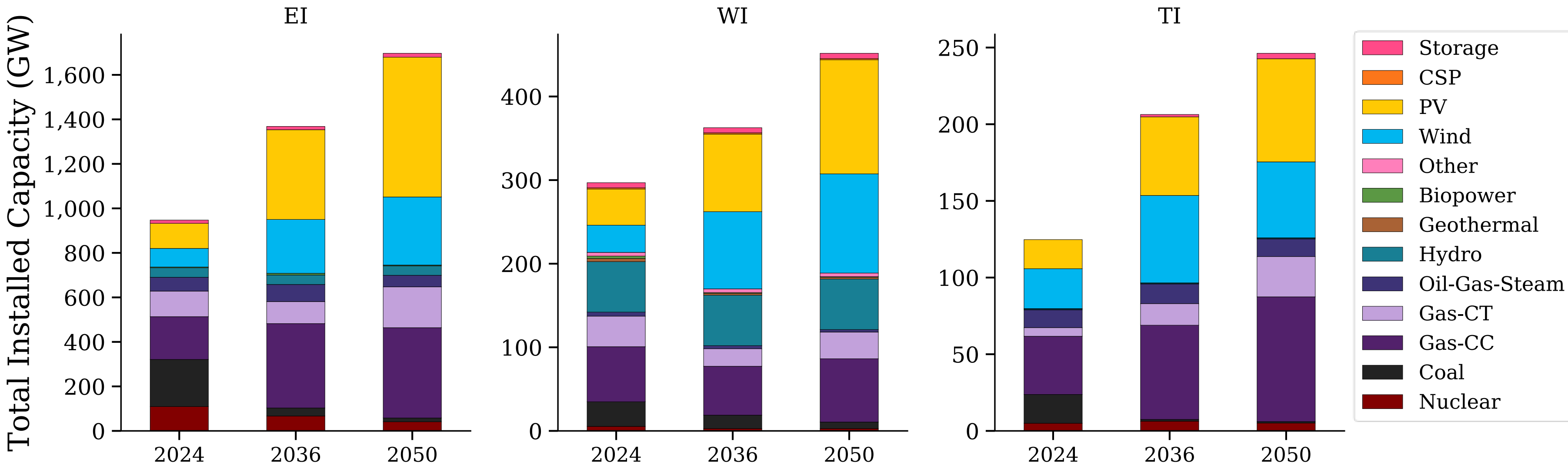

Figure 1. Total installed capacity for the EI (left), WI (middle), and TI (right) for the three study infrastructure plans

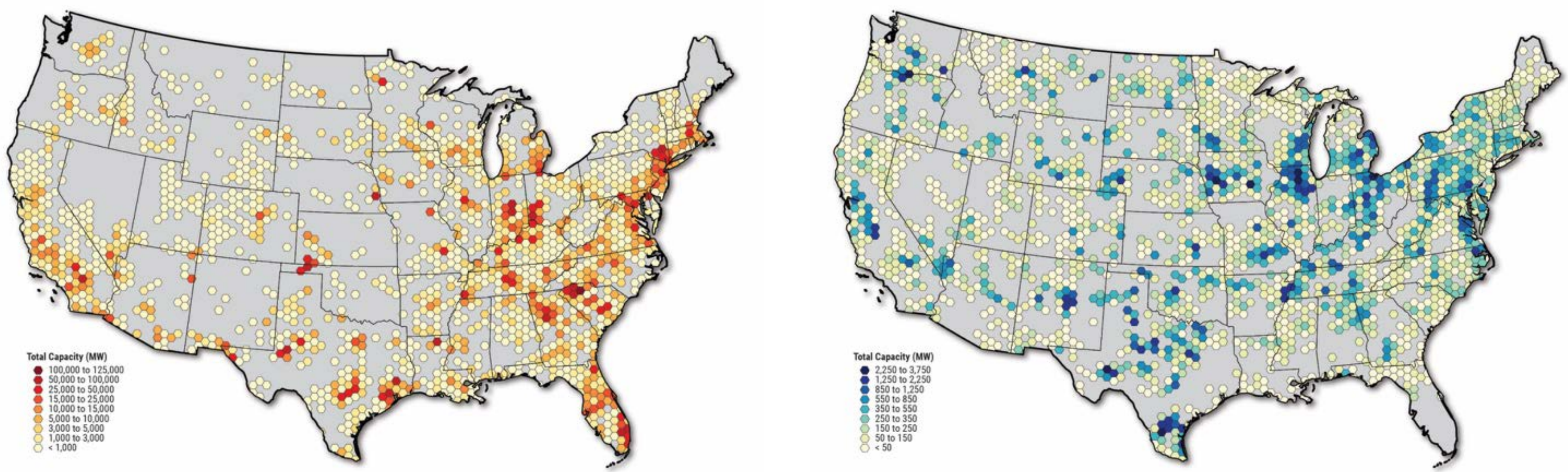

Figure 2. Locations and sizes of utility-scale PV (left) and wind (right) sites in the 2050 plan

ReEDS also builds new transmission between its balancing areas. To translate the results of the less granular transmission representation in the ReEDS model into the nodal production cost model (PCM), expanded pathways in ReEDS are converted into distinct transmission lines that connect to substations in the PCM (Brinkman et al. 2021). Table 2 shows the interzonal transmission expansion in the 2036 and 2050 plans and the percent increase in transmission capacity relative to the 2024 plan, which resulted from ReEDS and were translated into the nodal PCM. Intrazonal transmission is also expanded, but it is not shown in the table. Figure 3 shows the boundaries of the zones in Table 2. We also use the zones, in addition to the three interconnections, as a common spatial extent to report aggregated results from the PCM simulations.

Table 2. Expanded Transmission Capacity Between Zones in the PCM Nodal Model

Percentage value in parenthesis is the increase from 2024.

Zone From	Zone To	2036	2050
CAISO	West Connect	422 MW (9%)	4,424 MW (96%)
Columbia Grid	Canada	523 MW (349%)	523 MW (349%)
Columbia Grid	Northern Tier	1,027 MW (14%)	2,758 MW (36%)
Columbia Grid	West Connect	12 MW (24%)	532 MW (1064%)
ISO-NE	Canada	0 MW (0%)	3,051 MW (72%)
MISO	Canada	1,813 MW (76%)	3,786 MW (158%)
MISO	SPP	625 MW (11%)	1,313 MW (22%)
MISO	TVA	2,515 MW (73%)	4,450 MW (129%)
Mountain West	Northern Tier	3 MW (3%)	12 MW (13%)
Mountain West	SPP	1,604 MW (458%)	1,604 MW (458%)
Northern Tier	SPP	131 MW (31%)	131 MW (31%)
NYISO	Canada	792 MW (198%)	4,012 MW (1003%)
NYISO	ISO-NE	5,353 MW (611%)	5,573 MW (636%)
PJM	MISO	3,165 MW (27%)	5,013 MW (44%)
PJM	NYISO	6,702 MW (791%)	6,702 MW (791%)
SERC	FRCC	2,298 MW (64%)	3,566 MW (99%)
SPP	ERCOT	508 MW (69%)	508 MW (69%)
SPP	TVA	1,182 MW (23%)	1,677 MW (33%)
TVA	PJM	853 MW (106%)	853 MW (106%)
TVA	SERC	491 MW (68%)	522 MW (72%)
West Connect	Mountain West	0 MW (0%)	0 MW (0%)
West Connect	Northern Tier	929 MW (91%)	929 MW (91%)
West Connect	SPP	340 MW (110%)	340 MW (110%)

ERCOT: Electric Reliability Council of Texas; FRCC: Florida Reliability Coordinating Council; ISO-NE: ISO New England; MISO: Midcontinent Independent System Operator; NYISO: New York Independent System Operator; PJM: PJM Interconnection: SERC: SERC Reliability Corporation; SPP: Southwest Power Pool; TVA: Tennessee Valley Authority

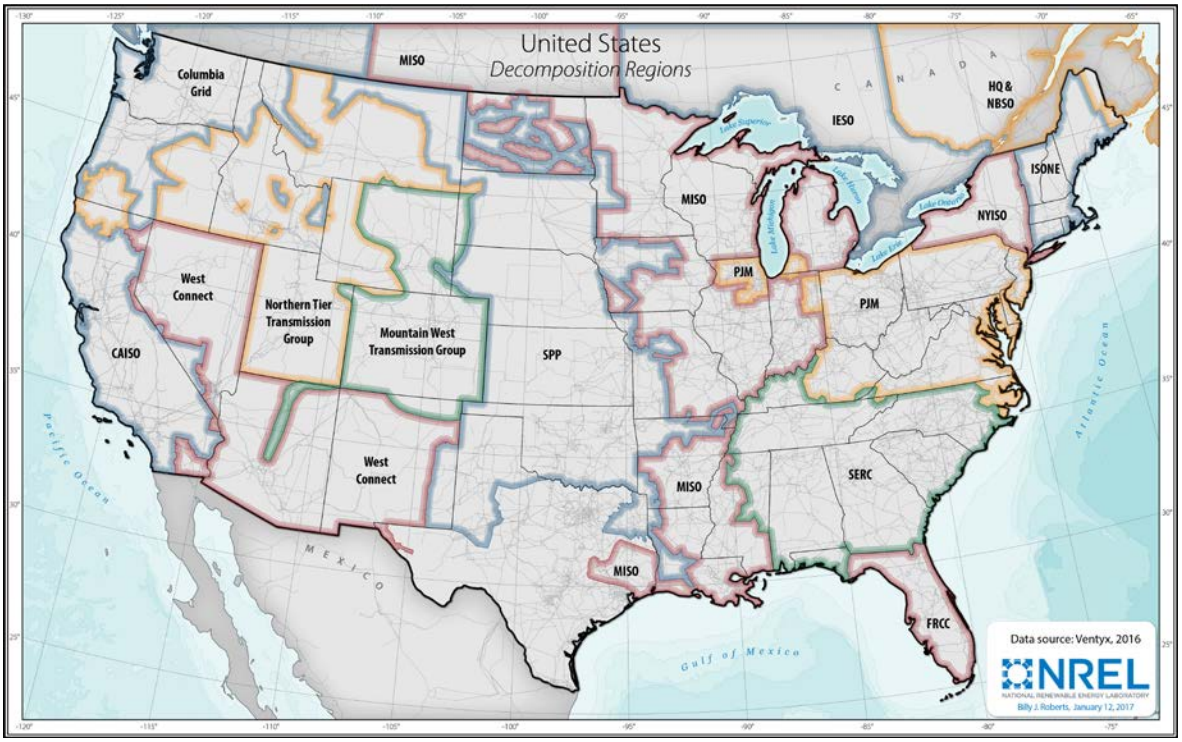

Figure 3. Regions defined with the PCM database of the WI, EI, and TI

Weather, Demand, and Renewable Resource Data

Our modeled future electric infrastructure plans were built by ReEDS using a single weather year with aggregated regional supply curves to represent wind and solar resource, but operational modeling and assessment requires higher geographic and spatial resolution data sets. Because correlations between weather variables that drive load and those that drive VRE (i.e., wind and solar generation) are central to the evaluation of weather-driven events in a high-penetration future, it is critical that coincidental data for wind, solar, other weather, and load is used.

The NREL Wind Integration National Dataset (WIND) Toolkit is a wind integration resource data set covering the United States (Draxl et al. 2015).[17] This data set provides gridded wind resource at 2-km spatial resolution. The original temporal interval is 5 minutes, though only 60-minute data was used for this project. The data set spans January 2007 through December 2013, and this defines the period of this study. Solar resource is available from the NREL National Solar Resource Database (NSRDB)[18] (Sengupta et al. 2018) as far back as 1998 and is regularly updated with new data. The native spatial resolution is 4 km, and the temporal resolution is 30 minutes.

[17] "Wind Integration National Dataset Toolkit," NREL, https://www.nrel.gov/grid/wind-toolkit.html
[18] "NSRDB: National Solar Radiation Database," NREL, https://nsrdb.nrel.gov

To create hourly generation profiles for new wind and solar plants for the three infrastructure plans, we utilized the combination of two NREL tools, the Renewable Potential Model (reV) (Maclaurin et al 2019) and the NREL System Advisor Model (SAM)[19]. reV determines the location of the new VRE using inputs from ReEDS, transmission infrastructure, and other geographic information and constraints. SAM then produces generation profiles for the sites chosen by reV using resource data from the WIND Toolkit and NSRDB and system configuration and technology assumptions for the turbines or PV systems. Wind turbine assumptions used to generate hourly profiles assumed future technology performance projections as described in the NREL ATB 2019 (Cole et al. 2019). We assumed PV systems were single axis tracking and had an inverter loading ration of 1.3. Distributed PV was modeled using a diversity of tilts and orientations as informed by the dGen modeling for the ReEDS scenario.

The National Oceanographic and Atmospheric Administration's (NOAA) collects and archives weather observations from weather stations around the country. NOAA's Local Climatological Data (LCD)[20] include hourly, daily, and monthly summaries at thousands of stations across the country. We used weather data for 90 cities spanning the CONUS, to capture weather at the largest U.S. load centers across different system operators in a semiregular geographic grid. Daily temperature deviations from climatology, heating degree days, and cooling degree days were examined, and these variables allowed us to identify anomalously warm and cold periods. The LCD also contains information about wind, pressure, precipitation, cloud cover, humidity and the currently occurring weather, which allows identification of important weather like snow, ice, and thunderstorms. Stations were selected that had a continuous record 2007–2013 to overlap with the WIND Toolkit and NSRDB data sets.

The regional load profiles for this study are based on the historical electricity demand for each event's corresponding meteorological year (2007–2013). To scale these profiles to the 2024, 2036, and 2050 infrastructure years, load multipliers taken from the 2018 ReEDS Standard Scenarios Mid-Case were applied. These multipliers were derived from yearly demand growth projections from the EIA AEO 2018 reference scenario. This simple scaling method neglects the potentially significant changes to the shape of electricity demand curves due to widespread electric vehicle adoption, demand response technologies, and behind-the-meter storage. Incorporating these effects requires a bottom-up approach to load shape projections, which is beyond the scope of this study.[21]

Taken together, these data sets comprise our own historical, high temporal and spatial resolution data set of weather, electricity demand, wind and solar resource data covering 2007–2013. Combining our data set with the assumed wind and solar generator locations for the 2024, 2036, and 2050 infrastructure years allows us to assess the magnitude and shape of increased VRE generation when subjected to the weather conditions of past events.

[19] "System Advisor Model (SAM)", NREL, https://sam.nrel.gov
[20] "Local Climatological Data (LCD)", NOAA, https://www.ncdc.noaa.gov/cdo-web/datatools/lcd
[21] Though demand that is due to vehicle electrification is weakly associated with external weather conditions, any electrification of building heating through adoption of heat pumps would strongly increase demand during extreme cold weather events. However, as this method uses demand based on historical demand during periods of extreme weather, it best captures the general correlation of weather-driven increases in load.

Net Load of 2024, 2036, and 2050 Infrastructure Plans

In this section, we explore the resulting net load for the 2024, 2036, and 2050 infrastructure plans for all 7 weather years (2007–2013) spanned by our wind, solar, and load data sets. As previously described in the Power Sector Infrastructure section, historical electricity demand from the study period was scaled to expectations for 2024, 2036, and 2050 using load multipliers taken from the 2018 Standard Scenarios Mid-Case. The first column in Table 3 shows the increase in the full system peak demand from 869 GW to 1,019 GW between 2024 and 2050. The table also shows how the increase is distributed among interconnections.

Table 3. Historical and Modeled Future Peak Demand by Interconnection

Infrastructure Plan Name	Peak Demand (GW)	Min Demand (GW)	Peak Net Load (GW)	Min Net Load (GW)	Wind Capacity (GW)	PV Capacity (GW)	Thermal and Hydro Capacity (GW)
Full System							
2024	869	374	749	252	156	175	1,101
2036	933	403	733	-35	407	548	1,042
2050	1,019	442	788	-148	494	833	1,131
Western Interconnection							
2024	177	85	164	44	33	43	806
2036	191	93	162	-3	92	93	772
2050	211	103	172	-25	119	136	811
Eastern Interconnection							
2024	658	254	589	179	87	113	215
2036	695	270	578	-36	257	403	172
2050	744	290	603	-142	325	630	191
Texas Interconnection							
2024	67	21	56	-11	26	19	80
2036	82	25	64	-51	57	51	98
2050	103	32	82	-41	50	67	129

Hourly wind and solar generation were calculated for all wind and solar plants using the weather data for the study period, and it was subtracted from the load for the same hour to calculate the net load for the entire period. Figure 4 shows the evolution of the distribution of net load from 2024 through 2036 to 2050; it indicates the additional wind and solar generation broadens the width of the distribution on both an hourly and a daily basis for the country as a whole, and each interconnection. The net load peak and minima are also shown in Table 3.

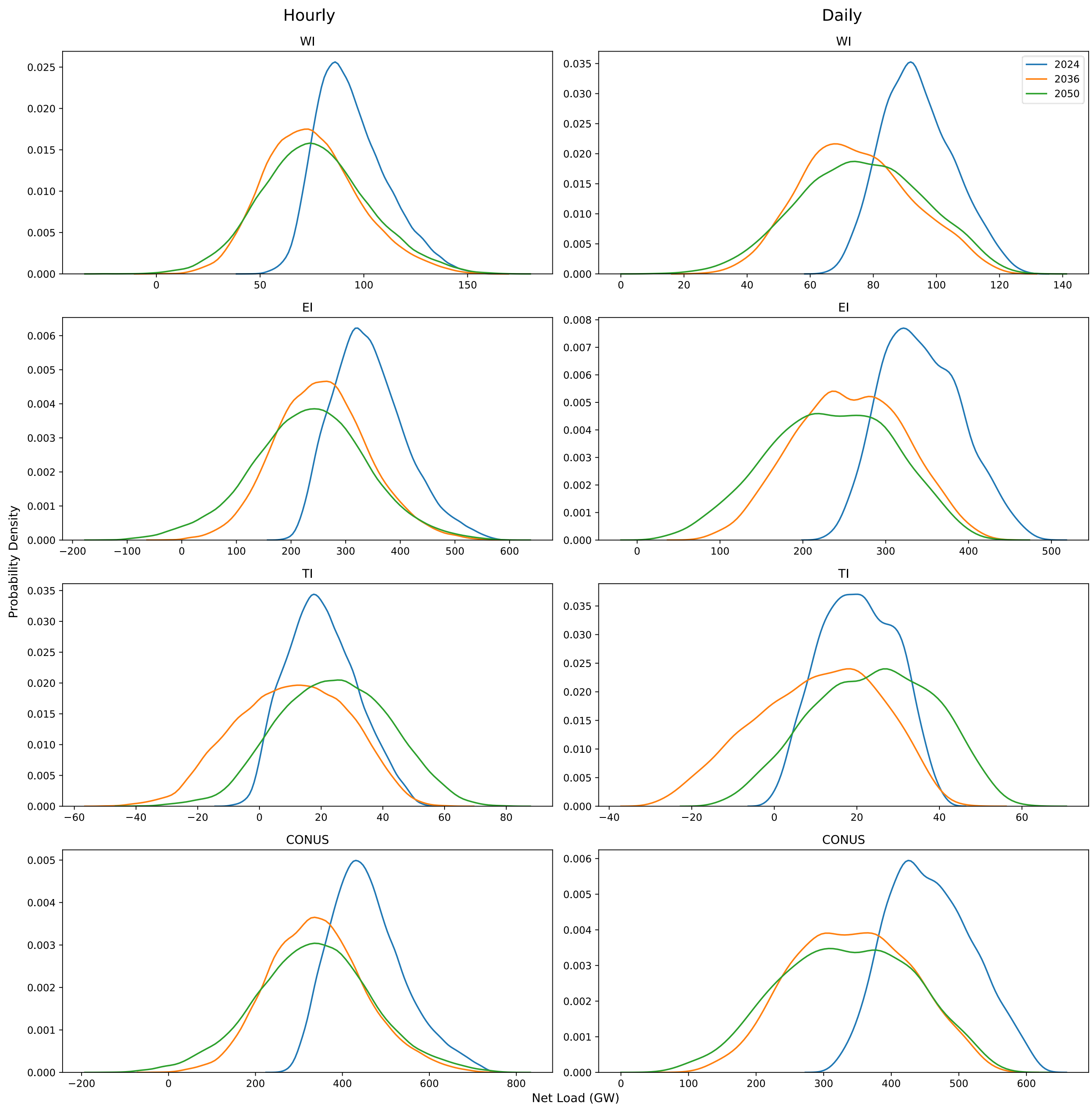

Figure 4. Distribution of hourly and daily average net load for 2007–2013 for the 2024, 2036, and 2050 plans

In 2050, the minimum hourly net load is negative across U.S. and Canada and for each interconnection. Though the distribution widens, it is important to note that, apart from the TI, the median net load moves lower, and except for the TI the upper tail does not move significantly higher. In all cases, the tail becomes thinner, meaning high net loads still occur, but their frequency decreases. Because thermal capacity increases slightly, this suggests—though full system modeling is required to confirm—that, from a resource adequacy perspective the system is operating under less stress on average in 2050 than in 2024, and it rarely becomes more constrained than it was in 2024 base case. It is also clear that far less nonrenewable generation is being used everywhere, and results from the ReEDS modeling that created the infrastructure plans suggest the VRE penetration by energy reaches 65% in 2050. Between 2024 and 2050, the share of installed capacity from VRE increases from 22.6% to 53.9%. Texas features the largest load growth (over 50%) from 2024 to 2050, and it has a smaller footprint and thus less resource diversity than the other two interconnections. These facts push the peak net load higher than 2024 peak load, and therefore the 2050 plan adds more thermal generation in the TI to ensure resource adequacy.

Further exploration of the load, net load, wind, and solar distributions and their relationship with weather is found in the appendix.

Identification of Events for the High-Penetration Tail Events Study

In this section, we describe how we identify extreme weather events for the period of our study (2007–2013). NOAA's long online historical archive of daily weather maps[22] was used to evaluate the significance of events within the meteorological record. We also used online news media to evaluate the newsworthiness of each event.

Identification Methodology

We used the data sets and four methodologies described in this section to identify extreme weather events that cover the categories in our Taxonomy section (page 1) and are of interest within the 2007–2013 time frame.

Demand Side Method 1.1: LCD Temperature Anomalies, heating Degree Days, and Cooling Degree Days

We obtained heating degree days, cooling degree days, and temperature deviations from normal from NOAA's Local Climatological Data (LCD) and organized them by date and region. This allowed cold waves and heat waves to be identified. In addition, it can be reasonably assumed periods of high heating degree days or cooling degree days correspond to high loads, and low heating degree days and cooling degree days typically have low loads. Thus, the LCD provided initial insight into expected system loads.

Demand Side Method 1.2: Load Data

Historical load data for the study period was obtained and used to identify periods of actual high system loads. The load magnitude was adjusted using simple scalars to account for expected load growth through 2050 in different regions. Load growth in some regions is expected to be faster

---

"Daily Weather Maps: Sunday, February 25, 2007," NOAA Weather Prediction Center, https://www.wpc.ncep.noaa.gov/dailywxmap/index_20070225.html.

than in others, so the shape of the load curves will therefore vary slightly from the load assumed here. Hourly data are available and could be aggregated to produce daily averages.

Supply Side Method 2.1: Spatial Average Resource Anomalies

To calculate resource deviations, the WIND Toolkit and NSRDB data sets were extrapolated onto a coincident grid, with hourly resolution, and these were used to produce daily averages. The deviation of this daily average from a seasonally "normal" day for the time of year across the full 7 years was calculated for every point on the grid. To reflect seasonality impacts, we used a moving 29-day window (14 days before and after plus the actual day) was applied across the 7 years of data to obtain the "normal" resource for each day at each point. This moving average was then subtracted from each day to produce a deviation from normal. These deviations could then be further averaged across any desired geographic region. The initial identification method looked at the CONUS and interconnection averages. These resource anomalies were then sorted and ranked.

Supply Side Method 2.2: Generation Anomalies

The methodology for assessing resource anomalies described above is limited as it does not consider how resource anomalies interact with the geographic distribution of potential future wind and solar generator sites. To resolve this issue, the hourly wind and solar generation data calculated with reV and SAM using the ReEDS build-out and corresponding resource data (as described in the Weather, Demand, and Renewable Resource Data section) was used to identify generation anomalies. As for Method 2.1, a 29-day by 7-year window was used to determine "normal" reference generation. The data set thus allowed the statistical attributes of wind and solar generation to be analyzed for each day on a national and regional basis. In addition, the use of expected generation data allowed hourly net load to be calculated and ranked to identify the days where demand and generation deviated in synergistic and antagonistic ways to yield low and high net loads.

Method 3: Identification of High-Impact Events

For events in the high-impact category, historical weather events within the study interval were selected that had significant adverse effects on the electric system and were large enough to make national news. Strong cold waves frequently have large societal impact as a result of attendant wintery precipitation, infrastructure impacts, or both. Strong heat waves across broad regions are also commonly reported in the national news because of infrastructure and public safety concerns, and as they are sometimes punctuated by strong thunderstorms. Thus, once heat and cold wave events were identified using temperature and/or load records using Methods 1.1 and 1.2, the dates of occurrence were searched in historical satellite imagery records, weather archives, and internet-based news records. This information was used to prioritize the highest-impact events and identify events where associated large-scale storm systems may have played a role. Many, but not all, events are catalogued as part of NOAA's "Billion-Dollar Weather and Climate Disasters" database.[23]

Tropical storm systems, even large hurricanes, tend to be much smaller in geographic scale than midlatitude storms and thus are more difficult to identify in the LCD because they impact fewer

[23] NOAA National Centers for Environmental Information (NCEI) U.S. Billion-Dollar Weather and Climate Disasters (2021). https://www.ncdc.noaa.gov/billions/, DOI: 10.25921/stkw-7w73

weather stations. However, tropical storm tracks are archived by NOAA and this archive[24] was used to shortlist storms that made landfall during the study interval. Storms with paths that would impact high wind and solar penetration because either their paths intersected with modeled generator locations or unusual weather patterns were identified.

Events Identified

The events identified by each individual method were compared to find events that were identified by multiple methods. As expected, high-load periods identified with Method 1.2 typically mapped to the extreme heat and cold events identified in the LCD with Method 1.1. Methods 2.1 and 2.2 did not identify similar events, which indicates specific placement of renewable generators significantly affects performance during extreme events. For this reason, Method 2.2, which used generation from modeled future capacity-specific locations, was deemed superior and given greater weight when selecting events. Further, Method 2.2 allowed net load to be calculated for specific events, by subtracting the wind and solar generation from the load data developed for Method 1.2. The final set of events were chosen to represent a diversity of events the future system may encounter rather than determine what the most extreme events or to rank the events against each other. Table 4 lists the final set of events we analyzed, which method or methods identified the event as being of interest, and any unique characteristics of an event. We focused PCM modeling and analysis across all three infrastructure plans to like weather events with different intensities (i.e., different intensity heat and cold waves) to better understand how the operations evolve as the VRE penetration changes. Finally, 2050 PCM sensitivity analysis concentrated on events where hydropower or the impact of turbine blade icing and cold temperature shutdown would have large impact.

Table 4. Summary of 2007–2013 Events Chosen for Analysis

Event Name	Event Dates	Identification Methods[25]	Unique Characteristics of the Event	Production Cost Modeling[26]
High-Impact Events				
Cold Wave	Feb 1–4, 2011	1.1, 1.2, 3	Intensity, record-breaking low temperatures, geographic extent, and southerly reach	2024, 2036, 2050 Plans
Heat Wave 1	July 19–24, 2011	1.1, 1.2, 3	Long-lasting heat wave, hottest summer countrywide in 75 years	2024, 2036, 2050 Plans
Heat Wave 2	June 29–Jul 7, 2012	1.1, 1.2, 3	Heat over much of the East, historic derecho storm event	—
Hurricane Irene	Aug 25–30, 2011	2.2, 3	Potential impact on wind and eastern solar	—

[24] "Historical Hurricane Tracks," NOAA, https://coast.noaa.gov/hurricanes/.
[25] Refers to methods described in the "Identification Methodology" section of the report.
[26] The "Power Sector Infrastructure" section of the report describes the characteristics of the scenarios, while the "Power Sector Event Modeling: Production Cost Modeling" describes the sensitivities.

Event Name	Event Dates	Identification Methods[25]	Unique Characteristics of the Event	Production Cost Modeling[26]
Hurricane Gustav	Sep 1–6, 2008	2.2, 3	Wide geographic extent and longevity over land	—
Winter Storms	Dec 4–12, 2013	1.1, 1.2, 2.2, 3	Three back-to-back storms with wide geographic impacts and long-lasting cold air reaching southern states	2050 Plan + Hydro Sensitivities + Icing Sensitivity
Events Posing Planning Challenges				
Winter Net Load 1	Feb 20–23, 2008	1.1, 1.2, 2.1, 2.2	Otherwise calm weather yielding extremely low-wind resource across CONUS and low-solar across south	2024, 2036, 2050 Plans
Winter Net Load 2	Dec 6–11, 2009	1.1, 1.2, 2.2	Concurrent high net load across all three interconnections, poor wind in the West and Texas	—
Winter Net Load 3	Feb 2–5, 2010	2.1, 2.2	Nationwide poor wind and solar	2050 + Icing Sensitivity
Summer Net Load 4	Aug 8–11, 2010	1.2, 2.2	High net load in the EI despite no extremes in either renewable resource or load	2024, 2036, 2050 Plans
Lowest Net Load	April 17, 2011	1.2, 2.1, 2.2	Widespread high wind and solar resource with low load results in lowest net load observed in data set	2050 Plan + Hydro Sensitivities + Icing Sensitivity
Wind Drought	Oct 1–24, 2010	2.2	Three weeks of well-below-normal wind CONUS-wide	—

Power Sector Event Modeling: Production Cost Modeling

To examine the impact of these extreme weather events on the operations of the future power systems of the WI, TI, and EI, we conducted a production cost modeling (PCM) analysis for seven of the twelve events we identified in Table 4 (page 17). The three grid infrastructure plans were translated into a detailed nodal PCM and simulated using a commercial software from Energy Exemplar called the PLEXOS Integrated Energy Model (PLEXOS) [27]. As a unit commitment and economic dispatch simulation model, PLEXOS optimizes operation of the generation mix to minimize overall production cost while observing various constraints such as generator minimum operating levels, ramp rates, reserve requirements, transmission thermal and interface flow limits, and more. Full details on assumptions and set up of the nodal WI, TI, and EI PCM can be found in the Brinkman et al. 2021. Figure 5 shows an example result from a

[27] "PLEXOS Market Simulation Software," Energy Exemplar, https://energyexemplar.com/solutions/plexos/

PCM simulation demonstrating the hourly unit commitment and economic dispatch of different generation technologies and fuel types to serve load in the EI.

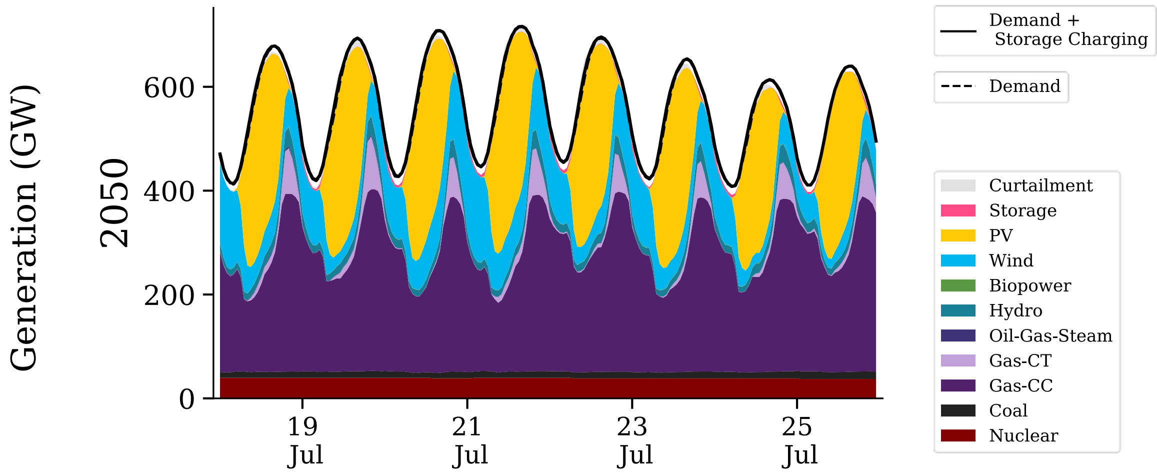

Figure 5. Example unit commitment and economic dispatch result from PCM simulation of the EI

To determine the impact of increasing penetration of renewable energy under extreme weather conditions, PLEXOS was run for all three infrastructure plans for four events. Three more events were used to run sensitivity analyses on parameters other than the grid infrastructure. The 2050 plan was used for all these sensitivities. The events and plans modeled are summarized in Table 4 (page 17). Often PCM is used to model a full year of system operations. However, we used PCM to focus on system operations during the pre-identified weather events. A key requirement to model a specific weather event in a future infrastructure is to provide synchronous wind, solar, and load time-series profiles, such that they all reflect the meteorology the system would experience if the event happened again. Applying the synchronous time-series data to a future system infrastructure allows investigation of that system's possible reaction to that historical weather event. In other words, the PCM has both a meteorological and an infrastructure year. The meteorological year is determined by providing wind, solar, load, and hydropower profiles and limits that reflect historical meteorology. Whereas the infrastructure year was determined by the three infrastructure plans of 2024, 2036, and 2050, which were summarized in the Power Systems Infrastructure section (page 7). The modeled generation and transmission capacity and the load growth differentiate the infrastructure years.

Recognizing the importance of weather on several aspects of the power system we integrated detailed weather dependent data into system components where we anticipated impacts. First, we used the most up-to-date hydro data to formulate our hydropower energy limits using U.S. Energy Information Administration's Form EIA-923[28] reported generation during the months around the event to better capture the hydrological conditions experienced during the weather events (Figure 6). This approach is similar to that taken by O'Connell et al. 2019. We also added a temperature dependence to each thermal generator's forced outage rates, rather than just maintaining the same constant forced outage rate for the entire year. Using temperature and outage rate correlations for different technologies within PJM (Murphy, Sowell, and Apt 2019),

[28] "Form EIA-923 Detailed Data with Previous Form Data (EIA-906/920)," EIA, October 29, 2020, https://www.eia.gov/electricity/data/eia923/.

we applied a daily forced outage rate based on the average temperature experienced by each thermal unit during the modeled events. For gas generators the impact is most pronounced during cold temperature events, leading to the highest outage rates during these periods. For steam generators, such as coal units, outage rates increase evenly between cold and hot temperatures.

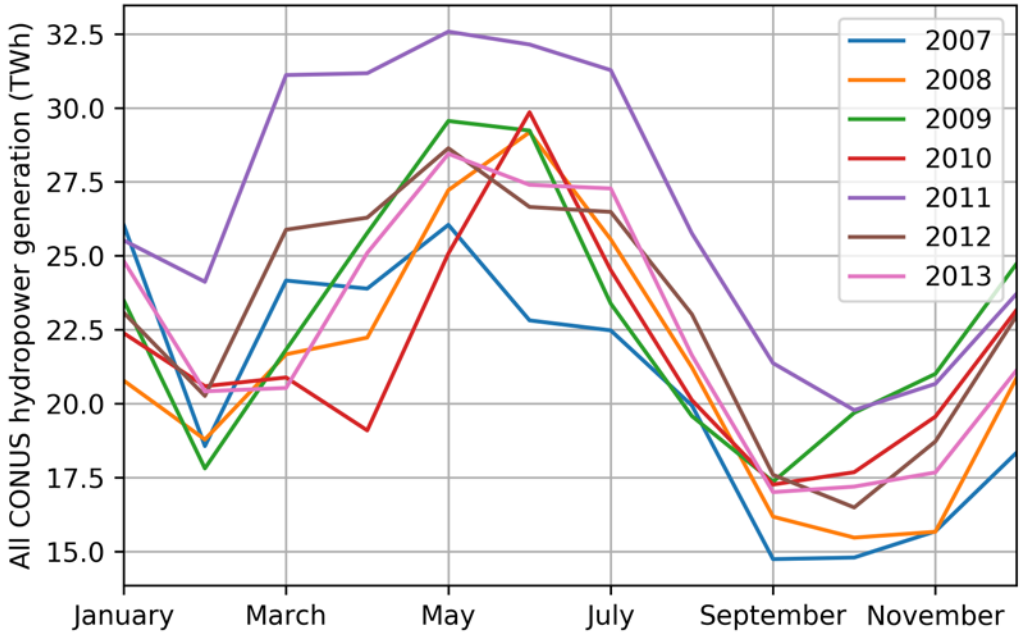

Figure 6. Total U.S. monthly hydropower generation for 2007–2013 based on EIA-923 data

For the Lowest Net Load event in the record (April 2011), three different hydropower sensitivities were compared with a base case plan: inflexible hydropower, wet hydropower and dry hydropower. These sensitivities govern the amount of energy available to each hydropower dam for each month of the year. In the Inflexible Hydro sensitivity, the monthly energy budget for dispatchable hydropower is converted to a flat hourly output for each hydropower unit. The wet and dry hydropower sensitivities use monthly energy limits from different hydrological years that reflect conditions that had more hydropower generation potential (wet) or less (dry) than the actual hydrological year for the particular event.

The December 2013 Winter Storms event included all three hydropower sensitivities and an additional “icing” sensitivity. This sensitivity captures the effect of wind turbine shutdowns that were due to blade icing or temperatures below -35°C. This is accomplished using the reV tool (see Weather, Demand, and Renewable Resource Data section for a description of reV). The Winter Net Load 3 also included an icing and cold temperature shutdown sensitivity for the 2050 plan.

Caveats and Limitations

This analysis has several important caveats and limitations:

- The analysis focuses on the impacts of extreme weather events on wind and solar generation; it *does not* fully cover other aspects of resilience to extreme weather. For example, it does not examine transmission and distribution outages or fully capture impacts on related fuel infrastructure such as natural gas pipelines.
- Certain impacts of extreme weather are not captured in the wind and solar generation assessment, most notably extended snow cover on PV. Wind turbine blade icing and low temperature shutdowns are only considered as sensitivities in the production cost modeling for select events.
- Net load evaluations look at whole interconnections and do not consider transmission constraints within the interconnections. However, in reality, regional transmission may limit effective transfer of renewable generation. The production cost modeling captures these constraints, but this was not conducted for every weather event or in event identification.
- The impact of any tropical storm on wind resource estimates is derived from numerical models and reanalysis. Numerical weather prediction simulation of hurricanes is difficult even when done retrospectively. Given the limited geographical extent of tropical storms, small errors in initial conditions can result in moderately large position and strength errors. Given the geographic aggregation of results in this study the impacts to our conclusions is limited. However, these nuances deserve greater attention in future work.
- The infrastructure plans have low deployment of storage, especially relative to newer versions of the Standard Scenarios.[29] Higher storage deployments may change which events create higher system stress and which do not.
- Besides wind turbine blade icing and temperature correlated outages of thermal units, we assume no physical damage to generation, transmission, or distribution infrastructure during the events.
- We ignore changes in the demand side that would impact the shape of the demand profile, like electrification and demand response.
- Because we only look at historical weather data, we do not capture any impacts of a changing climate on the types of events that might matter.
- Frequently production cost modeling includes forecast errors for wind and solar generation. However, we chose not to include forecast errors for the production cost modeling for this study. While NREL publishes high resolution wind and solar data for 2007–2013, at the time the modeling was completed the forecast data had only been robustly generated for 2012. The ability to forecast wind, solar, and load during extreme weather events should be a focus of further research and modeling should be done to understand its operational impacts.
- Operating reserves were modeled at an aggregated level for all regions. However, our analysis does not focus on reserve shortages. This should be a focus of future research.

[29] This report used assumptions from the 2018 Standard Scenarios. The cost of storage was revised down in the 2019 Standard Scenarios resulting in greater deployment of storage.

Findings

In this section, we present eight key findings. The findings are based on case studies of the three infrastructure plans using weather events from 2007 to 2013.

1. Wind and solar generation tend to be available during the extreme weather events of today and do not introduce new resource adequacy concerns or system operation stress as their annual energy penetration increases. Exceptions exist, but they tend to be short periods of elevated net load.
2. Mild weather conditions can produce extended periods of low wind and solar resource. Historically, the weather during these events would not be a reason for concern among system planners and operators, but with the increasing contribution of wind and solar generation, these events need to become a focus of planners in order to ensure system adequacy.
3. Because cold waves occur in winter when solar generation is already low, system operations during cold waves is most heavily influenced by the performance of wind generation. Generally, wind generation is abundant as the cold front moves through, but there is uncertainty in the extent of the wind lull that follows the front, both temporally and spatially. The severity of the lull determines the magnitude of the required response from the rest of the system.
4. Increased PV capacity drives system operational changes during summer months and this does not change during heat waves. However, the contribution from wind after sunset differentiates the level of system operation stress caused from one heat wave to another.
5. Understanding the characteristics and diversity of wind and solar resources—at small and large geographic scales—is key to assessing their contribution to resource adequacy. Operating existing and expanded transmission more flexibly than today enables that contribution.
6. In areas where hydropower is abundant, its availability and flexibility are key to mitigating system stress during extreme weather events.
7. Broad, interconnection-wide impacts from wind turbine blade icing and cold temperature shutdowns are rare. However, regional icing and cold temperature events can be significant and rely on local gas generation dispatch and interregional transmission flows to maintain adequate supply to meet demand.
8. Tropical storm impact on renewable resource availability is localized and of less impact than direct damage to generation, transmission, and distribution infrastructure.

These findings are specific and limited to the events from the historical data set and to the grid infrastructure futures considered, but they point to an overarching conclusion: the most concerning events to the resource adequacy of the future system are different than the concerning events of today. Future research is needed to investigate applicability of these findings to: (1) other weather conditions, beyond the limited sample of weather events from 2007–2013 explored here and including those that capture further influence of climate change in the coming decades; and (2) other grid infrastructure futures.

Finding 1. Wind and solar generation tend to be available during the extreme weather events of today and do not introduce new resource adequacy concerns or system operation stress as their annual energy penetration increases. Exceptions exist, but they tend to be short periods of elevated net load.

Impactful weather events that significantly impact grid infrastructure and operations can be divided into two rough categories: those that drive high load (e.g., heat waves and cold waves) and those that impact transmission and generation infrastructure (e.g., thunderstorms, ice storms and snowstorms, and windstorms). Some weather events fall into both categories. For example, extreme cold waves driving record wintertime load may be accompanied by ice, snow, and wind that damages transmission infrastructure and increases thermal generation outage rates. Similarly, heat waves can cause transmission and generation outages and derates, in addition to driving up load.

Here, we examine how the extreme weather of the "High-Impact Events" listed in Table 4 (page 17) impacts the wind and solar generation potential, and we assess whether increased VRE penetration could worsen capacity and energy concerns during these events. At the time these events occurred, the multiday cold or heat waves all drove load higher and often caused disruptions to the generation and transmission infrastructure. In this section, for each event, we compare load to net load, and we examine how the distribution of daily average load compares to the distribution of daily average net load, to isolate the impact of increased VRE. In each case, the distributions include the 29 days surrounding the middle of the event (fourteen days on either side and inclusive of the event) for all 7 years of available data. Each distribution is made up of at least 203 days (more depending on the length of the event) and will be referred to as the seasonal distribution. Table 5 (page 25) shows the percentile within the seasonal distribution of load and net load across the full data set for each day of each event across all three interconnections. In the table, values of 100 or close to that are examples of days with the highest load or net load in the data set for that time of year. The full meteorological summary and impact of each event is examined in detail in the appendix. As stated in the Caveats and Limitations section, the wind generation profiles used to support this finding are without the impact of turbine blade icing and low temperature shutdowns; The impact of blade icing and low temperature shutdowns is discussed in Finding 7. Also, we do not attempt to capture persistent snow cover on PV panels at any point in this report.

In general, the variable renewables added in these scenarios generate at statistically common levels for the season during the extreme weather events of today. Figure 7 compares the time series of 2050 load to net load for each infrastructure plan, across all four events. The shape of the load profile is assumed to be the same across all three infrastructure plans, but there is load growth moving from 2024 to 2036 to 2050. Since weather defines the amount of renewable generation, but only modulates total load, we expect more variability in net load, as can be seen in Figure 7. Often the generation from wind and solar can reduce the burden of extreme high loads that are typical of these extreme weather events. However, there are days and hours during these events when net load is still among the highest in the data set, suggesting wind and solar do not mitigate all periods of resource adequacy stress caused by these events. However, the periods of high net load are not as protracted as the periods of high load, and net load peaks are always well below load peaks. In some cases, adding wind and solar can change which day of a weather event would require the most thermal or hydropower generation to meet demand.

Comparing a shift in a day's load percentile to net load percentile helps determine whether renewable generation on that day was available and if it was significant enough to mitigate high loads. The data in Table 5 generally shows how available renewable resources change which days could be most challenging to meet net load during these weather events. In some cases, peaks in load and net load occur on the same day and at times reside together at the high end of the distribution of seasonal load and net load, respectively. But in these cases, the surrounding days fall outside of the high end of the net load seasonal distribution, while continuing to be in the high end of the load seasonal distribution. The TI during the Cold Wave event is an example of this, where both load and net load peak on February 3, but net load percentile falls much more than the load percentile during the other high load days of the event. In other events, renewable generation is available on the peak load day such that the peak net load occurs on a different day. This is seen in Heat Wave 1 in the EI. July 21 is the peak load day for the event, but the peak net load day has been shifted earlier to July 19.

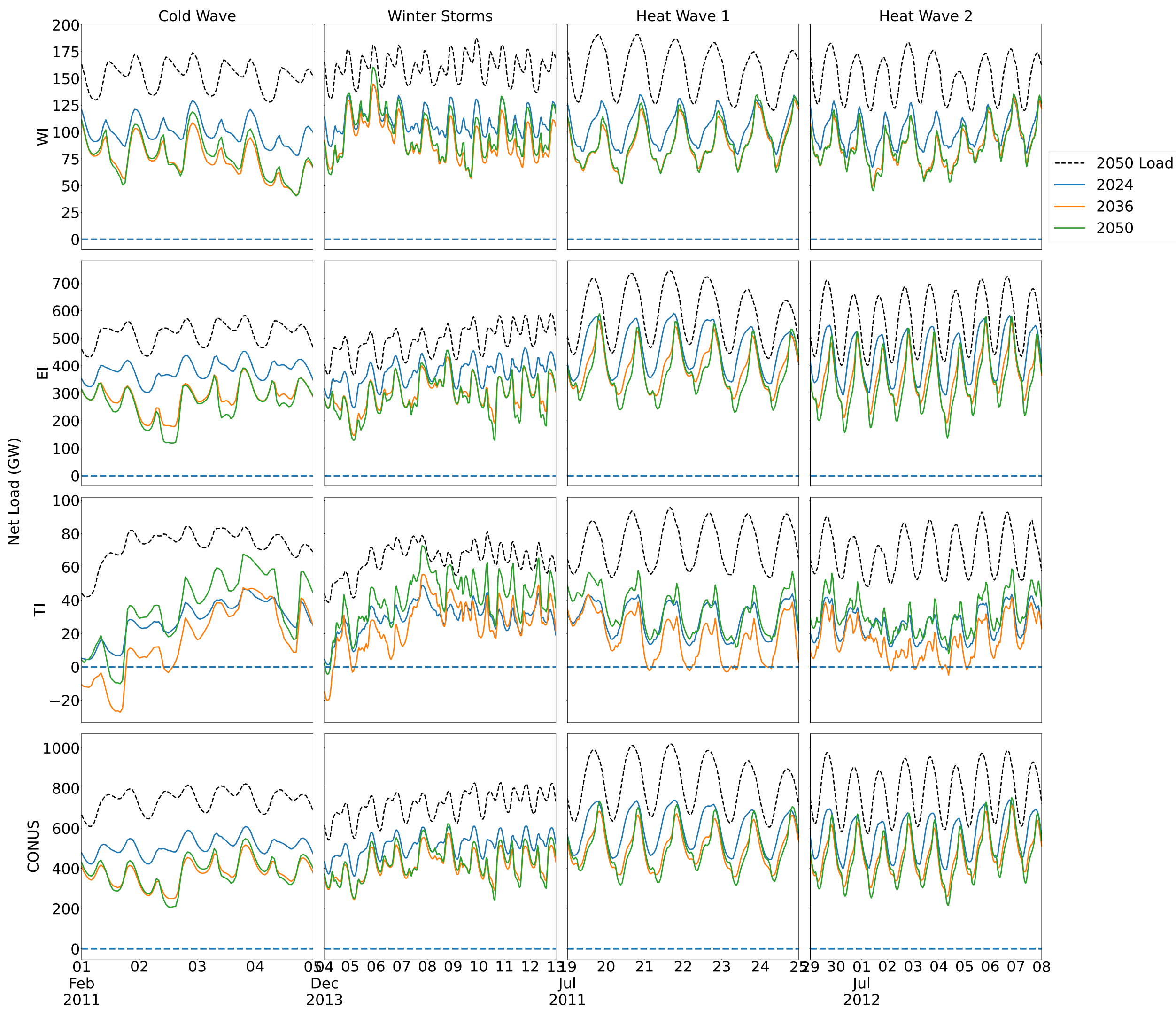

Figure 7. 2050 load (dashed lines), and net load for 2024 (blue), 2036 (orange), and 2050 (green) infrastructure years for the Cold Wave, Winter Storms, and Heat Wave events

Table 5. Comparison of Daily Average Load Percentile within Month around Date to Daily Average Net Load Percentile within Month around Date over the Full 7-Year Data Set for the 2050 Infrastructure Plan. Green shading indicates lower percentiles, while yellow indicates higher percentiles.

Interconnect		TI		EI		WI	
Event	Day	Load Percentile	Net load Percentile	Load Percentile	Net load Percentile	Load Percentile	Net load Percentile
Cold Wave	1-Feb	91.8	31.1	69.4	32.7	92.9	58.2
	2-Feb	99.5	81.1	71.9	21.9	98.0	70.4
	3-Feb	100.0	100.0	90.3	57.1	95.4	52.0
	4-Feb	99.0	87.2	82.7	62.2	74.0	4.6
Winter Storms	4-Dec	39.6	51.9	29.2	18.2	79.9	89.9
	5-Dec	81.2	83.8	40.3	46.8	84.2	100.0
	6-Dec	98.7	85.1	61.7	66.9	96.1	90.3
	7-Dec	100.0	100.0	67.5	90.9	91.6	77.3
	8-Dec	96.8	99.4	78.6	94.2	90.9	64.3
	9-Dec	98.1	98.1	91.6	72.7	98.7	49.4
	10-Dec	99.4	94.2	92.2	57.8	96.8	85.7
	11-Dec	97.4	95.5	96.5	70.8	92.9	72.7
	12-Dec	92.9	88.3	96.8	77.9	89.6	76.6
Heat Wave 1	19-Jul	59.5	91.1	97.6	99.4	75.0	13.1
	20-Jul	72.0	32.7	98.8	80.4	65.5	22.6
	21-Jul	85.7	13.1	100.0	95.2	49.4	26.2
	22-Jul	78.6	8.3	99.4	98.8	38.7	25.6
	23-Jul	71.1	5.4	87.5	83.3	13.1	50.0
	24-Jul	60.1	20.8	65.5	94.0	8.9	50.6
	25-Jul	92.3	54.8	81.0	97.0	51.2	28.6
Heat Wave 2	29-Jun	79.9	64.9	98.7	80.5	73.4	55.8
	30-Jun	29.2	55.8	79.2	80.5	34.4	48.7
	1-Jul	6.5	18.8	76.6	76.0	20.1	2.0
	2-Jul	45.5	15.6	96.1	89.0	58.4	57.8
	3-Jul	58.4	19.5	98.7	87.7	59.7	26.0
	4-Jul	38.3	13.6	90.9	66.2	10.4	36.4
	5-Jul	72.7	44.2	99.4	98.1	24.0	65.6
	6-Jul	75.3	68.8	100.0	99.4	42.2	82.5
	7-Jul	39.6	75.3	98.1	92.2	26.0	79.2
	8-Jul	20.8	75.3	76.0	83.8	26.6	76.0

Figure 8 shows the wind, solar, load, and net load for the 2050 infrastructure plan in the TI for the Cold Wave event, which is based on a record cold event from February 1 through February 4, 2011. The impact of the cold temperatures leads to well above-normal seasonal loads, with loads in the 91st to 100th percentile all 4 days. Wind generation is available early in the event as load rises rapidly. On February 1, net load is below normal because of well-above-normal wind and above-normal PV production. On February 2, load is nearly in the 100th percentile relative to the seasonal distribution, but net load is reduced to the 81st percentile, again because of above-normal wind. However, the following day, February 3, wind and solar generation decreases and the peak load and peak net load days occur on the same day. The TI experiences its 25th-highest net load on February 3 and is the highest load and net load day for this time of year across all 7 years studied. The extreme high load is driven by the cold air that remained in place, and net load peaked in the afternoon as the sun began to set and wind fell below normal. For the day, wind generation is still above the median seasonal availability, while solar drops to the 18th percentile. This example shows that while strong winds are associated with the arrival of cold weather at the onset of the event, there can be a reduction in wind generation to below normal after the front moves on. In this case there is a drop in the wind generation on the evening of February 3 into February 4 to below average levels, but not to statistically uncommon levels. The cold wave's impact on the wind resource will be discussed more in Finding 4.

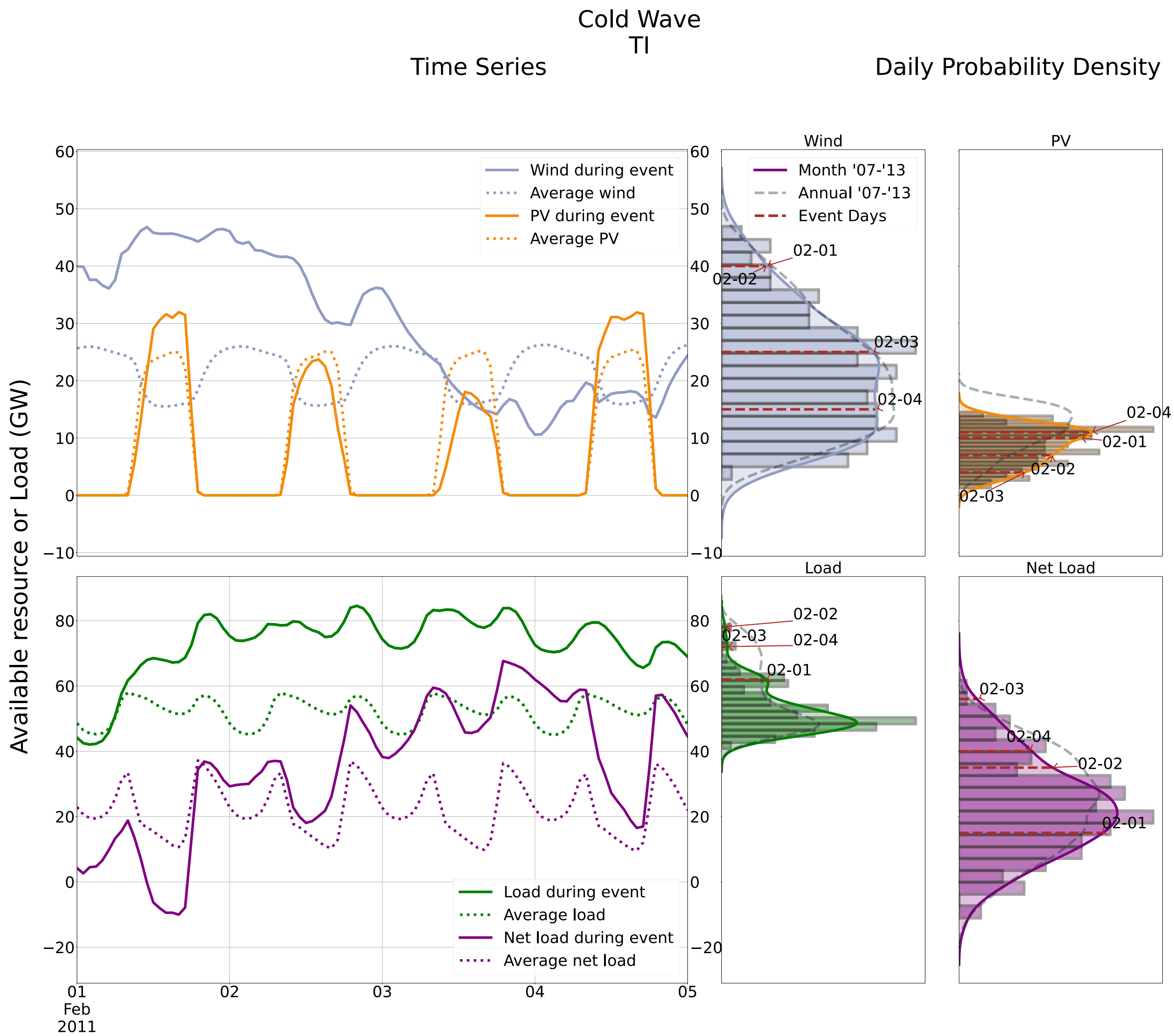

Figure 8. Wind (blue-gray), solar (orange), net load (purple), and load (green) hourly time series (left) and average daily generation probability densities (right) for the February 2011 Cold Wave event in the TI for the 2050 infrastructure plan in the TI

The time-series plot (left) shows the actual values during the event (colored time series) in relation to the average values for that time of year (dotted time series). The distribution (right) shows the average daily values (GW) for the time of year (colored distribution), the yearly distribution (gray dotted distribution), and the location of the event days in the distributions (red dotted lines with the day labels).

Another example of general availability of wind and solar during a High-Impact event was the December 2013 Winter Storms event. During this event, the historical load is well above normal in all three interconnections from December 7 through December 13, as seen in Table 5. In particular, in the WI, load is elevated above normal for the whole event, with a peak load at around 187 GW, 98th percentile of seasonal load, on the evening of December 9 and most of the days of the event above the 90th percentile for seasonal load. However, above-average wind and solar generation occur concurrently, on the peak load day of December 9, such that what is a 98th percentile load day is only a 49th percentile net load day. The peak net load day is December 5, which is 100th percentile for net load relative to the seasonal distribution, and it shifted to earlier in the event than load because of wind resources that were below normal at that time (Table 4). This is caused by the combination of cold surface air, radiational cooling, and high pressure aloft that all conspired to produce weak pressure gradients and a strong surface inversion across most of the West after cold air moved into the region on December 4.

For the EI, a similar switch occurs between the peak load day and the peak net load day. Figure 9 shows the time series and daily average distribution summary for the EI during the Winter Storms event. December 12 has the highest load of the event in the EI because of the cold, but net load is closer to average for the season. However, December 7 and 8 were near-normal load days, but they have very high net loads due to poor wind resource in normally wind rich regions sitting between two storms. This is similar to the Cold Wave event, with a period of cold stagnant weather following an initial cold wave, even when the cold was moderating, causing wind resource to diminish faster than load. Much of the EI also experiences poor solar resource because of fog and clouds on the days of the events. Thus, the period within this event that is of most concern is the peak net load day for the event in the 2050 plan, while the highest load periods during these storms are less concerning because of the availability of VRE.

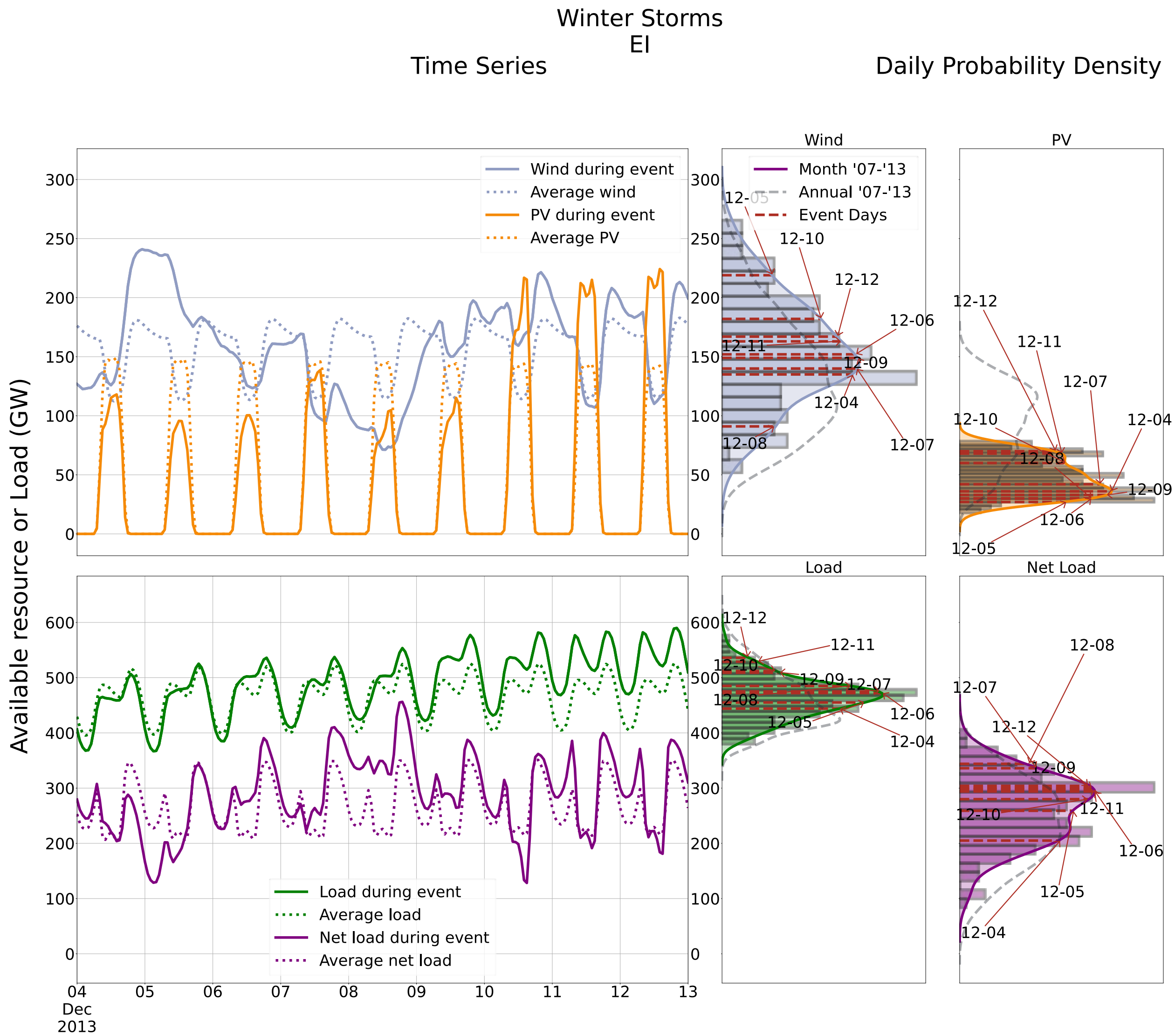

Figure 9. Wind (blue-gray), solar (orange), net load (purple), and load (green) hourly time series (left) and average daily generation probability densities (right) for the December 2013 Winter Storms event for the 2050 infrastructure plan in the EI

The time-series plot (left) shows the actual values during the event (colored time series) in relation to the average values for that time of year (dotted time series). The distribution (right) shows the average daily values (GW) for the time of year (colored distribution), the yearly distribution (gray dotted distribution), and the location of the event days in the distributions (red dotted lines with the day labels).

Heat wave events also show that wind and solar resources tend to be available on peak load event days, changing the distribution of which days are most extreme when comparing load to net load. For example, the EI peak load day for the entire seven year data set is July 21, 2011 and occurred during the Heat Wave 1 event. The event is summarized for the EI in Figure 10. This day experiences above-normal wind resource and slightly above-normal solar resource in the EI so that the overall net load in 2050 is no longer the peak day. However, 2 days before in the evening of July 19, despite loads being lower, the setting sun combined with below-normal wind generation leads to the peak in net load on July 19 for the event (Figure 10). Though the net load is 7% lower than the highest net load day in the seven year data set.

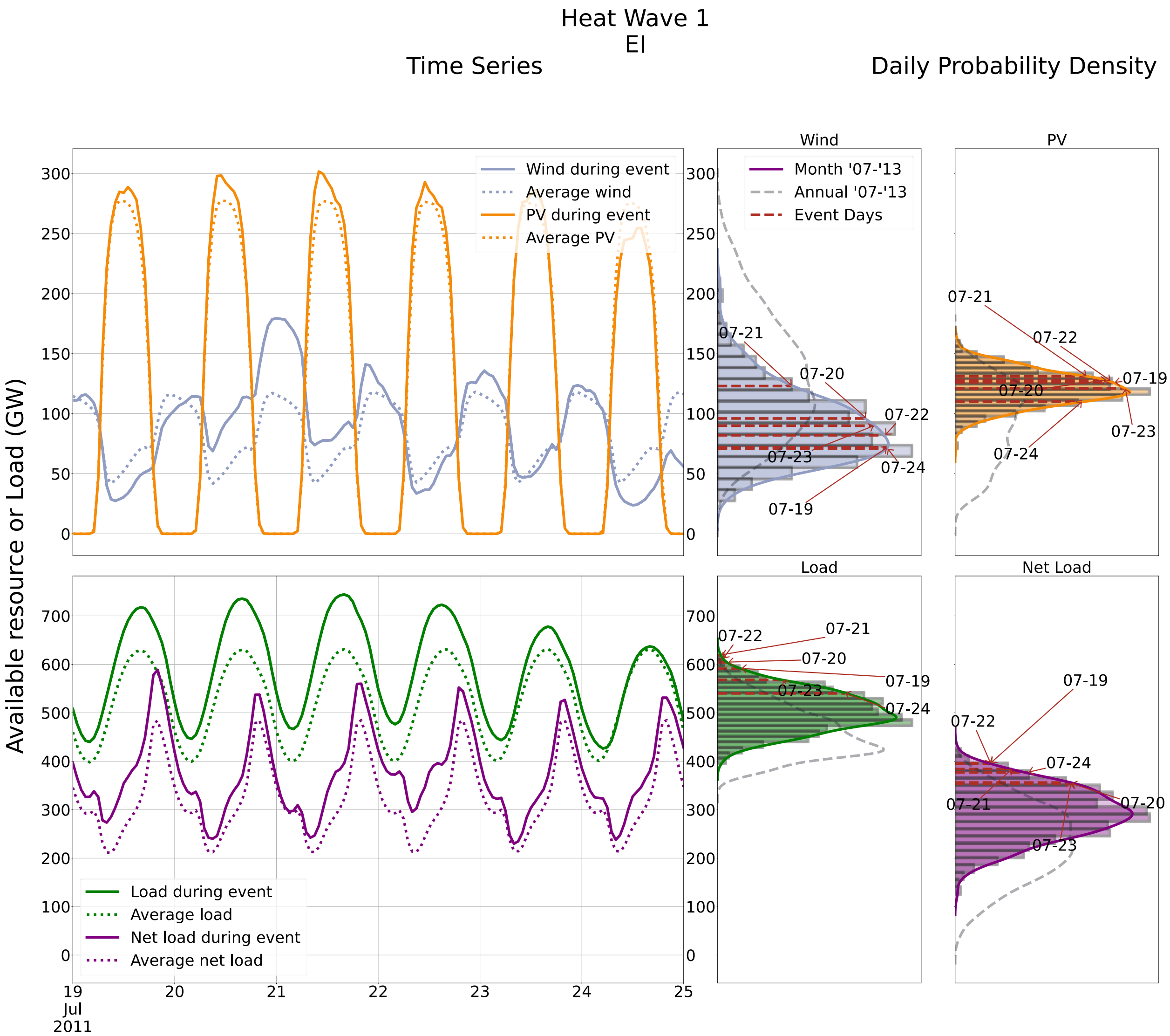

Figure 10. Wind (blue-gray), solar (orange), net load (purple), and load (green) hourly time series (left) and average daily generation probability densities (right) for the Heat Wave 1 event for the 2050 infrastructure plan in the EI

The time-series plot (left) shows the actual values during the event (colored time series) in relation to the average values for that time of year (dotted time series). The distribution (right) shows the average daily values (GW) for the time of year (colored distribution), the yearly distribution (gray dotted distribution), and the location of the event days in the distributions (red dotted lines with the day labels).

Heat Wave 2 in July 2012 has a similar effect on the EI, with many of the net load days being lower in the distribution than load days. However, in this case, days with low wind resource in the EI also coincided with the maximum demand on the EI on July 5 and 6.

As Finding 1 states, there are exceptions during these events that do lead to elevated net load for a short period. As seen in Table 5, the Winter Storms at different points hits the 100th percentile of the seasonal average net load in the TI and WI, and reaches the 94th percentile in the EI. The Cold Wave event in the TI also reaches the 100th percentile of the seasonal average net load. With the exception of the December 5 during the Winter Storms event in the WI, the elevated net loads are the same days as the highest load day during the event. This supports the finding that during the extreme weather events of today, VRE is not adding additional resource adequacy concerns. Variable renewable energy does shift the concerning day during the Winter Storms event in the WI. Load hits the 98th percentile of the seasonal distribution, the highest of the event, 5 days after the peak net load day. But after the peak net load day, the average daily net load drops out of the high end of the seasonal distribution. The case studies presented here support the finding that during the extreme weather events of today, variable renewable energy is not adding additional resource adequacy concerns and are available at common levels. Operators and planners should be aware that days like the exceptions we have described can occur, but they do not present the extended resource adequacy concerns of other weather events, which will be discussed in Finding 2.

In summary, there is a significant shift away from temperature-driven demand being the primary system stress and toward a more complex combination of wind resource and solar resource availability, combined with temperature-driven demand. In general, the addition of VRE in the quantities and regions modeled can mitigate extreme loads during extreme temperature events. In some cases, it can change which day would be most challenging to meet with dispatchable thermal and hydropower generation. Reasons for this include that summertime high loads occur on sunny days and wintertime high loads tend to coincide with the arrival of cold air that is brought in by strong winds. However, there is considerable nuance in these interactions, and as penetration increases, the details will become increasingly important.

Finding 2. Mild weather conditions can produce extended periods of low wind and solar resource. Historically, the weather during these events would not be a reason for concern among system planners and operators, but with the increasing contribution of wind and solar generation, these events need to become a focus of planners in order to ensure system adequacy.

As the penetration of variable renewable generation increases, a new type of "extreme" will become increasingly important to system planners and operators: widespread low wind and solar resource during moderate to high loads leading to extremely high net loads. These very high net load days may not be coincident with the summer or winter peak load, which tend to determine generation and transmission capacity needs under today's approach to system planning.

We identified four events characterized by periods of high net load driven by moderate to high load and very poor renewable resources. These are listed in Table 4 (page 17) as the Winter Net Load 1–3 events and the Summer Net Load event. The hourly net load profiles for these events are shown in Figure 11, along with 2050 load profile. Though the total demand is lower in these events than in the high-impact events covered in the section above, the gap between net load and load is narrower because VRE output is low for portions of all these events. We also compare the daily percentile load and net load for each day in the events in Table 6. The difference between the load and net load percentiles emphasizes how for these events, days with otherwise normal or above-normal load can become days with very high or extreme net load. In other words, load during these events is closer to the middle of the distribution of seasonal loads and therefore more common for the system to encounter. But due to low wind and solar output relative to normal, the net load during the event ends up in the high tail of the seasonal net load distribution, a system state that occurs infrequently.

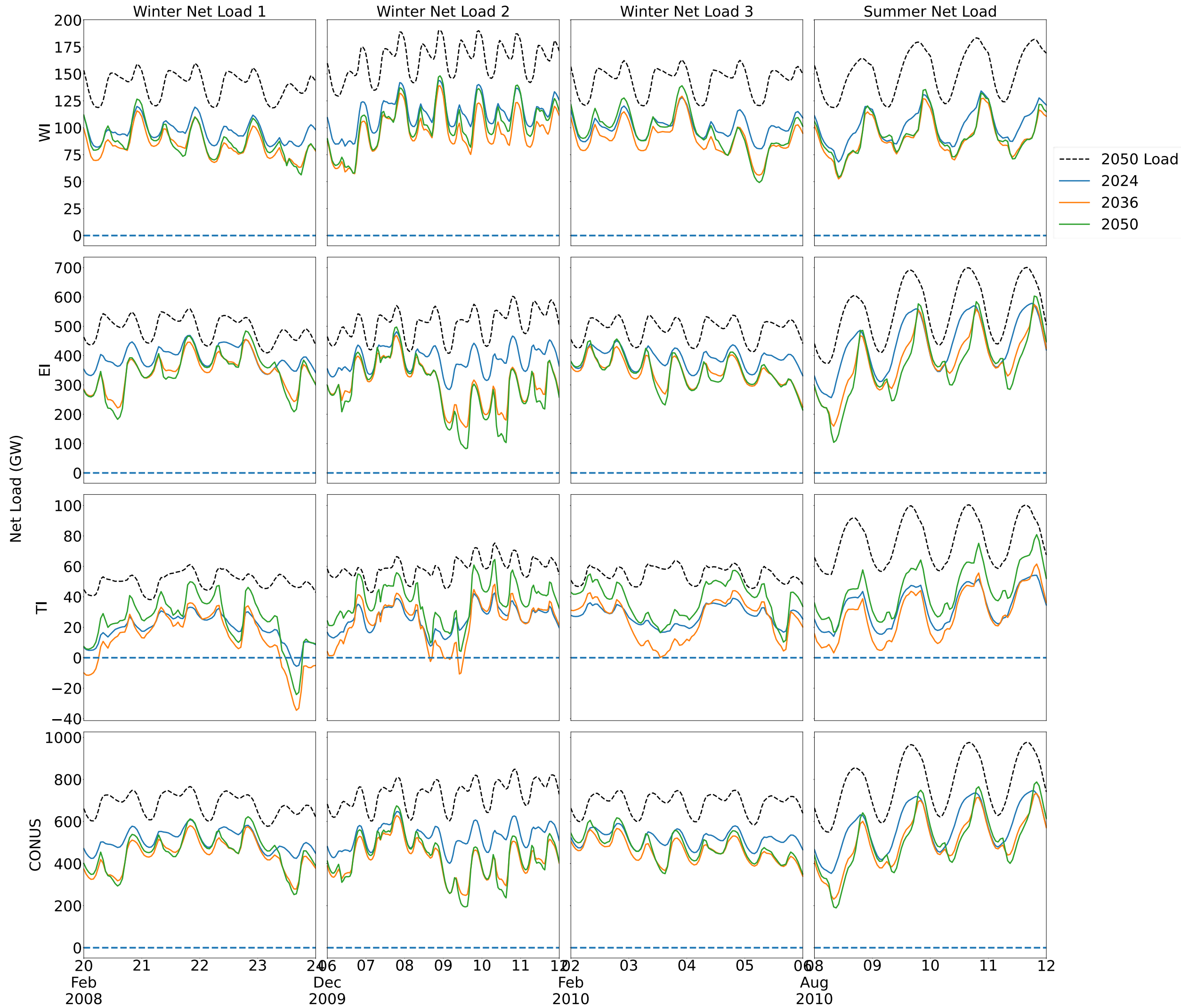

Figure 11. 2050 load (dashed lines), and net load for 2024 (blue), 2036 (orange), and 2050 (green) future years for the Winter Net Load 1 – 3 and Summer Net Load events.

Times are in Eastern Standard Time (EST).

The Winter Net Load 1 and 3 events are not noteworthy either meteorologically or from a load perspective: temperatures are not extreme, nor are there storm systems that would otherwise affect electric infrastructure. Winter Net Load 2 does see elevated loads, especially in the WI where the load is above the 95th percentile of the seasonal average daily load distribution for 5 consecutive days. The West Coast experienced very cold temperatures, which drove up load in the WI and is a weather event that may stress the contemporary system. However, the weather and load impacts in the EI and TI are not particularly noteworthy from the perspective of today's system. Compared to the Cold Wave and Winter Storms events highlighted with Finding 1, these three events tend to have lower loads but significantly higher net loads. For example, in the EI, the 2050 peak hourly net loads (Figure 11) are 484 GW, 497 GW, and 456 GW for the Winter Net Load 1, 2, and 3 events respectively, compared to 391 GW for the Cold Wave and 456 GW for the Winter Storms events. Table **6** shows the days of the event that have normal- to above-normal load and very high net load. In the EI during Winter Net Load 1 event, the load on February 22 reaches the 78th percentile of the seasonal load but the 100th percentile in seasonal net load. Similarly, in the WI during Winter Net Load 3 event, February 3 has load in the 56th percentile of seasonal load but net load in the 96th percentile.

Table 6. Comparison of Daily Average Load Percentile within Month around Date to Daily Average Net Load Percentile within Month around Date over the Full 7-Year Data Set for the 2050 Infrastructure Plan

Interconnection		TI		EI		WI	
Event	Day	Load Percentile	Net load Percentile	Load Percentile	Net load Percentile	Load Percentile	Net load Percentile
Winter Net Load 1	20-Feb	50.0	73.6	79.7	78	52.2	92.3
	21-Feb	71.4	93.4	89.6	98.9	61.5	90.7
	22-Feb	78.0	91.2	78.0	100.0	51.1	81.9
	23-Feb	50.5	30.8	34.1	96.2	16.5	62.6
	24-Feb	18.7	60.4	21.4	68.1	7.7	16.5
Winter Net Load 2	6-Dec	73.2	78.0	66.1	79.8	60.1	37.5
	7-Dec	75.0	95.2	85.1	100.0	95.8	95.2
	8-Dec	69.0	57.1	81.5	73.8	98.2	97.0
	9-Dec	87.5	75.6	82.1	10.1	100.0	92.9
	10-Dec	95.8	92.9	93.5	32.1	99.4	95.8
	11-Dec	89.3	88.1	98.2	54.2	97.6	94.0
	12-Dec	61.9	84.5	84.5	38.7	78.6	61.3
Winter Net Load 3	2-Feb	73.1	91.2	57.7	98.9	56.6	96.2
	3-Feb	78.0	58.2	51.6	85.2	58.2	97.8
	4-Feb	76.9	96.2	54.9	90.7	51.6	68.7
	5-Feb	56.0	79.1	42.3	55.5	42.3	64.8
	6-Feb	50.5	67.0	28.6	36.3	11.5	85.7
Summer Net Load 4	8-Aug	40.7	15.9	28.0	20.9	3.8	18.1
	9-Aug	81.3	57.7	90.7	96.2	23.6	54.9
	10-Aug	89.6	89.6	96.2	99.5	36.8	45.6
	11-Aug	97.3	98.4	97.3	100.0	40.7	31.3
	12-Aug	91.2	96.2	94.0	95.6	44.5	28.0

The high net load winter events are driven primarily by daily deviations in wind that are below the median coupled with high but not necessarily the high loads seen in the events in Finding 1. However, below average solar coupled with multiday low wind events during this time period combine to make a very high net load day. The Summer Net Load event also is particularly sensitive to low wind generation leading to high net loads relative to the seasonal distribution. This event, and others like it, tend to be clear days but stagnant air that produce average to above average solar generation and low wind output. As will be discussed in Finding 4, we did not investigate widespread wildfire haze that may limit the solar generation during events like the Summer Net Load event. This should be the focus of further research.

The time series of load, net load, wind, and solar generation in the EI for Winter Net Load 1, which occurred in February 2008, exemplifies this type of event and is shown in Figure 12. Here, cold weather led to slightly elevated loads and depressed wind generation. During this event a vigorous storm system tracking east opens the door to cold air moving south, with a second system following rapidly behind, reinforcing the cold. As the cold air spreads east and deepens, pressure gradients equilibrate, and wind generation gradually decreases. Even though there is little moisture to work with, the cold front still produces clouds. From February 21 – 23, a weak storm develops on the cold front over the deep south pushing moisture northward. This combined with the prevailing high pressure and light winds yields clouds and widespread light fog, dropping solar below average. The highest load occurs on February 21, but the peak net load occurs on February 22.

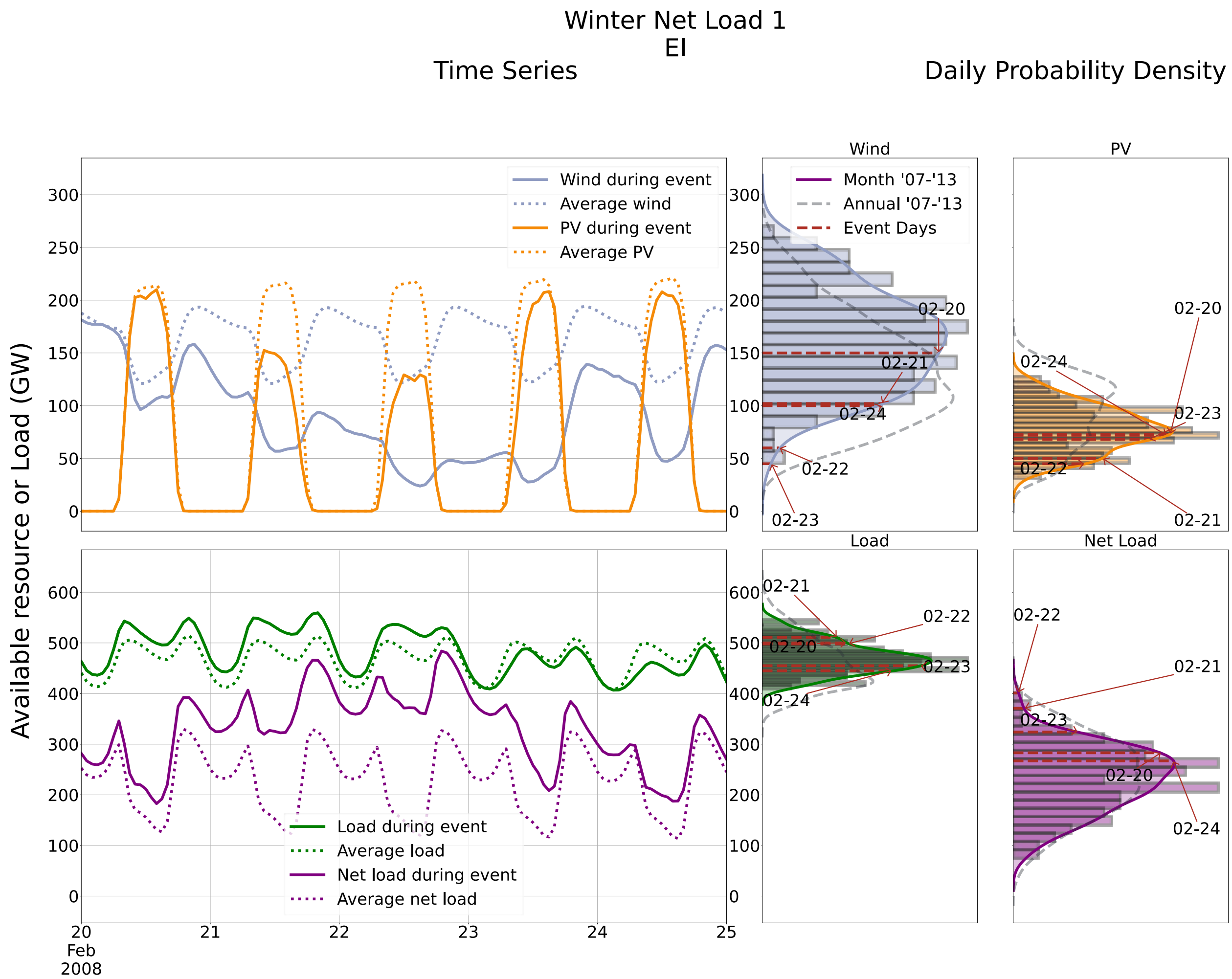

Figure 12. Wind (blue-gray), solar (orange), net load (purple), and load (green) time series in the EI for the Winter Net Load 1 event with surrounding period average shape shown as dashed lines

The time-series plot (left) shows the actual values during the event (colored time series) in relation to the average values for that time of year (dotted time series). The distribution (right) shows the average daily values (GW) for the time of year (colored distribution), the yearly distribution (gray dotted distribution), and the location of the event days in the distributions (red dotted lines with the day labels).

In extreme weather events like these with extended low wind, the widespread geographic extent of stagnant weather conditions limits the benefits of geographic resource diversity. The Winter Net Load 3 event, which occurred in February 2010, has extended low wind and solar resource across nearly all of the EI, with February 2 being both the lowest wind resource day in the seasonal distribution and only reaching the 7th percentile for solar generation. The geographic extent of the resource deficit is shown in Figure 13, including every region in the EI experiencing below average wind generation potential, except for small pockets of average wind potential in Missouri and North Carolina. These conditions arise from stagnant weather patterns. Overall, conditions appear to be mild with little precipitation or wind on February 2, and most of the country is cloudy and cool with conditions that remain largely unchanged until February 5. Periods like these will become increasingly important for system planning, as there is little contribution to resource adequacy from onshore wind or solar geographic diversity during such a widespread event. Larger deployment of offshore wind was not considered as part of the infrastructure plans and may add unique diversity value to offset the widespread low onshore wind during events such as Winter Net Load 3.

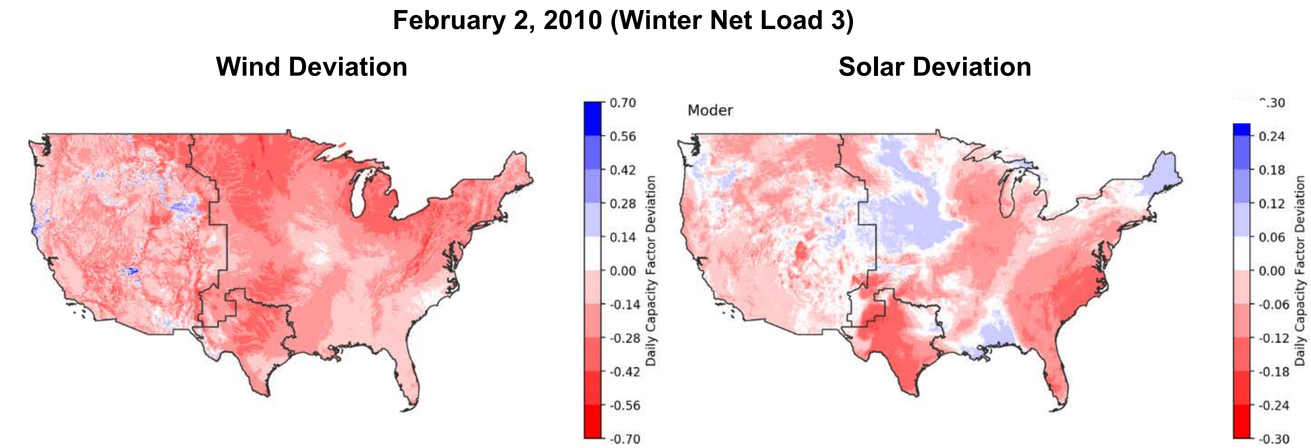

Figure 13. Daily wind and solar resource deviation for February 2, 2010 during the Winter Net Load 3 event

The deviation is difference between the capacity factor during the event to the average capacity factor for the 29 days around the event for all 7 years. Areas in red are below average capacity factors for that time of year, while areas in blue are above average.

The Summer Net Load event highlights how even though PV generation tends to be highest during this time of year, and is even higher than normal during the event, the combination of low wind and high load can produce an extremely high net load. In general, wind generation is lower during the summer months than in the winter months, and for this event, wind generation declines as the hot weather increases load. Figure 14 shows the time series and distribution for this event in the 2050 infrastructure year and demonstrates this combination for the EI. From the August 9 to August 12, declining wind generation drives each day's net load to be a higher percentile rank than that day's load (Table 6). While solar PV is not the primary driver for this event, the time series shows the peak net load on the August 11 occurs during the evening at sunset. The result is the highest net load hour and day in the EI for the entire data set.

The Summer Net Load event has 3 consecutive days with this combination of low wind and high load. Unlike cold waves, which are connected to changeable weather by atmospheric dynamics and thus have some synergy with wind generation and diverse solar resource, heat waves are associated with stable, quiescent conditions. Unless triggered by local scale circulations, such as canyon winds, sea breezes, and thunderstorm outflows, winds tend to be light. In addition, there is reduced vertical mixing, such that trapped aerosols and haze are prevalent, which have the potential to decrease solar generation. A shallow layer of stratus (most likely in winter) or fair weather cumulus (most likely in summer) clouds are often present. It is possible that in a larger meteorological data set there may be days where load is as high as the Heat Wave 1 event and which are accompanied by wind resource that is as bad, or slightly worse, than in the Summer Net Load event. Because wind is low and net load is occurring after sunset, additional wind and solar capacity would add little additional capability to serve load during the Summer Net Load event without supporting infrastructure, such as storage or responsive demand. As the diversity value of low-cost wind is saturated, events like these should be given increased attention for planning activities and as a motivation for research.

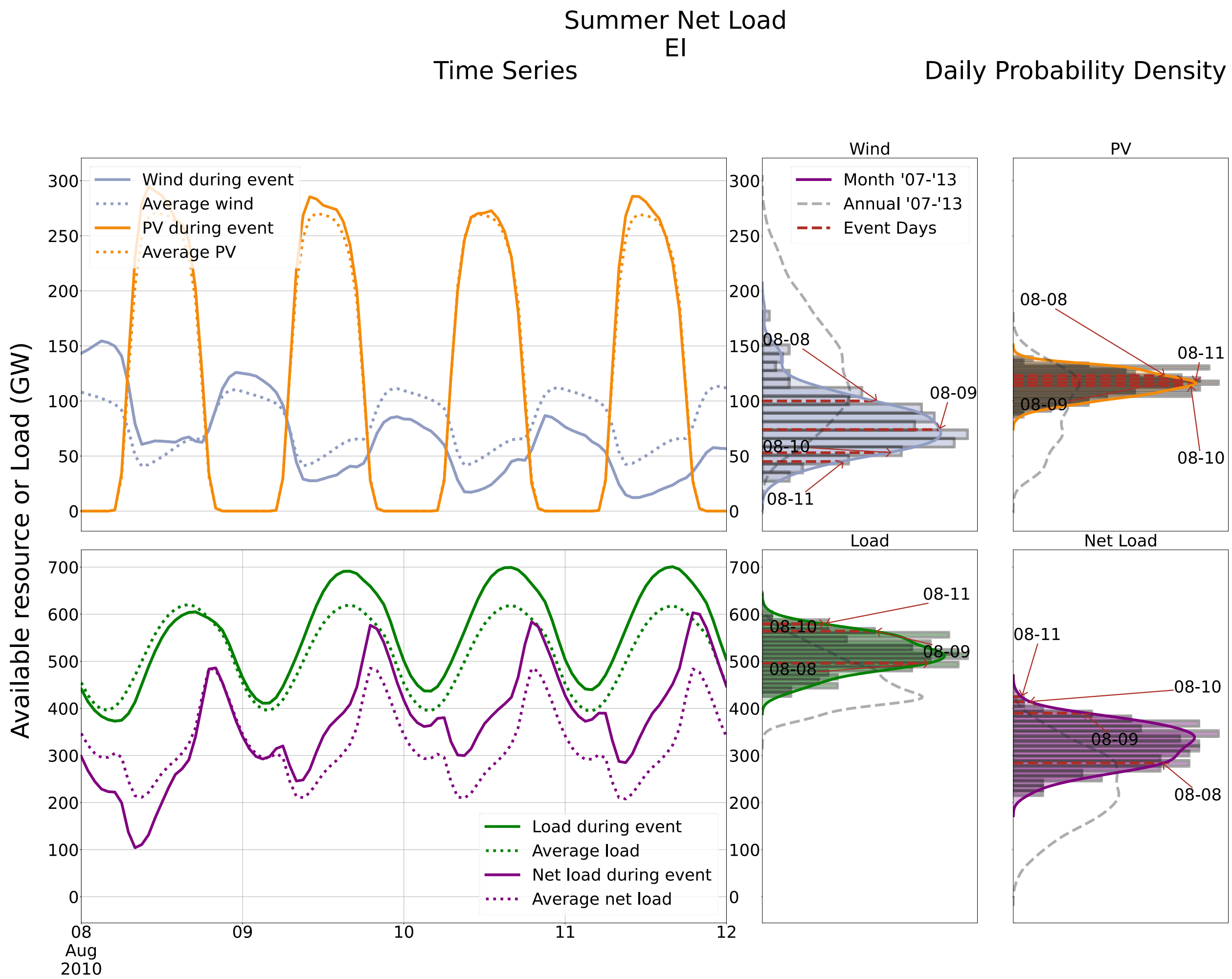

Figure 14. Wind (blue-gray), solar (orange), net load (purple), and load (green) time series in the EI for the Summer Net Load event with surrounding period average shape shown as dashed lines

The time-series plot (left) shows the actual values during the event (colored time series) in relation to the average values for that time of year (dotted time series). The distribution (right) shows the average daily values (GW) for the time of year (colored distribution), the yearly distribution (gray dotted distribution), and the location of the event days in the distributions (red dotted lines with the day labels).

Finding 3. Because cold waves occur in winter when solar generation is already low, system operations during cold waves is most heavily influenced by the performance of wind generation. Generally, wind generation is abundant as the cold front moves through, but there is uncertainty in the extent of the wind lull that follows the front, both temporally and spatially. The severity of the lull determines the magnitude of the required response from the rest of the system.

Operations during all types of events change due to an increasing contribution from variable renewable generation, but no type of event that we studied changed as much as cold waves. Historically, both cold and heat waves impact load magnitude and shape, but the timing and magnitude of the wind and solar resource during a cold wave changes the operations paradigm in important ways, and the impact is specific to the geography and meteorology of each region.

The Rocky Mountains roughly separate the EI and TI from the WI, and from a meteorological regime perspective, they divide the country. During the winter, they act as a guide that channels frigid pools of air that have formed in the Arctic and Canada southward and prevents them from dispersing toward the west. The typical evolution of a cold wave begins with storms moving inland from the Pacific. The storms then move across the Intermountain West, where their lower structure is disrupted by mountainous terrain, wringing out much of their moisture. An upper-air disturbance then emerges east of the Rocky Mountains, where the sudden drop in elevation helps reinvigorate the storm.[30] To the east of the low pressure system, warm air begins to move north and east, while cold air is pulled south in the region to the west of the center of the low pressure. The mountain barrier constrains the cold air leading to genesis and strengthening of a cold frontal zone that pushes south down the Front Range of the Rockies, drawing air out of Canada.

As such systems move eastward, guided by the jet stream, they will intensify if the conditions are right and thus open the door to allow cold air pooled on the Canadian Prairies to spin south and eventually east, as warm air flows north ahead of the system. As surface pressure drops in the strengthening storm, the pressure gradient between the cold dense air moving south and the warm air moving north intensifies and wind speeds increase, especially along the cold front. In simple terms, this is why cold waves are often observed moving down the Front Range urban corridor in Colorado and then off toward the east. The details of the evolution, such as how far the air moves south and how cold it is, vary from storm to storm depending on the storm's location and the depth and temperature of the cold air. These same variables also impact the strength of the wind at the cold front (which is where the air mass abruptly transitions) and behind it, into the colder air. They also define how long it will take before the pressure equilibrates and the wind dies down. Thus, a cold wave moving down the Rocky Mountains will bring wind, quickly followed by falling temperatures, possibly precipitation (or enhancement of precipitation if it has already developed in the warm sector ahead of the cold front), and then clearing skies and diminishing wind. The cold air will then either deepen or gradually moderate depending on the balance of nighttime cooling and solar heating, until another disturbance brings in air to replace it.

[30] The reasons for this are outside scope of this study but thinking of the increase in spin that occurs as a column of water is stretched down a drain is a reasonable analogy.

The southern United States is at a low enough latitude that even during the darkest winter days, cold air begins to moderate once it is no longer being transported in, so the extremely high wintertime loads rarely occur concurrently with really low wind resource, but above average loads can combine with very low wind resource and are sometimes exacerbated by low solar, to produce extremely high net loads. Such behavior means wind generation is very synergistic with conditions that increase the demand as cold waves move in, but it also means the wind will often diminish while demand remains high as the event decays. At this time, clear skies and cold temperatures can result in good solar production, but this is not always the case as moist air from the next system can start moving in on weak flow bringing clouds as it rides over the cold air. Fog and low clouds can also form if enough moisture is in contact with the cold ground. Thus, until the next storm arrives, even as temperatures moderate, wind and solar generation can remain low, yielding the highest net load after the coldest air has abated.

Figure 15 shows the relationship of 2050 daily average wind generation and 2050 daily average load for all days in the winter months for the EI. The day-to-day variability greatly increases as VRE penetration increases, and at first, it does not appear that there is a strong relationship between wind and load. However, one does exist; it is just buried in different regimes. In the appendix, we include analysis demonstrating that wind appears to be anticorrelated with load for CONUS when plotting the full 7-year time series on an hourly basis. However, looking at winter only and a daily average (Figure 15), we see that the bottom right corner of the plot is sparsely populated, indicating that when load is very high, there is usually some wind. Further, high loads are related to above-average wind generation. The lower plots of Figure 15 shows the relationship between load and net load trends to a less-steep gradient as load increases, suggesting that for peak wintertime loads, wind and solar tends to contribute when most needed. However, some days in the lower plot indicate that net load peaks not when loads are highest, but when they are moderately high. This is the impact of wind diminishing once the cold air is in place. These characteristics of wind influence wind's capacity credit, as discussed in Keane et al. 2011.

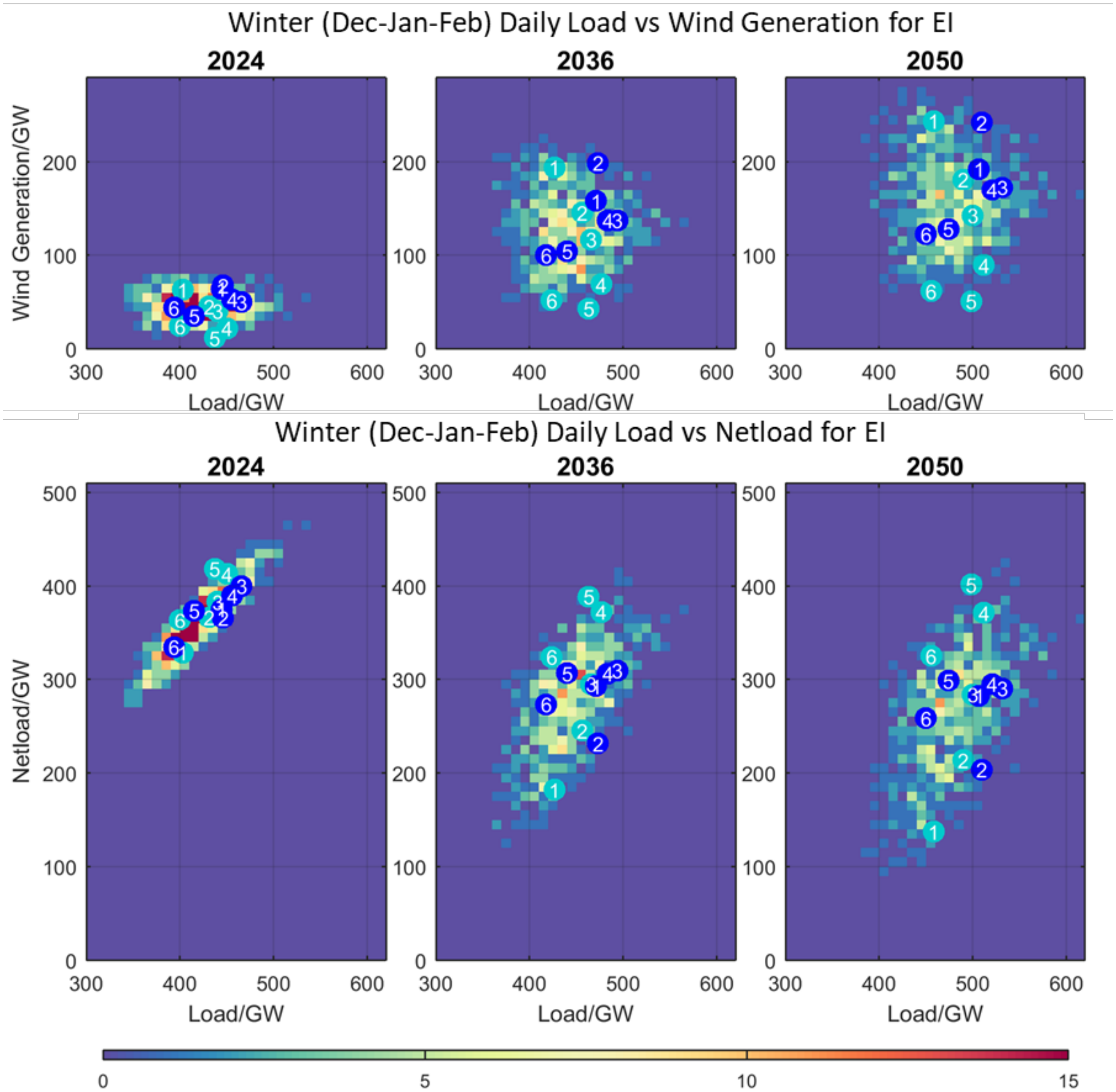

Figure 15. Relationship of load to wind generation (top) and load to net load (bottom) during the winter months for the EI for the 2024, 2036, and 2050 plans

The numbers show days from the start of two cold wave events, including the February 2011 Cold Wave event (blue dots) and the February 2008 Winter Net Load 1 event (Teal dots) (Table 4, page 17).

In addition to investigating the meteorology of cold waves and how they lead to changes to the wind and solar availability, we studied two different cold wave events in a PCM to understand how operations during those events change as the penetration of VRE on the system increased:

- The Cold Wave event: A "high-impact" event in early February 2011 (see Table 4, page 17)
- The Winter Net Load 1 event: a milder "planning-challenges" event in mid-to-late February 2008 (see Table 4, page 17).

While the Cold Wave event dropped temperatures across the county, the Winter Net Load event mostly reduced temperatures in the central and eastern United States, and both impacted system operations in the EI and TI.

Meteorologically, the Cold Wave event was notable for three key characteristics. First, the intensity and longevity of the cold in the southwestern and southern states was unusual as it lingered and was reinforced as it pushed south, west, and east. On February 2, 2011, the areal extent of the cold air was greatest, with almost a third of the CONUS experiencing low temperatures below 0°F (-18°C). Second, the intensity of the high pressure associated with the cold dense air reached 1,055 millibars (mb), which was close to the CONUS record of 1,058.5 mb. Last, the cold system spawned back-to-back storms that developed in the desert southwest, bringing snow and additional winter storm impacts to regions already affected by the cold.

Figure 16 shows the deviation of the daily wind capacity factor from normal for this time of year for February 1–4, 2011 during the Cold Wave event. As the cold sweeps across the EI and TI on February 1, it brings much stronger wind resource than normal to the Southwest Power Pool (SPP), Midcontinent Independent System Operator (MISO), and Electric Reliability Council of Texas (ERCOT) regions. As the cold lingers but the front moves out, some areas see a drop in the wind resource, which, as described earlier, is common when the wind is induced by a cold wave. However, the wind does not drop off as dramatically in the Upper Midwest, mitigating the system operations and adequacy challenges posed by this event.

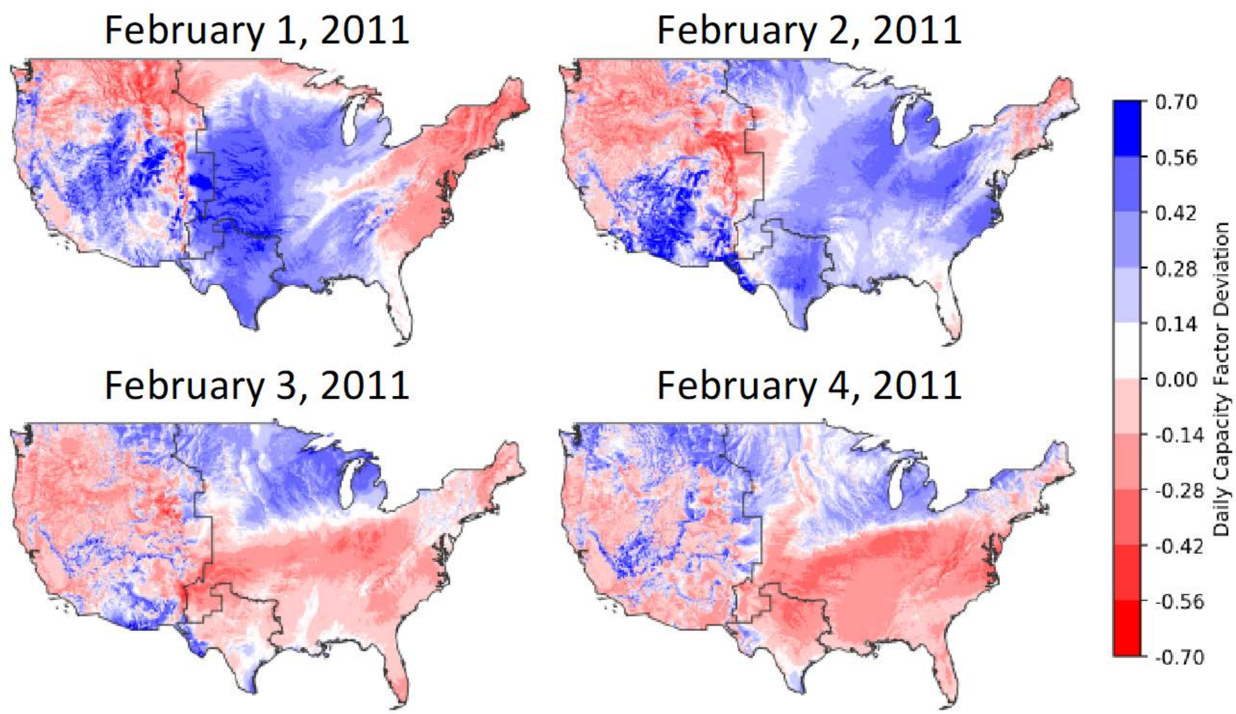

Figure 16. National daily average wind capacity factor deviation during the February 2011 Cold Wave event

The deviation is difference between the capacity factor during the event to the average capacity factor for the 29 days around the event for all 7 years. Areas in red are below average capacity factors for that time of year, while areas in blue are above average.

In contrast, the Winter Net Load 1 event, which occurred between February 18–23, 2008, is marked by rather unremarkable winter weather. A storm system moves through the Great Lakes area on February 18 and then continues north into the Canadian Maritime Provinces. Cold air is pulled out of Canada into the Midwest behind the storm. In the Upper Midwest, temperatures are cold enough to place major load centers like Minneapolis, Chicago, and Pittsburgh into the highest 2%–5% of heating degree days on February 19– 21, with moderation into the highest 15%–20% on February 22–23. Major East Coast load centers also experience temperatures that result in heating degree days in the highest 10% throughout the period. Further south, temperatures are cold but inconspicuous.

Figure 17 shows the wind deviation from normal in the days following the initial cold front during Winter Net Load 1. Not shown in the figure is a pickup in the wind resource as the front moved through, which is similar to the wind resource behavior observed in the Cold Wave event in 2011. However, throughout much of the EI, the wind resource drops and is well below normal in the days that follow and are the days shown in the figure.

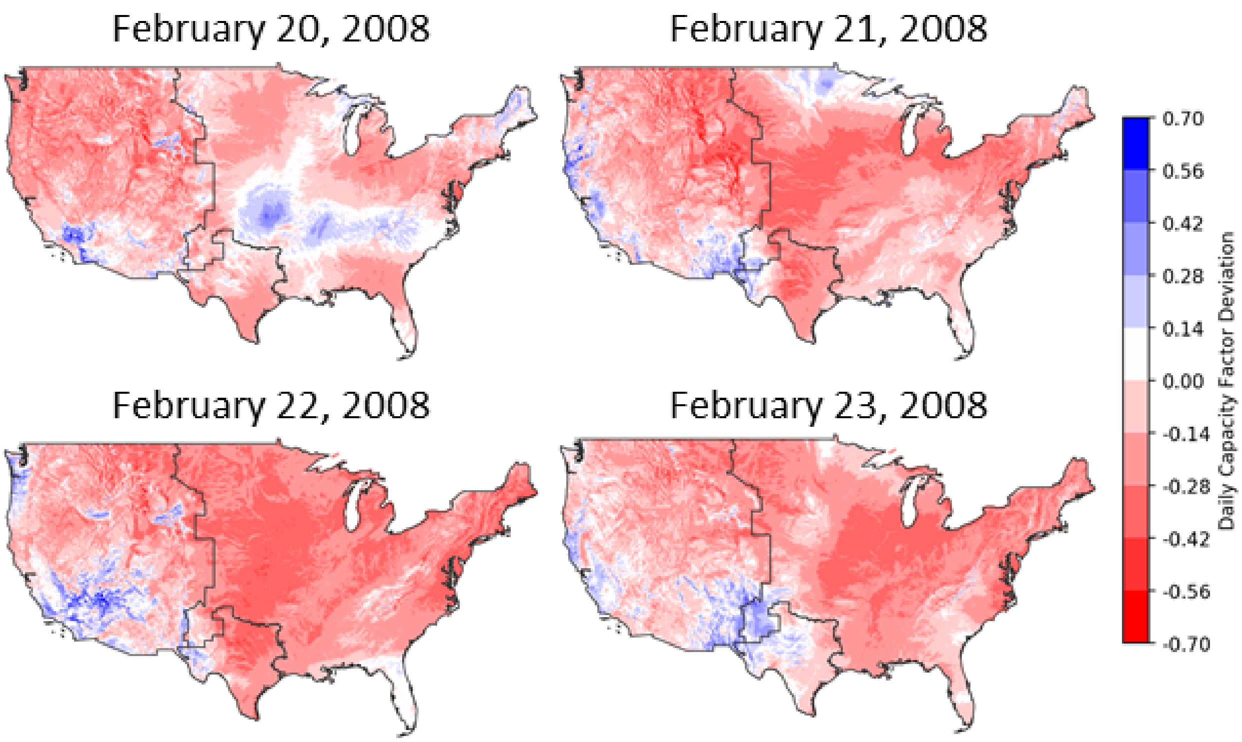

Figure 17. National daily average wind capacity factor deviation during the February 2008 Winter Net Load 1 event

The deviation is difference between the capacity factor during the event to the average capacity factor for the 29 days around the event for all 7 years. Areas in red are below average capacity factors for that time of year, while areas in blue are above average.

The difference in the way the wind resource recedes from its peak between the two events makes the Winter Net Load 1 event particularly challenging for future EI operations, while the resulting net load for the EI during the Cold Wave event is right at the average net load for that time of year. Figure 18 shows the net load time series of the 2050 system relative to normal and the daily average net load relative to the seasonal and yearly net load distributions. During the first days of the Cold Wave event in 2011, net load is depressed in the EI relative to normal because of the high wind resource; however, even as the wind resource dies down some, the net load only increases to be about normal for this time of year.

The net load in the TI is a different story. Because of the TI's smaller area and lack of large transmission connections with other interconnections, both events look challenging to TI operations as the cold wave dissipates. In the Cold Wave event, February 3, 2011—which is the third full day of cold temperatures in Texas but is well after the intrusion of the initial cold wave—is the 25th-highest net load day, and the 7th-highest among winter days, in the TI between 2007 and 2013 for the 2050 plan.

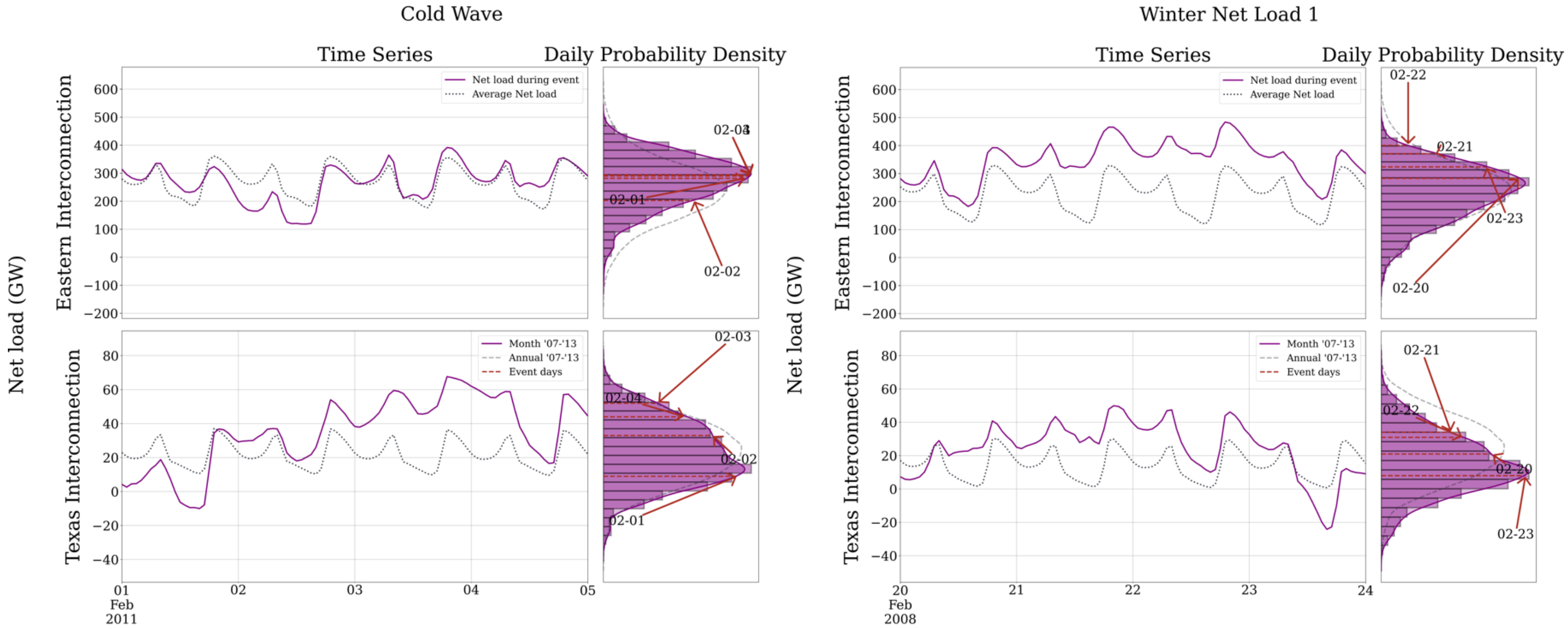

Figure 18. Net load time series in the EI and TI for the February 2011 Cold Wave event, modeled with the 2050 infrastructure, with surrounding period average shape shown as dashed lines

The time-series plot (left) shows the actual values during the event (colored time series) in relation to the average values for that time of year (dotted time series). The distribution (right) shows the average daily values (GW) for the time of year (colored distribution), the yearly distribution (gray dotted distribution), and the location of the event days in the distributions (red dotted lines with the day labels).

We simulated how the three future power system infrastructure plans (2024, 2036, and 2050) would operate during both cold waves. The resulting EI dispatch is shown in Figure 19. The respective cold waves hit the system on February 1, 2011, during the Cold Wave event and on February 18, 2008, during the Winter Net Load 1 event, and, most obviously in the 2036 and 2050 infrastructures, an increase in total wind generation comes with it. The system responds by reducing the gas-combined cycle (gas-CC) generation. In both events, wind generation decreases as load remains elevated in the following days. Given the dynamics of cold waves described earlier, the decrease in wind generation is expected in both events. However, the amount of decrease differs drastically between the two events.

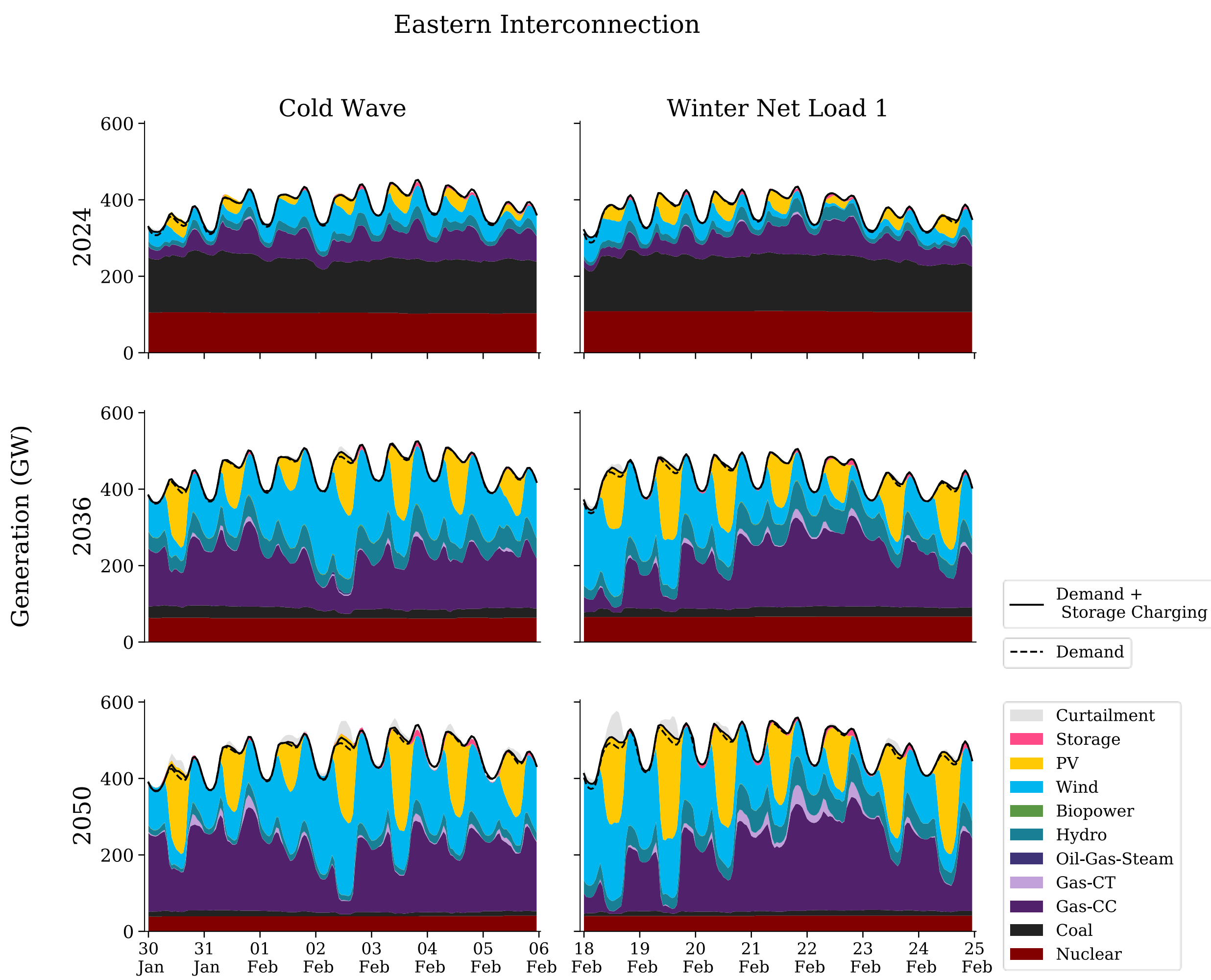

Figure 19. Generation dispatch for the EI during the February 2011 Cold Wave event (left column) and the February 2008 cold wave, or High Net Load 1 event (right column)

Both cold waves were simulated with three future infrastructure years: 2024 (top), 2036 (middle), and 2050 (bottom).

In the Cold Wave event in 2011, Upper Midwest wind generation remains above average (as was seen in Figure 16 (page 41)), which limits the need for a large ramp back up of the gas fleet. Transmission to export the Upper Midwest wind generation also serves as an enabling technology to ensure greater utilization of the wind generation in the following days. Figure 20 (page 47) shows the net interchange of power between MISO and its neighbors during the Cold Wave event. In 2024, the net interchange is not highly impacted by the changing wind generation. However, in both 2036 and 2050, when there is a higher wind penetration and an increase in transmission capacity, exports from MISO to PJM are more substantial. As wind generation in other parts of the EI decreases on the evening of February 2, MISO goes from importing 7 GW of power from PJM to exporting more than 15 GW to PJM in a matter of 24 hours. Exports to PJM quickly decrease from the peak, but MISO remains a net exporter to PJM for the next 2 days before the cold subsides.

However, the milder cold wave during the Winter Net Load 1 event in 2008 does not have the excess wind generation in any part of the EI. This event requires more thermal generation to come online, including an extended period of gas-combustion turbine (gas-CT) generation from the evening of February 20 through the evening of February 22. Typically, gas-CT capacity is used as a peaking unit, coming online for just a few hours before shutting back down. However, as the wind generation dies down but the cold persists in the Winter Net Load 1 event, available thermal capacity is tight enough that these gas-CTs need to stay on longer. Some staying on for about 36 hours.

Figure 21 (page 48) shows the TI dispatch during both cold waves. Wind is already a larger part of the Texas generation portfolio, so the impact of the cold wave on operations is seen even in the 2024 plan. During the Cold Wave event, load in the TI nearly doubled, while there was no noticeable change in load during the Winter Net Load 1 event. Because of the lack of significant ties between the TI and its neighbors, the TI mostly relies on its available thermal capacity to deal with the decrease in wind that follows as the initial front of the cold wave moves out of Texas. For both events in 2036, the year with the most wind capacity in the TI, large amounts of potential wind and PV generation are curtailed during the initial ramp-up of wind as the cold waves move through. Longer duration storage, on the order of a day, was not explored in this study, but could be a valuable technology for Texas to handle the days that follow the initial cold wave, charging off of the curtailed energy earlier in the event.

The limited sample size of weather events (2007–2013) we explored in this study suggest cold waves are among the weather events with the largest impact on system operations and adequacy as the system utilizes more VRE. This is predominately because of wind generation dynamics driven by the cold waves. Initially, the front that brings cold temperatures also brings high wind resource. In the two cold waves we studied, this means wind generation ramps up at the same time as a pick-up in load, if there is any. The Cold Wave event brought very cold temperatures that dramatically increased load in the EI and TI, whereas the Winter Net Load 1 event did not result in an as large of an increase in load. However, as the front moves on, but temperatures remain cold, the wind generation tends to decrease, requiring a response from the system. In some cases, such as the Cold Wave event in the EI, there is enough geographic diversity in the wind and solar resource and utilizable transmission to trade the available VRE between regions. However, the Winter Net Load 1 event had a widespread negative impact on the wind resource throughout the EI and necessitated a large ramp-up of the dispatchable thermal capacity. Two days during the Winter Net Load 1 event are among the highest net load days in the data set for the EI. This suggests the days following the onset of a cold wave may be among the most important for planners to consider when determining generation capacity needs for high VRE systems of the future. Our results also suggest the days following milder cold waves may be the most concerning, but more research on a larger sample size of cold waves is required to support that conclusion.

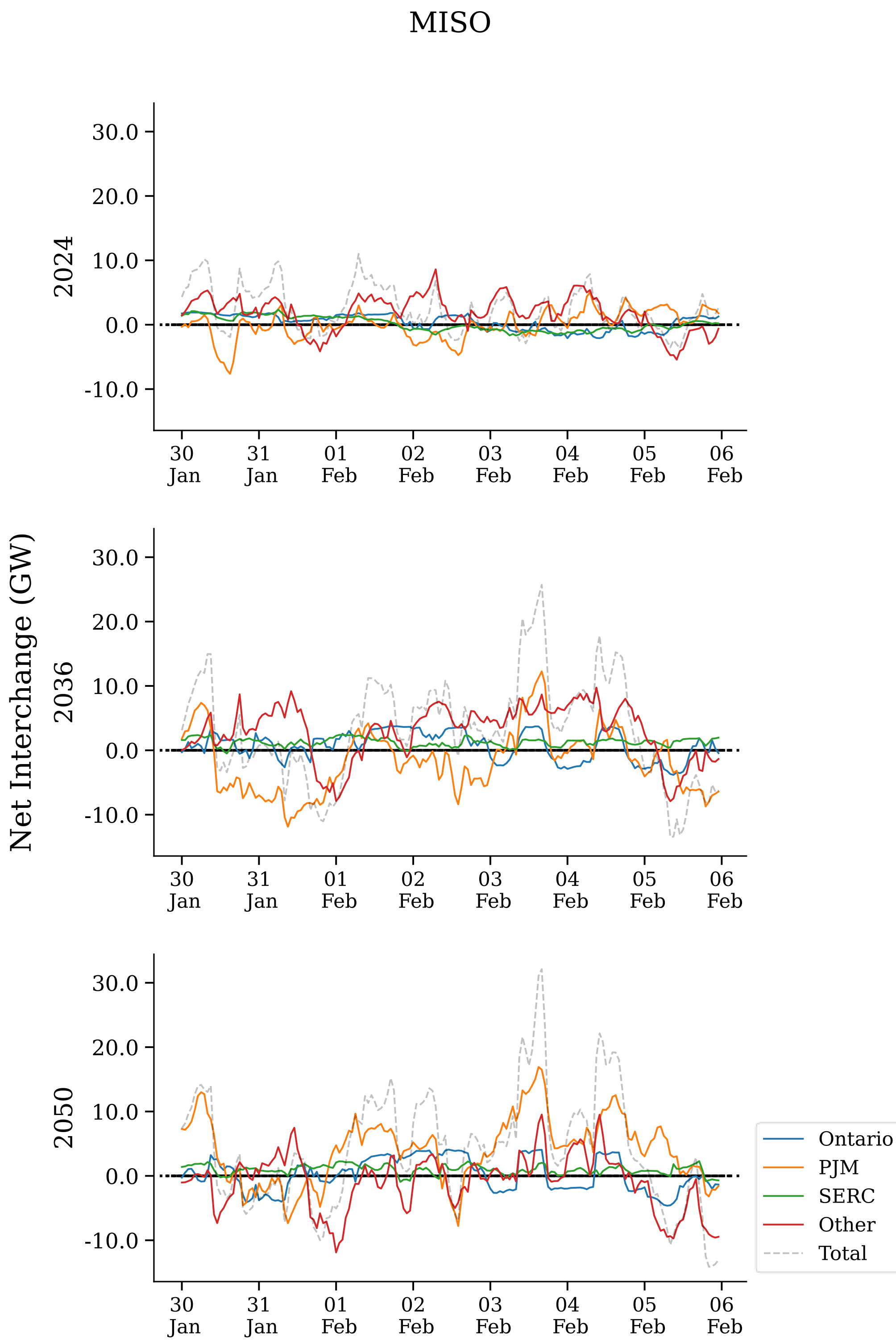

Figure 20. Net power flow between MISO and its neighbors during the February 2011 Cold Wave event

Positive flow means an export from MISO to its neighbor.

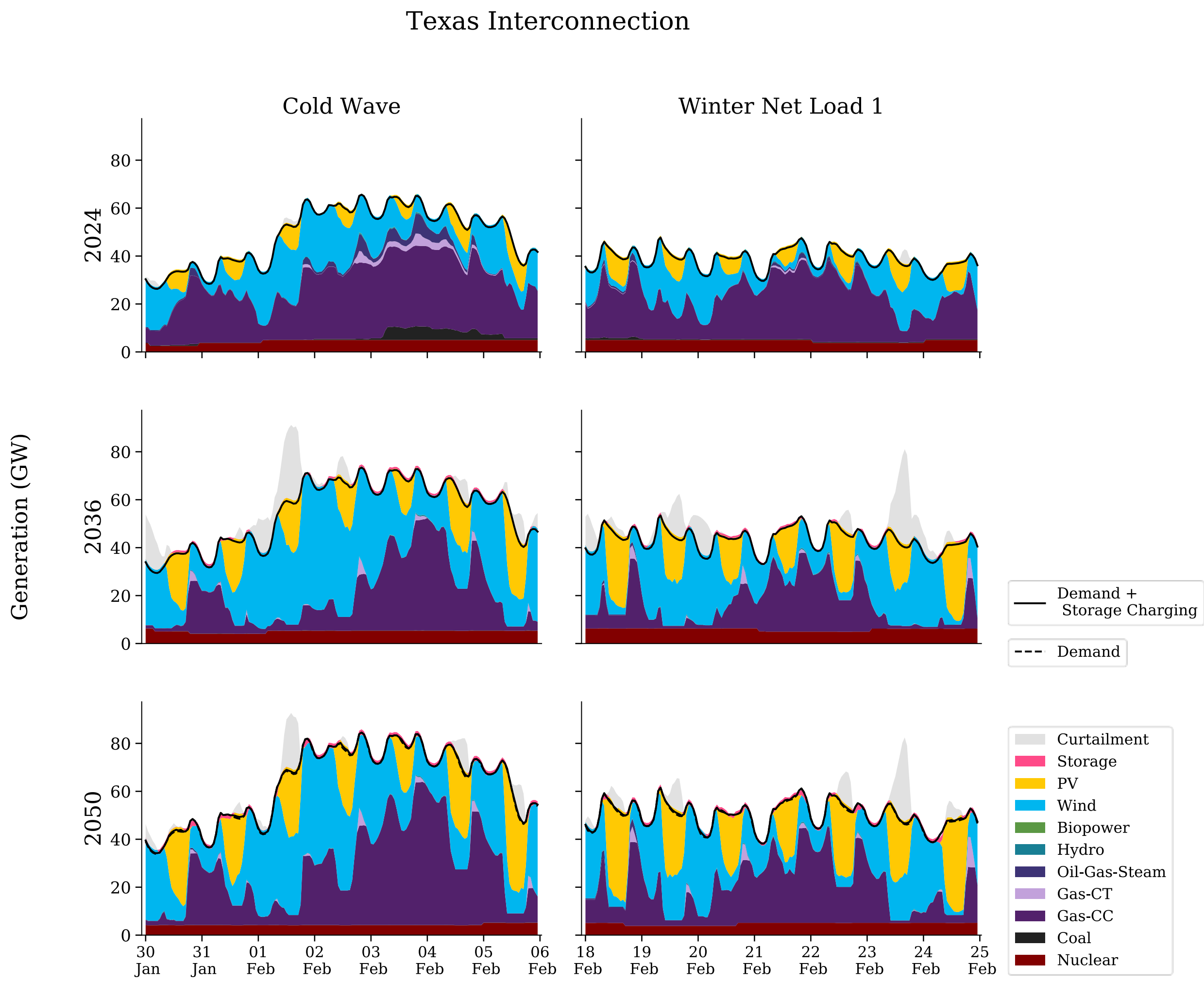

Figure 21. Generation dispatch for the TI during the 2011 Cold Wave event (left column) and the 2008 cold wave, or High Net Load 1 event (right column)

Both cold waves were simulated with three future infrastructure years: 2024 (top), 2036 (middle), and 2050 (bottom).

Finding 4. Increased PV capacity drives system operational changes during summer months and this does not change during heat waves. However, the contribution from wind after sunset differentiates the level of system operation stress caused from one heat wave to another.

Historically heat waves drive the highest load days in most regions in CONUS; they send temperatures climbing and consequentially electric load also. Day-to-day operations in heat waves are largely the same, but the wind generation contribution to peak net load is the major driver of system operations and resource adequacy stress. The magnitude and shape of the solar generation profile is largely the same from one day to the next, and the rest of the system ramps and cycles on and off to utilize as much solar generation as possible in the middle of the day. This causes major differences in the system dispatch as the solar PV capacity increases from 2024 to 2036 to 2050, as can be seen in Figure 23 (page 52) and Figure 24 (page 53). However, this is not unique to heat waves and constitutes typical operations, especially during summer months, in high VRE systems. What differentiates system stress between heat waves is the contribution from wind generation after sunset when solar PV is contributing nothing. To demonstrate this, we analyzed two distinct heat waves, a record-breaking heat wave in July 2011, named Heat Wave 1 in this paper, that had average wind generation and a moderate heat wave, the Summer Net Load event, mostly impacting the EI, in August 2010 that had below-average wind generation.

The weather of the Heat Wave 1 event is caused by the strengthening of a persistent dome of high pressure. The dome covers much of the country, with the exception of the Pacific Northwest, pushing high temperatures well into the 90s, and in some places to over 100°F. By July 23, 100°F heat is impacting the Mid-Atlantic states, including New York City. Though strong daytime heat associated with clear skies increases the likelihood of daytime thunderstorm formation, stable conditions such as those seen in July 2011 and August 2010 tend to inhibit significant storm outbreaks that provide relief from the heat. The Summer Net Load event, which occurred between August 8–11, 2010, is particularly unusual because the stable, unactive weather pattern leaves the country largely devoid of frontal boundaries, storms, pressure gradients, and areas of precipitation that led to higher-than-normal temperatures in the EI. Temperatures are generally 5°F –11°F above normal in the Great Plains and 3°F –10°F above normal in the eastern part of the country with the deviation increasing throughout the event. Southeastern Texas is 14°F –17°F above normal, with a weak warming trend.

The meteorological differences between Heat Wave 1 and the Summer Net Load events are subtle, but they result in differences in both load and wind generation potential. Figure 22 displays the load and net load impact of the two events. During the Heat Wave 1 event, load hits record highs throughout CONUS. In fact, July 21, 2011, has the highest load hour in the entire 2007–2013 data set. However, the net load is somewhat depressed due to contributions from above average wind and average solar. The Summer Net Load event, on the other hand, drives high—but not record high—loads. However, this event experiences the highest net load day in the data set on August 11, 2010, with August 10 not far behind. As is typical of summer load and net load profiles, there is little change in the diurnal shape of either profile. The main concern for system planners and operators is knowing how high the load—and, more importantly in a high VRE future, the net load—will get.

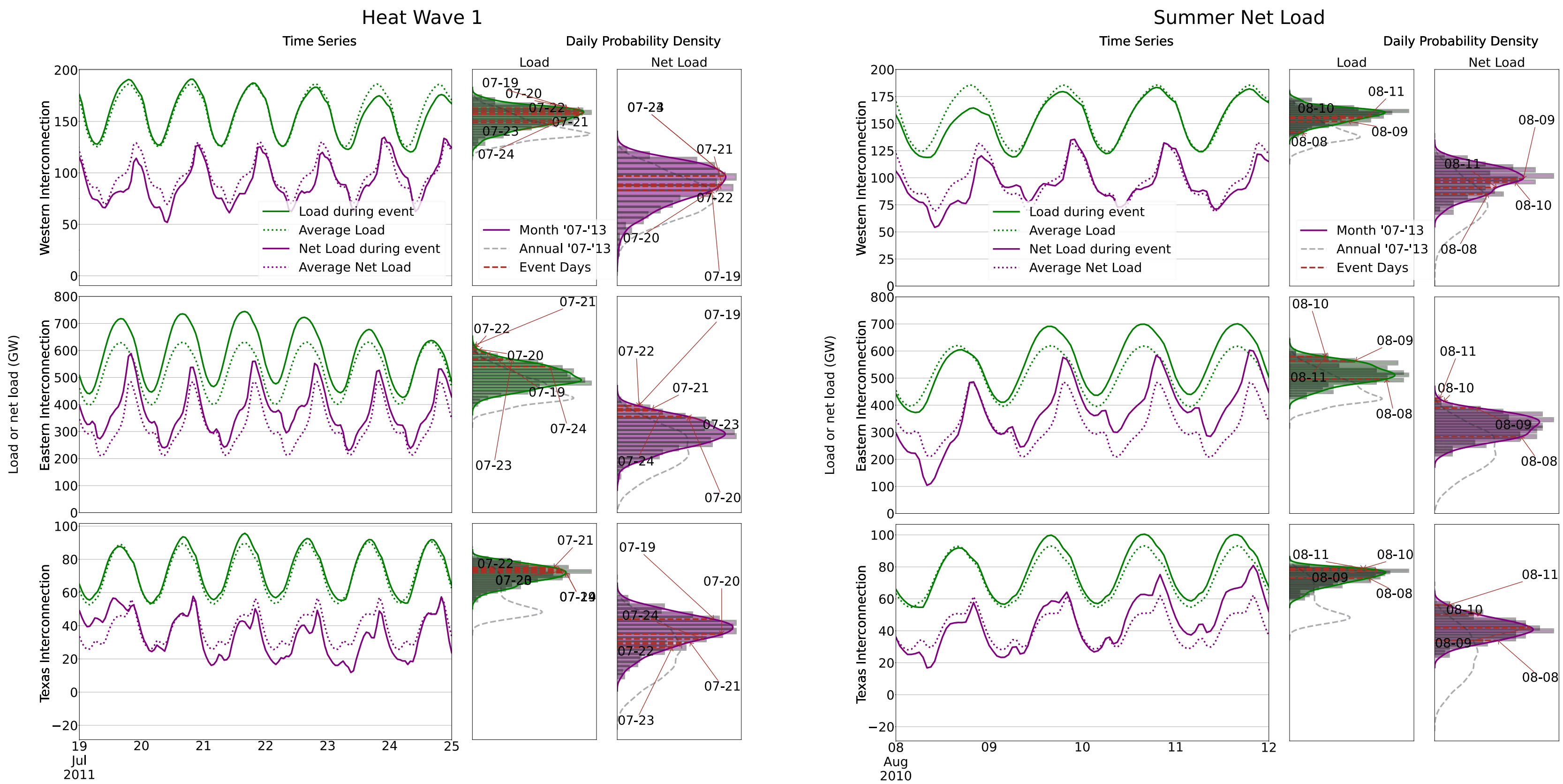

Figure 22. Load (green) and net load (purple) generation time series for the Heat Wave 1 (left) and the Summer Net Load (right) with surrounding period average shape shown as dashed lines

The time-series plot (left) shows the actual values during the event (colored time series) in relation to the average values for that time of year (dotted time series). The distribution (right) shows the average daily values (GW) for the time of year (colored distribution), the yearly distribution (gray dotted distribution), and the location of the event days in the distributions (red dotted lines with the day labels).

Figure 23 shows the total available wind and solar generation in the three interconnections. The diurnal pattern of wind is consistent both within the event and relative to the seasonal average; what changes is the total energy contribution from wind. During the record-breaking heat of Heat Wave 1, nearly every day in each interconnection has above-average wind generation. And, the TI's wind, which experienced some of the most intense heat during this event, is well above average.

The geographic diversity of solar and the typical clear skies that come with heat waves result in stable solar generation during these events. The main operational and resource adequacy concern about solar during heat waves is its diurnal generation profile. As PV penetration increases, less PV capacity can contribute at times of need as the net load peak is shifted to the evening. However, this is well understood and forecastable. Based on the heat waves we studied, operators will know what they will get from the PV resource, in terms of both the timing and the magnitude of generation. However, there is a major caveat relating to solar generation in heat waves: none of the heat waves we investigated between 2007 and 2013 coincided with major wildfires. Wildfire intensity, size, and correlation with high heat have increased over the last decade. Aerosols from wildfires spreading over large swaths of CONUS, which has become common in the summer, will negatively impact PV generation. Wildfires and their impact on VRE resource and system operations should be a focus of further research.

For both heat wave events (Heat Wave 1 and Summer Net Load), we modeled system operations for the 2024, 2036, and 2050 infrastructures. Figure 24 shows the EI generation dispatch during the Heat Wave 1 event on the left and the Summer Net Load event on the right. Figure 25 breaks out individual generation types to demonstrate changes to commitment and dispatch for Heat Wave 1. In both events, daily operations are largely the same and evolve similarly as the wind and solar penetration increases. As noted earlier, the shape of wind and solar generation are largely consistent day-to-day. The two resources are largely anticorrelated; solar generation maxes out in the middle of the day when wind is very low, and wind picks up in the evening as the sun is setting and the solar generation ramps down. However, in the EI, the wind evening ramp only fills in a fraction of the solar generation peak. There is very little curtailment, as there is typically plenty of load to consume the wind and solar energy, although in 2050 a small amount of solar curtailment occurs as its peak output. The major difference between the two heat waves is the amount of available thermal and hydropower capacity needed at the net load peak, which depends on the coincidence of the heat wave with reduced wind generation.

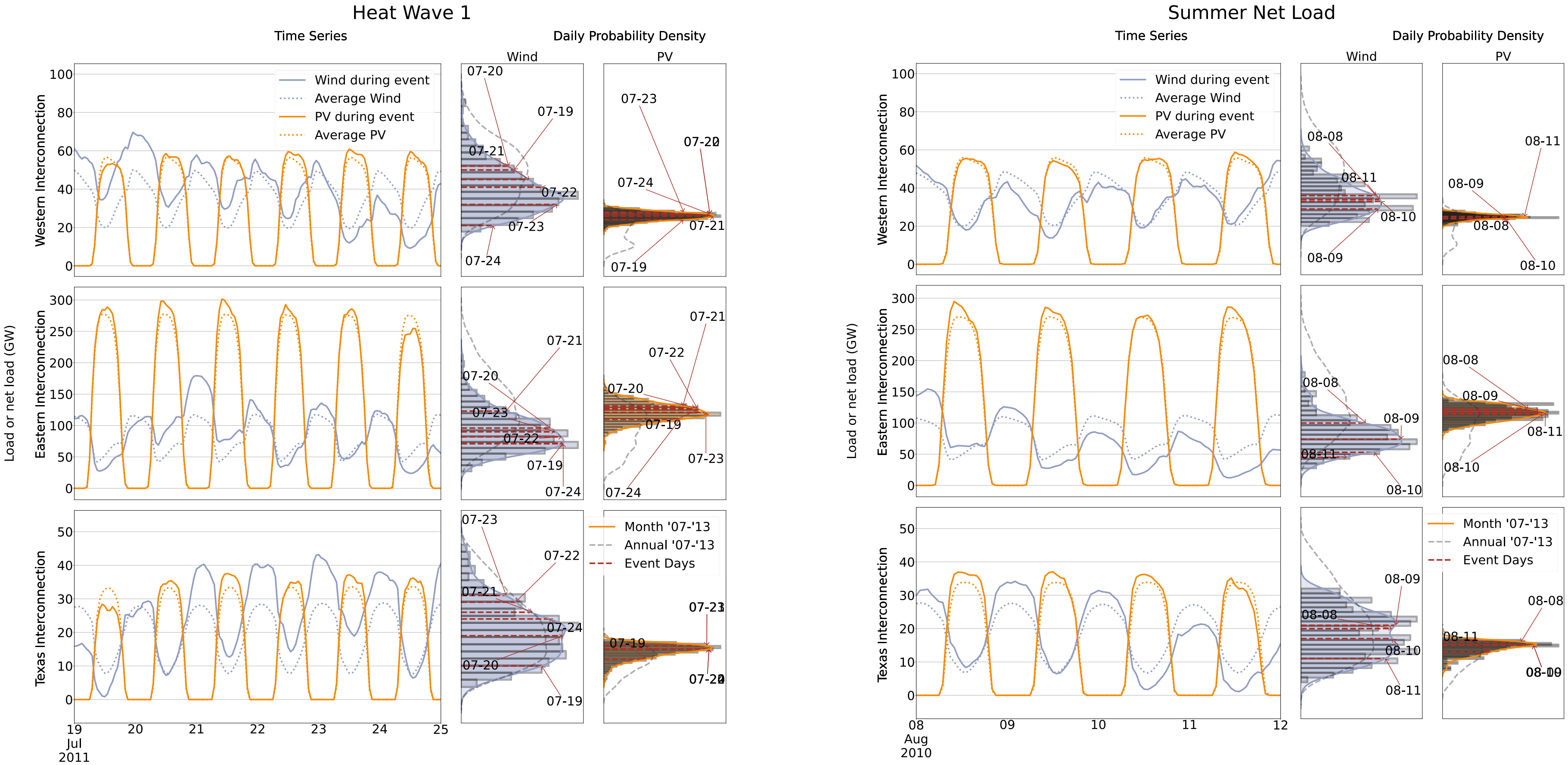

Figure 23. Wind (blue-gray) and solar (orange) generation time series for the Heat Wave 1 (left) and the Summer Net Load (right) with the surrounding period average shape shown as dashed lines

The time-series plot (left) shows the actual values during the event (colored time series) in relation to the average values for that time of year (dotted time series). The distribution (right) shows the average daily values (GW) for the time of year (colored distribution), the yearly distribution (gray dotted distribution), and the location of the event days in the distributions (red dotted lines with the day labels).

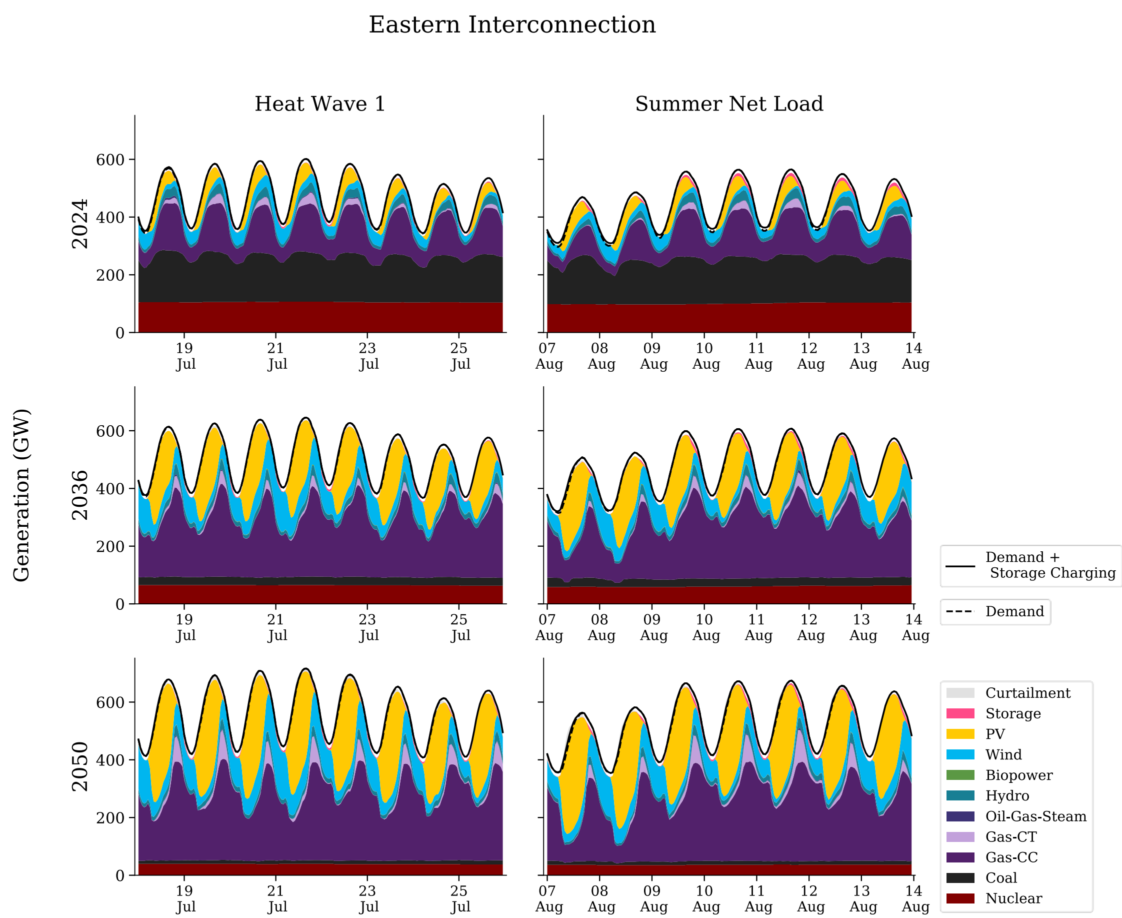

Figure 24. Generation dispatch for the EI during the Heat Wave 1 (left column) and the Summer Net Load (right column)

Both heat waves were simulated with three future infrastructure years: 2024 (top), 2036 (middle), and 2050 (bottom).

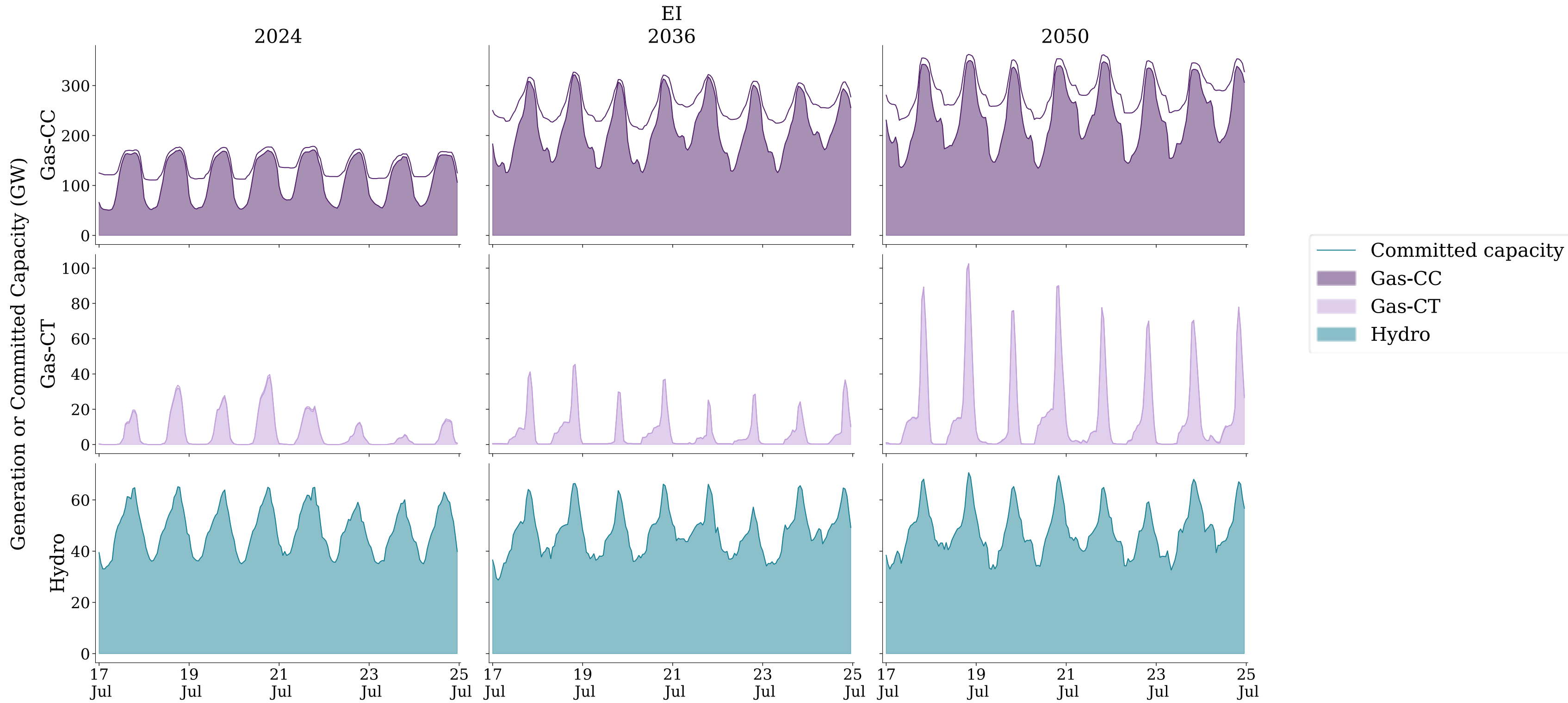

Figure 25. The committed capacity (solid line) and dispatch (filled area) for different generator types (along the vertical axis) in the EI for the three future infrastructure years—2024 (left), 2036 (middle), and 2050 (right)—during the Heat Wave 1 event

That day-to-day operations during a heat wave look largely the same does not mean each region within the EI is self-reliant. As an example, Figure 26 shows the net exports between MISO and its neighbors. During both heat waves, net exports are more dynamic with increased wind and solar penetration. Net exports in 2024 are relatively stable, rarely changing much hour-to-hour. In both 2036 and 2050, net exports change rapidly, largely following when solar generation increases and decreases throughout the EI. The 2036 average hourly rate of change of MISO's net exports is 53% and 90% higher than the 2024 rate of change in Heat Wave 1 and Summer Net Load events, respectively. The analogous values for 2050 are 100% and 133% higher. In both heat waves and in all infrastructure plans, MISO is a net importer, though in 2050 there are hours every day where MISO exports power. However, during the Summer Net Load heat wave, which had less impact on total load but unseasonably low wind generation, MISO relies more heavily on imports. On average, hourly MISO net imports are 2,100 MW and 1,600 MW higher during the Summer Net Load event than during Heat Wave 1 in 2036 and 2050, respectively.

In summary, the heat waves we studied had little to no impact on PV generation, but they do impact total wind generation. The increased PV capacity has a large impact on system operations, pushing more thermal and hydropower generation toward a tighter and tighter net load peak in the evening. In the summer, wind generation typically is at its lowest, but, over a wide enough area, wind plays a critical role to resource adequacy because it reliably increases its generation in the evening as solar decreases. Critically for system resource adequacy, when considering the heat waves we studied, there is little or no correlation between extreme heat that drives up load and heat waves that depress wind generation below what seasonably would be expected. However, based on the weather years of 2007–2013, the most pressing events for planners and operators to ensure sufficient capacity at the net load peak appear to be moderate heat waves, such as the Summer Net Load event, that bring with them persistent high pressure and very low wind generation.

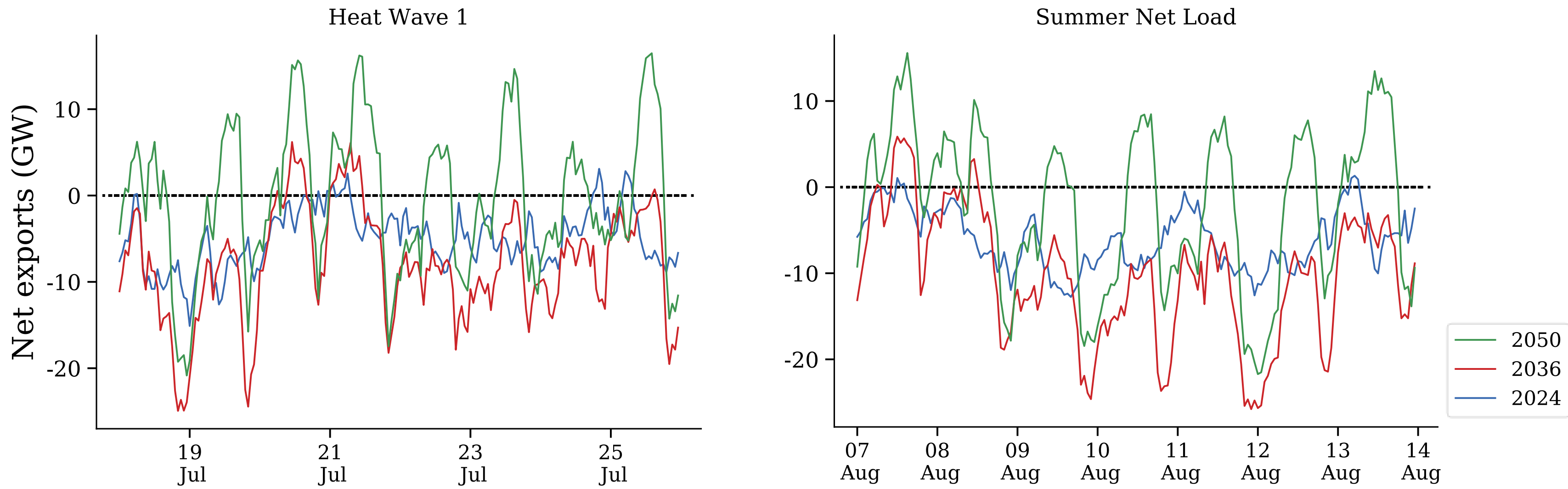

Figure 26. Net exports between MISO and its neighbors during Heat Wave 1 (left) and Summer Net Load (right) heat waves for the three infrastructure plans 2024 (blue), 2036 (red), and 2050 (green)

Positive net export means MISO is exporting more power to its neighbors than importing.

Finding 5. Understanding the characteristics and diversity of wind and solar resources—at small and large geographic scales—is key to assessing their contribution to resource adequacy. Operating existing and expanded transmission more flexibly than today enables that contribution.

Several of the weather events we identified include periods of low wind and solar resource. However, even in these events with low wind and solar output, these resources can still contribute to resource adequacy and system resilience through interregional coordination and flexible resources. We explored two events that feature extremely high net loads and demonstrate how careful planning and an understanding of regional variable resource can enable reliable operations without an overbuilt generation or transmission system.

The first example involves the wind and solar resource in SPP during the Summer Net Load event in early to mid-August 2010. On August 10 and August 11, 2010, the EI experienced nearly the highest net load days within the data set because of the very low wind generation throughout the interconnection. In the 2050 infrastructure plan, during the daytime hours on August 10 and August 11, the fleetwide capacity factor of wind in the EI fell to 5% and 4% respectively. This especially impacts SPP in our dispatch modeling. We modeled this event using 2024, 2036, and 2050 infrastructure plans. In these plans, wind and solar were modeled to account for 32% of SPP's installed capacity in 2024, increasing to 60% and 64% in 2036 and 2050 respectively. Figure 27 shows the SPP system dispatch during this event for all three plans.

For much of the Summer Net Load event, SPP relies on its transmission infrastructure to import power during the event. SPP also taps into nearly all its available thermal capacity in the evening hours after sunset. The left plot of Figure 28 (page 59) shows the offline available thermal capacity (i.e., thermal capacity that is not committed and not on a planned or forced outage) in SPP throughout the event. In the 2036 and 2050 infrastructure plans, at 8 p.m. EST on August 11, there is nearly no offline thermal capacity available in SPP. At the same time, imports from MISO drop to zero from a high of 9 GW a few hours earlier, as seen in the right hand plot of Figure 28. SPP is on its own, PV generation is quickly ramping down as the sun sets, and SPP lacks additional available thermal capacity. However, at the same time, wind ramped back up; at 8 p.m. EST, SPP's wind had a combined capacity factor of 22%, up from 5% only 6 hours earlier. During this event, SPP's wind followed a typical pattern for wind generation in the EI, picking up in the evening and overnight. This was not the case for MISO where wind reaches a maximum fleetwide capacity factor of only 9% overnight, while SPP reaches 58% in the early morning hours of August 12. SPP's wind recovers enough that it could turn thermal units off and export power to MISO.

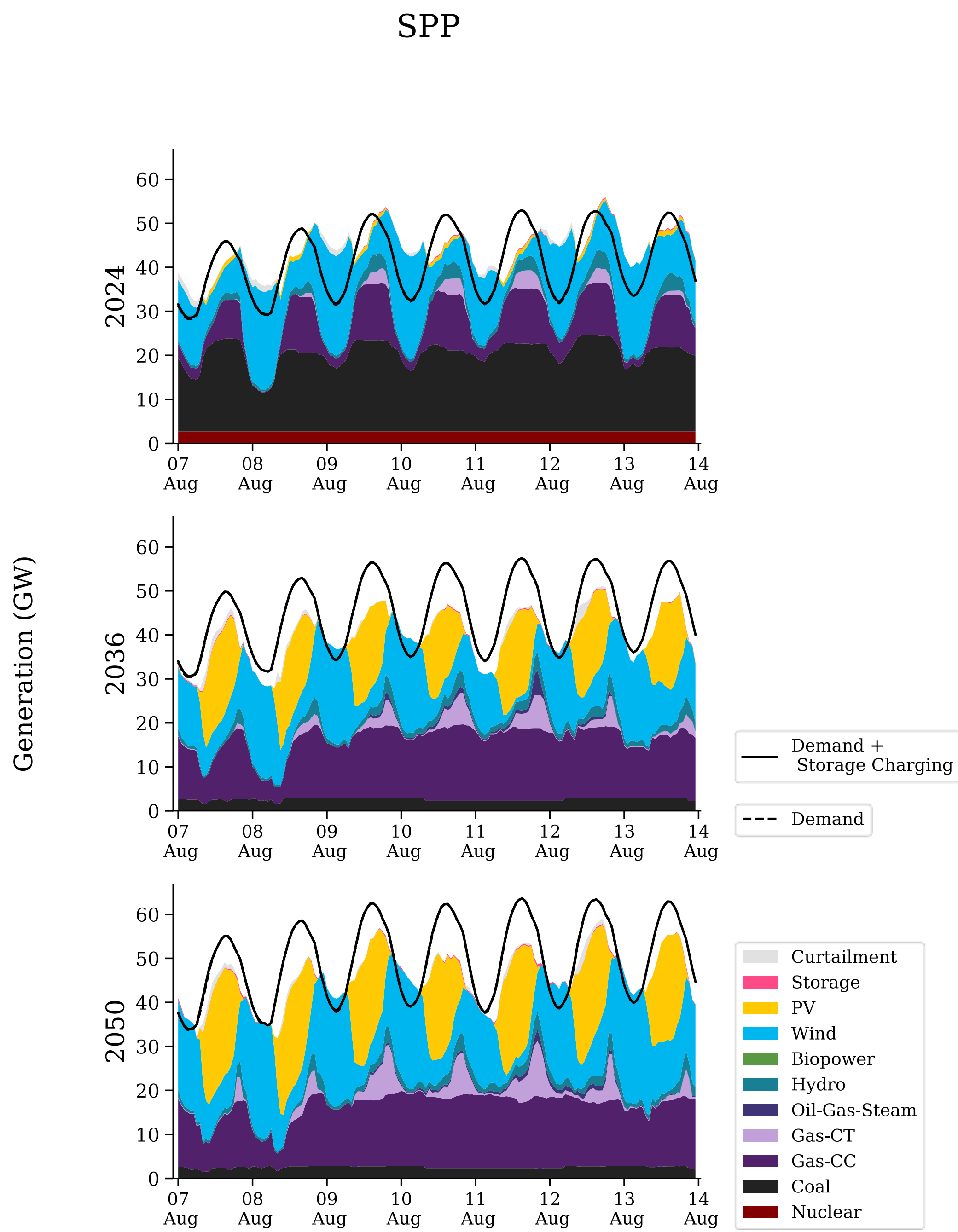

Figure 27. Generation dispatch for SPP for three future infrastructure years—2024 (top), 2036 (middle), and 2050 (bottom)—during a period of high net load for August 7–13, 2010

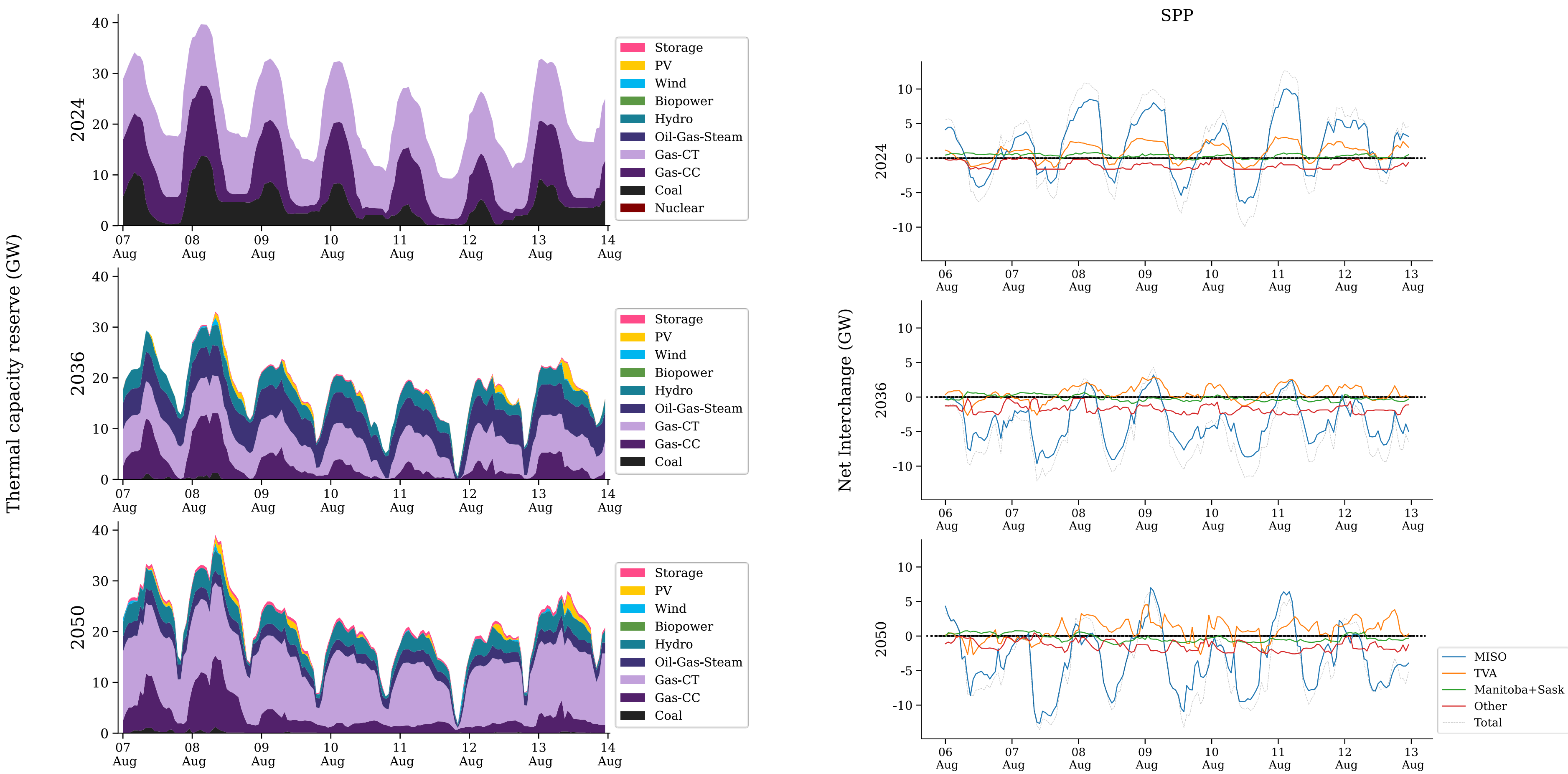

Figure 28. Offline thermal capacity reserve in SPP (left column) and net power flow between SPP and its neighbors (right column) during the Summer Net Load event

Positive flow means an export from SPP to its neighbor.

February 21–23, 2008 during the Winter Net Load 1 event is another example where the geographic diversity of VRE boosted its contribution to resource adequacy even though the overall and local wind and solar resource was low. During this period, the EI experiences cold temperatures that elevate load above normal. At the same time, stagnant air steadily reduces the wind generation output by more than 90% from the event high, hitting an extreme low output for the full data set on February 23. In addition, winter storm systems reduce PV output in the Southeast and in MISO on February 21, before extending into PJM the next day.

The impacts of the low wind and solar resource are seen in MISO, PJM, and the Southeast. The dispatch stacks of all three regions are shown in Figure 29. On February 21, cloud cover reduces the typical PV generation in the middle and southern parts of the interconnection, while the Mid-Atlantic experiences above-average PV output. Both MISO and the Southeast have low PV output on February 21, but it is balanced by a high output day from PJM, which covers the Mid-Atlantic. As the storms move east on February 22, PV output is low again in the Southeast and PJM, while MISO's PV output recovers to some degree. Though much of the PV generation in the EI is located in more-southern latitudes, geographic diversity of the build-out does provide value by dampening the aggregate PV generation reduction.

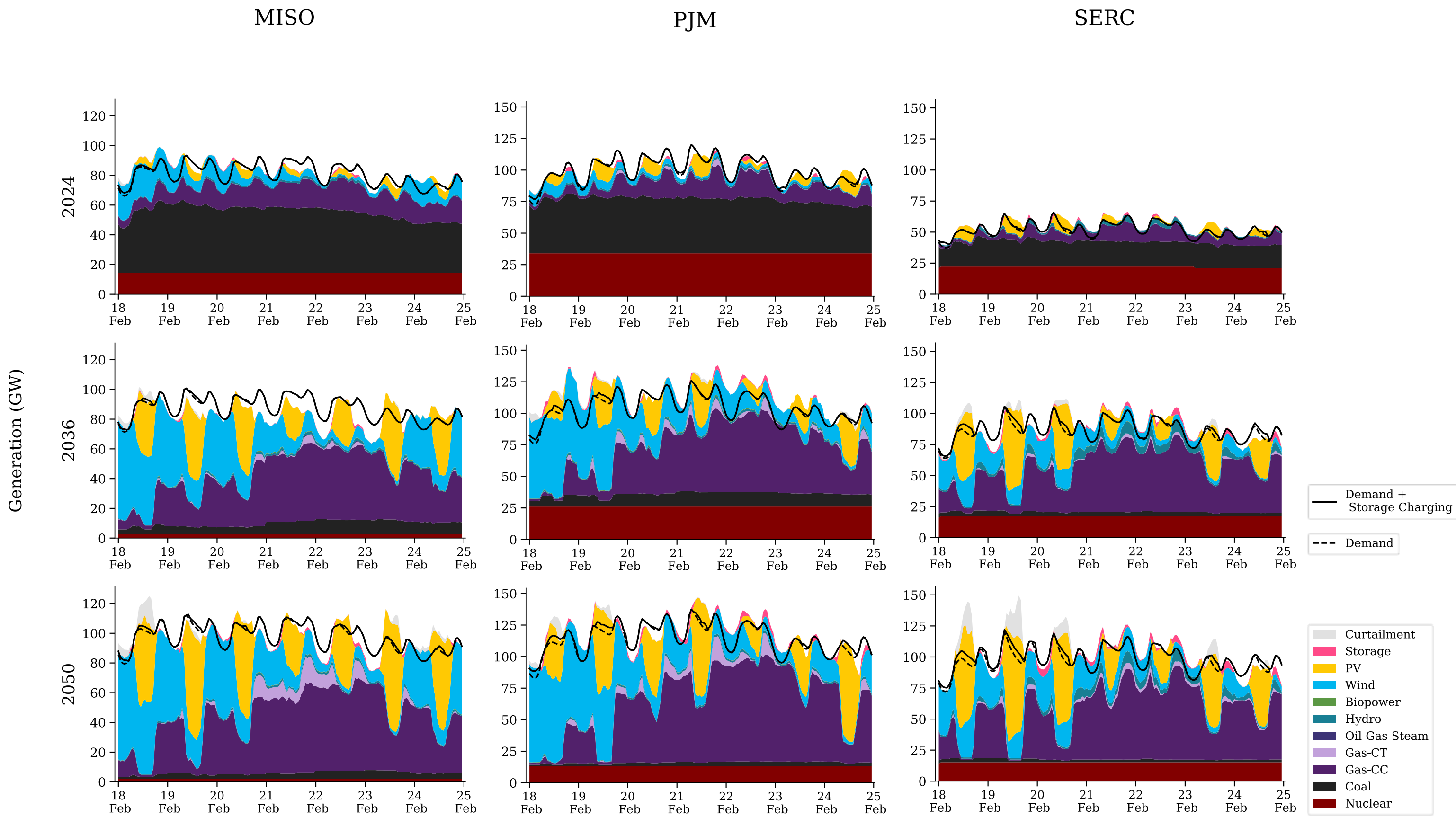

Figure 29. Generation dispatch for MISO (left column), PJM (middle column), and the Southeast (right column), for three future infrastructure years—2024 (top), 2036 (middle), and 2050 (bottom)—during the Winter Net Load 1 event in February 2008

Figure 30 shows the trading between the three regions, which generally becomes more dynamic with higher wind and solar penetrations. The trading pattern on February 22, at the height of the net load in the interconnection, highlights the use of transmission to capture the potential of the diverse PV resource. Particularly in 2050, the interchange between PJM and the NYISO has a strong diurnal pattern throughout the week. PJM exports more power to NYISO when PV output is high in the interconnection. This happens even on February 22, when PJM PV output is low. These exports are actually coming from FRCC and MISO with power wheeled through SERC and PJM to get to NYISO. Without the transmission capacity, which is expanded in 2036 and 2050 as summarized in Table 2 (page 10), and institutions in place to dynamically trade between regions, the interconnection would be unable to take advantage of the geographic diversity of the PV output, exacerbating an already challenging resource adequacy event.

Both events—the Summer Net Load in August 2010 event and the Winter Net Load 1 event in February 2008—demonstrate geographic diverse VRE contributing to resource adequacy and resilience of the system even though the overall resource is low, especially in local areas. It is key to system resilience to understand the behavior of the resource by studying multiple weather years' generation profiles and ensuring the infrastructure exists to take advantage of geographic diversity of the resource. It is also imperative to use modeling tools that capture the full geographic scale of the power system. In the Summer Net Load event, wind generation in SPP was very low around midday but recovered enough by the evening to maintain adequacy even though very little capacity remained in the offline thermal fleet. Trading with its neighbor in both directions was also critical to maintain adequacy in SPP and the EI more generally. In the Winter Net Load 1 event, transmission infrastructure and dynamic operations of transmission allowed for the sharing of diverse PV resource throughout the EI, thus enabling PV to contribute to adequacy and reducing the cost to provide that adequacy.

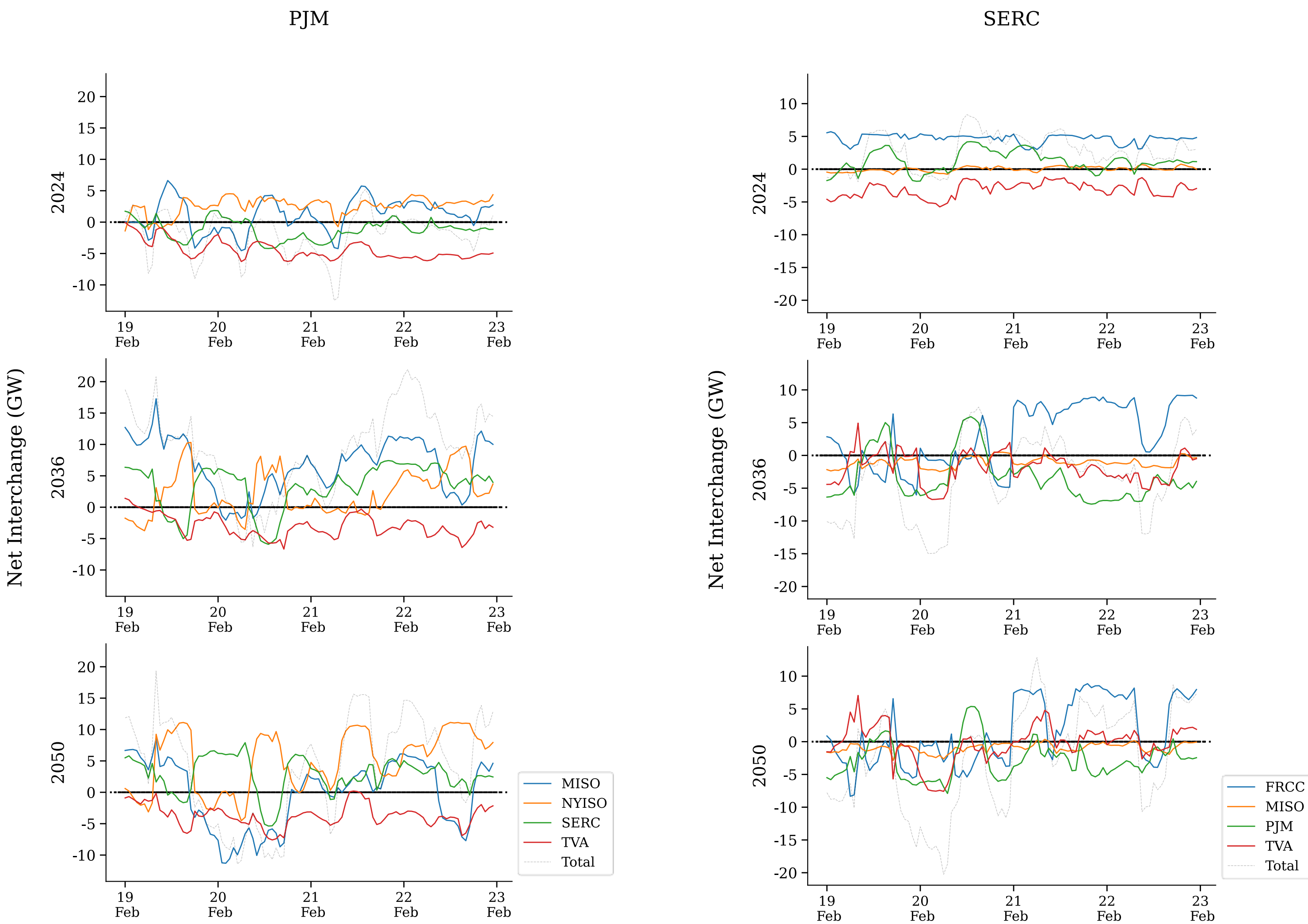

Figure 30. Net power flow between PJM (left) and the Southeast (right) and their respective neighbors for three future infrastructure years—2024 (top), 2036 (middle), and 2050 (bottom)—during the High Net Load 1 event in February 2008

Positive flow means an export from PJM/Southeast to its neighbor.

Finding 6. In areas where hydropower is abundant, its availability and flexibility are key to mitigating system stress during extreme weather events.[31]

Hydropower provides valuable flexibility for the WI when water availability allows it. The way this flexibility is best used changes as the penetration of wind and solar increases. Rather than strictly following the load profile, hydropower is best used to follow net load, which often means operating more as a peaking unit (i.e., ramping up quickly for a few hours after sunset before ramping back down). This shift in desired operations can be seen in Figure 31. However, several factors impact whether hydropower can achieve this new behavior. These factors include whether it is a wet, dry, or normal hydropower year or season and whether other water regulations, policies, and facility design that limit flexibility of dispatchable hydropower units (i.e., has a reservoir for water storage) to shift when to use the water stored in their reservoir.

Figure 31 shows the WI dispatch during the Heat Wave 1 event in July 2011 that drove up load throughout CONUS. Hydropower has a much larger capacity and energy contribution in the WI and the change to its operations between the 2024, 2036, and 2050 infrastructure plans is significant. With the increased PV penetration in 2036 and 2050, hydropower shifts energy when it provides as much capacity as possible during the net load peaks. In 2024, however, hydropower has a flatter peak output that more closely follows load rather than net load. Total daily energy provided from one day to the next is also more variable in 2036 and 2050 than in 2024.

[31] This finding focuses on WI operations and the role of hydropower during extreme weather events. Hydropower provides significant energy and capacity to regions within the EI, but it's role and significance are larger in the WI as a whole.

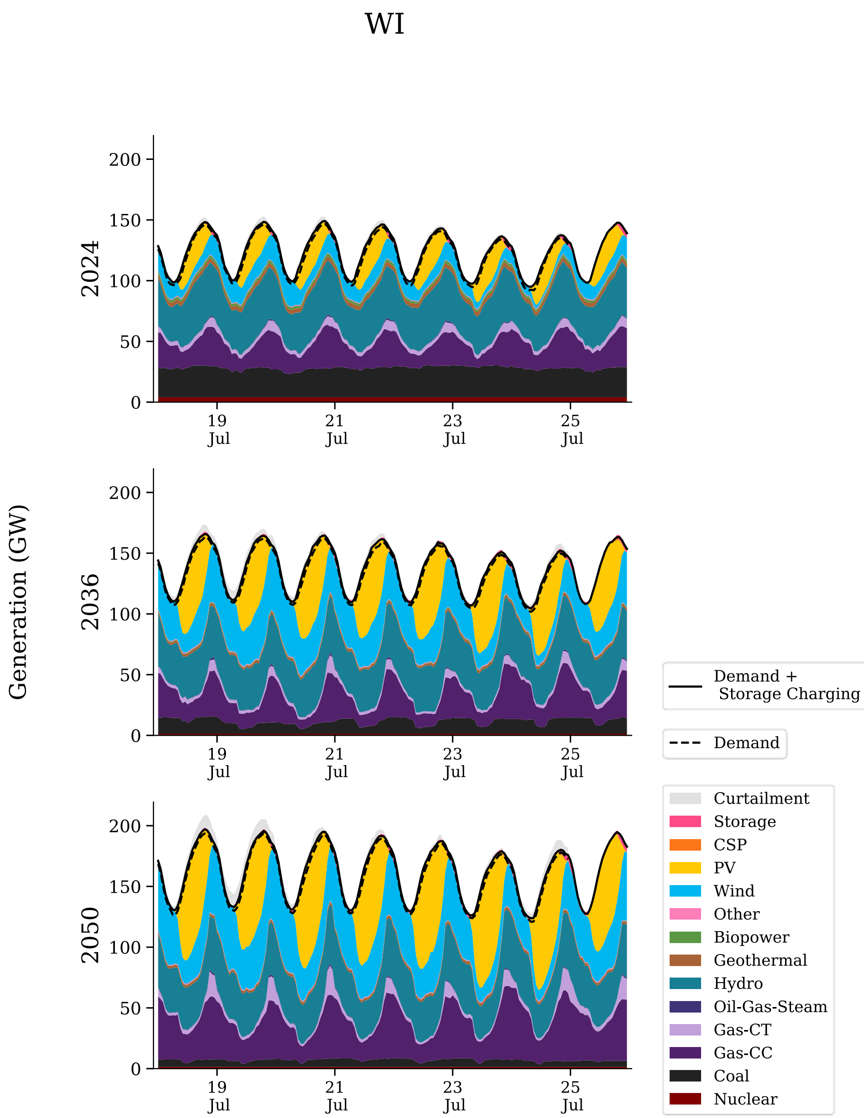

Figure 31. Generation dispatch for the WI for three future infrastructure years—2024 (top), 2036 (middle), and 2050 (bottom)—during the July 2011 heat wave

To more fully understand hydropower's value to the WI, we simulated system operations under different hydropower availability and flexibility assumptions. These sensitives were only run using the 2050 plan, and we focused the hydropower sensitivities on two weather events: a set of winter storms in December 2013 (the Winter Storms event) and the Lowest Net Load event in April 2011. Availability assumptions focused on wetter and dryer conditions than what were actually experienced, but they were still plausible conditions for the time of year. Figure 6 (page 20) in the Methods section shows how monthly hydropower generation changes seasonally and differs between the 7 years in the data set. Hydropower generation tends to be greatest in the United States in the spring and early summer, and it hits a low in the fall. The Inflexible Hydro sensitivity forced all dispatchable hydropower units to allocate their monthly or weekly hydropower water budgets equally for all hours and days. In other words, the dispatchable hydropower in the system was forced to operate at a constant output for the entire month or week, as determined by water availability. This is an aggressive assumption for reduced hydropower flexibility, but many hydropower units are at risk of losing this type of flexibility as they go through the relicensing process. For many units, power is one of the last uses of a dam's water to be considered, which limits the flexibility they might otherwise provide to the power system.

The change in total generation is shown for the Lowest Net Load event in Figure 32. Inflexible hydropower leads to increased gas-CC generation. Curtailment of wind and solar generation also increases, by 6%. Similarly, dry hydropower conditions reduce total hydropower output, which is mostly met by gas-CC generation. However, dry hydropower conditions also lead to a 10% decrease in wind and solar curtailment. The reduced curtailment is due to dry hydropower conditions offering more flexibility to the dispatchable hydropower fleet in the WI. April 2011 was already considered a wet year and for that reason we did not consider a wet hydropower sensitivity for this event.

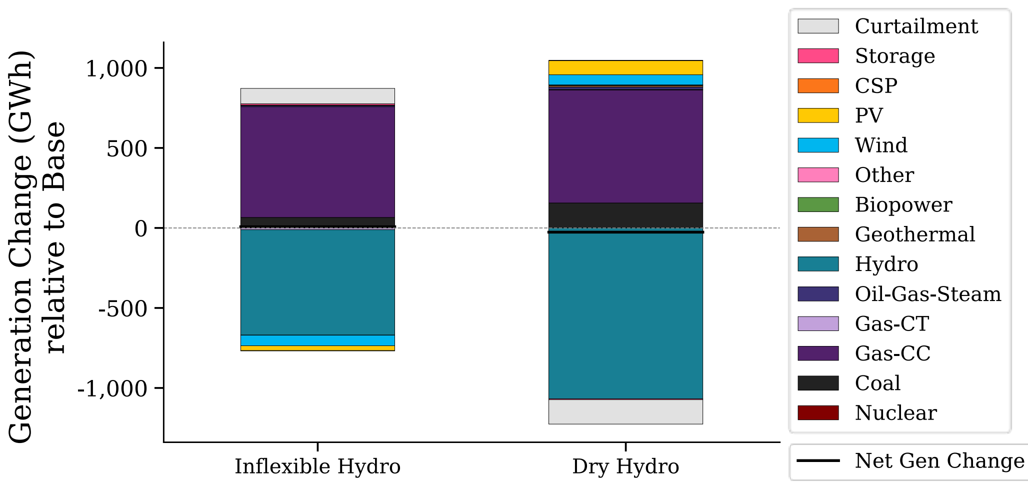

Figure 32. Change in total WI generation by type for different hydropower flexibility and availability assumptions during the April 2011 Lowest Net Load event, modeled with the 2050 infrastructure

Figure 33 demonstrates how the hourly operations of the WI hydropower fleet changes under inflexible and dry hydropower sensitivities for the Lowest Net Load event. Inflexible hydropower shows some of its greatest impact on the first 3 days of the event. In this sensitivity, hydropower is less capable of providing capacity at the peak net load hours in the evening, which leads gas-CCs to ramp-up more than they otherwise would; however, daytime hydropower generation leads to curtailment of the PV generation at its peak daily output. All of these effects of inflexible hydropower operations result in a 17% increase in production costs during this event. Dry hydropower conditions do not cause much change in the hourly generation shape, but they lead to less generation at all hours.

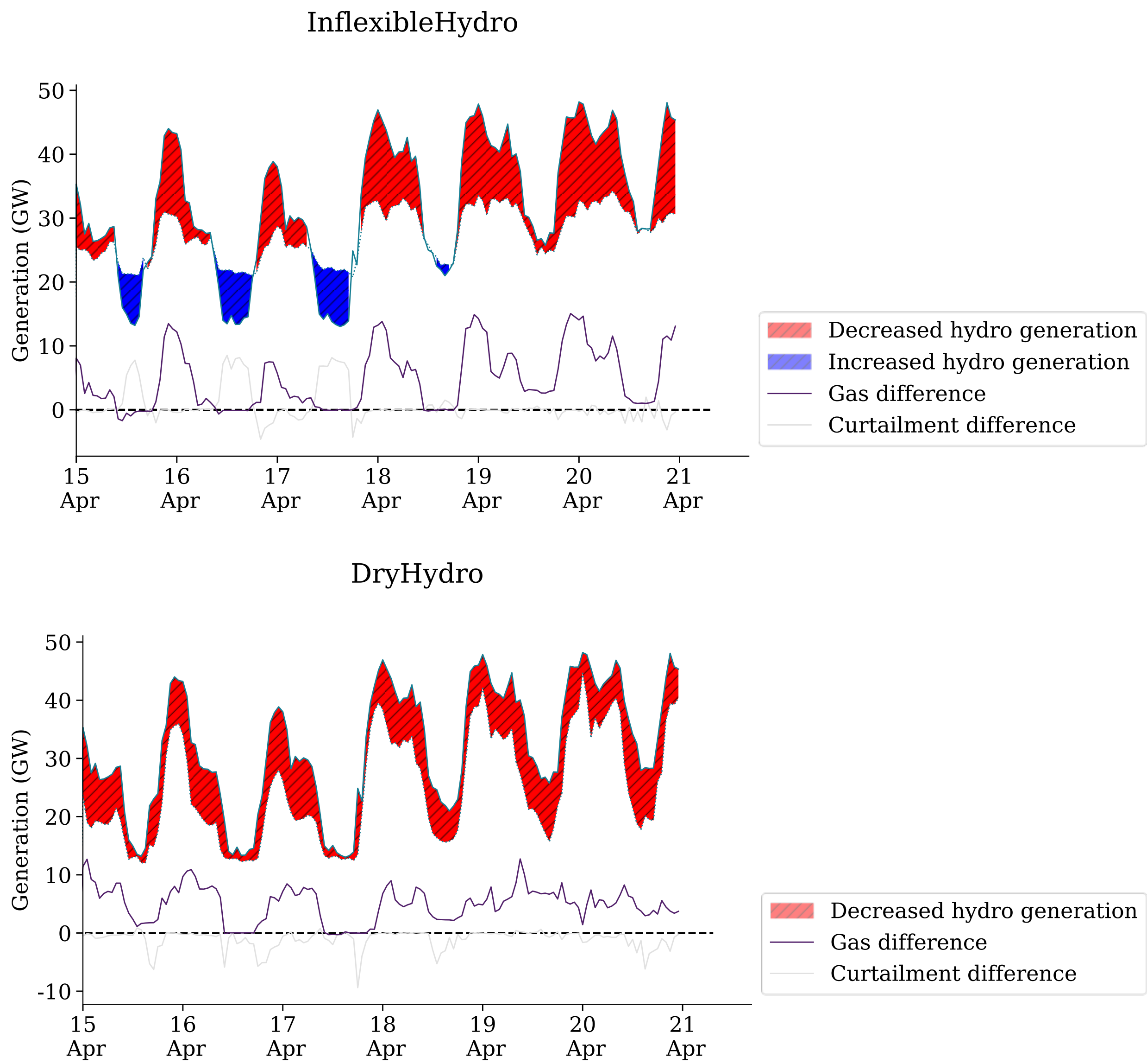

Figure 33. Impact of inflexible hydropower (top) and dry hydropower (bottom) conditions on hourly hydropower generation and associated changes in gas generation and curtailment of VRE for the WI during a low net load event in April 2011

The red crosshatched areas show times of reduced hydropower generation. Blue areas show increased hydropower generation.

Figure 34 shows the change in generation by type for dry and wet hydropower conditions and inflexible hydropower operations during the December 2013 Winter Storms event. Availability of hydropower had little impact during this event. The variability of hydropower availability is lower in December than in other months; a dry December does not look that different from a wet December. Inflexible hydropower, however, has a large impact on operations. Total hydropower generation decreased by 12% relative to the base 2050 plan during the Winter Storms event. The event had higher net load than the rest of the month, and the hydropower generation in the base case allocated more of December's hydropower generation to this event. Inability to shift more water for hydropower generation to the days of the Winter Storms event would be costly to the WI, leading to a large increase in peaker gas-CT usage (up 20%) and even imports from the EI. The 2050 plan modeled here does increase transfer capacity between the EI and WI some, and that extra capacity is utilized in this event.

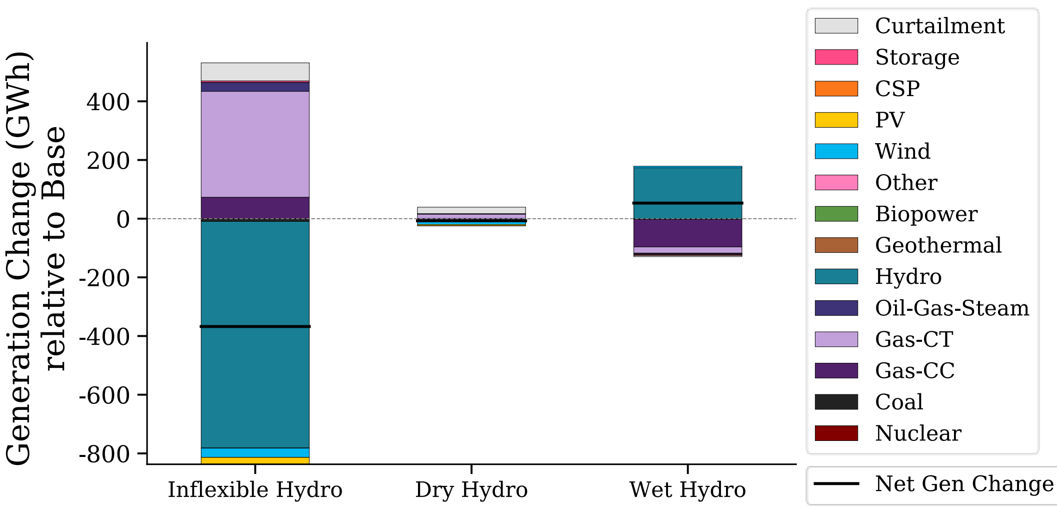

Figure 34. Change in total WI generation by type for different hydropower flexibility and availability assumptions during the 2013 Winter Storms event

Figure 35 emphasizes why inflexible hydropower leads to more peaking generation requirements. The base case profile for hydropower generation is highly variable and peaky in nature. It operates at low levels of around 20–25 GW of total generation before peaking most days close to 35–40 GW in a matter of an hour or two, before ramping back down a few hours later. The inflexible hydropower sensitivity disallows this type of behavior, and in response the WI relies on quick-start peaking units and net imports from the EI to provide the capacity lost from hydropower generation.

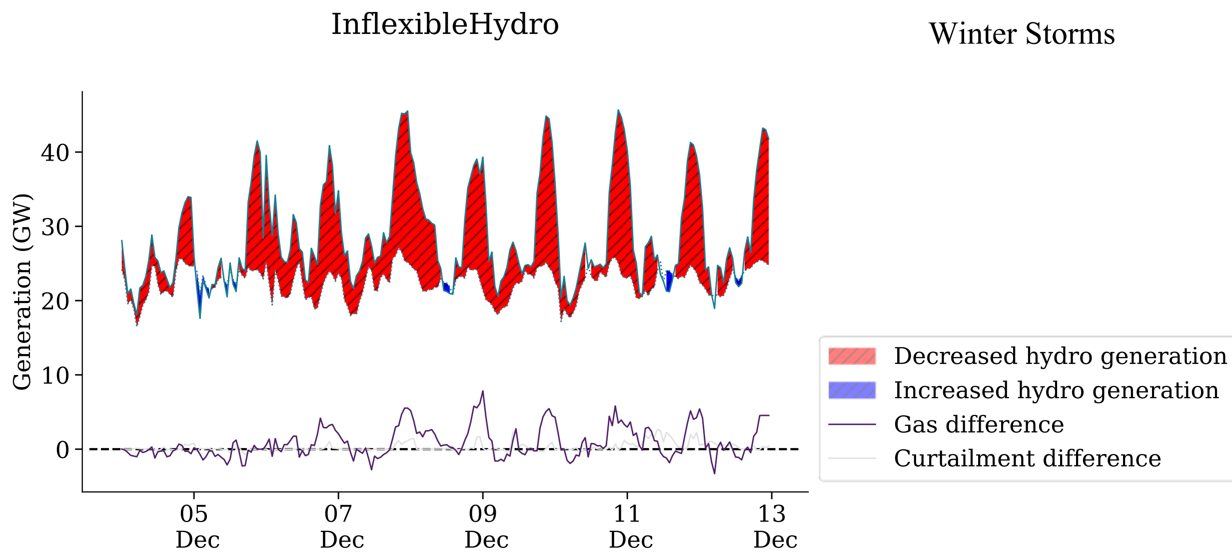

Figure 35. Inflexible hydropower's impact on hourly hydropower generation and associated changes in gas generation and curtailment of VRE for the WI during the December 2013 Winter Storms event

The red crosshatched area shows times of reduced hydropower generation. Blue areas show increased hydropower generation.

As stated earlier, water availability and flexibility to shift when water is used impact whether hydropower can achieve the change in operations desired by higher VRE penetration systems. In the Lowest Net Load event, dry hydropower led to less generation at peak, but hydropower was still shaped, subject to operational and regulatory constraints, to provide as much power as possible at the peak net load hours. While our modeling partially captured the coincident weather affecting hydropower availability and wind and solar generation, more research using a large weather data set is needed to more fully understand the correlation between hydropower, wind, and solar. Even more important than availability of water to hydropower's ability to provide value and resilience during key weather events is how much flexibility a hydropower unit has to shift energy day-to-day and hour-to-hour. The Inflexible Hydro sensitivity is quite costly to the WI as the system is unable to focus hydropower's water use during the events or hours of the event where it is most valued. Further research should be done to understand which is of higher value—shifting energy day-to-day or hour-to-hour—and how the type of event affects the value.

Finding 7. Broad, interconnection-wide impacts from wind turbine blade icing and cold temperature shutdowns are rare. However, regional icing and cold temperature events can be significant and rely on local gas generation dispatch and interregional transmission flows to maintain adequate supply to meet demand.

Two events—the December 2013 Winter Storms event and the February 2010 High Net Load 3 event—were used to investigate the impact of wind turbine blade icing and low temperature shutdowns on the 2050 infrastructure plan operations. Blade icing and low temperature shutdowns led to a 7% (3.5 GWh) and 10% (2.7 GWh) decreases in total wind generation for the December 2013 Winter Storms and the February 2010 Winter Net Load 3 events, respectively. In both cases the differences are made up almost entirely by the gas fleet: both gas-CCs and gas-CTs. This finding highlights the importance of planning for potential icing and cold temperature cut-outs in forecasting along with anticipating the increased forced outage rates of thermal units, in order to ensure needed capacity is available. Options for reducing icing and cold related derates through turbine cold weather packages should also be considered.

Figure 36 shows when icing or low-temperature shutdowns reduced wind generation capacity for the December 2013 Winter Storms event. Considering the entire resource throughout the three interconnections, wind generation derating due to icing and low temperature is pervasive throughout the event, but it never represented more than a 10% reduction in generation relative to the base case. That the aggregate resource rarely sees huge drops in wind generation means the effects of icing and cold temperature cut-outs on resilience and resource adequacy to broad areas are limited.

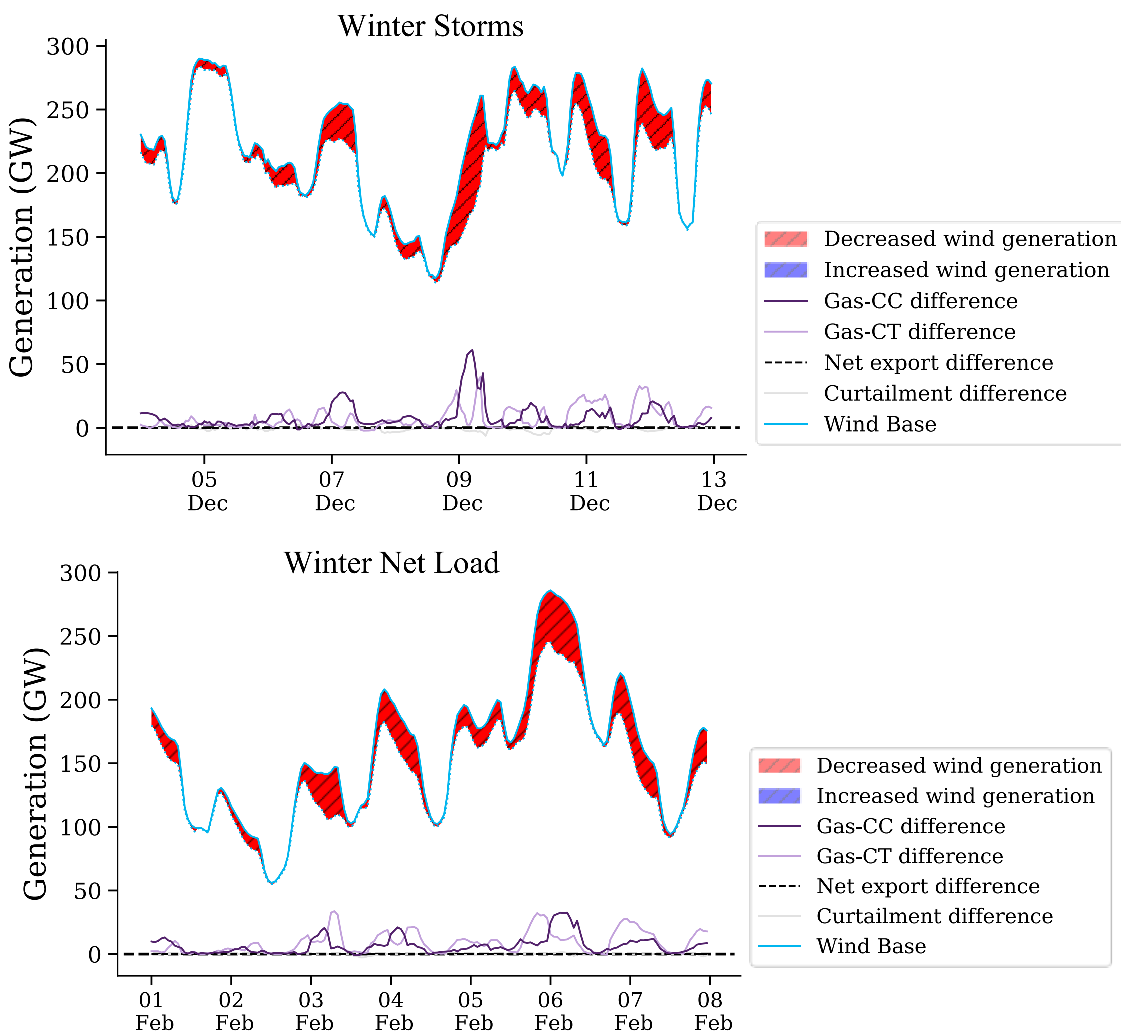

Figure 36. Total wind generation for the full system in the base plan and the blade icing and low temperature shutdown sensitivity for the December 2013 Winter Storms event (top) and the low VRE event in February 2010 (bottom)

The differences in gas-CC generation, gas-CT generation, and curtailment are also shown. The differences are between the base case run and the run that considered icing and low temperature shutdowns.

However, the system does react to the reduced wind generation. And a mix of increased gas-CC and gas-CT generation fills the gap. In the December 2013 Winter Storms event, the two technologies each meet about half the generation deficit; in the February 2010 Winter Net Load 3 event, gas-CTs meet about 58% of the deficit, and gas-CCs made up the rest.

Though system-wide icing does not lead to significant reductions in the wind generation, local impacts can be very large for long periods of time. Figure 37 shows the wind generation reduction in Minnesota and Wisconsin due to icing and low temperature shutdowns during the Winter Net Load 3 event. Starting late on February 3 and lasting until midday on February 4, the two-state region experiences a large icing event that reduces wind output. At the height of the event, wind output is reduced by 7,500 MW, about a 75% decrease relative to the base 2050 plan. The resulting gap is initially met by turning on quick start gas-CTs, but as the icing event continues and worsens, gas-CCs are also turned on. The region also reduces its exports to the Chicago area of PJM, meaning that region also must find other forms of generation to meet its load during this time.

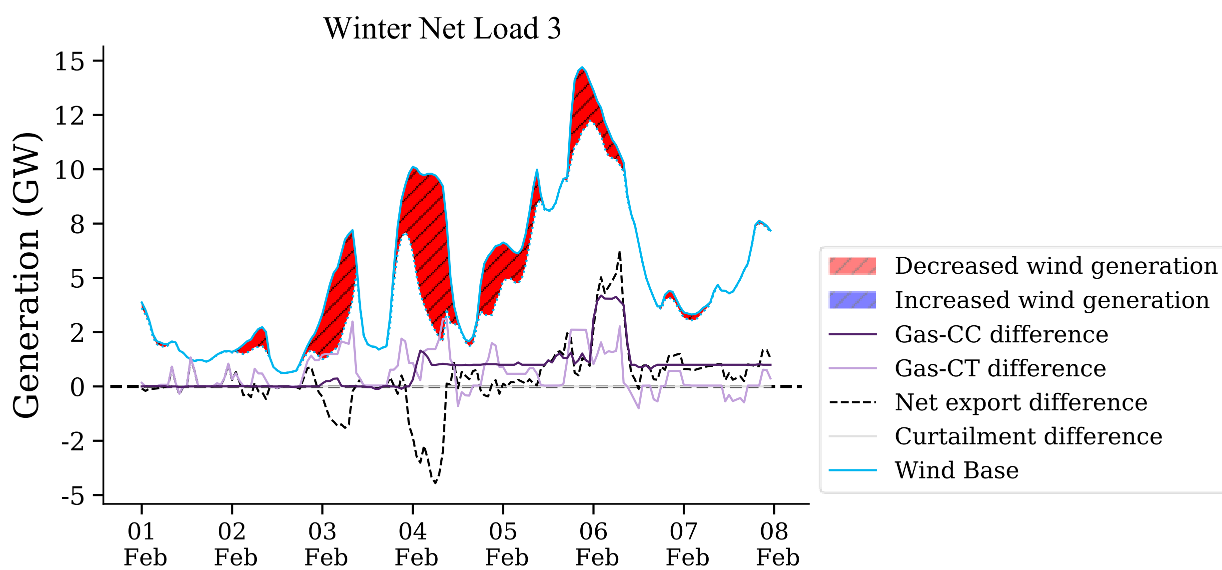

Figure 37. Icing and cold temperature cut-out's reduction of wind generation in Minnesota and Wisconsin for the Winter Net Load 3 event

The difference in gas-CC, gas-CT, curtailment of VRE, and net interchange between Minnesota and Wisconsin and their neighbors are also shown. The differences are between the base case run and the run that considered icing and cold temperature cut-outs.

Our modeled system responds to system-wide and local icing and low temperature shutdown events by turning on gas units and utilizing transmission flexibility; however, gas units have historically tended to be forced out more frequently at cold temperatures (Murphy, Sowell, and Apt 2019). Figure 38 shows the thermal forced outages during the December 2013 Winter Storms event. As the event progresses, a greater share of gas-CTs and gas-CCs begin to be forced offline, and at peak outage, about 10% of gas units are out in MISO. Enough reserve capacity is built such that the event can withstand both the reduced wind output from icing and low temperature shutdowns, and the increased gas outages. However, having this extra capacity to ensure adequacy comes at a cost.

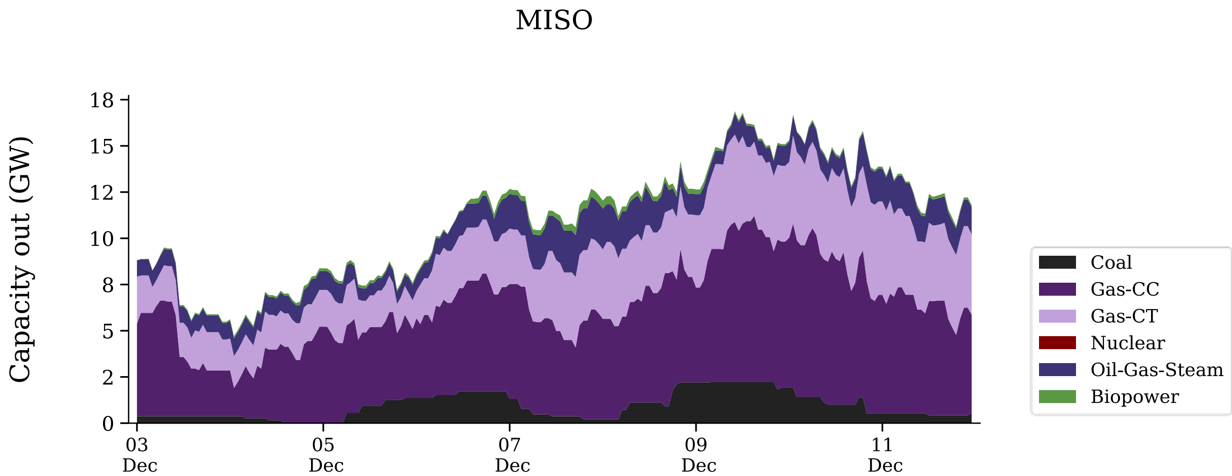

Figure 38. Total thermal capacity on an outage (forced or planned) in MISO during the December 2013 Winter Storms event in the 2050 system

Ability to forecast icing and cold temperature events and coordinate operations across regions will be key to determine how intense of a resilience and resource adequacy concern these events are. The cold or icing events were limited to reducing total wind generation in the EI by 10%. Though this is a significant reduction, it is not enough to force the event into the tail of the wind resource availability distribution. However, our modeling shows local icing and cold temperature shutdowns do reach more concerning levels, but with proper coordination with neighbors the event can be managed. We did not investigate the ability to forecast these types of wind generation derates, which should be a focus of future research.

Finding 8. Tropical storm impact on renewable resource availability is localized and of less impact than direct damage to generation, transmission, and distribution infrastructure.

Tropical storms and hurricanes can significantly impact the power sector. However, these storms primarily impact local transmission infrastructure, and the extent of the impact is small compared to both the size of the electrical system and the larger pressure systems that drive the extreme temperature events. Outside the band of damaging wind speeds, their impact on wind and solar generation is primarily through the broad extent of cloud cover and net increase in wind resource, even when accounting for the cut-out windspeed for the typical wind turbine.

For example, Figure 39 shows the time series of wind and solar generation in the EI and TI for September 1–4, 2008 as Hurricane Gustav made landfall and moved inland. Even though there is an area of good wind generation associated with the storm, the EI did not register wind generation that was outside what is seen in other events; the above-normal generation on September 1 and the early part of September 2 were more a function of the frontal zone in the northwest portion of the interconnection. This frontal zone dissipated on September 3, producing below-normal resource across the interconnection despite the presence of the weakening storm. The TI was small enough to see some impact from the storm, but it was no more dramatic than the impact from other events from more typical midlatitude storms.

The impact on solar was even smaller, and the cloud plume did not cover enough area to have an impact that was differentiable from the typical cloud cover, other than a slight change in the EI late on September 2 and early on September 3. In the case of Gustav and other tropical storms, we found that interconnection-wide changes in renewable resource were mostly in the noise and that the reduction in solar generation that was due to tropical storms was more than offset by increases in wind generation and reductions in load. Further, the strongest winds of a hurricane only extend a few tens of kilometers from the center of the storm, so even the most powerful storms will only cause high wind speed cutouts for wind turbines on a local level; again, these will be offset by increased generation elsewhere. Since hurricanes lose their strength rapidly upon landfall, their major impact on wind generation cutouts is limited to coastal regions.

For island systems, tropical storms and hurricanes are much more concerning, but for the conterminous United States the impact is minimal. We examined Hurricane Maria because it tracked up the East Coast and was found to have slightly beneficial impact on wind generation. However, there is a chance that a powerful Category 4 or 5 hurricane tracking through a dense area of offshore wind along the East Coast or through the Gulf of Mexico could have a major impact if it caused major infrastructure loss. Such an evaluation was outside the scope of this study and should be considered in future work.

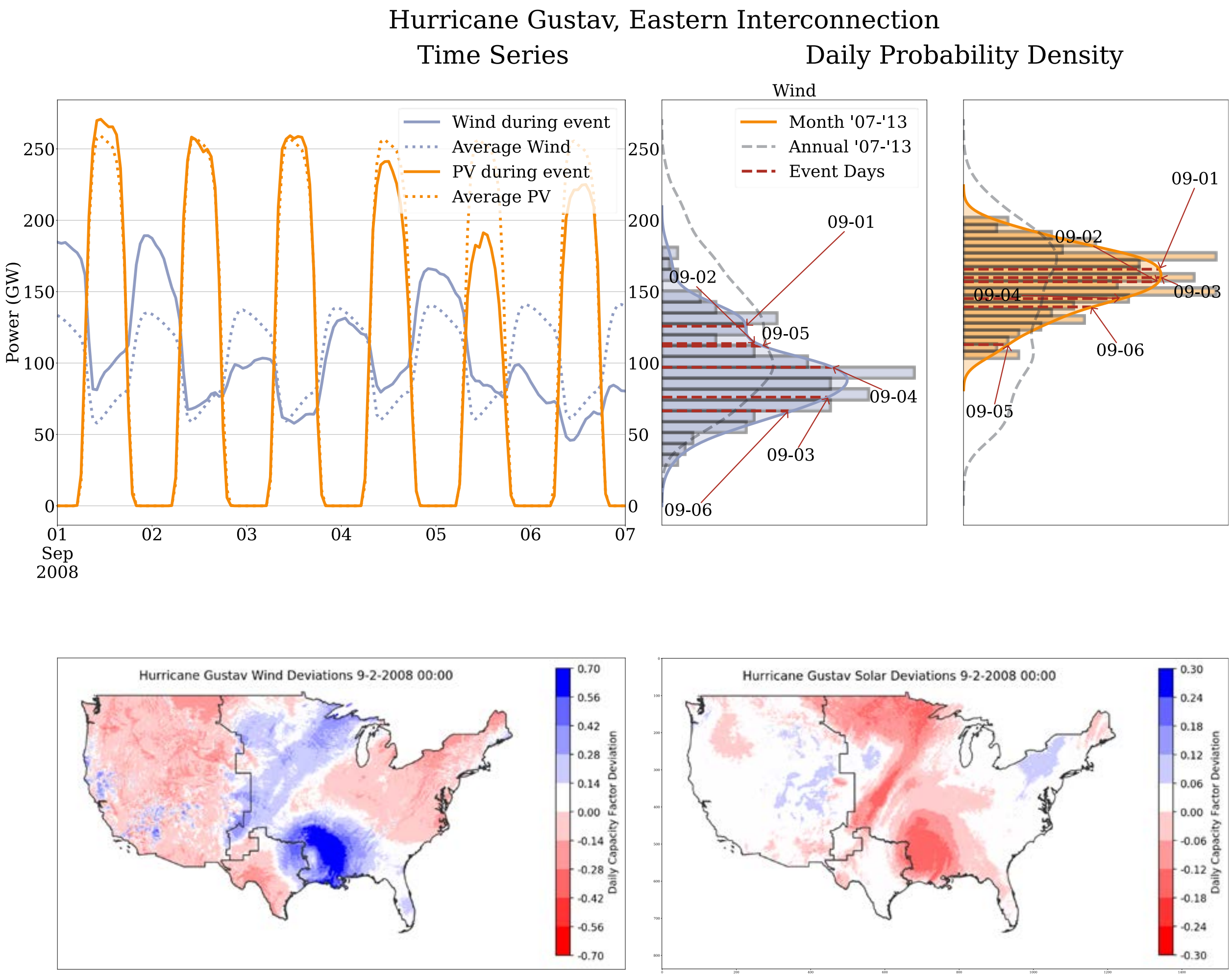

Figure 39. Spatial and temporal evolution of wind and solar resource during Hurricane Gustav

Top panels show 2050 infrastructure wind and solar simulated generation in the EI during Hurricane Gustav with bottom panels showing wind and solar resource deviation on September 2nd. This shows how the cloud cover from Gustav is relatively small as compared to the interconnect; solar generation during this day is near normal.

Conclusions

In this report, we presented a first of its kind analysis investigating how various weather events would impact U.S. power system operations when wind and solar are large contributors to the energy mix. Using case study weather events from 2007 to 2013, we found that this power system transition does not lead to new operational or resource adequacy concerns during the high-impact weather events of the past (e.g., extreme cold waves, extreme heat waves, and midlatitude storms). Wind and solar are generally available during these events. However, weather events that were not particularly concerning historically, and tend to be milder versions of the high-impact weather events, can lead to large and extended periods of wind and solar deficits. These events introduce new resource adequacy concerns and need to be a focus for planners and operators.

Cold waves, both extreme and mild, present a new dynamic for system operators to be aware of. In the EI and TI, wind generation potential tends to be high as the initial front of the cold wave sweeps across these interconnections, but then decreases in the days that follow even as temperatures remain cold. The extent, both temporally and spatially, of this wind generation lull will distinguish between cold waves that cause resource adequacy concerns for operators and planners. Based on the on the historical weather data set of 2007–2013, milder cold waves may have more severe lulls, presenting new weather conditions that cause resource adequacy concerns. Wind turbine blade icing and cold temperature shutdowns also introduce risk during cold waves, however, their impact tends to be local, while their interconnection-wide impact is less severe than the low wind generation caused by reduced wind speeds that can come after the initial cold front. Solar generation is lower in the wintertime, but winter precipitation and cloud cover can reduce solar generation even further. However, in the case study events we investigated, the impact tended to be spatially limited.

The resource adequacy risk of heat waves also evolves with greater penetrations of VRE. During heat waves, net load and resource adequacy risk tends to be highest after sunset when solar PV generation has gone to zero. During the record breaking heat waves within in our data set, there was enough wind generation potential to reduce the system stress at the daily net load peak. However, more mild heat waves that are associated with broad scale high pressure systems can lead to low wind generation potential in the evening and create higher net load periods than the record breaking heat waves of the past. A key limitation to our investigation of heat waves is that we did not include the impact of coincident large-scale wildfires that could have severe impact on solar PV generation potential. Given the wildfires and associated blackouts in California in the late summer of 2020, we recommend further research on how wildfires may change future system operations during heat waves.

For both cold and heat waves, a geographically diverse wind and solar fleet enabled by expanded and flexible transmission reduces regional resource adequacy risks, even when the negative impact to the wind and solar resource is widespread. Also, in regions with large contributions from hydropower, the flexible operations of those units reduce the operations cost and resource adequacy concerns associated with the weather events we studied. Other enabling technologies, such as storage of different durations, responsive demand, and offshore wind, should also be considered for their weather resilience value in future work.

For this report, we used case study weather events to provide initial insights on the evolving role of weather events to our power system operations and planning in the U.S. We encourage system planners, policy makers, and researchers to use these events to test the weather resilience and resource adequacy of future power system infrastructure, whether that is for an integrated resource plan or exploring tradeoffs between different policy decisions. This report also described a methodology for identify other events specific to different regions or weather years.

We also identified several areas where further research is required. Most importantly, we need to better understand how frequently the concerning events we identified occur, while capturing events we may have missed by only using a data set covering 2007–2013. This means creating wind, solar, hydropower, and load data sets for a larger historical period, but also creating data sets that capture the effects of climate change. As discussed in the Taxonomy of Extreme Weather Events section, climate change may vary the frequency and magnitude of the weather events we studied or introduce new types of weather events unexplored in this work. Using the expanded data sets, future work should also explore new methods to statistically quantify risks to system operations presented by these weather events by pairing PCM with other resource adequacy models and tool, while exploring a greater number of infrastructure plans.

References

Abatzoglou, J.T. and A.P. Williams. *Impact of Anthropogenic Climate Change on Wildfire Across Wester*n US Forests. Proceedings of the National Academy of Sciences. October 18, 2016 113 (42) 11770-11775. https://doi.org/10.1073/pnas.1607171113.

ABB. 2018. "ABB Velocity Suite." http://new.abb.com/enterprise-software/energy-portfolio-management/market-intelligence-services/velocity-suite.

Allen-Dumas, Melissa, Binita KC, and Colin I. Cunliff. *Extreme Weather and Climate Vulnerabilities of the Electric Grid: A Summary of Environmental Sensitivity Quantification Methods*. Oak Ridge, TN: Oak Ridge National Laboratory. ORNL/TM-2019/1252. https://doi.org/10.2172/1558514.

Blackport, Russell, and James Screen. 2020. Weakened evidence for mid-latitude impacts of Arctic warming, Nature Climate Change, Vol. 10. https://doi.org/10.1038/s41558-020-00954-y

Bloom, Aaron, and Josh Novacheck. 2017. *The Eastern Renewable Generation Integration Study: Insights on System Stress: Preprint*. Presented at the 6th International Workshop on Integration of Solar Power into Power Systems, Vienna, Austria, November 14–15, 2016. National Renewable Energy Laboratory. NREL/CP-6A20-67205. https://www.nrel.gov/docs/fy17osti/67205.pdf .

Bloomfield, H. C., C. C. Suitters, D. R. Drew, *Meteorological Drivers of European Power System Stress*, Journal of Renewable Energy, vol. 2020, Article ID 5481010, 2020. https://doi.org/10.1155/2020/5481010

Brinkman, Gregory, Dominique Bain, Grant Buster, Caroline Draxl, Paritosh Das, Jonathan Ho, Eduardo Ibanez, et al. 2021. *The North American Renewable Integration Study: A U.S. Perspective*. Golden, CO: National Renewable Energy Laboratory. NREL/TP-6A20-79224. https://www.nrel.gov/docs/fy21osti/79224.pdf.

Cohen, J, et al. 2020. *Divergent consensuses on Arctic amplification influence on midlatitude severe winter weather*, Nature Climate Change, Vol. 10. https://doi.org/10.1038/s41558-019-0662-y

Cohen, Stuart, Jon Becker, Dave Bielen, Maxwell Brown, Wesley Cole, Kelly Eurek, Will Frazier, et al. 2020. Regional Energy Deployment System (ReEDS) Model Documentation: Version 2019. Golden, CO: National Renewable Energy Laboratory. NREL/TP-6A20-74111. https://doi.org/10.2172/1606151.

Cohen, Stuart, Jon Becker, Dave Bielen, Maxwell Brown, Wesley Cole, Kelly Eurek, Will Frazier, et al. 2019. *Regional Energy Deployment System (ReEDS) Model Documentation: Version 2018*. Golden, CO: National Renewable Energy Laboratory. NREL/TP-6A20-72023. https://doi.org/10.2172/1505935.

Cole, Wesley, Daniel Greer, Katherine Lamb. *The potential for using local PV to meet critical loads during hurricanes.* Solar Energy, vol. 205, 2020. https://doi.org/10.1016/j.solener.2020.04.094

Cole, Wesley, Will Frazier, Paul Donohoo-Vallett, Trieu Mai, and Paritosh Das. 2018. *2018 Standard Scenarios Report: A U.S. Electricity Sector Outlook*. Golden, CO: National Renewable Energy Laboratory. NREL/TP-6A20-71913. https://doi.org/10.2172/1481848.

Cole, Wesley, Nathaniel Gates, Trieu Mai, Daniel Greer, and Paritosh Das. 2019. *2019 Standard Scenarios Report: A U.S. Electricity Sector Outlook*. Golden, CO: National Renewable Energy Laboratory. NREL/TP-6A20-74110. https://doi.org/10.2172/1580330.

Cole, Wesley, Sean Corcoran, Nathaniel Gates, Trieu Mai, and Paritosh Das. 2020. *2020 Standard Scenarios Report: A U.S. Electricity Sector Outlook*. Golden, CO: National Renewable Energy Laboratory. NREL/TP-6A20-77442. https://www.nrel.gov/docs/fy21osti/77442.pdf.

Denholm, Paul, Trieu Mai, Rick Wallace Kenyon, Ben Kroposki, and Mark O'Malley. 2020. *Inertia and the Power Grid: A Guide Without the Spin*. Golden, CO: National Renewable Energy Laboratory. NREL/TP-6120-73856. https://www.nrel.gov/docs/fy20osti/73856.pdf.

EIA (U.S. Energy Information Administration). 2018. "Annual Energy Outlook 2018 with projections to 2050." Washington, D.C.: U.S. Energy Information Administration. https://www.eia.gov/outlooks/aeo/pdf/aeo2018.pdf.

Francis, Jennifer and Stephen J Vavrus. 2015. Evidence for a wavier jet stream in response to rapid Arctic warming. Environ. Res. Lett. 10 014005

Handschy, Mark, Stephen Rose, Jay Apt. *Is it always windy somewhere? Occurrence of low-wind-power events over large areas.* Renewable Energy, vol. 101, 2017. https://doi.org/10.1016/j.renene.2016.10.004

Hardiman, Mike. 2011. *Intense Cold Wave of February 2011*. National Weather Service El Paso, Texas, Santa Teresa, New Mexico. https://www.weather.gov/media/epz/Storm_Reports/Cold11/Feb2011ColdWx.pdf.

Keane, Andrew; Milligan, Michael R.; Dent, Chris; Hasche, Bernhard; D'Annunzio, Claudine; Dragoon, Ken; Holttinen, Hannele; Samaan, Nader; Söder, Lennart; O'Malley, Mark. *Capacity value of wind power.* IEEE Transactions on Power Systems, 26 (2): 564-572, 2011. https://doi.org/10.1109/TPWRS.2010.2062543

Kretschmer et al 2018, *The different stratospheric influence on cold-extremes in Eurasia and North America.* Nature Clim. Atmos. Sci, 1. https://doi.org/10.1038/s41612-018-0054-4.

Li, Bowen, Sukanta Basu, Simon J. Watson, and Herman W.J. Russchenberg. *Mesoscale modeling of a "Dunkelflaute" event,* Wind Energy, vol. 24, issue 1, 2020. https://doi.org/10.1002/we.2554

Maclaurin, Galen, Nick Grue, Anthony Lopez, and Donna Heimiller. 2019. *The Renewable Energy Potential (reV) Model: A Geospatial Platform for Technical Potential and Supply Curve Modeling*. Golden, CO: National Renewable Energy Laboratory. NREL/TP-6A20-73067. https://doi.org/10.2172/1563140.

Murphy, Sinnott, Fallaw Sowell, and Jay Apt. "A Time-Dependent Model of Generator Failures and Recoveries Captures Correlated Events and Quantifies Temperature Dependence." *Applied Energy* 252 (November 2019). https://doi.org/10.1016/j.apenergy.2019.113513.

NERC (North American Electric Reliability Corporation). 2014. "Polar Vortex Review." Atlanta, GA. https://www.nerc.com/pa/rrm/Pages/January-2014-Polar-Vortex-Review.aspx.

NREL (National Renewable Energy Laboratory). 2018. "2018 ATB (Annual Technology Baseline)." Golden, CO: National Renewable Energy Laboratory. https://atb.nrel.gov/electricity/2018/.

O'Connell, Matt, Nathalie Voisin, Jordan Macknick, Fu. *Sensitivity of Western U.S. power system dynamics to droughts compounded with fuel price variability.* Applied Energy, vol. 247. 2019. https://doi.org/10.1016/j.apenergy.2019.01.156

Rose, Stephen. (2019, June 4–6). "MISO Market Operations during Weather Events." ESIG 2019 Meteorology & Market Design for Grid Services Workshop, Denver, CO, United States. https://www.esig.energy/event/meteorology-market-design-for-grid-services-workshop/.

Rossol, Michael, Grant Buster, and Mike Bannister. The Renewable Energy Potential Model (reV). https://github.com/NREL/reV (version v0.4.46), 2021. https://doi.org/10.5281/zenodo.4501717.

Sun, Yinong, Paige Jadun, Brent Nelson, Matteo Muratori, Caitlin Murphy, Jeffrey Logan, and Trieu Mai. 2020. Electrification Futures Study: Methodological Approaches for Assessing Long-Term Power System Impacts of End-Use Electrification. Golden, CO: National Renewable Energy Laboratory. NREL/TP-6A20-73336. https://www.nrel.gov/docs/fy20osti/73336.pdf.

Tsai, Chen-Hao, Armando Figueroa-Acevedo, Maire Boese, Nihal Mohan, James Okullo, Brandon Heath, and Jordan Bakke. *Challenges of Planning for High Renewable Futures: Experience in the U.S. Midcontinent Electricity Market.* Renewable and Sustainable Energy Reviews, Volume 131, October 2020. https://doi.org/10.1016/j.rser.2020.109992.

Appendix. Scenario Design, 2007-2013 Data Analysis, and Case Study Descriptions

ReEDS Scenario Assumptions

A customized set of these futures was run in ReEDS specifically for this study to create future infrastructure scenarios for 2024, 2036, and 2050. The Heritage ReEDS version was used. This version is run in 2-year increments in the sequential solve mode with foresight limited to natural gas price forecasts. It also included expansion and retirement decisions for Canada. This particular ReEDS version only consider a single weather year, 2012, for making planning decisions, current ReEDS versions use the full 2007–2013 weather years. The main constraint ReEDS uses to ensure adequate generation capacity exists to serve peak and extreme loads is by enforcing a regional planning reserve margin consistent with today's NERC recommendations. Between the two year solve intervals, ReEDS updates the capacity credit of wind and solar (i.e., the percent of installed capacity counted toward the planning reserve margin) for each region based on a top net load hour analysis. The scenario was run with most of the same assumptions as the 2018 Standard Scenarios' (Cole et al. 2018) Low RE Cost scenario, which includes:

- Reference demand growth rate from the EIA's Annual Energy Outlook 2018 (AEO2018) (EIA 2018)
- Reference natural gas price from the AEO2018 (EIA 2018)
- Low-case projections for solar photovoltaics (PV) and wind cost from the 2018 Annual Technology Baseline (ATB) (NREL 2018)
- Mid generation and storage technology cost projections from the 2018 ATB (NREL 2018)
- Financing values from the 2018 ATB with a 20-year capital recovery period
- Thermal lifetime retirements for non-nuclear plants based on the ABB Velocity Suite database (ABB 2018), at-risk nuclear retirements at 60 years, and all other nuclear at 80 years
- No feedback due to changes in the climate that would impact the wind, solar, and load profiles or water availability for hydropower.
- State, regional, and federal policies as of spring 2018.[32]

However, the scenarios differ from the 2018 Standard Scenarios Mid-Case because it uses the 2019 Standard Scenarios renewable energy supply curve assumptions. (Cohen et al. 2019). Figure 1 (page 9) plots the cost-optimal resource mixes determined by ReEDS for all three scenarios in the Eastern Interconnection (EI), Texas Interconnection (TI), and Western Interconnection (WI). The installed capacity for each generator type and locations of wind and solar build-out for each scenario are summarized in Figure 1 and Figure 2 (page 9).

Behind-the-meter, distributed PV capacity was included in the infrastructure with NREL's Distributed Generation Market Demand (dGen) model. It simulates customer adoption of

[32] See ReEDS documentation (Cohen et al. 2019) chapter 8 for a detailed explanation of policies modeled and their implementation.

distributed energy resources for residential, commercial, and industrial entities based on technology costs, local rate structures, and consumer behavior.[33]

Further Exploration of Net Load of 2024, 2036, and 2050 Infrastructure Scenarios

Figure A-1 shows three heat maps of the hourly load versus net load for all hours in the 2007–2013 data set for the 2024, 2036, and 2050 scenarios. The heat maps provide additional insight into how net load behavior changes as wind and solar penetration increases. In 2024, we see a tight distribution of load and net load, with a roughly linear correlation between them. As VRE penetration increases, the load-to-net load relationship becomes more diffuse because of the variability of both wind and solar. In addition, despite load increasing, the overall net load distribution moves downward and the occurance of hourly net loads above 700 GW reduces. The bifurcation that is seen is a result of an increasing amount of solar capacity. The upper part of the distribution contains more nighttime hours and the lower net load distribution is daytime where solar is present. Some of the densely populated area joining the two is associated with increased variability in solar relative to load, near sunset and sunrise, as well as the variability associated with the diurnal wind generation profile. The rest is a function of wind and solar variability associated with changes in weather at all time scales. The addition of VRE tilts the distribution away from a one-to-one relationship, especially at lower loads. It trends back toward equivalence at very high loads, but the relationship is complex, and is driven by multiple effects. To parse some of these impacts, we analyzed the data by interconnection and season, and we examined the relationship of load to wind generation, solar generation, and overall renewable generation on both an hourly basis and a daily average basis.

[33] "Distributed Generation Market Demand Model." NREL, https://www.nrel.gov/analysis/dgen/

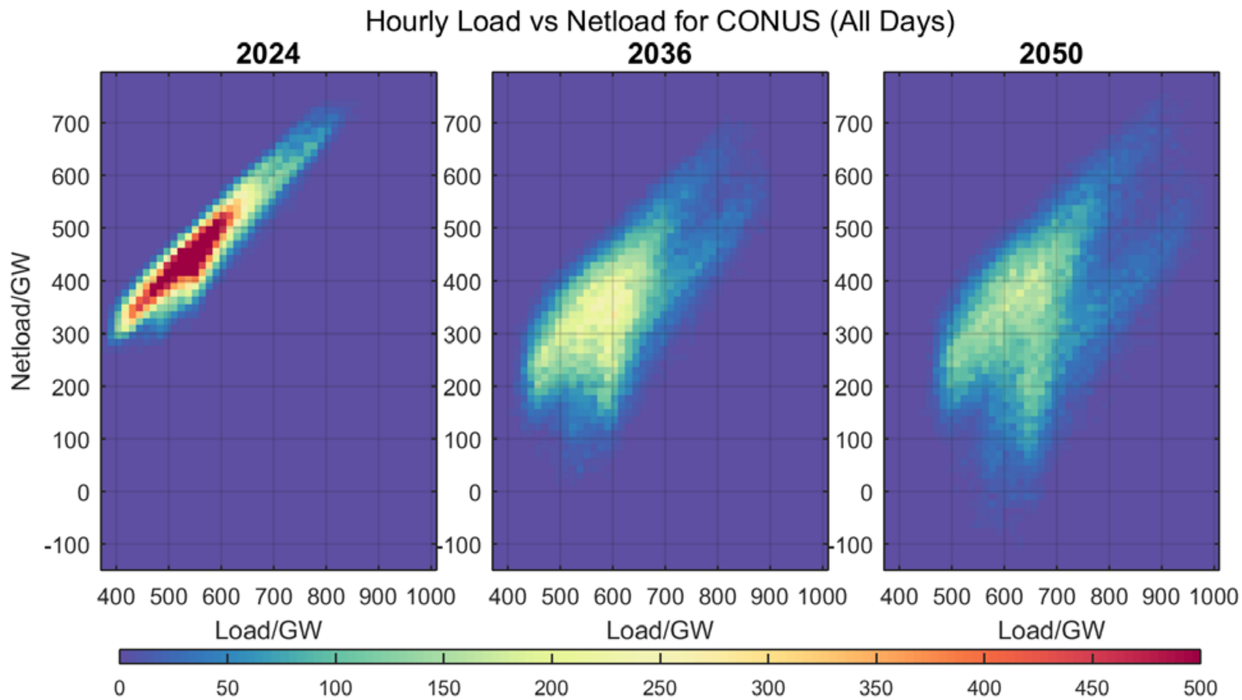

A-1. Distribution of hourly load versus net residual load across all days and years for the entire CONUS

Figure A-2 shows the relationship of wind generation to load for all hours. As expected, the distribution becomes more diffuse as wind capacity is added. There is a trend toward less wind generation for hours with higher load. This is because wind generation in most locations peaks at night, when load tends to be lower, and because on average across the CONUS typical wind generation is stronger during the spring and autumn when load is lower, and weaker during the summer months when loads are higher. Daily distributions (not shown here) reveal this. And we see that as load increases into the tail of the distribution, wind output does not continue to fall. There is a complicated relationship between the weather that creates demand spikes (especially in winter) and the coincident wind resource, as we discuss later in Finding 3.

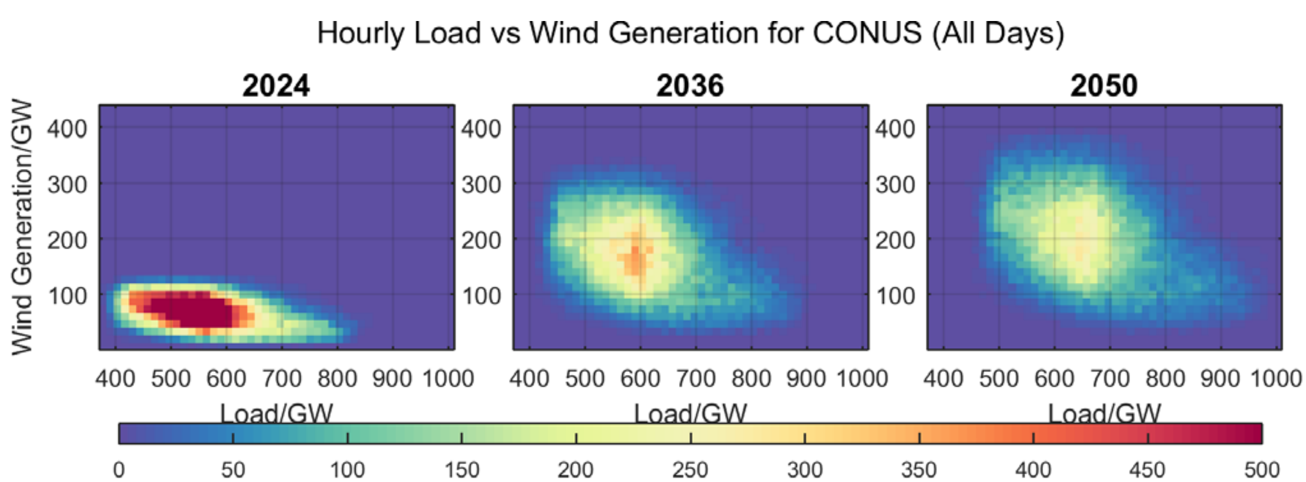

Figure A-2. Distribution of hourly load versus wind generation across all days and years for the entire CONUS

The relationship of PV generation (Figure A-3) to load also becomes more diffuse as diversity and peneteration increases. The large number of points at or close to zero are associated with nighttime and sunrise/sunset, while the spread is a function of sky cover, time of year, and other meteorological factors impacting solar potential. However, we do see high solar generation during periods of high loads. There are several reasons for this that are at play in different scenarios. First, solar resource in most locations peaks in summer on sunny days; these are also days when load tends to be high. However, at southerly latitudes (e.g., southern parts of California, Arizona, New Mexico, Texas, the Gulf States, and Florida), solar generation potential can also be high in winter and spring on cold, sunny days because of the relationship between PV panel temperature and efficiency. And such days are often high load days.

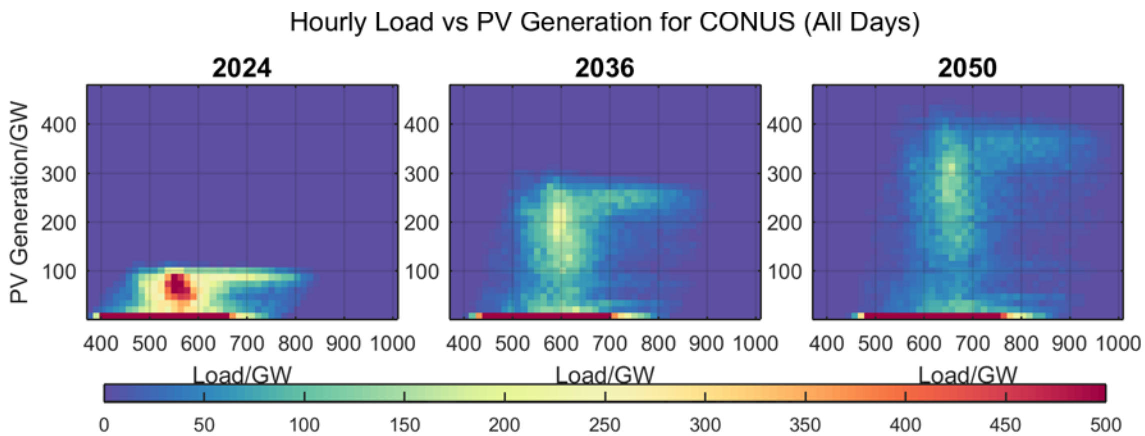

Figure A-3. Distribution of hourly load versus PV generation across all days and years for the entire CONUS

When the time-series data are broken down by season and region, additional patterns begin to emerge. For example, Figure A-4 and Figure A-5 highlight the differences between the winter and summer correlation of hourly wind to load in the EI. In these figures, we see that winter wind generation is better correlated to load than is summer generation. The overall wind generation is considerably higher in the winter months and the inverse correlation between wind generation and load disappears, while it is still obvious in summer months. This is because EI winter loads are initiated by transitions to cold weather and these transitions are intiated by storm systems that bring windy weather. Meanwhile, high loads in the summer are associated with large domes of high pressure that can bring stagnant conditions to much of the EI. Though these conditions can also promote the low-level jet, this is a nighttime phenomena and it is anticorrelated with EI load patterns.

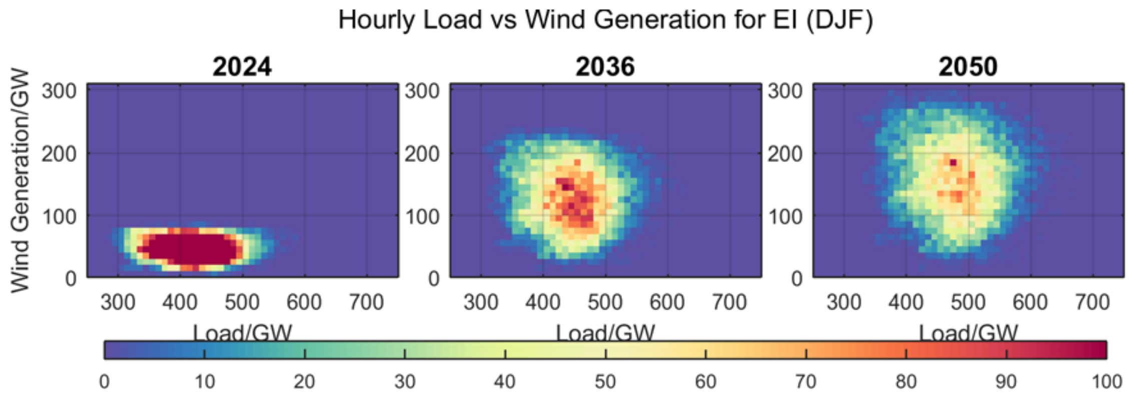

Figure A-4. Distribution of hourly load versus wind generation in winter months for the EI

DJF = All days in the months of December, January, and February

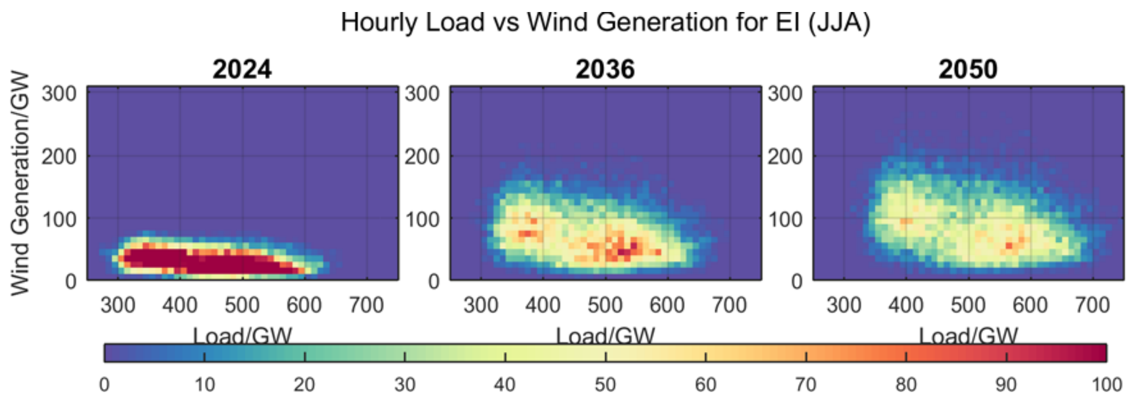

Figure A-5. Distribution of hourly load versus wind generation in summer months for the EI

JJA = All days in the months of June, July, and August

Our analysis here describes the evolution of the net load across the three infrastructure scenarios and the complex interrelationships involved in the weather driving the strength and timing of load and generation. The reminder of the paper focuses on extremes within the net load distributions and how those extremes differ between today and higher VRE penetration systems.

Event Description Structure

In this report, we used a standardized approach to report on each of the events we analyzed (Table 4, page 17), in which we describe each event's meteorology and its impacts on load, wind generation, and solar generation. And the section for each event concludes with a subsection examining the overall system impacts, where the nuances of the event can be highlighted and seen in the context of how an event's meteorology might impact the grid from a perspective focused on outage and resource sufficiency.

The following subsections are used for each event:

- **Meteorological Description:** summary of the historical weather event; features that make it unique, unusual, or challenging; and associated maps
- **Load Impacts:** an interconnection-level analysis of load during the event, in the context of the historical load shape and scaled to represent 2050 load data set to identify unusual impacts.

- **Wind and Solar Generation:** resource availability for wind and solar during the event; predicted modeled time series of generation by interconnection under a future with high variable renewable build-out; and a statistical analysis of the events position within the adjacent period and the overall data set.
- **Overall System Implications**: modeled future net load time series during the event and comparison to daily net load across the full data set; discussion of any other system impacts (e.g., outages of conventional generators, transmission system impacts, and other nonmodeled potential impacts on renewable generation)
- **System Modeling:** results from a full production cost modeling exercise for the event for each of the three interconnections, including comparisons for operations at progressively higher penetrations from 2024, 2036, and 2050.

Standardized visualizations are used to present the findings for each section for an event. A meta-description of each figure used is described below in the Meteorological Summary Figures section.

Note that meteorological events are unique in terms of geographical extent and longevity. For example, cold waves tend to last only a few days and translate from west to east across the country, but heat waves can last several weeks. For this reason, for each event, the number of panels presented in a figure that provides geographic information will vary to show the evolution of the weather as effectively as possible. Similarly, the date ranges that are averaged in plots showing statistical aggregation and the scale for time-series graphs will vary. Geographically, modeled generation is aggregated to the WI, EI, and TI footprints. Many of the figures will contain hyperlinks that allow readers to access additional graphics that would not be practical to incorporate here.

Meteorological Summary Figures

Figure A-6 shows examples of the two types of geographic weather maps that summarize each meteorological event. Subplot (a) shows a typical surface weather map detailing the sea-level pressure distribution, weather system locations and frontal boundaries, while subplot (b) shows maximum and minimum temperatures. In all cases presented here, these maps were obtained from the NOAA National Centers for Environmental Prediction online archives. The figures in the electronic version of this report contains embedded hyperlinks to the online archive for the event, which contain high-resolution data for each event, including detailed surface station plots, 500 mb height plots and quantitative precipitation plots.

Each event will typically show a series of panels for each map type to show the evolution of the event in time. Subplot (a) provides a meteorological synopsis valid at 7 a.m. EST (12 noon UTC). The information presented is a simplified version of a standard surface map and will be familiar to readers with a meteorological background. Key features have been labeled for non-meteorologists and are described in Table A-1.

Subplot (b) presents contour plots of maximum and minimum temperature. The maximum temperature is for the period from 7 a.m. through 7 p.m. LST the *previous* day and the minimum temperature is for the period from 7 p.m. LST the *previous* day through 7 a.m. LST on the indicated date of the surface map. Areas of excessive cold or heat drive generally drive increased electricity demand, are correlated with conventional generator outages, and in some cases can directly affect wind or solar generation.

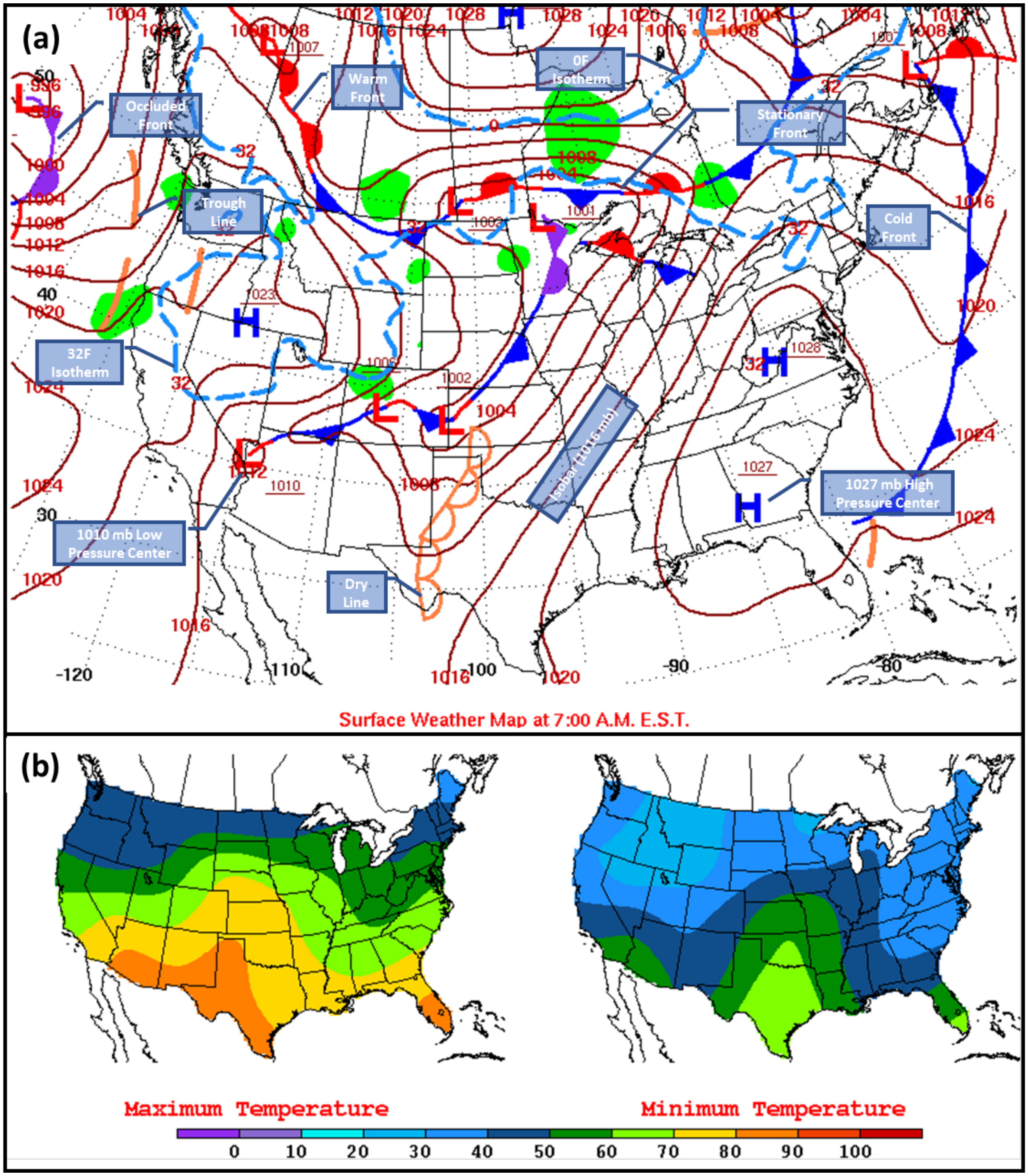

Figure A-6. Examples of weather map with labels (a) and min-max temperature maps (b)

Table A-1. Weather map symbol description

Name	Example	Meteorological Description	Electric Sector Impact
Isobars	1024	Lines of constant sea-level pressure	The closer the isobars are together, the stronger the pressure gradient force and the stronger the wind and associated wind generation
High pressure center	**H**	Local maxima in surface pressure and are generally associated with quiescent weather, sinking motion and clearing skies.	Low wind generation; typically, good solar, but can be associated with fog in the wintertime.
Low pressure center	**L**	These represent local minima in surface pressure and are associated with storm centers, rising motion, clouds and precipitation.	Poor solar generation, especially east of low pressure.
Fronts	Four types of fronts exist, outlined below, all representing zones of temperature contrast, clouds, and precipitation. A front shown with a dashed line is weakening. All fronts are marked by a wind shift and period of stronger wind		
	Cold Front 	Cold air moving into the region the triangle points toward.	Cooling behind front; passage often marks improving solar and wind resource
	Warm Front 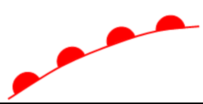	Warm air moving into the region the ahead of the semi-circle.	Approach brings lowering cloud deck and less solar resource, improving after passage. Warming.
	Stationary Front 	Zone of temperature gradient that is stationary.	Persistent poor solar resource; some wind
	Occluded Front 	Situation in a mature midlatitude cyclone where the cold front has caught up with and lifted the warm front so that the warm front is no longer observed at the surface	Improving wind and solar resource behind the front; cooling temperatures
Trough Line	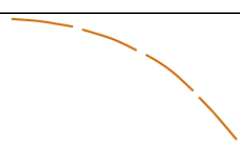	Line connecting local maxima in cyclonic curvature in the isobars. These areas are the locus of clouds and precipitation and are often decaying fronts where a strong temperature gradient is no longer present at the surface (all fronts have a trough along them).	Wind shift and increase as trough passes; decreasing solar resource upon approach, improving behind.

Name	Example	Meteorological Description	Electric Sector Impact
Dry Line	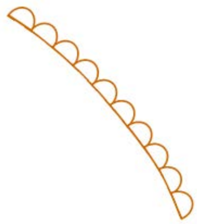	Zones where there is a large gradient in humidity but little gradient in temperature. Important in diagnosing and predicting severe thunderstorm (convective) activity	Highlights the boundary of increased air conditioner load due to humid conditions. Focus for deep convection => reduced solar and possible gusty variable winds.
Isotherms	32º F 0º F	Lines of constant temperature. The 32ºF line indicates the boundary between freezing and non-freezing conditions	Extreme low temperatures can cause wind to cut out. Freezing precipitation can linger on panels/blades, reducing generation after a storm.
Precipitation	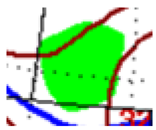	Areas where precipitation was occurring at the valid time of the map	Poor solar resource; less diurnal temperature fluctuation

Wind and Solar Total Resource Maps

Figure A-7 illustrates the wind and solar capacity factors averaged for a given day, along with the deviation (in absolute capacity factor) from the average resource obtained by subtracting the corresponding 29-day x 7-year window average described in the Identification Methodology section. The blue positive deviations represent above-average resource and the red negative deviations are below normal. The capacity factors were obtained by running the wind and solar resource data through power curves for standard technology turbines and panels, as described in the Weather, Demand, and Renewable Resource Data section.

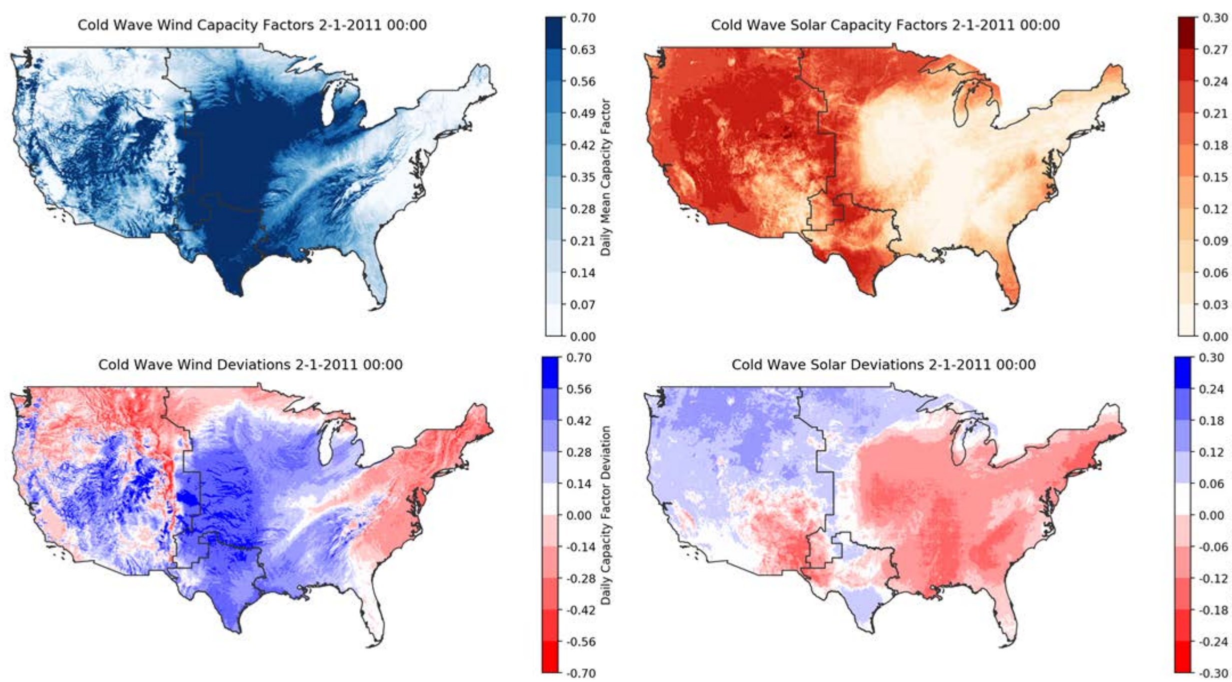

Figure A-7. Example of spatial wind and solar resource average and deviation maps

These plots represent the estimated daily average/deviation of wind and solar resource at each point on the 4-km resource grids. However, the actual impact of deviations on total generation is dependent on the specific locations of the existing and modeled future wind and solar generators as described in *Weather, Demand, and Renewable Resource Data.* Note the region outlines for the WI, EI, and TI.

Time-Series and Daily Probability Density Plots for Load, Wind Generation, Solar Generation, and Net Load

For the duration of the event, plots for wind and solar generation along with load and net load are created for each interconnection region. An example for load is shown in Figure A-8 (page 89). These combination plots show a time series on the left with hourly resolution that shows the evolution of each metric through the event along with a comparison to "normal" derived from the full data set.

The derivation of each metric is described below:

- *Load*: based on historical load for the 2007 through 2013 period. Each region is scaled according to the expected load growth in each region under standard EIA assumptions. The normal line is calculated by averaging all matching timestamps (e.g. all noon hours) across the 29-day period surrounding each event hour, taking into account all 7 meteorological years. This averaging does not take into account variability in the load shape due to weekends and holidays, as the data set is not long enough to do so in a statistically robust way.
- *Wind and solar generation*: estimated by running the WIND Toolkit and NSRDB data for the respective hour and location through the power curves of the generators built out by ReEDS; the 2050 Tech Break scenario is used unless otherwise noted. Moving windows 29-day windows are also used to calculate the typical wind and solar generation, which is not subject to weekend and holiday differences.
- *Net load*: calculated by subtracting the wind and solar generation from the load. The sum of wind and solar normal are subtracted from the load to obtain normal net load.

On the right is a statistical distribution to illustrate the attributes of an event in context of the broader data set. The distribution shows data for days surrounding the event from all 7 years. The actual days of the event are indicated on the plot to identify their location within the distribution. The number of days around the event will vary according to the event type to get the correct type of context. In the example shown here, the 14 days before and after the middle of a 4-day cold event are used, so the distribution contains 29*7 (years)=203 days. The smooth line is a best fit to the distribution, while the bars represent the actual data frequency. The dashed line shows the annual distribution (i.e., all data).

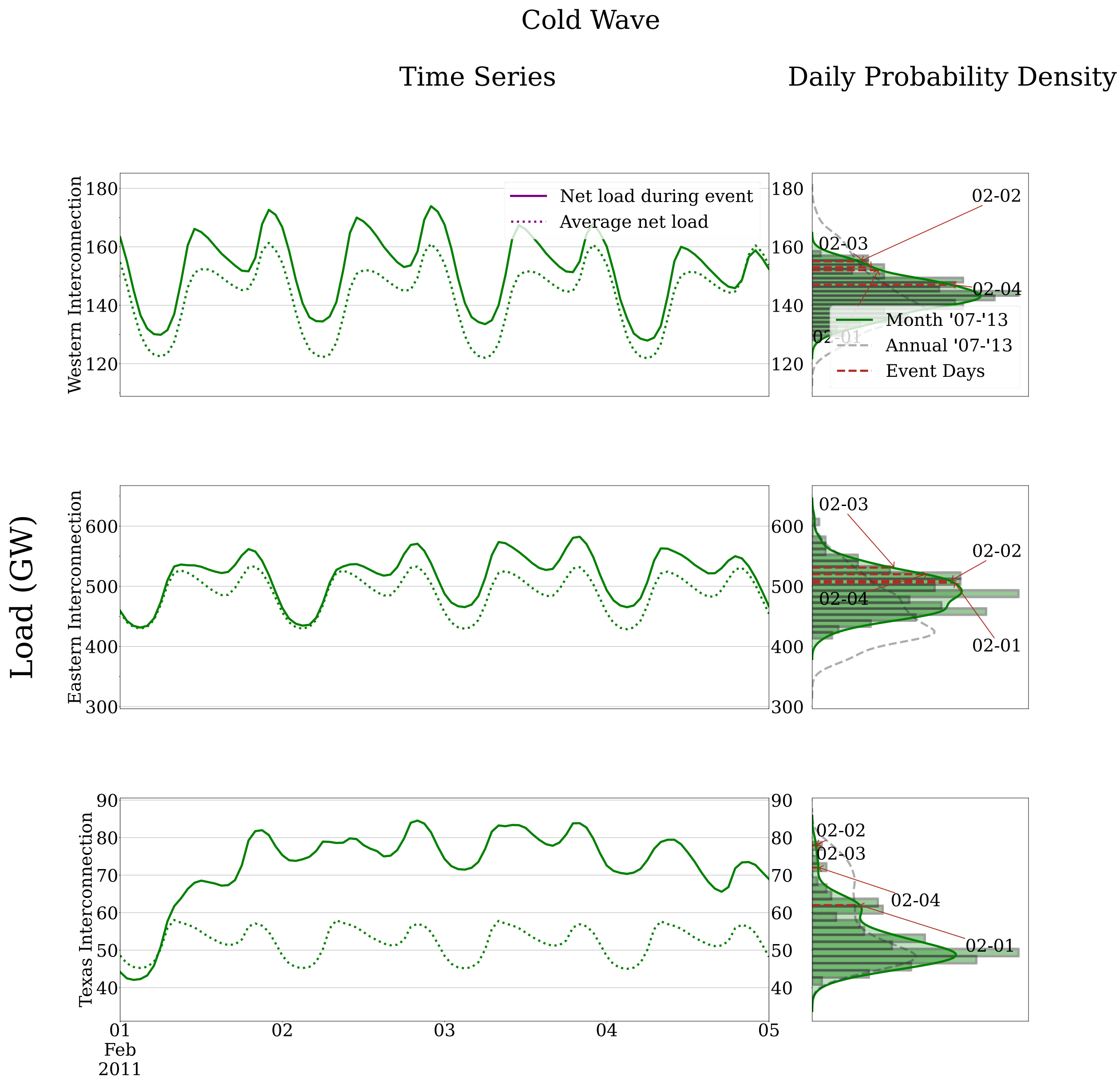

Figure A-8. Distribution of 2050 regional loads for the 29 days surrounding the middle of the event in green, and across the 7-year data set in gray, with the event days labeled (right); time series of regional load during the 4-day event in green, compared to load averaged across the 7-year data set for the month surrounding the event in gray (left)

Cold Wave: February 1–February 4, 2011

Event Summary

The beginning of February 2011 saw an intense cold wave impact much of the country, setting many records. The event was unusual in the southward penetration of cold air, with temperatures well below freezing reaching El Paso, Texas. The cold air was also deep enough to filter into the Intermountain West rather than simply channeling down the east side of the Rocky Mountains. The cold results in higher-than-normal and, in the TI's case, extreme load for this time of year. In some regions, the cold front that causes the low temperatures also contributes to higher-than-normal wind resources, especially at the beginning of the event.

In modeled future systems, this dynamic enables increased wind generation and a lower reliance on the thermal fleet to meet increased load. However, the cold persists for multiple days, keeping load high while wind generation decreases, leading to the need for increased Gas-CC generation, especially in the TI and the EI. For future study, it is critical to understand the value of storage to mitigate the need for thermal cycling, thermal capacity reserve, and reliance on long distance power transmission.

Meteorologically, the February 2011 cold wave was notable for three key characteristics. First, the intensity and longevity of the cold in the southwestern and southern tier states was unusual as it lingered and was reinforced as it pushed south, west, and east. Figure A-9 shows the daily maximum and minimum temperatures across CONUS for February 2, 2011, the day the areal extent of the cold air was greatest with almost a third of CONUS experiencing temperature minima below 0°F (-18°C). Second, the intensity of the high pressure associated with the cold dense air, which reached 1055 mb, which is close to the CONUS record of 1058.5 mb. Last, the cold system also spawned back-to-back storms that developed in the desert southwest, bringing snow and additional winter storm impacts to regions already affected by the cold.

Meteorological Description

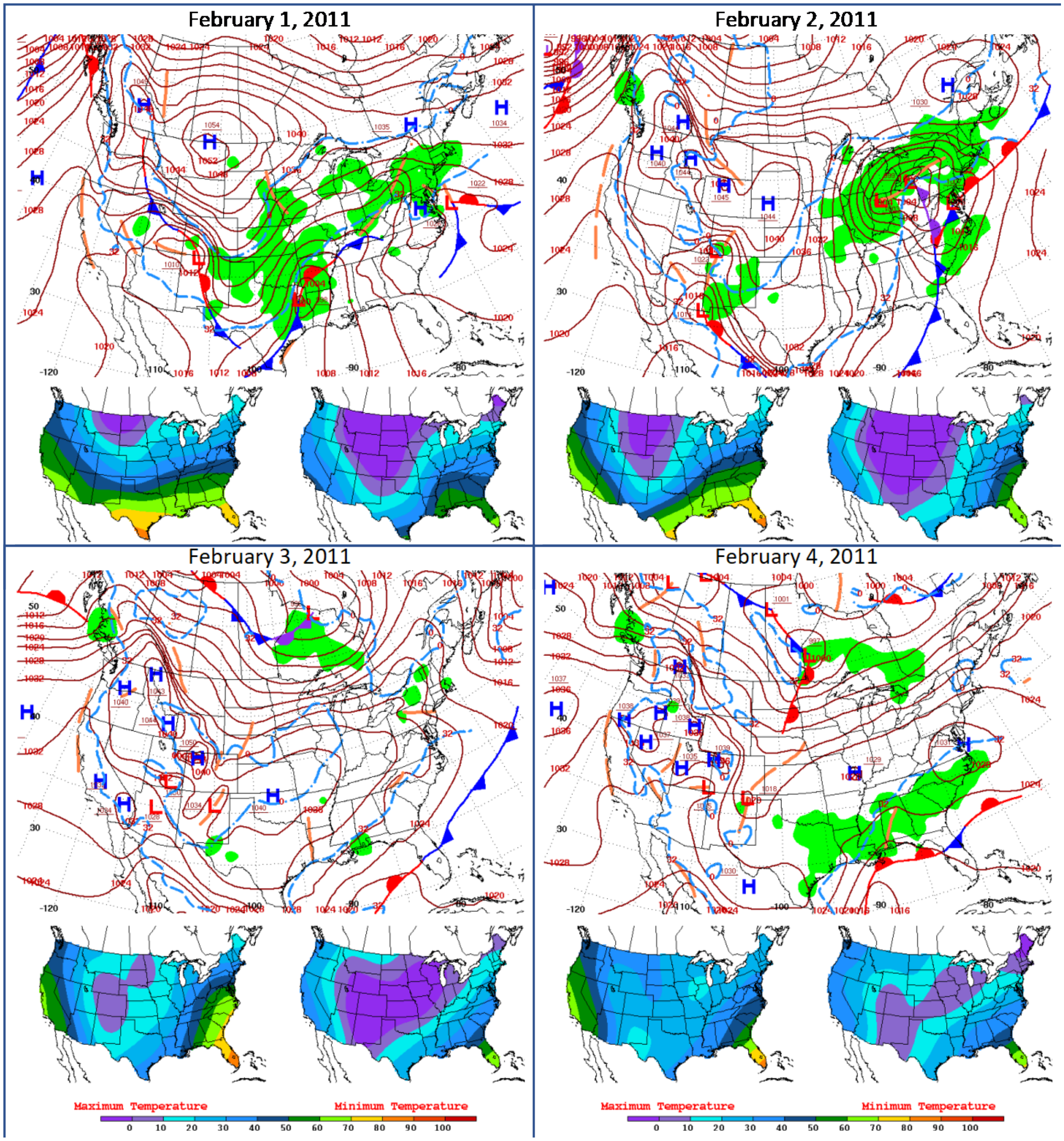

Figure A-9. Surface weather and temperature maps valid at 7 a.m. EST

See the Event Description Structure section for plot details.

Source: “Daily Weather Maps: Tuesday, February 1, 2011,“ NOAA Weather Prediction Center, https://www.wpc.ncep.noaa.gov/dailywxmap/index_20110201.html

The weather pattern that brought the cold air south began with a pressure ridge developing in the northern branch of the jet stream over the northeastern Pacific on January 28, 2011. This feature evolved to create a high amplitude wave pattern with southerly flow extending all the way into the Arctic Ocean, bringing frigid Arctic air to eastern British Columbia, Alberta, and Saskatchewan.

By January 31st, cold air coming down the Front Range of the Rockies caused temperatures to drop below 0º F (-18°C) in the northern plains. The cold air continued to move south, reaching all the way to the U.S.-Mexico border and deepening enough to start filtering across the Rocky Mountain passes and spreading westward. This brought some of the coldest-ever temperatures to locations like El Paso, Las Vegas, Phoenix and Albuquerque, and near-record cold reached the populous areas of Oklahoma, eastern Texas and the Southern tier states. El Paso set its record minimum high temperature of 15°F (-9°C), and remained below freezing for 78 hours, despite seeing almost full sun on February 3. Due to the severity of the event, the El Paso National Weather Service field office created a short summary of the storm and its impacts in Western Texas and New Mexico (Hardiman 2011).

Though the far west and east of the country did not reach record breaking cold, temperatures reached values well below normal in populated areas like Seattle, Los Angeles, Boston, and New York City as the cold air spread across the country.

Two storm systems were associated with the cold wave. The first and most significant developed in southeast Nevada and tracked through the Four Corners, into West Texas on January 31. Here it encountered the frigid air being channeled down the Rocky Mountains, leading to very unusual significant snowfall in El Paso and across the border in Mexico. The center of the storm tracked east across northern Texas on February 1 before arcing northeast toward the East Coast on February 2 (Figure A-9). It moved northeast bringing heavy precipitation to most areas east of the Rockies. The large pressure gradient on the western side of the storm caused robust northerly flow to occur behind the storm, which in turn brought cold air into the south (Figure A-9).

This storm had large impacts, including widespread distribution system outages. States of emergency were declared in Illinois, Missouri, Oklahoma, and Wisconsin. Ahead of the storm along its southern track, there were severe storms and some tornados. As the storm turned northeast, it moved over a region where cold air was trapped close to the surface, bringing over an inch of freezing rain and sleet to some places. Temperatures dropped behind the low-pressure center, which this combined with strong winds, brought blizzard conditions along the storm’s path, including major cities in the Upper Midwest, Northeast, and in the southern Plains.

A second, slower-moving disturbance developed in the Four Corners and West Texas. As the storm emerged in the lee of the Rockies, it moved into cold air and weakened substantially before redeveloping along the Gulf Coast as the upper-level trough lifted northeastward. This second system had a more minor impact, but it had a significant impact on solar resource across Texas and the southeastern United States.

Load Impacts

During the 4-day event, modeled 2050 load (based on historical load data) in all three interconnections was above the typical average for the time of year (Figure A-10). In the WI, three of the days were well above average, and in the TI, February 2nd, 3rd, and 4th were in the extreme tails of the load distribution with February 2nd and 3rd marking the highest load for the season across the 7-year data set.

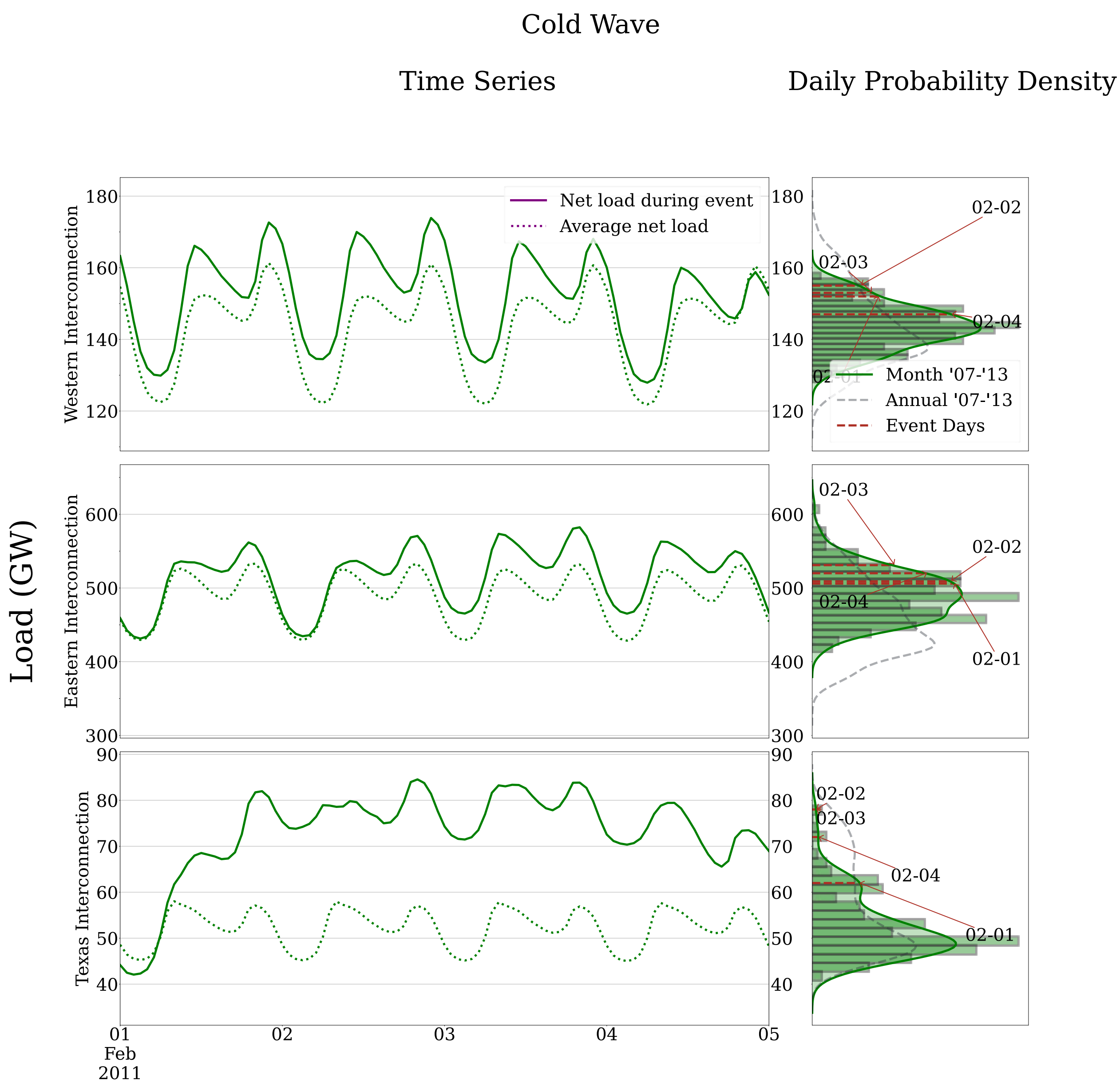

Figure A-10. Time series of regional load during the 4-day event in green, compared to load averaged across the 7-year data set for the month surrounding the event in grey (left) and distribution of 2050 regional loads for the 29 days surrounding the middle of the event in green, and across the 7-year data set in grey, with the event days labeled (right)

The time-series data on the left side of Figure A-10 shows that in each case the load during the event has the same shape as average (dashed line), but the amplitude is higher. WI load is above average throughout the period, and at times 15 GW (over 10%) above the typical load at this time of year. By the 4th, the cold in the west begins to moderate and loads return to normal levels. The EI initially shows elevated daytime loads with nighttime close to normal. However, as the colder air arrives from the west, nighttime loads increase and the load is at times close to 10% above typical. The extreme cold moderates on the 4th and loads begin to return to more typical levels.

Though the scale for the Texas generation is much smaller, the load deviation is very large with deviations of over 25 GW at a time when average load is typically 50 GW. This is consistent with the record cold temperatures noted in El Paso and other cities within the TI during this period, and the longevity of the cold in Texas and neighboring states.

Wind Generation

The same weather pattern that brings cold air into the region causes strong wind resources to develop, especially in the wake of the first storm that moves across Texas to the northeast on February 1st and 2nd. Figure A-11 shows the strong wind resource within Texas and across much of the central plains on those dates. While this diminishes by the 3rd and 4th, above-normal wind resources are present across much of the northern Plains. This correlation is not unique to this storm and indicates that wind generation associated with cold wave events could help meet increased load.

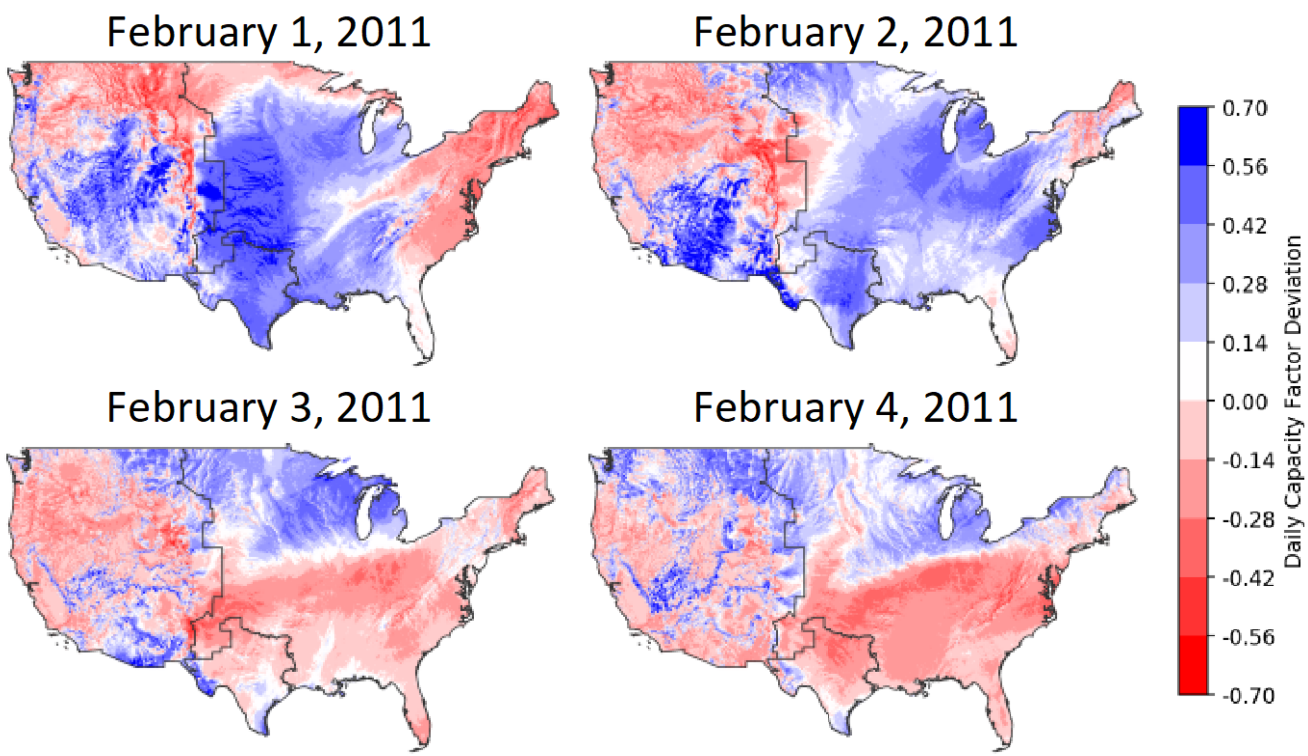

Figure A-11. National daily average wind resource deviation during the cold wave event

Daily aggregated wind generation was at or above normal during all 4 days of the event for each of the three interconnection regions (Figure A-12), except for being near normal on the 4th for Texas. Western wind generation clusters close to the statistical median for the time of year during the coldest period of the event for the west (February 1st–3rd) and is well above normal on the 4th. This is notable considering the weather pattern, which is conducive to below-normal west wind generation based on capacity, which is generally clustered in the northwest and California. That is, the capacity build-out modeled by 2050 occurs in the interior Southwest, which experiences better wind resource during this event, enhancing generation relative to the overall wind resource in the West.

Wind resource is extremely good to the east of the Rockies and throughout Texas on February 1 and February 2. Due to modeled wind generator placement within Texas and the great plains regions experience good wind resource during these days, this translates to the significantly above average generation on the TI on those days, and to the above average generation seen on the EI (Figure A-12). Once the storm moves off the east, the wind subsides and by the latter part of February 3rd, TI wind generation falls below normal. Generation in the EI remains close to normal mainly due to good resource in the Upper Midwest first associated with the weakening storm that has moved into Canada and then due to redevelopment along the old frontal boundary as upper-air conditions again become conducive to storm formation.

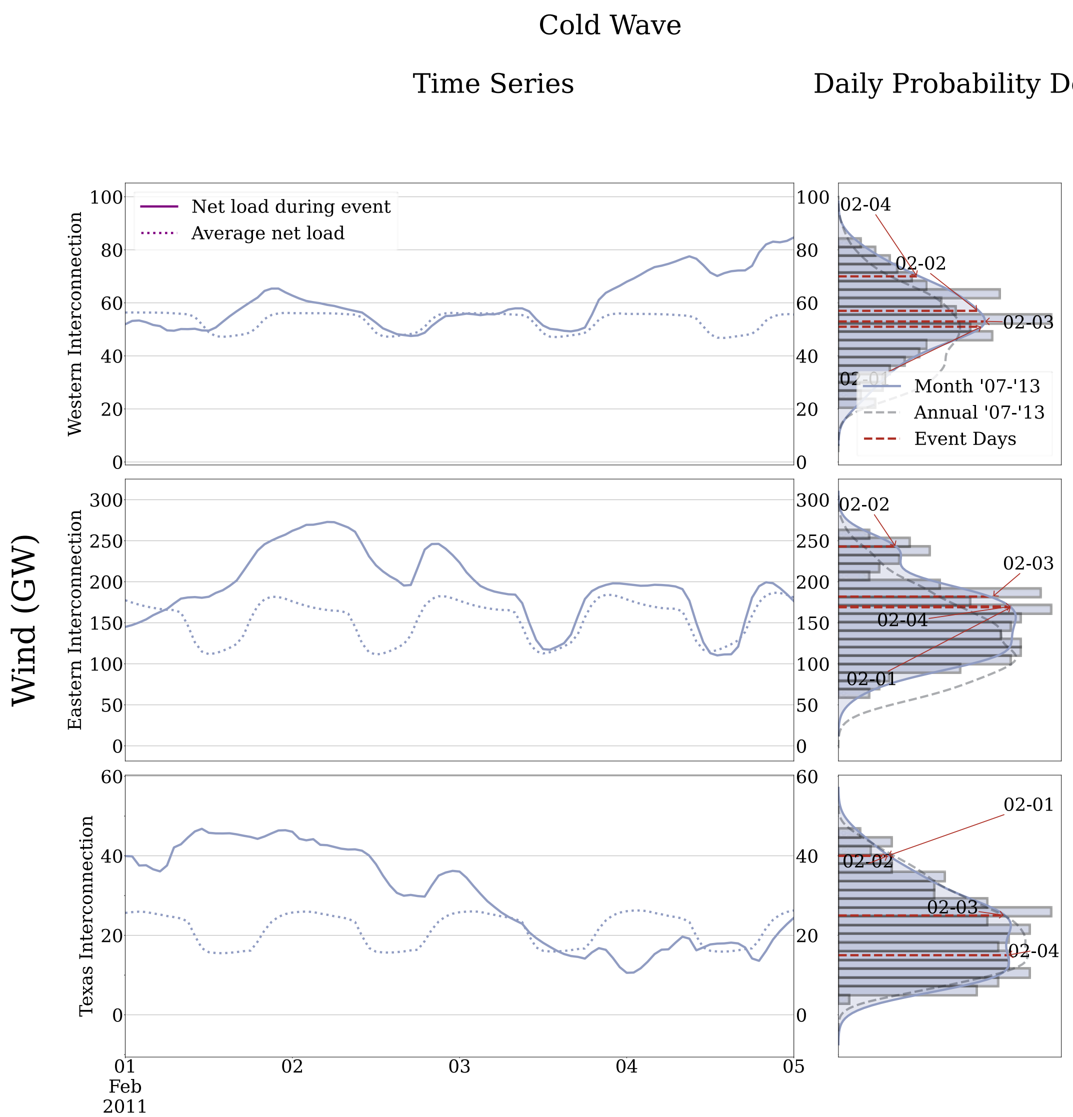

Figure A-12. Event regional wind generation (based on 2050) in context of the distribution of generation for the surrounding month (left) and time series plots of wind generation under the 2050 scenario, relative to normal for the season (right)

Solar Generation

Clouds associated with the two large-scale storm systems that cross the country during this event diminish the solar resource in some regions. Subsequently, as the storm weakens and moves into

Canada, high pressure builds in, bringing improving solar resource on the EI at a time when the wind resource is diminishing. The TI also benefits from good solar resource in the clearing conditions behind the first storm, but only briefly due to the second weak storm system. It should be noted that cold temperatures and snow covered ground increase overall panel efficiency.

The blizzard caused by the storm system dramatically reduces PV resource east of the Rockies on February 1st and still impacts a large swath of the eastern part of the country on February 2nd (Figure A-13). The weaker and slower-moving second storm that tracks across the southern-tier states impacts the Four Corners on February 1st and Texas on the 2nd, and it lingers in east Texas and the Southeast on the 3rd and 4th. Solar resource is good in the west on February 1st and 2nd due to the strong high-pressure system, and this region of good resource extends further east as cold, dry air pushes east behind the first storm.

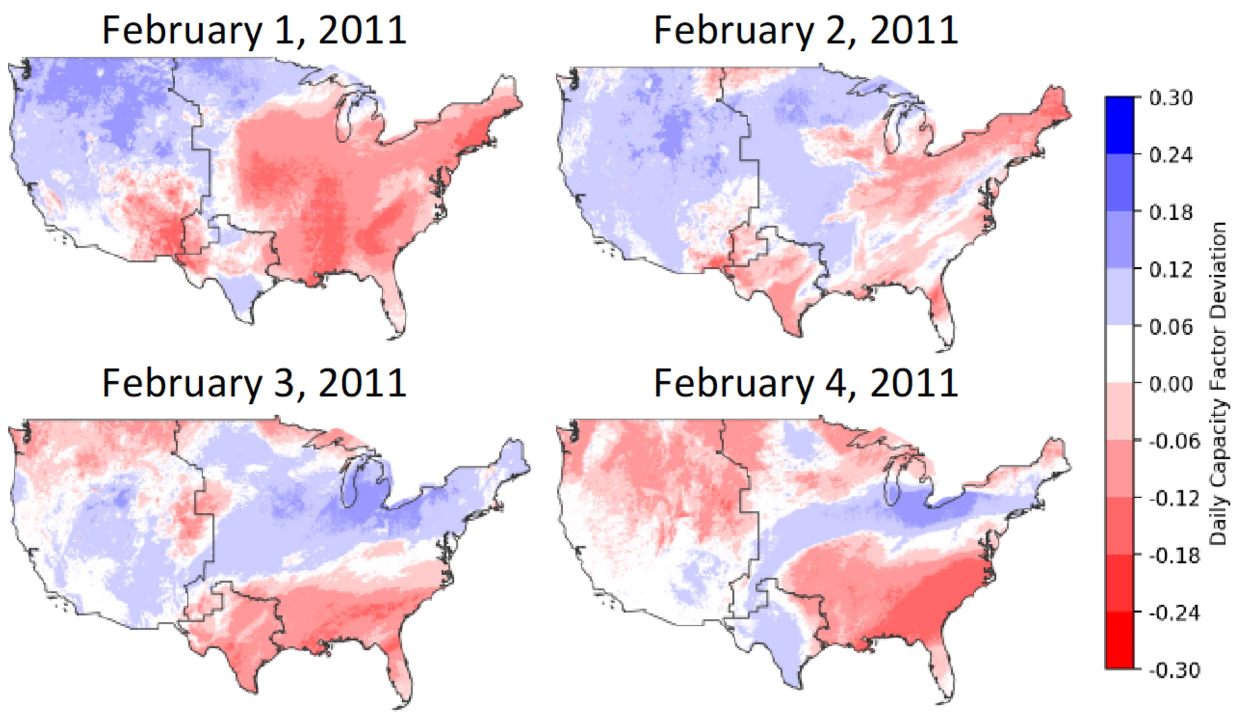

Figure A-13. National daily average solar resource deviation during the cold wave event

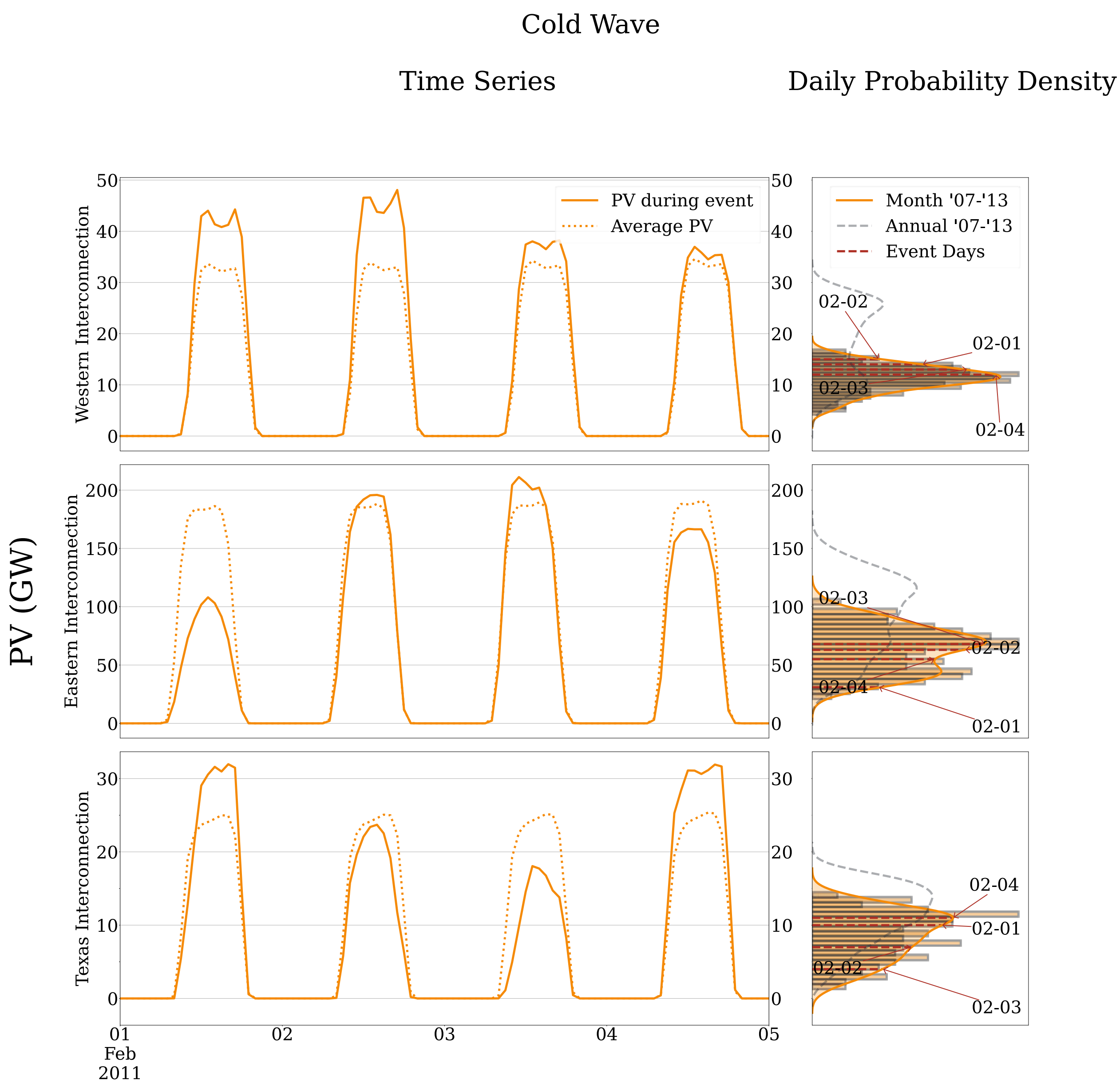

Figure A-14. Event regional modeled 2050 PV generation in context of the distribution of generation for the surrounding month (left) and time series plots of PV generation under the modeled 2050 scenario, relative to normal for the season (right)

The north-central states then come under the influence of the decaying storm, which has rotated into Canada, while a subsequent Pacific storm begins to affect the west on the 3rd and 4th. The good resource in the west on the 1st and 2nd is clearly seen in the statistical distribution and times series plot (Figure A-14) as is the poor generation in the east that is due to the first storm system.

Net Load

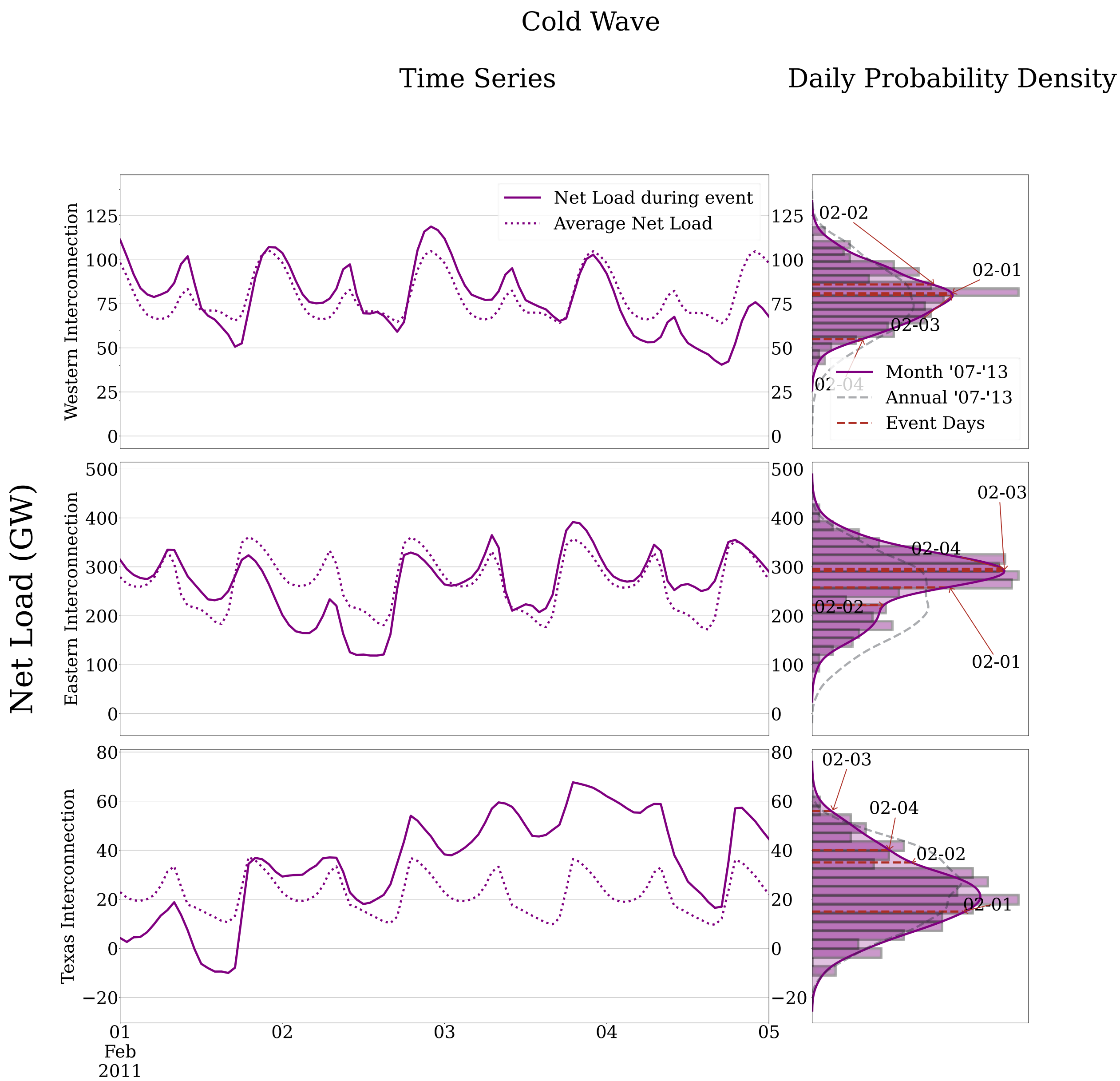

Figure A-15. Event regional modeled net load context of the distribution of generation for the surrounding month (left) and time series plots of modeled net load under the modeled 2050 scenario, relative to normal for the season (right)

In general, the location of net load for the event days within the distribution is significantly closer to the mean than the location of load within the load distribution. This is especially clear for the TI, where the impact of the cold wave on load is most impactful. February 2nd, 3rd, and 4th are all on the extreme upper end of the distribution of load for the month surround the event (Figure A-10). However, net load for both February 2nd and 4th are significantly closer to the mean net load distribution, and only February 3rd remains in the extreme upper tail of the net load distribution. February 1st also moves from being well above the most probable load in the load distribution to being below the most probable net load in the net load distribution. This reflects the enhanced wind generation in the TI on February 1st and 2nd and the higher-than-average solar generation of February 4th.

In general, this effect is also observed in the WI and the EI for this event when comparing the location of event days in the distribution of net load and the distribution of load, albeit with a smaller magnitude. Within both the WI and the EI, load is above the most probable load in the distribution for all 4 days of the event (Figure A-10). For the WI, two net load days fall within the most probable net load of the distribution (February 1st and 3rd) and another day (February 4th) falls to the very low side of the net load distribution. Similarly, for the EI, two net load days fall within the most probable net load of the distribution (February 3rd and 4th) and the other 2 days (February 1st and 2nd) are well below that.

The mitigating impact of renewables during cold waves are partially due to the meteorological conditions that resulted in the cold air coming south down the eastern side of the Rocky Mountains, as this resulted in a robust wind resource. As the pressure gradient driving the air south diminishes, atmospheric subsidence typically occurs, yielding clearing and improving solar resource. Cold surface conditions and clear skies are then conducive to good solar generation, which partially offsets the reducing wind generation. The February 2011 case was somewhat unusual in that a second weak storm immediately impacted Texas and the southeast thus reducing the benefit of solar in these areas.

System Modeling

Though the examination of load, wind and PV generation, and net load data can reveal some general relationships between the cold weather event and potential impact on grid operations, full production cost modeling of grid operations is needed to provide a more complete picture. Here we examine the operation of each of the three interconnections during the cold weather event at three points in time that reflect different penetrations of variable renewable energy and grid infrastructure: 2024, 2036, and 2050.

Texas Interconnection Operations

The system operations impacts from this event are most intense in the TI. As was shown in Figure A-10, 2 days from this event have the highest average daily load in the entire data set, and a third day is in the extreme high end of the tail of the distribution of the load. Figure A-16 shows the evolution of the TI's generation dispatch from 2024 to 2036 to 2050 as wind and solar PV capacity increases. In 2036, there is 2.2 times more wind capacity and 1.9 times more solar PV capacity than in 2024. In 2050, wind capacity is 1.9 times greater and PV is 3.5 times greater than in 2024. The increase in weather-driven generation leads to significant changes in the response to this event to meet load.

Texas Interconnection

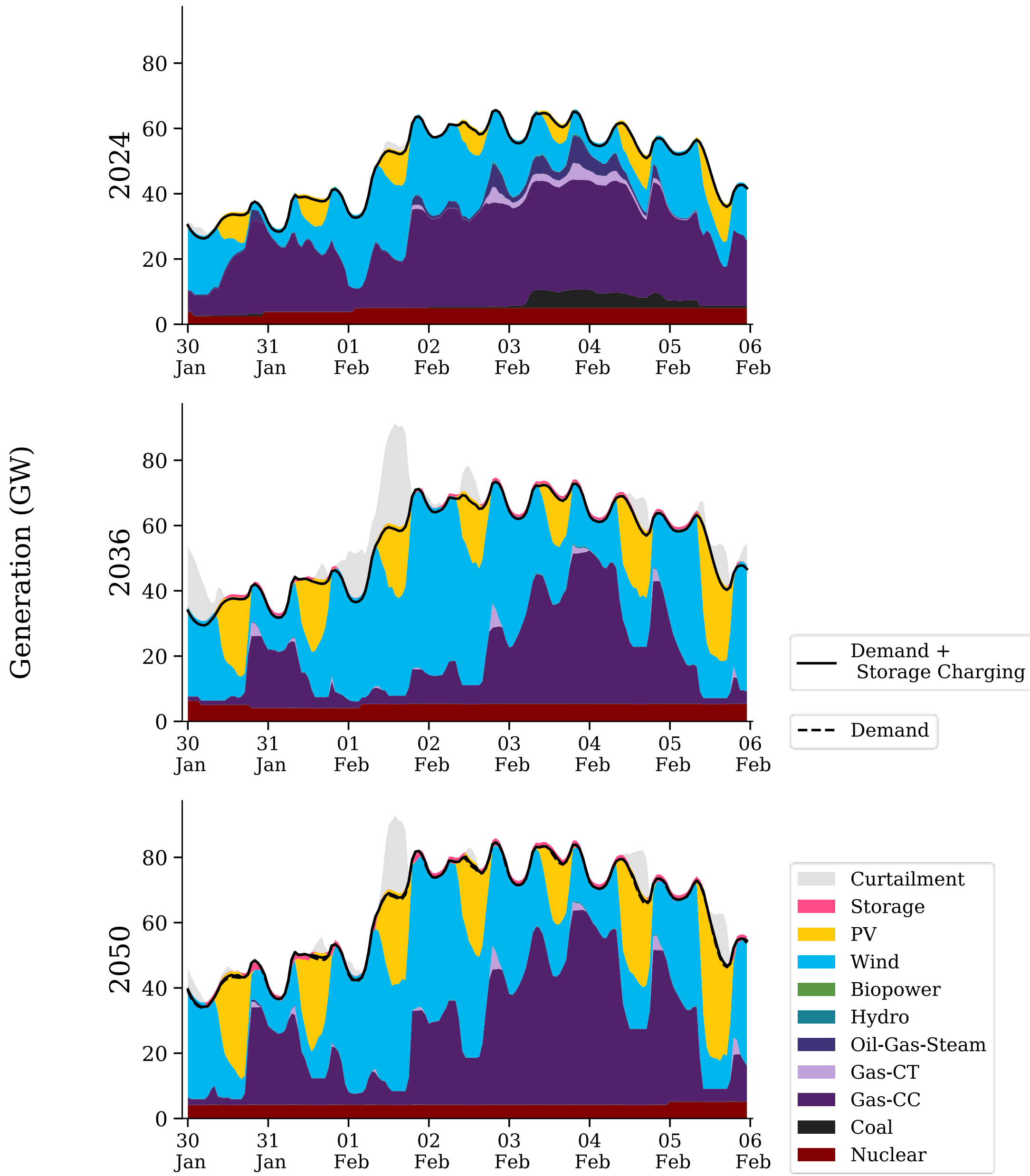

Figure A-16. Generation dispatch for the TI for three future infrastructure years—2024 (top), 2036 (middle), and 2050 (bottom)—during an extreme cold wave beginning February 1, 2011

There are two main periods of time during this event. The first is ramping up generation over the day of February 1st when the cold air arrives in Texas and load nearly doubles over the 24-hour period. The second is after peaking out, when the load plateaus at this high level for the next 48 hours while the cold and winter weather persists.

In the first period (2024), this ramp-up is met primarily by natural gas-CC, and by some natural gas-CT and oil generators as the peak is reached, meeting about 50% of all demand during the load ramp-up and in the early morning hours of the 2nd. While the wind resource is strong, generation in 2024 is mostly constant during this period and does not contribute much to meeting the load growth.

However, in the 2036 and 2050 infrastructure years, this load increase is met more by a concurrent increase in wind and PV generation rather than natural gas-CC, and gas-CT and oil generation at peak demand is almost completely reduced. As demonstrated in , the wind resource on February 1st and 2nd is some of the strongest in the data set for the TI. In all years, wind reaches nearly 100% capacity factors on the evening of the 1st. PV also contributes to meeting the rising load on the 1st, however, VRE curtailment in 2036 is greater than total PV generation, while in 2050, PV generation is only slightly larger than total curtailment.

After rising steadily, the load plateaus and remains almost 50% above normal through the 4th. Over this time, the wind resource ramps down steadily from a peak on midnight of February 2nd to a low point at midnight of the 4th. Concurrent cloud cover from the blizzard limits PV resources until clearing on the 4th.

Using the 2024 capacity mix, wind reaches a maximum instantaneous penetration by generation of 42.4% at midnight EST on February 2nd, and it diminishes to 8.3% two days later, at midnight on February 4th. Over that time frame, natural gas-CC meets the majority of load, and a significant amount of natural gas CT, oil, and coal generation turns on and runs continuously just to meet the total load volume. In the 2036 and 2050 infrastructure years, wind generation still decreases but contributes a greater amount, with penetration decreasing from 80.0% to 17.2%, and 61% to 14.5% respectively, between the 2nd and the 4th. Natural gas CC generators are online to provide the rest of the generation, but they ramp more frequently than in 2024 rather than stay on continuously. Similarly, quick start units (oil, gas, steam) and CTs only come online for a few peak hours rather than run through the whole load plateau.

These changes in operations are reflected in the production cost modeling. Increased wind and solar capacity reduce the normalized production cost to operate during this event, primarily by reducing fuel cost to operate all the natural gas units that ran throughout the event in 2024 (Figure A-16). The 2036 system is cheapest to operate primarily because of the large contribution of wind generation especially on the first 2 days of the cold wave. Throughout this event in the TI, PV generation is limited because of the shorter days and the persistent cloud cover for most of the elevated load days. Even so, the 2050 system, which has a larger share of PV capacity than 2036, has a lower normalized production cost than the 2024 system. The contribution of start costs to the normalized production cost are highest in the 2050 system, as more cycling on and off of Gas-CC units is required to balance the system around the solar generation in midday.

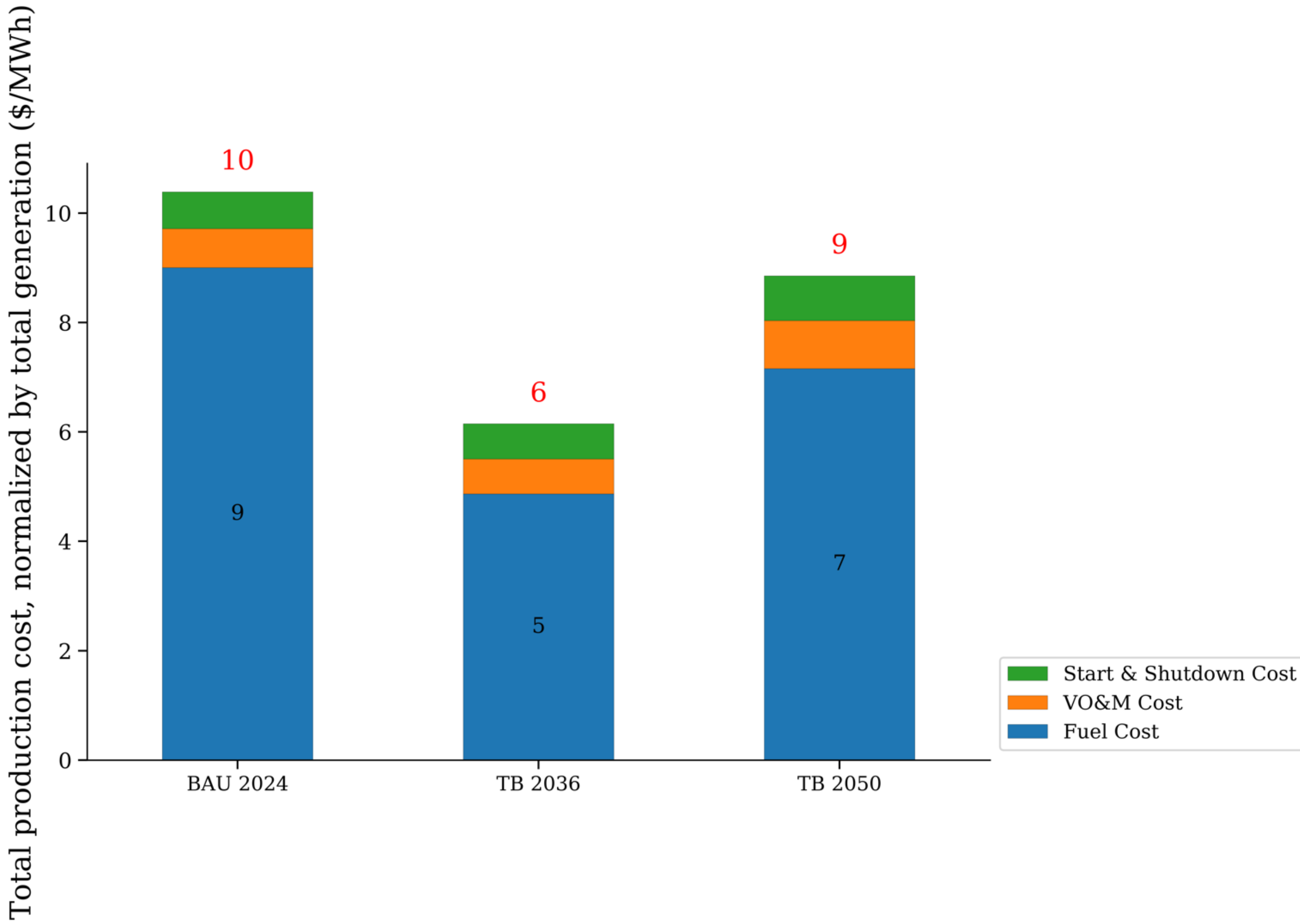

Figure A-17. Total production cost to operate the system in the TI for each infrastructure scenario for the cold wave in early February 2011

Eastern Interconnection Operations

The cold wave also changes operations in the EI as the cold sweeps across the plains, bringing with it strong wind resource as the front moves through. However, the wind and solar resource remains more constant in PJM, MISO, and SPP throughout the event, and trading between these regions leads to a reduced reliance on cycling of thermal units to balance the system. Figure A-18, Figure A-19, and Figure A-20 show the evolving dispatch for 2024, 2036, and 2050 for MISO, SPP, and PJM respectively. The cold wave coming off of the Rocky Mountains hits SPP first, which has a large pickup in wind generation in the late evening hours of January 31st. SPP already has large wind capacity in its footprint in 2024 and the ramp-up of wind can be seen in all three infrastructures. The cold front later brings a ramp-up of wind in MISO in the morning of February 1st. This is most obvious in the 2036 and 2050 systems. Finally, the cold wave hits PJM's wind capacity regions late on February 1st.

Of the three EI regions shown here, MISO's combined wind and PV resource stays relatively stable throughout the event. The cold wave brings a pickup in the wind on February 1st, leading to a shutdown of some of the Gas-CC fleet. Though the load does not increase as dramatically in

MISO as it did in the TI, wind's increased output is well correlated to the cold induced increase in load in MISO. Unlike in the TI, little to no curtailment of wind and PV is needed.

As the event unfolds, cycling of the Gas-CC fleet does increase in 2036 and 2050 relative to 2024. In the middle of the day on February 2nd in the 2036 and 2050 infrastructures, Gas-CC generation reaches a minimum in MISO. At this time, wind output has decreased from its peak around midnight of the 2nd, but PV generation is significant at this time after the two previous days saw below average output. On the 3rd and 4th, PV generation is also high, although the midday ramp down in Gas-CCs is less significant as MISO exports reach 25 GW in 2036 and over 30 GW in 2050 at their peak midday on the 3rd. As the cold leaves MISO in the early morning hours on February 5th, wind dies down, but the ramp down is well correlated with strong PV, limiting the need to turn on more thermal units. MISO also switches to being a net importer of power on the 5th after 4 straight days of net exports.

The beginning of the event in SPP plays out similarly to the TI. SPP already has a large wind penetration in 2024, which peaks at about 30 GW in all years on February 1st and 2nd. Unlike the TI, the wind stays at an average output with a diurnal pattern strongly anticorrelated to solar for the remainder of the event.

Between 2024 and 2036, SPP is modeled to retire much of its coal and nuclear generation and expand solar generation. Wind and gas stay mostly flat, as some retirements of Gas-CTs are balanced by Gas-CC expansion. This leads to large imports of power into SPP, especially overnight, in the 2036 system. By 2050, SPP has again expanded some gas and wind generation, making it a net exporter for nearly the entire event, with the exception of the days leading into the event when wind generation is low.

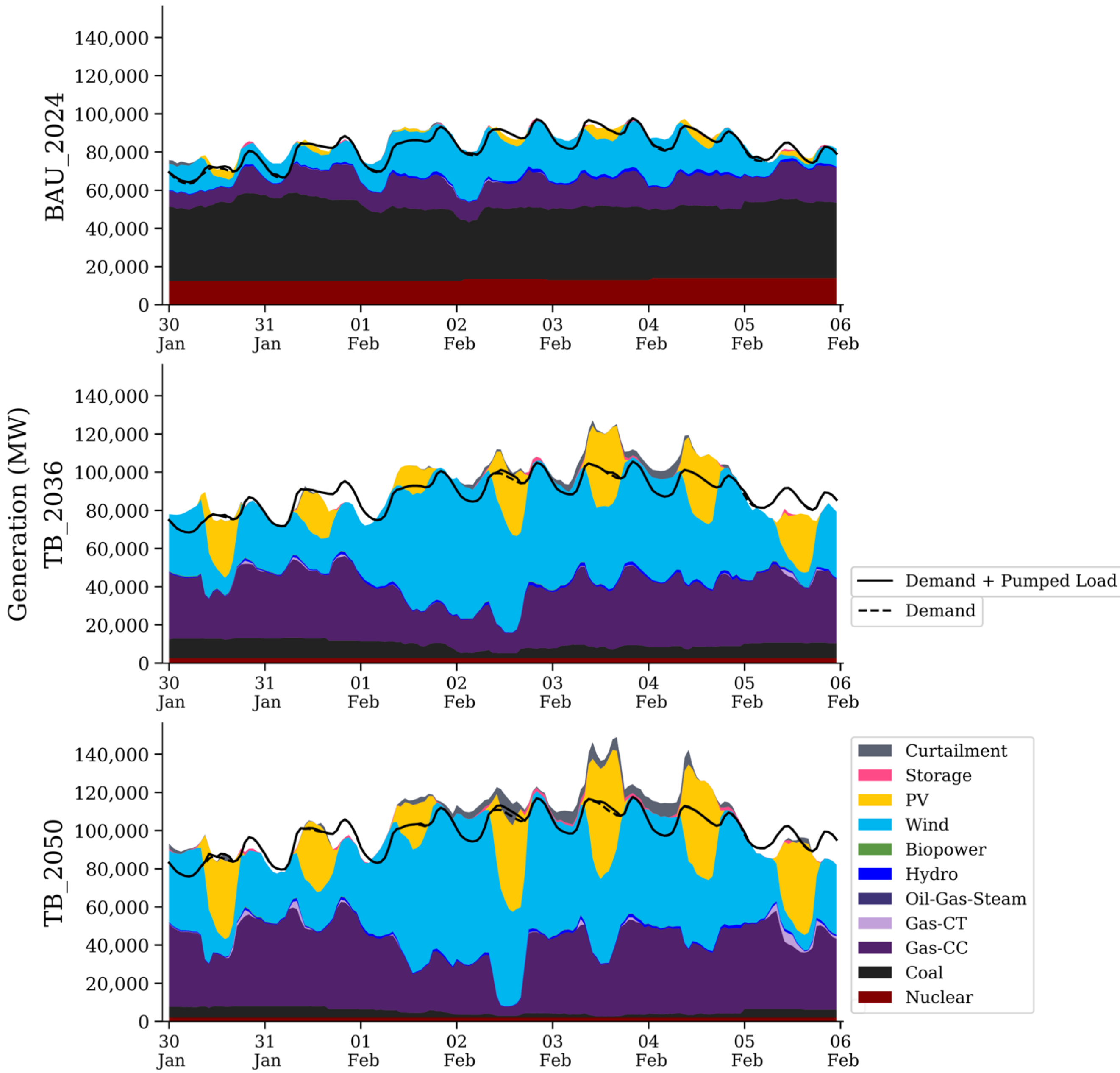

Figure A-18. Generation dispatch for MISO for three future infrastructure years—2024 (top), 2036 (middle), and 2050 (bottom)—during an extreme cold wave beginning February 1, 2011

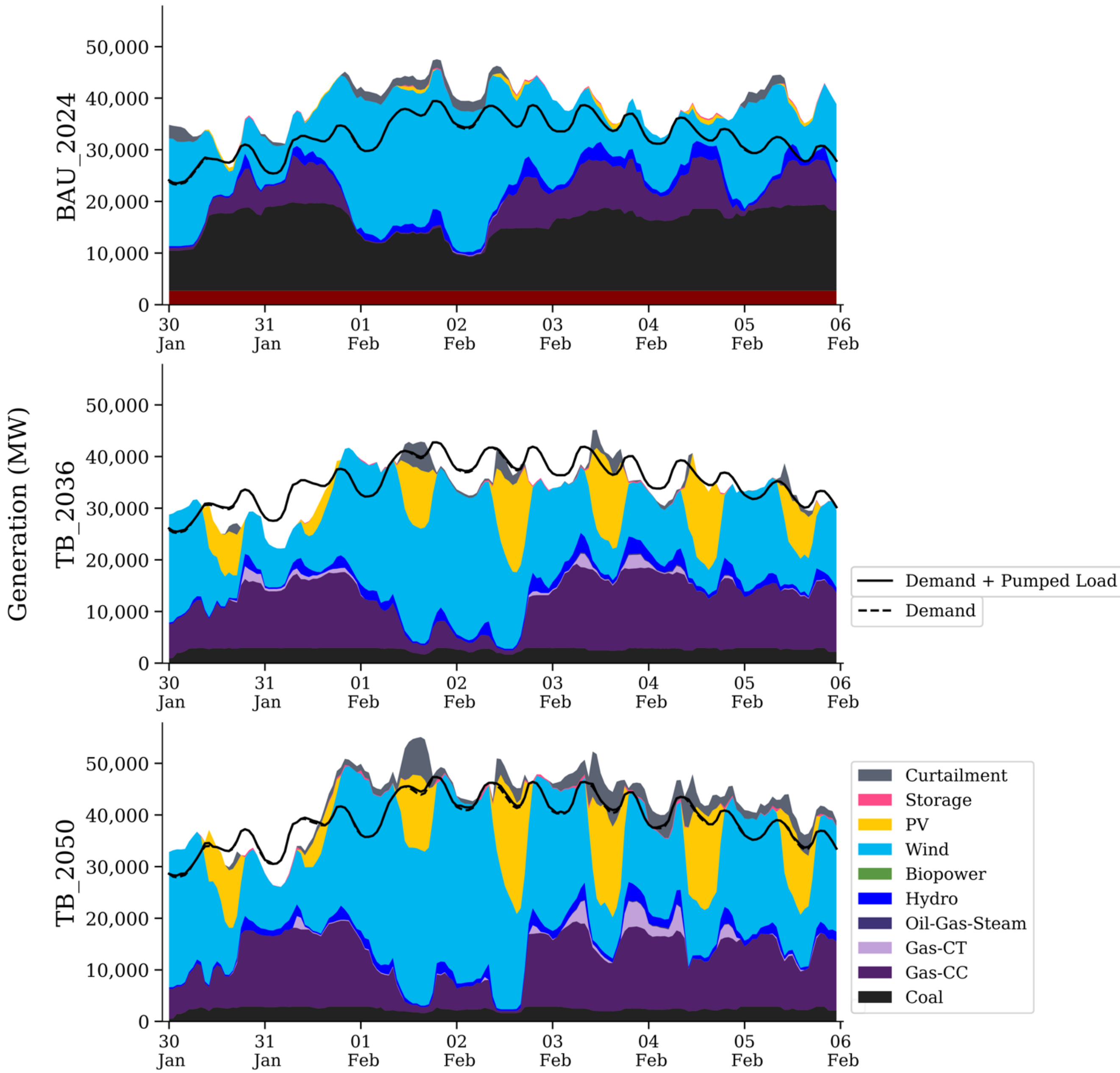

Figure A-19. Generation dispatch for SPP for three future infrastructure years—2024 (top), 2036 (middle), and 2050 (bottom)—during an extreme cold wave beginning February 1, 2011

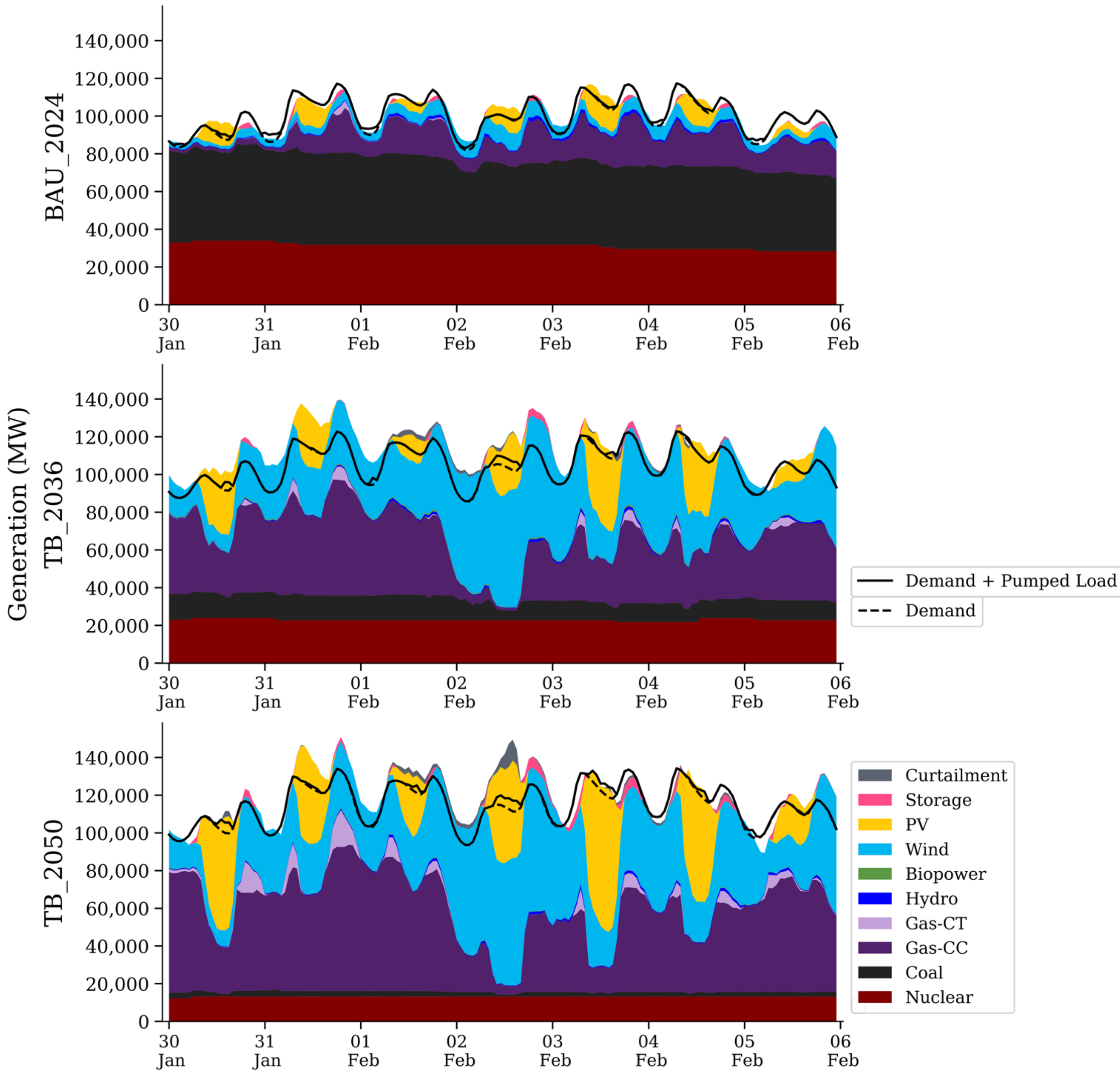

Figure A-20. Generation dispatch for PJM for three future infrastructure years—2024 (top), 2036 (middle), and 2050 (bottom)—during an extreme cold wave beginning February 1, 2011

PJM experiences one of the largest shifts in generation type used to meet load during this event across the three infrastructures. In 2024, nuclear and coal generation account for over 12.5 terawatt-hours (TWh) of generation, about 75% of generation, during the event, decreasing to 5 TWh in 2036 (about 30%) and 2.5 TWh in 2050 (about 10%). Gas, wind, and solar make up the difference in addition to serving the 2.5 TWh of load growth. By 2050, wind and PV make up approximately 45% of all generation. Storage operations also change. In 2024, pumping from pumped storage units occurs overnight and generation occurs mostly to help meet the evening peaks and sometimes the elevated morning peak caused by the cold temperatures. Whereas in 2036 and 2050, pumping and charging from existing pumped storage and new battery energy storage occurs exclusively midday, when PV generation is high.

In 2024, operations are not particularly dynamic in PJM. Nuclear and coal operate as baseload, while Gas-CCs follow net load. Weather impacts are mostly limited to causing 5–10 GW of coal and nuclear outages throughout the event, along with some gas. PJM imports a small amount of power for most of the event, except for about a 36-hour period where it is mostly exporting on February 2nd. This corresponds with a small drop in load in PJM and is not necessarily caused by a change in generation. Trading with SERC is the most impacted interface (Figure A-21).

Operations in 2036 and 2050 are much more dynamic. Wind picks up steadily as the cold front moves into PJM on February 1st, from about 35 GW up to 70 GW over a period of 12 hours. Gas-CCs are decommitted almost entirely by the afternoon of February 2nd. Midday on the 2nd, wind and PV make up about 85% of all generation in PJM in 2050. The same decommitment of Gas-CCs and high VRE penetrations occur in MISO and SPP, limiting trade between the three regions. However, PJM is able to export its excess generation to its neighbors to the north and south. Wind returns to normal on the 3rd and 4th, ramping down midday and turning back up overnight. The 3rd and 4th are also strong solar generation days in PJM. In 2036, the decrease in wind generation in the morning is met almost exactly by PV and vice versa at sunset. In 2050, PV capacity makes up a larger proportion of the installed capacity, making the wind-solar balance a little more extreme during the day. In 2050 on the 3rd, PV generation peaks at 75 GW, when it accounts for about two-thirds of all generation at midday.

Net exports become more dynamic with large swings in flow direction and magnitude in 2036 and 2050, as demonstrated in Figure A-21. Leading into the event, PJM exports until the morning of the 3rd, when a large ramp down in net exports occurs. In 2036, PJM was exporting about 25 GW late on the 2nd, but by the morning of the 3rd, it is net-neutral in power exchange with its neighbors. In 2050, net exports reach 20 GW midday on the 2nd, but by the morning of the 3rd, PJM is a net importer of around 13 GW. In both 2036 and 2050, the large ramp down occurs between all three neighbors, but MISO has the most consistent and extreme ramp in net interchange. During the remainder of the event, net exports look very similar to 2024.

MISO’s exchange with its neighbors is shown in Figure A-22. The trade between MISO and SPP is the most impacted between 2024 and 2050. As wind generation picks up significantly in SPP on January 31st, SPP goes from importing 7,500 MW from MISO to exporting nearly 10,000 MW in about 18 hrs.

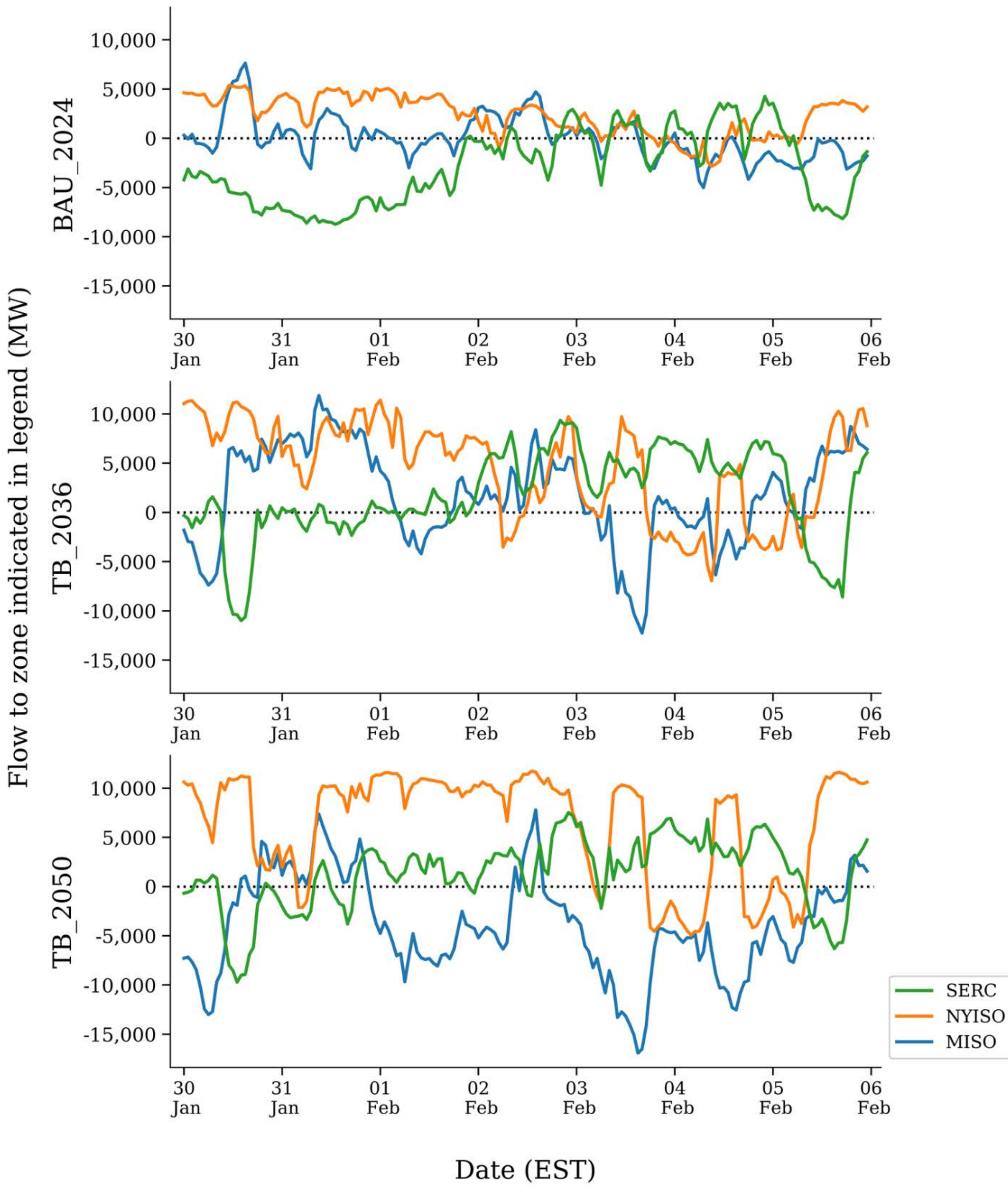

Figure A-21. Net power flow between PJM and its neighbors during the cold wave event in early February 2011

Positive flow means an export from PJM to its neighbor.

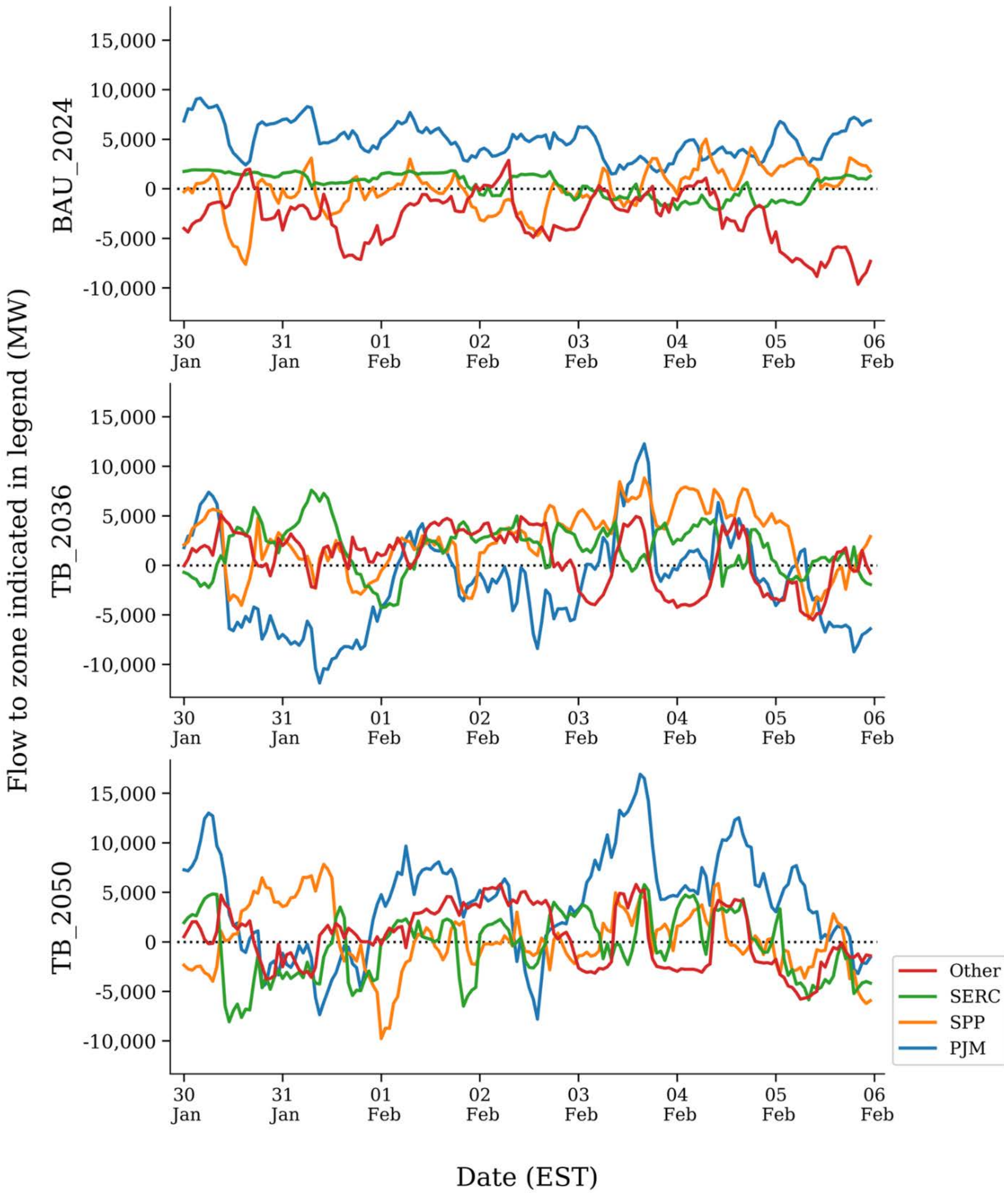

Figure A-22. Net power flow between MISO and its neighbors during the cold wave event in early February 2011

The orange series shows the exchange with SPP and the blue series shows the exchange in PJM. Positive flow means an export from MISO to its neighbor.

Impacts Summary

In summary, the higher-than-normal and, in the TI's case, extreme load that is seen in some regions in response to the extreme cold is met with high wind generation especially at the beginning of the event. This allows for lower reliance on the thermal fleet to ramp up with the increased load in 2036 and 2050 relative to the 2024 system. However, the cold persists for multiple days after the front moves through, keeping load high while wind generation decreases. In the EI, wind generation is still above average and it is anticorrelated with solar generation. However, the decreased wind generation in the IE and the TI relative to its peak at the beginning of the event still leads to the need for regions to ramp up their Gas-CC fleets in 2036 and 2050. The load for this time of year and this event and PV generation during this event are not well correlated. This leads to cycling of thermal units—both turning units off and on and ramping units down to minimum stable levels during the daytime hours—to meet both morning and evening load peaks. Also, during daytime hours, there is economic curtailment of wind and PV.

During the height of the event, strong solar resource is present in the WI, while the EI exhibits very poor solar resource due to the strong storm. Cold waves are typically associated with a high amplitude upper flow pattern that brings cold, dry, clear conditions on the west side of the Rocky Mountains, and clouds and precipitation farther downstream. The existing electrical connection between the EI and the WI is insufficient to take advantage of this, nor does the modeling add additional interties between the interconnections.

For future study, the value of storage to mitigate the need for thermal cycling, thermal capacity reserve, and reliance on long distance power transmission could be assessed. In the case of the TI, 24-hour or multiday storage may reduce the need to ramp up much of the thermal fleet when the cold wave persists for multiple days after the initial cold front moves through. In this case, curtailment of wind and solar would be available for charging in both the 2036 and 2050 systems at the beginning of the event. Shorter-duration storage in the EI would assist during the morning and evening load peaks, which tend to occur before sunrise and after sunset this time of year.

Heat Wave 1: July 19–August 6, 2011

Event Summary

In summer 2011, North America experienced an unusually strong and long-lived heat wave. Nationally, it was the hottest summer in 75 years, and in Texas, New Mexico, Oklahoma and Louisiana, it was the hottest summer (June through August) in the 117-year record. June 24, 2011, through September 6, 2011, saw only one day where a triple-digit temperature was not recorded in a major Texas load center and only a few days when this was true in Oklahoma. The average temperature in Oklahoma for June through August was 86.9°F, which is the highest for any state, in any season. It was also drier than normal across most of the country, with Texas experiencing its driest summer on record, and New Mexico and Oklahoma coming in second- and third-driest respectively.[34]

[34] Details about the summer of 2011 can be found at "National Climate Report: Annual 2011," NOAA, https://www.ncdc.noaa.gov/sotc/national/201113.

Meteorological Description

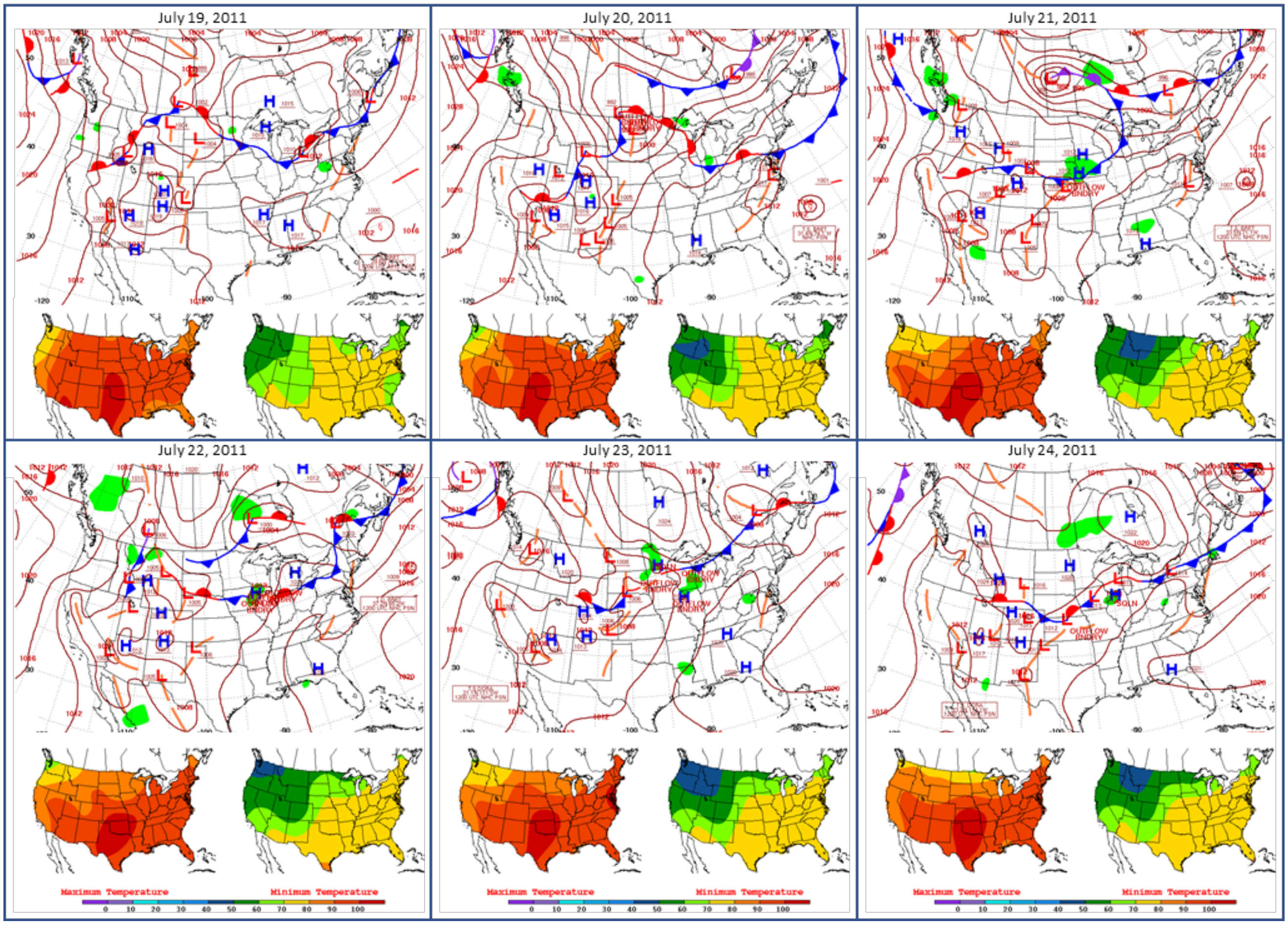

Figure A-23. Surface weather and temperature maps valid at 7 a.m. EST

See Event Description Structure section for plot details.

Source: “Daily Weather Maps: Tuesday, July 19, 2011,“ NOAA Weather Prediction Center, https://www.wpc.ncep.noaa.gov/dailywxmap/index_20110719.html

The summer of 2011 was marked by a persistent upper-level ridge east of the Rocky Mountains. This type of pattern creates subsidence and stable atmospheric conditions, steers away large-scale storm systems, and yields high surface pressure with generally clear skies. Though strong day time heat associated with clear skies increases the likelihood of daytime thunderstorm formation, the stable conditions tend to inhibit significant storm outbreaks that provide relief from the heat.

Beginning July 14, 2011, this dome of high pressure began to further strengthen and push north while expanding both east and west. As can be seen in Figure A-23, by July 19, there was little pressure gradient across much of the country and a swath of 90º F+ maximum temperatures covered over 80% of the CONUS, with areas of Texas, Oklahoma, and Kansas seeing temperatures over 100°F. While a weak weather system moved into the Pacific Northwest and brought thunderstorm activity and slightly cooling conditions to the northern tier states over the next 5 days, the rest of the country remained under the high pressure dome with high temperatures well into the 90s to over 100°F. By the 23rd, 100°F heat was impacting the mid-

Atlantic states and all the way to New York City. On the 24th, a cold front began to push into the eastern third of the country from Canada, cooling the northeast into the 80s by the 25th, but the heat continued for weeks across Texas and the Southern Plains.

Load Impacts

The heat wave's impact on load is concentrated in the EI, where load is well above normal. Load on July 20, July 21, and July 22 are the top-three loads days for the EI in the 7-year data set. Analysis ranking the average number of cooling degree days at major load centers across the country indicated that the top-four days in the record all occurred between July 20 and July 23. This is driven by cities on the EI. This picture is also borne out in Figure A-24, which shows a time series of loads through the event. EI loads are way above the average for that period, while the other regions are near normal.

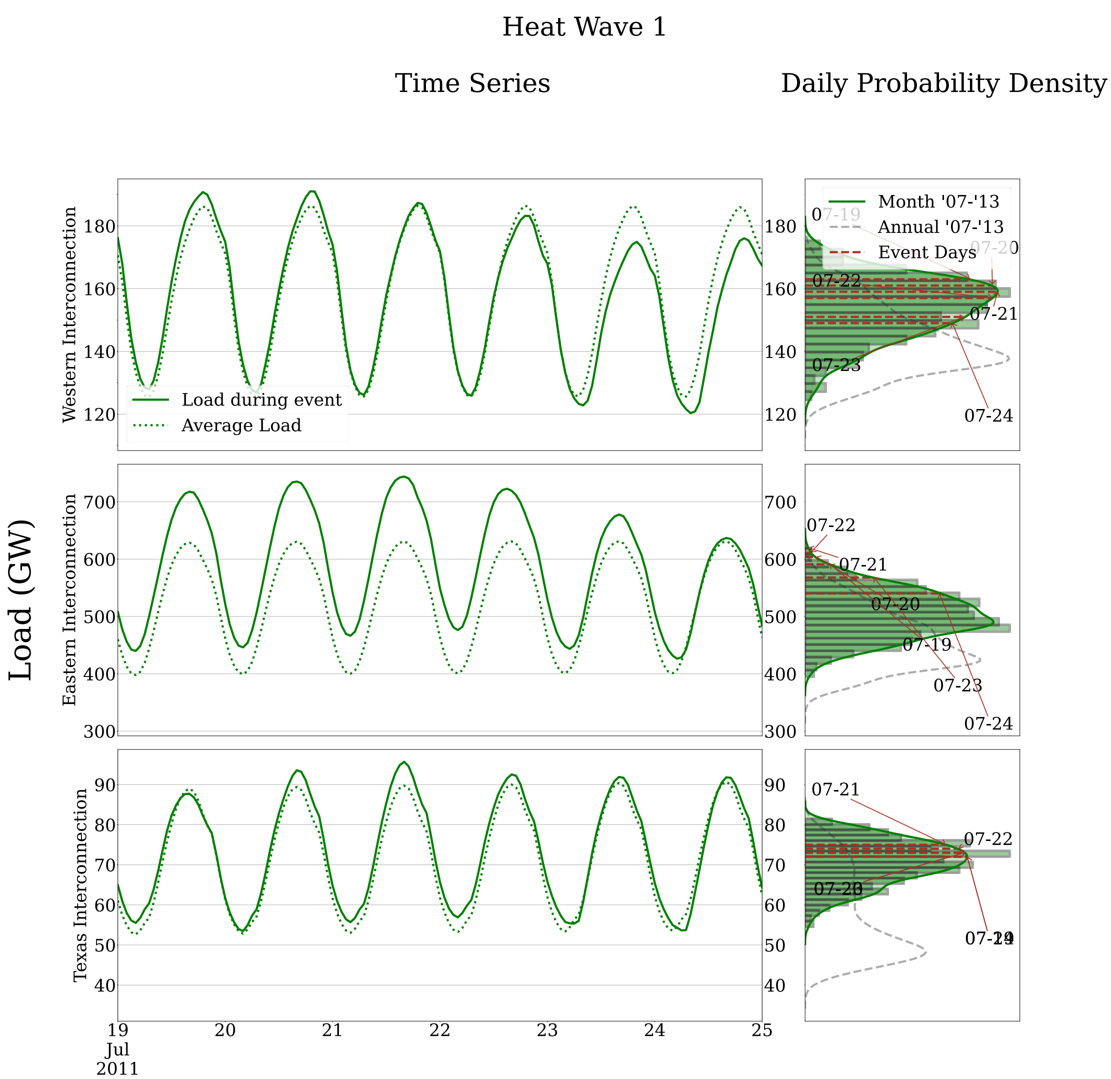

Figure A-24. Time series of regional load during the 4-day event in green, compared to load averaged across the 7-year data set for the month surrounding the event in grey (left) and distribution of 2050 regional loads for the 29 days surrounding the middle of the event in green, and across the 7-year data set in grey, with the event days labeled (right)

Load in the WI is close to the median for the period. This is mostly as expected, as the Pacific Northwest is being impacted by a weak storm system and California and the desert southwest is seeing near normal temperatures. Only the eastern part of the WI is seeing the well-above-normal temperatures. TI loads are above normal but not exceptionally hot given the time of year.

Wind Generation

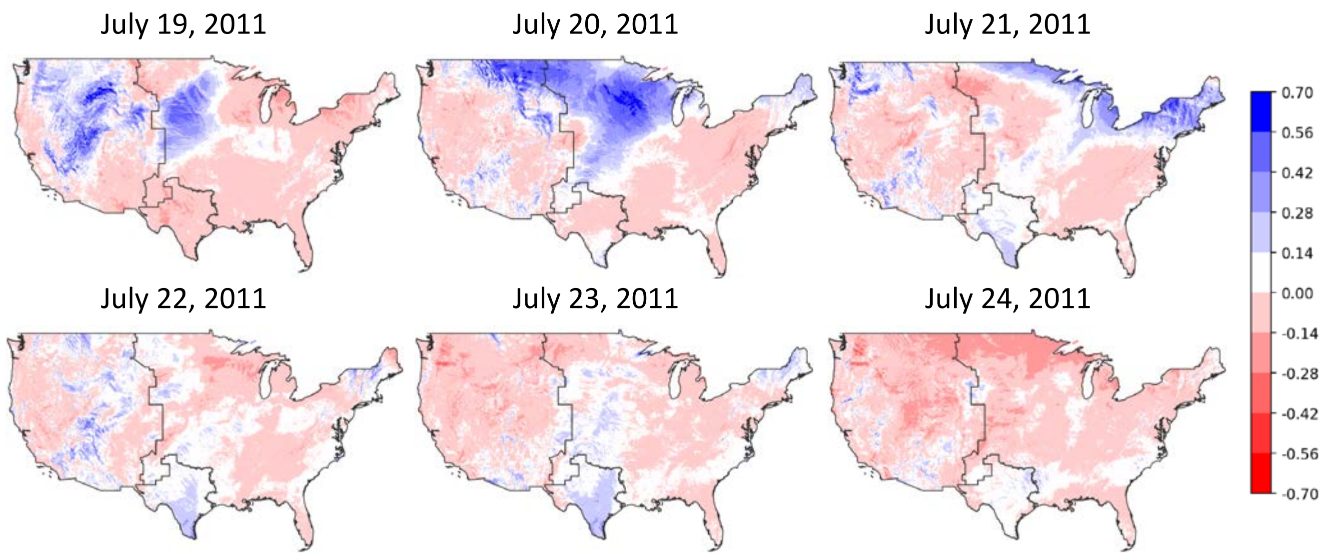

Figure A-25. National daily average wind resource deviation during the heat wave event

In the context of the broader record (Figure A-26), the wind generation is fairly unremarkable, and there does not seem to be any correlation between this heat event and a coincident reduction in wind resource. The TI and the EI both see above average wind conditions throughout the hottest period. And on the 21st, which was one of the hottest days, EI wind was well above normal.

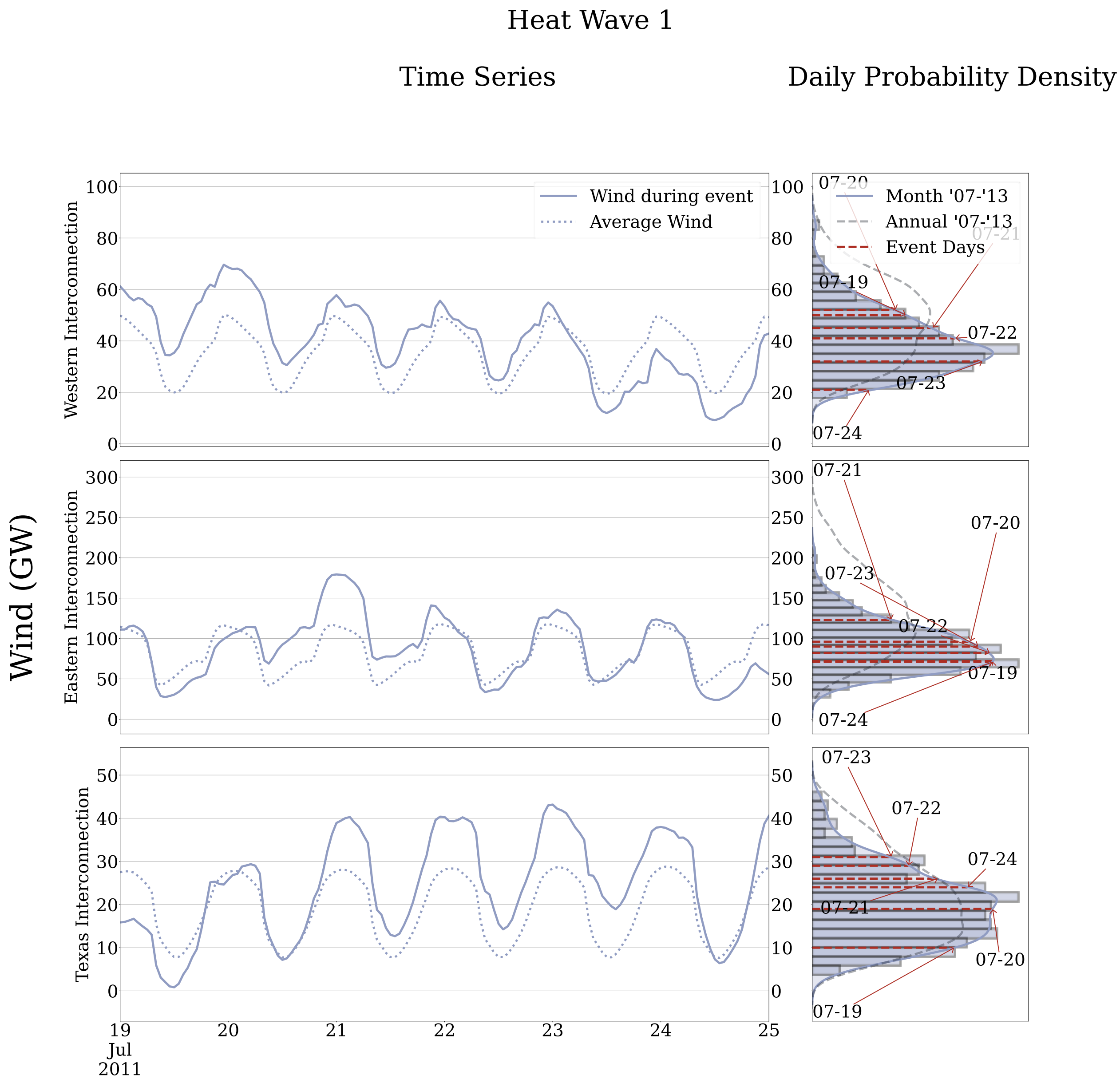

Figure A-26. Event regional wind generation (based on 2050) in context of the distribution of generation for the surrounding month (left) and time series plots of wind generation under the 2050 scenario, relative to normal for the season (right)

However, the EI wind is generally low relative to the annual average at this time of year. While poor wind resource is not in this case found to correlate with high loads, the period where loads are highest generally is not well matched with the wind resource built out in the east. The converse is true for Texas, indicating Texas wind is generally better matched to seasonal load shape.

The geographic distribution of wind deviation in Figure A-25 is uneven across the EI. Much of the east is seeing below-normal wind resource, as expected given the weak pressure gradients seen in Figure A-23. This is made up for by above average wind in the northern part of the EI, which is impacted by the storm system passing through Canada and the northern Plains, implying robust transmission availability would be needed to serve load for those areas with higher wind resource. Also, increased wind generation occurs mostly during the overnight hours, especially in Texas on the 21st and in the East. Last, the wind in the west is in the tail of the distribution on the 24th, and it really drops in the second part of the day in the EI. Even though the highest temperatures are over, loads are still very high during this period across the country.

Solar Generation

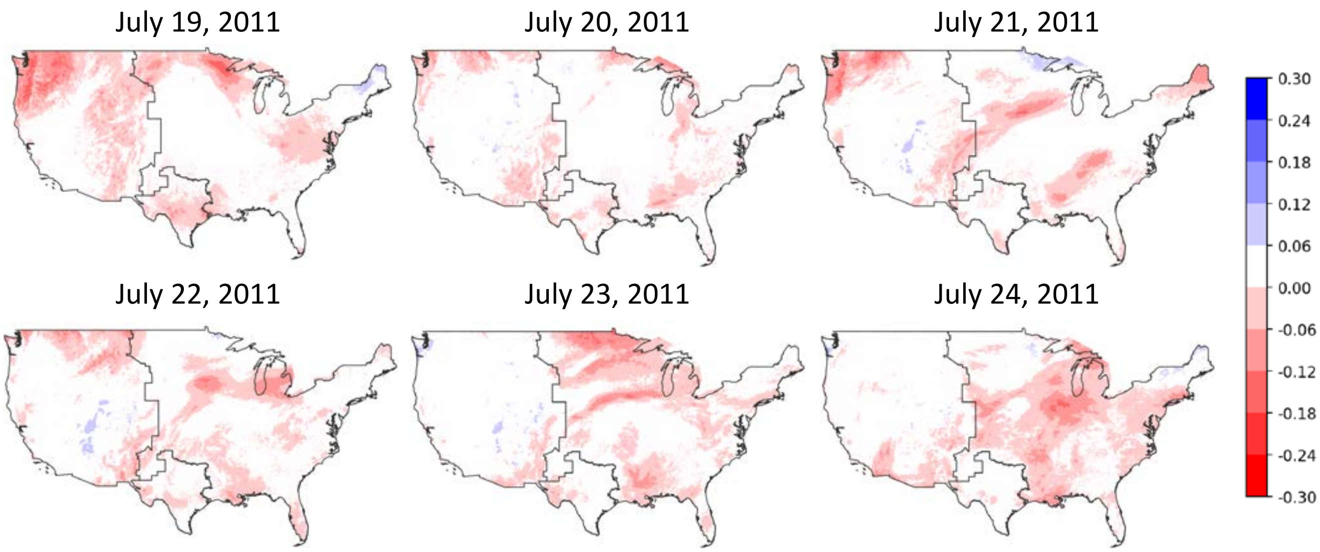

Figure A-27. National daily average solar resource deviation during the heat wave event

Nationwide, with the exception of July 24 and July 19, the solar resource is close to, or slightly above normal. This is as expected; it is summer and there are few deep clouds, and beyond the exceptions below, the overall resource is dictated by haze, afternoon fair weather cumulus, and possible pop-up thunderstorms in the late afternoon, and with high pressure dominating, convection is suppressed. On the 19th, the impact of the storm system moving onshore in the west beings to impact the Intermountain West. There are also some thunderstorms in Texas that day. Through the rest of the week, the impact of the storm system is tracking along the U.S.-Canada border, with thunderstorms kicking off on the frontal boundary. On the 24th, there is more organized thunderstorm activity in the east as a frontal boundary sags south.

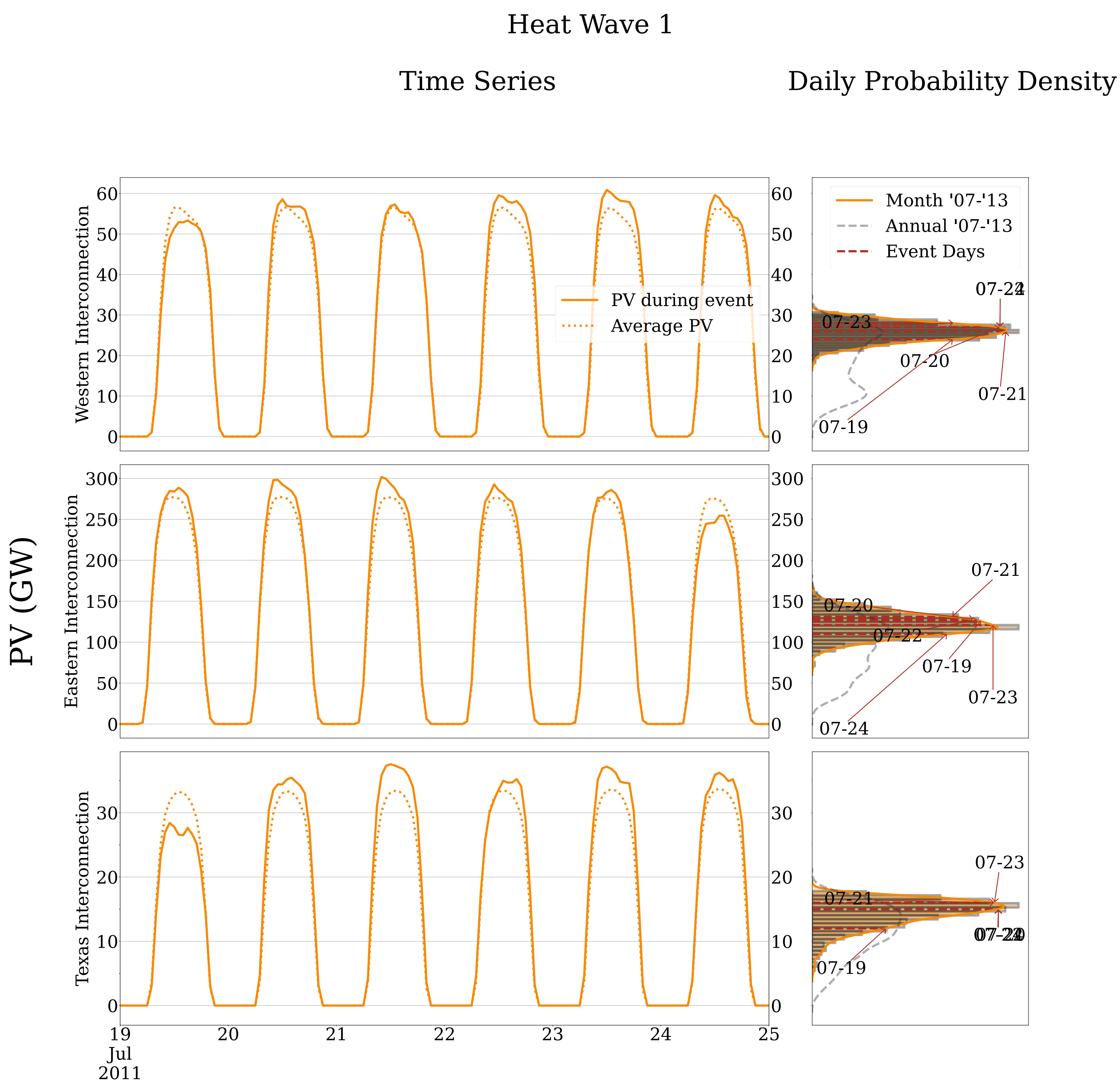

Figure A-28. Time series plots of solar generation under the 2050 scenario

Looking at PV in context of the typical multiyear distribution for the time of year, the event days cluster quite tightly around the mean and that the distribution is well above the average for July. The one notable exception is the 19th in Texas. On this day, the heat combined with moist flow from the Gulf of Mexico fueled some significant thunderstorms in the Houston area.

Net Load

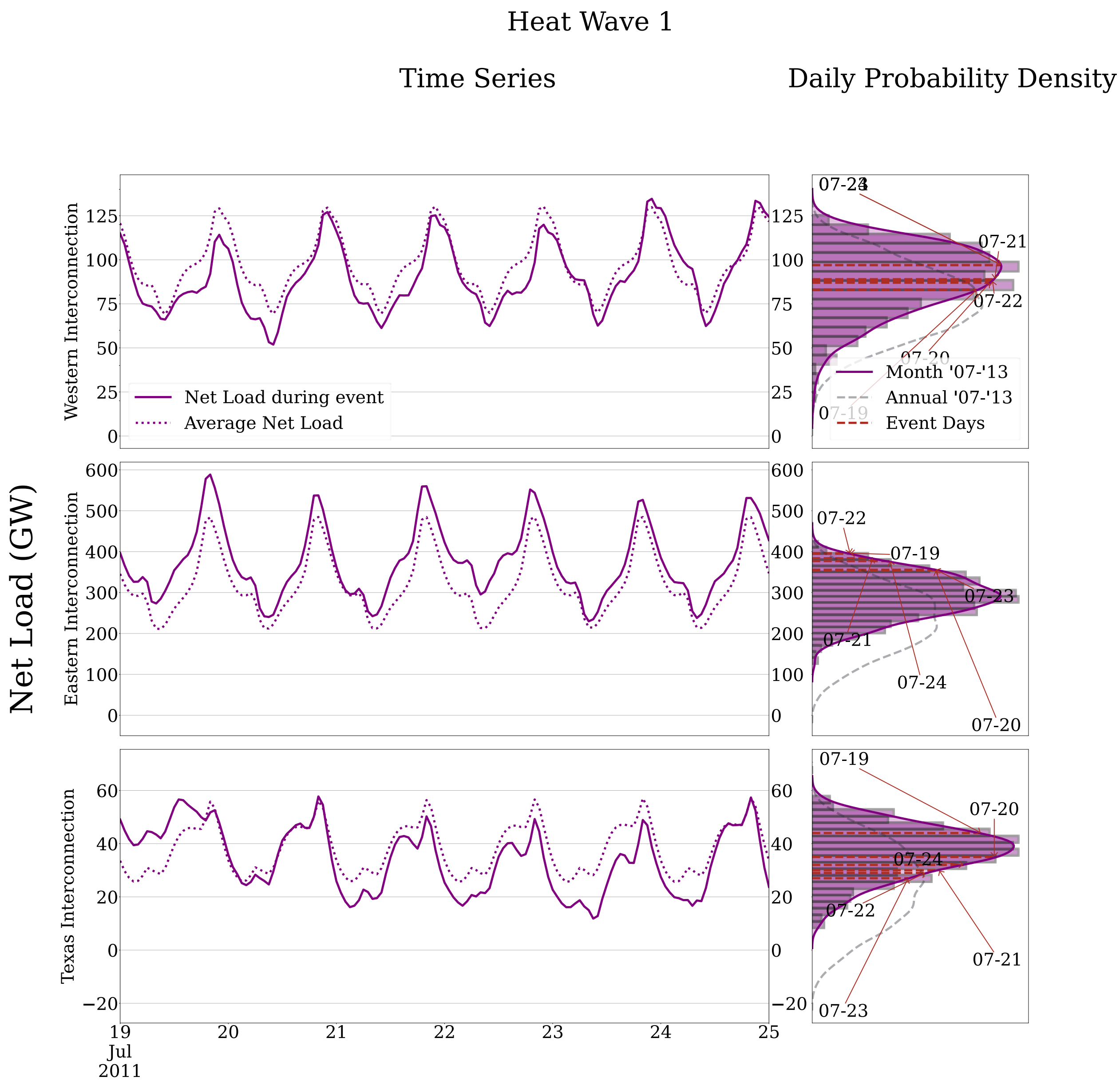

Figure A-29. Event regional modeled net load context of the distribution of generation for the surrounding month (left) and time series plots of modeled net load under the modeled 2050 scenario, relative to normal for the season (right)

In the EI, while the daily average net load values are high, they do not define the upper limit as the load distribution does. However, when looking at the hourly time series, there are significant peaks in net load above what is typical, both during afternoon peaks, such as on the 19th and overnight from the 21st to the 22nd (Figure A-29).

The average net load in both the West and Texas is near or below typical for that time of year during the days of the event with one exception: on the 19th in the TI, net load is significantly above the median largely due to lower than average wind that day. While there is a reduction in

PV generation from the clouds and thunderstorms in East Texas that day, the load is also lower, likely for the same reason.

System Modeling

Operations during this event remain largely the same day-to-day, although the specifics change from 2024 to 2050. Across all infrastructure years, wind and PV total generation and the shape of the generation are largely average. Wind ramps up in the evening, when PV decreases at sunset. Both the shape and magnitude of the load in all three interconnections is constant.

Eastern Interconnection Operations

Figure A-30 shows the EI generation dispatch and commitment over the 1-week period in the heart of the heat wave at the end of July 2011. Under 2024 infrastructure, the EI sees large cycling of Gas-CC to meet the daytime peak, shifting slightly away from the actual peak to max out during the net load peak as PV decreases. About 25% of Gas-CC capacity online in the middle of the day turns off overnight, while the remaining online capacity ramps down to an aggregate Gas-CC fleet capacity factor of less than 50%. Coal also has some small cycling, but it is almost exclusively from ramping down rather than turning off. Hydropower ramps up gradually throughout the day, maxing out at the peak net load in the early evening. CTs are also used throughout the extent of the daytime hours, and not just at peak load.

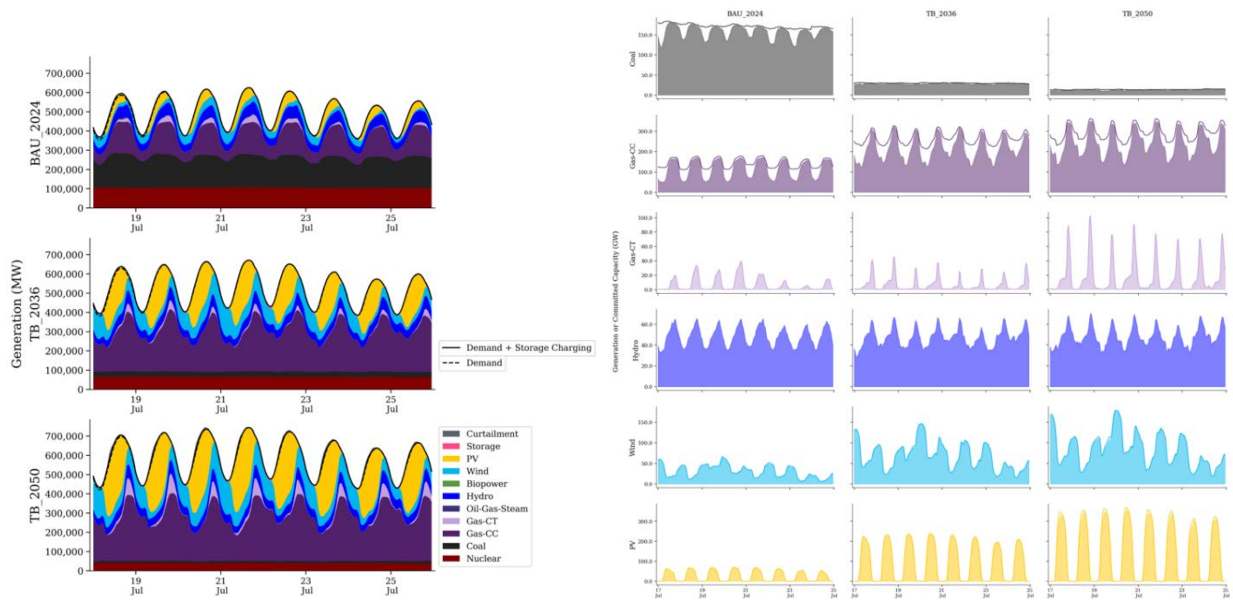

Figure A-30. (a) Generation dispatch for the EI for three future infrastructure years: 2024 (top), 2036 (middle), and 2050 (bottom) and (b) Committed capacity (solid line) and dispatch (filled area) for different generator types (along the vertical axis) for the three future infrastructure years—2024 (left), 2036 (middle), and 2050 (right)—during an extreme heat wave in mid to late July 2011

In 2036, the largest change in operations is due to the increased PV penetration. In the EI, the proportion of Gas-CC cycling on/off each day and those that ramp remains about the same as in 2024; however, the capacity turned on and ramped up in the day is meeting a much tighter peak net load in the evening. The tighter peak output from Gas-CCs leads to these units operating at their minimum generation level 30% of the time in 2036 compared to only 20% of the time in 2024 (Figure A-31). Also in 2036, there is a lot more Gas-CC generation, filling some of the gap left by coal that retired between 2036 and 2024. This leads to more total Gas-CC capacity started in 2036 (Figure A-31). Gas-CTs are almost exclusively used for an hour or two at net peak load, and the total Gas-CT capacity started increases by 50% in 2036 (Figure A-31). Hydropower is slightly peakier in 2024 but still ramps up throughout the day toward net peak load.

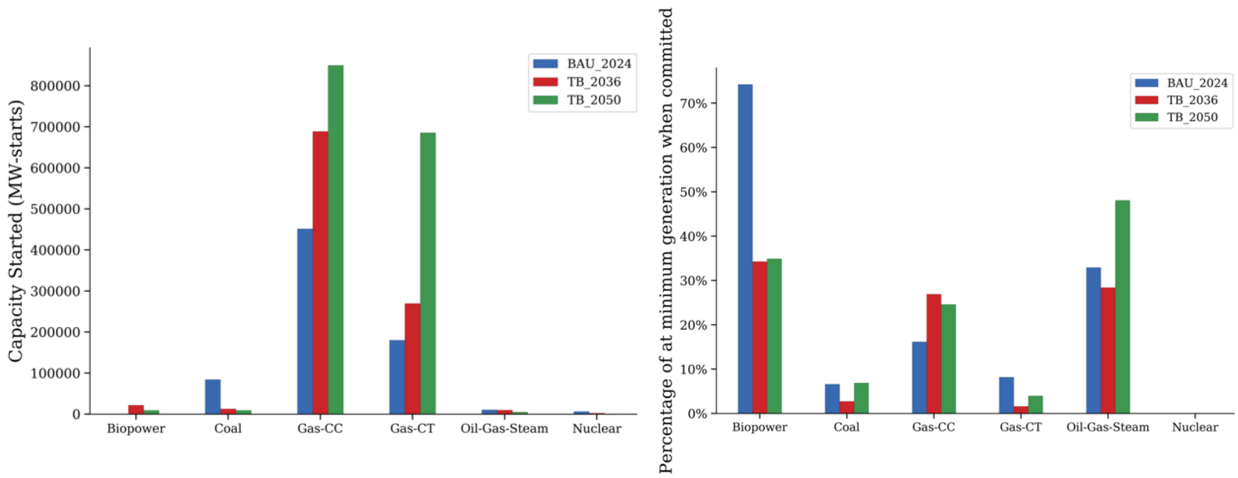

Figure A-31. Total capacity started and percent time spent at minimum generation from July 18 to July 25, 2011

By 2050, PV penetration has increased in the EI. In 2036, PV has an instantaneous penetration of about 33% compared to a nearly 50% peak penetration in 2050. Gas-CC operation is very similar to 2036, but there is slightly more total Gas-CC generation in 2050. There is more reliance on Gas-CTs at peak net load. In 2050, peak generation from Gas-CTs hits about 100 GW in the EI, whereas in 2024 and 2036, peak Gas-CT output was only 40 GW. About 80% of the 100 GW of Gas-CTs are used for an hour or two each day of the event, and then shutdown again.

Western Interconnection Operations

In the WI, a larger PV penetration in 2024 leads to the same resources having a tighter peak around net peak load, but the high-level takeaways are largely similar to those of the EI. Though much of the Southwest and California experience hot temperatures, load is not elevated like it is in the EI. Wind and PV generation is right about average for this time of year. Together this leads to a lower than typical net load for this time of year in the West. There is even a small amount VRE curtailment early in the event.

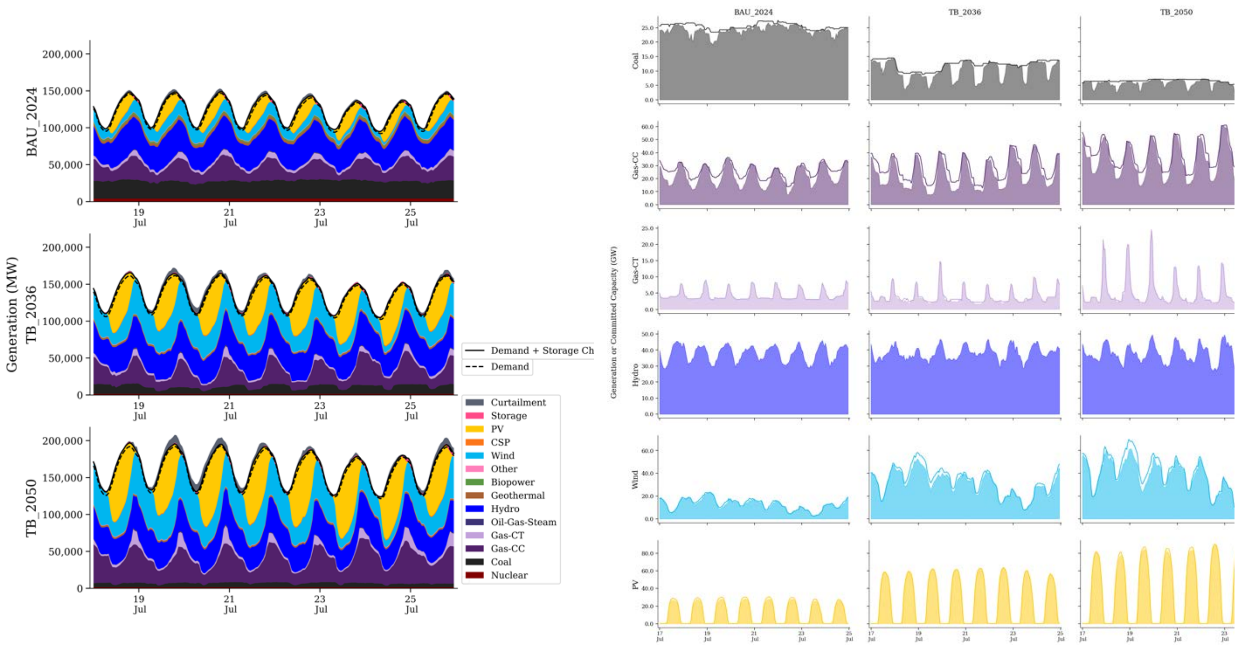

Figure A-32. (a) Generation dispatch for the WI for three future infrastructure: years 2024 (top), 2036 (middle), and 2050 (bottom) and (b) Committed capacity (solid line) and dispatch (filled area) for different generator types (along the vertical axis) for the three future infrastructure years—2024 (left), 2036 (middle), and 2050 (right)—during an extreme heat wave in mid to late July 2011

Even though this event does not suggest increased VRE penetration causes more system stress, there are significant changes in the way the system operates as the infrastructure changes. The changes are most noticeable in the hydropower operations and the interchange between regions. Figure A-32 shows hydropower's change throughout the WI. In 2024, hydropower follows load almost exactly, but in 2036 and 2050, hydropower starts to follow net load instead. Rather than ramping up at the beginning of the day and maintaining a level output for much of the day as in 2024, hydropower ramps up quickly and ramps down quickly again in both 2036 and 2050. Hydropower's operations are particularly peaky in 2050, with more solar PV throughout the interconnection, especially in the hydropower-rich Pacific Northwest (Figure A-33).

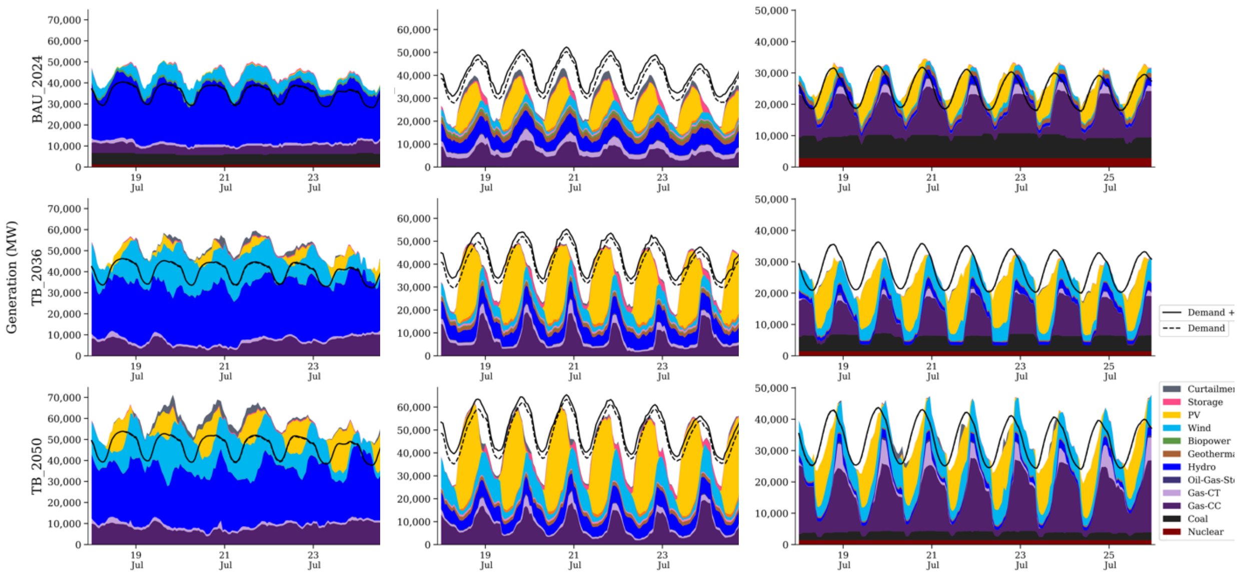

Figure A-33. Generation dispatch for the Pacific Northwest (left column), CAISO (middle column), and the Southwest (right column), for three future infrastructure years—2024 (top), 2036 (middle), and 2050 (bottom)—during an extreme heat wave in mid to late July 2011

Figure A-33 shows the dispatch in three regions of the WI: the Pacific Northwest, CAISO, and the Southwest. Figure A-34 shows the interchange between CAISO and its neighbors, including the Pacific Northwest (blue) and Southwest (green). The timing of changes in the interchange between regions does not change between the three infrastructure years. However, as the wind and solar penetration increases, particularly as the solar penetration increases, the magnitude of the change increases. The change is most obvious between CAISO and the Southwest. In 2024, CAISO is always importing from the Southwest, save a few hours where the net interchange is zero. In both 2036 and 2050, CAISO exports in the middle of the day to the Southwest when PV generation is highest. The Southwest exports to CAISO after sunset with significant ramp ups of Gas-CCs and Gas-CTs. The pattern of the Pacific Northwest interchange is similar, although the Pacific Northwest is always a net exporter. Also, instead of a ramp-up of gas units, hydropower is operated more flexibly to respond to the net load peak in CAISO.

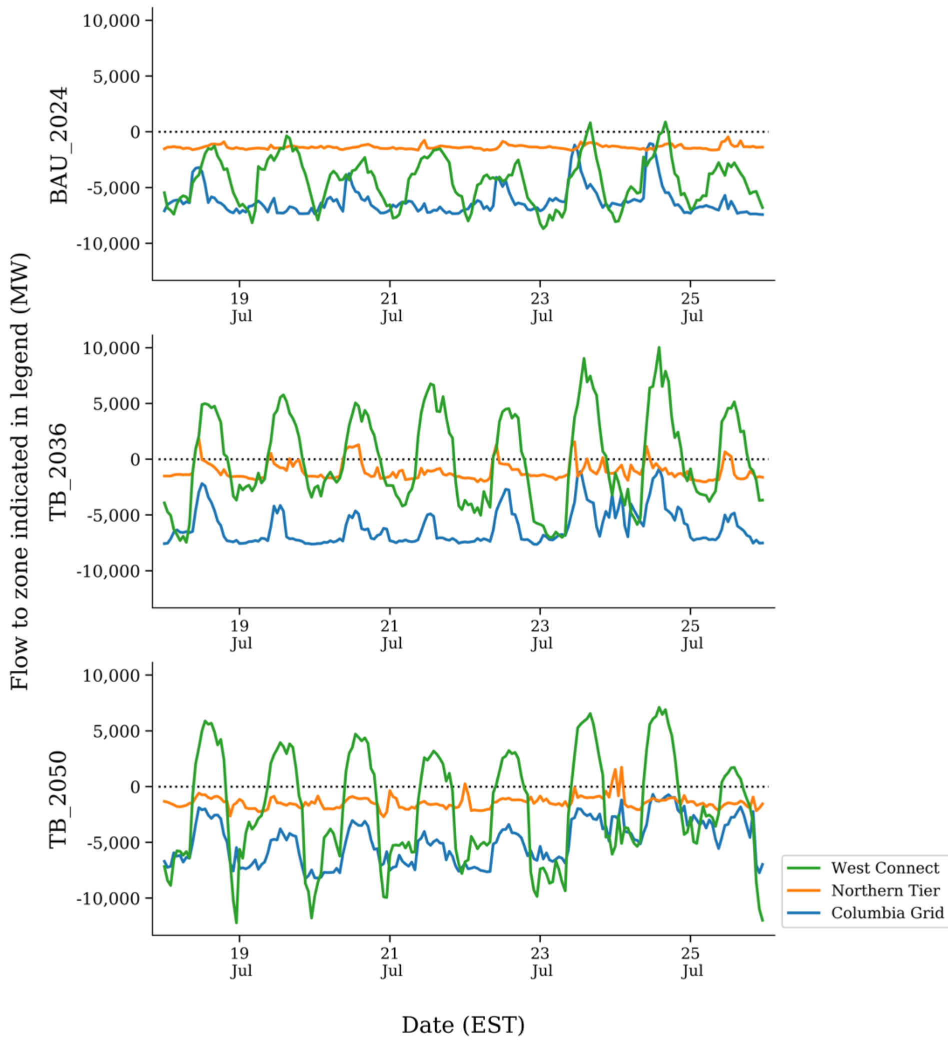

Figure A-34. Net power flow between CAISO and its neighbors during an extreme heat wave in mid to late July 2011

Positive flow means an export from CAISO to its neighbor.

Impacts Summary

During the historic heat wave in July 2011, the load in the EI is in the extreme high end of the load distribution tail. The WI also experiences historic high temperatures, but load is about average for that time of year. In both cases, VRE production is about as expected for that time of year, but operations do change as the penetration increases. Cycling on/off among Gas-CCs and Gas-CTs and ramping of Gas-CCs is key to balancing (1) throughout the EI and (2) in CAISO and the Southwest in the WI. In the WI, specifically in the Pacific Northwest, hydropower's operations also change to provide more capacity for shorter intervals after sunset.

In the EI, VRE serves 11% of load over the 7-day period in 2024, increasing to 38% of load in 2050. Similarly, VRE goes from 20% of load to 45% of load in the WI between 2024 and 2050. However, this increase in VRE did not lead to a decrease in normalized production costs, as seen in Figure A-35. Some of this is due to the increase in gas generation as well, especially in the EI.

However, this highlights the cost impacts of the more generators spending time at their minimum generation levels.

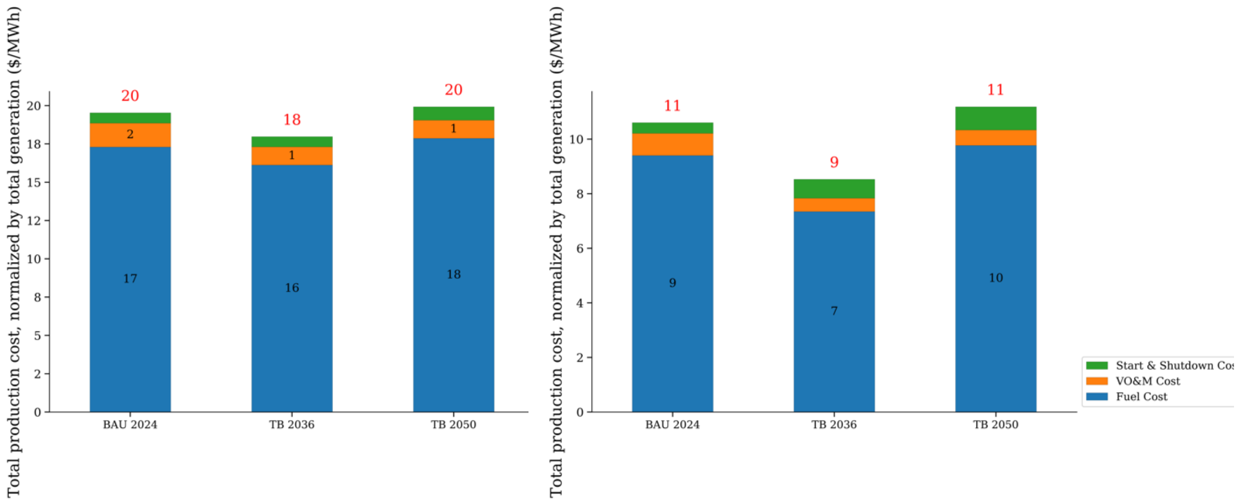

Figure A-35. Normalized production cost for the EI (left) and WI (right) for three future infrastructure years—2024, 2036, and 2050—during an extreme heat wave in mid to late July 2011

Heat Wave 2: June 29–July 7, 2012

Event Summary

Meteorological Description

The heat wave in 2012, which is well documented in the meteorological record, is notable especially for the longevity of the heat in the southern part of the country, with many places recording their warmest July, many temperature records being broken, and the broad region experiencing temperatures in the upper 90s and 100s both east and west of the Rocky Mountains around the Fourth of July holiday.[35] Also, the period includes the historic June 29, 2012, derecho that was directly fueled by the warm, humid temperatures.

Upper-level high pressure began to expand northward out of Texas on June 23, 2012, creating a blocking pattern in the upper-level winds so that the storm track was diverted well north into Canada. By the June 28, triple-digit temperatures extended through Southern Arizona, New Mexico, most of Texas, and all of Oklahoma and Kansas. By the 29th, a weak frontal boundary left behind by a low-pressure system that had moved through Canada was draped from Idaho, almost directly east to Pennsylvania (upper left of Figure A-36), and weak winds around the surface high pressure system centered in the Gulf of Mexico were pushing hot, humid air into the midsection of the country.

Strong upper-level high pressure then remained parked over the center of the country for the next 8 days with temperatures reaching into the upper 90s across almost the entire of the country east of the Rockies and into the 100s over much of the mid-south and Upper Midwest. The contours in the maximum temperatures in Figure A-36 do not capture the 100-degree heat on every day of the record, but station data indicate it is present across a huge part of the central United States every day.[36] Because the upper-level high pressure was centered there, Iowa, Illinois, Missouri, Nebraska, South Dakota, and Wisconsin were all hotter than Texas. Chicago saw 4 days over 100°F.

The June 29th derecho system is the most notable and impactful storm to occur during this time frame. A thunderstorm complex formed on the frontal boundary on in Iowa and developed explosively into the derecho mentioned above, racing across the country roughly following the frontal boundary. The bow-echo thunderstorm system moved at about 60 mph across 800 miles and brought straight-line winds that peaked at over 90 mph across a huge swath of its path. The storm knocked out power to more than 3.7 million people and killed 22 people.[37]

---

[35] See https://www.wpc.ncep.noaa.gov/dailywxmap/index_20120629.html
[36] https://www.wpc.ncep.noaa.gov/dailywxmap/dwm_minmax_20120705.html
[37] (National Weather Service) https://www.weather.gov/media/publications/assessments/derecho12.pdf

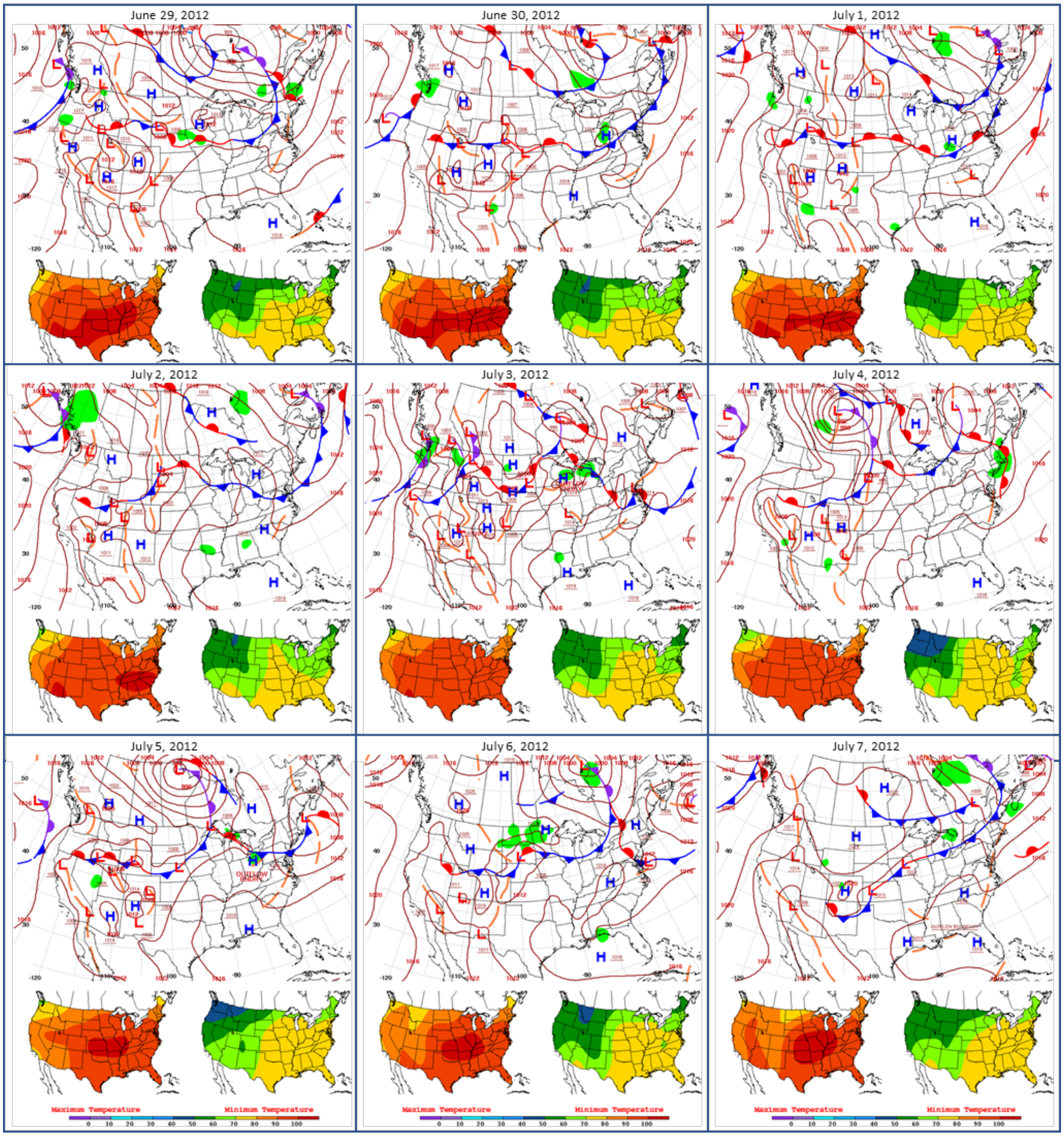

Figure A-36. Surface weather and temperature maps valid at 7 a.m. EST

See the Event Description Structure section for plot details.

Source: "Daily Weather Maps: Wednesday, June 29, 2012" NOAA Weather Prediction Center, https://www.wpc.ncep.noaa.gov/dailywxmap/index_20120629.html

Load Impacts

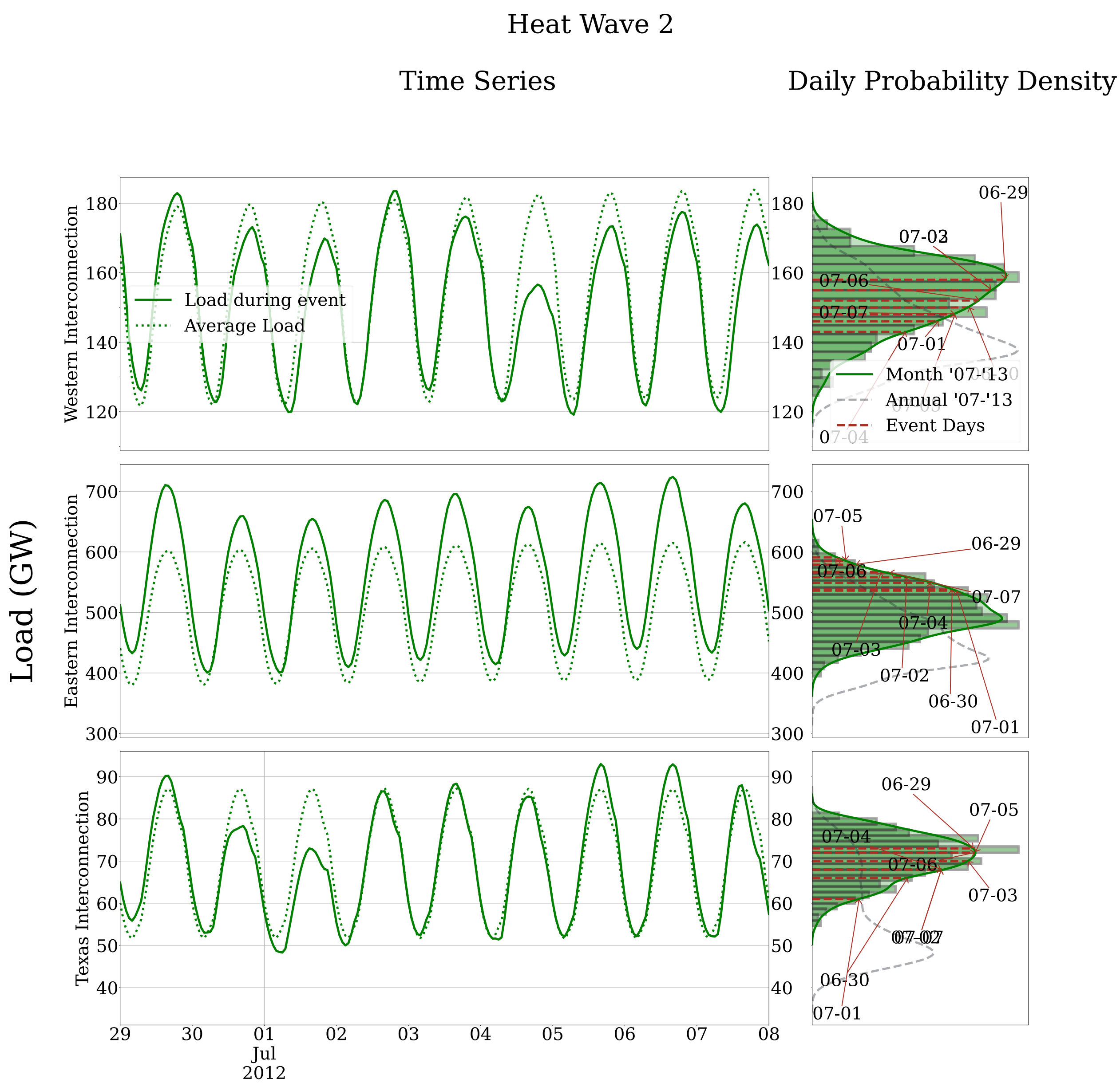

Figure A-37. Time series of regional load during the 4-day event in green, compared to load averaged across the 7-year data set for the month surrounding the event in grey (left) and distribution of 2050 regional loads for the 29 days surrounding the middle of the event in green, and across the 7-year data set in grey, with the event days labeled (right)

The heat wave drove high loads in the EI, with the whole time frame being well above average and most notably July 5 and July 6 being near the upper end of the distribution for this time of year. These days had not only elevated peaks but also higher load during the overnight ours. Though temperatures on July 4 were also very high, loads were lower due to the holiday, which fell on a Wednesday. Loads on the WI and the TI were normal to below normal for this time of year, as the heat was not as widespread over both of these regions.

Wind Generation

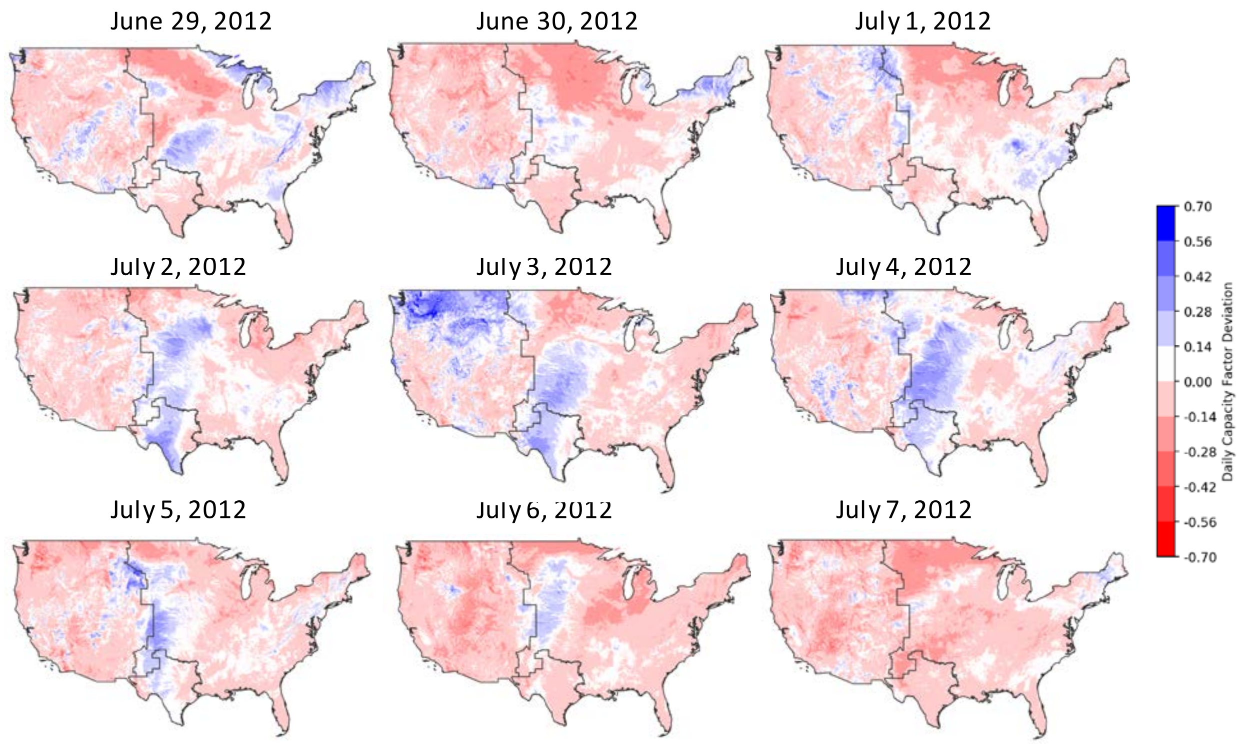

Figure A-38. National daily average wind resource deviation during the 2012 heat wave event

During the heat wave, large areas are close to normal wind resource (-14 to +14 capacity factor points) as seen in Figure A-38, with slight enhancement evident in the Great Plains region on the hottest days of July 5 and July 6. Almost all the enhancement of wind resource appears to be due to a strengthening of the plains low-level jet. The enhancement is driven by pressure gradients set up by differences in the rates of heating and cooling of the air column over the higher terrain further west, relative to the lower terrain to the east. It would be expected that during particularly hot, humid days across the entire continent this pressure gradient would increase and the increase would be most prevalent at night because the drier near-surface air at higher elevations in the center of the continent will cool faster than air at the same pressure level further east, where surface elevations are lower and the air is very moist.

This enhancement is generally seen in wind generation across all three interconnections from the 2nd through the 5th in Figure A-39. On the 6th and 7th, the EI wind falls below normal. The western part of the EI is still seeing above-normal resource due to the strengthening of the nocturnal low-level jet; however, north of the frontal boundary (Figure A-38), high pressure has built in and counteracts the diurnal pattern leading to a reduction in resource in the northern plains at a time when EI loads are still very high. Overall during this time, the wind generation on the EI and the TI clusters around the median, and similar to the 2011 event, higher wind generation occurs overnight, which is not well correlated to peak load.

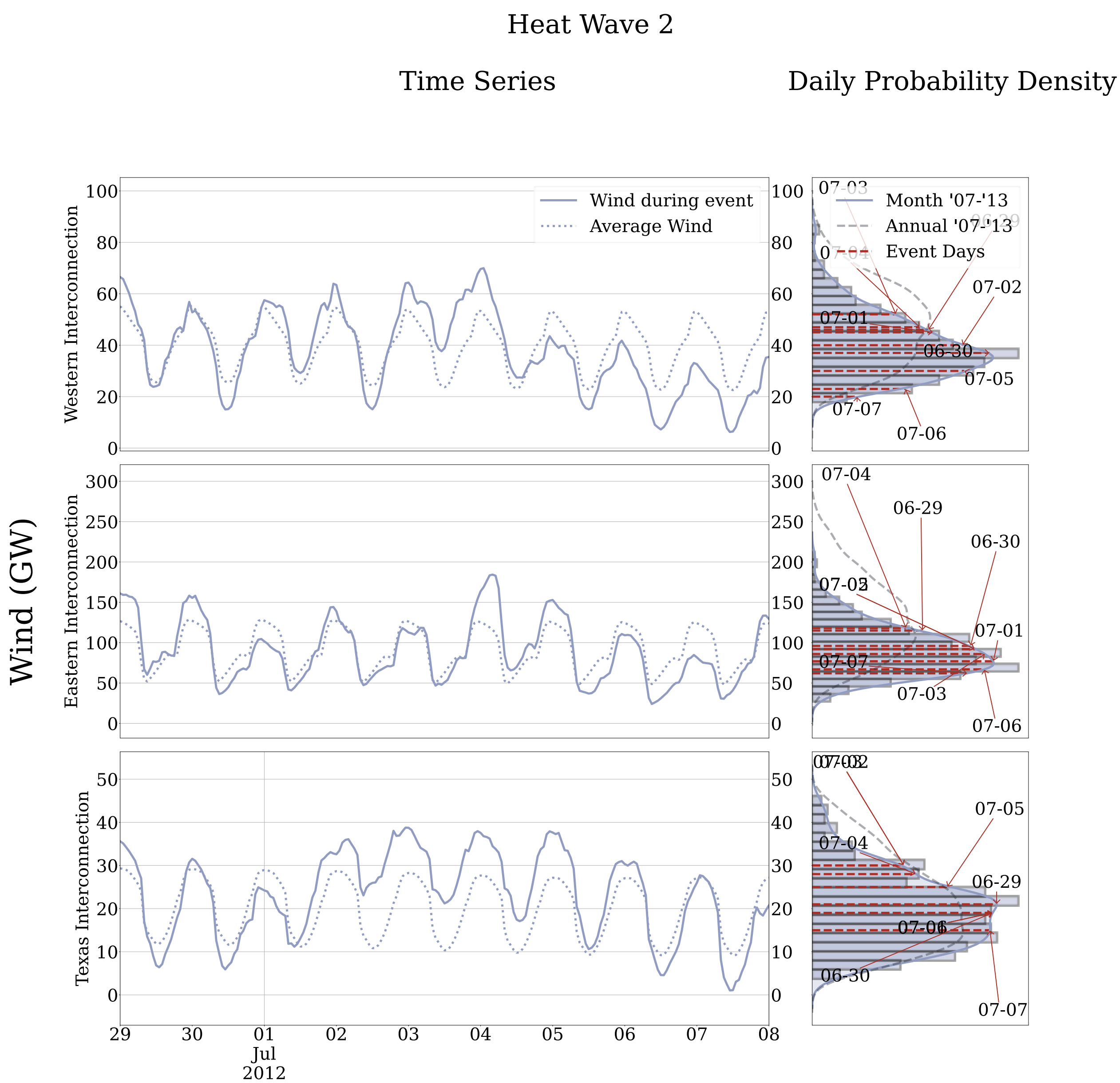

Figure A-39. Event regional wind generation (based on 2050) in context of the distribution of generation for the surrounding month (left) and time series plots of wind generation under the 2050 scenario, relative to normal for the season (right)

Wind resource in the WI is much more variable during the event than in the EI or the TI. Though WI loads are not exceptionally high compared to seasonal normal during this period, wind generation falls off precipitously from the 4th through the 7th, and the resource on the 7th is in the tail of the distribution. This is due to a trough of low pressure that begins to move north up California's Central Valley into Oregon. This turns flow offshore and tends to not be conducive for good wind generation in the west, and it results in warm temperatures in major West Coast cities from Seattle to Portland to San Francisco to Los Angeles.

Though the derecho on the 29th was short-lived and not very observable in the generation data, it had the potential to damage to wind facilities in its path. Derechos bring very rapidly increasing winds along their gust front, and wind turbine control systems may be unable to react rapidly enough to pitch blades or yaw the nacelles to angles that do not subject them to extreme forces. More research into wind response to derecho events would be needed to understand their impact in high wind penetration scenarios.

Solar Generation

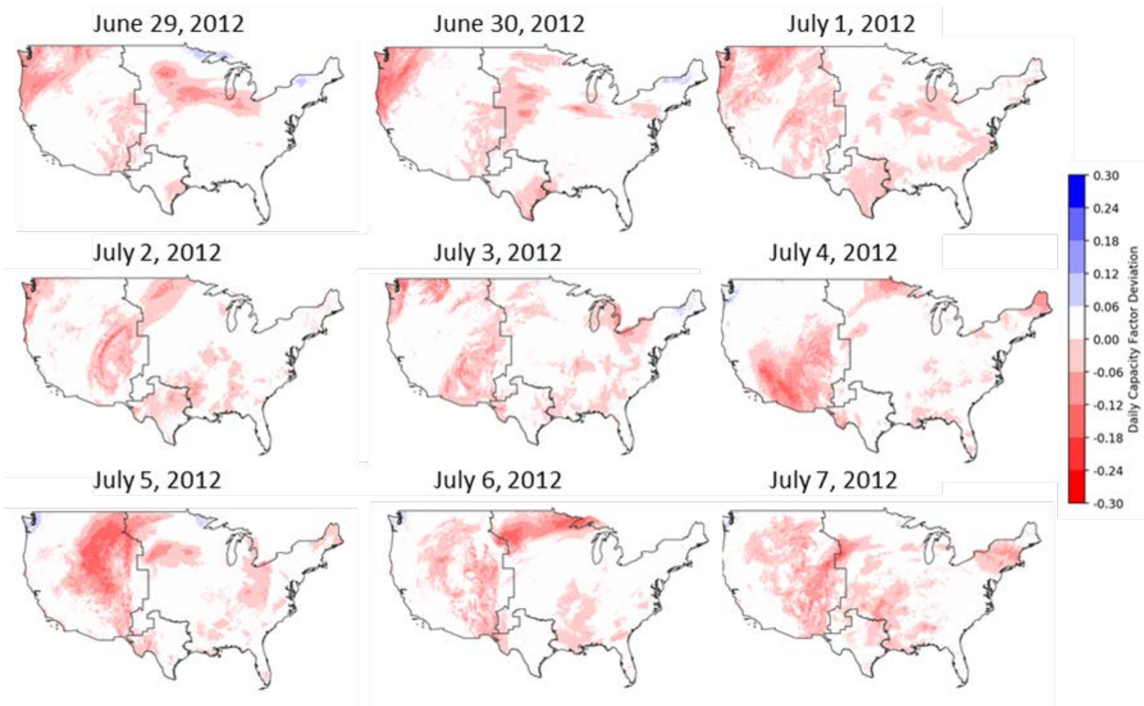

Figure A-40. Event regional modeled 2050 PV generation in context of the distribution of generation for the surrounding month (left) and time series plots of PV generation under the modeled 2050 scenario, relative to normal for the season (right)

Many of the key features for solar generation are similar to the 2011 heat wave. Specifically, the variability between days is low, the heat wave days fall in the main part of the distribution, and the overall summertime distribution is tight and well on the high side of the annual resource distribution. Overall, resource is slightly higher in the EI due to less clouds under the high pressure are associated with the heat system, and this is somewhat correlated with the increased load peaks.

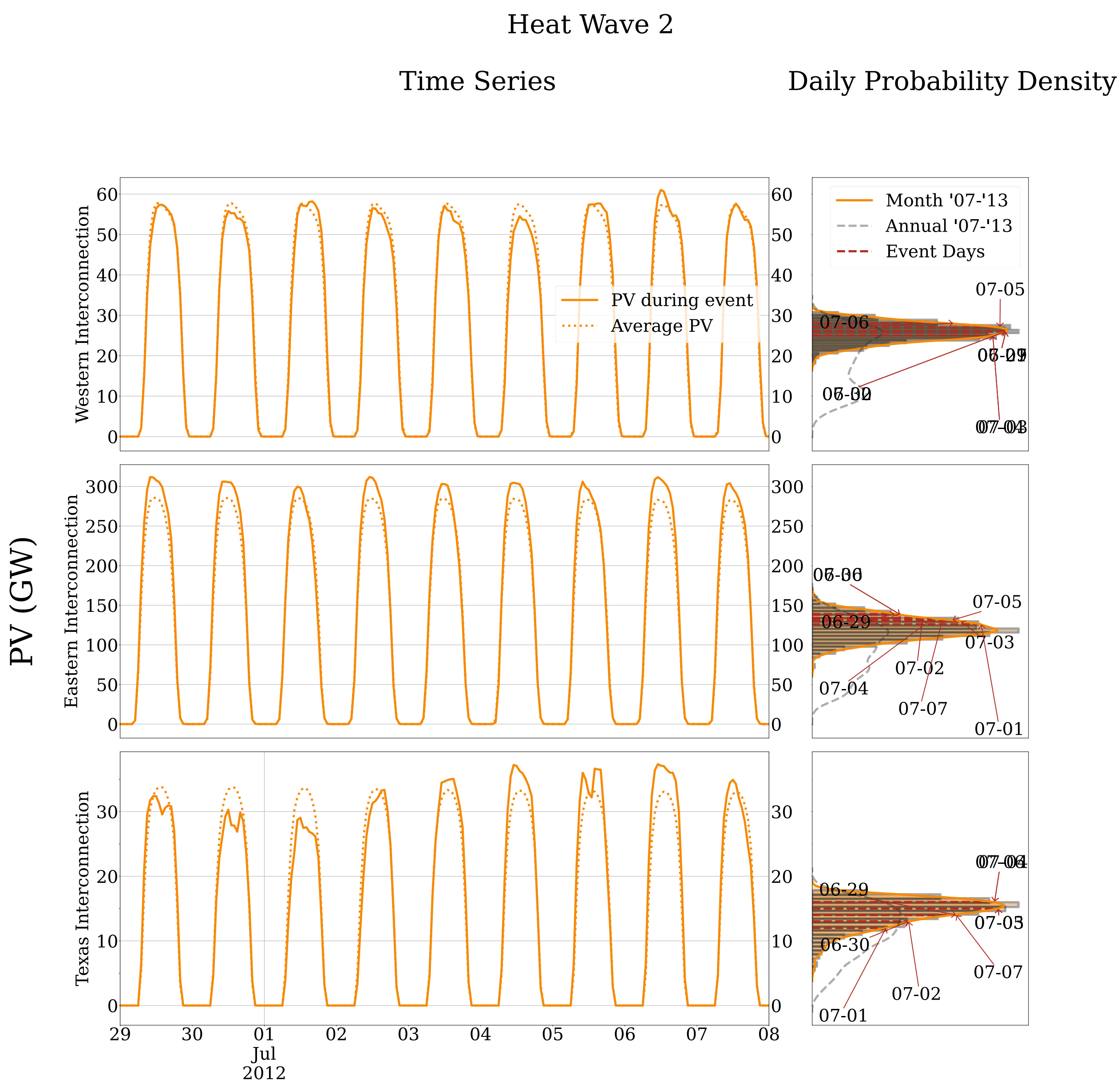

Figure A-41. Event regional modeled 2050 PV generation in context of the distribution of generation for the surrounding month (left) and time series plots of PV generation under the modeled 2050 scenario, relative to normal for the season (right)

Texas sees slightly below-normal resource at the beginning of the period owing to clouds and thunderstorms in the southern part of the state, and like in 2011, the lower solar resource period is roughly correlated with lower loads owing to the reduced insolation and correspondingly lower maximum temperature in the vicinity of the major load centers such as Houston, San Antonio, and Dallas.

Net Load

For this heat wave, the meteorological features driving higher loads are not correlated with features that result in significantly below-normal renewable generation at modeled generation sites. Through most of the period, the higher loads are coincident with higher average daily renewable generation, especially on the EI, where solar is above normal due to decreased clouds, and wind is near normal.

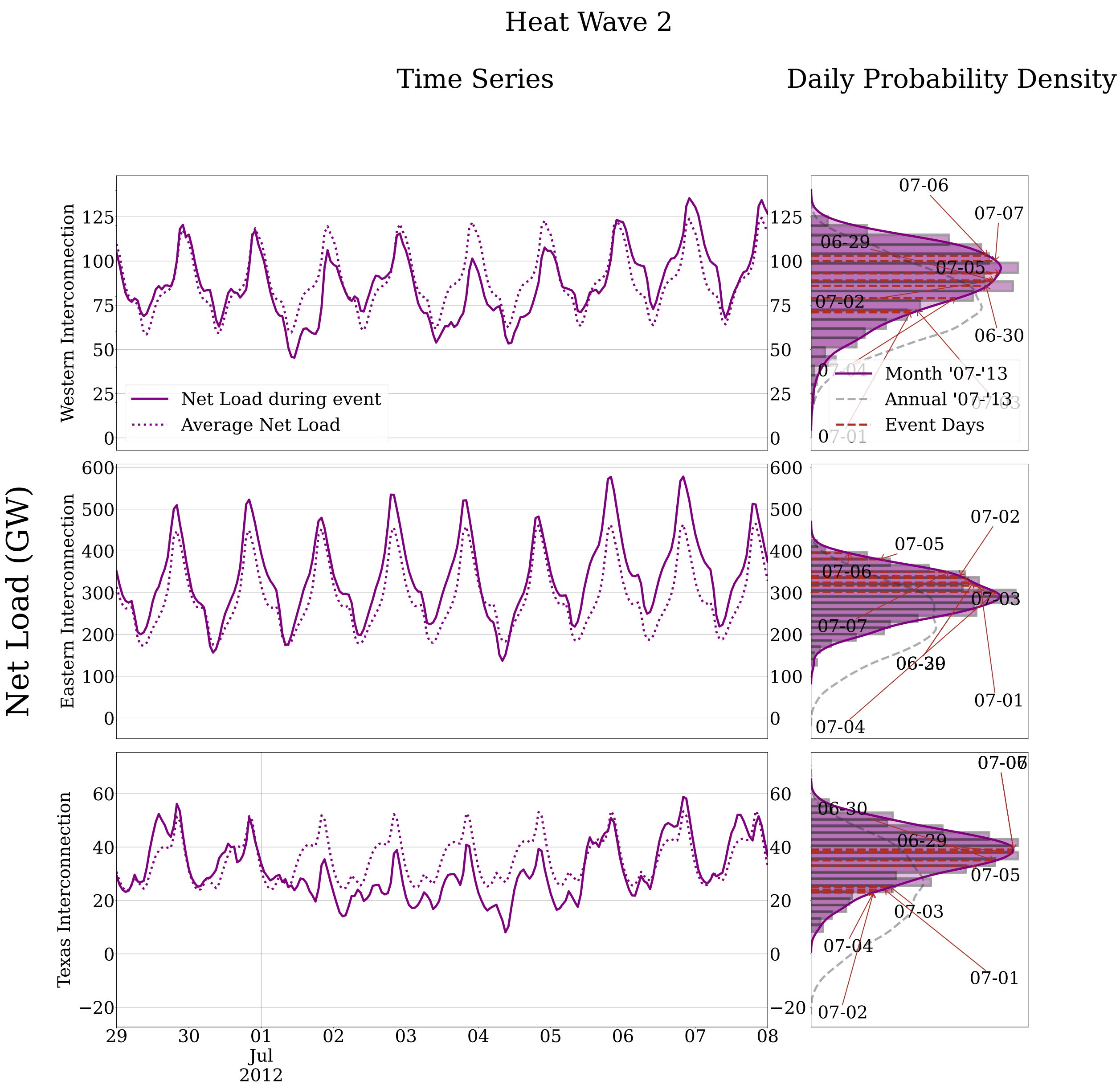

Figure A-42. Event regional modeled net load context of the distribution of generation for the surrounding month (left) and time series plots of modeled net load under the modeled 2050 scenario, relative to normal for the season (right)

Comparing the distribution of net load during the event (Figure A-42) to the distribution of load (Figure A-37), the distribution can be seen to be generally shifted toward the left relative to the median in all regions. However, in the EI where impacts of the heat wave are highest, all days are still above the median, and July 5 and July 6 are still within the high end of the net load distribution. In the TI, we see even more impact, with net load decreasing through the highest load period, relative to the average for the time of year. However, as in the summer period in general, during the event, the net load pattern contains sharp spikes where the need for fast ramping generation is needed.

Hurricane Irene: August 25–30, 2011

Event Summary

Irene was a large hurricane that reached Category 3 but weakened to Category 1 before making landfall on the Outer Banks of North Carolina. The event was selected for its potential to impact offshore and near shore wind generation and PV generation in the Southeast.[38]

Irene made landfall as a Category 1 hurricane on August 27, 2011, in North Carolina and then tracked up the East Coast and moved inland over New York where it interacted with a frontal system and became extratropical as it moved northward into Canada. Rainfall of 10–15” in many coastal counties of North Carolina result in extensive flooding. Winds associated with the storm and tornadoes spawned as it approached caused widespread power outages due to downed trees.

Meteorological Description

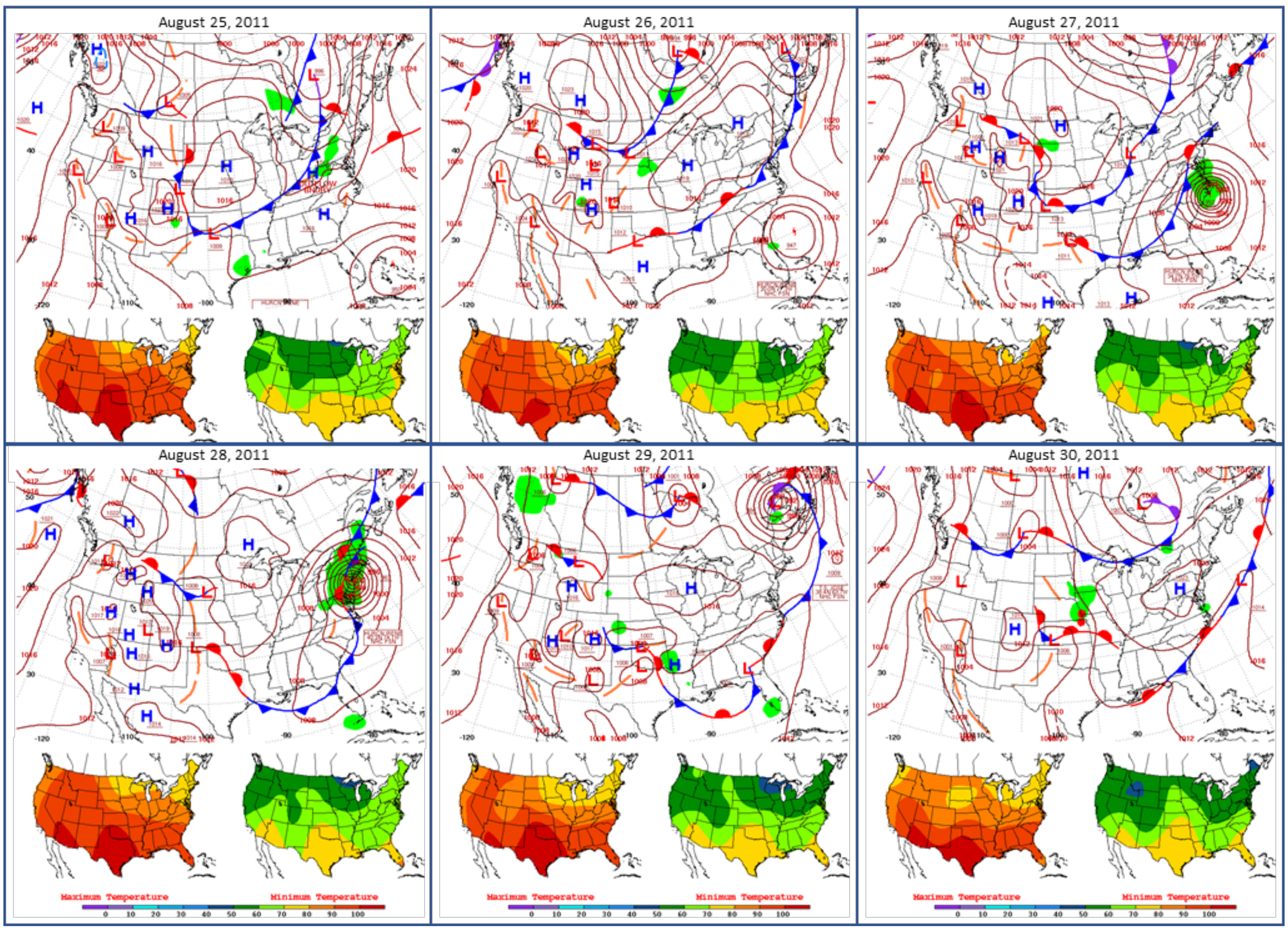

Figure A-43. Surface weather and temperature maps valid at 7 a.m. EST

See the Event Description Structure section for plot details.

Source: “Daily Weather Maps: Thursday, August 25, 2011,” NOAA Weather Prediction Center, https://www.wpc.ncep.noaa.gov/dailywxmap/index_20110825.html

[38] See https://www.wpc.ncep.noaa.gov/dailywxmap/index_20110825.html

Figure A-43 shows the weather across the United States as Irene approaches and during its track up the East Coast. As the storm approached, most of the southern half of the country was still experiencing very hot weather associated with the Summer 2011 heat wave that was described previously. A moderate frontal system pushing through Canada was bringing relief from the heat to northeastern United States. Clouds from Irene began to impact eastern Florida on the 25th, extending into Georgia and South Carolina on the 26th. The main impacts of the storm were seen along the coast from North Carolina north on the 27th and then inland and along the East Coast on the 28th and 29th.

Load Impacts

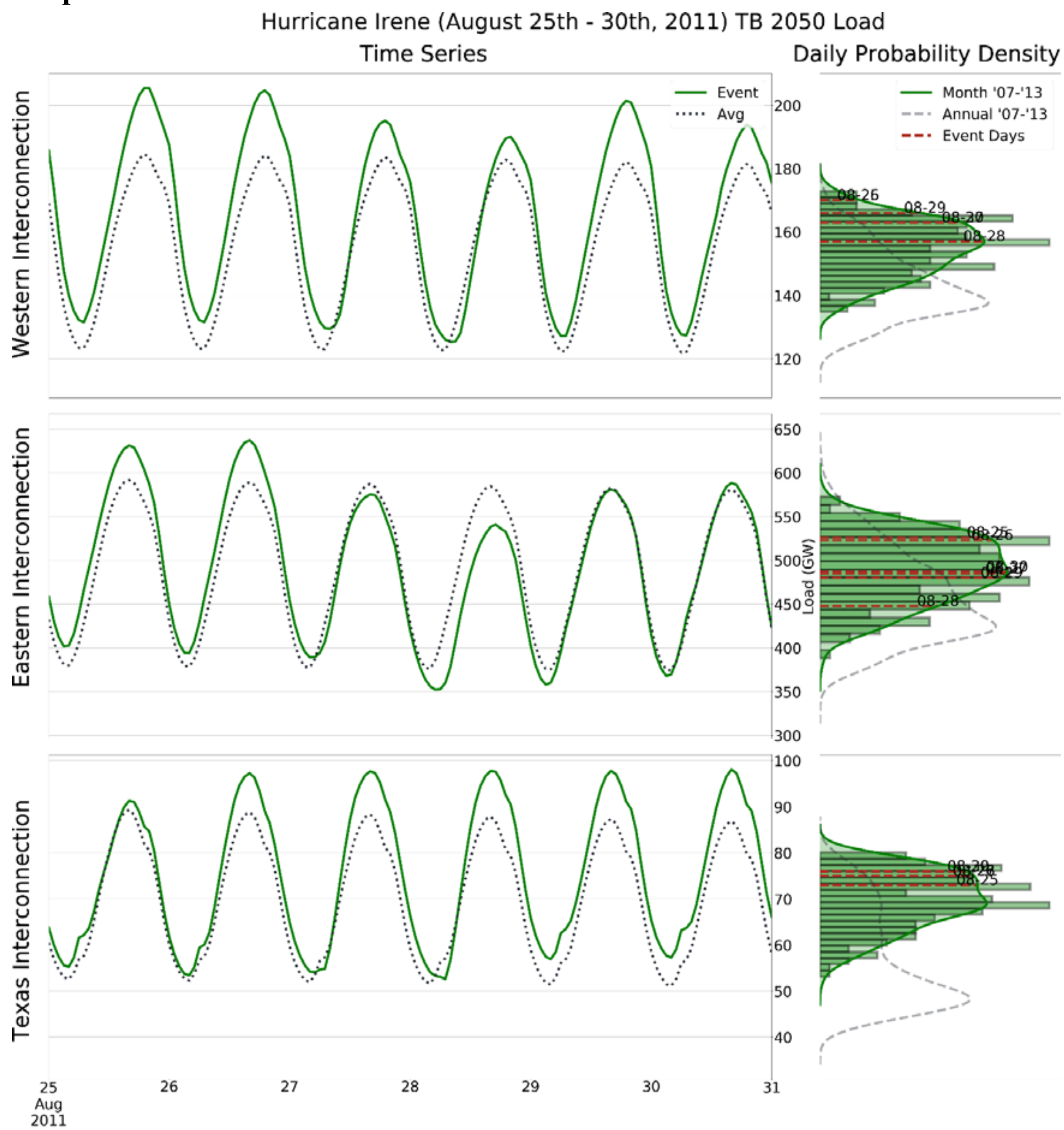

Figure A-44. Time series of regional load during the 4-day event in green, compared to load averaged across the 7-year data set for the month surrounding the event in grey (left) and distribution of 2050 regional loads for the 29 days surrounding the middle of the event in green, and across the in grey, with the event days labeled (right)

The impacts of the hurricane on load were all localized in the EI as seen in Figure A-44. Load was beginning to reduce on the EI on the 27th and became still significantly lower than normal on the 28th. Some of this drop is due to cooler air moving into the northeast, but much of it was likely due to a cool wet day on the 28th in the major East Coast cities from Charlotte, North Carolina, to Washington D.C., to New York City. Loads were by no means in the tail of the distribution for the time of year, though it should be noted that the month surrounding the event includes the transition into fall and the attendant cooler temperatures. To the west and in Texas, above-normal load was still being experienced due to the ongoing heat wave.

Wind Generation

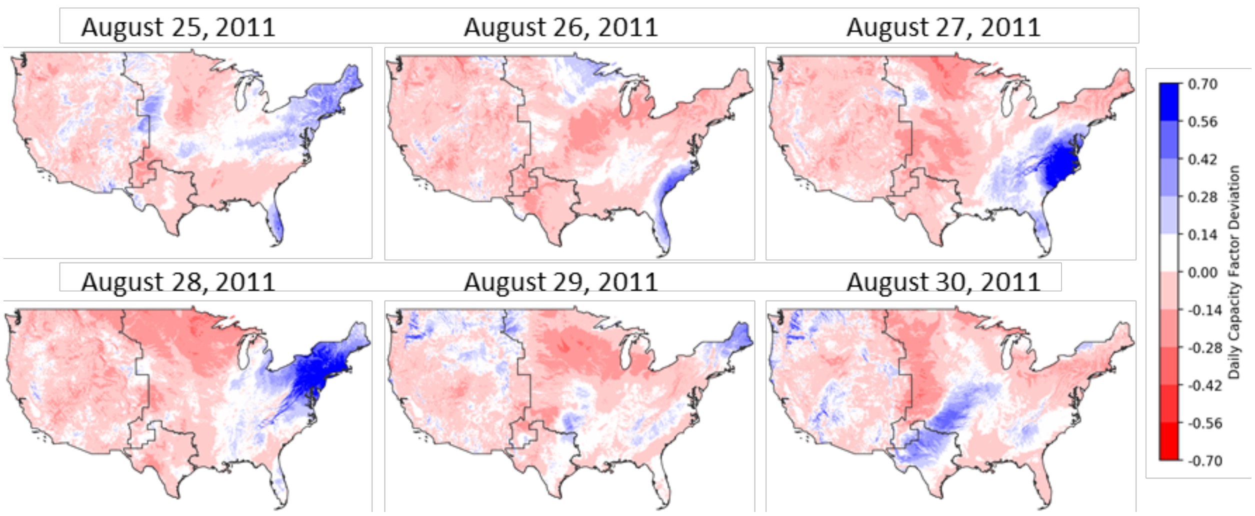

Figure A-45. National daily average wind resource deviation Hurricane Irene

The track of the storm is clearly visible in the spatial plots (Figure A-45), where it shows up as a fairly compact area of significantly enhanced resource that first impacts Florida and then moves northward. Hurricane force winds for this storm extend only a few miles inland and therefore would not be expected to result in extensive high wind cutouts and could otherwise boost wind generation. Though the storm does increase EI wind generation (Figure A-46), it is limited due to the small geographic area it affects, the lower concentration of wind generators on the East Coast than the central plains, and concurrent reduced wind resource in the central plains, which offsets enhancement from the storm, especially on the 27th. The 28th sees significantly higher-than-normal wind generation due to the storm moving into the northeast, but this is surpassed by generation on the 25th, which is before the storm has begun to affect the region.

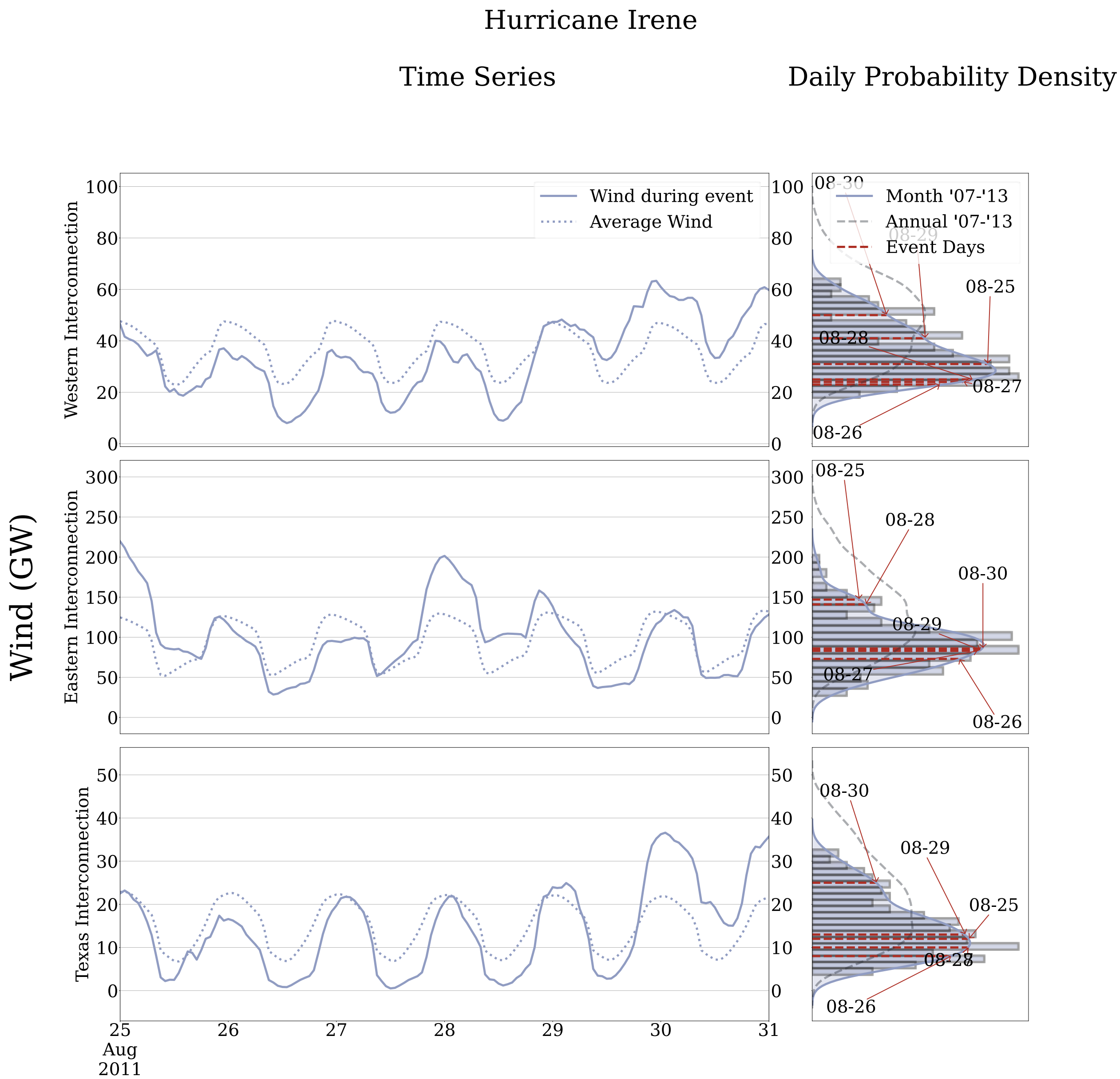

Figure A-46. Event regional wind generation (based on 2050) in context of the distribution of generation for the surrounding month

The typical weather conditions occurring in the TI and the WI may have a more significant impact in a high-penetration future than Hurricane Irene. The west and Texas remain hot through the period and the daytime wind is considerably below normal. High pressure over the Intermountain West acts to reduce WI wind as the region enters a regime where air flow is from the continent toward the ocean. This is not the prevailing direction, and few wind plants are located in places that can take advantage of it.

Solar Generation

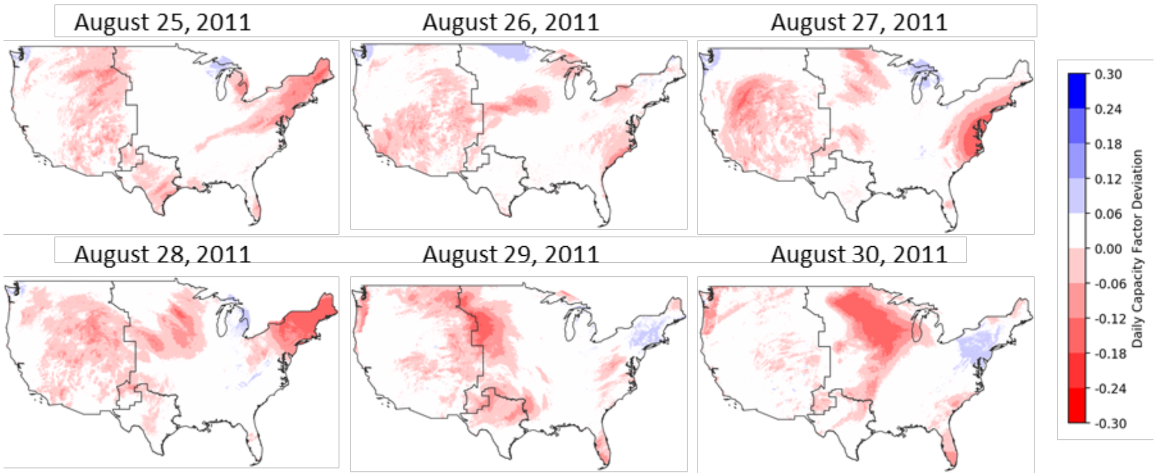

Figure A-47. National daily average solar resource deviation during Hurricane Irene

The storm cloud shield decreases solar PV, but the impacts are localized and not as significant as the effects of the larger-scale weather, which is generally less disturbed than average yielding overall better PV resource. As a result, PV generation is above normal throughout most of the period in all regions, and most notably is enhanced on the 28th across the EI, which is concurrent with the drop in load that is due to the storm moving into the northeast.

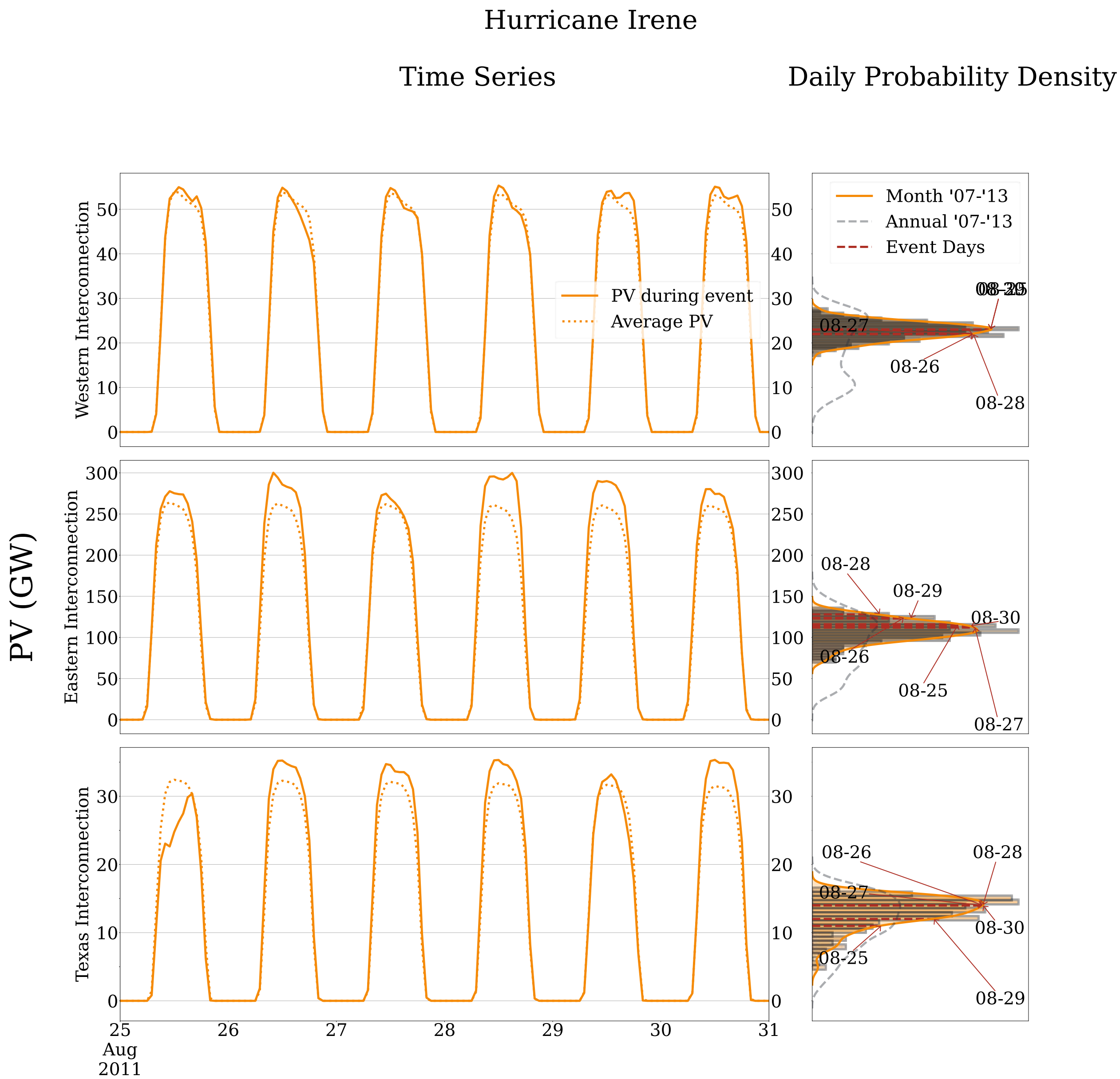

Figure A-48. Event regional solar generation (based on 2050) in context of the distribution of generation for the surrounding month

Net Load

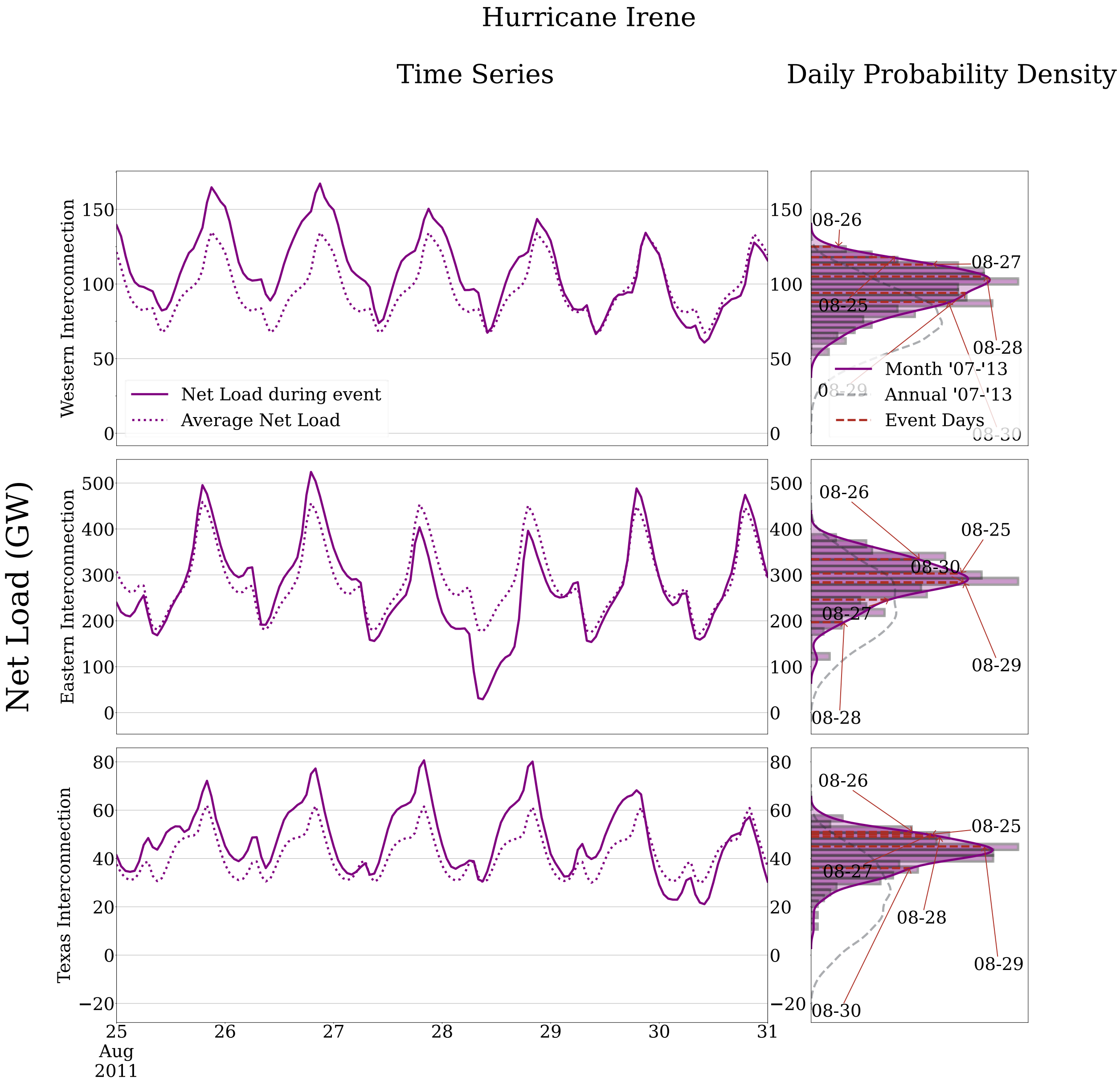

Figure A-49. Statistical distribution of net load in the month surrounding the event for 2024 and 2050 scenarios

Hurricane Irene did not produce strong enough winds over land to cause widespread high wind speed cut-out, and it would not have caused damage to wind plant infrastructure normally designed to withstand winds equivalent to a Category 3 storm. The main impact of the storm was reduced load as the storm made its way past major load centers on the East Coast. Net load (Figure A-49) indicates that on the 28th in the EI, the combination of enhanced wind generation due to the storm enhanced solar generation in the plains away from the storm cloud cover, and the reduced load leads to net load in the tens of gigawatts during the day of the 28th. Net load recovers to 400 GW in less than a day from this point, and it may tax the ability of the rest of the fleet to ramp, especially if generators were impacted by outages due to the storm.

Hurricane Gustav: September 1–6, 2008

Event Summary

Hurricane Gustav was notable for its size and long overland track, which impacted a wide swath of the wind and solar resources in the EI. Gustav cloud cover caused a significant solar deficit, but it was countered by improved wind generation across the same region. As the hurricane moved through the Midwest, strong high pressure east of the hurricane over the mid-Atlantic that yielded clear skies and led to good solar resource and poor wind generation.[39]

Gustav moved inland from the Gulf of Mexico into Louisiana on September 1, 2008, as a Category 2 storm. Once overland, the wind weakened rapidly, as is typical for hurricanes, but a broad cloud shield, heavy precipitation, and moderate winds persisted for several days. A very weak upper-level environment allowed the storm to remain intact despite being cut off from the warm water fuel source. On the 4th, it interacted with an approaching cold frontal boundary and the storm transitioned to having extratropical characteristics. The remaining low-pressure system swept rapidly north on the 4th and 5th into Missouri, Illinois, and Michigan.

Weather across the rest of the country was typical for the beginning of the transition into fall. The cold front that ultimately picked up Gustav brought some of the first cool air into the northwest and interior west, with nighttime temperatures dropping in parts of Idaho, Montana, Wyoming, and the Upper Midwest. Nationwide, temperatures were fairly seasonal, with typical oscillations around the median temperature. The northeast was warm, but not exceptionally so, and the major California coastal cities were experiencing a moderately strong late summer heat wave.

[39] See "Daily Weather Maps, Monday September 1, 2008," https://www.wpc.ncep.noaa.gov/dailywxmap/index_20080901.html

Meteorological Description

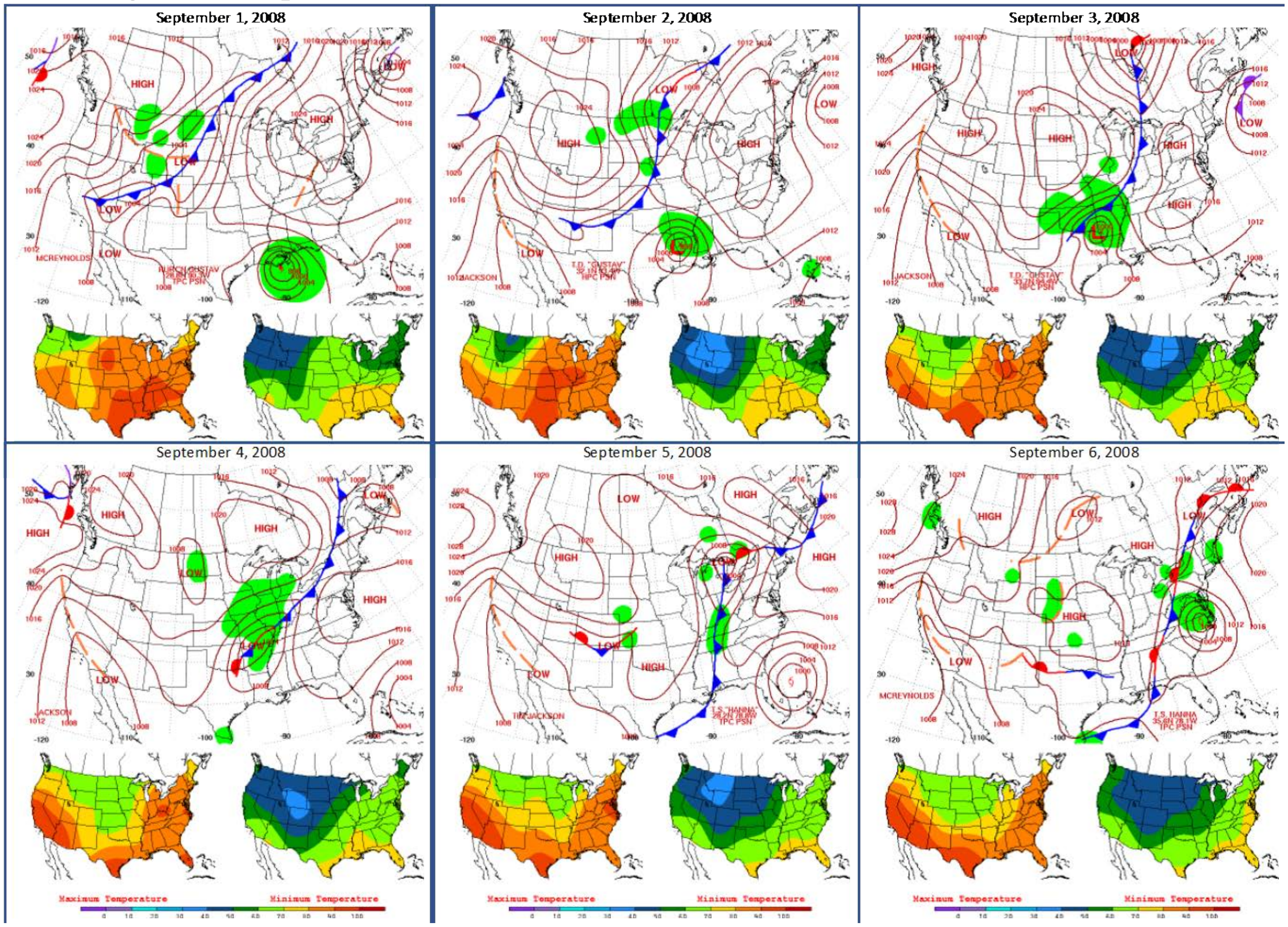

Figure A-50. Surface weather and temperature maps valid at 7 a.m. EST

See the Event Description Structure section for plot details.

Source: "Daily Weather Maps: Monday, September 1, 2008," NOAA Weather Prediction Center, https://www.wpc.ncep.noaa.gov/dailywxmap/index_20080901.html

Load Impacts

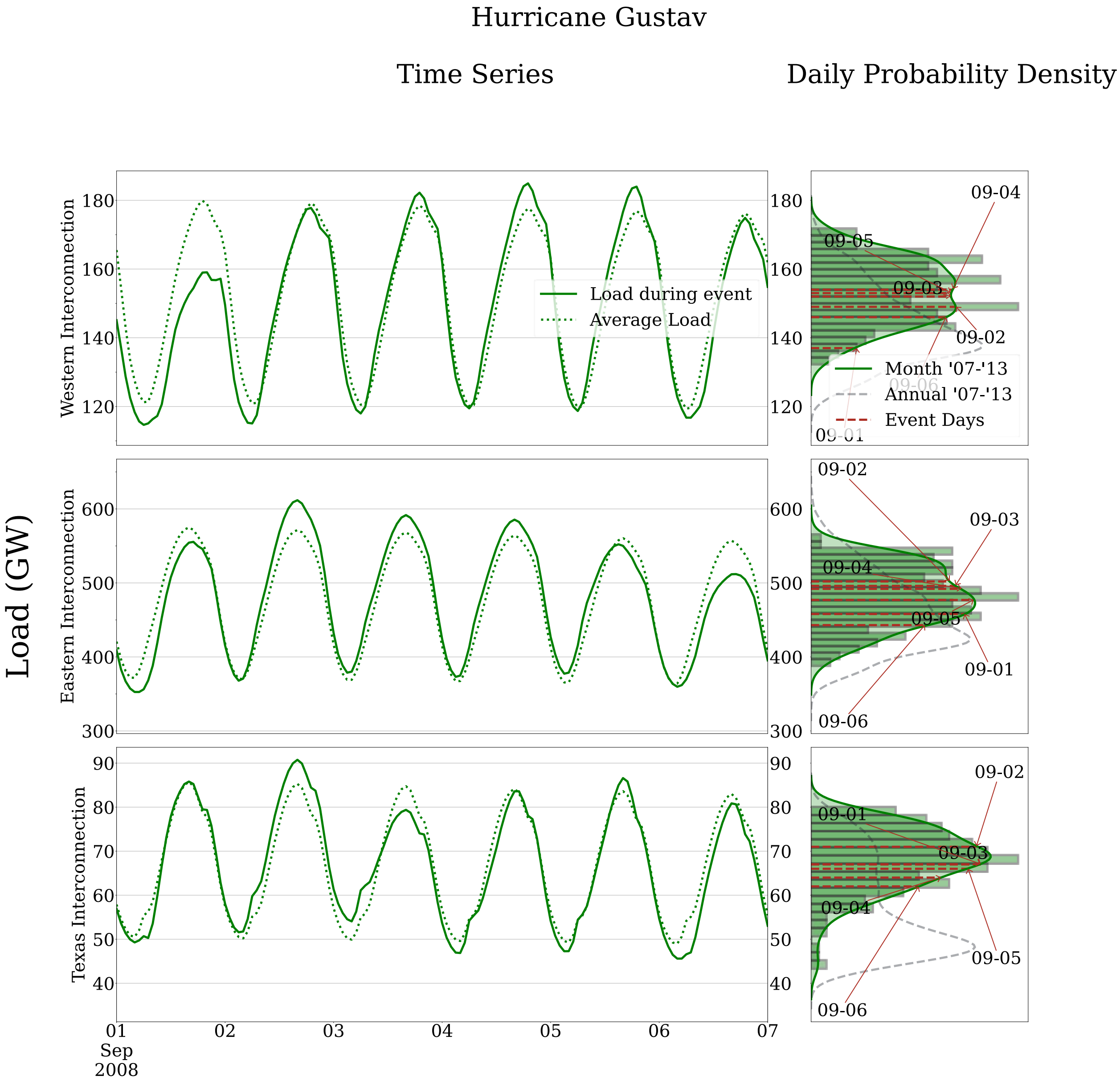

Figure A-51. Time series of regional load during the 4-day event in green, compared to load averaged across the 7-year data set for the month surrounding the event in grey (left) and distribution of 2050 regional loads for the 29 days surrounding the middle of the event in green, and across the 7-year data set in grey, with the event days labeled (right)

The impacts of Gustav on load are mostly unremarkable (Figure A-51). East Coast loads were somewhat above normal, especially on the 2nd and the 3rd, as they were driven by the above-normal temperatures in the eastern third of the country, and the moderation at the end of the period is due to the cold front moving eastward. The cloud shield from Gustav might have had a minor impact, reducing load in major cities like New Orleans and Baton Rouge on the 1st as the hurricane made landfall, but the impact is minimal relative to interconnection-wide load.

TI loads were generally near normal, tapering to slightly below normal toward the end of the period. This was much more a function of the cooler air arriving from the north than reduced solar heating due to Gustav's cloud shield, which did not extend far into Texas.

The hurricane did not impact the WI at all, and with the exception of September 1st, loads there were typical for the time of year. On the 1st, a cold front from a mid-latitude storm system was bringing the first cool air of the season to the west and loads were well below normal. Later in the period, cooling demand was higher on the West Coast, but it was largely offset in the aggregate by cooler temperatures in the Intermountain West.

Wind Generation

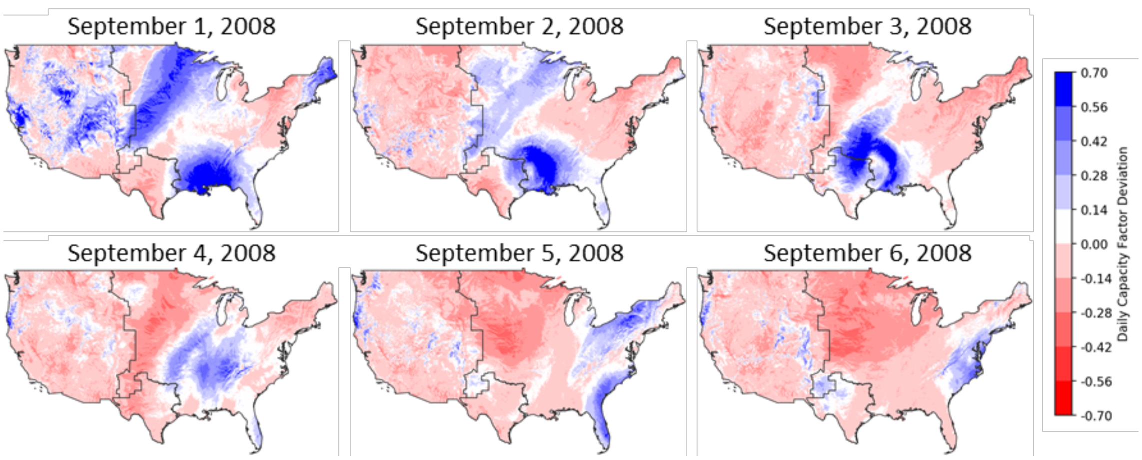

Figure A-52. National daily average wind resource deviation during Hurricane Gustav

The impact of Gustav can clearly be seen in Figure A-52 as a circular area of well above-normal resource on the 1st through the 3rd. This enhancement, combined with the impact of the cold front sweeping south through the western side of the EI yields much above-normal wind generation on the 1st and 2nd (Figure A-53). However, on the 3rd, EI wind generation falls below the normal for the time of year. This is because—despite the presence of a good-sized region of enhancement due to Gustav—the wind is below normal over a broader area of the east where other significant wind capacity is located. Once the hurricane is sheared apart by the cold front on the 4th, the enhancement becomes more diffuse, and on the 5th it is more characteristic of typical enhancement along a frontal zone. During this period, wind generation on the EI recovers to near and above-normal values as the cold front moves past large areas of wind capacity. The enhancement along the coast of Florida on the 5th and along the mid-Atlantic coast on the 6th is due to the approach of tropical storm Hanna.

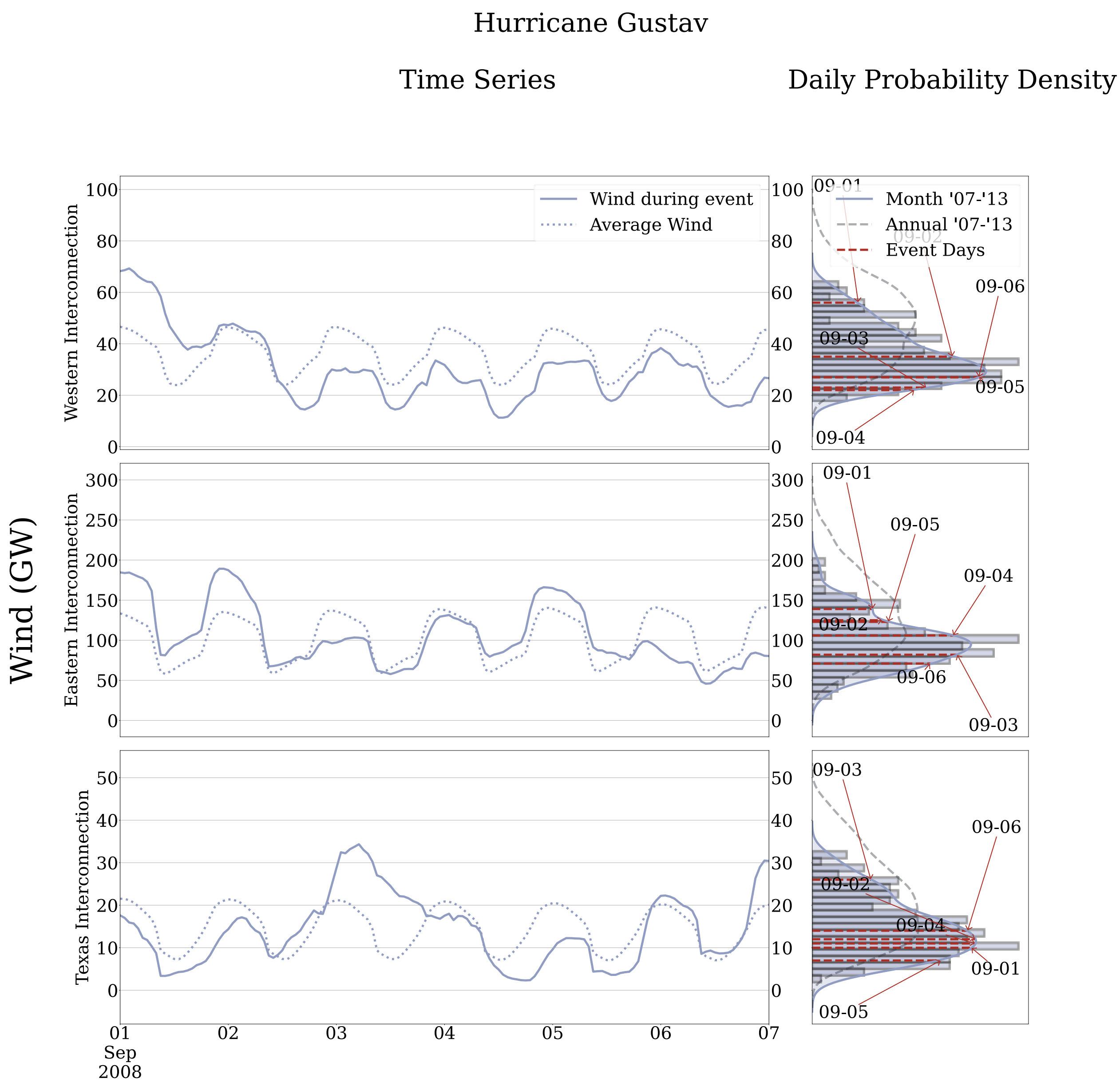

Figure A-53. Event regional wind generation (based on 2050) in context of the distribution of generation for the surrounding month (left) and time series plots of wind generation under the 2050 scenario, relative to normal for the season (right)

Despite the western part of Gustav impacting Texas, the TI wind generation is below normal on the 1st and 2nd because the storm, combined with high pressure building to the north, weakens the low-level jet in western Texas. On the 3rd, Texas sees an enhancement in wind generation as the cold front sweeps through the region.

WI wind is unaffected by Gustav. It peaks on the 1st in response to cold air being advected southward behind the cold front as high pressure builds in. Once the high pressure is established inland, the flow goes offshore producing the downslope east winds in California that are characteristic of hot days there. This type of pattern is also associated with lower wind generation, as even though winds occurring during offshore flow are strong, they are infrequent and do not tend to drive wind plant siting.

Solar Generation

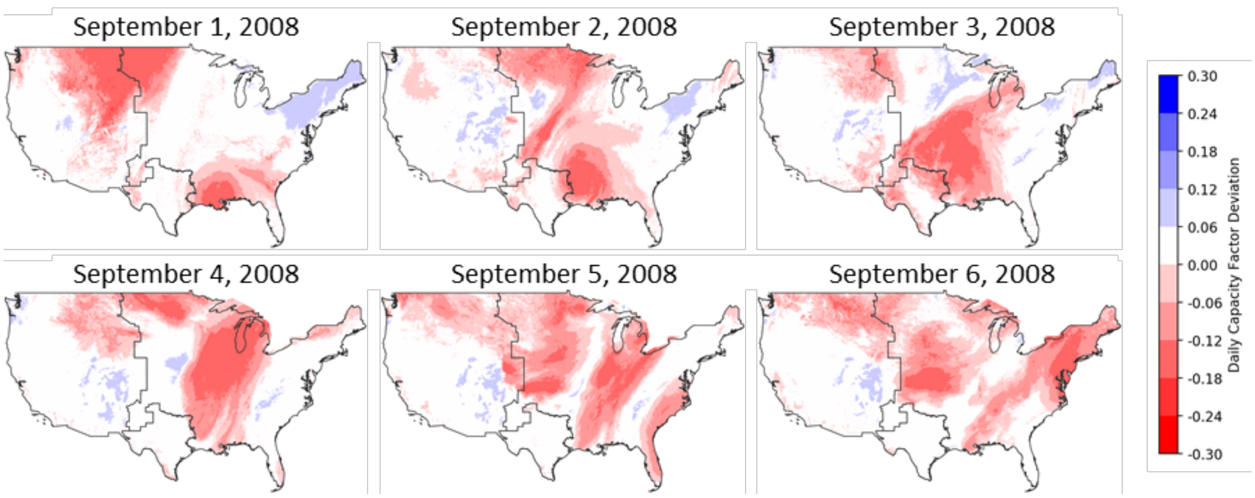

Figure A-54. National daily average solar resource deviation during Hurricane Gustav

The cloud shield from Gustav can clearly be seen in Figure A-54. The organized structure of the storm is visible in the solar resource reduction on the 1st and 2nd, and it becomes more diffuse as the moisture from the storm is spread out as it interacts with the frontal system. However, the only day that saw a significant deviation from the typical solar generation for the time of year was the 5th, when EI experiences a low generation day in the distribution in Figure A-55 at roughly 25% below normal. Though the cloud shield from a large hurricane has a significant impact on solar resource, the geographic extent of a hurricane is not large enough for the impact to be profound on an interconnection-wide perspective relative to typical weather variability.

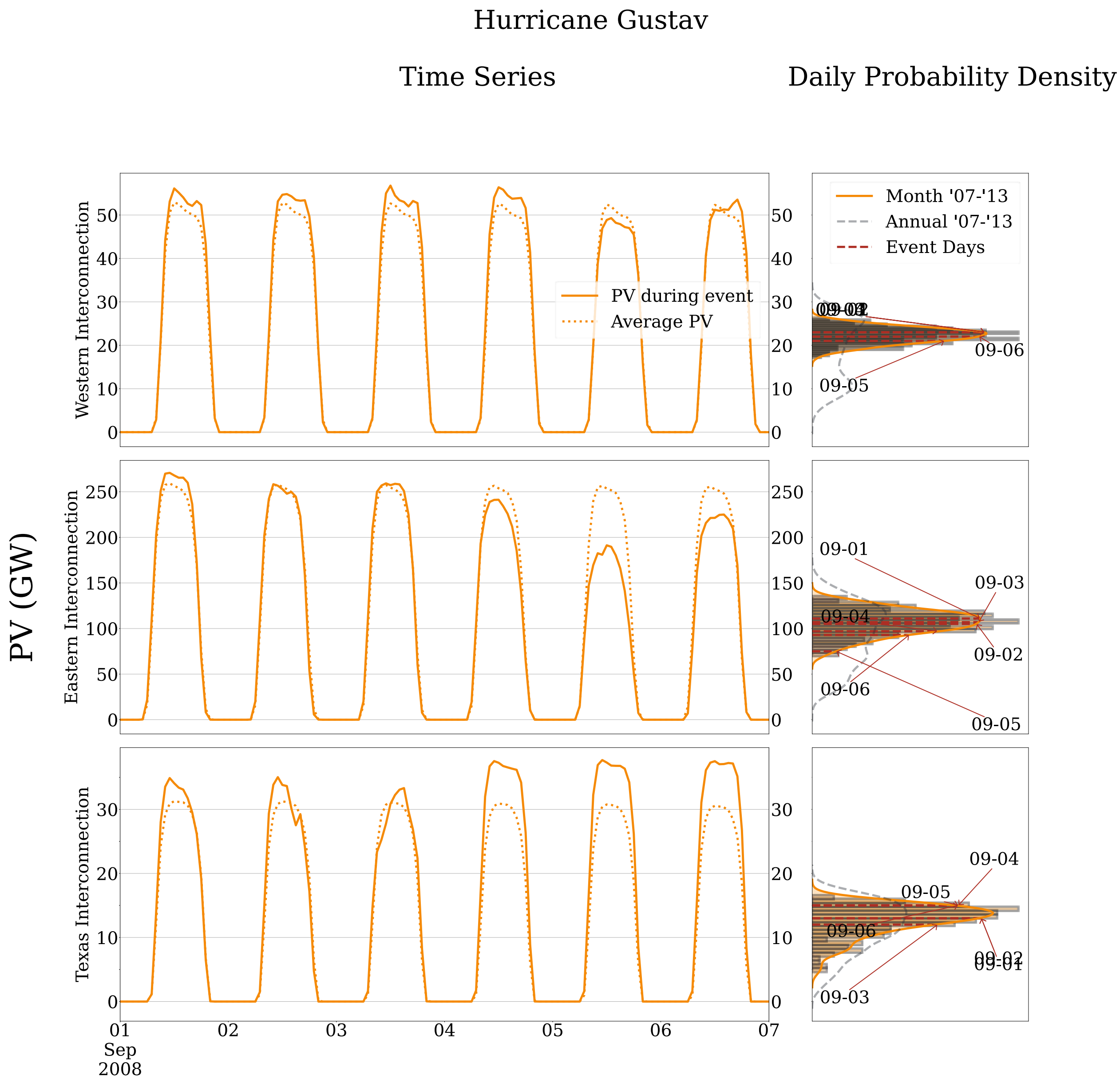

Figure A-55. Event regional modeled 2050 PV generation in context of the distribution of generation for the surrounding month (left) and time series plots of PV generation under the modeled 2050 scenario, relative to normal for the season (right)

Net Load

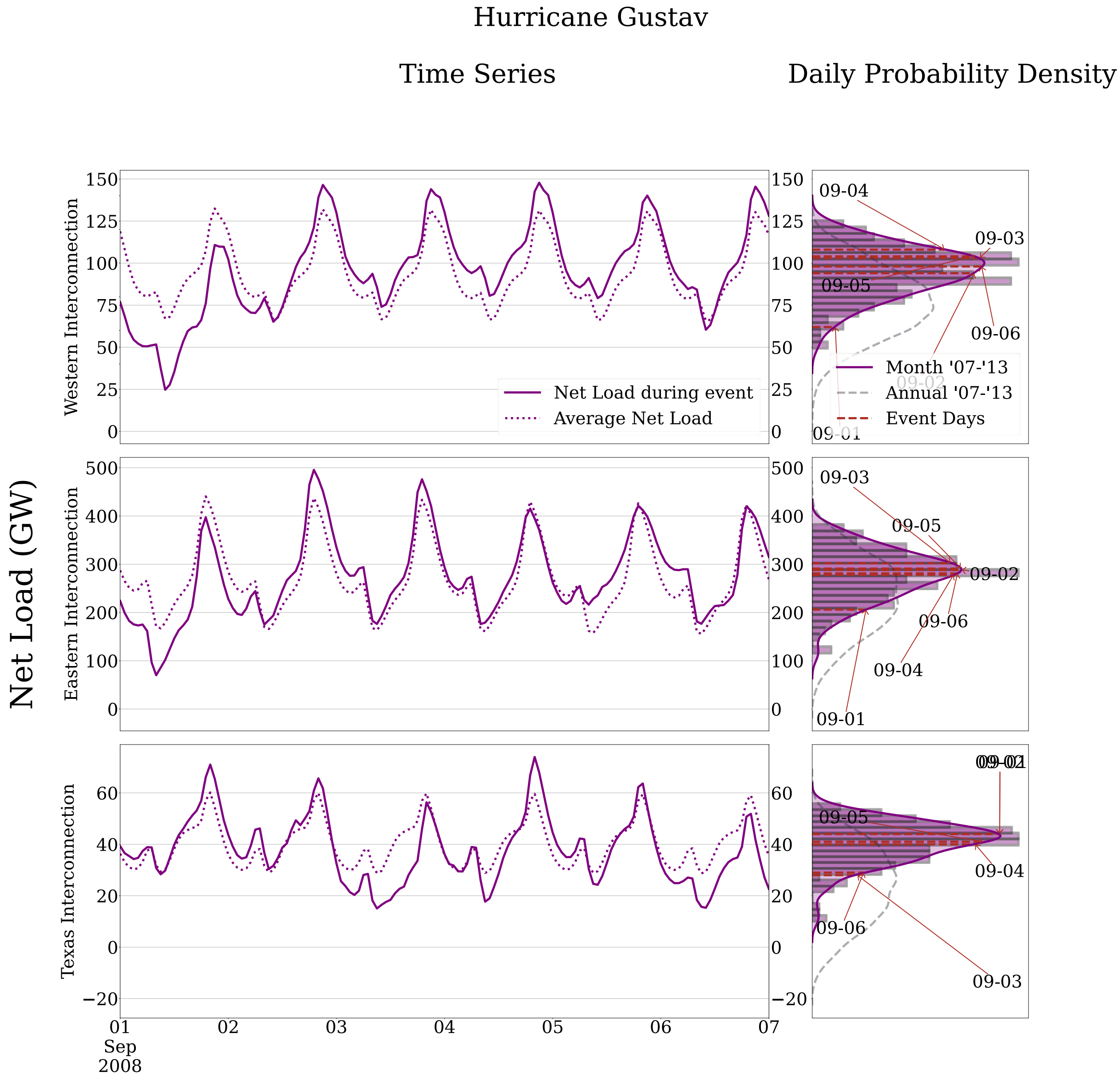

Figure A-56. Event regional modeled net load context of the distribution of generation for the surrounding month (left) and time series plots of modeled net load under the modeled 2050 scenario, relative to normal for the season (right)

Figure A-56 indicates all regions have near-normal or below-normal net loads when Gustav is impacting the country, as interconnection-wide wind and solar resource variability is only slightly correlated with the landfall of Gustav. This result is similar to that of Irene. The combination of a high penetration system and a hurricane landfall does not necessarily lead to profound interconnection-wide excursions of net load, and the variability that results from the diurnal cycles and larger weather patterns in wind and solar output is more impactful.

Hurricanes like Gustav would likely result in more local impacts not explored here. For example, significant amounts of wind capacity are built in coastal Louisiana in the modeled 2050 scenario, and the hurricane likely would cause output there to peak as it approached, cut out as the strongest winds reached the wind plants, and then come back at full capacity soon afterward, assuming most facilities were undamaged. Though solar resource is within normal variation over the whole interconnection, it would also be well below normal locally under the area affected by the clouds of the storm. Such effects could create local balancing and transmission usage issues, and full grid simulations would be needed to analyze them.

Winter Storms: December 4–12, 2013

Event Summary

The first half of December 2013 was an historic period for U.S. weather. Three back-to-back winter storms brought snow, sleet, and freezing rain to large swaths of the country, impacting infrastructure, including the electric system. Frigid air pushed well south behind each storm, driving high loads especially on the TI.[40]

Meteorological Description

Figure A-57 shows the evolution of each storm, as well as the advancement of cold air behind each system. Note, however, that (1) storms crossing the mountainous terrain of the west are disrupted by the terrain and are difficult to track on surface maps and (2) Dion and Electra were relatively weak storms through much of their lives and the daily resolution of the surface maps makes Electra particularly difficult to discern.

Cleon moved inland in British Columbia early on December 1, 2013, and brought rain and snow to the West Coast, and mostly snow to the Great Basin area. Very cold arctic air from Canada emerged behind the storm and moved south into the Great Basin and west, toward the West Coast, where it impacted Seattle, Portland, and even cities as far south as Los Angeles. By midnight on the 3rd, Cleon had drifted to the South Dakota-Minnesota border and its circulation brought cold Canadian air down the Rocky Mountain Front Range. A second low pressure system rapidly developed and merged with Cleon on the 4th, and the storm intensified rapidly and arced northeast, bringing heavy snow to regions near the center of the low. The storm brought rain and then snow or freezing rain all the way south to Texas, Oklahoma, and Arkansas on the 5th and 6th. On the 6th and 7th. The storm also brought wintry weather to the East Coast.

By the time the storm was done, parts of Minnesota had received close to three feet of snow, two feet to Wisconsin, and a foot to the Dakotas, Nebraska, Missouri, Iowa, and Illinois. Areas farther south saw a wintry mix, with Oklahoma City picking up 3” of snow, higher elevations in Arkansas seeing close to 12”, and places in Texas and Mississippi getting significant ice and sleet. Parts of Dallas saw over 1” of sleet and ½” of ice accumulation.

As Cleon’s effects were moving toward the East Coast, Dion was coming onshore late in the day on December 6, along the Oregon-California border. Between December 7 and 9, Cleon moves through the mountains, and Dion moves rapidly on the same basic trajectory as Cleon. With cold air already in place from Cleon, almost all the precipitation from Dion is frozen. Dion results in snow from coast to coast and to low lying areas of the northwest that infrequently see snowfall. Further south, at low elevations, it is freezing rain; to the north or at higher elevations, it is snow. Though snowfall amounts were moderate, they were on top of the snow still on the ground from Cleon.

Electra was the weakest of the three storms, and it mostly impacted a region from Ohio north and east to the East Coast. As the cold front from Dion moved off the East Coast on the 10th, cold air that pulled south behind Dion remained across most of the country. On the 11th, a third low

[40] See https://www.wpc.ncep.noaa.gov/dailywxmap/index_20131203.html

pressure system formed in the lee of the Rockies and intersected with a weak front, with the jet stream steering winds moving this storm on a rapid path eastward.

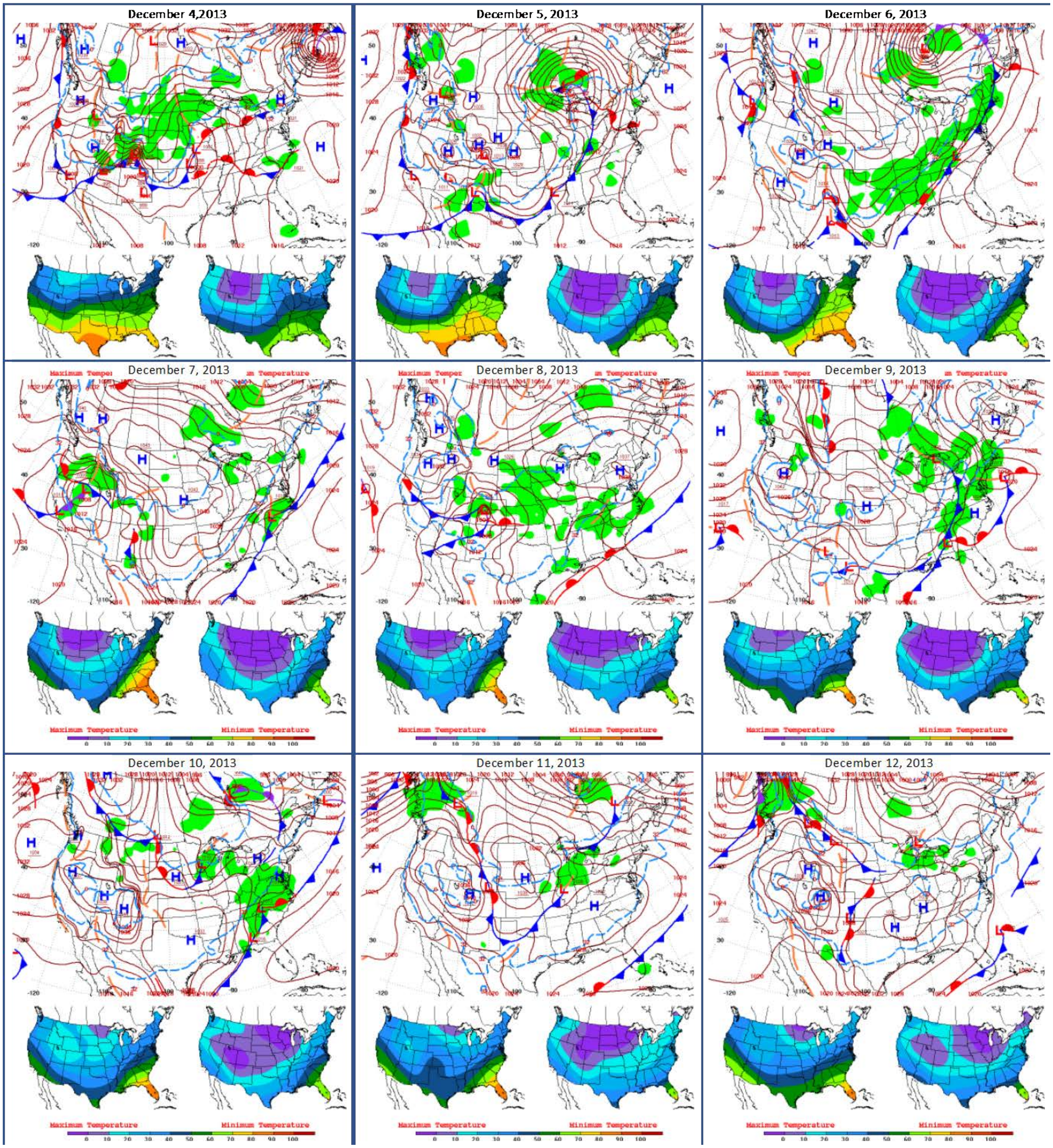

Figure A-57. Surface weather and temperature maps valid at 7 a.m. EST

See the Event Description Structure section for plot details.

Source: "Daily Weather Maps: Wednesday, December 4, 2013," NOAA Weather Prediction Center, https://www.wpc.ncep.noaa.gov/dailywxmap/index_20131204.html

Load Impacts

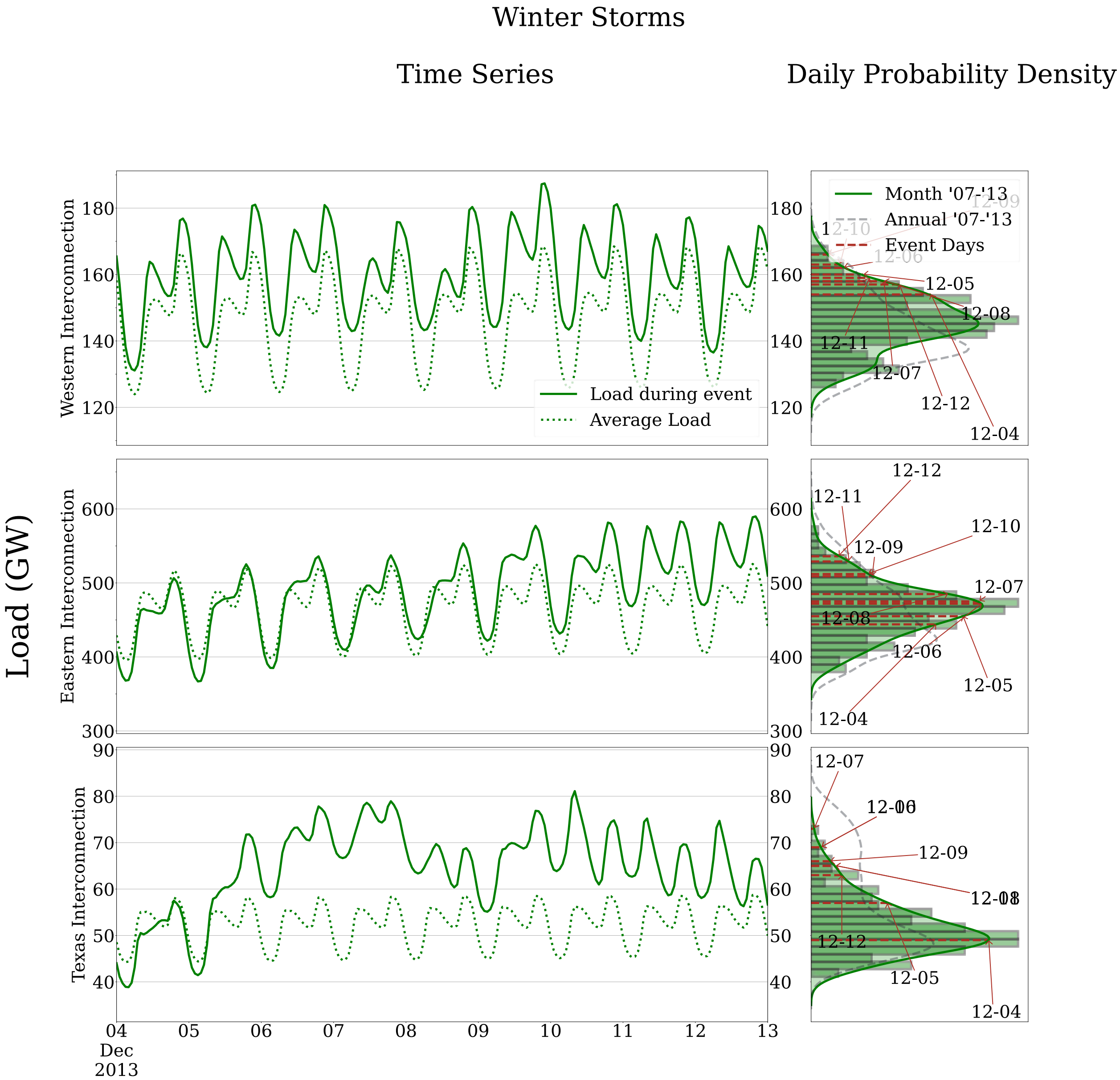

Figure A-58. Time series of regional load during the 4-day event in green, compared to load averaged across the 7-year data set for the month surrounding the event in grey (left) an distribution of 2050 regional loads for the 29 days surrounding the middle of the event in green, and across the 7-year data set in grey, with the event days labeled (right)

Load is above the median, for most days, across all regions as anticipated from widespread cold weather. The two exceptions are December 4th and 5th, where EI loads are slightly below normal and TI loads are near normal due to the cold air is only just beginning to filter into these regions at this point. Load in the west is well above normal for the whole period with the 6th, 9th, and 10th being within the upper tail of the distribution. The 9th was an especially cold day across the whole of the west as can be seen in the min/max plots (Figure A-58), and in heating degree days from the LCD (not shown). The morning load rise is particularly increased by the cold, and the deviation on the 9th is close to 27 GW on top of the typical 150-GW load.

The highest EI loads occur toward the end of the period as the cold air migrates eastward into the major East Coast load centers. Even though it is cold on the 9th across a big area of the EI, from a population-weighted perspective, the second half of this event is the most important on the EI. Though not in the extreme tail, the 11th and 12th are noteworthy, especially in context of high loads across the rest of the country.

The impact on Texas is the most noticable. This is likely because of the prevalence of electric heating, combined with the longevity of the event relative to a typical cold snap that makes it to Texas. On the TI, loads are in the extreme tails of the typical seasonal distribution on at least 3 days, with December 7, 2013 being the highest load observed across the entire data set for the 29-day window centered on December 8. Load on the 7th is close to 50% above normal (Figure A-58) and following the reinforcing shot of cold air drawn south behind Dion on the 10th, the load briefly peaks at over 80 GW at a time when it is more typically about 54 GW.

Wind Generation

Wind resource across each interconnection shows increased variability throughout the event, with days exhibiting generation within both the high and low ends of the distribution across all three interconnections. This is expected given the active weather with storms moving across the country and high pressure systems building in behind them.

In general, the wind generation on the WI and the EI is close to the median expected at this time of year. The median is also above the annual average, as this is normally a windy time of year. However, December 5th and 6th are both low wind generation days on the WI, and December 8th is well below normal and close to the tail on the EI. Also notable is the well-above-normal generation on the EI on December 5th. On the TI, 3 days are significantly below normal, and the 8th and 9th are in the extreme low generation tail.

Figure A-59 shows that the 5th and 6th saw extremely low wind resource throughout the WI. This is when cold air had moved into the west. The combination of cold surface air, radiational cooling, and high pressure aloft all conspire to produce weak pressure gradients and a strong surface inversion. Both features tend to lead to air stagnation at the surface in winter. Where there is wind, it tends to be offshore, through gaps and passes, and because this is not a prevailing direction, wind facilities usually are not built in these locations. This is confirmed in Figure A-60, where wind generation can be seen to tail off from over 70 GW on the 4th to less than 20 GW late on the 5th and then remains below 30 GW until late on the 6th before ramping back to normal values around 50 GW. As mentioned in the load impacts subsection, the 5th and 6th saw well-above-normal loads, and the impact of this coincident high load and low wind will be discussed in the system impacts section.

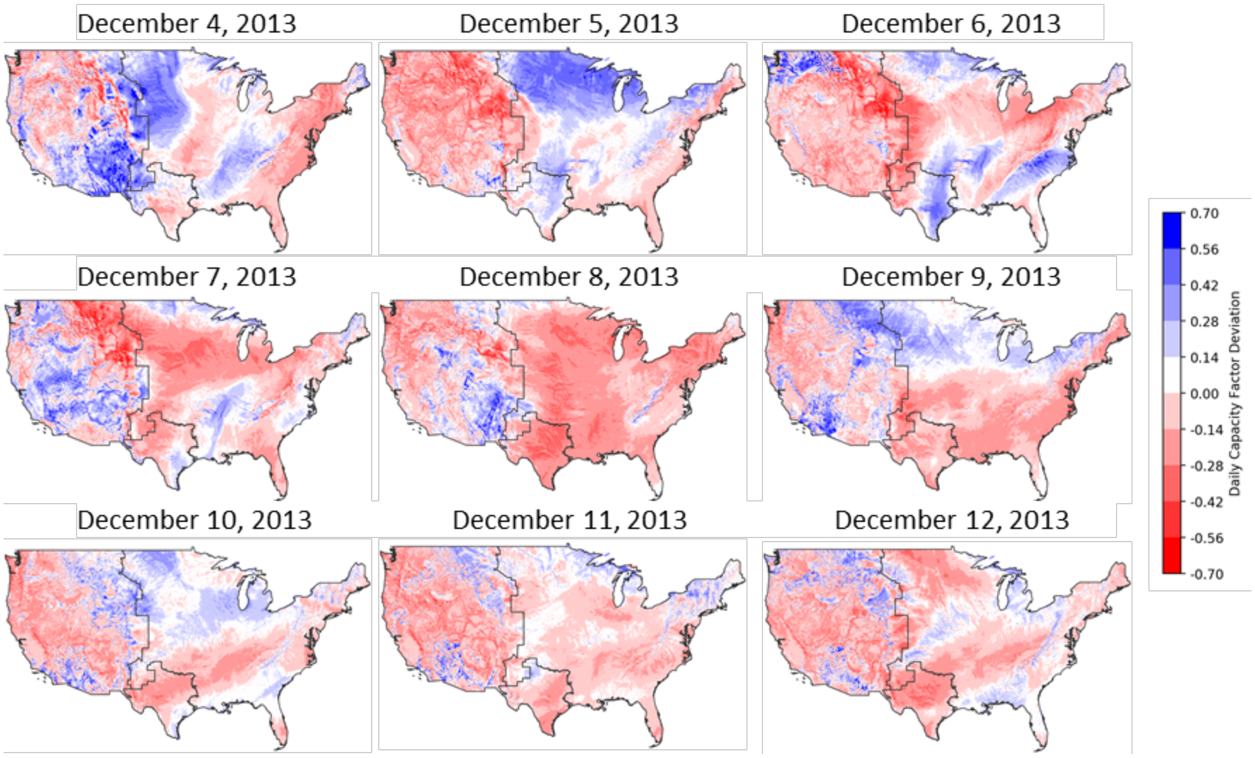

Figure A-59. National daily average wind resource deviation during the December 2013 winter storms event

Almost the entire EI has below-normal wind resource on the 8th as seen in Figure A-60. This is the period following Cleon's cold front clearing the East Coast and high pressure building in before Dion passes. The low gradients, combined with a surface inversion that is due to subsidence and strong radiational cooling over snow cover and under clearing skies, yields a period where wind is well below normal. This is concurrent with above-normal load on the EI.

The same influences are responsible for the low wind resource on the TI on the 8th, but they remain through the 9th. Things moderate on the 10th, but somewhat below-normal output continues on the TI through the end of the period. This is again coincident with above-normal load.

Both the TI and the EI see better than normal wind resource during the period where the cold air is arriving, and loads are rising, indicating some similar synergy between cold waves and wind generation that was seen in the February 2011 cold wave event. However, in the case of this event, the stagnant pattern that occurs in between storms yields a period where higher loads and lower wind resource coincide in Texas.

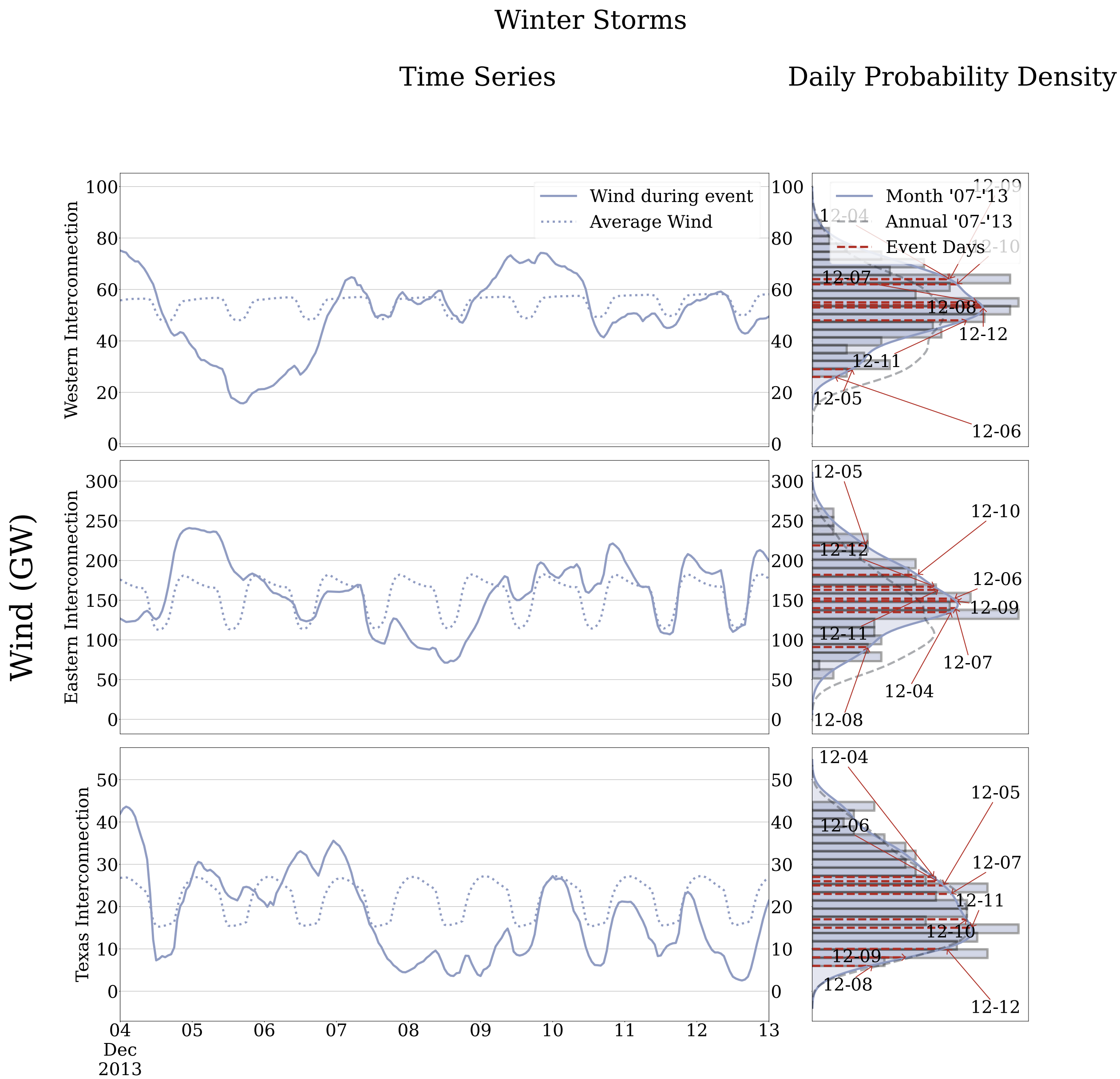

Figure A-60. Event regional wind generation (based on 2050) in context of the distribution of generation for the surrounding month (left) and time series plots of wind generation under the 2050 scenario, relative to normal for the season (right)

Solar Generation

During much of this event, solar does not contribute much generation to the TI or the EI, and it should be noted that the numbers presented here represent upper limits. Many panels may be underproducing due to snow and ice coverage, which could be long-lasting due to the extended cold periods.

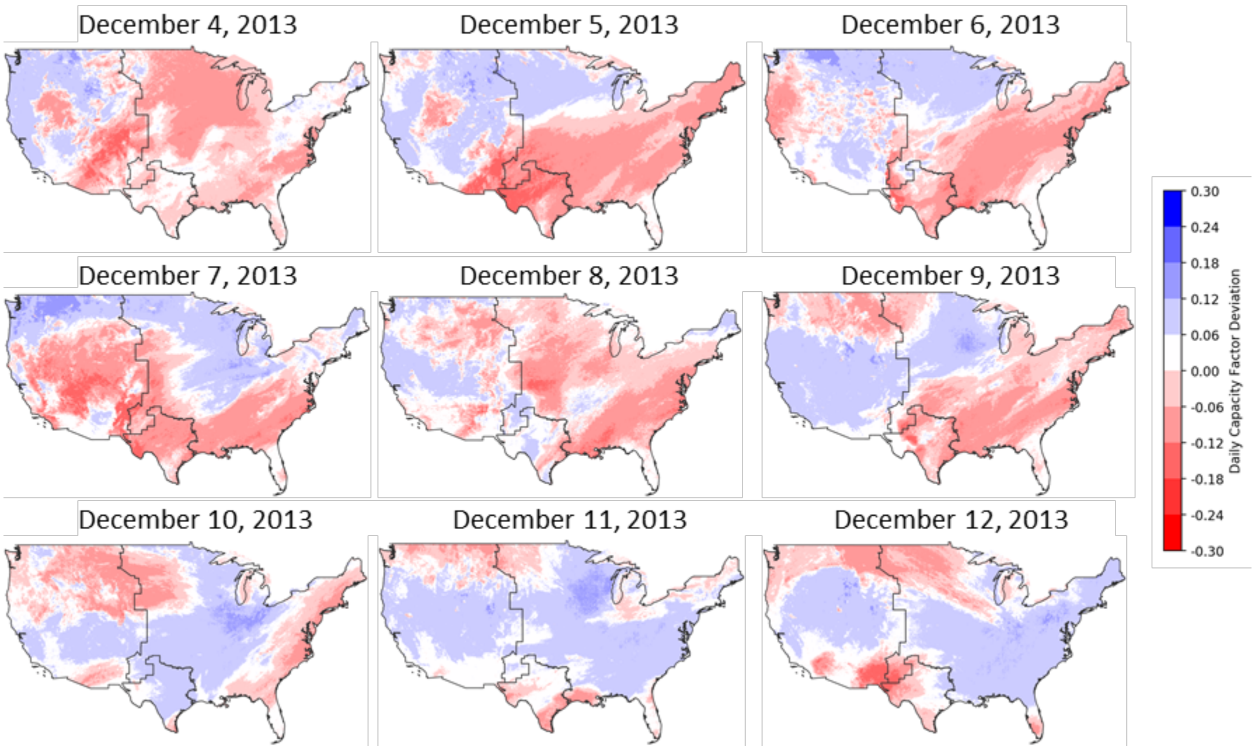

Figure A-61. National daily average solar resource deviation during the December winter storms event

As expected for December, close to the winter solstice, solar is well below the annual average there should lower impact from deviations due to the storms. In the WI, solar output is generally above normal. On the EI, clouds associated with Cleon and Dion reduce the available solar generation in the first half of the event. High pressure over most of the EI brings clear conditions from the 10th through the 12th, except for the Northeastern states, which Electra is impacting. As a result, EI solar is well above normal during the latter days of this event. On the TI, the deficit during much of the period is more pronounced especially on the 6th through the 8th, and on the 10th.

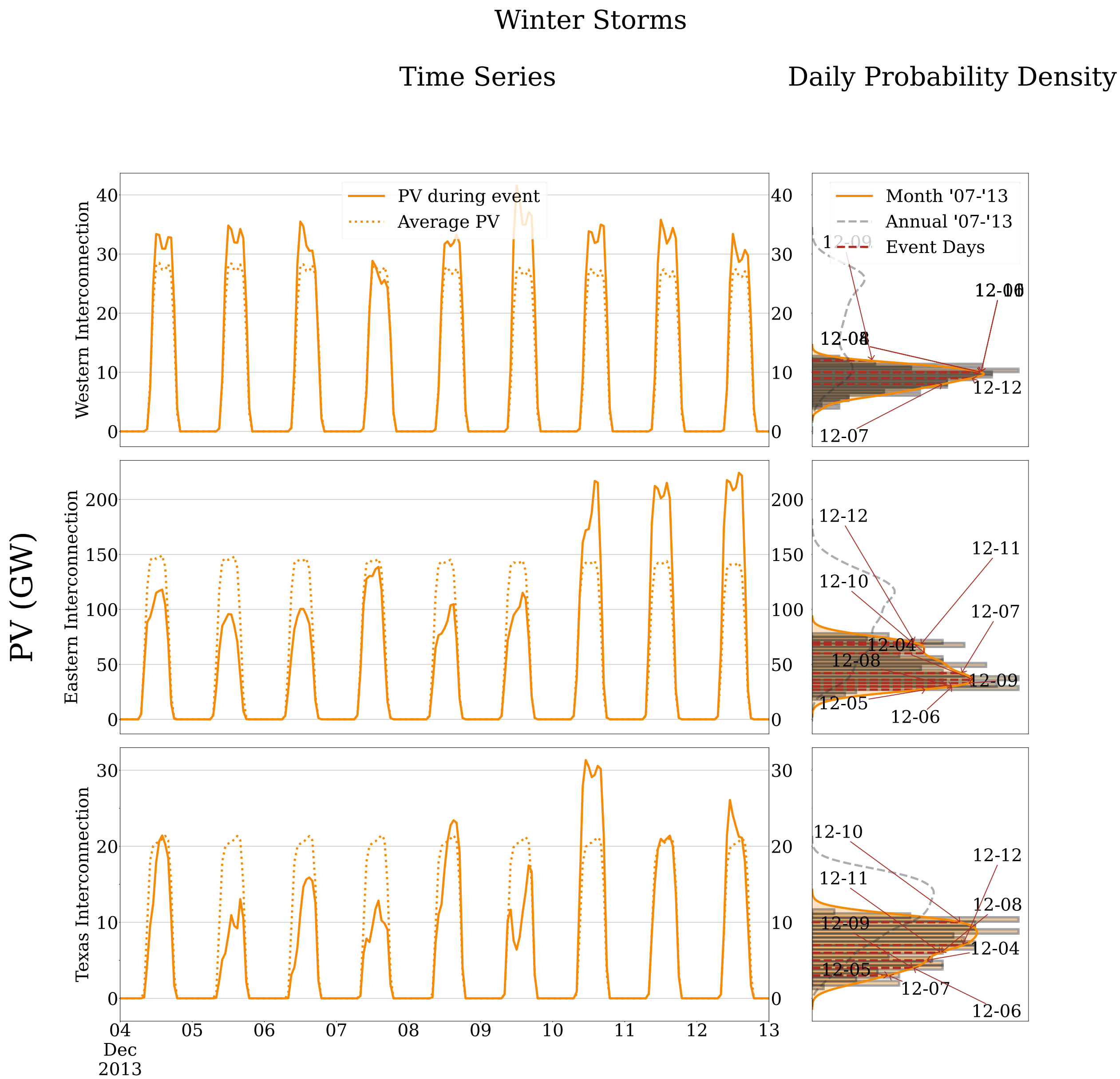

Figure A-62. Event regional modeled 2050 PV generation in context of the distribution of generation for the surrounding month (left) and time series plots of PV generation under the modeled 2050 scenario, relative to normal for the season (right)

Net Load

The combination of high loads and low wind resource on the WI push the 5th and 6th to the extreme tails of the net load distribution. The effect can be starkly seen in the time series plots of Figure A-63, where the minimum daily net load exceeds the typical daily maximum. The 5th is also at the upper end of the annual distribution and not just the seasonal distribution. In the load distribution, the 5th is high but not at the extreme upper bound.

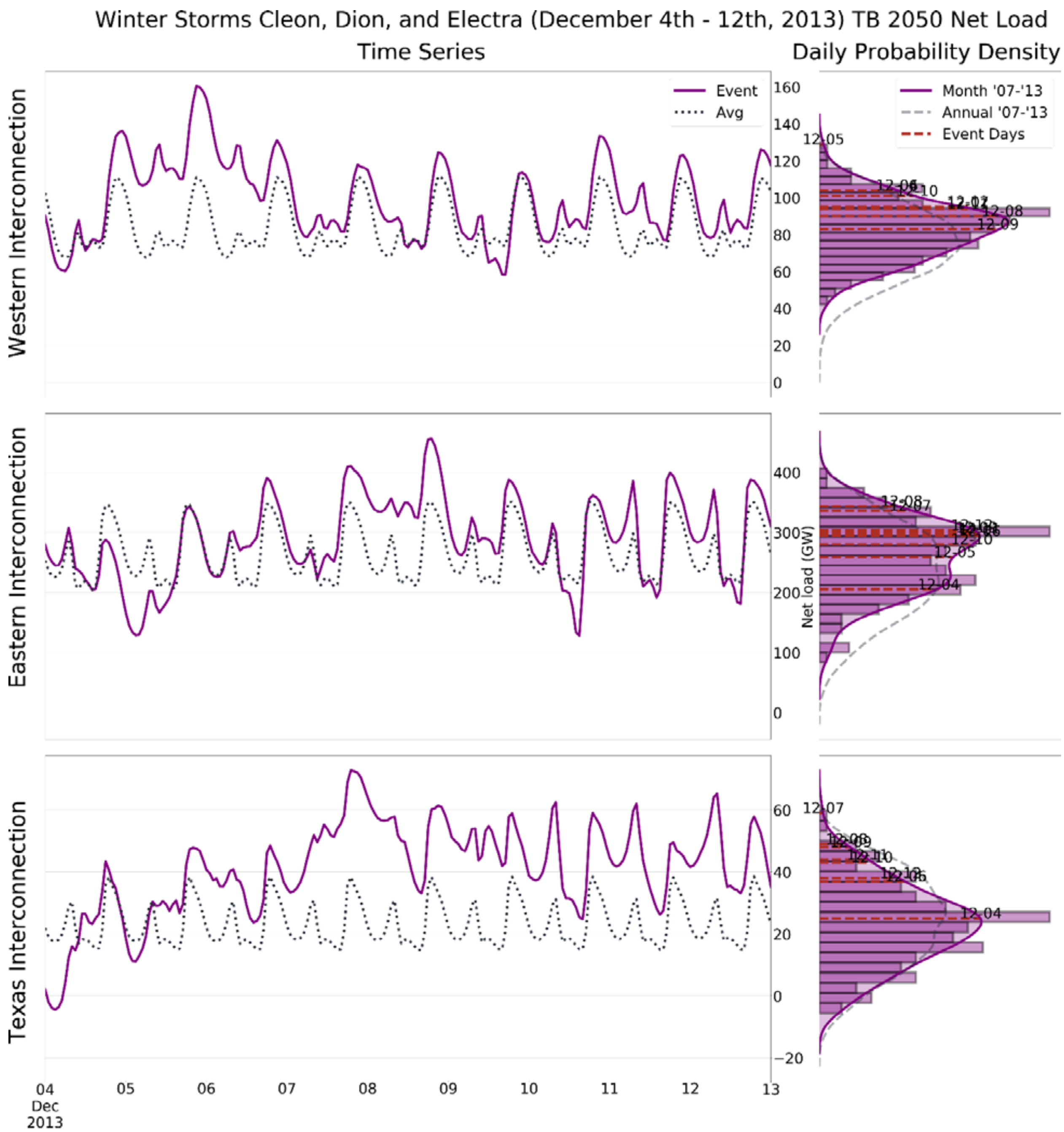

Figure A-63. Event regional modeled net load context of the distribution of generation for the surrounding month (left) and time series plots of modeled net load under the modeled 2050 scenario, relative to normal for the season (right)

High load and low resource are also responsible for pushing the TI into the extreme upper end of the net load distribution on the 7th. Weak pressure gradients and stable air close to the surface prevent wind aloft from mixing down, resulting in unusually weak wind resources starting on the 7th. Cloudy conditions on the 9th further exacerbate the situation. We see a period of 4 days from the middle of the 5th through midday on the 10th where the minimum net load is higher than the typical peak, and on the 8th and 9th, there are periods where peak net load is more than double what is typical for the time of year in both scenarios. While Texas loads peak in the summer, the net load values observed in this case are close to the annual peak. Further, the main reason for the brief dip in net load observed on the 8th is slightly above-normal solar generation. It is unclear how much of this solar generation may actually be diminished due to snow and ice cover on panels, as this is the day after Cleon dropped large amounts of frozen precipitation in Texas. Similarly, the 8th and 9th may have much lower wind generation than shown here, again due to icing.

The 7th and 8th sees maximum weather impacts across all the interconnections. On these days, loads are high due to the cold, and wind resource is below normal in the west at the beginning of the 2-day stretch and drops through the day on the 7th on the EI and the TI. Meanwhile, solar is below normal in Texas and somewhat below on the EI. At the same time, Cleon has produced a major snowfall and icing event, and pulled Arctic air into the Upper Midwest that is close to cut-out temperatures, and Dion has dropped snow throughout the Intermountain West.

Across all three interconnections, the net load is at or above the median with just a few exceptions at the beginning of the period before the coldest air arrives in most of the country. The statistical distribution in Figure A-63 shows a similar effect to other events that day, with very high loads in the distribution being shifted away from the upper extreme. Conversely, a few days that are near the median for load days are shifted up and become higher in the net load distribution. Most notably, these are December 5th and 6th on the WI, December 8th on the EI, and December 8th and 9th on the TI.

System Modeling

For this event, we completed PCM simulations for the 2050 infrastructure year. In addition to the base 2050 infrastructure, we considered five sensitivities on the 2050 base case. One sensitivity focuses on derated wind output that is due to blade icing or temperatures below 35 degrees Celsius. The other four scenarios adjust the availability or flexibility of hydropower plants. We included different hydrological years to change the energy available to dispatchable hydropower units that reflect a dry and a wet year. For flexibility changes, we included a scenario where dispatchable hydropower units are more or less flexible than the base case.

Western Interconnection Operations

Figure A-64 shows the dispatch results of the WI regions during the Winter Storms event. The WI is most impacted by the initial storm Cleon. Load was elevated due to cold temperatures throughout the interconnection and as the storm moves to the EI, the wind generation plummets throughout the WI. Stagnant high-pressure system settled over the Western United States on the 5th and 6th, creating the low wind resource. However, skies are clear during these low wind days throughout the WI following the exit of winter storm Cleon, allowing PV to contribute significant energy and capacity in the middle of the day.

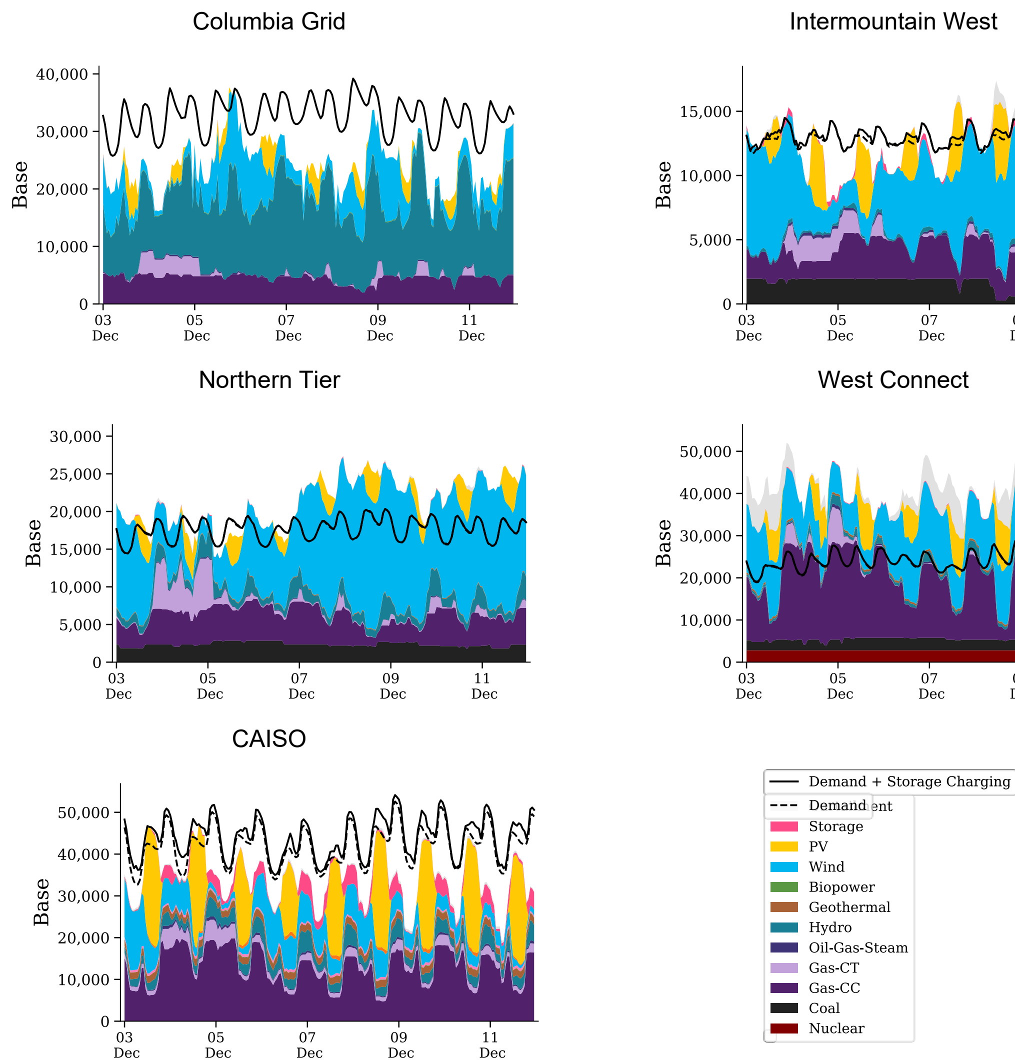

Figure A-64. Generation dispatch for the various regions of the WI

The results shown here are from the base 2050 infrastructure scenario during the winter storm events in December 2013.

However, the stagnant air is significant, and lacking substantial storage to shift the high PV availability to the evening and overnight hours requires other resources to maintain adequacy during this period. In response to the low wind output, nearly all available thermal units (i.e., thermal units not on an outage) are called to come online. Figure A-65 shows the offline, but available, thermal capacity throughout the WI during this event. In the evening on the December 5, all but 4 GW of thermal units remain available but offline. Due to the cold temperatures brought by Cleon, thermal outages are higher than normal, further tightening the available resources to maintain adequacy in the WI. For example, on December 5, the Intermountain West region, which is primarily Colorado and Wyoming, lost 2,100 MW of its 3,500 MW of gas-CC capacity for much of the day due to forced outages. The remaining 1,400 MW of gas-CC were operating at full capacity. Much of the forced out capacity became available again the next day and was brought online immediately.

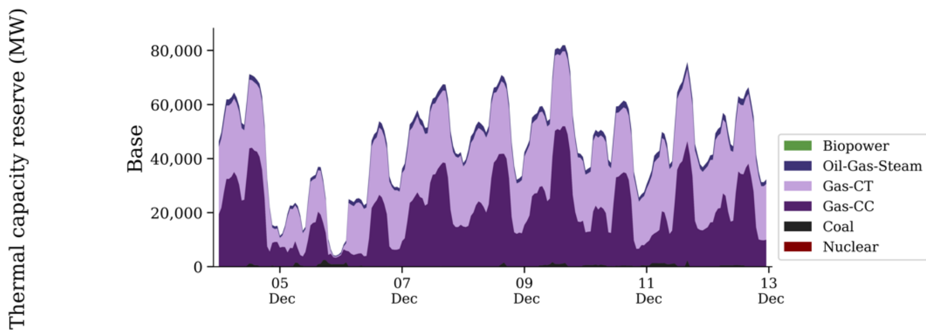

Figure A-65. Offline available (not on a forced or planned outage) thermal capacity in the WI during the Winter Storms event

Hydropower from the Pacific Northwest also plays a large role throughout the event. December typically has low energy availability, but dispatchable hydropower has flexibility to shift that energy to periods of need. This flexibility will be explored in detail in the hydropower sensitivity analysis.

Sensitivity Analysis

As described earlier, five sensitivities were run on the base 2050 infrastructure. Figure A-66 shows the impact of each sensitivity on total generation change by type from the base case for the three interconnections combined. Including wind turbine blade icing and cold temperature cutoff shifts generation between generation types the most. The decreased wind output is met by an equal mix of gas-CCs and gas-CT generation. The hydropower availability sensitivities either increase or decrease total hydropower generation. The increase or decrease is offset almost entirely by gas-CC generation, and the decreased hydropower operational flexibility sensitivity does lead to less hydropower generation being allocated to the event. This is also met with an increase in a mix of gas-CCs and gas-CTs.

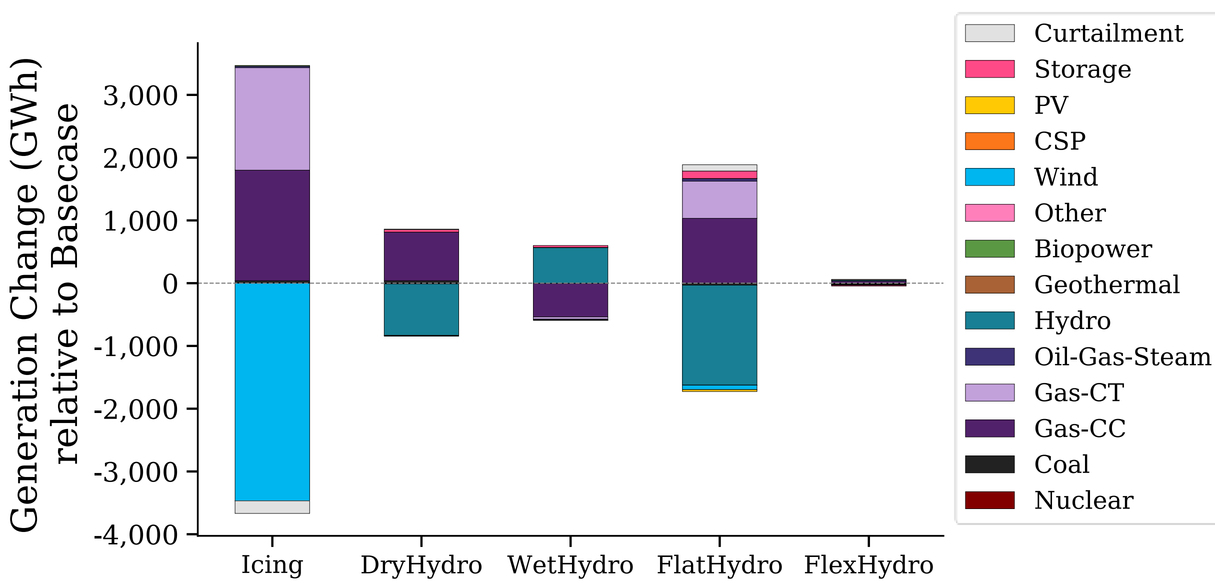

Figure A-66. Change in generation between sensitivities and the base case during the Winter Storms event

The Winter Storms event brought freezing precipitation to many areas of the CONUS in early December 2013. Due to the diversity in the wind resource, the total wind fleet never saw more than a 10% derate in generation that was due to blade icing and cold temperatures. However, areas such as SPP experienced much larger impacts throughout the event. Cleon and Dion brought cold temperatures and freezing precipitation to SPP's footprint between December 5th and 10th. Figure A-67 shows the associated wind generation reduction during those periods. Late in the day on December 8 and throughout much of the day on December 9, as Dion made its way through the middle of the country, SPP wind is reduced 33%–50%. The gap is filled by a mix of local gas-CTs and gas-CCs, and by increased net imports from neighbors.

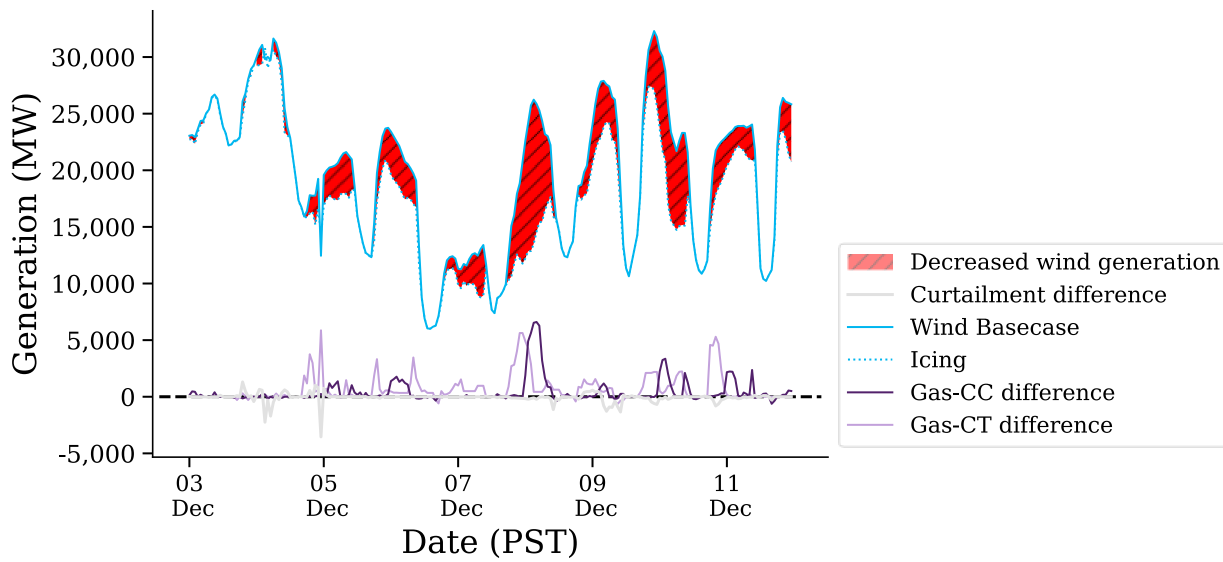

Figure A-67. Decreased wind generation due to icing and cold temperature cut-out in SPP during the Winter Storms event

Of the hydropower sensitivities, less-flexible operation sensitivity leads to the largest change in operations. Figure A-68 shows the importance of the base case hydropower flexibility during the event in the WI. Throughout the event, hydropower provides significant peaking capacity, given the elevated load throughout the event. Even though December is low hydropower generation month due to limited water availability, flexible operations still benefit the system during extreme weather events, such as these winter storms. The most constrained operations also make the system more costly to operate. During the Winter Storms event, the WI production costs increase 8.2% with less-flexible hydropower operations.

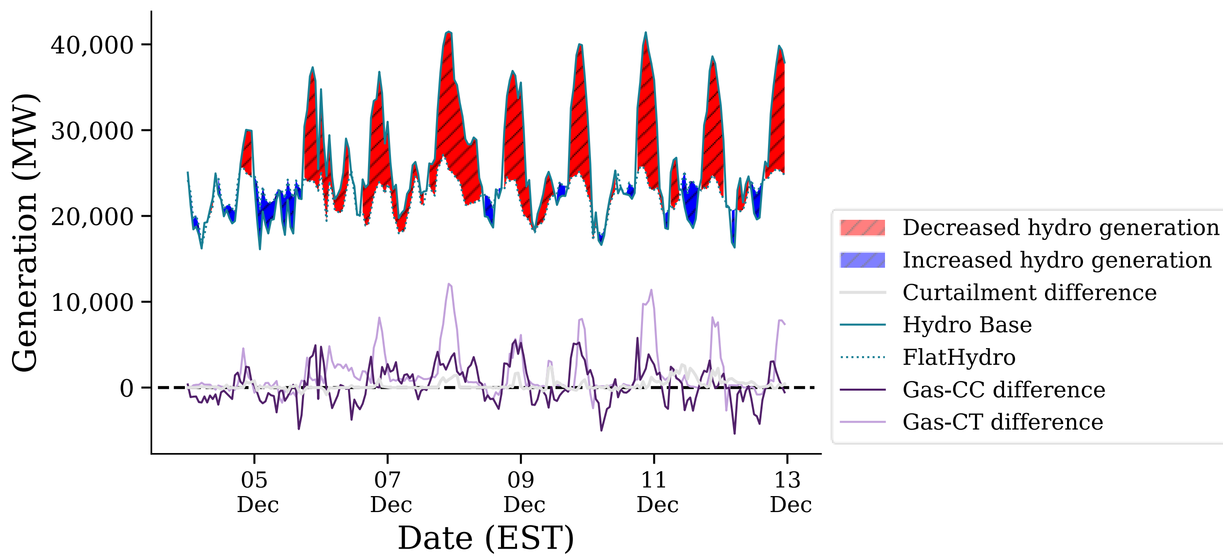

Figure A-68. Change in hydropower operations due to less flexible hydropower operation assumptions in the WI during the Winter Storms event.

Impacts Summary

The Winter Storms event is a good example of a highly impactful weather event on today's system that has unequal impacts throughout the event, both temporally and geographically when studied on a high VRE penetration system. Most days have near average wind and PV generation available, meaning the system can maintain system adequacy without much stress. However, some days end up in either end of the tails of the wind and solar potential distribution leading to a diversity of operational outcomes from day-to-day.

This event is unique because it not only brought cold to much of the country, but also because large swaths of the country experienced snow or other forms of freezing precipitation. These conditions increase the risks of turbine blade icing and natural gas fueled generator outages. We demonstrated with sensitivity analysis that blade icing and cold temperature cut-outs of wind generation are costly, especially for smaller areas. However, even with this continental-scale storm, icing and cold had a limited impact on the overall wind resource.

Especially in the WI, the cold's impact to the natural gas fleet was a cause for concern over a 2-day stretch, with very low wind generation availability throughout the interconnection. The low wind meant there was a greater reliance on other generating sources. Forced outages of gas-CCs and gas-CTs due to the cold were elevated, meaning very little dispatchable capacity was kept offline. Hydropower and solar PV both played outsized roles to support the system during this time. In the days that followed the 2-day stretch of low wind, load continued to be well above normal, but wind recovered while PV and hydropower kept up a similar level of energy and capacity contributions.

This event was made neither "worse" nor "better" when simulated on a higher VRE penetration system. However, new risks and opportunities present themselves with the future grid infrastructure. Future research is needed to better understand options for mitigating the risk even further.

Winter Net Load 1: February 20–23, 2008

Event Summary

Stable weather over the west and generally low pressure gradients developing behind a weak cold wave in the east led to somewhat below average temperatures, light winds, and widespread clouds and fog. And these conditions led to an event where the combination of below average resource and above average load combined to result in high residual load once renewable generation had been subtracted from demand. The 21st and 22nd ranked in the 91st and 88th percentile of net loads respectively.[41]

Meteorological Description

February 20–23, 2008 was marked by rather unremarkable winter weather. A storm system moved through the Great Lakes area on the 18th and then continued north into the Canadian Maritime provinces. Cold air was pulled out of Canada into the Midwest behind the storm. The upper-level jet stream wave pattern was highly amplified with a blocking ridge over the western half of the country, preventing Pacific storm systems from moving into the east half of the country. This pattern promoted high surface pressure and stable conditions across the entire eastern part of the continent, resulting in lower wind resources.

Temperatures during the period were somewhat below normal (roughly 70th to 85th percentile of days heating degree days) across most of the west where the air was stagnant and nights were still long enough to form a strong temperature inversion. To the east, almost everywhere north of the cold front saw below-normal temperatures. In the Upper Midwest, temperatures were cold enough to place major load centers like Minneapolis, Chicago, and Pittsburg into the highest 2%–5% of cooling degree days on the 19th through the 21st, with moderation into the highest 15-20% on the 22nd and 23rd. Major East Coast load centers also saw temperatures that resulted in cooling degree days in the highest 10% throughout the period. Further south, temperatures were cold but unremarkable.

Because the atmospheric dynamics were so weak, the pressure gradients were weak on the 20th and 21st and very weak on the 22nd and 23rd. Higher surface pressure brought weak winds diverging outward from it as the cold air filtered in and slowly moved east and moderated.

[41] See https://www.wpc.ncep.noaa.gov/dailywxmap/index_20080220.html

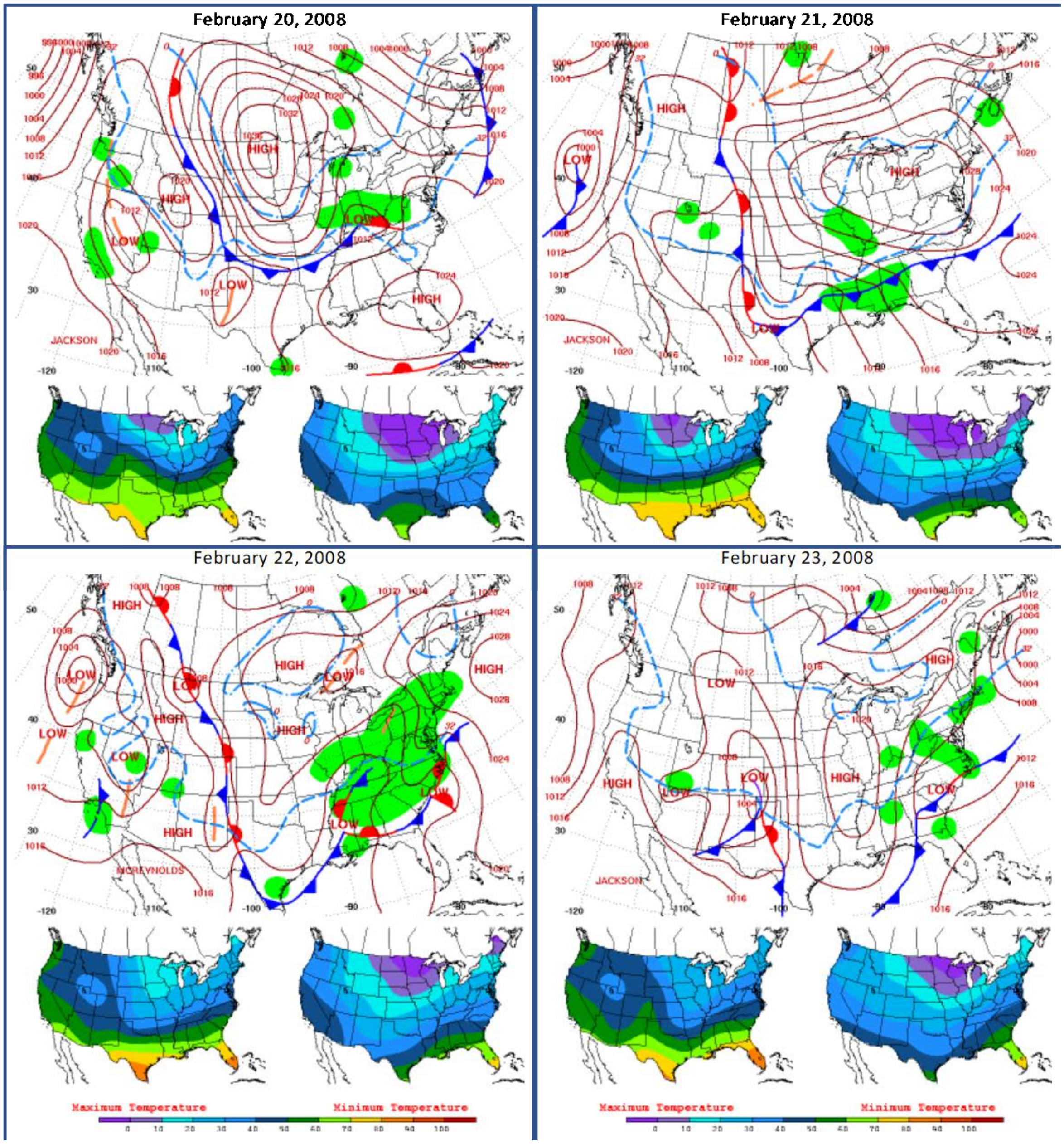

Figure A-69. Surface weather and temperature maps valid at 7 a.m. EST

See the Event Description Structure section for plot details.

Source: "Daily Weather Maps: Wednesday, February 20, 2008," NOAA Weather Prediction Center, https://www.wpc.ncep.noaa.gov/dailywxmap/index_20080220.html

Load Impacts

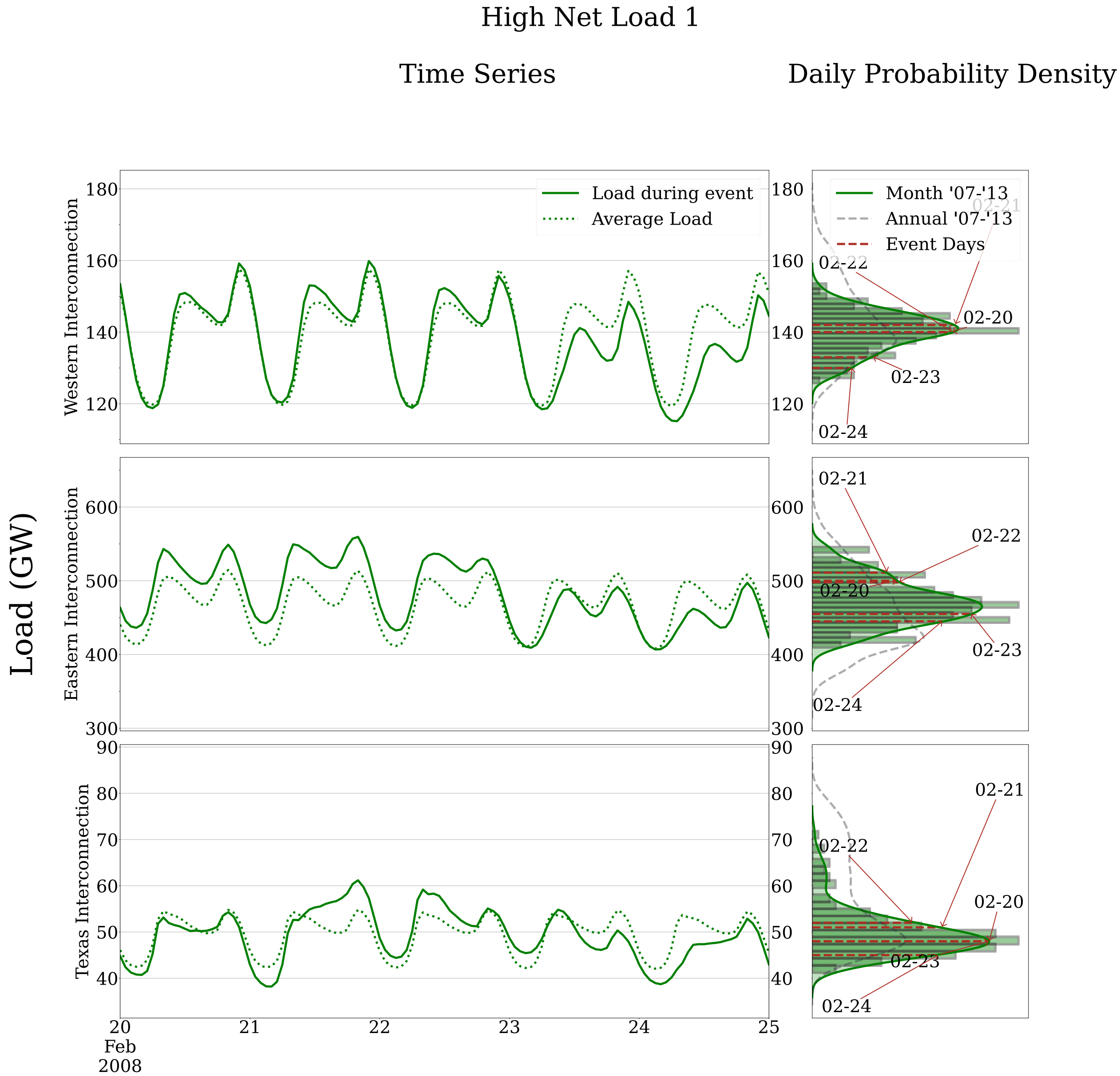

Figure A-70. Time series of regional load during the 4-day event in green, compared to load averaged across the 7-year data set for the month surrounding the event in grey (left) and distribution of 2050 regional loads for the 29 days surrounding the middle of the event in green, and across the 7-year data set in grey, with the event days labeled (right)

Loads on all the interconnections were somewhat above normal most of the time through the period. Note that the 23rd is a Saturday so lower load is expected. WI loads are near normal to slightly above normal, which is expected given the cooler than normal temperatures. On the EI, the temperature excursion is larger and this is reflected in the position of the days well above of the median, but these days are not in the tail of the distribution. The cold air reaches the Texas interconnection on the 21st and is reflected in a rapid rise in daytime load, presumably associated with heating. The front pushes all the way to Southern Texas on the 22nd, but the cold air begins moderating quickly and by the 23rd loads start to decline.

Wind Generation

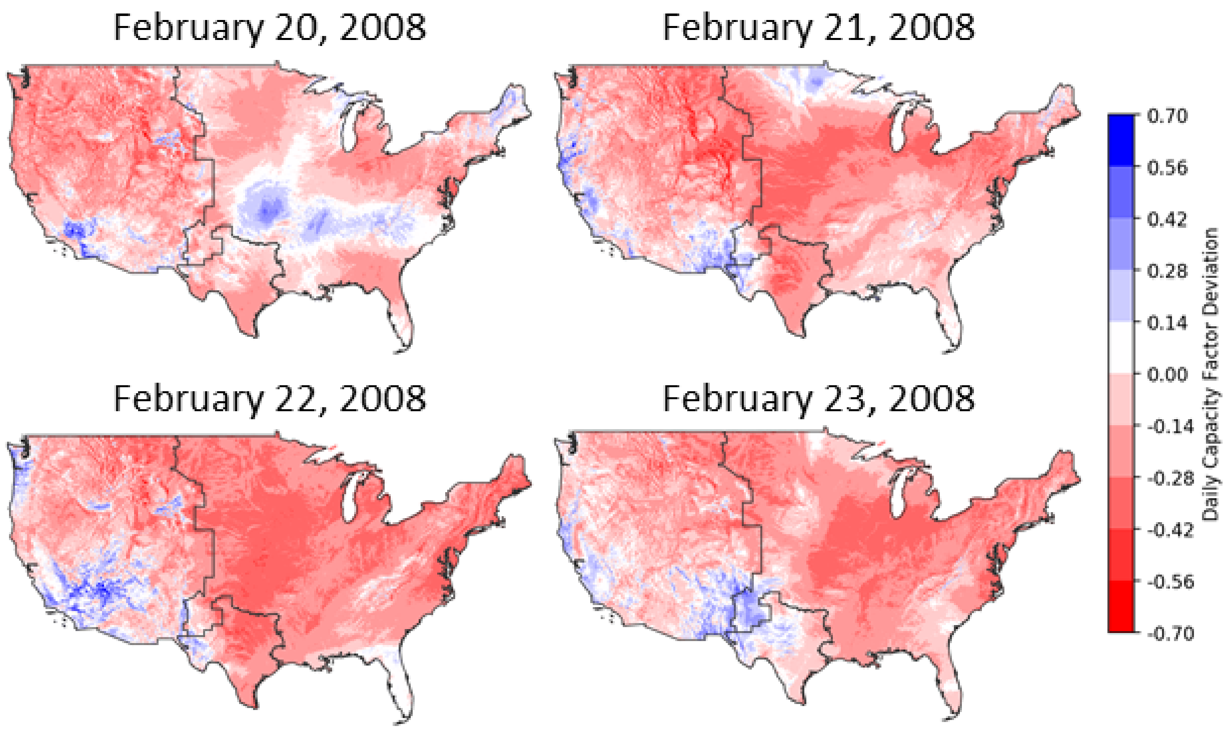

Figure A-71. National daily average wind resource deviation during the February 2008 high net load event

Wind resource is below normal to well below normal across most of the country for the entire period (Figure A-71). The 22nd and 23rd are particularly wind-poor across as reflected in Figure A-72, which shows that daily wind generation is lower than the median for the time of year on all three interconnections and is at the very tail of the distribution on the 22nd and 23rd on the EI. The 21st and 22nd are very low wind days on the TI but not quite so close to the far tail as on the EI.

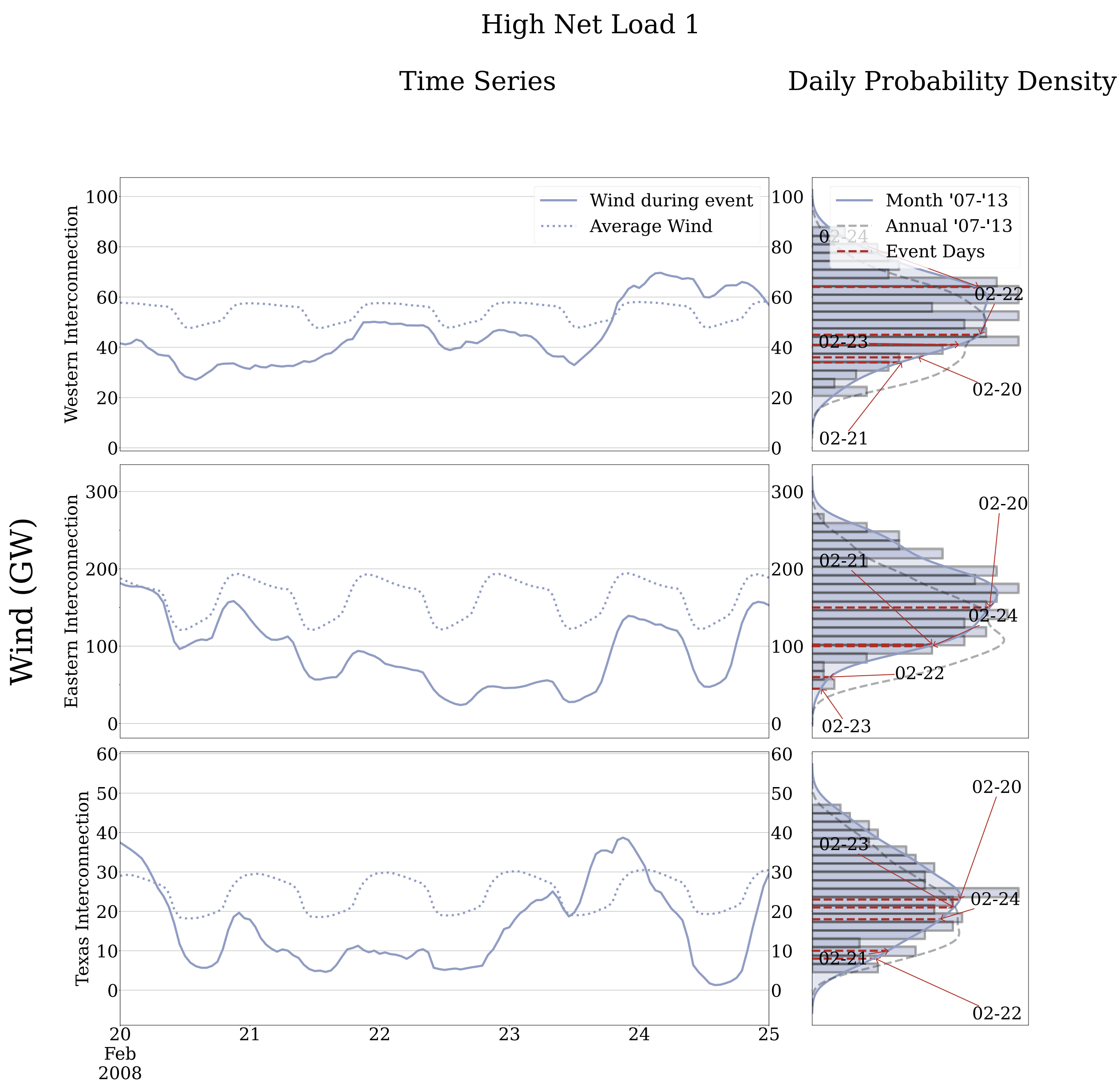

Figure A-72. Event regional wind generation (based on 2050) in context of the distribution of generation for the surrounding month (left) and time series plots of wind generation under the 2050 scenario, relative to normal for the season (right)

The time series plots in Figure A-72 show just how significant the deviation in wind output is. In Texas, generation is 15–20 GW below the normal diurnal range, which is about 20–30 GW. On the 20th and 21st, the west deficit is on the order of 20 GW, where the typical range is 48–58 GW. The deficit on the EI is the main driver. It normally oscillates at from about 125 GW to 185 GW at this time of year, but on the 22nd, the output drops to just 25 GW and even during the evening maximum only reaches 50 GW.

Solar Generation

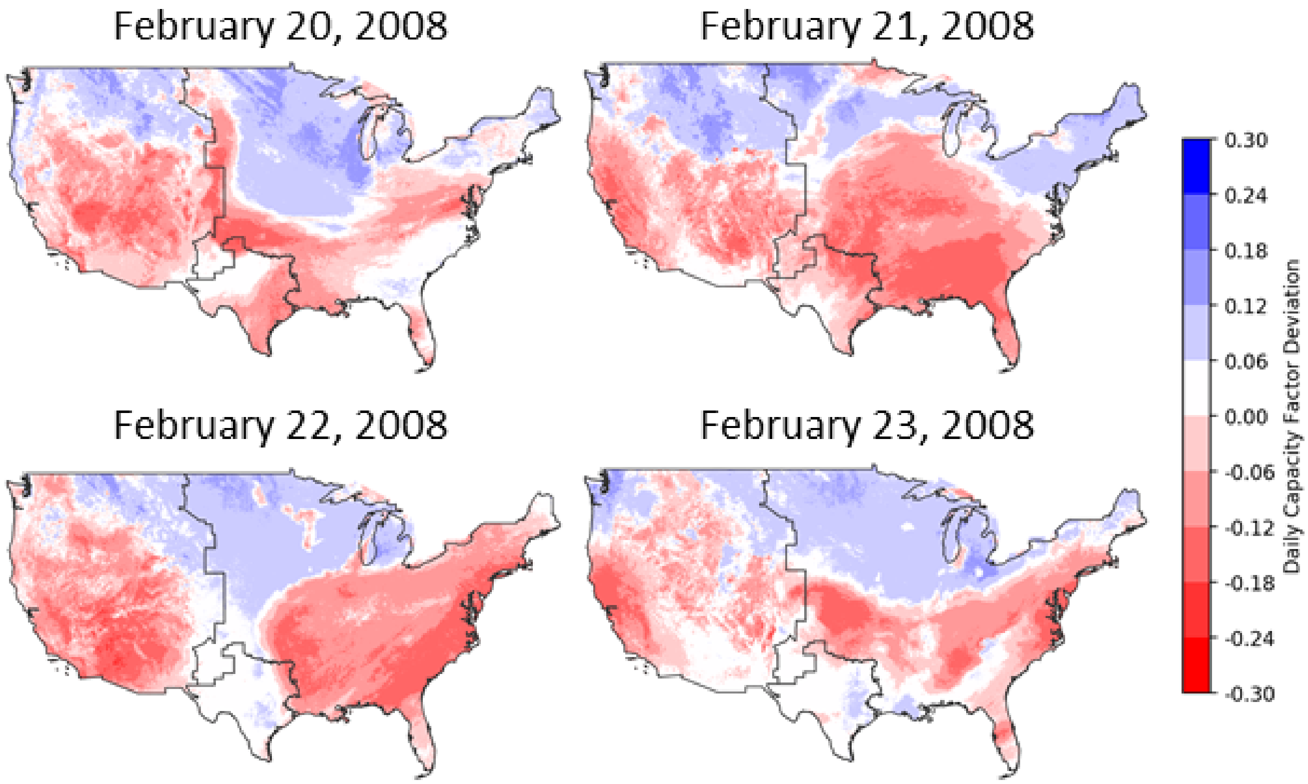

Figure A-73. National daily average solar resource deviation during the February 2008 high net load event

During this event, there is a general north-south split between better and worse than normal resource as seen in Figure A-73. The assumed placement of future solar generators at more locations in the south than the north results in below-normal generation (Figure A-74), although not as far into the tail of the distribution as wind generation.

The region of well above-normal resource in the northern part of the country is associated with the cold dry air arriving from Canada and the strong high pressure causing subsidence and clearing of clouds. Further south, several factors are at play. Even though there is little moisture with which to work, the cold front still has enough lift to produce clouds. This is the cause of the arc of low solar capacity seen on the 20th. From the 21st through the 23rd, a weak storm developing on the cold front over the deep south pushes moisture northward. This, combined with the prevailing high pressure and light winds, yields clouds and widespread light fog. Over the west, there is considerable fog and haze in the stagnant air and moisture from a decaying Pacific storm that makes landfall on the 22nd also brings clouds across a large area.

The time series plots in Figure A-74 show that the impact is considerable, with WI solar dropping to about 60% of typical on the 21st and 22nd, and the shoulders around sunrise and sunset being clipped considerably by the impact of fog. Solar resource is also low in the west on the 20th through the 22nd and in the TI on the 20th and 21st.

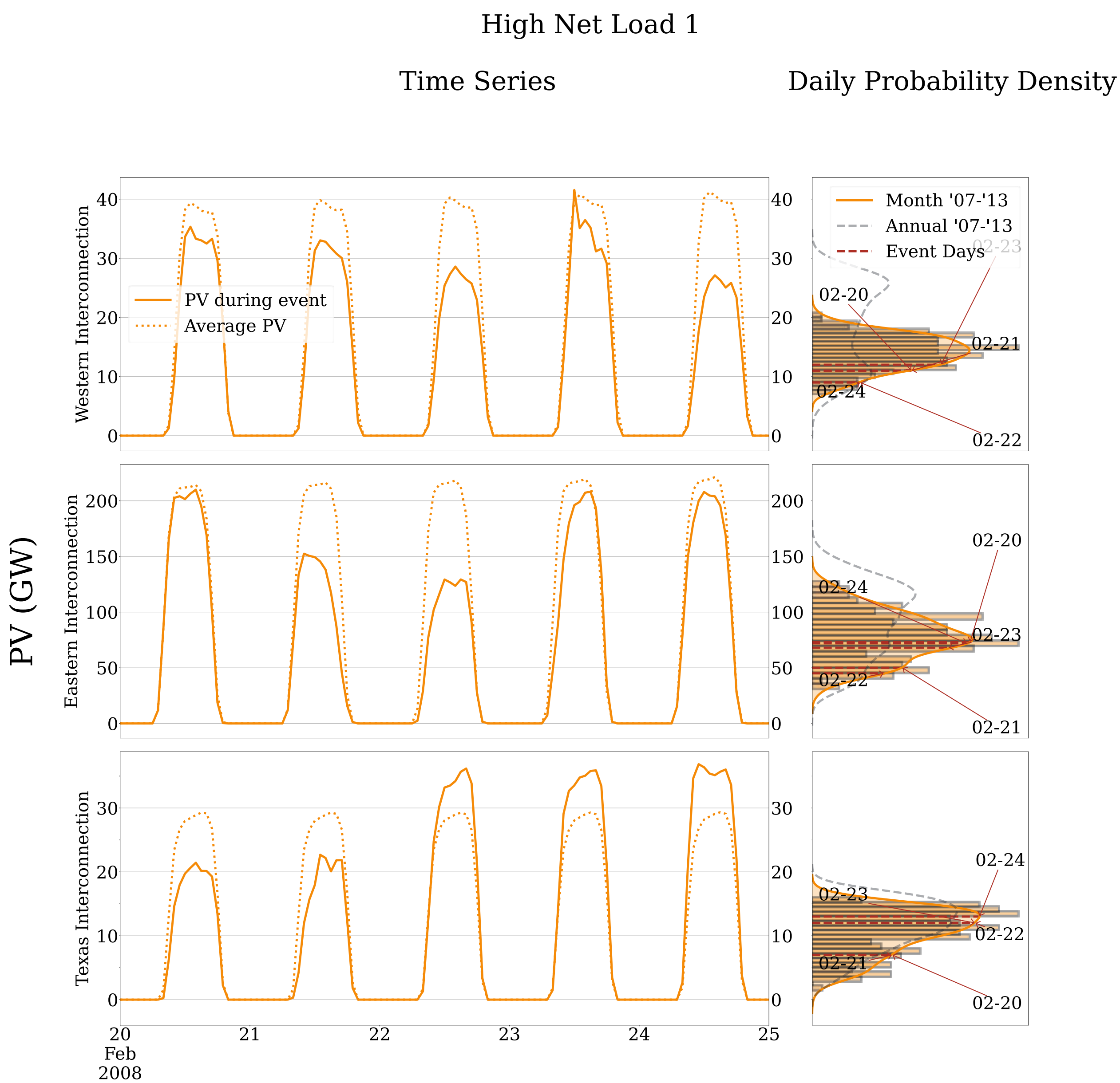

Figure A-74. Event regional modeled 2050 PV generation in context of the distribution of generation for the surrounding month (left) and time series plots of PV generation under the modeled 2050 scenario, relative to normal for the season (right)

Net Load

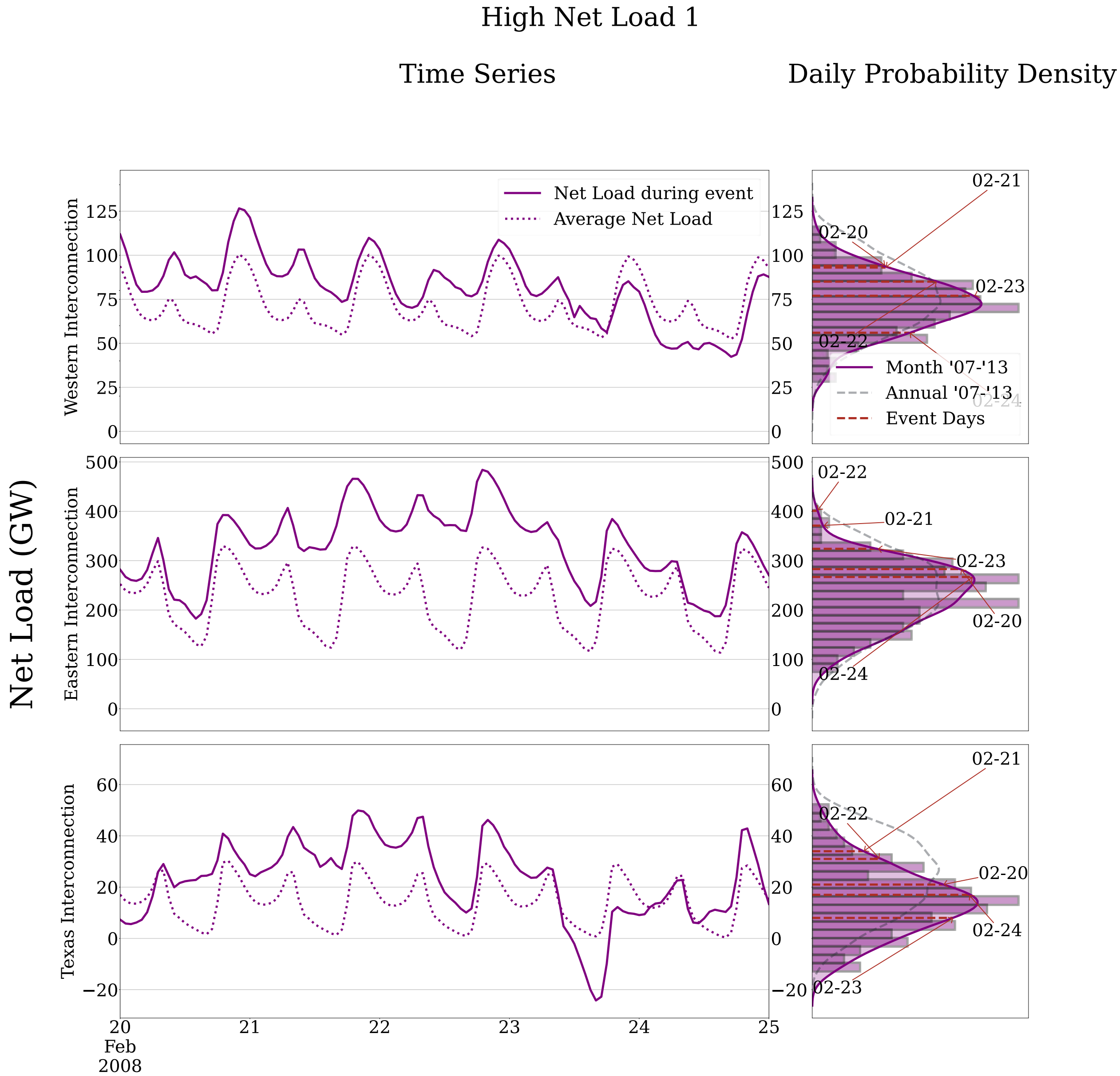

Figure A-75. Event regional modeled net load context of the distribution of generation for the surrounding month (left) and time series plots of modeled net load under the modeled 2050 scenario, relative to normal for the season (right)

The February 2008 event saw high net loads across all three interconnections, as a result of the coincidence of moderate to high load driven by cold temperatures, poor wind resource throughout the region, and poor solar resource where PV build-out is dense. The impacts on the EI are significant, with the 22nd being the upper bound of net load for the EI across the entire data set in 2050 (Figure A-75). This is despite the fact that the 22nd is not near the maximum load day in the load distribution data set (Figure A-70). Over the entirety of the 21st through the 23rd, net load in the EI never drops below the seasonal average daily peak net load. On the night of the 22nd, for a period, net load is close to 200 GW above the typical value. Net load in the WI and the TI are also above average for nearly the whole time period, with only a few hours at the beginning and end of the event dropping below normal.

System Modeling

As described above, the relatively benign weather created conditions that may stress system operations in a high variable renewable energy future. The high net load is observed across the continent, but this section will focus on operations in the EI where high load, extreme low wind resource, and low solar resource all combine on February 22, 2008.

Eastern Interconnection Operations

Figure A-76 shows the system dispatch and commitment for the full EI. In 2024, there is little day-to-day change. Wind generation ramping down throughout the week is met by a gradual increase in the number of Gas-CCs online. Very few, but some, Gas-CTs are used to meet afternoon peaks. However, in 2036 and 2050, operations at the beginning of the week look very different from those of February 22nd, the peak net load day in the interconnection. Over the course of 5 days in 2050, wind drops from a high of nearly 300 GW of available generation to a low of 24 GW. On the same days, winter storms over the solar generation regions create the lowest solar output for the interconnection of the modeled week. In response, Gas-CCs are turned on and stay online through the peak of the event. Gas-CTs come online to help meet morning and evening net load peaks, and they even stay online during the day.

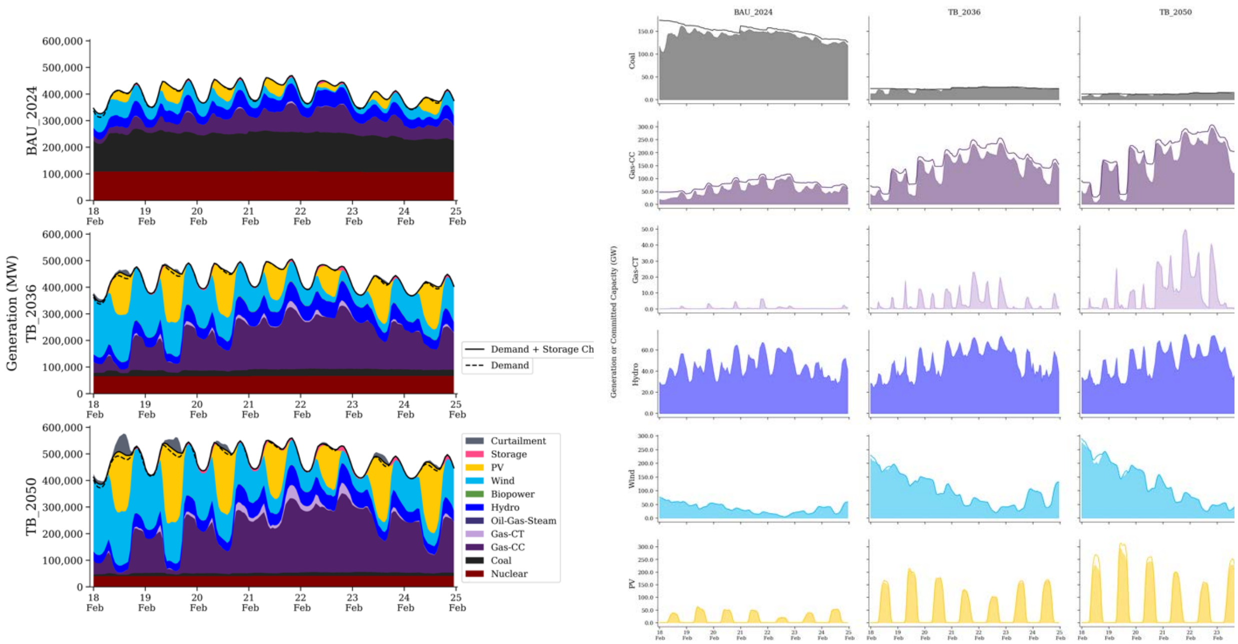

Figure A-76. (a) Generation dispatch for the EI for three future infrastructure years: 2024 (top), 2036 (middle), and 2050 (bottom) and (b) Committed capacity (solid line) and dispatch (filled area) for different generator types (along the vertical axis) for the three future infrastructure years—2024 (left), 2036 (middle), and 2050 (right)—during a high net load winter event in February 2008

The impacts of the low wind and solar resource are seen in MISO, PJM, and the Southeast. The dispatch of all three regions are shown in Figure A-77. The general takeaways from the full interconnection discussion above hold for these regions as well, but broken down, there are unique impacts of the events weather on each region. As shown in Figure A-73, on February 21st, cloud cover reduces the typical PV generation in the middle and southern parts of the interconnection, while the mid-Atlantic experiences above average PV output. Both MISO and the Southeast have low PV output on the 21st, but it is balanced by a high output day from PJM, which covers the mid-Atlantic region. As the storms move east on February 22nd, PV output is low again in the Southeast and PJM, and MISO's PV output recovers to some degree. Though much of the PV generation in EI is located in farther south, geographic diversity of the build-out does provide value by dampening the aggregate PV generation reduction.

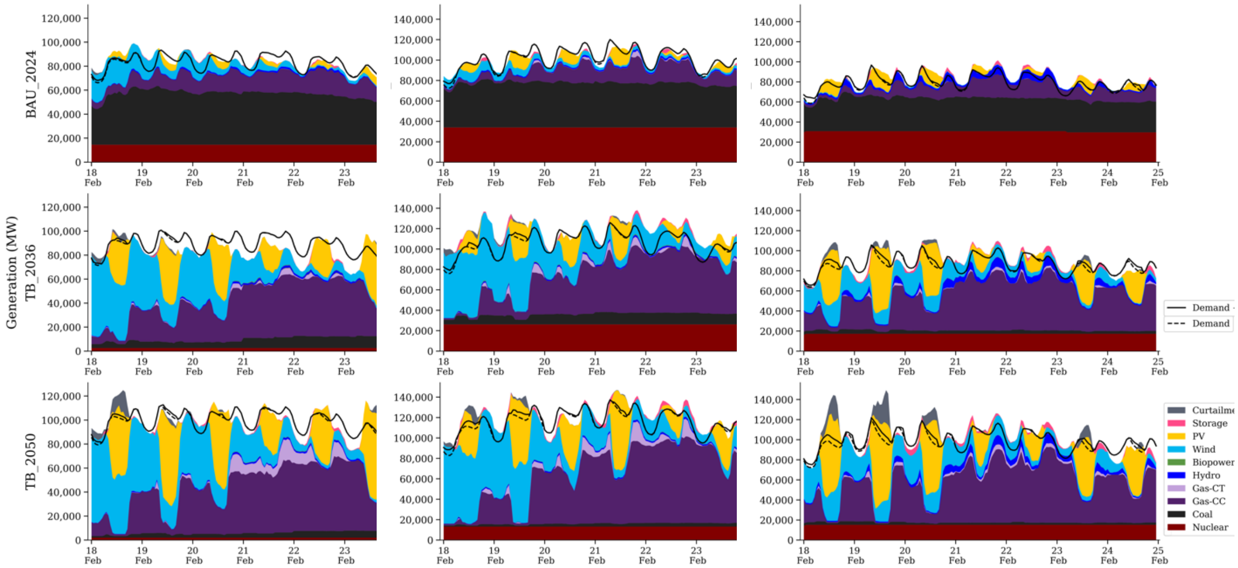

Figure A-77. Generation dispatch for MISO (left column), PJM (middle column), and the Southeast (right column), for three future infrastructure years—2024 (top), 2036 (middle), and 2050 (bottom)—during a high net load winter event in February 2008

Figure A-78 shows the trading among the three regions. As has been seen in many of the system operations analysis in this report, trading among regions becomes more dynamic with higher wind and solar penetrations. Also of interest, is trading on February 22nd and specifically, the height of the net load in the EI. And particularly, the interchange between PJM and NYISO in 2050 has a strong diurnal pattern, where PJM exports more power to NYISO when PV output is high in the interconnection. This happens even on the 22nd, when PJM PV output is low. These exports are actually coming from FRCC, which exports its excess PV generation to SERC, which wheels it to NYISO through PJM. Without the transmission capacity or institutions in place to dynamically trade between regions, the interconnection would be unable to take advantage of the geographic diversity of the PV output.

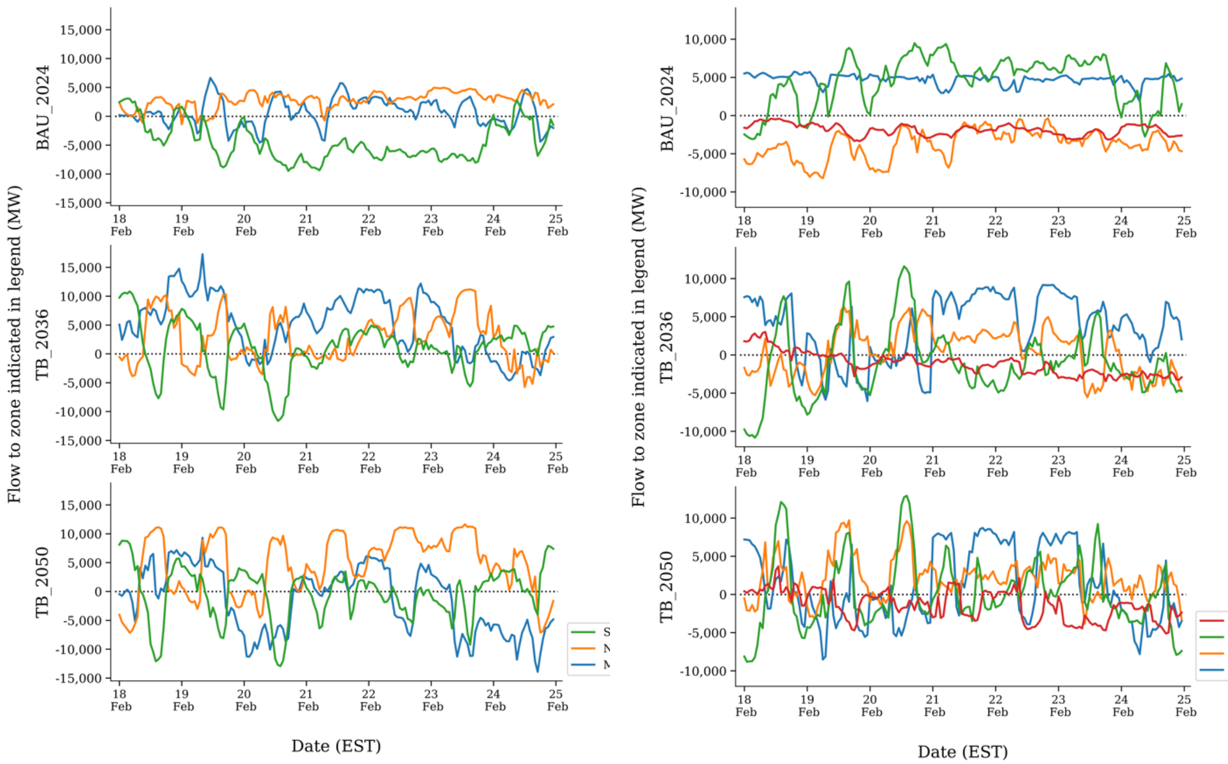

Figure A-78. Net power flow between PJM (left) and the Southeast (right) and their respective neighbors for three future infrastructure years—2024 (top), 2036 (middle), and 2050 (bottom)—during high net load winter event in February 2008

Positive flow means an export from PJM/Southeast to its neighbor.

Finally, Figure A-79 shows the regionally prices within MISO, PJM, and the Southeast during the high winter net load period. Prices in 2024, which show some divergence at the daily peaks, are largely homogeneous. The infrastructure years 2036 and 2050 show more divergence, particularly at the height of the net load between the 21st and 23rd. In MISO (left column), in regions farther south with less wind and more PV, prices are largely stable, while the peakier prices occur in the north. In PJM, regions closer to the East Coast have depressed prices on the 21st, as their solar generation is less affected by the cloud cover in the south and Midwest. Prices in the Southeast also diverge during the period with significantly depressed wind output. The price divergence suggests the 2036 and 2050 infrastructures could benefit from some additional transmission capacity to better manage an event like this one.

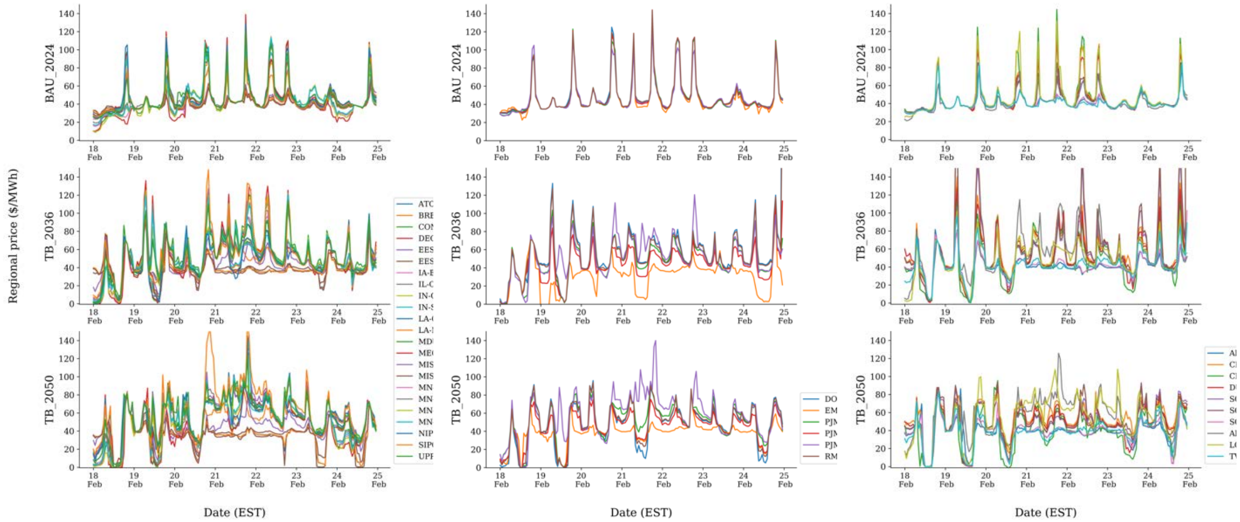

Figure A-79. Regional power prices in MISO (left column), PJM (middle column), and the Southeast (right column), for three future infrastructure years—2024 (top), 2036 (middle), and 2050 (bottom)—during a high net load winter event in February 2008

Impacts Summary

Between February 21 and February 23, 2008, the EI experienced meteorological conditions that may stress the operations in a system with high penetrations of wind and solar. Cold temperatures elevated load to be above normal during this period. At the same time, stagnant air steadily reduced the wind generation output by more than 90%, which hit an extreme low output relative to the full data set on the 23rd. In addition, winter storm systems reduced PV output in the Southeast and in MISO on the 21st, before extending into PJM on the next day. All this leads to a very different style of system operations between the modeled 2024 system and the 2036 and 2050 systems. Gas-CC and Gas-CT capacity ramped up and stayed on throughout the peak of the event. At the same time, diversity in the location of the PV resource and dynamic transmission operations reduced the intensity of system stress that may have been caused if regions relied exclusively on local resources.

Winter Net Load 2: December 6–11, 2009

Event Summary

High net load occurred for several days due to benign weather conditions that promoted low wind and solar resource. High net loads were present across all three interconnections on December 7, 2009, resulting in a tail event for the EI and the entire country. Wind and solar were below normal to well below normal on average across all three interconnections.[42]

Meteorological Description

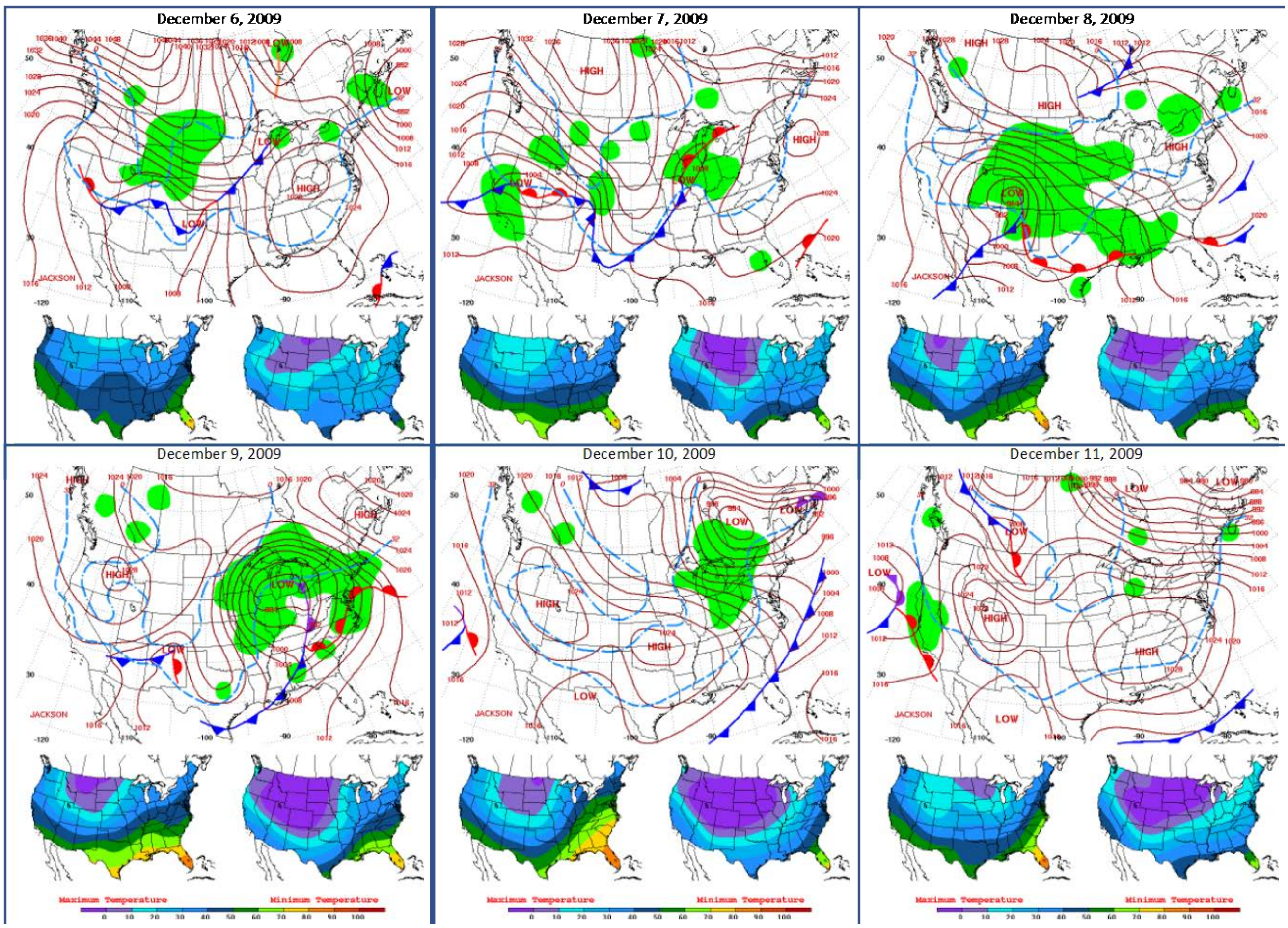

Figure A-80. Surface weather and temperature maps valid at 7 a.m. EST

See the Event Description Structure section for plot details.

Source: "Daily Weather Maps: Sunday, December 6, 2009," NOAA Weather Prediction Center, https://www.wpc.ncep.noaa.gov/dailywxmap/index_20091206.html

[42] See https://www.wpc.ncep.noaa.gov/dailywxmap/index_20091206.html

At the beginning of December 2009, the upper-air pattern amplifies so that a strong upper-level ridge of high pressure forms across the west and a deep upper-level low forms across the rest of the country. This pattern continues to amplify through the 5th, blocking the Pacific storm track and allowing the Rocky Mountains to channel cold, dry air south from Canada. By the 5th, the cold air reaches all the way to southern Texas and pushes west to the Oregon coast and east to a line running from about Louisiana northeast to New York City.

Heating degree days ranks range from about the 70th to 95th percentile; it is cold, but temperatures are not unprecedented across a broad area. On the 6th, the upper-level pattern moves west, allowing cold air trapped in British Columbia to enter the Intermountain West. The air is deep enough to move through mountain passes and into the Great Basin; it then pushes through gaps in the Cascades into the maritime west and can be seen advancing southward into California (Figure A-80, first four panels). Across the eastern half of the country, a broad area of surface high pressure is in control on the 6th, bringing a crisp day with plenty of sunshine and moderating temperatures.

By the 7th, cold air is pushing south all the way to Los Angeles. The land-sea contrast together with a sharp trough (low pressure) in the upper-level flow lead to the rapid formation of a storm in Northern California that tracks west through the 7th, bringing rain and snow to California, Nevada, and the Four Corners. Meantime, a weak system also forms on the Iowa-Missouri border. The system is weak but produces clouds and light precipitation across a broad area. The western storm system deepens rapidly as it moves through the mountainous terrain of the west, and on the 8th it emerges into the Plains and arcs northeast into the eastern Great Lakes area. The storm taps into warm air from the Gulf of Mexico and brings much precipitation to everywhere east of a line from Minnesota to Louisiana; it also brings warmer temperatures.

To the west, high pressure builds in behind the storm and a reinforcing blast of cold air moves south so that the 8th and 9th ranks in the top-10 coldest days in the record in Seattle, Portland, San Francisco, Los Angeles, and Salt Lake. As the storm's cold front sweeps south and east across the rest of the country, temperatures fall rapidly but are not record-setting like they are in the west. Skies clear and high pressure dominates the entire country on the 10th and 11th. The nighttime low temperatures on the 10th are extremely low, with a huge swath of the country seeing temperatures below 0°F and the teens and twenties that extend deep into Texas. Temperatures in the west remain well below normal through the 11th, when an approaching Pacific storm scours out the cold air.

Load Impacts

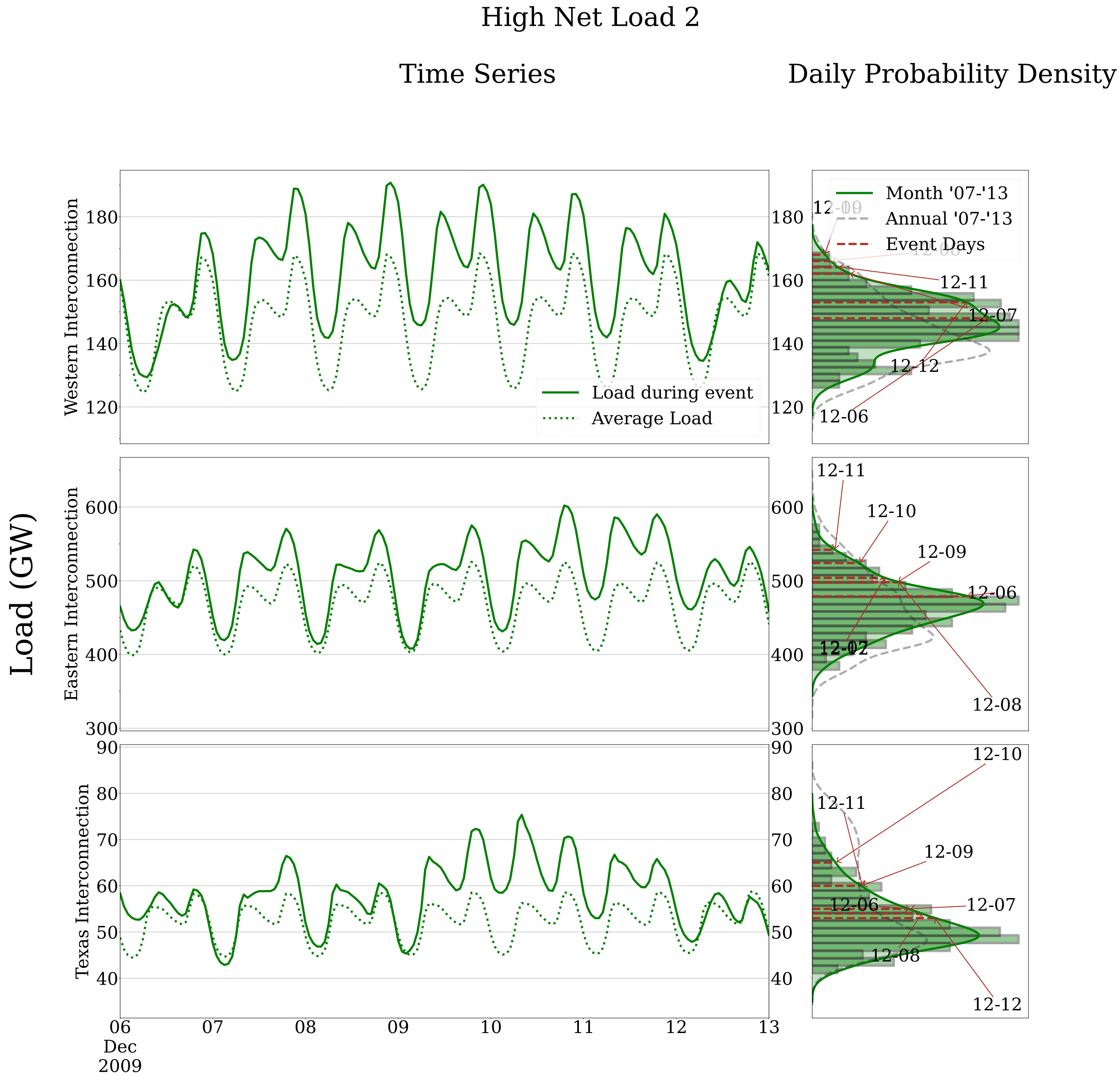

Figure A-81. Time series of regional load during the 4-day event in green, compared to load averaged across the 7-year data set for the month surrounding the event in grey (left) and distribution of 2050 regional loads for the 29 days surrounding the middle of the event in green, and across the 7-year data set in grey, with the event days labeled (right)

This is a cool period across the country so, as expected, load is above normal for days in the surrounding multiyear 29-day window. WI loads on the 7th through the 11th are in the tail of the distribution in the west, and the 8th, 9th, and 10th are in the extreme tail. Coincidently, this is consistent with the ranking of these days as close to the coldest in the data set at all major western load centers.

These loads are also in the tails of the annual distribution (the Pacific Northwest is one of the few wintertime peaking loads), so this period is challenging for the WI. The loads in the other interconnections are also close to the tail of the distribution on the 10th and 11th, where very cold nights drive minimum loads above normal.

Wind Generation

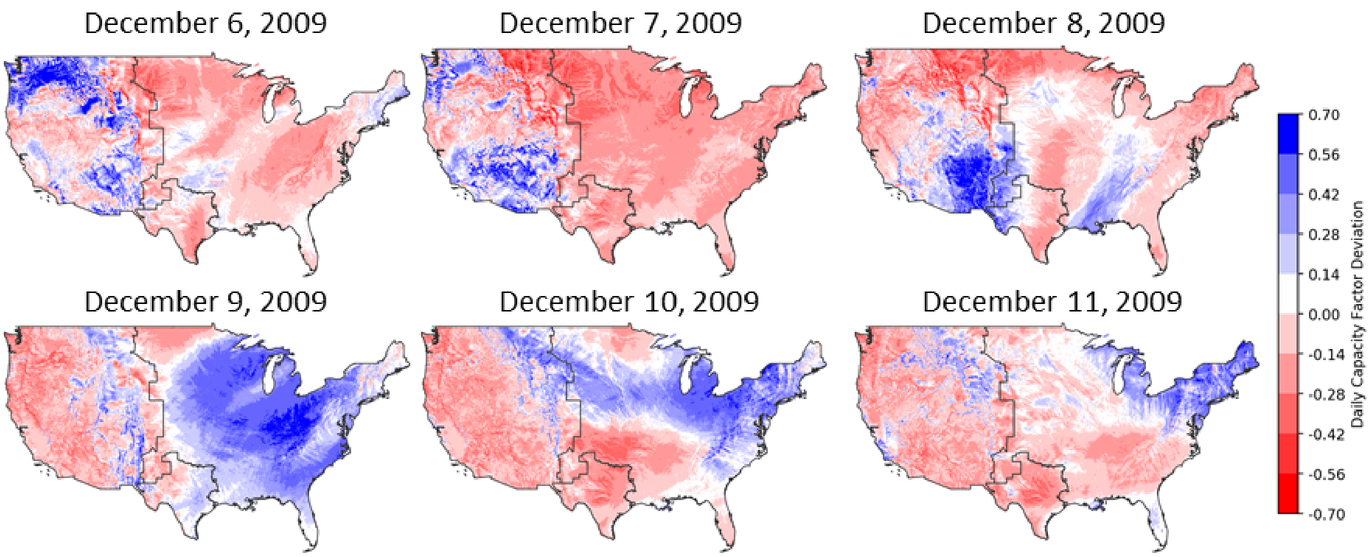

Figure A-82. National daily average wind resource deviation during the December 2009 high net load event

The distribution of event days relative to the multiyear window in Figure A-83 indicate that west wind is generally slightly lower than normal, with the exception of the 6th and to some degree the 7th. This is confirmed in the time series plot of Figure A-83, which indicates a generally low wind period once the strong generation on the 6th has faded.

Figure A-82 shows this stronger generation is driven from the Pacific Northwest on the 6th, and this is typical when then is cold air surges into the Columbia Basin from Canada. This region is modeled to contain many wind plants in order to capture prevailing onshore flow, but during a cold surge, the northerly flow is funneled into the Columbia Gorge, which results in a period of strong generation until cold air piling up against the Cascades produces enough localized high pressure to block further inflow and the wind resource could often remain low for days.

A strong east wind usually blows west of Cascades, concurrent with high loads, during this period. However, capacity is not modeled to be significantly built in this area. Still, the small amount that is built helps prevent wind output from decreasing farther into the tails.

A secondary bump early on the 7th is associated with the storm system crossing the mountains through Nevada. Following this, wind output remains below normal for the rest of the period, coincident with high load.

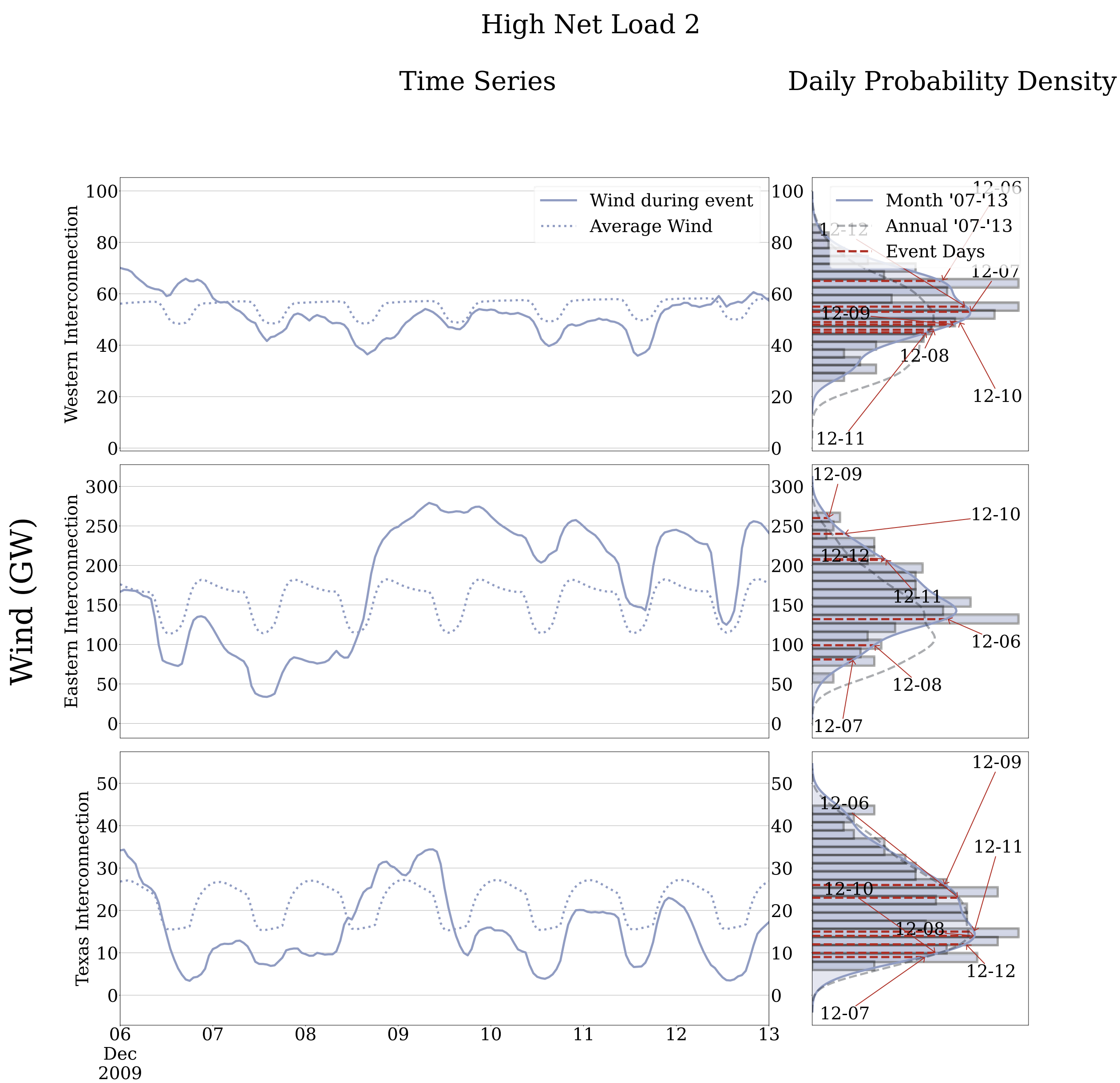

Figure A-83. Event regional wind generation (based on 2050) in context of the distribution of generation for the surrounding month (left) and time series plots of wind generation under the 2050 scenario, relative to normal for the season (right)

The EI sees an extremely volatile period of wind production during this event, as wind ranges from less than half the average on the 7th to more than double on the 9th. Though they are not in the extreme tails, the 7th and 8th are periods of very poor production. The ramp-up on the 9th fits with a pattern of good wind generation in the EI during a cold wave, where wind capacity can shore up generation needs by capturing the energy associated with northerly winds driving cold air south; and the 9th is followed by a day or two of poor generation once the cold air is in place and quiescent weather dominates.

The weak storm system that forms over Iowa and tracks east on the 7th barely produces any wind enhancement. However, the big storm that emerges from the Rockies on the 8th rapidly ramps production and by the 9th almost the entire eastern interconnection sees above to well above-normal wind resource as a direct result of the storm system. Production remains above normal on the 10th as the storm continues to impact the Northeast and northerly winds push cold air south behind the system; even though Figure A-82 indicates much of the EI has below-normal wind resource on the 11th as high pressure builds in, there is still enough above-normal wind in the northeast, which has a significant amount of modeled capacity to offset the reduction further west and south.

The TI does not have the diversity described above. Like in the EI, the wind drops off rapidly in the TI as the surge of cold air dies on the 6th, and the 7th is a very low generation day. Generation surges above normal again on the 8th and 9th as the major storm passes and cold air is driven in on the west side of it, but it then diminishes again so that the 10th also sees low wind generation across the entire state.

Solar Generation

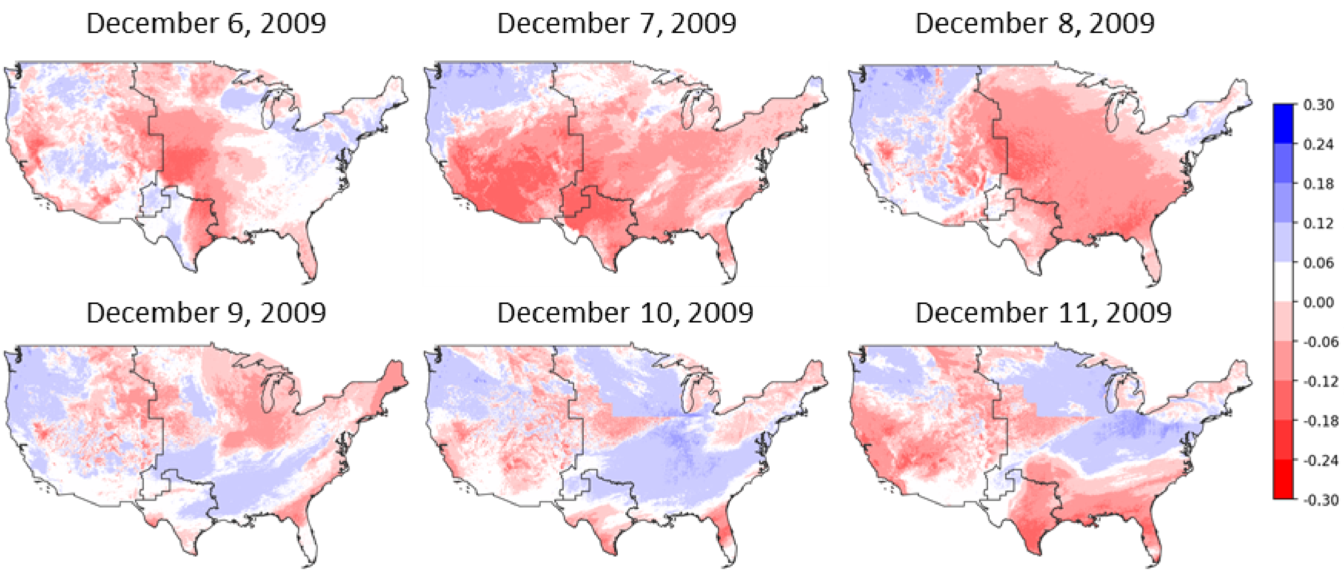

Figure A-84. National daily average solar resource deviation during the high net load event

This event occurs a couple of weeks before the winter solstice, so maximum daily solar resource is close to its seasonal minimum and represents a considerably smaller fraction of the weather-driven generation than wind. Also, as expected for the time of year and given the passage of a major storm system from coast to coast, the solar resource is quite variable in time and space as seen in Figure A-84 and Figure A-85. In general, there is enough asset diversity and spatial weather variability that the solar generation amounts cluster around the median for each interconnection.

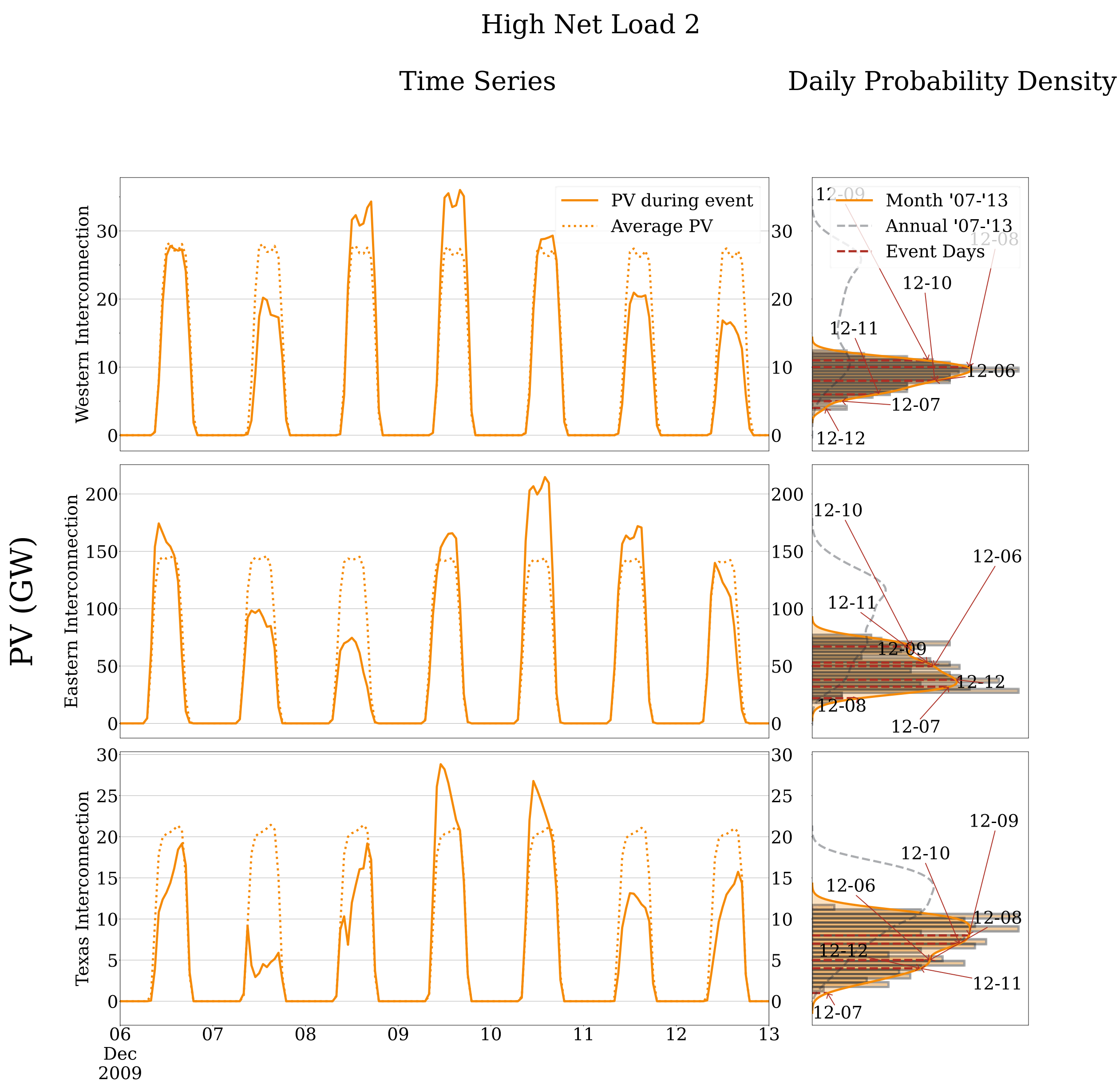

Figure A-85. Event regional modeled 2050 PV generation in context of the distribution of generation for the surrounding month (left) and time series plots of PV generation under the modeled 2050 scenario, relative to normal for the season (right)

However, the 7th and 8th both see major impacts on solar generation from the storm system. On the 7th, the system crosses the west and drastically reduces solar output there. It also reduces generation on west part of the TI, but it is fog that has the largest impact in Texas, presumably due to the cold air overlying warm moist ground. At the same time, the weak system in the Midwest also reduces EI output. This is concurrent with low wind output on all the interconnections.

Net Load

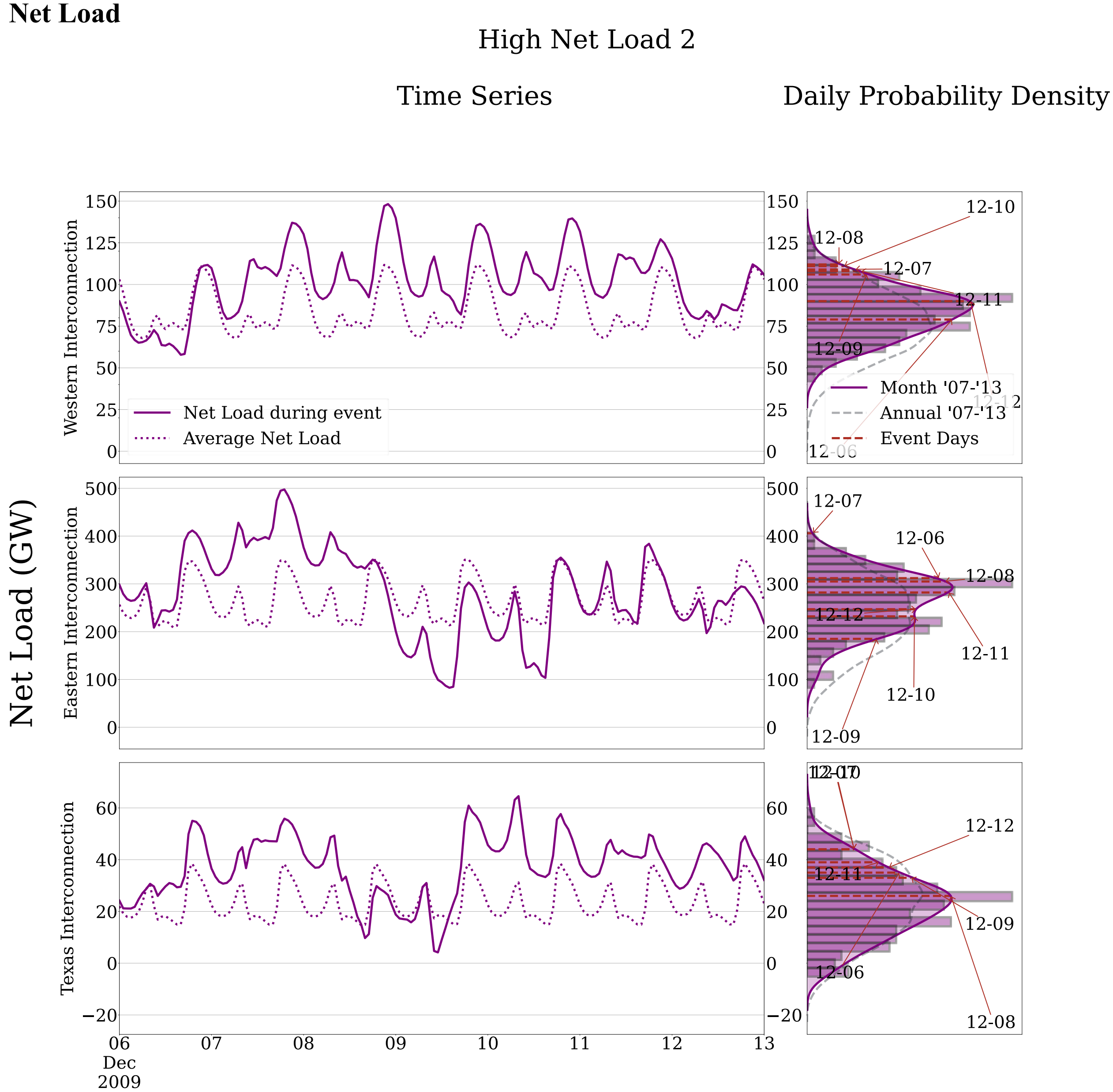

Figure A-86. Event regional modeled net load context of the distribution of generation for the surrounding month (left) and time series plots of modeled net load under the modeled 2050 scenario, relative to normal for the season (right)

In the WI, load is much above normal for the whole period, and the combination of poor wind resource and seasonally low solar resource result in residual loads deviations from normal that are larger than those of just the load deviation presenting additional challenges. While the event does bring close to record breaking cold to the Pacific Northwest and coastal California, from a national perspective, it is cold but not exceptional.

On the EI, the 7th and 8th are not extremely high load events relative to the distribution, and the temperature record does not indicate this would be an extreme event. However, the combination of moderate loads, combined with very poor wind and solar resource, drives net load to the extreme high tail of both the seasonal and annual distributions. These deviations are close to 50%/150 GW of excursion in residual load relative to typical for the period. The very high load days on the 10th and 11th on the EI are mitigated by enhanced renewable generation in the region, and what was a high load event on those 2 days becomes a situation where the residual load is actually near or below normal.

The TI exhibits similar attributes. The combination of high loads and poor wind and solar conspire to push net loads to high levels. Like for the EI, this is true in the days following the initial cold wave, but in the case of Texas, it also occurs again on the 10th and 11th when high pressure limits the wind and clouds across much of the state reduce solar output.

In this event, near-record cold in the west results in the WI having elevated but not extreme net load over the whole period. However, in the EI, moderate cold combined with poor wind and solar results in the 7th being the upper bound of net load over the whole data set. As the EI is summer load peaking, planning margins could provide for excess generation in winter, but any additional constraints on the system due to gas outages or gas supply limitations might also impact reliability during this time.

Winter Net Load 3: February 2–5, 2010

Event Summary

A weather pattern conducive to high pressure and weak pressure gradients both east and west of the Rocky Mountains leads to 4 days of otherwise benign weather with low temperatures and extremely poor wind resources across CONUS. A storm moving across the southern part of the country dramatically reduces solar output from west to east through the period. Despite loads on each interconnection being close to normal, weak wind and solar resource results in net load that is well above normal, with some days being near the top of the net load distribution.[43]

Meteorological Description

February 2–5, 2010 was relatively calm from a weather perspective. A weak cold front moved down the Front Range of Colorado on the 2nd, bringing temperatures that were below the mean but not unusual to the Midwest. Temperatures in the region ranged from 1°F to 7°F below normal on the west side of the low-pressure system, as seen close to Chicago on February 2nd, with cold air moving southward. On the east side of the low-pressure system, there was a compensating area of above average temperatures in locations like Chicago, Detroit, and Pittsburgh. Meanwhile, cool air introduced behind the last frontal system to move across the East Coast was still in place on the East Coast, yielding temperatures that were on average 1°F–5°F below normal in that region through the time period.

Earlier in the period, on January 31, high pressure dominates at the surface, with cool air extending south all the way to Texas in the wake of a previous frontal system. Weak and splitting upper-level flow and high pressure ridging over western Canada was conducive to reinforcing cool surface flow down the Rockies and weak front strengthening. On the 2nd, a frontal system approaches the Pacific Northwest, where temperatures are generally 1°F–5°F above the period mean. Cold air again filters into upper western plains and drives south to Northern Texas, but it does not extend eastward due to warmer air flowing from the southeast around the large high-pressure system. A trough in the jet stream helps develop the weak low pressure system seen on the first map in Figure A-87; this system has no access to a moisture source and weakens once the jet stream feature moves eastward. By the 3rd, the freezing line has again reached Texas but circulation around the large high-pressure system over the East Coast is now pushing warmer air into the mid-south and Ohio Valley.

On the West Coast, the split jet stream flow and weak dynamics mean the storm approaching the Pacific Northwest weakens while another storm forms on a trough in the southern jet stream branch. This southern low produces lots of rain across western Texas on the 3rd due to moisture circulating over the Gulf of Mexico around the high pressure system. By the 4th, the rain has spread east over Texas, Oklahoma, Louisiana, Arkansas, Kansas, and Mississippi.

The rest of the east is in an upper pattern conducive to continued surface high pressure with little interesting weather as a result. By the 5th, the storm system moving across the southern states finally gets some upper-level support and strengthens. This improves the wind resource over east, but the large cloud shield dramatically reduces the solar resource.

[43] See https://www.wpc.ncep.noaa.gov/dailywxmap/index_20100202.html

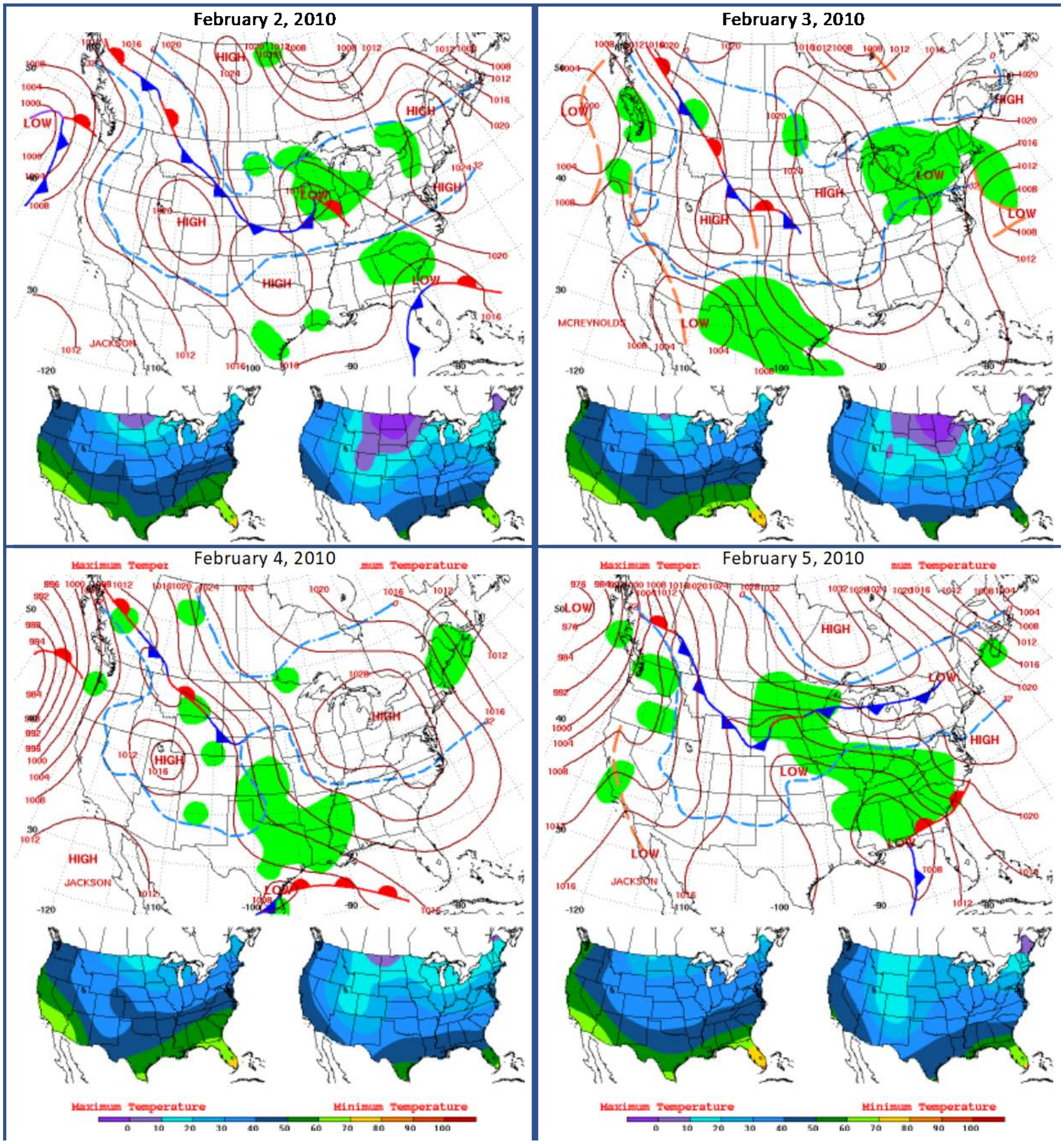

Figure A-87. Surface weather and temperature maps valid at 7 a.m. EST

See the Event Description Structure section for plot details.

Source: "Daily Weather Maps: Wednesday, February 20, 2010," NOAA Weather Prediction Center, https://www.wpc.ncep.noaa.gov/dailywxmap/index_20100202.html

Load Impacts

Figure A-88 shows the loads during this period were comparable with typical loads for the period. We see that the event days fall close to the median in the WI and the EI and moderately above normal in the TI. The time series plot shows that daytime loads were slightly above normal in the west, while nighttime loads were slightly below normal. This deviation may reflect cool daytime temperatures and little sunlight, combined with warmer than average nighttime temperatures. On the EI, loads were tightly clustered in the middle of the distribution and again the time series shows slightly elevated daytime and decreased nighttime loads that are likely due to the widespread cloud cover.

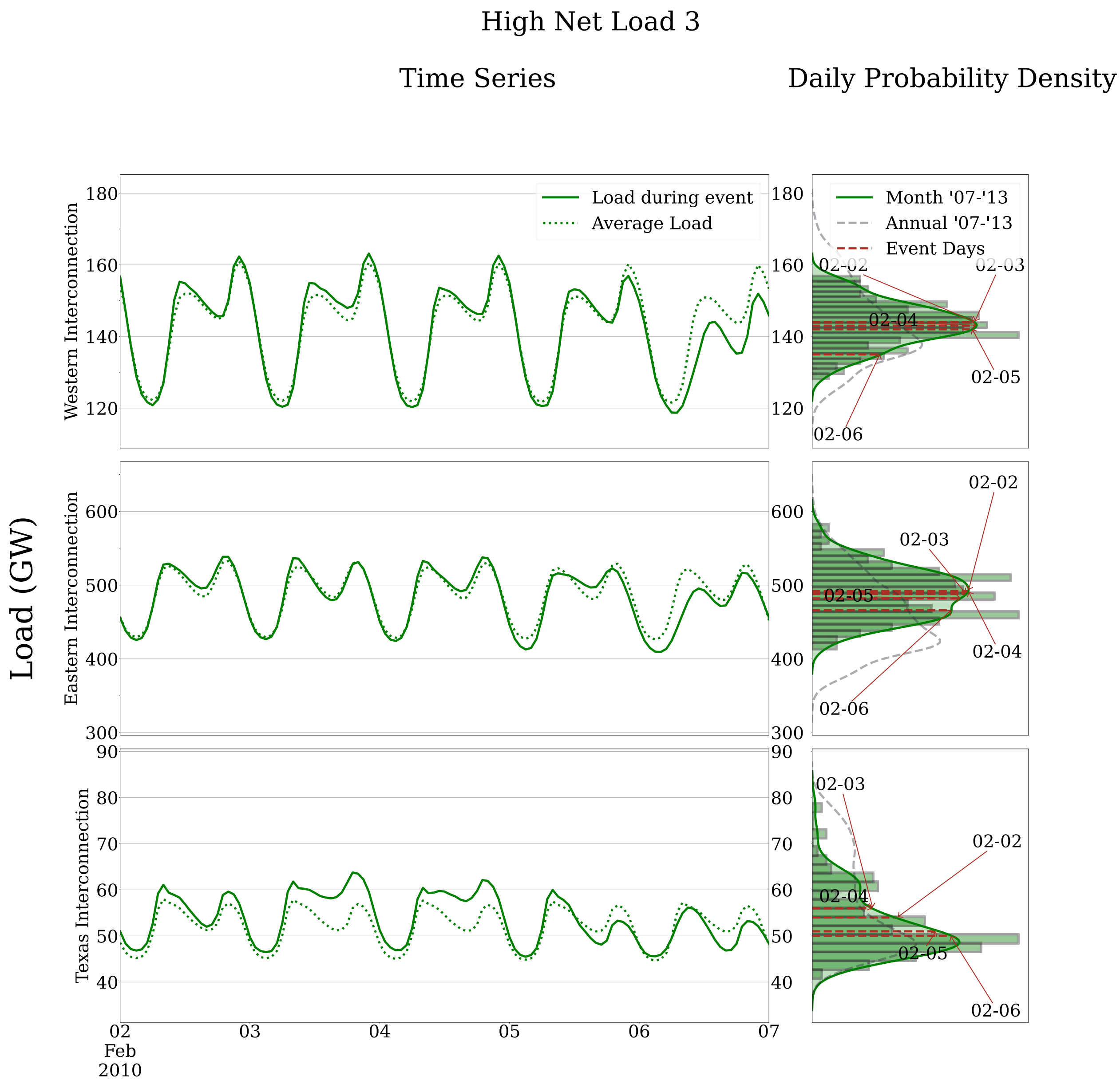

Figure A-88. Time series of regional load during the 4-day event in green, compared to load averaged across the 7-year data set for the month surrounding the event in grey (left) and distribution of 2050 regional loads for the 29 days surrounding the middle of the event in green, and across the 7-year data set in grey, with the event days labeled (right)

Daytime loads in the TI are well above normal on the two coldest days (3rd and 4th), while nighttime loads are close to normal. The larger deviations in Texas are (1) likely a function of the climate diversity is lower in the TI than in the EI and the WI and (2) because typical February temperatures in Texas tend to be in a zone where air conditioning and heating loads are low on average, but cold excursions can rapidly increase use of resistive heating load.

Wind Generation

Figure A-89 vividly show the poor wind resource during this period. February 2nd is extremely poor across the entire CONUS, with only a few spots showing near or slightly above-normal wind. In the statistical distribution in Figure A-90, February 2 is in the tail of distribution for all three regions, and it is the lowest wind resource day for the seasonal distribution for the EI and the TI. The wind drought continued across both the east and the west on the 3rd, though Texas saw above average resource due to the low pressure system transiting across the state.

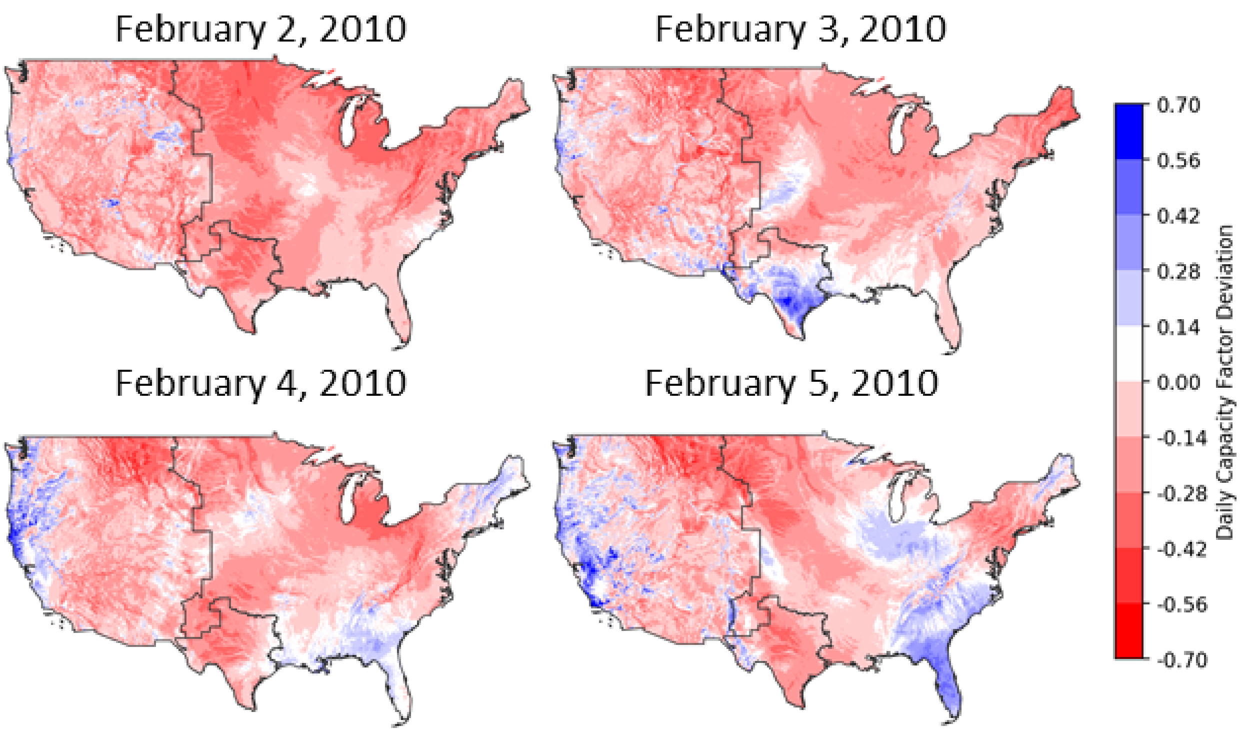

Figure A-89. National daily average wind resource deviation during the high net load event

Wind begins to return to the west on February 4 as a frontal system moves through the Northwest and a more active weather pattern returns. However, it is not until the February 5 that the EI sees a return to near normal wind conditions as the storm system that had crossed Texas and the southern states strengthens and impacts wind facilities along the eastern ridgetops and produces an area of enhanced gradient between the high and low pressure extending across Virginia, West Virginia, Ohio, Indiana, and Illinois.

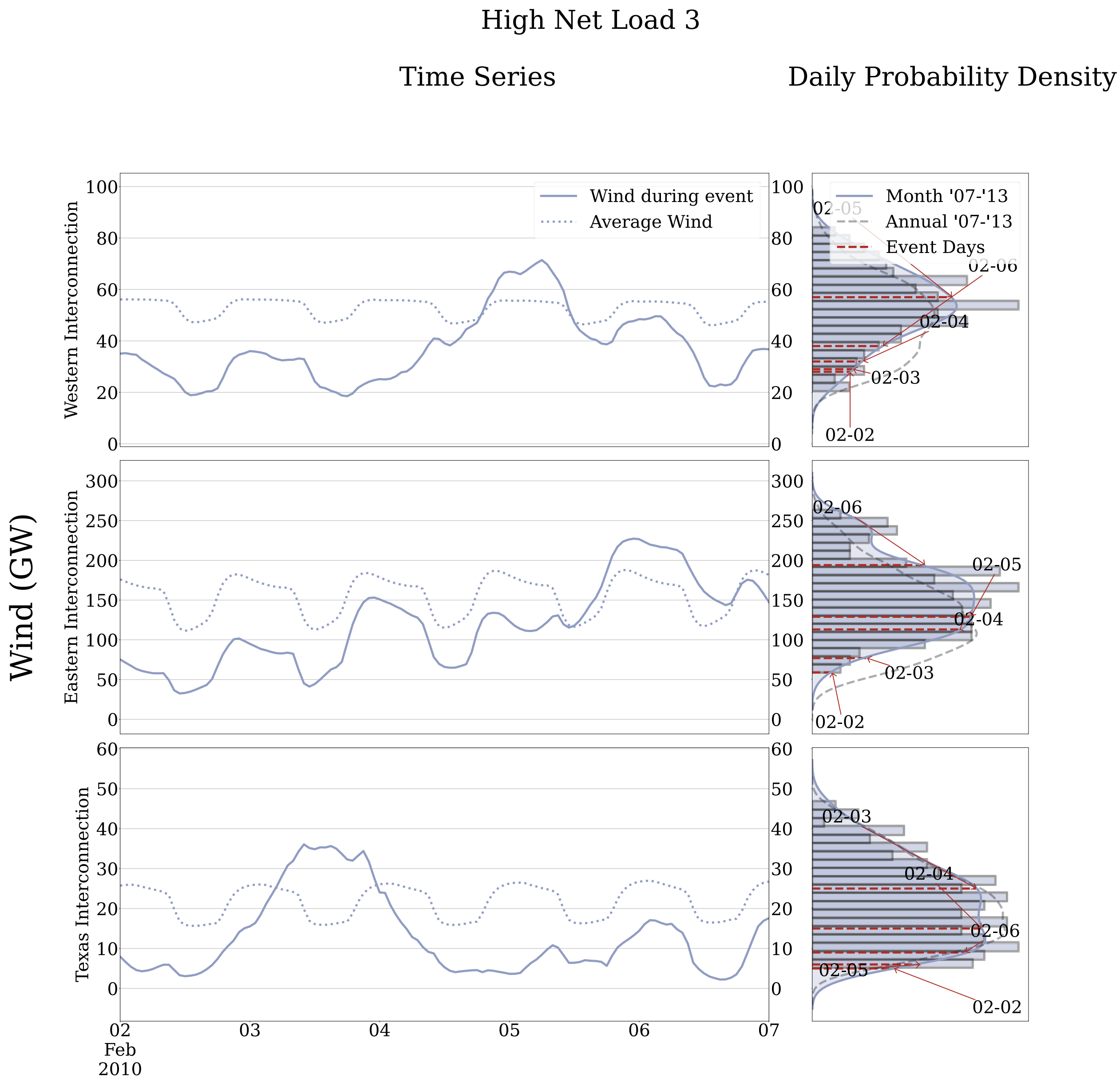

Figure A-90. Event regional wind generation (based on 2050) in context of the distribution of generation for the surrounding month (left) and time series plots of wind generation under the 2050 scenario, relative to normal for the season (right)

Solar Generation

Solar resource was also well below normal during the period. Figure A-91 indicates February 3 is a reasonable day for solar on the EI. Though there are some area of higher resource availability in the EI on February 2 and 4, there is less modeled solar capacity built in the Dakotas, Nebraska, and Northern New England. This results in EI solar generation in Figure A-92 being lower on February 2 than on February 4 even though resource maps indicate a broader area of above-normal resource on February 2 than February 4. February 5 has poor solar resource across almost the entire eastern interconnection except for parts of Oklahoma and Northern New England.

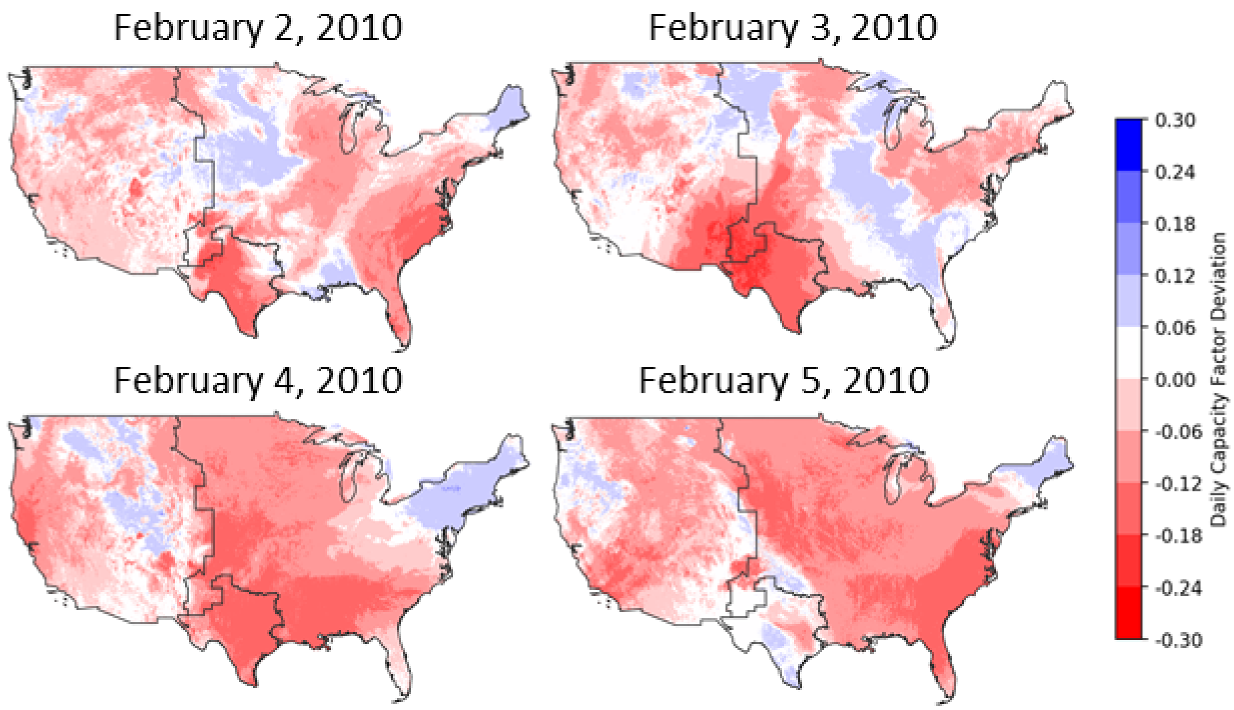

Figure A-91. National daily average solar resource deviation during the high net load event

The chief causes of the poor solar resource in the east on February 4 and 5 are that:

- The storm system passes through Texas and the southern states.
- Upsloping southwesterly flow from the Gulf brings clouds to the Midwest, and the storm system is combined with flow around the high pressure centered over the northeast
- Near the center of the high-pressure system, the flow is stagnant and persistent fog is present on February 4, while on the February 5, moist flow associated with the low-high pressure couplet brings clouds to the area of the east.

February 5 is the lowest solar resource day in the distribution for the EI and despite not being in the tail of the WI distribution and being above normal in the TI, it is the fifth-lowest solar generation day CONUS-wide based on the 2050 build-out.

Western solar during the period is below normal on all days, with February 5 showing the lowest solar, but none of the days is in the tail of the distribution. However, with very poor solar generation elsewhere, the negative deviations are important.

The solar deviation in Texas is especially important because the normal output during daytime hours is around 25 GW; however on February 3 and 4, solar output is only 5 GW or lower. February 2–4 were all low solar generation days in the tail of the distribution, with the 3rd and the 4th representing the lowest days in the data set.

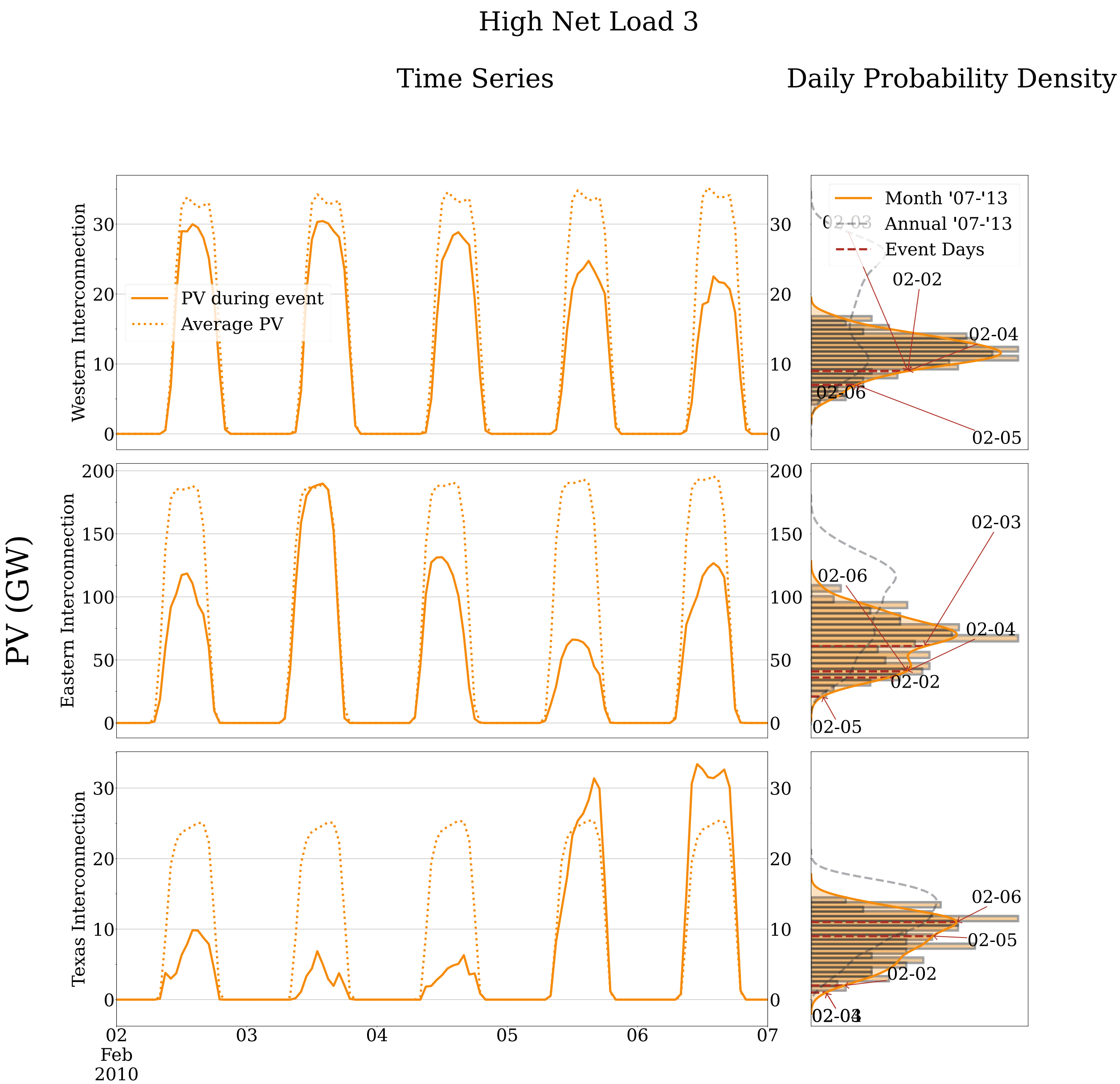

Figure A-92. Event regional modeled 2050 PV generation in context of the distribution of generation for the surrounding month (left) and time series plots of PV generation under the modeled 2050 scenario, relative to normal for the season (right)

Net Load

From a traditional weather event perspective, nothing is notable about the period: the weather is typical for the season with nothing more than some moderately heavy rain in the south and a few cool days in the Midwest.

In this case, net load is in the high tail of the distribution in each interconnection on at least one day during the period. Though February 5 is notable for the poor solar resource in the EI, this is compensated for by low loads and improving wind generation. February 2 stands out in Figure A-93, especially when looking across all three interconnections. Despite near median load in the EI and WI, and moderately above-normal load in the TI, the event is close to the tail of the net load distribution in all three interconnections. In Texas where load is highest relative to normal, the net load is furthest from the tail on February 5 due to better than average wind generation associated with a passing storm system.

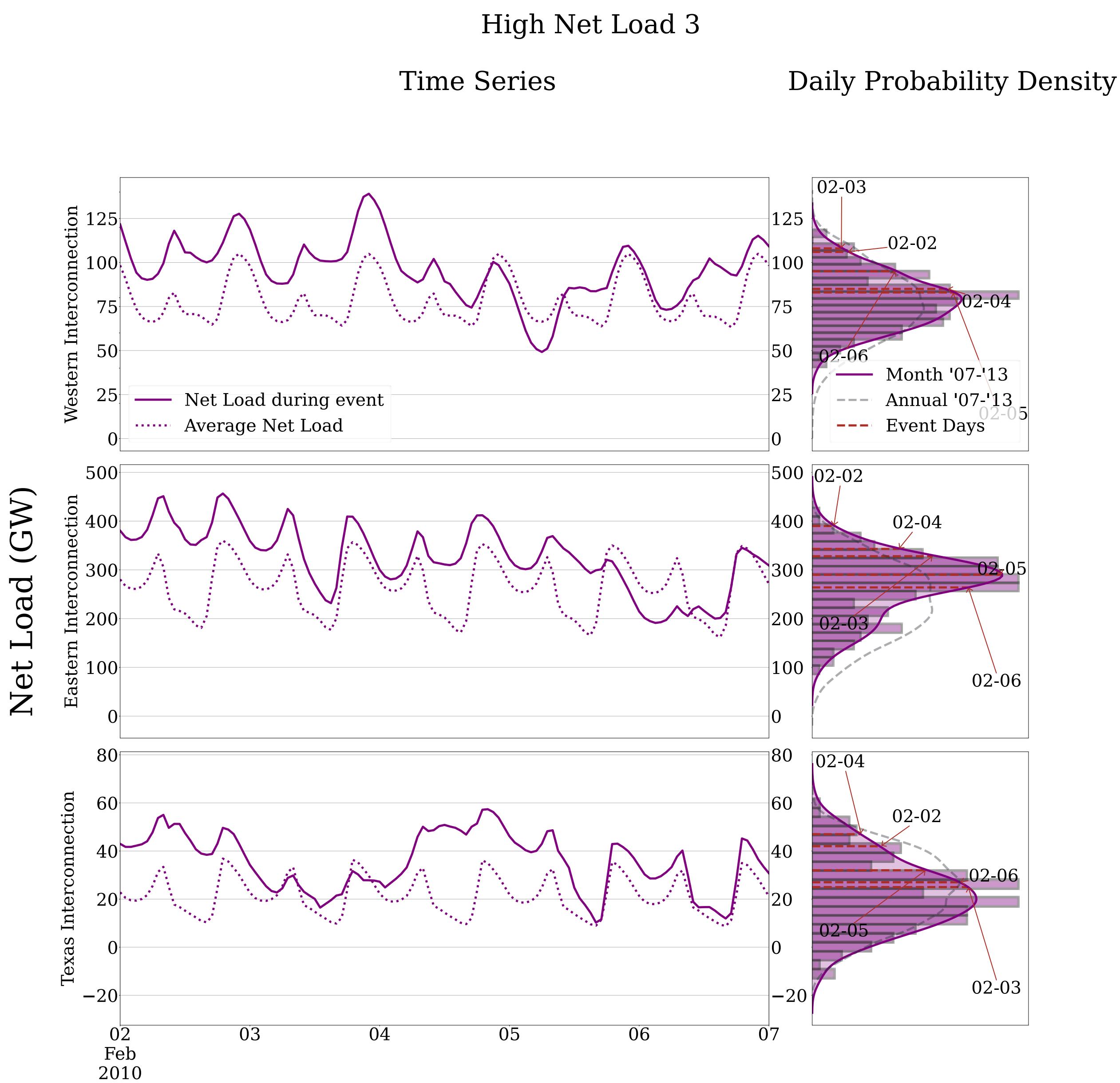

Figure A-93. Event regional modeled net load context of the distribution of generation for the surrounding month (left) and time series plots of modeled net load under the modeled 2050 scenario, relative to normal for the season (right)

System Modeling

Across the three interconnections, the low VRE conditions during this moderately high net load event is met by adequate dispatchable thermal and hydropower generation. Figure A-94 shows the system dispatch in 2050 for the WI, EI, and TI. In the WI and the EI in particular, though wind and solar generation are both below average for this time of year, the diurnal shape of the resource and the geographic diversity of the resource in both interconnections leads normal diurnal cycle of the thermal and hydropower fleet. The TI experiences more day-to-day variability in the net load, leading to more significant cycling of the gas-CC fleet.

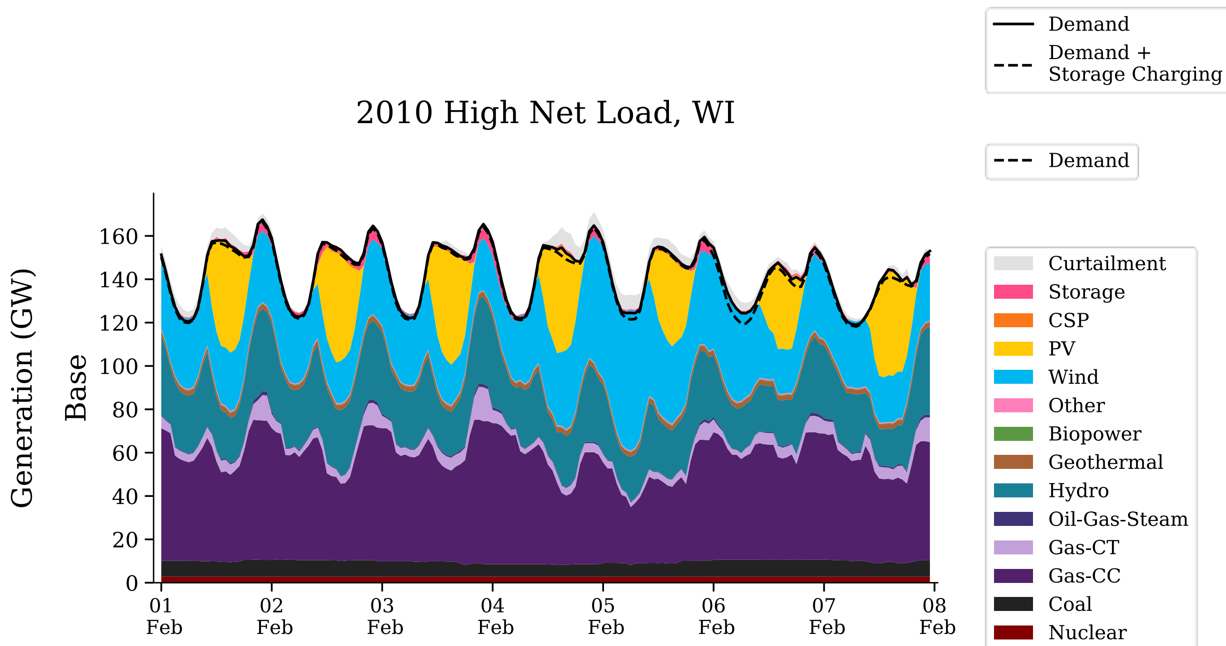

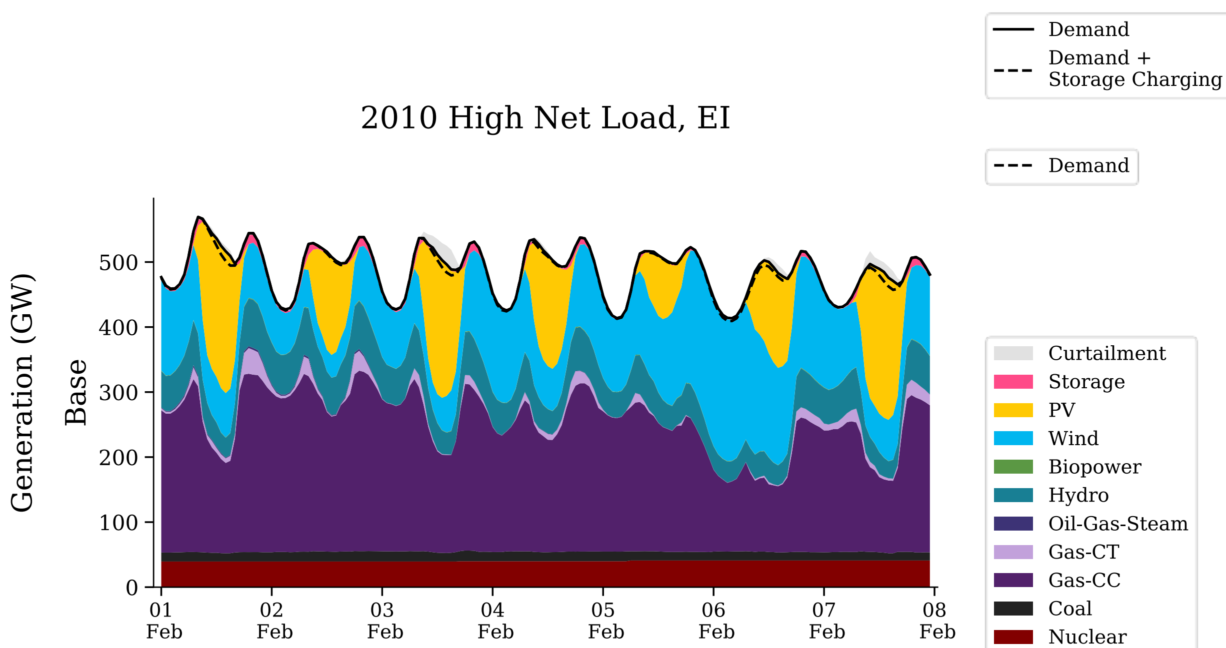

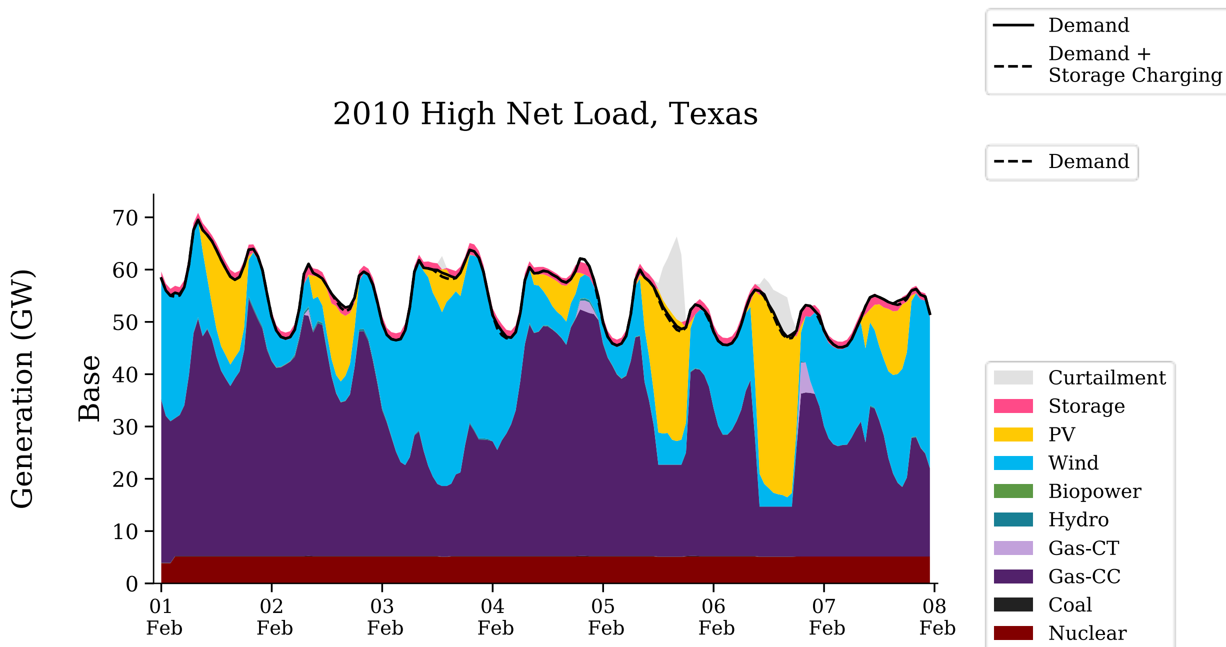

Figure A-94. System dispatch during the Lowest Net Load event for the WI (top), TI (middle), and EI (bottom)

This event caused periods of low wind and solar output across the continent, but it also brought with it below- or near-freezing temperatures, which could further reduce wind generation potential due to blade icing derates. The results from Figure A-94 show the base case assumptions, but we also investigated this event with wind generation impacted by blade icing. Figure A-95 demonstrates the impact of blade icing in the red areas of the time-series plot. During the event, icing does decrease wind generation. This might be a combination of gas-CCs and gas-CTs increasing the cost to serve load. However, icing never reduces wind generation by more than 10%. System-wide, geographic diversity provides ample resilience to icing events, but local impacts are more significant.

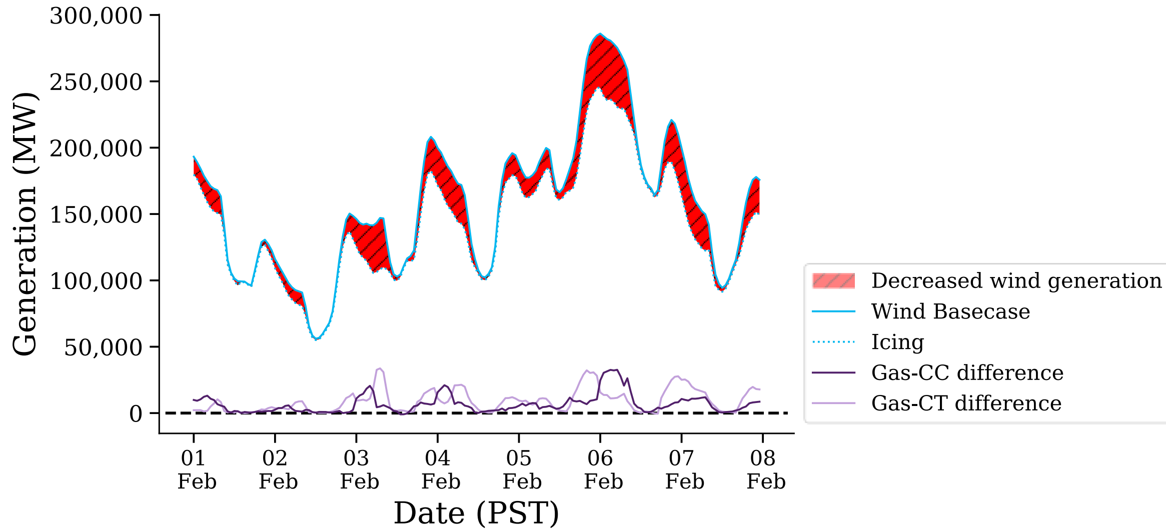

Figure A-95. Total wind generation for the full system in the base scenario and the blade icing and low-temperature shutdown scenario

The differences in gas-CC generation, gas-CT generation, and curtailment are also shown. The differences are between the base case run and the run that considered icing and low-temperature shutdowns.

Figure A-96 shows the impact to wind generation just within SPP, where the impact is much larger than the EI as a whole. On February 3 and 4, as described in the Meteorological Description, the SPP region experienced widespread precipitation events, which played a role in blade icing derates. The region experiences an even larger icing event on February 6 and 7. In this case, the region relied most on quick-start gas-CTs to fill the gap of the icing derated wind generation. Further modeling is needed to explore the impacts of forecasting icing events in order to fully understand the costs and resilience implications of widespread icing in particular areas of the interconnection.

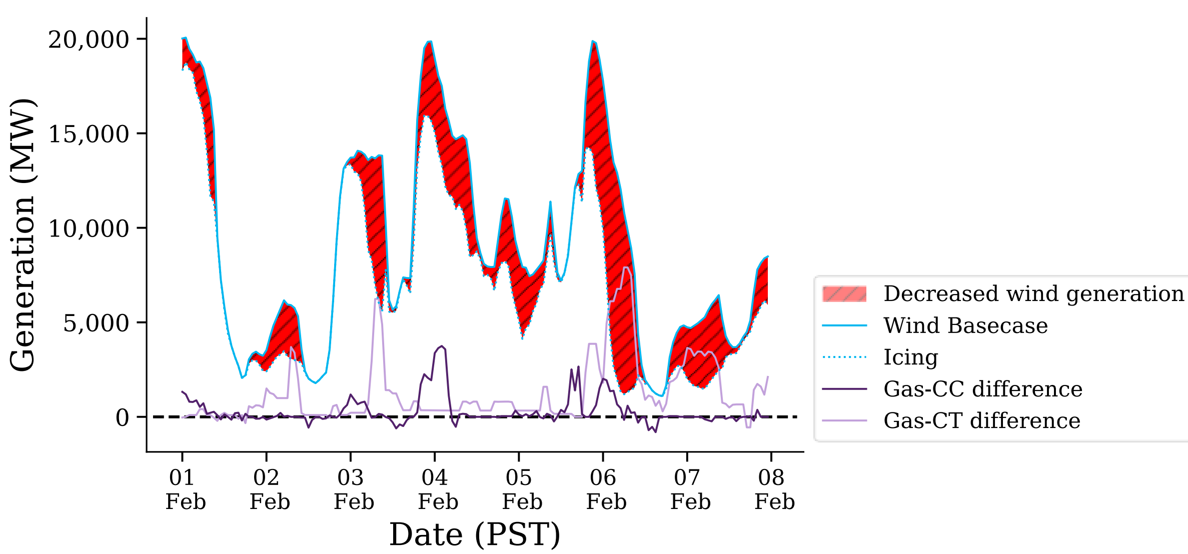

Figure A-96. Total wind generation for the full system in the base scenario and the blade icing and low temperature shutdown scenario.

The differences in gas-CC generation, gas-CT generation, and curtailment are also shown. The differences are between the base case run and the run that considered icing and low temperature shutdowns.

Summer Net Load: August 8–11, 2010

Event Summary

This event features a period of otherwise benign weather where temperatures are warm but not extreme, resulting in above normal but not extreme demand, low wind generation, and near normal solar generation. Together, these factors result in net loads on the EI that are in the upper end of the seasonal and annual distribution of net loads.[44]

Meteorological Description

From the perspective of the mid-latitude climate that the CONUS typically experiences, the period of August 8th through the 11th is unusual because of the stagnant, inactive weather pattern. The upper-level jet stream flow largely migrates northward into Canada, leaving almost the entire country under a strong upper-level high pressure system, with very little pressure gradient from the surface or at any level (Figure A-97).

There are essentially no dynamics driving the weather, and Figure A-97 shows that the country is largely devoid of frontal boundaries, storms, pressure gradients, and areas of precipitation, especially on the 8th and 9th. In short, the situation is more suggestive of the tropics than the midlatitudes. Note, however, that moderate to heavy precipitation (not shown) does occur each day along the weak features that are marked on each map. This precipitation, which is all convective, is driven by daytime heating destabilizing the atmosphere, and the weak troughs and fronts serve as triggers where convection can break through the atmospheric "cap" and develop into local thunderstorms. The primary areas affected are the Great Lakes, Florida, the Gulf Coast, the Four Corners, and the Intermountain West, where weak monsoon flow is occurring. On the 10th, the thunderstorms also impact the western Plains.

The temperature plots, even given the inactive nature of the weather pattern, are remarkably consistent from day to day. Temperatures across the west are generally running 1°F–6°F below normal during the first 2 days of the period, and trending toward normal in the second 2 days, with the desert southwest warming above normal by the 11th. The Plains are generally 5°F–11°F above normal and the eastern part of the country is 3°F to 10 °F above normal with an upward trend in both areas, especially the east. Southeastern Texas is 14°F–17 °F above normal with a weak upward trend. Meanwhile, major cities in Florida are slightly below normal due to thunderstorm activity early in the period and return to normal in the last 2 days of the period.

[44] See "Daily Weather Maps, Sunday August 8, 2010," https://www.wpc.ncep.noaa.gov/dailywxmap/index_20100808.html.

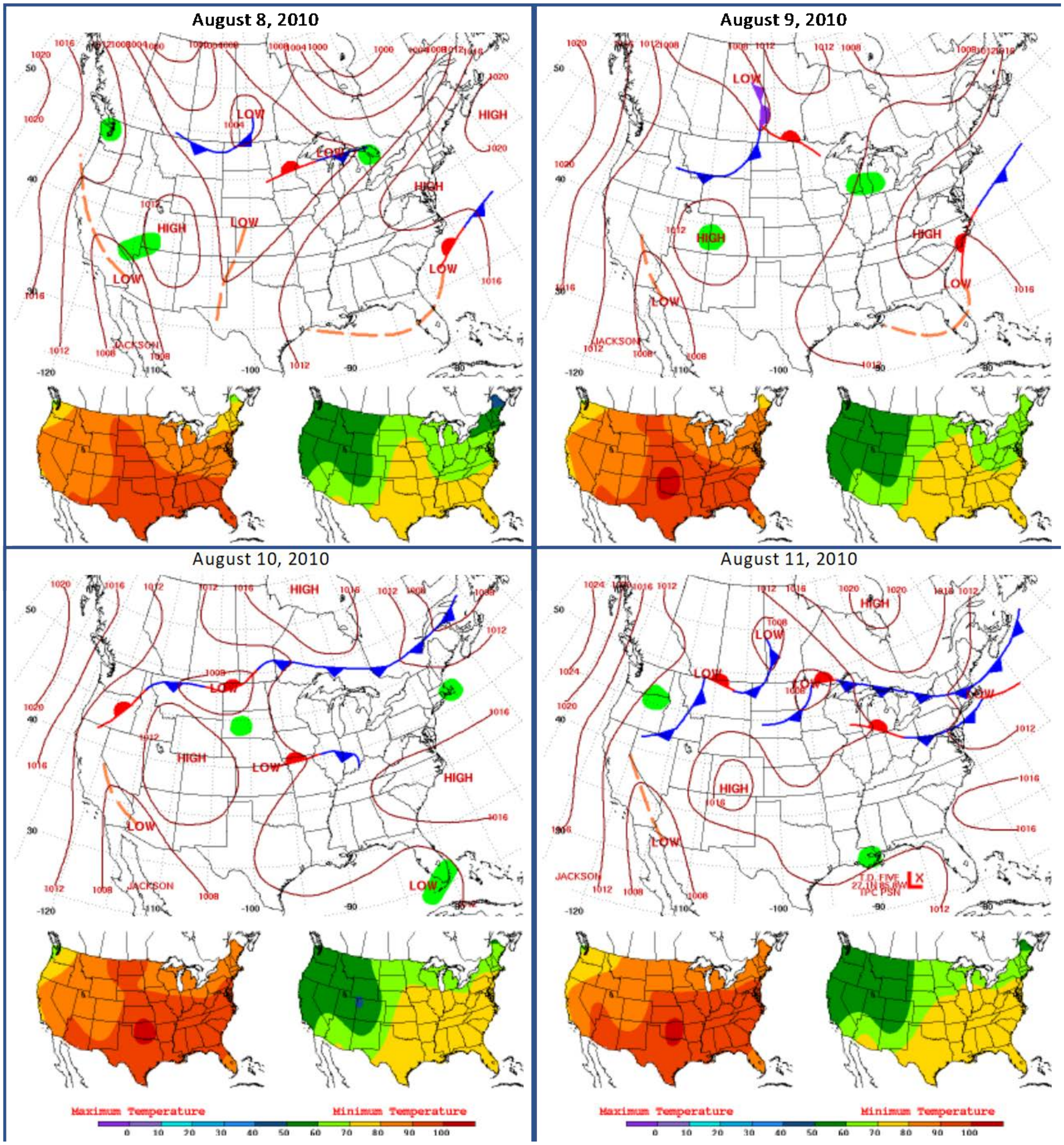

Figure A-97. Surface weather and temperature maps valid at 7 a.m. EST

See the Event Description Structure section for plot details.

Source: "Daily Weather Maps: Sunday, August 8, 2010," NOAA Weather Prediction Center, https://www.wpc.ncep.noaa.gov/dailywxmap/index_20100808.html

Load Impacts

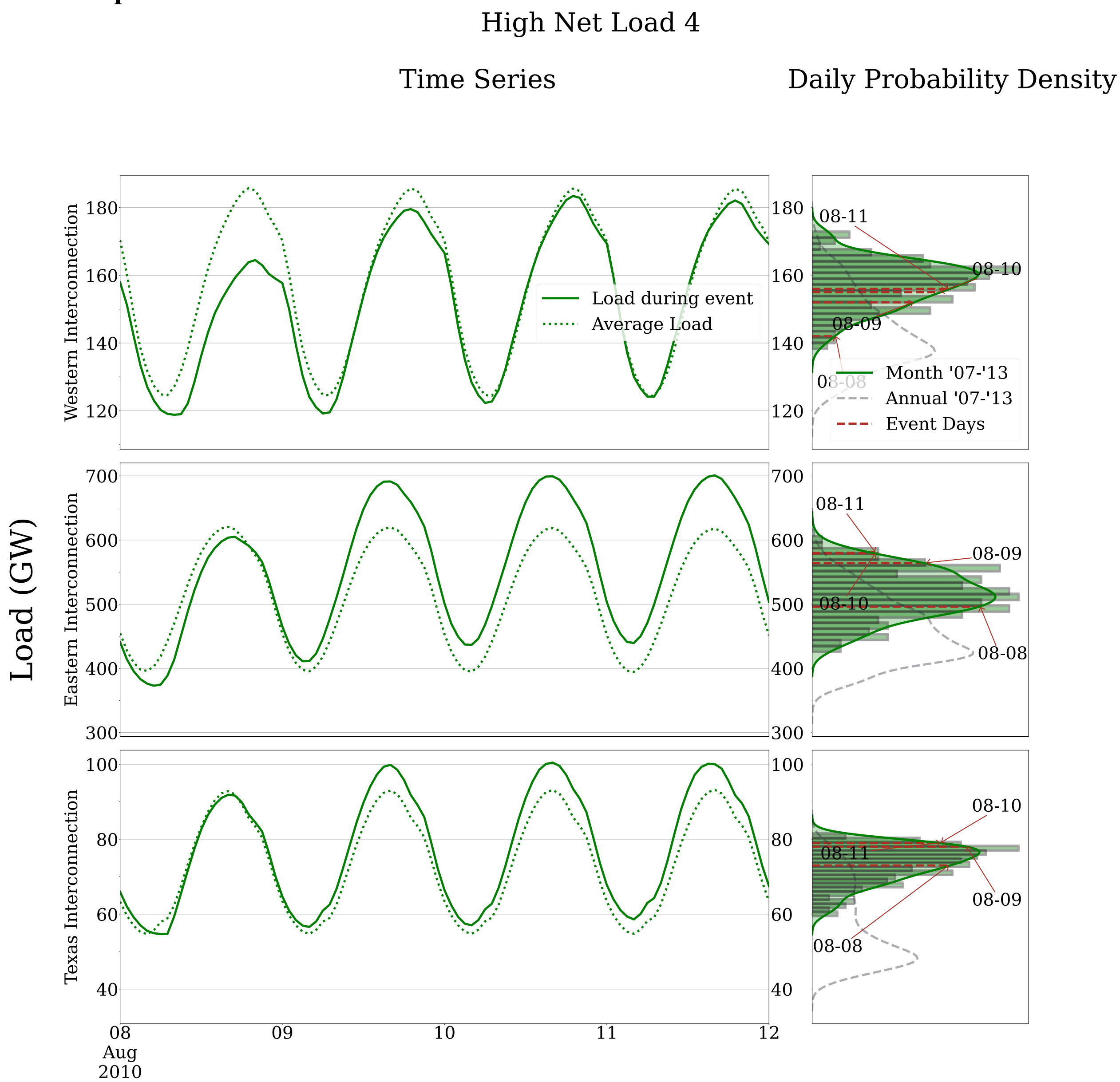

Figure A-98. Time series of regional load during the 4-day event in green, compared to load averaged across the 7-year data set for the month surrounding the event in grey (left) and distribution of 2050 regional loads for the 29 days surrounding the middle of the event in green, and across the 7-year data set in grey, with the event days labeled (right)

As expected, based on the consistent countrywide temperature profile, load in the WI is below normal but increasing. Load in the EI is below normal on the 8th and trends higher to become well above normal on the 10th and 11th as the heat increases in the major East Coast load centers. The load evolution is similar in the TI, with slightly below-normal load on the 8th that migrates above normal on the 9th and increases through the 11th, though it is much closer to typical than in the EI.

Wind Generation

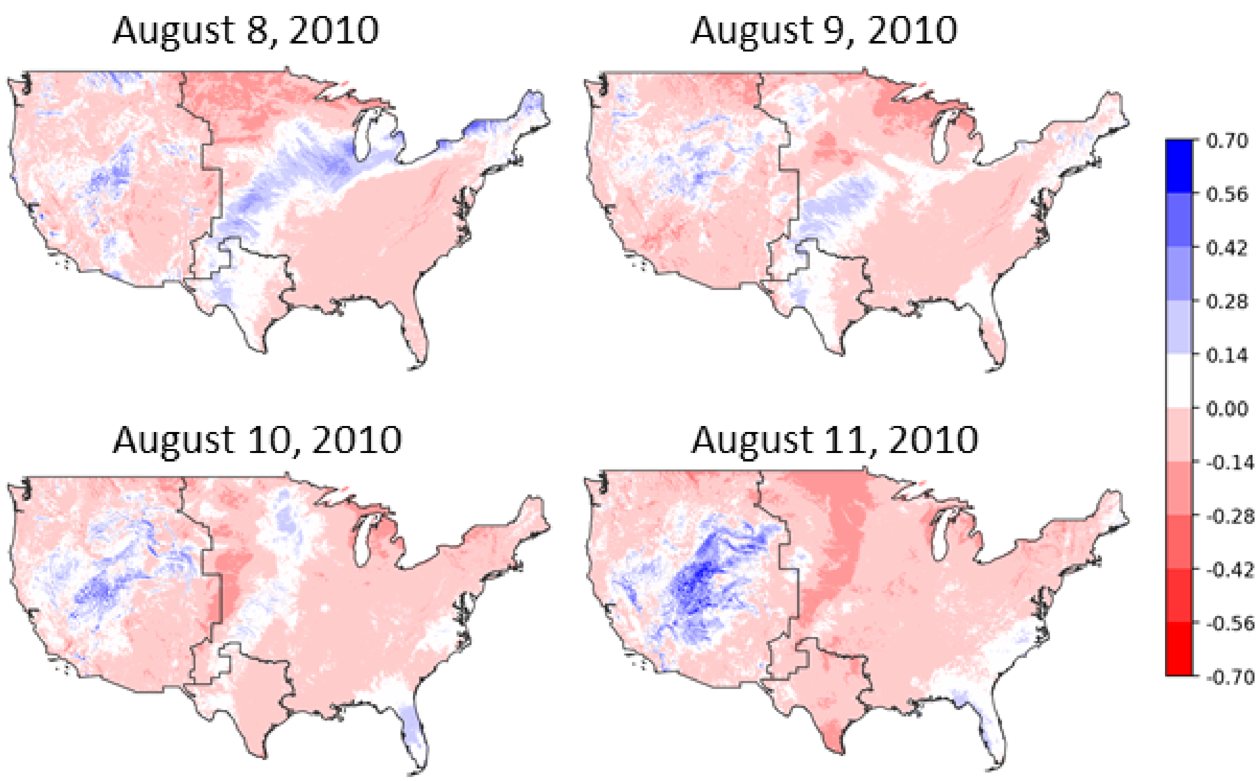

Figure A-99. National daily average wind resource deviation during the high net load event

The EI sees below-normal wind resource deviations covering a large area on all days of the event (Figure A-99), and the largest impacts occur on the 10th and the 11th. Generation on those 2 days is well below normal, with a minimum on the 11th around 10 GW at midday. The deviations are not as large on the 8th and 9th, and they are partially mitigated by a large area of above-normal wind resource across a swath of the Midwest and New England that is home to a large amount of modeled 2050 wind capacity.

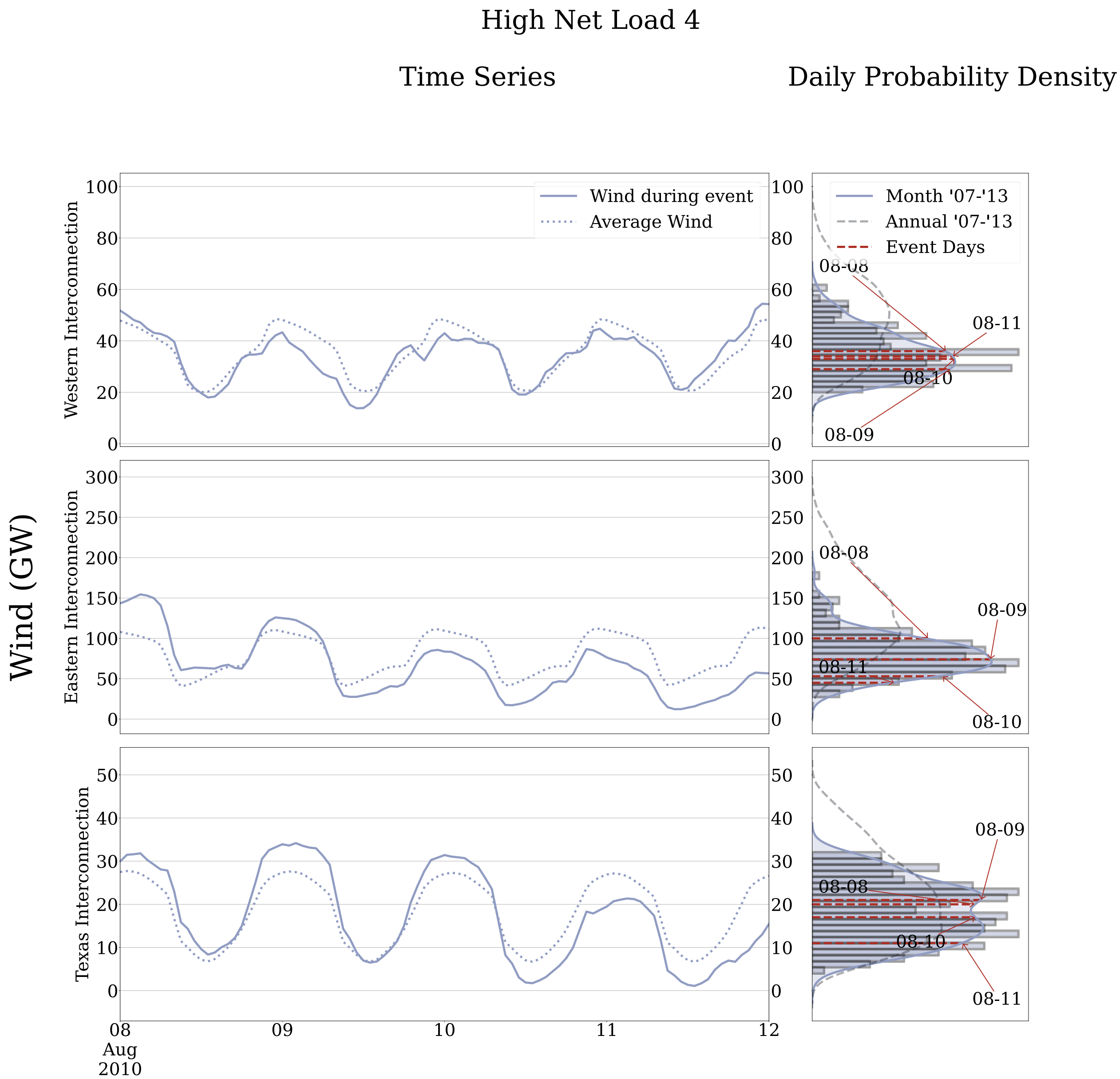

Figure A-100. Event regional wind generation (based on 2050) in context of the distribution of generation for the surrounding month (left) and time series plots of wind generation under the 2050 scenario, relative to normal for the season (right)

TI wind is generally near normal through the period, though it does move from slightly above normal to slightly below normal. As anticipated given the lack of mid-latitude storms throughout the period, the wind pattern follows the diurnal average, and only the amplitude changes as conditions become less favorable for the prevailing low-level jet activity across the Midwest. Wind in the WI is near normal, as much of the wind generation in the west in the summer is driven by regional sea-breeze and mountain-valley circulations, and the overall pattern is onshore and conducive to generation.

Solar Generation

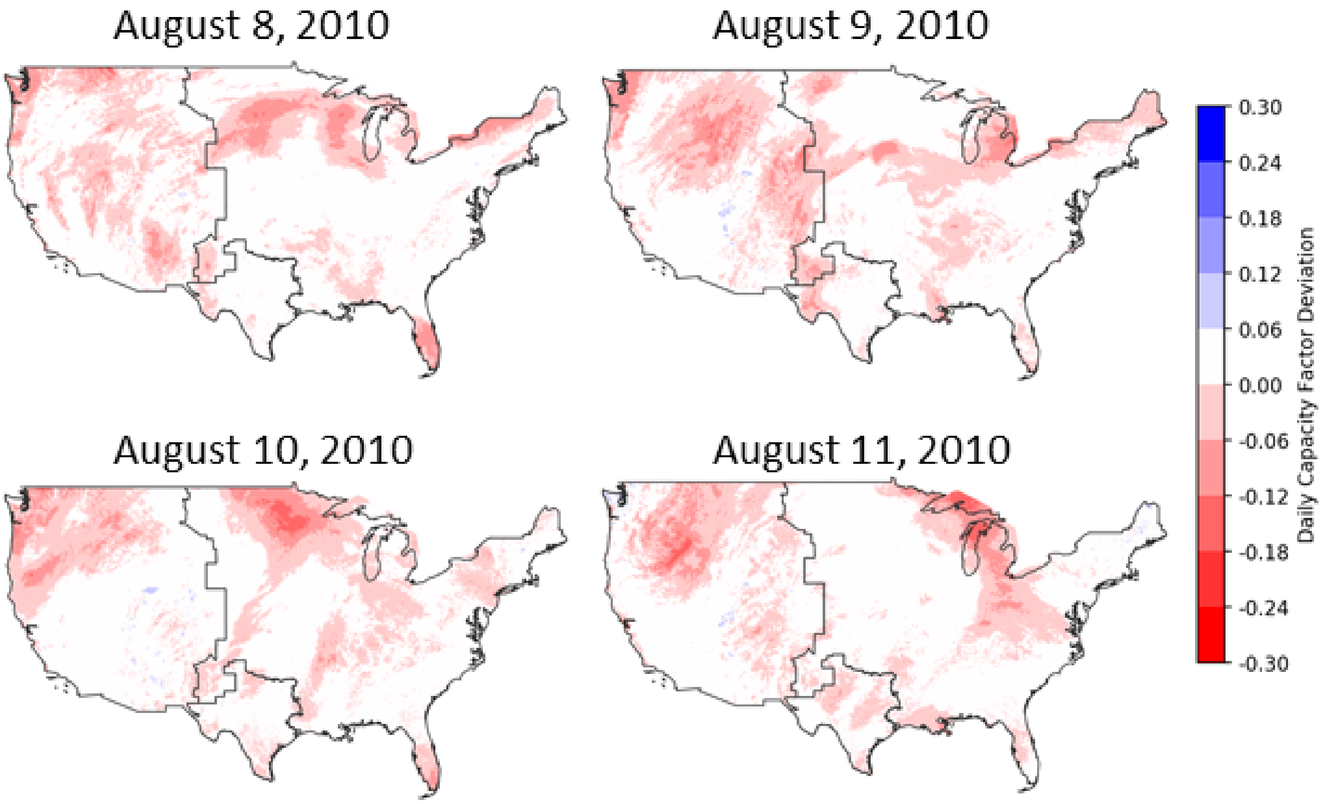

Figure A-101. National daily average solar resource deviation during the high net load event

As should be expected given the season and the lack of weather across the country, solar generation is slightly above normal across the CONUS. The broad high pressure yields cloud-free skies in the morning. However, the lack of any weather systems is a double-edged sword for solar resource. While low-pressure systems bring clouds and precipitation, the sinking air and building high pressure behind them create stable conditions that inhibit the daytime cumulus formation. Shallow cumulus in of itself reduces solar generation, but when uninhibited, the humid air that tends to exist across the United States due to flow off the warm Gulf of Mexico and the East Coast Gulf Stream commonly leads to thunderstorm development. During this period, the impact of the clearer skies due to lack of active large-scale storm systems is somewhat offset by the reduction in insolation in the afternoon due to afternoon cumulus and thunderstorm clouds. This can be seen in Figure A-102 where generation is seen to decrease faster than the average curve during the afternoon hours.

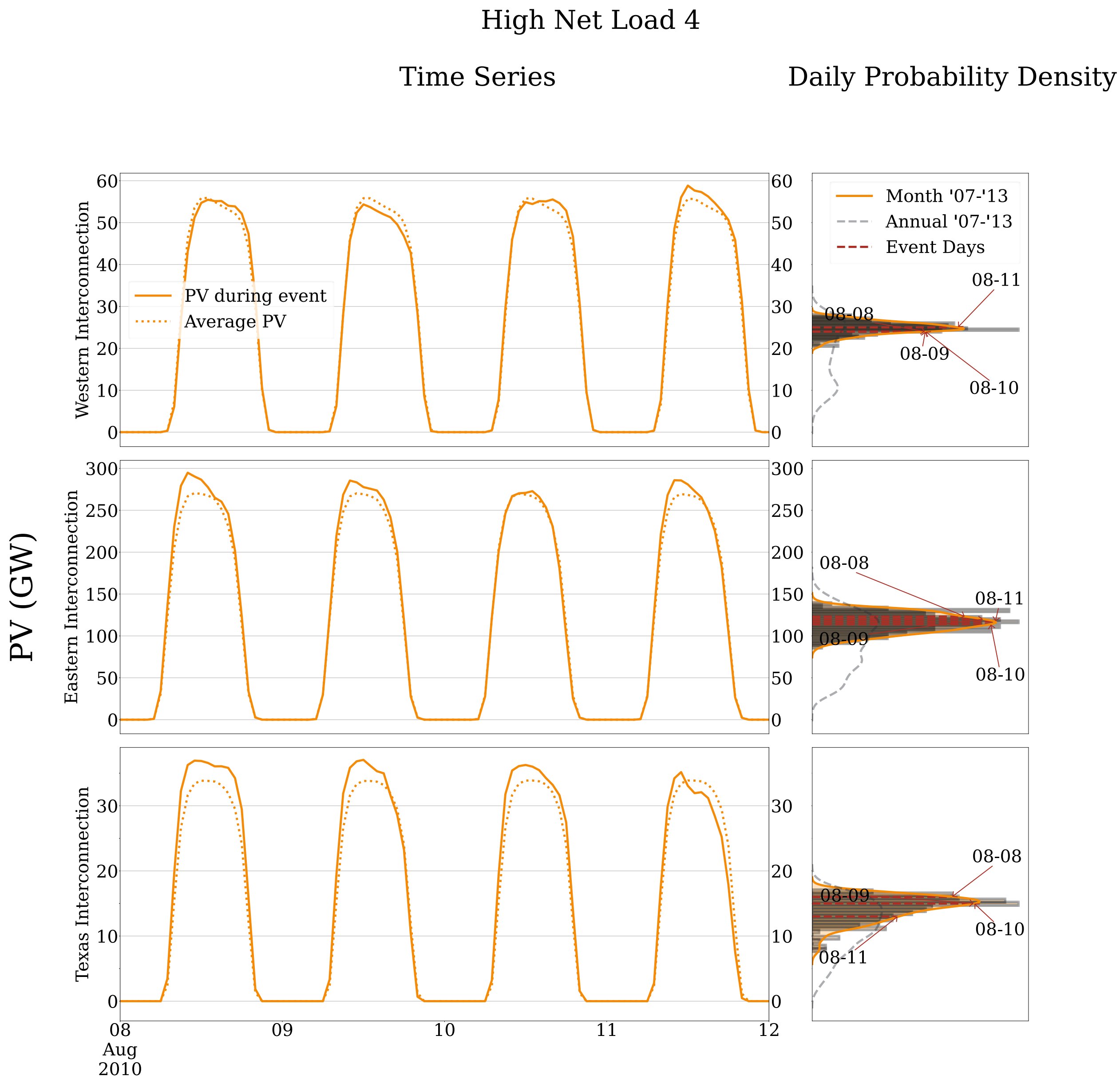

Figure A-102. Event regional modeled 2050 PV generation in context of the distribution of generation for the surrounding month (left) and time series plots of PV generation under the modeled 2050 scenario, relative to normal for the season (right)

Net Load

This event is of interest because while load is high, especially on the EI, it is not extreme. At the same time, while wind resource is low, it is also not extremely low relatively to the surrounding month in the multiyear data set and solar is near normal on all interconnections. Yet Figure A-103 shows net load is in the extreme tail of the distribution on the EI for the 11th and the 10th is also very high, while concurrently the 11th is also a very high net load day in the TI.

These days are in the high net load distribution tail, even though they are not extreme load, wind, or solar days, because in the late summer months wind generation on the EI is at a seasonal low, with a median of only about 75 GW compared to double that in the winter months and has a tight distribution that declines steeply to the left of the median; the median generation on the 11th was less than 45 GW. Meanwhile, summer has periods where load peaks on the EI, with a rapidly declining tail. This means a large-but-not-extreme downward deviation in renewable generation can push a high-but-not-extreme load into the extreme tail of the net load distribution.

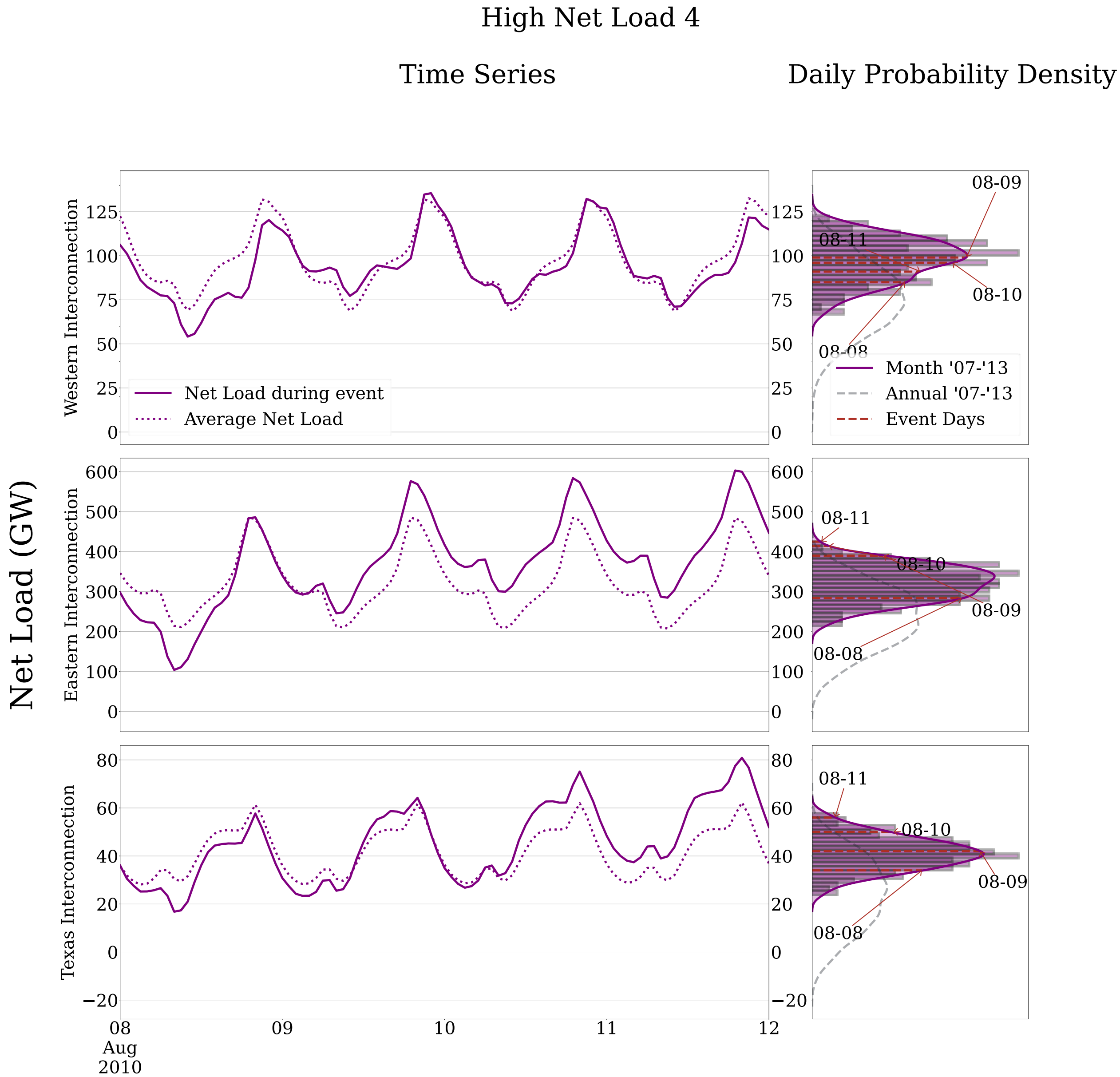

Figure A-103. Event regional modeled net load context of the distribution of generation for the surrounding month (left) and time series plots of modeled net load under the modeled 2050 scenario, relative to normal for the season (right)

Further, the diurnal amplitude of the load is high at this time of year at about 220 GW from lowest to highest point on a typical day as compared to winter where it is closer to 100 GW. Therefore, rapid changes in available wind, and to a lesser extent solar, can create large requirements for additional generation. This is best observed in the EI in Figure A-103 from the morning through the evening of the 8th where the reduction in wind output combined with the diurnal load and solar pattern led to a 400 GW swing in net load over a period of about 15 hours.

System Modeling

As demonstrated in the previous sections, this event causes particular issues in the EI. High, but not extreme high load, coupled with low, but not extreme low wind resource, create two of the highest EI net load days in the data set on August 10th and 11th 2010. The following analysis will focus on the EI to explore how the system's response changes as the VRE penetration increases.

Eastern Interconnection Operations

Figure A-104 shows the generation dispatch of the EI during this period. On a whole, operations do not look to be all that distinct from other high load events in the summer. Cycling diurnal of Gas-CC and Gas-CT units is common balance the system around the daytime PV generation, while hydropower shifts its operations as the penetration of wind and solar increase to more closely track a tighter and peakier net load peak in the late afternoon.

However, what makes this event unique is how low the wind resource gets across the EI. During the daytime hours on August 10th and 11th, the fleetwide capacity factor of wind in the EI falls to 5% and 4% respectively. Fortunately, from a balancing and resilience perspective, PV generation is normal for this time of year across the interconnection and fills in the gap left by the wind. As the sun sets across the interconnection between 7pm-9pm EST, the wind resource has picked back up, never dropping below a fleetwide capacity factor of 11% (August 11th at 7pm) and averaging 25%. This pickup is key, particularly in regions with large shares of wind generation capacity.

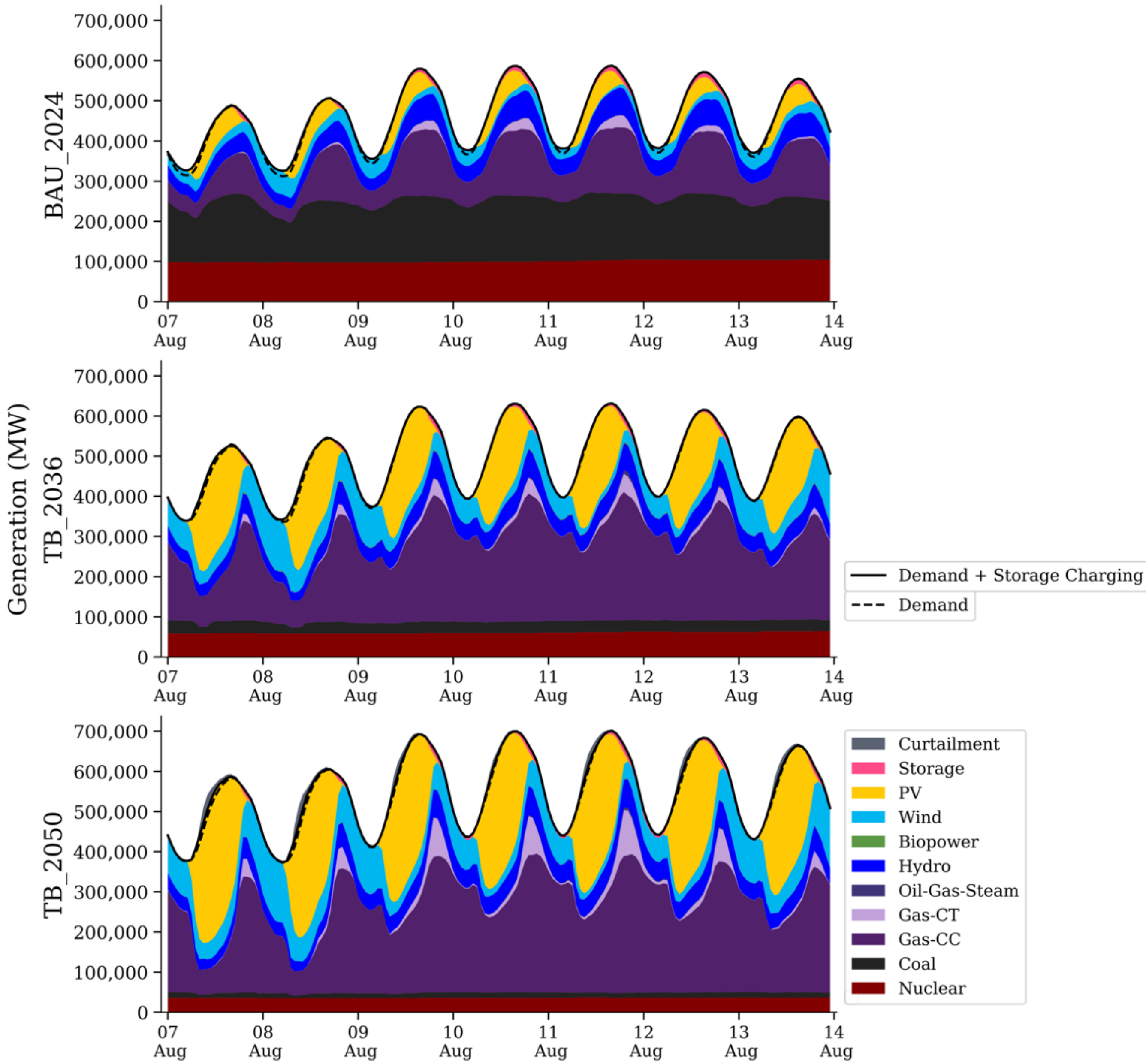

Figure A-104. Generation dispatch for the EI for three future infrastructure years—2024 (top), 2036 (middle), and 2050 (bottom)—during a period of high net load from August 7 to August 13, 2010

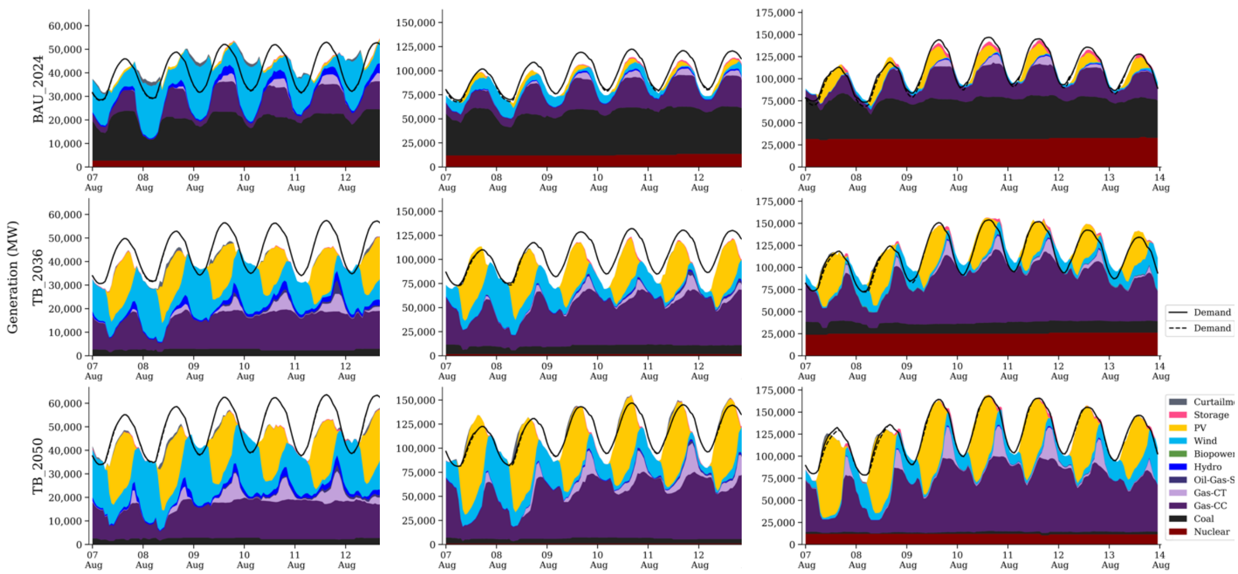

Figure A-105. Generation dispatch for SPP (left column), MISO (middle column), and PJM (right column), for three future infrastructure years—2024 (top), 2036 (middle), and 2050 (bottom)—during a period of high net load from August 7 to August 13, 2010

Figure A-105 shows the dispatch stacks for SPP, MISO, and PJM. All three regions have high penetrations of wind, SPP in particular. For MISO and PJM, operations look similar to the rest of the interconnection, strong PV resource makes up for the very little to no wind generation in the middle of day. Gas-CCs are cycled around the PV resource and quick start Gas-CTs turn on at the net load peak as the wind picks up a bit in the evening and overnight hours.

SPP, on the other hand, ends up closer to dropping load during this event than any other region. Figure A-106(a) shows the offline available thermal capacity (i.e. thermal capacity that is not committed and not on a planned/forced outage), in SPP throughout the event. In 2036 and 2050, at 8pm EST on August 11th there is nearly no offline thermal capacity available in SPP. Also as this time, imports from MISO have dropped to zero from a high of 9 GW a few hours earlier, as seen in Figure A-106(b). SPP is on its own, PV generation is quickly ramping down as the sunsets, and it lacks additional thermal capacity to turn on. At this same time, wind is ramping back up; at 8pm EST SPP's wind has a combined capacity factor of 22%, up from 5% only 6 hours earlier. During this event, SPP's wind follows a more typical pattern for wind generation in the EI, picking up in the evening and overnight. This is not the case for MISO. MISO wind reaches a maximum of 9% fleetwide capacity factor overnight, while SPP reaches 58% in the early morning hours of the 12th. SPP's wind recovers enough that it actually is able to both turn thermal units off and export power to MISO.

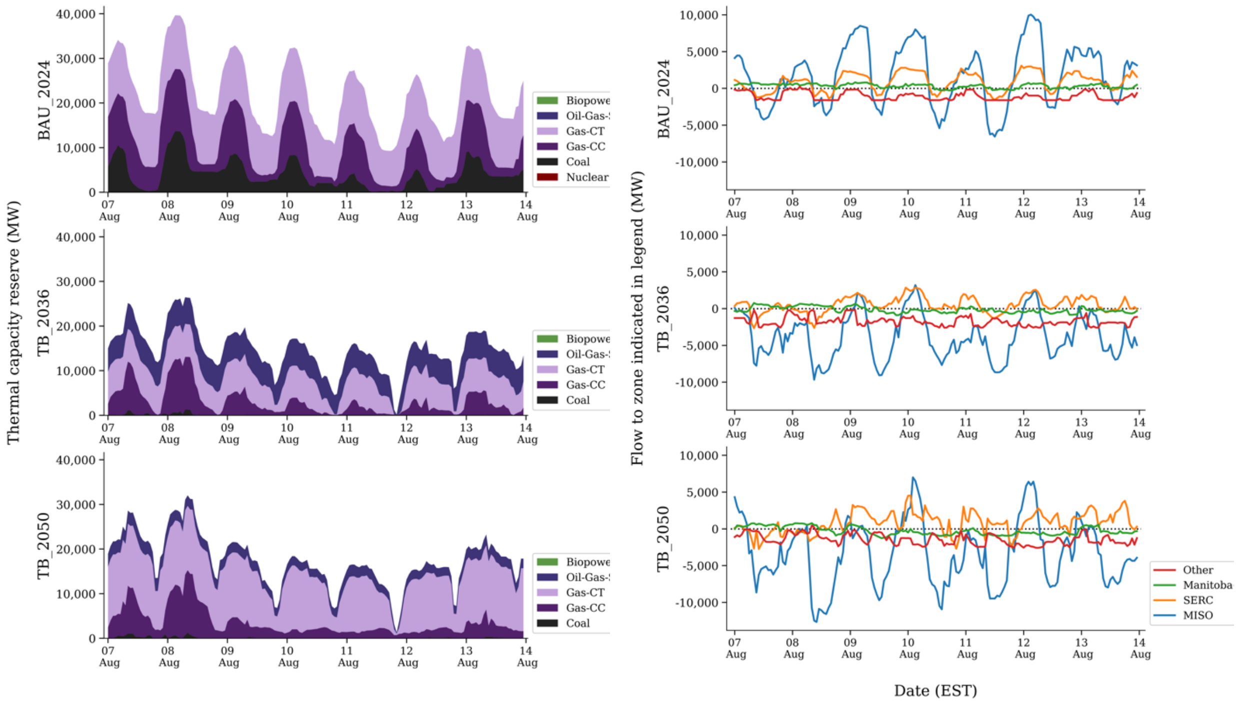

Figure A-106. (a) Offline thermal capacity reserve in SPP, and (b) Net power flow between SPP and its neighbors during a period of high net load from August 7 to August 13, 2010

Positive flow means an export from SPP to its neighbor.

Impacts Summary

In the EI, nearly the highest net load days within the data set on August 10th and the 11th in 2010. The high net load is driven by low wind resource and high load. In most regions, there is adequate thermal capacity to turn on, particular in the hours after sunset, to serve all load. SPP, however, exhausts its thermal capacity on the evening of the 11th in both the 2036 and 2050 infrastructure scenarios, relying on their stronger wind resource to ensure balancing. This case demonstrates how careful planning and an understanding of the regions VRE resource can ensure reliable operations without an overbuilt generation or transmission system. However, to truly understand the risk and system stress this type of weather event may cause to a system like SPP, we recommend more uncertainty analysis to ensure the system is truly robust and resilient. Only hours earlier to SPP exhausting its available offline thermal reserve, the wind resource was hovering near zero at 4-5% fleetwide capacity factor. While SPP's wind recovered by the time the net load peak hit, MISO's wind had not. If the timing of SPP's evening wind ramp-up occurred even an hour later, or was forecasted differently, SPP may have been forced to drop load to maintain system stability.

Lowest Net Load: April 17, 2011

Event Summary

The type of conditions present on April 17, 2011, were not unusual, but the combination of seasonally mild temperatures, low demand, and widespread strong generation from both wind and solar resulted in the lowest CONUS-wide net load observed in the 7-year data set.[45]

Meteorological Description

On April 16th, the western CONUS is under the influence of a weak, low-amplitude upper-level ridge with moderate zonal (west-to-east) flow north of 40 degrees. A shortwave trough (area of cyclonic vorticity) is moving into the Pacific Northwest. This is conducive to generally quiet conditions across the west, except for a weak surface low and cold front moving through the Pacific Northwest. East of the Rockies, a moderately strong upper-level trough that is lifting northeast is responsible for the fairly strong but occluding surface low over the Great Lakes region. The Gulf of Mexico is open (i.e. there is access to lots of moisture), and the east is experiencing lots of clouds and precipitation. Except for the lee of the Rocky Mountain and northern Midwest, most of the country is above freezing all day on the 16th.

The low-amplitude jet stream pattern continues into the 17th, with the East Coast trough weakening and lifting north, pushing the surface low into Canada and the cold front out over the Atlantic Ocean. Weak high pressure builds into the eastern part of the country behind the cold front and south of about 40 degrees latitude. When combined with high pressure in the southwest, this causes clear skies across most of the southern part of the country, with a weak frontal zone delimiting a transition to more cloudy and unsettled conditions across the northern tier. As expected with the low-amplitude flow, temperatures are stratified from south to north and are generally mild, with high temperatures mostly ranging from 50s in the northern states to low 80s in the southern part of the country. Overnight low temperatures are also mild, ranging from mostly 30s and 40s in the north to 60s and low 70s in the south.

[45] See https://www.wpc.ncep.noaa.gov/dailywxmap/index_20110417.html

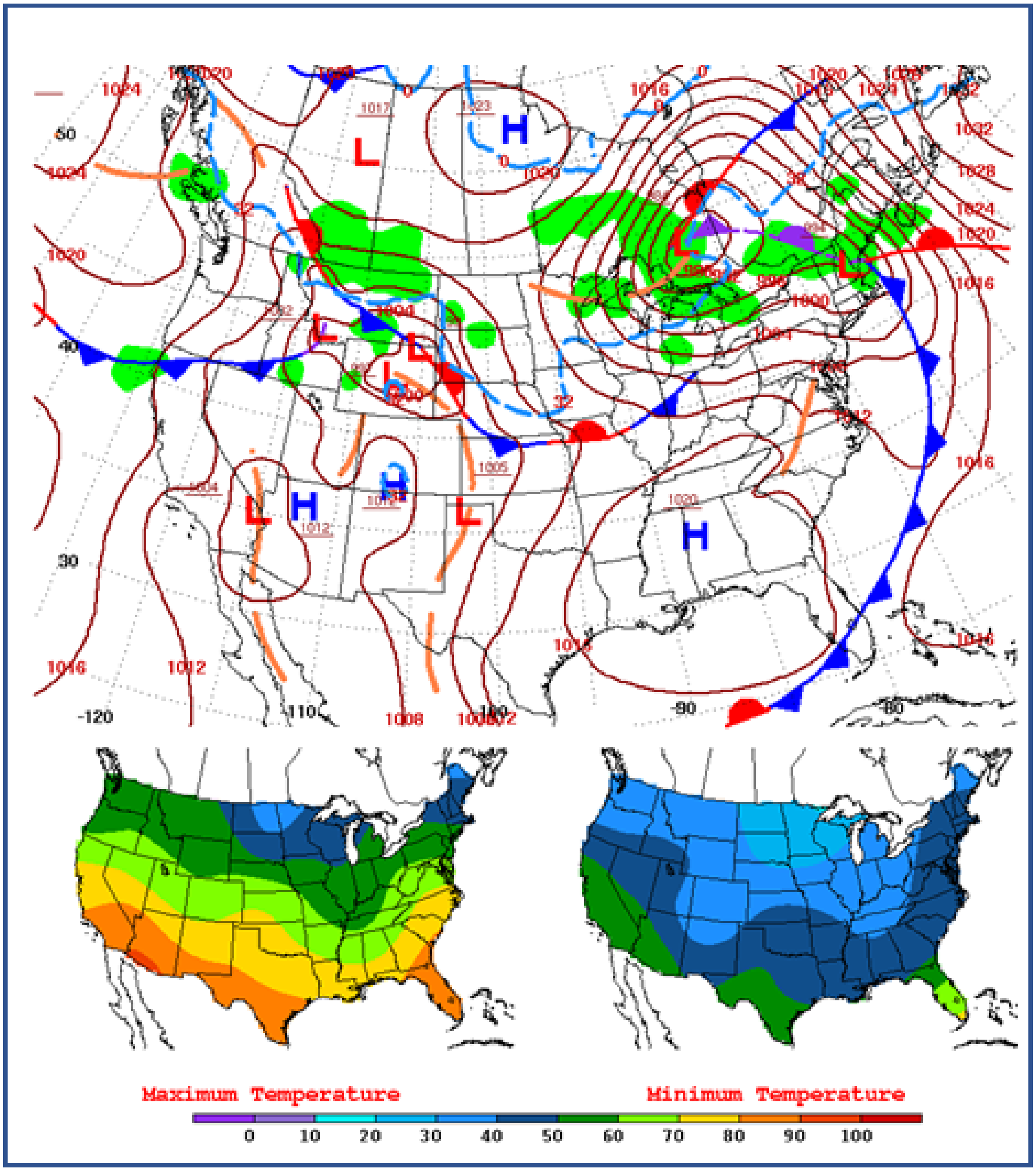

Figure A-107. Surface weather and temperature maps valid at 7 a.m. EST

See the Event Description Structure section for plot details.

Source: "Daily Weather Maps: Sunday, April 17, 2011," NOAA Weather Prediction Center, https://www.wpc.ncep.noaa.gov/dailywxmap/index_20110417.html

Load Impacts

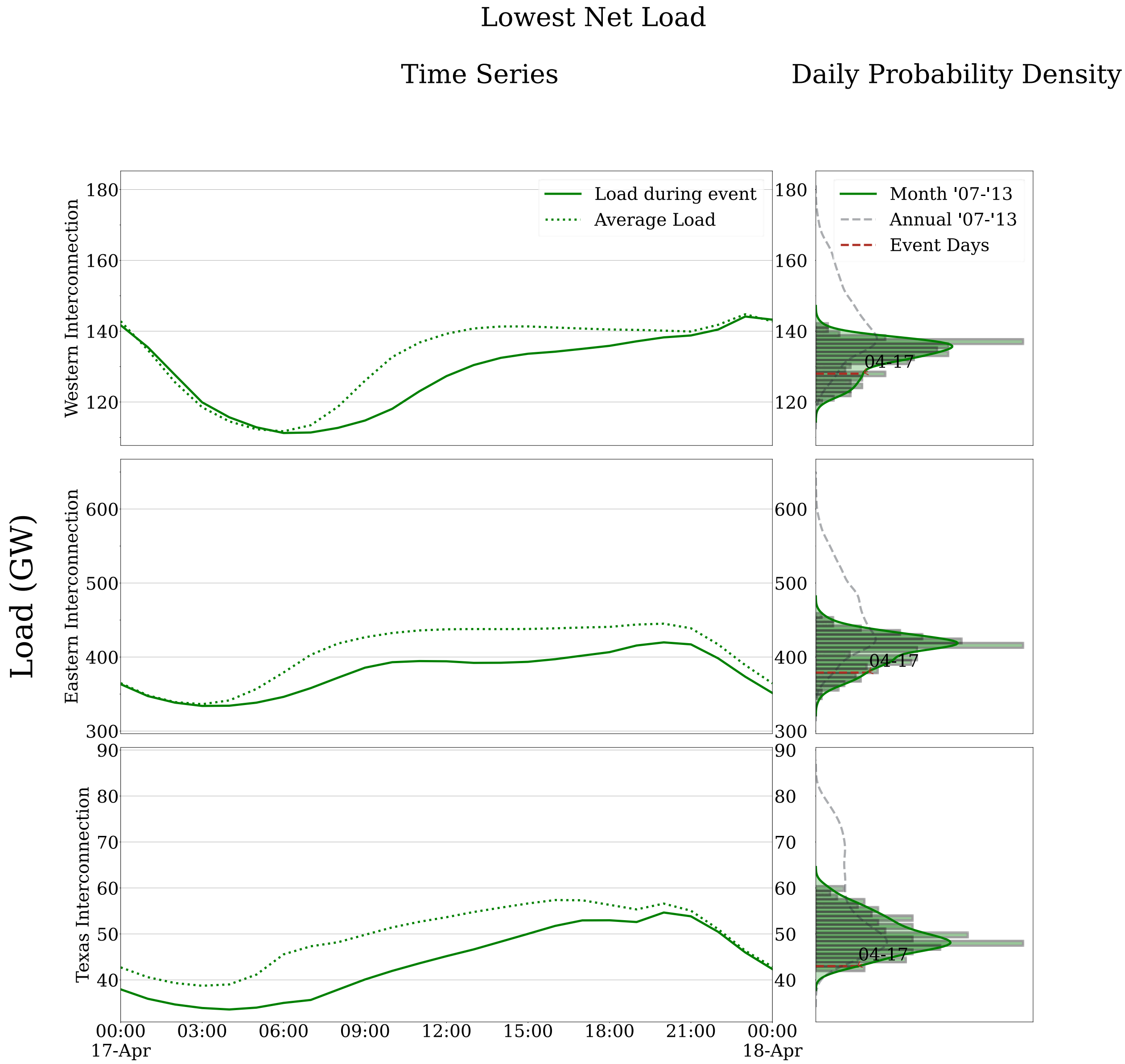

Figure A-108. Time series of regional load during the 4-day event in green, compared to load averaged across the 7-year data set for the month surrounding the event in grey (left) and distribution of 2050 regional loads for the 29 days surrounding the middle of the event in green, and across the 7-year data set in grey, with the event days labeled (right)

The meteorological factors described above result in mild temperatures and produce little heating or cooling demand, along with lots of sunshine. In addition, the 17th was a Sunday. These factors all coincide to drive low loads in all three interconnections. The load is low relative to the surrounding month, which being a shoulder month, is well below the annual median anyway. In the TI, the load is close to the lowest in the data set.

Wind Generation

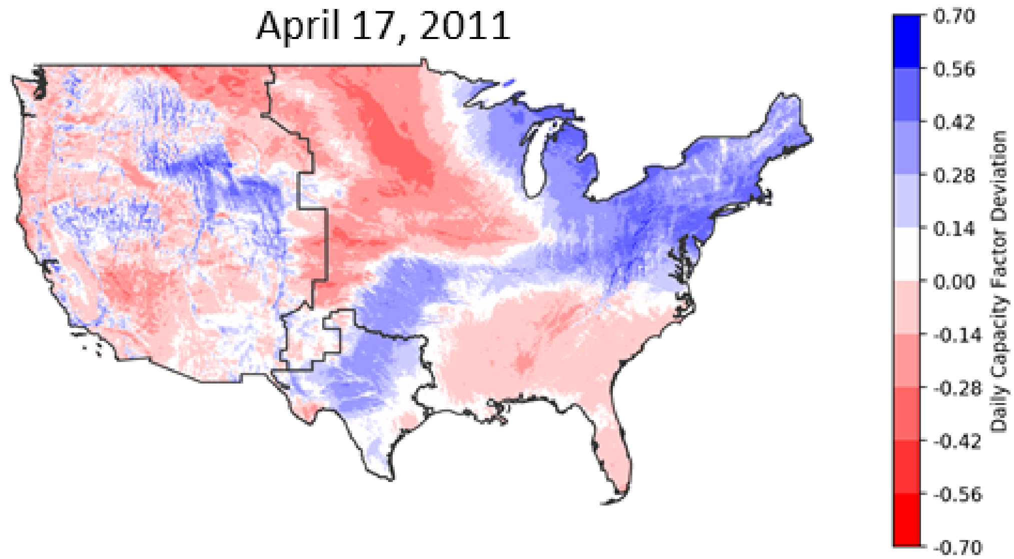

Figure A-109. National daily average wind resource deviation during the lowest net load in the record

No fill is at or up to 14 percentage points slightly above normal.

Though surface high pressure dominate the southern part of the country and there are no major storms to speak of, the wind resource across much of the country is at or slightly above-normal (Figure A-109). Although the Dakotas and Nebraska and southeast see below-normal wind resource, the positioning of high pressure in the south east and low pressure in the lee of the Rockies combined with daytime heating, work to strengthen the plains low level jet, resulting in enhanced wind generation in both the southwestern part of the EI and the TI. In addition, the area between the storm moving into Canada and the southeast high-pressure center features an enhanced pressure gradient that strengthens winds over the Ohio Valley, Great Lakes region and Northeast. These areas produce well-above-normal wind generation in the EI on the 17th based on the modeled placement of new generators.

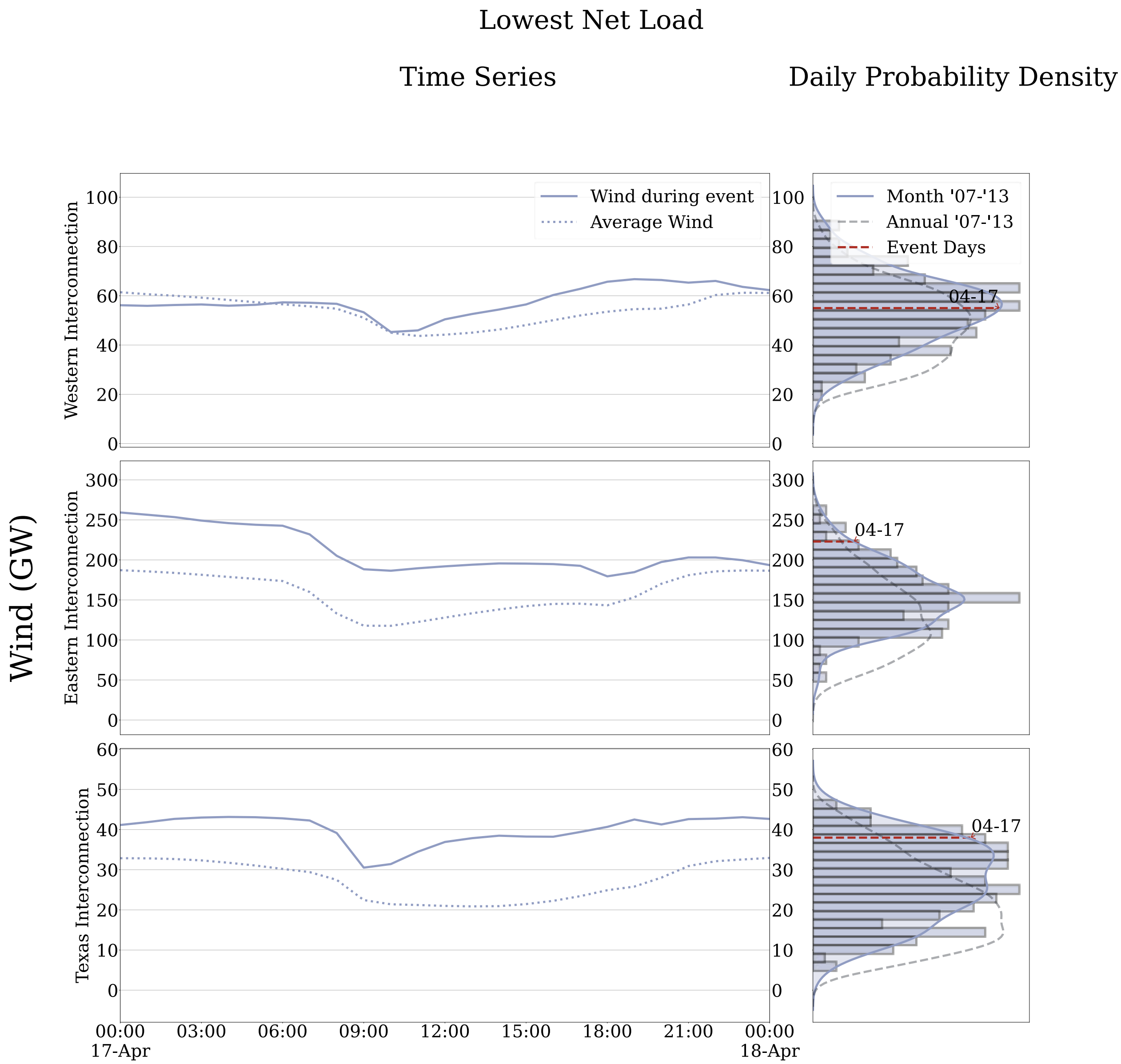

Figure A-110. Event regional wind generation (based on 2050) in context of the distribution of generation for the surrounding month (left) and time series plots of wind generation under the 2050 scenario, relative to normal for the season (right)

The wind resource in the WI is more variable, with a large area of below-normal generation ahead of the cold front moving south. However, this is compensated for by slightly above-normal generation in central and southern California under onshore flow, and in the strong onshore flow behind the front in the Pacific Northwest. As this front moves south, onshore flow strengthens behind it and this is likely the cause of the large increase in generation from just before noon. In addition, Arizona and New Mexico see enhanced resource, and all these areas have increased concentrations of modeled wind generators in 2050.

Solar Generation

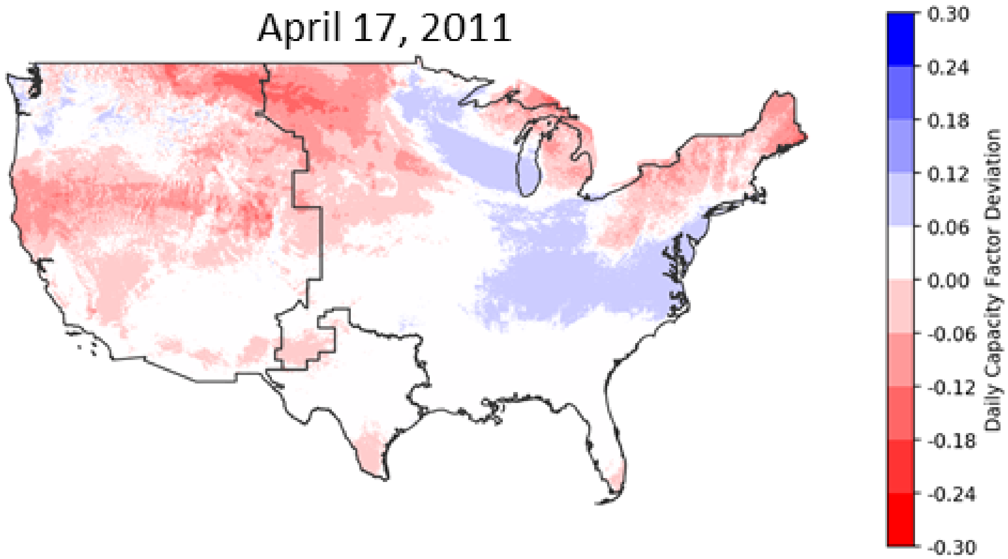

Figure A-111. National daily average solar resource deviation during the lowest net load in the record

The largely cloud-free conditions and moderate temperatures across the south provide for good PV production across a broad area (Figure A-111). Solar production is only slightly better than normal in the southwest. However, this area contains a lot of generating capacity that typically produces at high levels this time of year, so good resource here more than compensates for the reduction due to the cloud field associated with the cold front moving across northern California.

PV generation (Figure A-112) is at or considerably better than normal across most of the EI and most of the TI due to the cloud-free skies and moderate temperatures. Importantly, the best solar resource is colocated with the regions where most of the modeled 2050 PV build-out occurs; this means EI solar production is well above the median for the time of year and annually, and Texas is a little above normal.

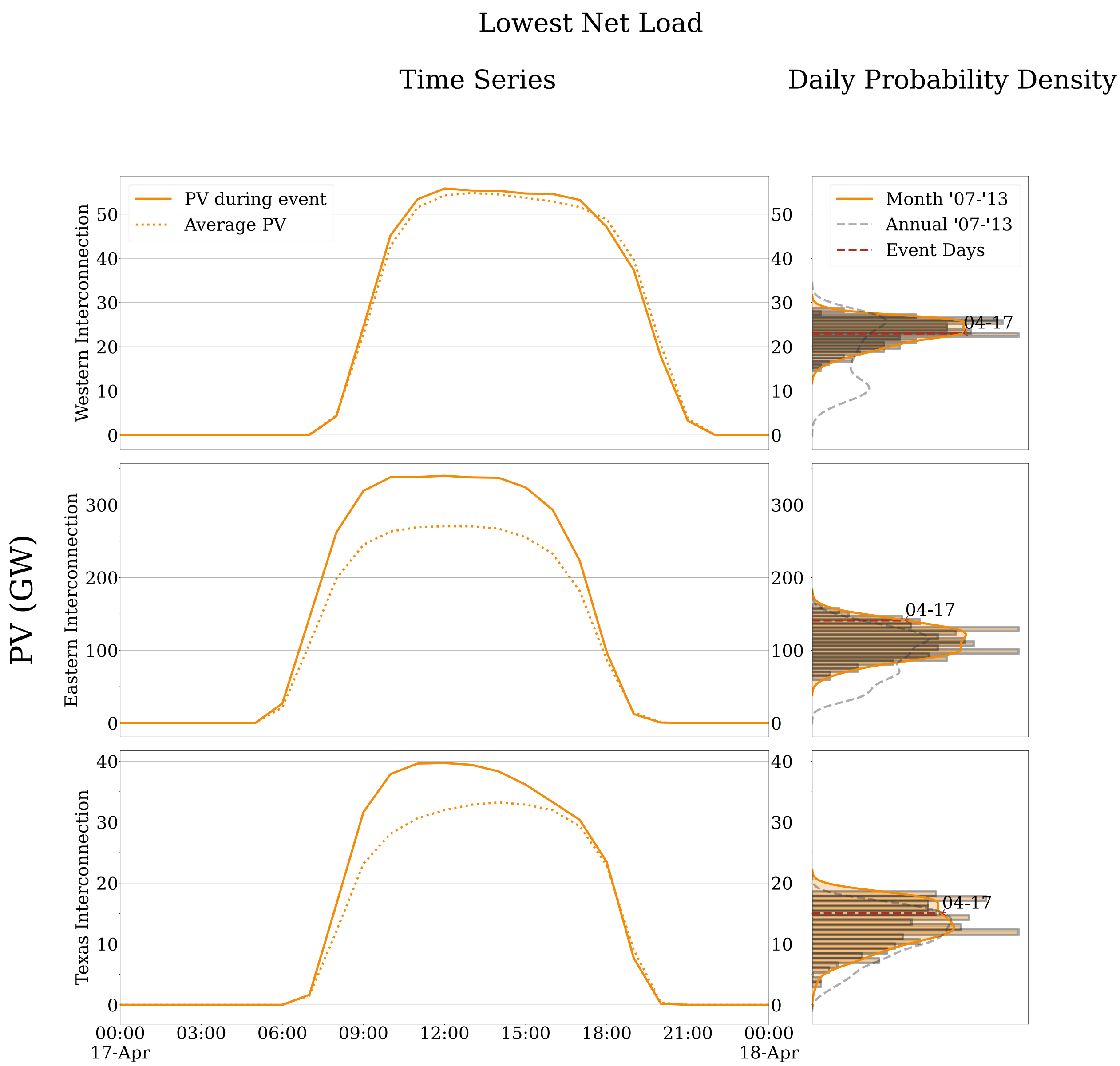

Figure A-112. Event regional modeled 2050 PV generation in context of the distribution of generation for the surrounding month (left) and time series plots of PV generation under the modeled 2050 scenario, relative to normal for the season (right)

Net Load

Mild temperatures along with typically lower weekend loads result in below-average loads on all three interconnections, though only the TI experiences load in the tail of the distribution. Also, the period experiences well above-normal renewable resources, especially in the EI and the TI. The combination of strong generation from both wind and solar pushes the net load for the CONUS to the lowest level in the entire 7-year data set. Net load in Figure A-113 is at the far low end of both the annual distribution and the surrounding monthly distribution for both the TI and EI, and they experience surplus generation of over 20 GW and over 100 GW respectively in the middle of the day. In the WI where both wind and solar were close to normal, the net load is near the median for the period, reaching a minimum of 20 GW during the middle of the day, when solar generation is greatest.

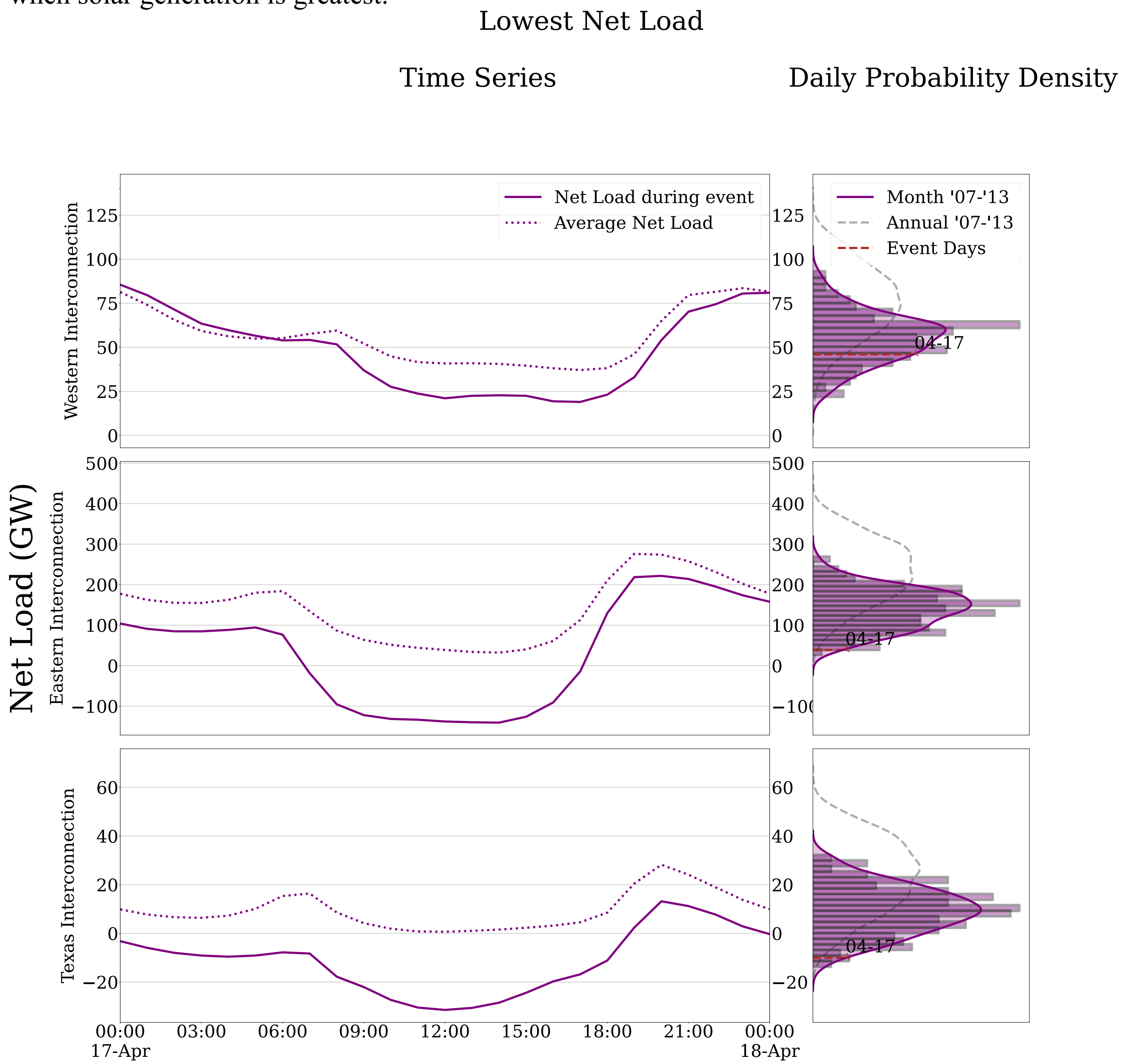

Figure A-113. Event regional modeled net load context of the distribution of generation for the surrounding month (left) and time series plots of modeled net load under the modeled 2050 scenario, relative to normal for the season (right)

An interesting feature seen in Figure A-113 is that during the multiyear period surrounding April 17, the daily volume of renewable supply is equal to demand on many days, and renewable supply exceeds load in a significant part of the TI, implying generation would be exported, curtailed, or stored if possible.

System Modeling

For this event, we completed PCM simulations for the 2050 infrastructure year and two sensitivities on the 2050 base case. The other two scenarios adjusted the availability or flexibility of hydropower plants. We included different hydrological years to change the energy available to dispatchable hydropower units that reflect a dry year (2011) was already a "wet" hydropower year. For flexibility changes, we included a scenario where dispatchable hydropower units were less flexible than the base case.

Figure A-114 shows the system dispatch for the week around the lowest net load day for all three interconnections. During this week, wind and solar meet 65% of all load. During such low net load conditions, VRE curtailment is high. System-wide curtailment for the week is 13%, and it is highest in the TI, where curtailment reaches 17% for the week. Curtailment is highest in the middle of the day, coincident with high wind and solar generation. In the EI and the WI, very little curtailment occurs overnight; however, the TI continues to see high, but lower, curtailment overnight even with nearly all non-nuclear thermal generation shut down. Curtailed wind and solar provide all operating reserve during these hours.

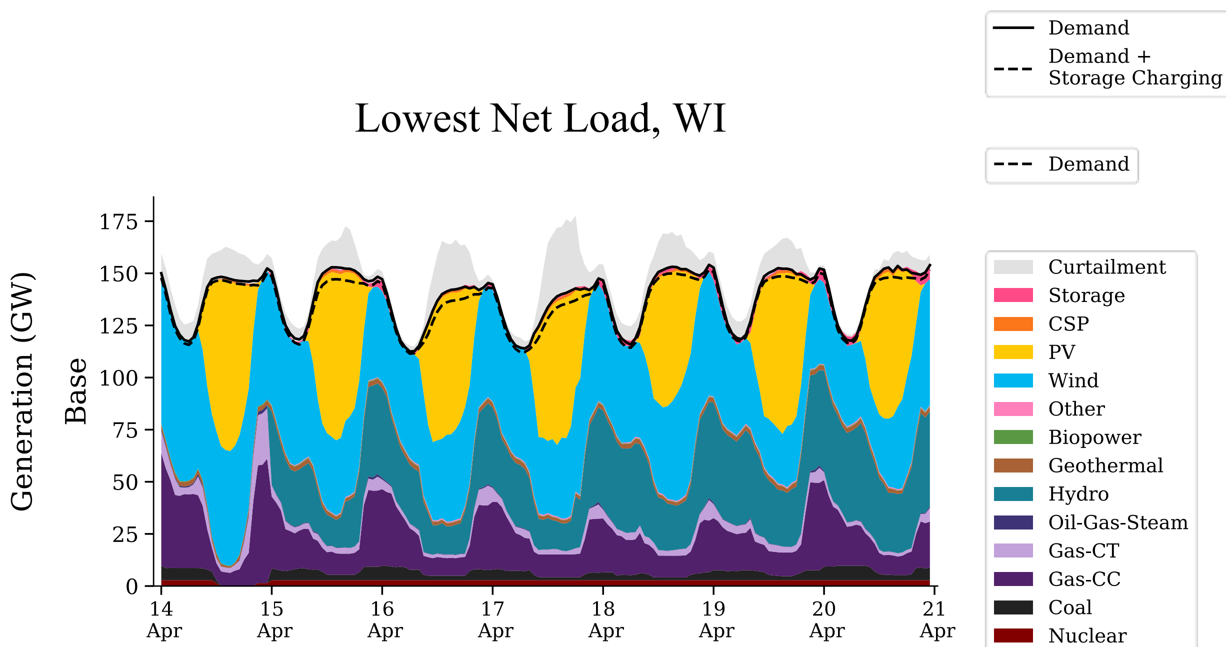

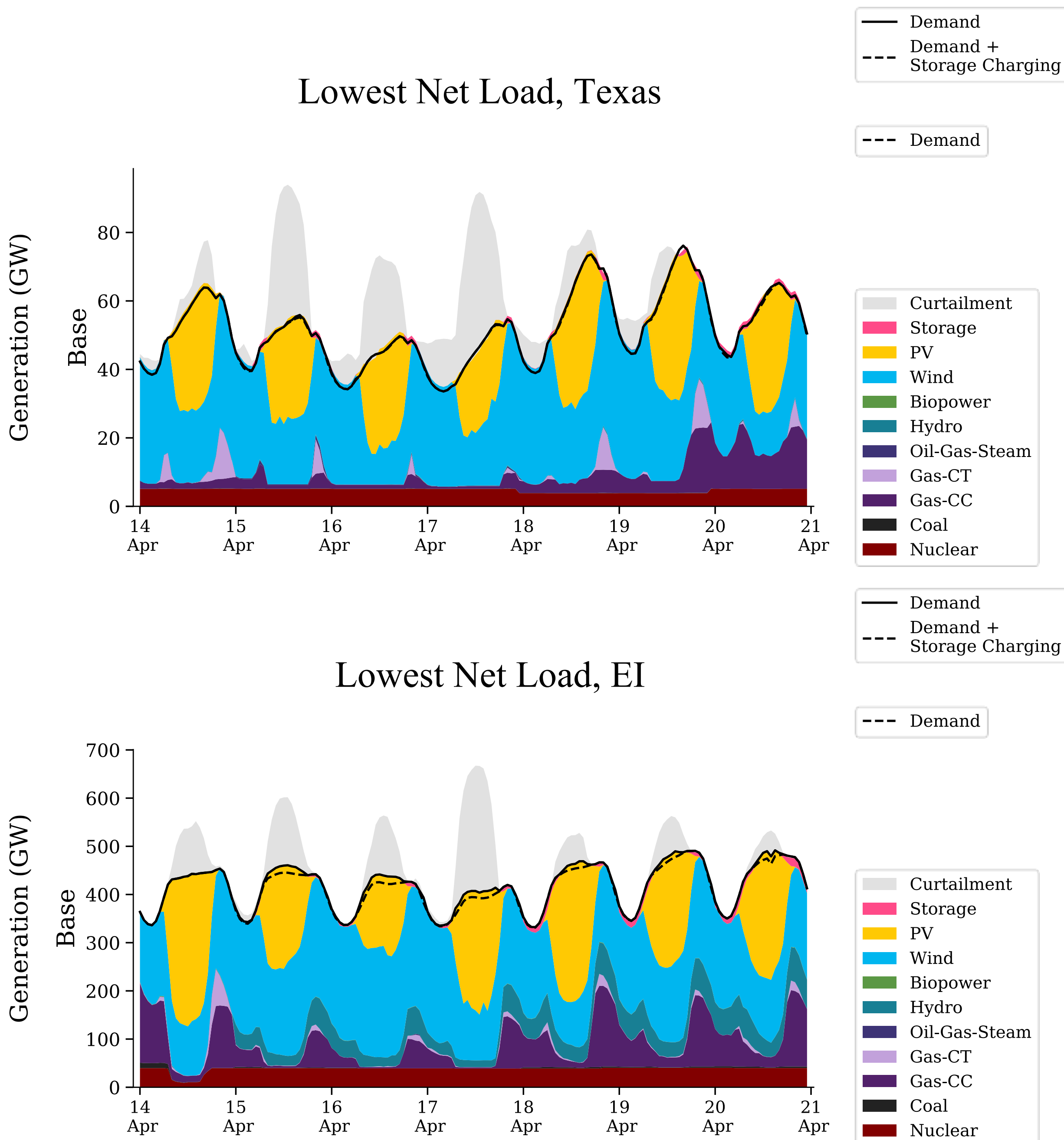

Figure A-114. System dispatch during the Lowest Net Load event for the WI (top), TI (middle), and EI (bottom)

Despite the high penetration and low load in all three interconnections, hours of peaking net load still occur. They occur at sunset and are met by a combination of reduced VRE curtailment, gas-CCs, hydropower, and quick-start gas-CTs. In the WI, which has a large fraction of energy from hydropower, solar and hydropower generation are strongly anticorrelated. The behavior of hydropower requires flexibility from hydropower to shift its energy to the higher-value overnight hours during this period.

Figure A-115 shows the total system-wide generation change relative to the base case hydropower generation assumptions. In both cases, the sensitivity reduces hydropower generation and gas-CC makes of much of the resulting gap. The Dry Hydro sensitivity reduces some VRE curtailment, and reducing the hydropower flexibility requires an increase in VRE curtailment.

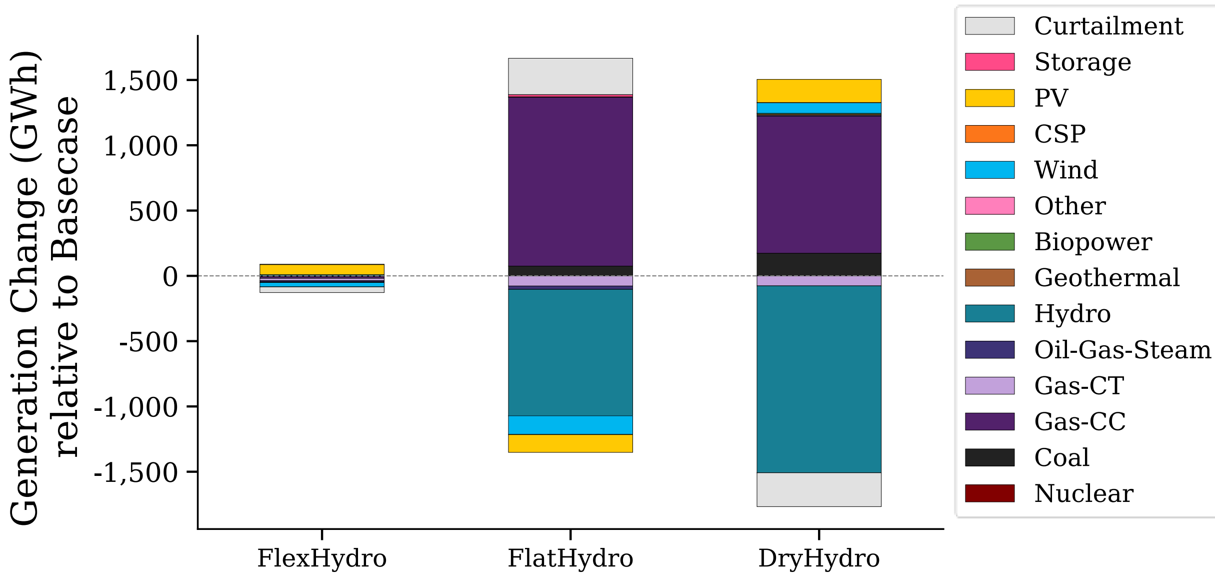

Figure A-115. Change in system-wide generation relative to the base 2050 system for the Inflexible Hydro and Dry Hydro sensitivities

Figure A-116 shows the change in hydropower generation in the Dry Hydro sensitivity. The shape of hydropower generation remains largely the same. Hydropower generation peaks at the daily net load peak and stays available for the overnight hours when there is no solar PV generation; there is just less hydropower generation dedicated to those hours. This reduced energy is planned for, and thus the gap can be met by gas-CCs, as opposed to gas-CTs, which may have been required had the hydropower reduction been unplanned.

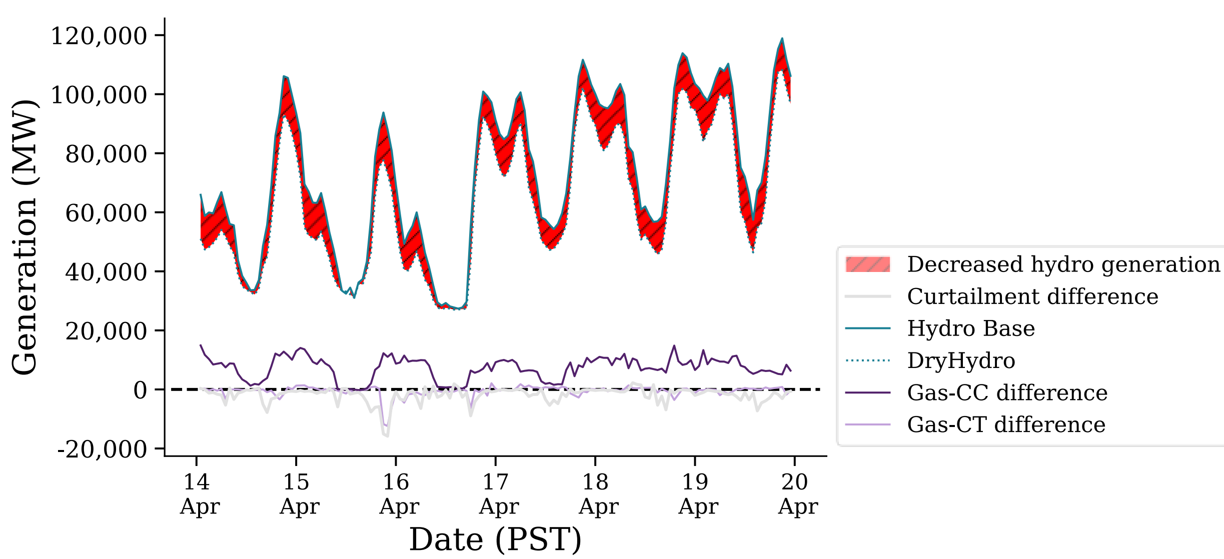

Figure A-116. Change in system-wide hydropower operations due to drier hydropower conditions during the Lowest Net load event

Similarly, Figure A-117 shows the change in hydropower generation due to less flexible hydropower generation. Similar to Dry Hydro conditions, less hydropower is available for peak net load times, but more hydropower is available midday. The mid-day hydropower leads to curtailment as hydropower plants are unable to ramp down at times of high coincident wind and solar generation. The increased curtailment and need for gas-CC generation overnight leads to a 17% increase in production costs in the WI.

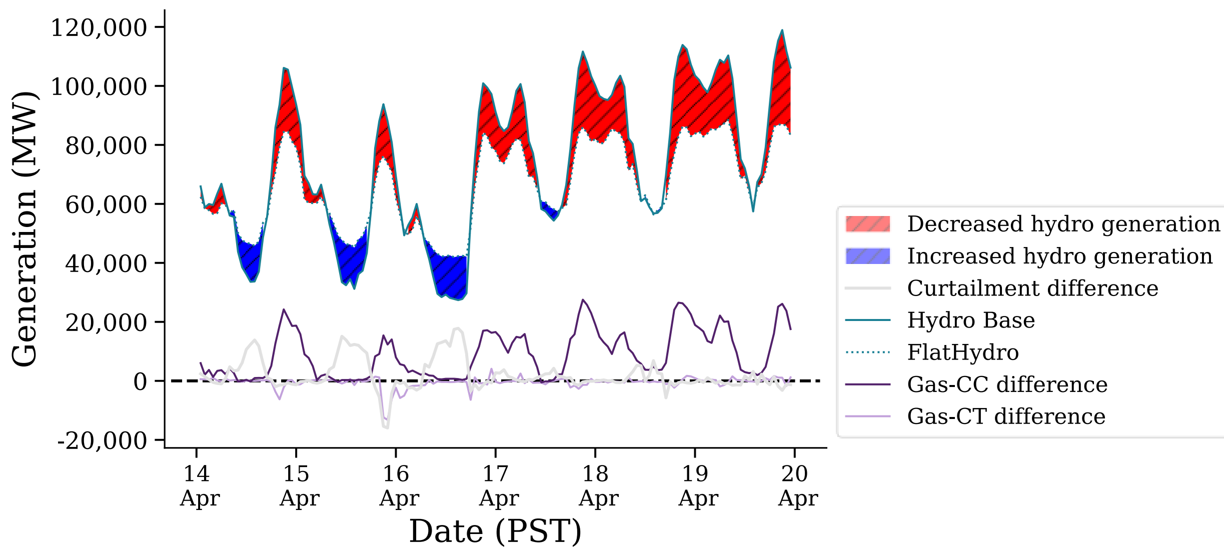

Figure A-117. Change in system-wide hydropower operations due to drier hydropower conditions during the lowest net load event

Wind Drought: October 1–24, 2010

Event Summary

Persistent high pressure at the surface and upper levels blocks the storm track and yields a three week period of low wind across most of the country.[46]

[46] See https://www.wpc.ncep.noaa.gov/dailywxmap/index_20101001.html

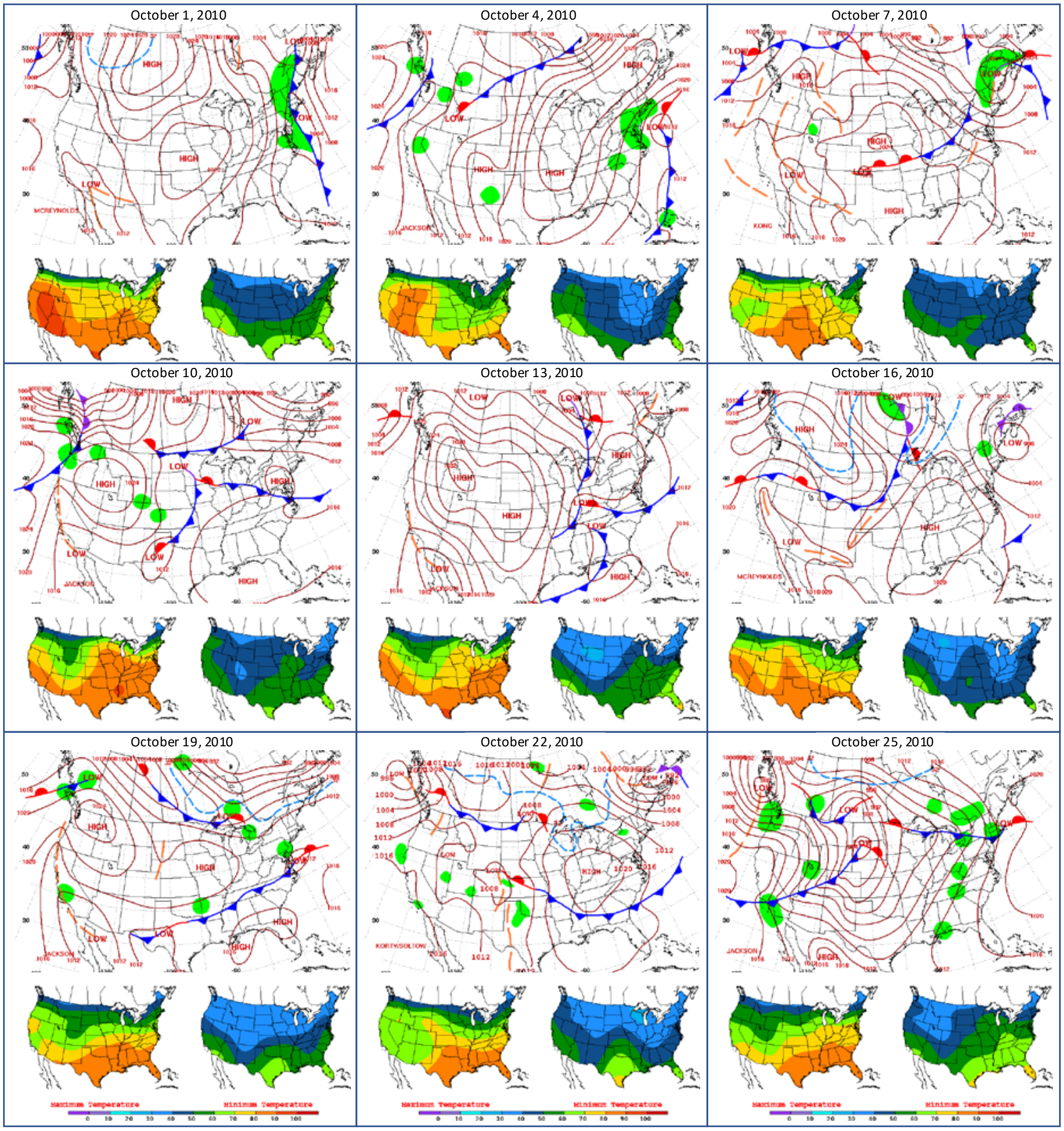

Figure A-118. Surface weather and temperature maps valid at 7 a.m. EST every third day of the wind drought

Note the dramatic change on the 25th when the drought has ended.
See the Event Description Structure section for plot details.

Source: "Daily Weather Maps: Friday, October 1, 2010," NOAA Weather Prediction Center, https://www.wpc.ncep.noaa.gov/dailywxmap/index_20101001.html

Meteorological Description

The period October 1 through 24, 2010 featured an anomalous continuation of a summertime like upper-level flow pattern into autumn. Upper-level high pressure dominated the midsection of the country, with weak upper low pressure to the west and east. This type of pattern blocks the storm track and, in this case, forced most of the weather systems northward into Canada with the CONUS being dominated by weak high pressure at the surface and almost no pressure gradient, and little weather or wind. Surface charts for a subset of the days, every third day, are shown in Figure A-118 and illustrate how little weather was occurring. Combined with shorter days bringing less solar heating, and more cooling at night, this type of pattern is not conducive to good wind resource as regions with summertime peaking resource tend to be driven by differential heating, which rapidly reduces in the transition season, and regions where the resource is driven by large-scale storm systems also see no wind.

Load Impacts

October is a transition month with cooler than average temperatures resulting in steadily reducing air conditioning load and in more northern locals an increase in heating related load during cool days. Overall in Figure A-119 shows load generally at or below the annual median, with no major excursions to extremely high levels. Left of the median, we see that there is a fat tail of below average load days.

WI loads are close to normal through most of the period with some mild excursions that can be explained by temperature effects. The high load day on the 1st is due to high temperatures in the Desert Southwest and Los Angeles area, and the above-normal period from the 11th through the 15th. The interior west also sees relatively cold nights, which may also drive increased nighttime load. In the east, we see that load is generally below normal.

There is a period of well above-normal temperatures that impacts a broad area and large load centers like Chicago, Detroit, Pittsburg, New York, Boston, and Washington D.C. and moves west to east from the 6th through the 15th, but at this time of year 5 F above drives loads down in the northern states, while 10–15°F above creates only moderate air conditioning load so only a few days show up as above-normal load. Texas experiences a cool period throughout the event except for the 11th and 12th and 18th through 22nd and consequently has well below average load.

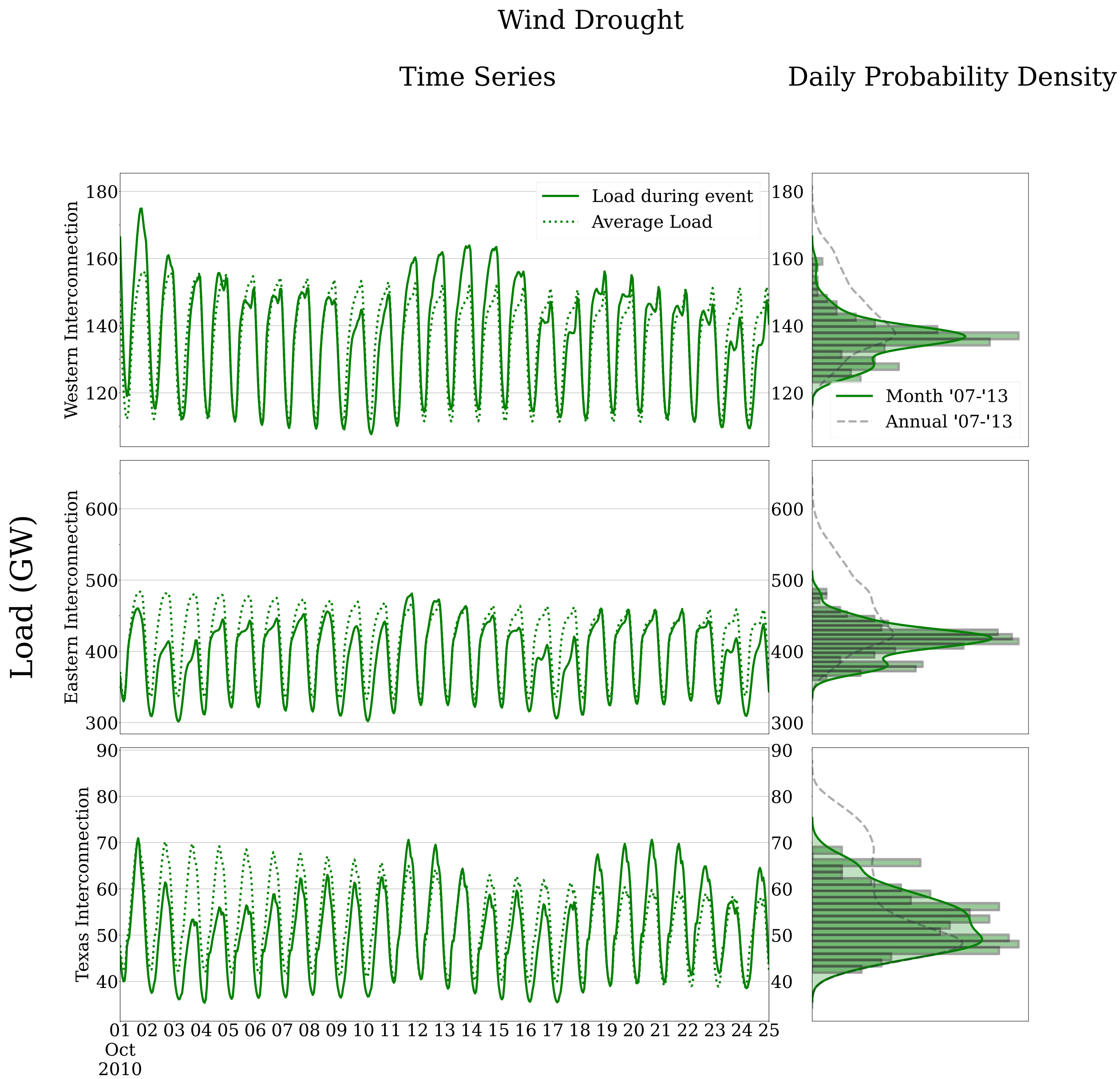

Figure A-119. Time series of regional load during the 4-day event in green, compared to load averaged across the 7-year data set for the month surrounding the event in grey (left) and distribution of 2050 regional loads for the 29 days surrounding the middle of the event in green, and across the 7-year data set in grey, with the event days labeled (right)

Wind Generation

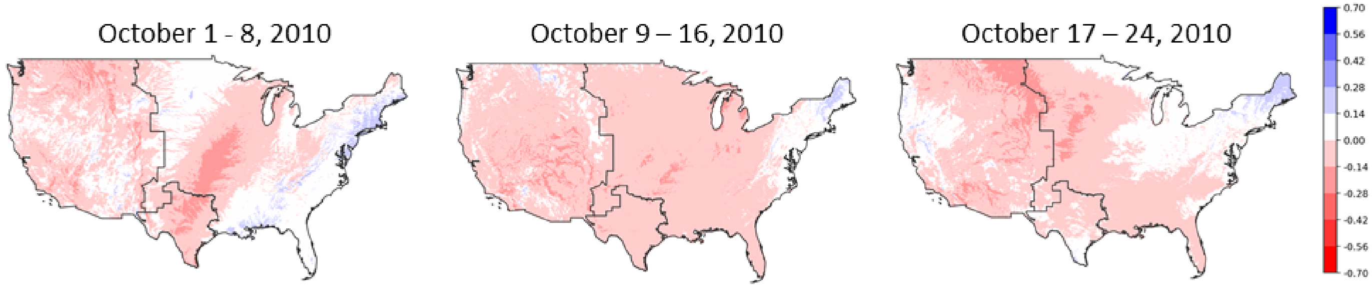

Figure A-120. Average wind resource deviation across three 8-day periods during the wind drought

National wind resource during this event is well below normal as seen in Figure A-120, especially for the period October 9 through October 16 when almost the entire country apart from the Northeast and a few spots in the west sees below average wind resource.

The time series in Figure A-121 shows that the wind drought is most consistent in the WI, with 19 of 25 days in the period having below-normal wind generation, with 7 days being 50% or less of normal for the period. The plot also shows the rapid recovery as weather systems start impacting the WI again during the day of the 24^{th}. On the EI, the 1^{st} through the 8^{th} has above average generation, and this is also reflected in Figure A-120. The period from October 9^{th} through 14^{th} sees much below average wind generation, with several days of approximately 50% of normal generation across the EI. The 12^{th} and 13^{th} are significant because wind is well below normal on the WI and TI as well. The last period is closer to normal on average, though the 19^{th} is noteworthy because of the coincidence with low wind on the other two interconnections.

Texas wind during the period is interesting because while it is below normal, it also shows a dramatic increase in diurnal variability with periods of stronger nighttime generation on the same days that daytime generation drops close to zero output. This suggests that the pattern is conducive to strengthening the nighttime low-level jet but weakening it more completely during this day. This fits with clear skies in fall conditions since the mechanism driving the low-level jet is related to differential heating of the dry high elevation plains and Rocky Mountain foothills relative to the lower elevations in the east. In the fall, under clear skies one expects both the heating and cooling to be more dramatic in the western part of the interconnection.

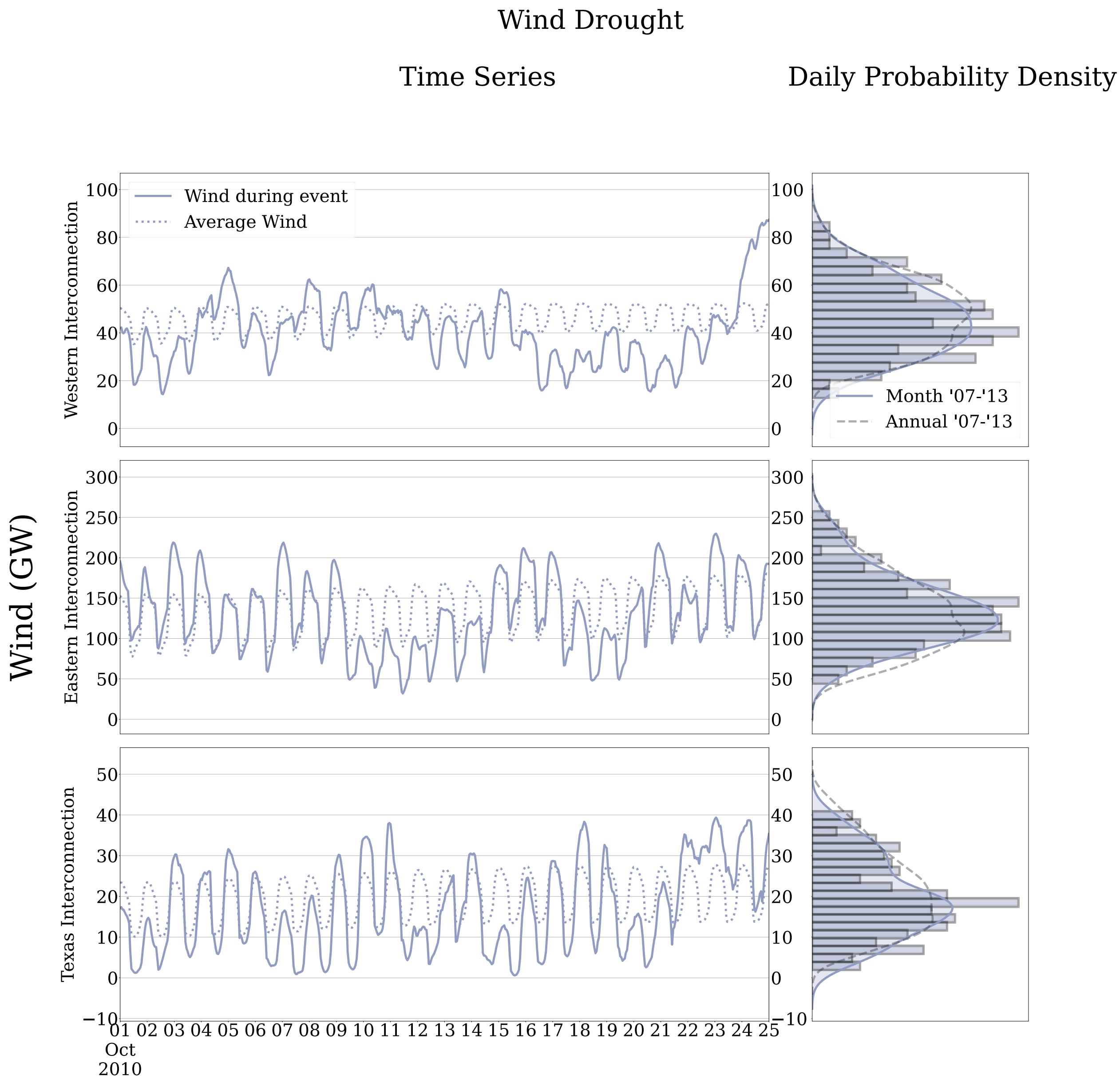

Figure A-121. Event regional wind generation (based on 2050) in context of the distribution of generation for the surrounding month (left) and time series plots of wind generation under the 2050 scenario, relative to normal for the season (right)

Solar Generation

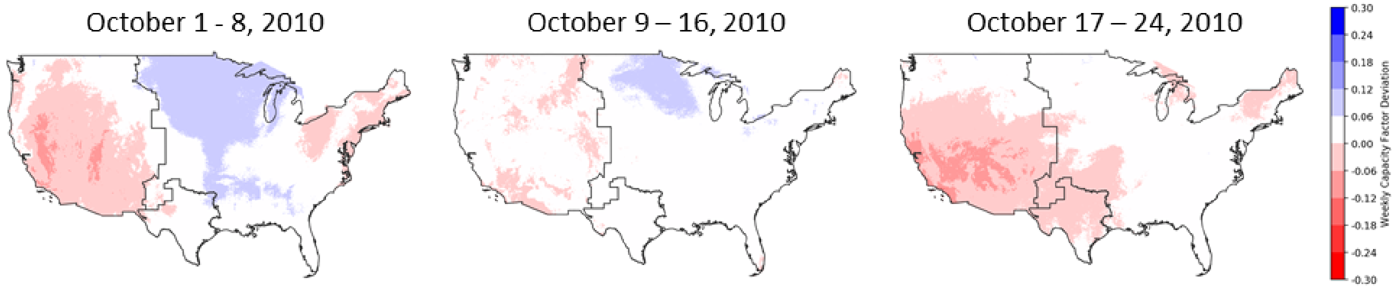

Figure A-122. Average PV resource deviation across three 8-day periods during the wind drought

The solar resource in the EI is above normal throughout the period as seen in Figure A-122.[47] The same is true of the TI for the first two 8-day periods, but the latter period sees below-normal resource. However, in the WI, the first and last periods see diminished solar resource. This is also reflected in Figure A-123. Reference to the weather maps in Figure A-118 show that this reduction is related to late season monsoon flow and at the end of the period by an upper-level low. Both spread clouds and rain into the southwest where significant modeled solar capacity is located in 2050.

[47] The white fill represents 0 to 6 capacity factor points above average capacity factor.

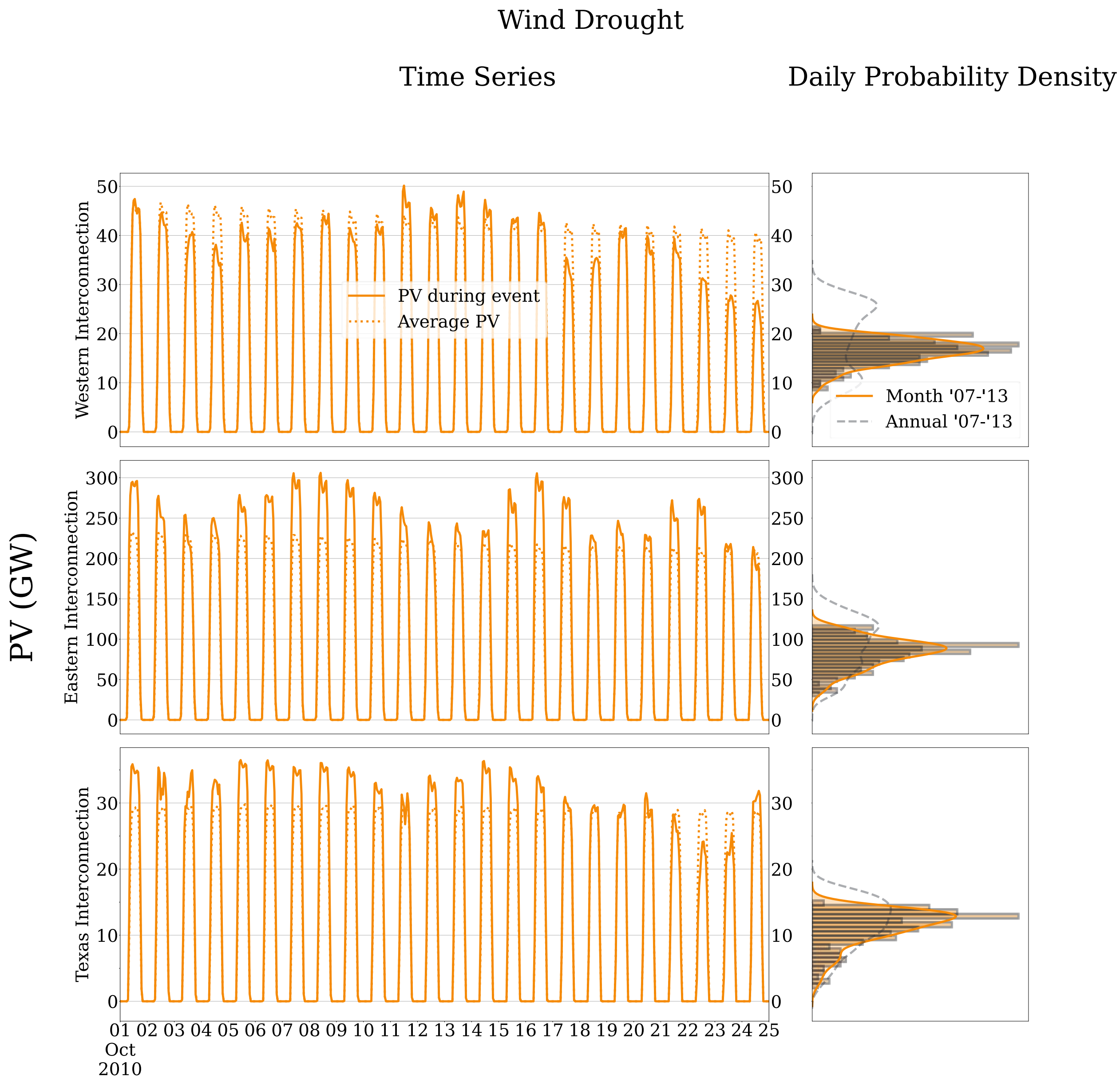

Figure A-123. Event regional modeled 2050 PV generation in context of the distribution of generation for the surrounding month (left) and time series plots of PV generation under the modeled 2050 scenario, relative to normal for the season (right)

Net Load

Despite historically low wind generation, the net load, while above average for the same period, is typically quite low, as is typical for the shoulder seasons. Indeed, on days when wind generation is near or above normal, the net load falls close to zero on all interconnections and on the EI and TI it falls below zero on two occasions. As these shoulder seasons typically allow time for thermal generators to go off-line for scheduled maintenance, these type of events may impact the timing of planned outages.

An operational issue that is worthy of mention for October is the frequent occurrence of downslope winds that bring hot dry conditions to regions west of the Sierra Nevada and California Coastal Mountains. The same conditions responsible for the wind drought also promote such flow and may cause transmission constraints to move generation (renewable or otherwise) to load, which could be exacerbated as the number of traditional assets declines.

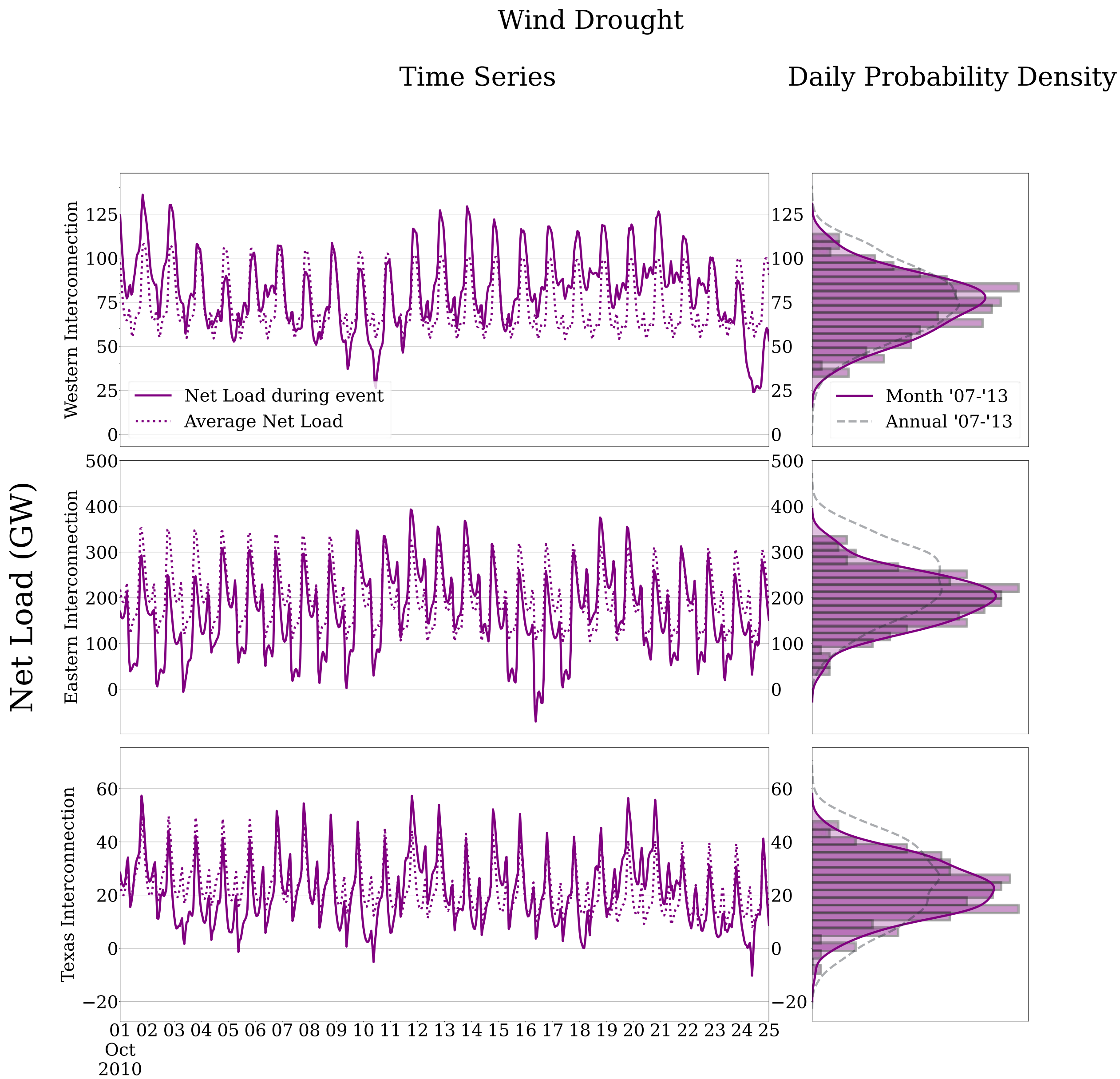

Figure A-124. Event regional modeled net load context of the distribution of generation for the surrounding month (left) and time series plots of modeled net load under the modeled 2050 scenario, relative to normal for the season (right)